Lecture Notes in Electrical Engineering 407

Artur Babiarz
Adam Czornik
Jerzy Klamka
Michał Niezabitowski
Editors

Theory and Applications of Non-integer Order Systems

8th Conference on Non-integer Order Calculus and Its Applications, Zakopane, Poland

Springer

Lecture Notes in Electrical Engineering

Volume 407

About this Series

"Lecture Notes in Electrical Engineering (LNEE)" is a book series which reports the latest research and developments in Electrical Engineering, namely:

- Communication, Networks, and Information Theory
- Computer Engineering
- Signal, Image, Speech and Information Processing
- Circuits and Systems
- Bioengineering

LNEE publishes authored monographs and contributed volumes which present cutting edge research information as well as new perspectives on classical fields, while maintaining Springer's high standards of academic excellence. Also considered for publication are lecture materials, proceedings, and other related materials of exceptionally high quality and interest. The subject matter should be original and timely, reporting the latest research and developments in all areas of electrical engineering.

The audience for the books in LNEE consists of advanced level students, researchers, and industry professionals working at the forefront of their fields. Much like Springer's other Lecture Notes series, LNEE will be distributed through Springer's print and electronic publishing channels.

More information about this series at http://www.springer.com/series/7818

Artur Babiarz · Adam Czornik
Jerzy Klamka · Michał Niezabitowski
Editors

Theory and Applications of Non-integer Order Systems

8th Conference on Non-integer Order Calculus and Its Applications, Zakopane, Poland

Springer

Editors
Artur Babiarz
Institute of Automatic Control
Silesian University of Technology
Gliwice
Poland

Jerzy Klamka
Institute of Automatic Control
Silesian University of Technology
Gliwice
Poland

Adam Czornik
Institute of Automatic Control
Silesian University of Technology
Gliwice
Poland

Michał Niezabitowski
Institute of Automatic Control
Silesian University of Technology
Gliwice
Poland

ISSN 1876-1100 ISSN 1876-1119 (electronic)
Lecture Notes in Electrical Engineering
ISBN 978-3-319-45473-3 ISBN 978-3-319-45474-0 (eBook)
DOI 10.1007/978-3-319-45474-0

Library of Congress Control Number: 2016949579

Printed on acid-free paper

This Springer imprint is published by Springer Nature
The registered company is Springer International Publishing AG
The registered company address is: Gewerbestrasse 11, 6330 Cham, Switzerland

Preface

The non-integer order calculus is as old as the integer one although up to recently its application was exclusively in mathematics. Many real systems are better described with non-integer order differential equations. This characteristic has attracted the engineers' interest in the later years and now it is a tool used in almost every area of science. The book presents high-quality research papers presented at the 8th Conference on Non-integer Order Calculus and Its Applications that was organized by the Institute of Automatic Control, Silesian University of Technology, Gliwice, Poland. The book is broadly divided into four parts reflecting particular aspects of the fractional-order calculus methods: mathematical foundations, modeling and control, controllability and stability, and applications.

The first part contains papers focus on general concepts of non-integer order calculus and differential equations such as existence of solutions of fractional impulsive integro-differential equations, approximation of non-integer order integrator with the use of diffusive realization of pseudo-differential operator, approximation of non-integer order integrator with the use of diffusive realization of pseudo-differential operator, Cayley–Hamilton theorem for fractional linear systems, composition properties of output-additive switching scheme with fractional constant-order differ-integral, dynamic properties of the variable-, fractional-order oscillation (inertial) element, properties of the discrete Mittag-Leffler two parameter function, output-additive switching strategy for a new variable type and order difference, large deviation principle for stochastic fractional differential equation and mean square stability of discrete-time fractional-order systems.

The second part provides new elements to the systems modeling and control using the theory of fractional-order systems. In particular the following topics are discussed: conformable fractional wave-like equation, parallel algorithm for reconstruction the boundary condition for the heat conduction equation with derivative of fractional order, Voigt models, optimal control problem for fractional discrete-time systems with quadratic performance index, maximum and minimum principles for the generalized fractional diffusion problem, transfer function forms for implementing a new class of fractional-order phase-lead compensators of analog type, optimal control for the fractional continuous-time Cucker–Smale model,

fractional-order integrators and differentiators using Tustin-based approximations, fractional model of transient current in organic semiconductor layers, heat transfer process in grid-holes structure, tuning non-integer order controllers, fractional-order backstepping sliding-mode controller, fractional-order transfer function models with delay and digital fractional-order PID controller.

In the third part of this volume, a bunch of new results in controllability, stability, detectability, and stabilizability of non-integer systems are given. Among others controllability of nonlinear fractional delay dynamical systems with multiple delays in control, controllability criteria for fractional systems with varying delays, controllability of nonlinear stochastic fractional integro-differential systems, realizations for fractional one-dimensional systems with digraph-based algorithm, relative controllability of nonlinear fractional delay dynamical systems, computation of the initial data of finite dimension and inputs for given outputs of linear stationary fractional differential-algebraic with delay system are presented.

The fourth part presents applications of non-integer models to: path control with Al-Alaoui rule for fractional calculus discretization, bi-fractional filtering on the Arduino Uno hardware platform, describe anomalous dielectric properties of materials whose behavior obeys to the Havriliak–Negami model, determination of state matrices of fractional-order dynamic system by use of digraphs, PI controller based on an optimal loop shape approach, mode controller design for blood glucose regulation, and methyl alcohol mass transfer in silica.

Gliwice, Poland
July 2016

Artur Babiarz
Adam Czornik
Jerzy Klamka
Michał Niezabitowski

Organization

The RRNR 2016—8th Conference on Non-integer Order Calculus and its Applications is organized by the Institute of Automatic Control, Silesian University of Technology in Gliwice in Poland.

Program Committee

Conference Chair
Tadeusz Kaczorek, Faculty of Electrical Engineering, Bialystok University of Technology, Poland

Conference Co-Chairs
Adam Czornik, Institute of Automatic Control, Silesian University of Technology, Poland
Jerzy Klamka, Institute of Automatic Control, Silesian University of Technology, Poland

Organizing Committee

Organizing Chair
Adam Czornik, Institute of Automatic Control, Silesian University of Technology, Poland

Organizing Co-Chairs
Artur Babiarz, Institute of Automatic Control, Silesian University of Technology, Poland
Michał Niezabitowski, Institute of Automatic Control, Silesian University of Technology, Poland

Contents

Part I
Mathematical Foundations

Existence of Solutions of Abstract Fractional Impulsive Integrodifferential Equations of Sobolev Type

Natarajan Annapoorani

Abstract In this paper, we prove the existence of solutions of fractional impulsive integrodifferential equations of Sobolev type. The results are obtained by using fractional calculus and fixed point techniques.

Keywords Fractional calculus · Integrodifferential equations · Sobolev type · Impulsive conditions · Fixed point theorems

1 Introduction

In the past few decades, fractional calculus has proved its efficiency in modeling the anomalous behaviors observed in various fields of science and engineering, so the theory of fractional differential equations has been extensively studied by several authors [1–10]. Fractional differential equations draw a great application in nonlinear oscillations of earthquakes [11], many physical phenomena such as seepage flow in porous media and in fluid dynamic traffic models. Fractional derivatives can eliminate the deficiency of continuum traffic flow.

The Sobolev type semilinear integrodifferential equation serves as an abstract formulation of partial integrodifferential equation which arises in various applications such as in the flow of fluid through fissured rocks [12], thermodynamics and shear in second order fluids and so on. Moreover, the fractional integrodifferential equations of Sobolev type appear in the theory of control of dynamical systems, when the controlled system or/and the controller is described by a fractional integrodifferential equation of Sobolev type. Furthermore, the mathematical modeling and simulations of systems and processes are based on the description of their properties in terms of fractional integrodifferential equation of Sobolev type. These new models are more adequate than previously used integer order models, so fractional order

N. Annapoorani (✉)
Bharathiar University, Coimbatore 641046, India
e-mail: pooranimaths@gmail.com

A. Babiarz et al. (eds.), *Theory and Applications of Non-integer Order Systems*,
Lecture Notes in Electrical Engineering 407, DOI 10.1007/978-3-319-45474-0_1

integrodifferential equations of Sobolev type have been investigated by many researchers. We refer the reader to [13–18] and the references therein.

On the other hand, the study of impulsive differential equations has attracted a great deal of attention in fractional dynamics and its theory has been treated in several works [15, 19, 20]. The differential equations involving impulsive effects appear as a natural description of observed evolution phenomena introduction of the basic theory of impulsive differential equations, we refer the reader to [21] and the references therein. The impulsive condition is a combination of traditional initial value problems and short-term perturbations whose duration is negligible in comparison with the duration of the process. Impulsive fractional differential equations are used to describe many practical dynamical systems including evolutionary processes characterized by abrupt changes of the state at certain instants. Nowadays, the theory of impulsive fractional differential equations has received great attention, devoted to many applications in mechanical, engineering, medicine, biology, ecology and etc. Motivated by the above, in this paper we study the existence of solutions of fractional impulsive integrodifferential equations of Sobolev type in Banach spaces.

2 Preliminaries

We need some basic definitions and properties which are used in this paper. Let X and Y be Banach spaces with norms $|\cdot|$ and $\|\cdot\|$ respectively and $\mathcal{R}_+ = [0, \infty)$. Suppose $f \in L_1(\mathcal{R}_+)$. Let $\mathcal{C}(J, X)$ be the Banach space of continuous functions $x(t)$ with $x(t) \in X$ for $t \in J = [0, a]$ and $\|x\|_{\mathcal{C}(J,X)} = \max_{t\in J} \|x(t)\|$. Also consider the Banach Space

$$\mathcal{PC}(J, X) = \{u : J \to X : u \in \mathcal{C}((t_k, t_{k+1}], X),\ k = 0, \ldots, m \text{ and there exist } u(t_k^-) \text{ and } u(t_k^+),\ k = 1, \ldots, m \text{ with } u(t_k^-) = u(t_k)\},$$

with the norm $\|u\|_{\mathcal{PC}} = \sup_{t\in J} \|u(t)\|$. Set $J' := [0, a]\backslash\{t_1, \ldots, t_m\}$.

Definition 1 The Riemann–Liouville fractional integral operator of order $\alpha > 0$, of function $f \in L_1(\mathbb{R}_+)$ is defined as

$$I_{0+}^{\alpha} f(t) = \frac{1}{\Gamma(\alpha)} \int_0^t (t - s)^{\alpha-1} f(s) ds,$$

where $\Gamma(\cdot)$ is the Euler gamma function.

Definition 2 The Riemann–Liouville fractional derivative of order $\alpha > 0, n - 1 < \alpha < n, n \in N$, is defined as

$${}^{(R-L)}D_{0+}^{\alpha} f(t) = \frac{1}{\Gamma(n - \alpha)} \left(\frac{d}{dt}\right)^n \int_0^t (t - s)^{n-\alpha-1} f(s) ds,$$

where the function $f(t)$ have absolutely continuous derivatives up to order $(n - 1)$.

The Riemann–Liouville fractional derivatives have singularity at zero and the fractional differential equations in the Riemann–Liouville sense require initial conditions of special form lacking physical interpretation [5], but the Caputo defined the fractional derivative in the following way, over come such specific initial conditions.

Definition 3 The Caputo fractional derivative of order $\alpha > 0$, $n-1 < \alpha < n$, is defined as

$$^{C}D^{\alpha}_{0+}f(t) = \frac{1}{\Gamma(n-\alpha)}\int_0^t (t-s)^{n-\alpha-1} f^n(s)ds,$$

where the function $f(t)$ have absolutely continuous derivatives up to order $(n-1)$. If $0 < \alpha < 1$, then

$$^{C}D^{\alpha}_{0+}f(t) = \frac{1}{\Gamma(1-\alpha)}\int_0^t \frac{f'(s)}{(t-s)^{\alpha}}ds,$$

where $f'(s) = Df(s) = \frac{df(s)}{ds}$ and f is an abstract function with values in X.

For basic facts about fractional integrals and fractional derivatives and in particular the properties of the operators I^{α}_{0+} and $^{C}D^{\alpha}_{0+}$ one can refer to the books [6, 7, 9, 10].

Consider the following nonlinear fractional impulsive integrodifferential equation of Sobolev type of the form

$$\begin{aligned} ^{C}D^{q}(Bu(t)) &= Au(t) + f\Big(t, u(t), \int_0^t h(t,s,u(s))ds\Big), \quad t \in J = [0,a], t \neq t_k \\ \Delta u\,\big|_{t=t_k} &= I_k(u(t_k^-)), \\ u(0) &= u_0, \end{aligned} \tag{1}$$

where $0 < q < 1$, A and B are a linear operator with domains contained in a Banach space X and ranges contained in a Banach Space Y and the operators $A : D(A) \subset X \to Y$ and $B : D(B) \subset X \to Y$ satisfy the following hypotheses:

(H1) A and B are closed linear operators,
(H2) $D(B) \subset D(A)$ and B is bijective,
(H3) $B^{-1} : Y \to D(B)$ is compact,
(H4) $B^{-1}A : X \to D(B)$ is continuous.

The nonlinear operators $f : J \times X \times Y \to Y$ and $h : \Omega \times X \to Y$ are given abstract functions, $I_k : X \to Y$, $k = 1, 2, \cdots, m$ and $u_0 \in X$, $0 = t_0 < t_1 < \cdots < t_m < t_{m+1} = a$, $\Delta u|_{t=t_k} = u(t_k^+) - u(t_k^-)$, $u(t_k^+) = \lim_{h\to 0^+} u(t_k + h)$ and $u(t_k^-) = \lim_{h\to 0^-} u(t_k + h)$ represent the right and left limits of $u(t)$ at $t = t_k$. Here $\Omega = \{(t,s) : 0 \le s \le t \le a\}$. For brevity, let us take $Hu(t) = \int_0^t h(t,s,u(s))ds$. It is easy to prove that the Eq. (1) is equivalent to the integral equation

$$u(t) = \begin{cases} u_0 + \dfrac{1}{\Gamma(q)} \displaystyle\int_0^t (t-s)^{q-1} B^{-1} Au(s)ds \\ + \dfrac{1}{\Gamma(q)} \displaystyle\int_0^t (t-s)^{q-1} B^{-1} f(s, u(s), Hu(s))ds, \text{ if } t \in [0, t_1], \\ u_0 + \dfrac{1}{\Gamma(q)} \displaystyle\sum_{i=1}^{k} \int_{t_{i-1}}^{t_i} (t_i - s)^{q-1} B^{-1} Au(s)ds \\ + \dfrac{1}{\Gamma(q)} \displaystyle\int_{t_k}^t (t-s)^{q-1} B^{-1} Au(s)ds \\ + \dfrac{1}{\Gamma(q)} \displaystyle\sum_{i=1}^{k} \int_{t_{i-1}}^{t_i} (t_k - s)^{q-1} B^{-1} f(s, u(s), Hu(s))ds \\ + \dfrac{1}{\Gamma(q)} \displaystyle\int_{t_k}^t (t-s)^{q-1} B^{-1} f(s, u(s), Hu(s))ds \\ + \displaystyle\sum_{i=1}^{k} B^{-1} I_i(u(t_i^-)), \text{ if } t \in (t_k, t_{k+1}]. \end{cases} \quad . \quad (2)$$

By a local solution of the abstract Cauchy problem (1), we mean an abstract function u such that the following conditions are satisfied:

(i) $u \in \mathcal{PC}(J, X)$ and $u \in D(A)$ on J';
(ii) $\dfrac{d^q u}{dt^q}$ exists and continuous on J', where $0 < q < 1$;
(iii) u satisfies Eq. (1) on J' and satisfies the conditions $\Delta u \big|_{t=t_k} = I_k(u(t_k^-))$, $u(0) = u_0 \in X$ or that it is equivalent u satisfying the integral Eq. (2).

We assume the following conditions to prove the existence of solution of the Eq. (1):

(H5) The functions $I_k : X \to Y$ are continuous and there exists a constant $L > 0$, such that

$$\|I_k(u) - I_k(v)\|_Y \leq L\|u - v\|_X, \forall\, u, v \in X \quad \text{and} \quad k = 1, 2 \ldots, m.$$

(H6) $f : J \times X \times Y \to Y$ is continuous and there exists a constant $L_1 > 0$, such that

$$\|f(t, x_1, y_1) - f(t, x_2, y_2)\|_Y \leq L_1(\|x_1 - x_2\|_X + \|y_1 - y_2\|_Y),$$

$\forall\, (t, x_i, y_i) \in J \times X \times Y$.

(H7) $h : \Omega \times X \to Y$ is continuous and there exists a constant $L_2 > 0$, such that

$$\left\| \int_0^t [h(t, s, u) - h(t, s, v)]ds \right\|_Y \leq L_2\|u - v\|_X, \forall\, u, v \in X.$$

For brevity let us take $\gamma = \dfrac{a^q}{\Gamma(q+1)}$ and $R = \|B^{-1}A\|$, $R^* = \|B^{-1}\|$, $N = \max_{t\in J} \|f(t,0,0)\|$, $N^* = \max_{(t,s)\in\Omega}\left[\left\|\int_0^t h(t,s,0)ds\right\|\right]$.

3 Main Results

Theorem 1 *If the hypotheses (H1)–(H7) are satisfied and if* $\gamma(m+1)\big(R + R^*L_1(1+L_2)\big) + mR^*L \le \frac{1}{2}$, *then the problem (1) has a unique solution continuous on* J.

Proof Let $Z = \mathcal{PC}(J, X)$. Define the mapping $\Phi : Z \to Z$ by

$$\begin{aligned}\Phi u(t) = u_0 &+ \frac{1}{\Gamma(q)}\sum_{0<t_k<t}\int_{t_{k-1}}^{t_k}(t_k-s)^{q-1}B^{-1}Au(s)ds\\ &+\frac{1}{\Gamma(q)}\int_{t_k}^{t}(t-s)^{q-1}B^{-1}Au(s)ds\\ &+\frac{1}{\Gamma(q)}\sum_{0<t_k<t}\int_{t_{k-1}}^{t_k}(t_k-s)^{q-1}B^{-1}f(s,u(s),Hu(s))ds\\ &+\frac{1}{\Gamma(q)}\int_{t_k}^{t}(t-s)^{q-1}B^{-1}f(s,u(s),Hu(s))ds\\ &+\sum_{0<t_k<t}B^{-1}I_k(u(t_k^-))\end{aligned} \tag{3}$$

and we have to show that Φ has a fixed point. This fixed point is then a solution of the Eq. (1). Choose $r \ge 2(\|u_0\| + \gamma(m+1)R^*(N + L_1N^*))$. Then we can show that $\Phi B_r \subset B_r$, where $B_r := \{u \in Z : \|u\| \le r\}$. From the assumptions we have

$$\|\Phi u(t)\| \le \|u_0\| + \frac{1}{\Gamma(q)}\sum_{0<t_k<t}\int_{t_{k-1}}^{t_k}(t_k-s)^{q-1}\left\|B^{-1}A\right\|\|u(s)\|ds$$

$$+\frac{1}{\Gamma(q)}\int_{t_k}^{t}(t-s)^{q-1}\left\|B^{-1}A\right\|\|u(s)\|ds$$

$$+\frac{1}{\Gamma(q)}\sum_{0<t_k<t}\int_{t_{k-1}}^{t_k}(t_k-s)^{q-1}\left\|B^{-1}\right\|\|f(s,u(s),Hu(s))\|ds$$

$$+\frac{1}{\Gamma(q)}\int_{t_k}^{t}(t-s)^{q-1}\left\|B^{-1}\right\|\|f(s,u(s),Hu(s))\|ds + \sum_{0<t_k<t}\left\|B^{-1}\right\|\left\|I_k(u(t_k^-))\right\|$$

$$\leq \|u_0\| + \frac{1}{\Gamma(q)} \sum_{0<t_k<t} \int_{t_{k-1}}^{t_k} (t_k - s)^{q-1} \left\| B^{-1}A \right\| \|u(s)\| \, ds$$

$$+ \frac{1}{\Gamma(q)} \int_{t_k}^{t} (t - s)^{q-1} \left\| B^{-1}A \right\| \|u(s)\| \, ds$$

$$+ \frac{1}{\Gamma(q)} \sum_{0<t_k<t} \int_{t_{k-1}}^{t_k} (t_k - s)^{q-1} \|B^{-1}\| \big[\|f(s, u(s), Hu(s)) - f(s, 0, 0)\|$$

$$+ \|f(s, 0, 0)\| \big] ds + \frac{1}{\Gamma(q)} \int_{t_k}^{t} (t - s)^{q-1} \|B^{-1}\| \big[\|f(s, u(s), Hu(s)) - f(s, 0, 0)\|$$

$$+ \|f(s, 0, 0)\| \big] ds + \sum_{0<t_k<t} \|B^{-1}\| \|I_k(u(t_k^-))\| \leq \|u_0\|$$

$$+ \frac{a^q}{\Gamma(q+1)} \Big[(m+1)Rr + (m+1)R^*L_1(r + L_2 r + N^*) + (m+1)R^*N) \Big]$$

$$+ mrR^*L \leq \|u_0\| + r \Big[\gamma(m+1)\big(R + R^*L_1(1 + L_2)\big)$$

$$+ mR^*L \Big] + \gamma(m+1)R^*(N + L_1 N^*) \leq r.$$

Thus, Φ maps B_r into itself. Now, for $u, v \in Z$, we have

$$\begin{aligned}
\|\Phi u(t) - \Phi v(t)\| \leq{}& \frac{1}{\Gamma(q)} \sum_{0<t_k<t} \int_{t_{k-1}}^{t_k} (t_k - s)^{q-1} \|B^{-1}A\| \|u(s) - v(s)\| ds \\
&+ \frac{1}{\Gamma(q)} \int_{t_k}^{t} (t - s)^{q-1} \|B^{-1}A\| \|u(s) - v(s)\| ds \\
&+ \frac{1}{\Gamma(q)} \sum_{0<t_k<t} \int_{t_{k-1}}^{t_k} (t_k - s)^{q-1} \|B^{-1}\| \|f(s, u(s), Hu(s)) \\
&- f(s, v(s), Hv(s))\| ds \\
&+ \frac{1}{\Gamma(q)} \int_{t_k}^{t} (t - s)^{q-1} \|B^{-1}\| \|f(s, u(s), Hu(s)) \\
&- f(s, v(s), Hv(s))\| ds \\
&+ \sum_{0<t_k<t} \|B^{-1}\| \|I_k(u(t_k^-)) - I_k(v(t_k^-))\| \\
\leq{}& \frac{a^q}{\Gamma(q+1)} [(m+1)R\|u - v\|] + mR^*L\|u - v\|
\end{aligned}$$

$$+\frac{a^q}{\Gamma(q+1)}(m+1)R^*L_1(\|u-v\|+L_2\|u-v\|)]$$
$$\leq [\gamma(m+1)(R+R^*L_1(1+L_2))+mR^*L]\|u-v\|.$$

Hence Φ is a contraction mapping and therefore there exists a unique fixed point $u \in B_r$ such that $\Phi u(t) = u(t)$. Any fixed point of Φ is a solution of Eq. (1). □

Now we discuss the existence of solution of the fractional impulsive Sobolev type Eq. (1) with nonlocal condition of the form

$$u(0) + g(u) = u_0 \tag{4}$$

where $g : \mathcal{PC}(J, X) \to X$ is a given function which satisfies the following condition.

(H8) $g : \mathcal{PC}(J, X) \to X$ is continuous and there exists a constant $G > 0$, such that

$$\|g(u) - g(v)\| \leq G\|u - v\|_{\mathcal{PC}} \quad \text{for } u, v \in \mathcal{PC}(J, X)$$

Theorem 2 *If the hypotheses (H1)–(H8) are satisfied and if* $\gamma(m+1)\big(R + R^*L_1(1+L_2)\big) + G + mR^*L \leq \frac{1}{2}$ *then the problem (1) with nonlocal condition (4) has a unique solution continuous on* J.

Proof We want to prove that the operator defined by $\Psi : Z \to Z$ by

$$\Psi u(t) = u_0 - g(u) + \frac{1}{\Gamma(q)}\sum_{0<t_k<t}\int_{t_{k-1}}^{t_k}(t_k - s)^{q-1}B^{-1}Au(s)ds$$
$$+\frac{1}{\Gamma(q)}\int_{t_k}^{t}(t-s)^{q-1}B^{-1}Au(s)ds$$
$$+\frac{1}{\Gamma(q)}\sum_{0<t_k<t}\int_{t_{k-1}}^{t_k}(t_k - s)^{q-1}B^{-1}f(s, u(s), Hu(s))ds$$
$$+\frac{1}{\Gamma(q)}\int_{t_k}^{t}(t-s)^{q-1}B^{-1}f(s, u(s), Hu(s))ds$$
$$+\sum_{0<t_k<t}B^{-1}I_k(u(t_k^-)) \tag{5}$$

has a fixed point. This fixed point is then a solution of the Eqs. (1) and (4). Choose $r \geq 2(\|u_0\| + \|g_0\| + \gamma(m+1)R^*(N + L_1N^*))$. Then we can easily show that $\Psi B_r \subset B_r$.

$$\|\Psi u(t) - \Psi v(t)\| \leq \Big(\gamma(m+1)\big(R + R^*L_1(1+L_2)\big) + G + mR^*L\Big)\|u - v\| \leq \frac{1}{2}.$$

The result follows by the application of contraction mapping principle. □

4 Conclusion

In this paper I have proved a set of sufficient conditions for the existence of solutions of fractional impulsive integrodifferential equations of Sobolev type. Also I have discussed the existence of solution of fractional impulsive integrodifferential equations of Sobolev type equation with nonlocal condition.

References

1. Balachandran, K., Trujillo, J.J.: The nonlocal Cauchy problem for nonlinear fractional integrodifferential equations in Banach spaces. Nonlinear Anal. **72**, 4587–4593 (2010)
2. Cheng, Y., Guozhu, G.: Existence of fractional differential equations. J. Math. Anal. Appl. **310**, 26–29 (2005)
3. Cheng, Y., Guozhu, G.: On the solution of nonlinear fractional order differential equation. Nonlinear Anal. **63**, 971–976 (2005)
4. Hilfer, R.: Applications of Fractional Calculus in Physics. World Scientific, Singapore (2000)
5. Kilbas, A.A., Srivastava, H.M., Trujillo, J.J.: Theory and Applications of Fractional Differential Equations. Elsevier, Amsterdam (2006)
6. Lakshmikantham, V., Leela, S., Vasundhara Devi, J.: Theory of Fractional Dynamic Systems. Cambridge Academic Publishers, Cambridge (2009)
7. Miller, K.S., Ross, B.: An Introduction to the Fractional Calculus and Fractional Differential Equations. Wiley, New York (1993)
8. Mophou, G.M., N'Guérékata, G.M.: On integral solutions of some nonlocal fractional differential equations with nondense domain. Nonlinear Anal. **71**, 4668–4675 (2009)
9. Podlubny, I.: Fractional Differential Equations. Academic Press, New York (1999)
10. Samko, S.G., Kilbas, A.A., Marichev, O.I.: Fractional Integrals and Derivatives: Theory and Applications. Gordan and Breach, Amsterdam (1993)
11. He, J.H.: Some applications of nonlinear fractional differential equations and their approximations. B. Sci. Technol. Soc. **15**, 86–90 (1999)
12. Barenblat, G., Zheltor, J., Kochiva, I.: Basic concepts in the theory of seepage of homogeneous liquids in fissured rocks. J. Appl. Math. Mech. **24**, 1286–1303 (1960)
13. Balachandran, K., Park, D.G., Kwun, Y.C.: Nonlinear integrodifferential equations of Sobolev type with nonlocal conditions in Banach spaces. Commun. Korean Math. Soc. **14**, 223–231 (1999)
14. Balachandran, K., Kiruthika, S.: Existence of solutions of abstract fractional integrodifferential equations of Sobolev type. Comput. Math. Appl. **64**, 3406–3413 (2012)
15. Balachandran, K., Kiruthika, S., Trujillo, J.J.: On fractional impulsive equations of Sobolev type with nonlocal condition in Banach spaces. Comput. Math. Appl. **62**, 1157–1165 (2011)
16. Balachandran, K., Uchiyama, K.: Existence of solutions of nonlinear integrodifferential equations of Sobolev type with nonlocal condition in Banach spaces. Proc. Indian Acad. Sci. **110**, 225–232 (2000)
17. Brill, H.: A semilinear Sobolev evolution equation in Banach space. J. Differ. Equ. **24**, 412–425 (1977)
18. Showalter, R.E.: Existence and representation theorem for a semilinear Sobolev equation in Banach space. SIAM J. Math. Anal. **3**, 527–543 (1972)
19. Balachandran, K., Kiruthika, S.: Existence of solutions of abstract fractional impulsive semilinear evolution equations. Electron. J. Qual. Theory Differ. Equ. **4**, 1–12 (2010)
20. Benchohra, M., Slimani, B.A.: Existence and uniqueness of solutions to impulsive fractional differential equations. Electron. J. Differ. Equ. **10**, 1–11 (2009)
21. Lakshmikantham, V., Bainov, D.D., Simeonov, P.S.: Theory of Impulsive Differential Equations. World Scientific, Singapore (1989)

Quadrature Based Approximations of Non-integer Order Integrator on Finite Integration Interval

Jerzy Baranowski

Abstract Implementation of non-integer order systems is the subject of an ongoing research. In this paper we consider the approximation of non-integer order integrator with the use of diffusive realization of pseudo differential operator. We propose a transformation of variables allowing easier approximation with use of quadratures. We then analyze the convergence and discuss the consequences of reduction in the integration interval.

Keywords Diffusive realization · Approximation · Non-integer order integrator · Quadratures

1 Introduction

Non-integer order systems take an increasing part in science and engineering. Their applications include, among the others, modeling, control and signal processing. In most of the problems the infinite memory of non-integer order systems introduces problems with realization. Because of that realizations cannot come directly from the definition but have to take form of integer order realizations.

In this paper, the problem of realization of non-integer order integrator, i.e., $1/s^{\alpha}$ is considered. A method based on diffusive realization of pseudo differential operators is investigated.

Currently realizations on non-integer order systems are focused in four areas. First area is based on approximating the s^{α} operator in the frequency domain. The most popular approaches are the Oustaloup's method [1, 2] and CFE (*Continuous fraction expansion*) method [3–5]. Both these methods are based on different premises

Work realised in the scope of project titled "Design and application of non-integer order subsystems in control systems". Project was financed by National Science Centre on the base of decision no. DEC-2013/09/D/ST7/03960.

J. Baranowski (✉)
AGH University of Science and Technology, Al. Mickiewicza 30, 30-059 Cracow, Poland
e-mail: jb@agh.edu.pl

A. Babiarz et al. (eds.), *Theory and Applications of Non-integer Order Systems*,
Lecture Notes in Electrical Engineering 407, DOI 10.1007/978-3-319-45474-0_2

but both allow obtaining relatively easy approximations. CFE method is generally considered as worse of the two in the aspect of frequency response representation [6]. Ostaloup's method gives a very good representation of frequency response at the cost of high numerical sensitivity. This sensitivity can be lessened with use of time domain realizations [7, 8].

Second method of approximation relies on discrete realizations based on truncation of series representations. In particular, the methods include truncation of Grünwald–Letnikov derivative definitions or power series expansions (PSE) in the z variable (discrete frequency) domain. These methods give good approximations only at high frequencies. Examples of the method can be found in [9]. Improvements on PSE methods with better band of correct approximation were investigated by Ferdi [10, 11].

Third method of approximation is based on approximation of non-integer order system impulse response with Laguerre functions. Early works in this area were unsuccessful in approximation of α order integrators [12, 13]. In [14] it was shown that under certain assumptions method is convergent in L^1 and L^2 norms when approximating asymptotically stable non-integer transfer functions of relative degree equal or greater than one. Most applications of the methods are in filtering and parametric optimization [15–18].

Fourth type of approximation that recently rises in popularity is the method using diffusive realization of pseudo differential operators [19] for approximation. First works in the area used finite dimensional approximation with trapezoidal integration [20]. Later works used simple diagonal matrix time domain realization with modified Oustaloup nodes from frequency domain method [21, 22]. This method is especially useful in analysis of infinite dimensional systems using operator theory. It can be used, for example, to prove such properties as stability of closed loop system [23].

In this paper, diffusive realization is used for construction of approximation using quadrature methods. In particular, frequency domain representation of non-integer order integral will be used, i.e., $1/s^\alpha$. For such system the input-output mapping will be approximated using two quadratures on finite integration intervals allowing creation of finite dimensional approximation in the form of sum of first order lags.

The rest of the paper is organized as follows. Next section presents a theorem that is a basis of investigation along with its proof. Next, the approximation method is presented and a variable transformation allowing effective use of quadratures. Then two types of quadratures are analyzed. Operation of both quadratures is investigated with the use of H^∞ norm as an indicator of approximation quality. Then results are discussed and future works directions are presented.

2 Diffusive Realization of Non-integer Order Integrator

As the basis for diffusive realization we consider the following theorem (see e.g. [21]) which determines equivalent form for integrator of order α.

Theorem 1 *For* $\alpha \in (0, 1)$ *and* $s \in \mathbb{C}$ *we have:*

$$\frac{1}{s^\alpha} = \int_0^\infty \frac{\sin \alpha\pi}{\pi} \frac{1}{x^\alpha} \frac{1}{s + x} x. \tag{1}$$

Proof Proof will be omitted, however it relies on computing inverse Laplace transform of $1/s^\alpha$ using contour integration using Bromwich contour (see Fig. 1).

Remark 1 Grabowski in [23] proved the same result in a different way. The given proof is based on direct calculation of right-hand side of (1) using integration contour as in Fig. 2. This proof, however, is not constructive.

The main advantage of the method used in Theorem 1 is that we do not need to integrate non-integer power of s. It allows to approximate the integral.

3 Approximation of Diffusive Realizations

The basic approach to approximation of integrals relies on using infinite sum of form

$$\int_0^\infty \frac{\sin \alpha\pi}{\pi} \frac{1}{x^\alpha} \frac{1}{s + x} x \approx \sum_{i=0}^{n} \frac{b_i}{s + x_i} \tag{2}$$

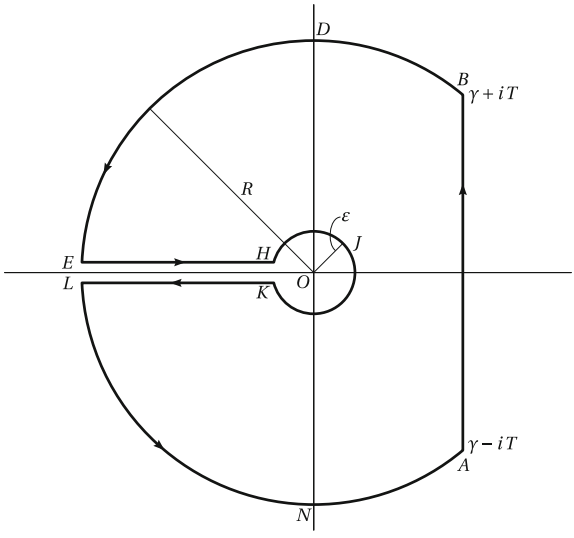

Fig. 1 Bromwich contour

Fig. 2 Contour from [23]

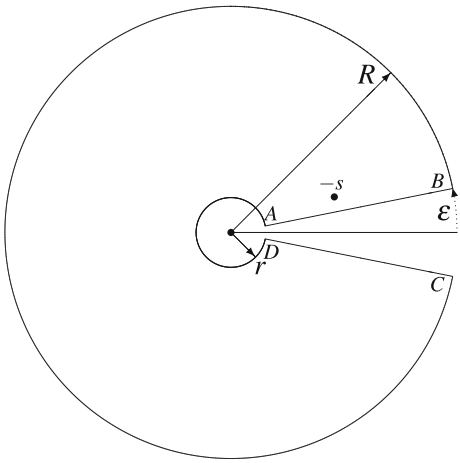

where x_i, are denote nodes of quadrature while b_i are products of quadrature weights and integrand values. The choice of quadrature for approximation is not straightforward. In [20] the authors used trapezoidal rule. In [21], rectangle rule with non-uniform nodes was considered. Both approaches transform the integration interval from $[0,\ \infty]$ to $(0,\ \omega_{max}]$ as x_i are important only for high frequencies. It causes, however, errors in integrating, especially near ω_{max}.

Despite the fact that integral (2) is defined on infinite interval, multiple authors had considered limiting the interval only to the one including the interesting frequency band. In this paper we will focus on such bounded intervals, but using more advanced quadratures.

It can be inferred, that because approximant (2) is a sum of first order low pass filters the quality of frequency response representation will depend on time constants. Because we are interested in good representation of frequencies for different orders of magnitude a following transformation is proposed. Let us set

$$x = 10^{\theta}$$

Integrating (1) for $x \in [10^a, 10^b]$ reduces to

$$\int_a^b \frac{\sin \alpha\pi}{\pi} \log(10) 10^{\theta(1-\alpha)} \frac{1}{s + 10^{\theta}} \mathrm{d}\theta. \tag{3}$$

This formula, while at first glance complicated allows balancing high and low frequencies. Following section contains analysis of quadratures for finite intervals.

4 Quadratures on Infinite Intervals

In this section we will consider two types of quadratures on finite intervals, originating from interval $[-1, 1]$. We will however present very elegant matlab code examples given originally by Trefethen [24]. Provided programs are fully functional and self explanatory.

The first quadrature we consider is the Gauss quadrature, also known as Gauss–Legendre quadrature. It is a quadrature, nodes of which are roots of Legendre polynomials, while formulas for weights one can find for example in [25]. Main advantage of the Gauss–Legendre quadrature comes from the orthogonality of Legendre polynomials. In particular, let us consider a polynomial $p(x)$ of order $2N + 1$. Such polynomial can always be written as $p(x) = q(x) \cdot l_{N+1}(x) + r(x)$, where $q(x)$ is a polynomial of degree $N + 1$, $l_{N+1}(x)$ is a Legendre polynomial of degree $N + 1$ and $r(x)$ is a polynomial of degree N. When considering interpolation quadrature of degree $N + 1$ on nodes, we can easily see that $\int_{-1}^{1} q(x) \cdot l_N(x)\mathrm{d}x = 0$ because of orthogonality of Legendre polynomials and the integral of $r(x)$ is exact because of uniqueness of interpolation polynomials. These facts give that Gauss–Legendre quadratures on $N + 1$ nodes are exact for polynomials of order $2N + 1$. Following code uses eigenvalue decomposition to obtain both weights and nodes.

```
function I = gauss(f,n) % (n+1)-pt Gauss quadrature of f
beta = .5./sqrt(1-(2*(1:n)).^(-2)); % 3-term recurrence coeffs
T = diag(beta,1) + diag(beta,-1); % Jacobi matrix
[V,D] = eig(T); % eigenvalue decomposition
x = diag(D); [x,i] = sort(x); % nodes (= Legendre points)
w = 2*V(1,i).^2; % weights
I = w*feval(f,x); % the integral
```

The second quadrature is the Clenshaw–Curtis quadrature. It is an interpolation quadrature on Chebyshev nodes. In certain aspects it is also equivalent to discrete cosine transform, and can be computed using FFT. Again code given by Trefethen:

```
function I = clenshaw_curtis(f,n) % (n+1)-pt C-C quadrature of f
x = cos(pi*(0:n)'/n); % Chebyshev points
fx = feval(f,x)/(2*n); % f evaluated at these points
g = real(fft(fx([1:n+1 n:-1:2]))); % fast Fourier transform
a = [g(1); g(2:n)+g(2*n:-1:n+2); g(n+1)]; % Chebyshev coeffs
w = 0*a'; w(1:2:end) = 2./(1-(0:2:n).^2); % weight vector
I = w*a; % the integral
```

While theory gives us, that Gauss quadratures, thanks to orthogonality, are exact for polynomials of twice higher order than interpolation quadratures it is observed that in practice Clenshaw–Curtis quadrature gives very similar precision [24]. Moreover it has much smaller computational complexity. It should be also noted, that while based on interpolation both of these quadratures are immune to Runge's phenomenon, as both Legendre and Chebyshev nodes have asymptotic distribution of $1/(1 - x^2)$ for $[-1, 1]$ interval.

5 Approximation Analysis

In order to analyze the approximation performance we conducted error analysis using H^∞ norm. We considered the difference

$$e(s) = \frac{1}{s^\alpha} - \sum_{i=0}^{n} \frac{b_i}{s + x_i}$$

for frequency $[10^{-5},\ 10^5]$ rad/s. The order of quadrature was increased in order to observe the change of norm of $\|e\|_\infty$. For initial analysis we have considered the integration interval of $[-5, 5]$ for (3) corresponding to $[10^{-5}, 10^5]$ rad/s for original integral. Both quadratures were tested simultaneously. In illustrated results $\alpha = 1/2$ was considered.

In the Fig. 3 we depicted this analysis. As it can be observed after initial convergence error stops decreasing and fixes on a certain value. This error is caused by the limitation of infinite interval into a finite one. Indeed one can observe in the Fig. 4 that increasing the interval to $[-7, 7]$ results in dropping of error by an order of magnitude.

The fixed error is connected to the phase errors at low frequencies. As one can observe in the Fig. 5, 50th order approximate has a phase error, especially noticeable at low frequencies, where the gain of the integrator is the largest. Because of that any

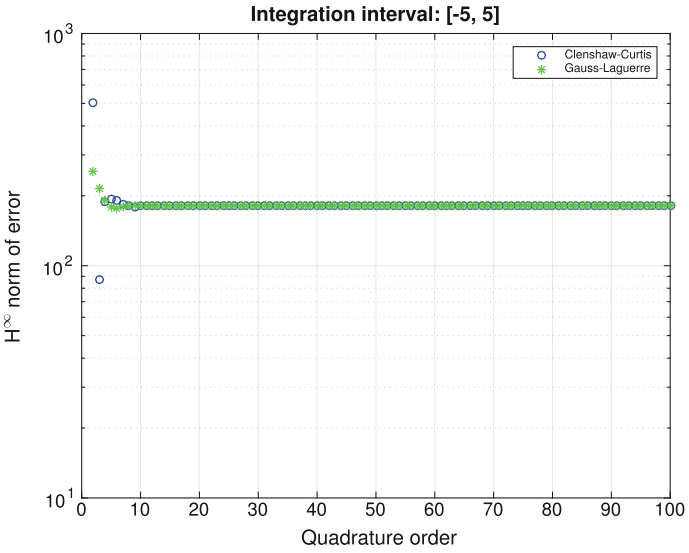

Fig. 3 Analysis of $\|e\|_\infty$ norm with increasing order of quadrature for the integration interval of $[-5, 5]$

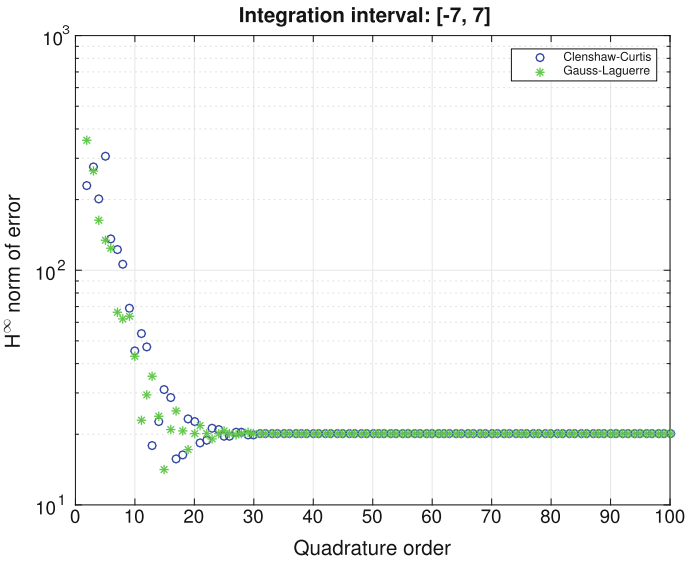

Fig. 4 Analysis of $\|e\|_\infty$ norm with increasing order of quadrature for the integration interval of $[-7, 7]$

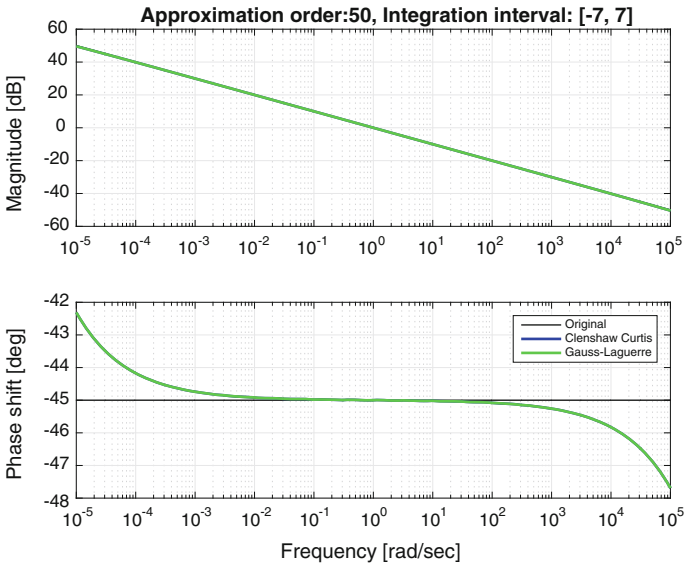

Fig. 5 Analysis of frequency response of 50th order approximation with the integration interval of $[-7, 7]$. Clenshaw–Curtis and Gauss–Legendre quadratures are overlapping

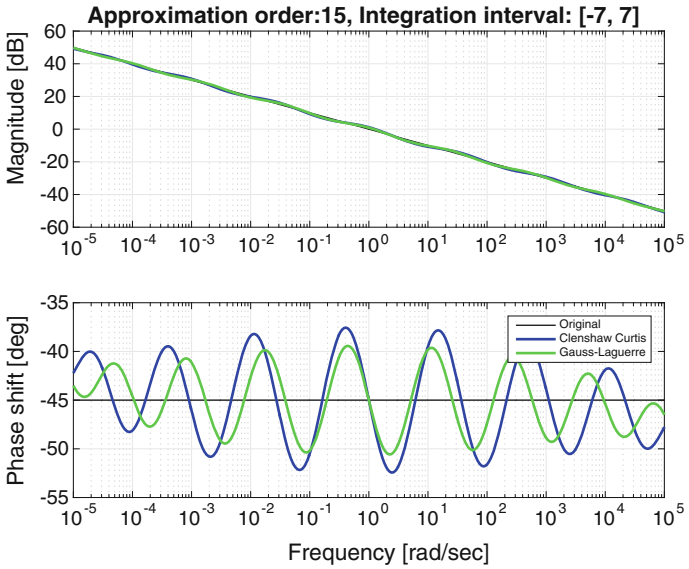

Fig. 6 Analysis of frequency response of 15th order approximation with the integration interval of $[-7, 7]$

error in phase is multiplied by approximately 300. What is interesting the magnitude is almost ideally represented.

As one can observe in the Fig. 4 there are values, where the error is smaller than the observed bias. For example such value is $N = 15$. In that case Gauss–Laguerre quadrature gives much better result. It is however caused by not obtaining convergence yet. It can be seen in Fig. 6, that the phase fluctuates strongly, and for such N and this type of quadrature is very close to the ideal value for low frequencies. Such approximation, however, is obviously not acceptable for use.

6 Conclusion

In this paper, we considered diffusive realization of integrator of order α and its approximation with use of quadratures on finite intervals. It can be observed, that initial convergence is relatively quick but bias caused by reduction of integration interval is fixed. This bias depends on integration interval, and as a-rule-of-a-thumb integration interval has to be greater than the band pass where the approximation is needed.

The performance indicator taken as the error of H^∞ norm is dominated by low-frequency terms, especially the phase errors. Nevertheless, the method should be further considered, especially in order to accelerate the convergence as there are

certain methods which show better performance for lower orders (see, e.g. Oustaloup method). It is probably due to the slow decay of function in diffusive realization (1). However, high order of approximation should not be feared, as system is directly realized with independent linear differential equations of order one which are very easily discretized.

It should be also noted, that Oustaloup approximation, which has only geometric justification outperforms this approximation significantly for bounded intervals. This suggests, that this type of approximation has only the theoretical significance.

Further works should be concentrated on using quadratures on finite intervals along with asymptotic approximation on the 'tail' of the function.

References

1. Oustaloup, A.: La Commande CRONE: Commande Robuste D'ordre Non Entier. Hermes (1991)
2. Oustaloup, A., Levron, F., Mathieu, B., Nanot, F.M.: Frequency-band complex noninteger differentiator: characterization and synthesis. IEEE Trans. Circuits Syst. I, Fundam. Theory, **47**(1), 25–39 (2000)
3. Vinagre, B.M., Chen, Y.Q., Petráš, I.: Two direct Tustin discretization methods for fractional-order differentiator/integrator. J. Franklin Inst. **340**(5), 349–362 (2003)
4. Vinagre, B., Podlubny, I., Hernandez, A., Feliu, V.: Some approximations of fractional order operators used in control theory and applications. Frac. Calc. Appl. Anal. **3**(3), 231–248 (2000)
5. Chen, Y., Vinagre, B.M., Podlubny, I.: Continued fraction expansion approaches to discretizing fractional order derivatives-an expository review. Nonlinear Dyn. **38**(1–4), 155–170 (2004)
6. Monje, C.A., Chen, Y., Vinagre, B.M., Xue, D., Feliu, V.: Fractional-order Systems and Controls. Fundamentals and Applications. Advances in Industrial Control. Springer, London (2010)
7. Baranowski, J., Bauer, W., Zagórowska, M., Dziwiński, T., Piątek, P.: Time-domain Oustaloup approximation. In: IEEE 20th International Conference on Methods and Models in Automation and Robotics (MMAR), pp. 116–120 (2015)
8. Baranowski, J., Bauer, W., Zagórowska, M.: Stability properties of discrete time-domain Oustaloup approximation. In Domek, S., Dworak, P. (eds.) Theoretical Developments and Applications of Non-Integer Order Systems, vol. 357 of Lecture Notes in Electrical Engineering, pp. 93–103. Springer International Publishing (2016)
9. Tseng, C.C.: Design of FIR and IIR fractional order Simpson digital integrators. Signal Process. **87**(5), 1045–1057 (2007)
10. Leulmi, F., Ferdi, Y.: Improved digital rational approximation of the operator S^{α} using second-order s-to-z transform and signal modeling. Circuits Syst. Signal Process. **34**(6), 1869–1891 (2015)
11. Ferdi, Y.: Computation of fractional order derivative and integral via power series expansion and signal modelling. Nonlinear Dyn. **46**(1), 1–15 (2006)
12. Maione, G.: Laguerre approximation of fractional systems. Electron. Lett. **38**(20), 1234–1236 (2002)
13. Aoun, M., Malti, R., Levron, F., Oustaloup, A.: Synthesis of fractional Laguerre basis for system approximation. Automatica **43**(9), 1640–1648 (2007)
14. Bania, P., Baranowski, J.: Laguerre polynomial approximation of fractional order linear systems. In: Mitkowski, W., Kacprzyk, J., Baranowski, J. (eds.) Advances in the Theory and Applications of Non-integer Order Systems: 5th Conference on Non-integer Order Calculus and Its Applications, vol. 257 of the series Lecture Notes in Electrical Engineering, pp. 171–182. Springer (2013)

15. Zagórowska, M., Baranowski, J., Bania, P., Piątek, P., Bauer, W., Dziwiński, T.: Impulse response approximation method for "fractional order lag". In: Latawiec, K.J., Łukaniszyn, M., Stanisławski, R. (eds.) Advances in Modelling and Control of Noninteger-order Systems - 6th Conference on Non-Integer Order Caculus and its Applications, vol. 320 of the series Lecture Notes in Electrical Engineering, pp. 113–122. Springer, Heidelberg (2014)
16. Zagórowska, M., Baranowski, J., Bania, P., Bauer, W., Dziwiński, T., Piątek, P.: Parametric optimization of PD controller using Laguerre approximation. In: IEEE 20th International Conference on Methods and Models in Automation and Robotics (MMAR), pp. 104–109, (2015)
17. Zagórowska, M.: Parametric optimization of non-integer order PD^{μ} controller for delayed system. In: Domek, S., Dworak, P. (eds.) Theoretical Developments and Applications of Non-Integer Order Systems, vol. 357 of Lecture Notes in Electrical Engineering, pp. 259–270. Springer, Heidelberg (2016)
18. Baranowski, J., Bauer, W., Zagórowska, M., Piątek, P.: On digital realizations of non-integer order filters. Circuits Syst. Signal Process (2016)
19. Montseny, G.: Diffusive representation of pseudo-differential time-operators. ESAIM: Proc. **5**, 159–175 (1998)
20. Heleschewitz, D., Matignon, D.: Diffusive realisations of fractional integrodifferential operators: Structural analysis under approximation. In: IFAC conference Systems Structure and Control, vol. 2, Nantes, France pp. 243–248 (1998)
21. Trigeassou, J., Maamri, N., Sabatier, J., Oustaloup, A.: State variables and transients of fractional order differential systems. Comput. Math. Appl. **64**(10), 3117–3140 (2012) (Advances in FDE, III)
22. Liang, S., Peng, C., Liao, Z., Wang, Y.: State space approximation for general fractional order dynamic systems. Int. J. Syst. Sci. **45**(10), 2203–2212 (2014)
23. Grabowski, P.: Stabilization of wave equation using standard/fractional derivative in boundary damping. In: Mitkowski, W., Kacprzyk, J., Baranowski, J. (eds.) Advances in the Theory and Applications of Non-integer Order Systems: 5th Conference on Non-integer Order Calculus and Its Applications, vol. 257 of the series Lecture Notes in Electrical Engineering, pp. 101–121. Springer International Publishing, Heidelberg (2013)
24. Trefethen, L.N.: Is Gauss quadrature better than Clenshaw-Curtis? SIAM Rev. **50**(1), 67–87 (2008)
25. Abramowitz, M., Stegun, I.A.: Handbook of Mathematical Functions with Formulas, Graphs, and Mathematical Tables. Dover, New York (1964)

On the Fractional Continuous-Time Hegselmann–Krause's Type Consensus Model

Ewa Girejko, Dorota Mozyrska and Małgorzata Wyrwas

Abstract The consensus problem of fractional-order multi-agent continuous-time systems is considered. In the system, interactions between opinions are defined like in Hegselmann–Krause models but with included memory by fractional-order operator on the left side of nonlinear system. In the paper we investigate various models for the dynamics of fractional order opinions by analytical methods as well as by computer simulations.

Keywords Consensus problem · Fractional order systems · Hegselmann–Krause models

1 Introduction and Preliminaries

Opinion dynamics is a field that recently draws attention of diverse researchers: mathematicians, physicians, biologists, sociologists and others. There are different approaches to modeling and analyzing the situation in which a group of individuals (calling agents) interacting with each other achieves a consensus. One way is to apply an appropriate model and examine the problem in a deterministic way. Very well known model in opinion dynamics, which treats about such phenomena is the Hegselmann–Krause model. Intensive investigation has been made in the classical approach for this model, see [1–3] and references therein. However, to the best of our knowledge, there are only few papers devoted to the subject in which fractional calculus was applied. In this paper models with Caputo and Grünwald–Letnikov operators in both, continuous and discrete cases, are studied. Grünwald–Letnikov operator is a very convenient tool for numerical approaches, while Caputo one is

E. Girejko (✉) · D. Mozyrska · M. Wyrwas
Bialystok University of Technology, Wiejska 45A, 15-351 Białystok, Poland
e-mail: e.girejko@pb.edu.pl

D. Mozyrska
e-mail: d.mozyrska@pb.edu.pl

M. Wyrwas
e-mail: m.wyrwas@pb.edu.pl

A. Babiarz et al. (eds.), *Theory and Applications of Non-integer Order Systems*,
Lecture Notes in Electrical Engineering 407, DOI 10.1007/978-3-319-45474-0_3

the most useful for direct calculations thanks to simple initial condition if one considers system involving Caputo operator. Fractional Comparison Principle gives us possibility of applying these two operators together in our consideration.

Let $c \in \mathbb{R}$. We introduce the notation $\mathbb{N}_c := \{c, c+1, c+2, \ldots\}$ and $(h\mathbb{N})_c := \{c, c+h, c+2h, \ldots\}$. Define the following sequence by its values:

$$a_k^{(\alpha)} := \begin{cases} 1 & \text{for } k = 0 \\ (-1)^k \frac{\alpha(\alpha-1)\ldots(\alpha-k+1)}{k!} & \text{for } k \in \mathbb{N}_1 \,. \end{cases} \tag{1}$$

Since $\frac{\alpha(\alpha-1)\ldots(\alpha-k+1)}{k!} = \binom{\alpha}{k}$, the sequence $\left(a_k^{(\alpha)}\right)_{k\in\mathbb{N}_0}$ can be rewritten using the generalized binomial as follows $a_k^{(\alpha)} = (-1)^k \binom{\alpha}{k}$. The following properties of the sequence $\left(a_k^{(\alpha)}\right)_{k\in\mathbb{N}_0}$ have been proven in [4]:

Proposition 1 ([4]) *Let $\alpha \in (0,1)$. Then the sequence $\left(a_k^{(\alpha)}\right)_{k\in\mathbb{N}_1}$ is increasing and $a_k^{(\alpha)} < 0$ for $k \in \mathbb{N}_1$. Moreover, $\lim_{k\to\infty} a_k^{(\alpha)} = 0$.*

Using the sequence (1) one can define the following operators.

Definition 1 Let $\alpha \in \mathbb{R}$. The Grünwald–Letnikov-type difference operator Δ_h^α of order α for a function $y : (h\mathbb{N})_0 \to \mathbb{R}$ is defined by

$$\left(\Delta_h^\alpha y\right)(kh) := h^{-\alpha} \sum_{s=0}^{\frac{t}{h}} a_s^{(\alpha)} y(kh - sh) \,, \tag{2}$$

where $h > 0$, $t = kh$, $k \in \mathbb{N}_0$ and $a_k^{(\alpha)}$ is the sequence given by (1).

Definition 2 Let $\alpha \in \mathbb{R}$. The Grünwald–Letnikov-type differential operator ${}^{GL}D^\alpha$ of order α for a function $x : \mathbb{R} \to \mathbb{R}$ is defined by

$$\left({}^{GL}D^\alpha x\right)(t) := \lim_{h\to 0} h^{-\alpha} \sum_{s=0}^{\frac{t}{h}} a_s^{(\alpha)} x(t - sh) \,, \tag{3}$$

where $h > 0$, $t = kh$, $k \in \mathbb{N}_0$ and $a_k^{(\alpha)}$ is the sequence given by (1).

Definition 3 ([5, 6]) Let x be defined on the interval $[0, t_1]$. The left-sided Caputo derivative of order $\alpha \in (0, 1]$ and the lower limit 0 is defined as follows:

$$\left({}^{C}D_{0+}^\alpha x\right)(t) := \frac{1}{\Gamma(1-\alpha)} \int_0^t x'(s)(t-s)^{-\alpha} ds \,. \tag{4}$$

Let us define the following Mittag-Leffler function, i.e. a one-parameter function defined by:

$$E_\alpha(z) := \sum_{k=0}^{\infty} \frac{z^k}{\Gamma(\alpha k + 1)}, \tag{5}$$

where the parameter $\alpha > 0$. It is known (see [5, 6]) that for the following fractional differential equation of order α with the left-sided Caputo derivative:

$$\left({}^C D^\alpha_{0+} x\right)(t) = ax(t) \;\; t \geq 0, \tag{6}$$

the function $t \mapsto E_\alpha(at^\alpha)$ is its solution.

In [8, Lemma 6.1] the following comparison of solutions of fractional order systems has been proven.

Lemma 1 (Fractional Comparison Principle) *If* $\chi(0) = \psi(0)$ *and*

$$\left({}^C D^\alpha_{0+} \chi\right)(t) \leq \left({}^C D^\alpha_{0+} \psi\right)(t),$$

where $\alpha \in (0, 1)$, *then* $\chi(t) \leq \psi(t)$.

Note that the following relation between the Caputo derivative and the Grünwald–Letnikov-type differential operator holds (see for instance [9]).

$$\begin{aligned} \left({}^C D^\alpha_{0+} x\right)(t) &= \lim_{h \to 0} \frac{1}{h^\alpha} \sum_{j=0}^{\left[\frac{t}{h}\right]} (-1)^j \binom{\alpha}{j} x(t - jh) - \frac{t^\alpha}{\Gamma(1-\alpha)} x(0) \\ &= \left({}^{GL} D^\alpha x\right)(t) - \frac{t^\alpha}{\Gamma(1-\alpha)} x(0), \end{aligned} \tag{7}$$

Usually there are considered the following fractional order systems of order $\alpha \in (0, 1]$ with the Grünwald–Letnikov-type differential operators:

$$\left({}^{GL} D^\alpha x\right)(t) = f(x(t)), \quad t \in \mathbb{R}, \tag{8}$$

with initial condition $x(0) = x_0 \in \mathbb{R}^n$, where $x = (x_1, \ldots, x_n)^{\mathrm{T}} : \mathbb{R} \to \mathbb{R}^n$ is a vector function and $f : \mathbb{R}^n \to \mathbb{R}^n$ and the Grünwald–Letnikov-type difference operators:

$$\left(\Delta^\alpha_h y\right)((k+1)h) = \bar{f}(y(kh)), \quad h > 0, \; k \in \mathbb{N}_0, \tag{9}$$

with initial condition $y(0) = x_0 \in \mathbb{R}^n$, where $y = (y_1, \ldots, y_n)^{\mathrm{T}} : (h\mathbb{N})_0 \to \mathbb{R}^n$ is a vector function and $\bar{f} : \mathbb{R}^n \to \mathbb{R}^n$.

The solutions to Eqs. (8) and (9) exist according to given initial conditions.

Moreover, the left hand side of system (9), could be recursively rewritten. Particularly, in (9) we can write the left hand side as:

$$\left(\Delta^\alpha_h y\right)((k+1)h) = h^{-\alpha} y((k+1)h) + h^{-\alpha} \sum_{s=1}^{k+1} a_s^{(\alpha)} y((k+1-s)h).$$

Then Eq. (9) takes the form

$$y((k+1)h) = -\sum_{s=1}^{k+1} a_s^{(\alpha)} y((k+1-s)h) + h^\alpha f(y(kh)) \quad \text{for} \quad k \in \mathbb{N}_0 \tag{10}$$

or equivalently, $y(kh) = h^\alpha f(y((k-1)h)) - \sum_{s=0}^{k-1} a_{k-s}^{(\alpha)} y(sh)$ for $k \in \mathbb{N}_1$ with given initial condition $y(0)$. From Proposition 1 for $\alpha \in (0, 1)$ we see that

$$y(kh) = h^\alpha f(y((k-1)h)) + \sum_{s=0}^{k-1} \left| a_{k-s}^{(\alpha)} \right| y(sh) \text{ for } k \in \mathbb{N}_1 \tag{11}$$

and if $f(\cdot)$ is positive function and initial conditions are positive then solutions are positive.

Proposition 2 *Let $\alpha \in (0, 1]$. The solution x of system (8) is approximated by the solution of system (9) in values via the following limit:* $\lim_{h\to 0} y(kh) = x(t)$, *where* $k = \left[\frac{t}{h}\right]$.

Proof The proof follows directly from the definition of the Grünwald–Letnikov-type differential operator.

2 Consensus Formation

Similarly as in [3, 4], let us consider a group of experts who have made an assessment of a certain magnitude. Let $x_i : \mathbb{R} \to [0, +\infty) =: \mathbb{R}_{\geq 0}, i = 1, \ldots, n$. Denote by $x_i(t)$ the assessment made by expert $i \in N := \{1, \ldots, n\}$ at time $t \in \mathbb{R}$ of the nonnegative magnitude under consideration.

Suppose expert i takes at a profile x of opinions only those experts j into account for which $|x_i - x_j| < \epsilon$, where $\epsilon > 0$ is a certain level of confidence level of agents i and j. Let us define $I_i(\epsilon) := \{j \mid 1 \leq j \leq n, |x_i - x_j| < \epsilon\}$. Note the set $I_i(\epsilon)$ is finite and the number of its elements will be denoted by $|I_i(\epsilon)|$.

Let $\epsilon > 0$ and $\alpha \in [0, 1]$. Therein we consider the fractional order Hegselmann–Krause's type models of the following form

$$\left({}^{GL}D^\alpha x_i\right)(t) = \frac{\sum_{j\in I_i(\epsilon)} (x_j(t) - \alpha x_i(t))}{(1-\alpha)|I_i(\epsilon)| + \alpha}, \quad i \in N \tag{12}$$

with initial condition $x(0) \in [0, 1]^n \subset \mathbb{R}^n$ that is the random vector.

Remark 1 Let us notice that system (12), which we propose, is covered with classical ones dependently on order α: for $\alpha = 0$ we get difference system considered by Krause in [3], while for $\alpha = 1$ we get the continuous version of the model examined by Blondel et al. in [1].

Note that discrete version of system (12) has the following form

$$\left({}^{GL}\Delta_h^{\alpha} y_i\right)((k+1)h) = \frac{\sum_{j\in I_i(\epsilon)}(y_j(kh) - \alpha y_i(kh))}{(1-\alpha)|I_i(\epsilon)| + \alpha}, \quad i \in N \tag{13}$$

From Eq. (11) we can directly write the recurrence for solutions for each separate agent $i \in N$:

$$y_i(kh) = h^{\alpha}\frac{\sum_{j\in I_i(\epsilon)}(y_j(kh) - \alpha y_i(kh))}{(1-\alpha)|I_i(\epsilon)| + \alpha} + \sum_{s=0}^{k-1}\left|a_{k-s}^{(\alpha)}\right| y_i(sh) \quad \text{for} \quad k \in \mathbb{N}_1 . \tag{14}$$

Remark 2 It is easy to see that for $\alpha = 0$ and $h = 1$ one gets the classical Hegselmann–Krause's model, i.e.

$$y_i(k+1) = \frac{\sum_{j\in I_i(\epsilon)} y_j(k)}{|I_i(\epsilon)|}, \quad i \in N,$$

that is considered for instance in [7].

By (6), the functions $t \mapsto E_{\alpha}((1-\alpha)t^{\alpha})$ and $t \mapsto E_{\alpha}((1-\alpha)nt^{\alpha})$ are the solutions of systems $\left({}^{C}D_{0+}^{\alpha}\chi\right)(t) = (1-\alpha)\chi(t)$ and $\left({}^{C}D_{0+}^{\alpha}\psi\right)(t) = (1-\alpha)n\psi(t)$, respectively with initial conditions $\chi(0) = \psi(0) = 1$. Let $\overline{x} := \frac{1}{n}(x_1 + \cdots + x_n)$. Then the following proposition holds true.

Proposition 3 *Let $\overline{x}$ be the average opinion. Then the following relation holds:*

$$E_{\alpha}((1-\alpha)t^{\alpha})\overline{x}(0) \le \overline{x}(t) \le E_{\alpha}((1-\alpha)nt^{\alpha})\overline{x}(0), \tag{15}$$

for $t \ge 0$.

Proof Since $(1-\alpha)|I_i(\epsilon)| + \alpha \le |I_i(\epsilon)|$ for $\alpha \in [0,1]$ and $\sum_{i=1}^{n}\sum_{j\in I_i(\epsilon)}(x_j(t) - x_i(t)) = 0$, we get

$$\begin{aligned}
\left({}^{C}D_{0+}^{\alpha}\overline{x}\right)(t) &= \frac{1}{n}\left({}^{C}D_{0+}^{\alpha}\left(\sum_{i=1}^{n} x_i\right)\right)(t) = \frac{1}{n}\sum_{i=1}^{n}\left({}^{C}D_{0+}^{\alpha}x_i\right)(t) \\
&= \frac{1}{n}\sum_{i=1}^{n}\frac{\sum_{j\in I_i(\epsilon)}(x_j(t) - \alpha x_i(t))}{(1-\alpha)|I_i(\epsilon)| + \alpha} \\
&\ge \frac{1}{n}\sum_{i=1}^{n}\frac{\sum_{j\in I_i(\epsilon)}(x_j(t) - x_i(t)) + \sum_{j\in I_i(\epsilon)}(1-\alpha)x_i(t)}{|I_i(\epsilon)|} \\
&= \frac{1-\alpha}{n}\sum_{i=1}^{n} x_i(t) = (1-\alpha)\overline{x}(t),
\end{aligned}$$

for $\alpha \in (0, 1]$. Moreover, since $(1-\alpha)|I_i(\epsilon)| + \alpha \geq 1$ for $\alpha \in [0, 1]$, we have

$$\begin{aligned}\left({}^{C}D^{\alpha}_{0+}\overline{x}\right)(t) =& \frac{1}{n}\left({}^{C}D^{\alpha}_{0+}\left(\sum_{i=1}^{n} x_i\right)\right)(t) = \frac{1}{n}\sum_{i=1}^{n}\left(D^{\alpha}_{0+}x_i\right)(t)\\ =& \frac{1}{n}\sum_{i=1}^{n}\frac{\sum_{j\in I_i(\epsilon)}(x_j(t) - \alpha x_i(t))}{(1-\alpha)|I_i(\epsilon)| + \alpha}\\ \leq& \frac{1}{n}\sum_{i=1}^{n}\left[\sum_{j\in I_i(\epsilon)}(x_j(t) - x_i(t)) + \sum_{j\in I_i(\epsilon)}(1-\alpha)x_i(t)\right]\\ =& \frac{1-\alpha}{n}|I_i(\epsilon)|\sum_{i=1}^{n} x_i(t) = (1-\alpha)|I_i(\epsilon)|\overline{x}(t) \leq (1-\alpha)n\overline{x}(t)\,,\end{aligned}$$

for $\alpha \in (0, 1]$. Hence, we get the following inequalities for the mean value $\overline{x}$:

$$(1-\alpha)\overline{x}(t) \leq \left({}^{C}D^{\alpha}_{0+}\overline{x}\right)(t) \leq (1-\alpha)n\overline{x}(t)\,. \tag{16}$$

Finally, using Lemma 1 we get the thesis.

Remark 3 Observe that directly from Proposition 3 we get the explicit formulas in some particular cases. And so, for $n = 1$ one gets $\overline{x} = x_1$ and $\left({}^{C}D^{\alpha}_{0+}x_1\right)(t) = (1-\alpha)x_1(t)$. Next, for $n = 2$, since $|I_1(\epsilon)| = |I_2(\epsilon)| = \{1, 2\}$ one can check that it holds

$$\left({}^{C}D^{\alpha}_{0+}\overline{x}\right)(t) = \begin{cases} \frac{2(1-\alpha)}{2-\alpha}\overline{x}(t), & |I_1(\epsilon)| = |I_2(\epsilon)| = 2;\\ (1-\alpha)\overline{x}(t), & |I_1(\epsilon)| = |I_2(\epsilon)| = 1.\end{cases}$$

Moreover, for $\alpha = 1$ we get $\overline{x}(t) = \overline{x}(0)$.

The next definition of an ϵ-profile was firstly stated in [3] and mentioned in many paper, as for example in [2].

Definition 4 An opinion profile $x = (x_1, \cdots, x_n)$ is called an ϵ-profile if there exists an ordering $x_{i_1} \leq x_{i_2} \leq \ldots \leq x_{i_n}$ of the components of x such that two adjacent components have a distance less or equal to ϵ, i.e.

$$x_{i_{k+1}} - x_{i_k} < \epsilon \quad \text{for all} \quad 1 \leq k \leq n-1\,.$$

For an opinion profile $x = (x_1, \ldots, x_n)$ we say that there is a split (or crack) between agents i and j if $|x_i - x_j| \geq \epsilon$.

In order to show the correctness of model (13) below we prove positivity of its trajectories $y_i(\cdot) = y_i(kh)$, $k \in \mathbb{N}$, $i \in N$ and $h > 0$.

Proposition 4 *Assume that $h^{\alpha} \leq 1 - \alpha$ holds for $\alpha \in [0, 1]$ and $h \geq 0$. If $y_i(0) \geq 0$ for each $i \in N$, then $y_i(kh) \geq 0$, for $i \in N, k \in \mathbb{N}_1$.*

Proof We will lead the proof by the induction principle. Firstly, observe that by (14) for $k = 1$ we get

$$y_i(h) = \alpha y_i(0) + h^\alpha \sum_{j \in I_i(\epsilon)} \frac{(y_j(0) - \alpha y_i(0))}{(1-\alpha)|I_i(\epsilon)| + \alpha} = \tag{17}$$
$$= \alpha y_i(0) \frac{(1 - \alpha - h^\alpha)|I_i(\epsilon)| + \alpha}{(1-\alpha)|I_i(\epsilon)| + \alpha} + h^\alpha \sum_{j \in I_i(\epsilon)} \frac{y_j(0)}{(1-\alpha)|I_i(\epsilon)| + \alpha}.$$

By assumption $h^\alpha \leq 1 - \alpha$ we get $y_i(h) \geq 0$.

Now let us assume that for $m = 1, \ldots, k-1$, $y_i(mh) \geq 0$. Then let us prove that $y_i(kh) \geq 0$. From (11) we get for $t = (k-1)h$

$$y_i(t+h) = h^\alpha \sum_{j \in I_i(\epsilon)} \frac{(y_j(t) - \alpha y_i(t))}{(1-\alpha)|I_i(\epsilon)| + \alpha} + \sum_{s=1}^{k+1} \left|a_s^{(\alpha)}\right| y_i(t + h - sh).$$

Hence

$$y_i(t+h) = h^\alpha \sum_{j \in I_i(\epsilon)} \frac{y_j(t)}{(1-\alpha)|I_i(\epsilon)| + \alpha} - \frac{h^\alpha I_i(\epsilon) \alpha y_i(t)}{(1-\alpha)|I_i(\epsilon)| + \alpha}$$
$$+ \sum_{s=2}^{k+1} \left|a_s^{(\alpha)}\right| y_i(t + h - sh) + \alpha y_i(t),$$

and consequently,

$$y_i(t+h) = h^\alpha \sum_{j \in I_i(\epsilon)} \frac{y_j(t)}{(1-\alpha)|I_i(\epsilon)| + \alpha} + \left(\alpha - \frac{h^\alpha I_i(\epsilon)\alpha}{(1-\alpha)|I_i(\epsilon)| + \alpha}\right) y_i(t)$$
$$+ \sum_{s=2}^{k+1} \left|a_s^{(\alpha)}\right| y_i(t + h - sh)$$
$$= h^\alpha \sum_{j \in I_i(\epsilon)} \frac{y_j(t)}{(1-\alpha)|I_i(\epsilon)| + \alpha} + \alpha \frac{(1 - \alpha - h^\alpha) I_i(\epsilon) + \alpha}{(1-\alpha)|I_i(\epsilon)| + \alpha} y_i(t)$$
$$+ \sum_{s=2}^{k+1} \left|a_s^{(\alpha)}\right| y_i(t + h - sh).$$

Using the assumptions we get $y_i(t+h) \geq 0$. Therefore by induction principle we get the thesis.

Our goal is to find such parameters that can establish "consensus" in the systems.

Definition 5 Let $\mathcal{A} = \{i_1, \ldots, i_s\} \subset N$ and $s < n$. The consensus with leaders from $\mathcal{A}$ of system (12) is said to be achieved if, for each agent $i \in N$ there exists $j \in \mathcal{A}$ such that

$$\lim_{t\to\infty} \left|x_i(t) - x_j(t)\right| = 0 \tag{18}$$

for any initial condition $x(0) = (x_1(0), \ldots, x_n(0))$. If $\mathcal{A} = \{i_0\}$ and $i_0 \in N$, then we say that system (12) achieves a consensus.

A consensus for system (13) can be defined similarly, and one has to change x_i to y_i and t to kh in condition (18).

Let $x_M(t) := \max_{i\in N} x_i(t), x_m(t) := \min_{i\in N} x_i(t), y_M(kh) = \max_{i\in N} y_i(kh)$ and $y_m(kh) = \min_{i\in N} y_i(kh)$. In what follows, we present results on achieving a consensus in both, continuous and discrete cases.

Proposition 5 *Let $\epsilon > 0$. If*

$$x_M(t) - x_m(t) < \epsilon\,, \tag{19}$$

for $t \in \mathbb{R}$, then system (12) tends to a consensus.

Proof Directly from the formulation of system (12) we can write

$$\begin{aligned}\left({}^C D^{\alpha}_{0+}(x_M - x_m)\right)(t) &= \frac{1}{(1-\alpha)n+\alpha} \sum_{j=1}^{n} \left(x_j(t) - \alpha x_M(t) - x_j(t) + \alpha x_m(t)\right) \\ &= \frac{-\alpha n}{(1-\alpha)n+\alpha} \left(x_M(t) - x_m(t)\right)\,.\end{aligned}$$

Taking $e(t) := x_M(t) - x_m(t)$, for $t \geq 0$, we get the following fractional order equation:

$$\left({}^C D^{\alpha}_{0+} e\right)(t) = \frac{-\alpha n}{(1-\alpha)n+\alpha} e(t)\,. \tag{20}$$

Then $t \mapsto E_\alpha\left(\frac{-\alpha n}{(1-\alpha)n+\alpha} t^\alpha\right)$ is the solution to (20) and since $\frac{-\alpha n}{(1-\alpha)n+\alpha} < 0$, we get $\lim_{t\to+\infty} e(t) = \lim_{t\to+\infty} E_\alpha\left(\frac{-\alpha n}{(1-\alpha)n+\alpha} t^\alpha\right) = 0$ and consequently, the thesis holds.

Proposition 6 *Let $\epsilon > 0$. If*

$$y_M(0) - y_m(0) < \epsilon\,, \tag{21}$$

then system (13) tends to a consensus.

Remark 4 Conditions (19) and (21) imply the opinion profiles x and y, respectively, are ϵ-profile.

Observe that for $n = 1$ the consensus of systems (12) and (13) is achieved by Definition 5.

Now we will focus on the situation when $n = 2$. First we show that consensus is always achieved for two agent, even though they are not in ϵ-profile at the beginning.

Proposition 7 *If $n = 2$, then system (12) achieves a consensus.*

Proof By Proposition 5, putting $x_M(\cdot) \equiv x_2(\cdot)$, $x_m(\cdot) \equiv x_1(\cdot)$ and $n = 2$ we get the thesis.

Next we show the property concerning the order of opinions is preserved for two agents.

Proposition 8 *Let $y_1(0) \geq 0$ for each $i = 1, 2$ and $h^\alpha \leq 1 - \alpha$ for $\alpha \in [0, 1]$ and $h \geq 0$. Then if for some i, $j \in N$ we have the relations $y_1(0) \leq y_2(0)$, then $y_1(kh) \leq y_2(kh)$ for $k \in \mathbb{N}_1$ and $h > 0$.*

Proof Firstly, observe that for two agents $|I_1(\epsilon)| = |I_2(\epsilon)|$ always holds and $|I_i| := |I_i(\epsilon)|$ equals to 1 or 2 for $i = 1, 2$. Since $h^\alpha \leq 1 - \alpha$, $y_1(0) \leq x_2(0)$ and $|I_1| = |I_2|$, we get

$$\begin{aligned} y_1(h) &= \alpha y_1(0)\frac{(1-\alpha-h^\alpha)|I_1|+\alpha}{(1-\alpha)|I_1|+\alpha} + h^\alpha \frac{\sum_{j\in I_1} y_j(0)}{(1-\alpha)|I_1|+\alpha} \\ &\leq \alpha y_2(0)\frac{(1-\alpha-h^\alpha)|I_2|+\alpha}{(1-\alpha)|I_2|+\alpha} + h^\alpha \frac{\sum_{j\in I_2} y_j(0)}{(1-\alpha)|I_2|+\alpha} = y_2(h)\,. \end{aligned}$$

Assume now that $y_1(rh) \leq y_2(rh)$ for $r = 0, \ldots, k_0$. Then since $h^\alpha \leq 1 - \alpha$, $y_1(0) \leq x_2(0)$, we get

$$\begin{aligned} y_1((k_0+1)h) &= \alpha y_1(k_0h)\frac{(1-\alpha-h^\alpha)|I_1|+\alpha}{(1-\alpha)|I_1|+\alpha} + h^\alpha \frac{\sum_{j\in I_1} y_j(k_0h)}{(1-\alpha)|I_1|+\alpha} + \mathcal{O}_1(k_0) \\ &\leq \alpha y_2(k_0h)\frac{(1-\alpha-h^\alpha)|I_2|+\alpha}{(1-\alpha)|I_2|+\alpha} + h^\alpha \frac{\sum_{j\in I_2} y_j(k_0h)}{(1-\alpha)|I_2|+\alpha} + \mathcal{O}_2(k_0) \\ &= y_2((k_0+1)h)\,, \end{aligned}$$

where $\mathcal{O}_1(k_0) := \sum_{s=0}^{k_0-1} \left|a^{(\alpha)}_{k_0+1-s}\right| y_1(sh)$ and $\mathcal{O}_2(k_0) := \sum_{s=0}^{k_0-1} \left|a^{(\alpha)}_{k_0+1-s}\right| y_2(sh)$ are defined in the proof of Proposition 8. Therefore, $y_i((k_0+1)h) \leq y_j((k_0+1)h)$. Hence using the induction principle we get that $y_1(sh) \leq y_2(sh)$ for all $s \in \mathbb{N}_0$.

3 Numerical Examples

First we consider system with $N = 2$ agents for the following orders $\alpha \in \{0.01, 0.5, 0.9\}$, where $h = 0.01$. The graphs are numerical simulations for approximations for 100 steps. In Fig. 1a–c we see that the consensus is reached by the system with orders from $(0, 1]$ and it does not depend on the fact whether the opinions are in ϵ profile or not. In Fig. 1 we have the situation where $x_2(0) - x_1(0) = 0.25 > \epsilon = 0.2$.

We also observe the similar behaviour for systems with $N = 50$ agents for the following orders $\alpha \in \{0.01, 0.5, 0.9, 1\}$, where $h = 0.01$. The graphs are numerical simulations for approximations for 100 steps. In Fig. 2b we see that for $\alpha = 0.5$ a consensus is reached while the system achieves the consensus with two leaders for $\alpha \in \{0.01, 0.9, 1\}$, see Fig. 2a, c and d.

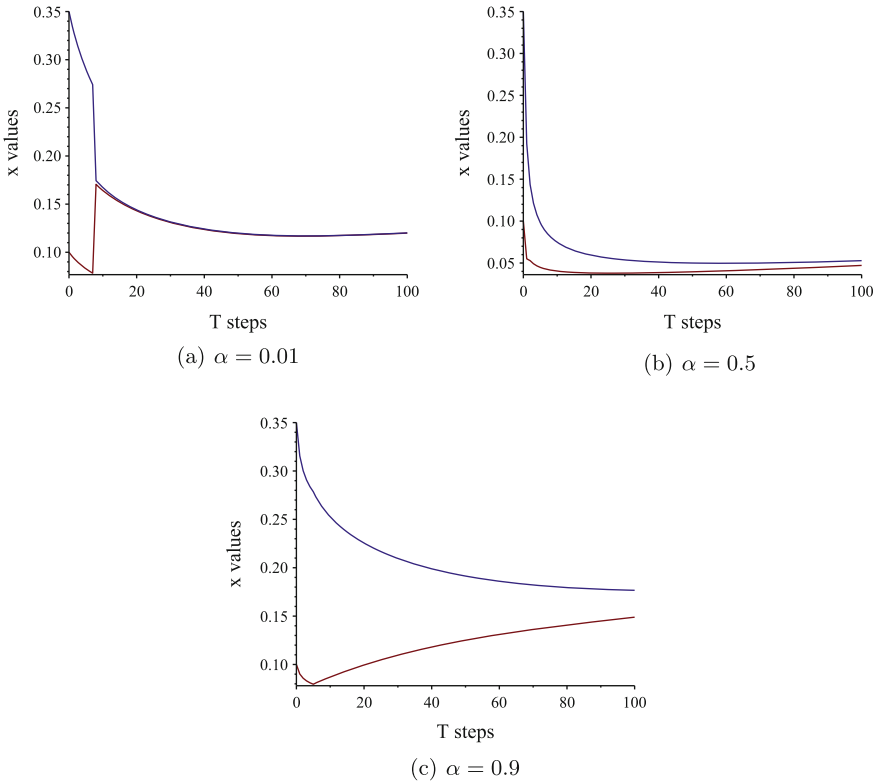

(a) $\alpha = 0.01$

(b) $\alpha = 0.5$

(c) $\alpha = 0.9$

Fig. 1 The graphs of approximations of solution for two agents with $\alpha \in \{0.01, 0.5, 0.9\}$ and $h = 0.01$, $n = 100$ steps, $\epsilon = 0.2$

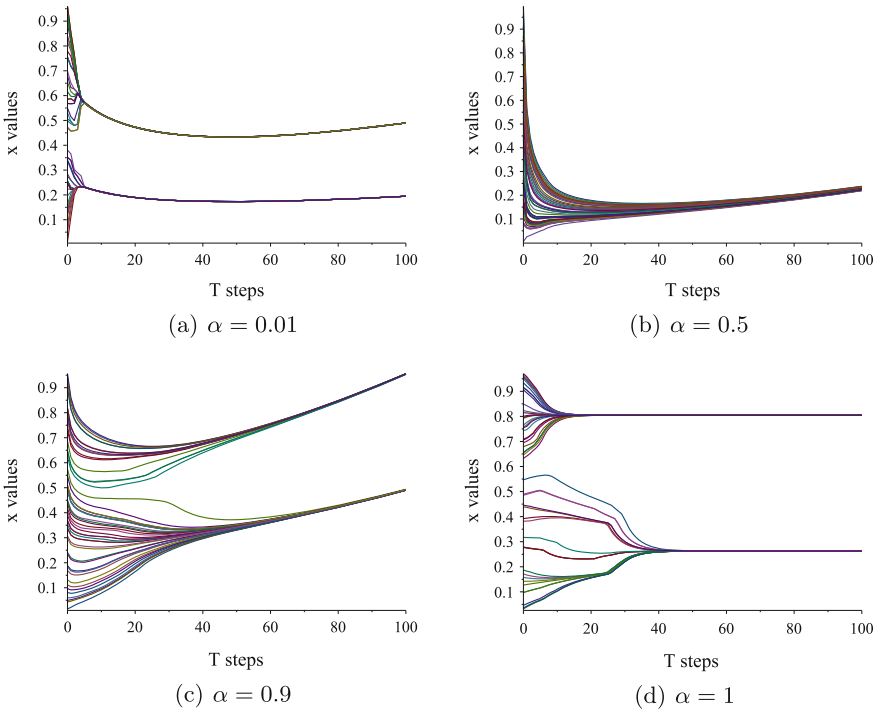

Fig. 2 The graphs of approximations of solution for 50 agents with $\alpha \in \{0.01, 0.5, 0.9, 1\}$ and $h = 0.01$, $n = 100$ steps, $\epsilon = 0.2$

Acknowledgments The work was supported by Polish founds of National Science Center, granted on the basis of decision DEC-2014/15/B/ST7/05270.

References

1. Blondel, V.D., Hendrickx, J.M., Tsitsiklis, F.N.: Continuous-time average- preserving opinion dynamics with opinion-dependent communications. SIAM J. Control Optim. **48**(8), 5214–5240 (2010)
2. Hegselmann, R., Krause, U.: Opinion dynamics and bounded confidence models, analysis, and simulations. J. Artif. Soc. Soc. Simul. **5**(3), 227–236 (2002)
3. Krause, U.: A discrete nonlinear and non-autonomous model of consensus formation. Proc. Commun. Differ. Equ. pp. 227–236 (2000)
4. Mozyrska, D., Wyrwas, M.: Fractional discrete-time of Hegselmann–Krause's type consensus model with numerical simulations. Submitted into Neurocomputing (2016)
5. Kilbas, A.A., Srivastava, H.M., Trujillo, J.J.: Theory and Applications of Fractional Differential Equations. North–Holland Mathematics Studies, 204. Elsevier Science B. V., Amsterdam (2006)
6. Podlubny, I.: Fractional Differential Equations. Academic Press, San Diego (1999)
7. Blondel, V.D., Hendrickx, J.M., Tsitsiklis, F.N.: On Krause's multi-agent consensus model with state-dependent connectivity. IEEE Trans. Automat. Contr. **5**(11), 2586–2597 (2009)

8. Li, Y., Chen, Y.Q., Podlubny, I.: Mittag-Leffler stability of fractional order nonlinear dynamic systems. Automatica **45**, 1965–1969 (2009)
9. Mozyrska, D., Girejko, E., Wyrwas, M.: Fractional nonlinear systems with sequential operators. Cent. Eur. J. Phys. **11**(10), 1295–1303 (2013)

Harmonic Numbers of Any Order and the Wolstenholme's-Type Relations for Harmonic Numbers

Edyta Hetmaniok, Piotr Lorenc, Mariusz Pleszczyński, Michał Różański, Marcin Szweda and Roman Wituła

Abstract The concept of harmonic numbers has appeared permanently in the mathematical science since the very early days of differential and integral calculus. Firsts significant identities concerning the harmonic numbers have been developed by Euler (see Basu, Ramanujan J, 16:7–24, 2008, [1], Borwein and Bradley, Int J Number Theory, 2:65–103, 2006, [2], Sofo, Computational techniques for the summation of series, 2003, [3], Sofo and Cvijovic, Appl Anal Discrete Math, 6:317–328, 2012, [4]), Goldbach, and next by the whole gallery of the greatest XIX and XX century mathematicians, like Gauss, Cauchy and Riemann. The research subject matter dealing with the harmonic numbers is constantly up-to-date, mostly because of the still unsolved Riemann hypothesis – let us recall that, thanks to J. Lagarias, the Riemann hypothesis is equivalent to some "elementary" inequality for the harmonic numbers (see Lagarias, Amer Math Monthly, 109(6):534–543, 2002, [5]). In paper (Sofo and Cvijovic, Appl Anal Discrete Math, 6:317–328, 2012, [4]) the following relation for the generalized harmonic numbers is introduced

$$H_n^{(r)} := \sum_{k=1}^{n} \frac{1}{k^r} = \frac{(-1)^{r-1}}{(r-1)!} \left(\psi^{(r-1)}(n+1) - \psi^{(r-1)}(1) \right), \tag{1}$$

for positive integers n, r. The main goal of our paper is to derive the generalization of this formula for every $r \in \mathbb{R}$, $r > 1$. It was important to us to get this generalization in possibly natural way. Thus, we have chosen the approach based on the discussion of the Weyl integral. In the second part of the paper we present the survey of results concerning the Wolstenholme's style congruence for the harmonic numbers. We have to admit that we tried to define the equivalent of the universal divisor (the polynomial, some kind of the special function) for the defined here generalized harmonic numbers.

E. Hetmaniok (✉) · P. Lorenc · M. Pleszczyński · M. Różański · M. Szweda · R. Wituła
Institute of Mathematics, Silesian University of Technology,
Kaszubska 23, 44-100 Gliwice, Poland
e-mail: edyta.Hetmaniok@polsl.pl

M. Pleszczyński
e-mail: Mariusz.Pleszczynski@polsl.pl

A. Babiarz et al. (eds.), *Theory and Applications of Non-integer Order Systems*,
Lecture Notes in Electrical Engineering 407, DOI 10.1007/978-3-319-45474-0_4

Did we succeed? We continue our efforts in this matter, we believe that such universal divisors can be found.

Keywords Harmonic numbers · Weyl integral · Wolstenholme relations

1 New Definition of the Generalized Harmonic Numbers

1.1 The Weyl Integral

One of the possible definition of the fractional derivative is based on the Weyl integral (see [6]) given by formula

$$W^{-\alpha} f(x) = \frac{1}{\Gamma(\alpha)} \int_x^\infty (\xi - x)^{\alpha-1} f(\xi) \mathrm{d}\xi, \ \alpha > 0, \ x > 0. \tag{2}$$

Moreover we take $W^0 f(x) := f(x)$. If $f(x) = O(x^{-\beta})$ as $x \to \infty$, then the integral is convergent for $0 < \alpha < \beta$.

Let us present now some properties of the Weyl integral. Assuming the existence of the appropriate integrals, the following equalities hold

$$\begin{aligned} W^{-\alpha}\left(W^{-\beta} f(x)\right) &= W^{-\beta}\left(W^{-\alpha} f(x)\right), \ \alpha, \beta > 0, \\ \frac{d^n}{dx^n}\left(W^{-\alpha} f(x)\right) &= W^{-\alpha}\left(\frac{d^n f(x)}{dx}\right), \ \alpha > 0, \ n \in \mathbb{N}, \\ E^n\left(W^{-\alpha} f(x)\right) &= W^{-\alpha}(E^n f(x)), \ \alpha > 0, \ n \in \mathbb{N}, \end{aligned}$$

where $Ef(x) := -\frac{df(x)}{dx}$.

Definition 1 Let f be a function being integrable in any compact interval $I \subset [0, \infty)$ and let $f(x) = O(x^{-\beta})$ as $x \to \infty$, for some $\beta > 0$. Then for each $\alpha > -\beta$ there exists the Weyl fractional derivative of function $f(x)$ of order α and

$$dW^\alpha f(x) = \begin{cases} W^\alpha f(x), & \alpha < 0, \\ f(x), & \alpha = 0, \\ W^{\alpha - \lceil \alpha \rceil}\left(E^{\lceil \alpha \rceil} f(x)\right), & \alpha > 0. \end{cases} \tag{3}$$

Example 1 We determine the Weyl fractional derivative of function e^{-px}, $p > 0$:

$$\begin{aligned} W^{-\alpha} e^{-px} &= \frac{1}{\Gamma(\alpha)} \int_x^\infty (\xi - x)^{\alpha-1} e^{-p\xi} \mathrm{d}\xi = \begin{bmatrix} \xi - x = u \\ d\xi = du \end{bmatrix} \\ &= \frac{1}{\Gamma(\alpha)} e^{-px} \int_0^\infty u^{\alpha-1} e^{-pu} \mathrm{d}u = p^{-\alpha} e^{-px} \end{aligned}$$

for $\alpha > 0$, $p > 0$. Hence we obtain

$$dW^{\alpha}e^{-px} = W^{\alpha-\lceil\alpha\rceil}\left(E^{\lceil\alpha\rceil}e^{-px}\right) = W^{\alpha-\lceil\alpha\rceil}\left(p^{\lceil\alpha\rceil}e^{-px}\right) = p^{\alpha}e^{-px}$$

for $\alpha > 0$.

Example 2 Now, we derive the Weyl fractional derivative of function $\frac{1}{x^p}$, $p > 0$:

$$\begin{aligned} W^{-\alpha}\left(\frac{1}{x^p}\right) &= \frac{1}{\Gamma(\alpha)}\int_x^{\infty}\frac{(\xi-x)^{\alpha-1}}{\xi^p}\mathrm{d}\xi = \frac{1}{\Gamma(\alpha)}\int_x^{\infty}\frac{(1-\frac{x}{\xi})^{\alpha-1}}{\xi^{p-\alpha+1}}\mathrm{d}\xi \\ &= \left[\begin{array}{c}\frac{x}{\xi}=u \\ \frac{x}{\xi^2}d\xi=-du\end{array}\right] = \frac{1}{\Gamma(\alpha)}\cdot\frac{1}{x^{p-\alpha}}\int_0^1(1-u)^{\alpha-1}u^{p-\alpha-1}\mathrm{d}u \\ &= \frac{B(\alpha,p-\alpha)}{\Gamma(\alpha)}\cdot\frac{1}{x^{p-\alpha}} = \frac{\Gamma(p-\alpha)}{\Gamma(p)}\cdot\frac{1}{x^{p-\alpha}} \end{aligned} \tag{4}$$

for $p > \alpha > 0$, where $B(x, y)$ denotes the beta function. Thus we get

$$\begin{aligned} dW^{\alpha}\left(\frac{1}{x^p}\right) &= W^{\alpha-\lceil\alpha\rceil}\left(E^{\lceil\alpha\rceil}\left(\frac{1}{x^p}\right)\right) \\ &= W^{\alpha-\lceil\alpha\rceil}\left(\frac{\Gamma(p+\lceil\alpha\rceil)}{\Gamma(p)}\cdot\frac{1}{x^{p+\lceil\alpha\rceil}}\right) = \frac{\Gamma(p+\alpha)}{\Gamma(p)}\cdot\frac{1}{x^{p+\alpha}} \end{aligned}$$

for $\alpha > 0$, $p > 0$.

1.2 Poligamma Functions and Their Modifications

Definition 2 The poligamma function of order m is defined as follows

$$\psi^{(0)}(x) := \psi(x) = \frac{d}{dx}\ln\Gamma(x), \qquad \psi^{(m)}(x) := \frac{d^m}{dx^m}\psi(x), \qquad m \in \mathbb{N}.$$

This function satisfies the recurrence relation (the basic facts concerning the ψ function, including formulas (5)–(7) are presented in monograph [7]):

$$\psi^{(m)}(x+1) = \psi^{(m)}(x) + \frac{(-1)^m m!}{x^{m+1}} \tag{5}$$

and from this relation we can get the equality (1). The poligamma function possesses also the integral representation

$$\psi(x) = \int_0^{\infty}\left(\frac{e^{-t}}{t} - \frac{e^{xt}}{1-e^{-t}}\right)\mathrm{d}t, \quad \psi^{(m)}(x) = (-1)^{m+1}\int_0^{\infty}\frac{t^m e^{-xt}}{1-e^{-t}}\mathrm{d}t,\ x > 0, \tag{6}$$

and can be presented in the form of series

$$\psi(x+1) = -\gamma + \sum_{n=1}^{\infty} \frac{x}{n(n+x)}, \qquad \psi^{(m)}(x) = (-1)^{m+1} m! \sum_{n=0}^{\infty} \frac{1}{(x+n)^{m+1}}. \quad (7)$$

Let us define now the modified poligamma functions

$$\psi_*^{(0)}(x) := \psi(x), \quad \psi_*^{(\alpha)}(x) := dW^{\alpha}\left(\psi(x)\right), \quad \alpha > 0. \quad (8)$$

Remark 1 The Weyl integral of function $\psi(x)$ is divergent, whereas for any $\alpha \in (0, 1)$, $m \in \mathbb{N}$ the integral $W^{-\alpha}\left(\psi^{(m)}(x)\right)$ is convergent, thereby the function

$$\psi_*^{(\beta)}(x) = dW^{\beta}\left(\psi(x)\right) = W^{\beta-\lceil\beta\rceil}\left(E^{\lceil\beta\rceil}\psi(x)\right) = (-1)^{\lceil\beta\rceil} W^{\beta-\lceil\beta\rceil}\left(\psi^{(\lceil\beta\rceil)}(x)\right)$$

is correctly defined for every $\beta > 0$.

By using definitions (8), (3), (2) and formula (4) we can derive the following recurrence relation (which is a generalization of formula (5)):

$$\begin{aligned} \psi_*^{(\alpha)}(x+1) &= dW^{\alpha}\left(\psi(x+1)\right) = dW^{\alpha}\left(\psi(x) + \frac{1}{x}\right) \\ &= dW^{\alpha}\left(\psi(x)\right) + dW^{\alpha}\left(\frac{1}{x}\right) = \psi_*^{(\alpha)}(x) + \frac{\Gamma(\alpha+1)}{x^{\alpha+1}}. \end{aligned} \quad (9)$$

Some Representations of the $\psi_*^{(\alpha)}$ Function

First we present the *integral representation of* $\psi_*^{(\alpha)}$ *function*. Let $m \in \mathbb{N}$, then

$$\psi_*^{(m)}(x) = E^m\psi(x) = (-1)^m\psi^{(m)}(x) = -\int_0^{\infty} \frac{t^m e^{-xt}}{1-e^{-t}}\mathrm{d}t$$

hence we have

$$\begin{aligned} &\psi_*^{(\alpha)}(x) = W^{\alpha-\lceil\alpha\rceil}\left(E^{\lceil\alpha\rceil}\psi(x)\right) \\ &= \frac{1}{\Gamma(\lceil\alpha\rceil-\alpha)} \int_x^{\infty} (\xi - x)^{\lceil\alpha\rceil-\alpha-1} \left(-\int_0^{\infty} \frac{t^{\lceil\alpha\rceil} e^{-\xi t}}{1-e^{-t}}\mathrm{d}t \right) \mathrm{d}\xi \\ &= -\int_0^{\infty} \left(\frac{1}{\Gamma(\lceil\alpha\rceil-\alpha)} \int_x^{\infty} (\xi - x)^{\lceil\alpha\rceil-\alpha-1} e^{-\xi t}\mathrm{d}\xi \right) \frac{t^{\lceil\alpha\rceil}}{1-e^{-t}}\mathrm{d}t = -\int_0^{\infty} \frac{t^{\alpha} e^{-xt}}{1-e^{-t}} \end{aligned}$$

where $\alpha > 0$.

The *series representation of* $\psi_*^{(\alpha)}$ *function* is of the form

$$\psi_*^{(m)}(x) = E^m\psi(x) = (-1)^m\psi^{(m)}(x) = -\sum_{n=0}^{\infty}\frac{m!}{(x+n)^{m+1}}, \quad m \in \mathbb{N},$$

$$\begin{aligned}
&\psi_*^{(\alpha)}(x) = W^{\alpha-\lceil\alpha\rceil}\left(E^{\lceil\alpha\rceil}\right)\\
&= \frac{1}{\Gamma(\lceil\alpha\rceil-\alpha)}\int_x^{\infty}(\xi-x)^{\lceil\alpha\rceil-\alpha-1}\left(-\Gamma(\lceil\alpha\rceil+1)\sum_{n=0}^{\infty}\frac{1}{(\xi+n)^{\lceil\alpha\rceil+1}}\right)\mathrm{d}\xi\\
&= -\Gamma(\lceil\alpha\rceil+1)\sum_{n=0}^{\infty}\frac{1}{\Gamma(\lceil\alpha\rceil-\alpha)}\int_x^{\infty}\frac{(\xi-x)^{\lceil\alpha\rceil-\alpha-1}}{(\xi+n)^{\lceil\alpha\rceil+1}}\mathrm{d}\xi\\
&= -\sum_{n=0}^{\infty}\frac{\Gamma(\alpha+1)}{(x+n)^{\alpha+1}},
\end{aligned} \tag{10}$$

for every $\alpha > 0$. From this relation we get also

$$\psi_*^{(\alpha)}(1) = -\Gamma(\alpha+1)\zeta(\alpha+1) \tag{11}$$

for $\alpha > 0$, where $\zeta(\cdot)$ denotes the zeta function.

1.3 Harmonic Numbers of Order r > 1

From formula (9) we obtain the following relations

$$\psi_*^{(\alpha)}(k+1) - \psi_*^{(\alpha)}(k) = \frac{\Gamma(\alpha+1)}{k^{\alpha+1}}, \tag{12}$$

$$H_n^{(r)} := \sum_{k=1}^{n}\frac{1}{k^r} = \frac{1}{\Gamma(r)}\left(\psi_*^{(r-1)}(n+1) - \psi_*^{(r-1)}(1)\right), \quad r > 1. \tag{13}$$

The last formula can be considered as the generalization of formula (1) for $r > 1$. The numbers $H_n^{(r)}, n \in \mathbb{N}, r \in \mathbb{R}, r > 1$ will be called the n-th harmonic numbers of order r.

Moreover, we set

$$H_n^{(r)}(x) := \sum_{k=1}^{n}\frac{1}{(k+x)^r} = \frac{1}{\Gamma(r)}\left(\psi_*^{(r-1)}(n+1+x) - \psi_*^{(r-1)}(x)\right). \tag{14}$$

We define also the generalized odd harmonic numbers of order $r > 1$ in the following way

$$O_n^{(r)} := \sum_{k=1}^{n} \frac{1}{(2k-1)^r} = H_{2n}^{(r)} - \sum_{k=1}^{n} \frac{1}{(2k)^r} = H_{2n}^{(r)} - \frac{1}{2^r} H_n^{(r)}. \tag{15}$$

Let us note that in paper [8] (see also [9]) the following interesting relation is proven

$$\sum_{k=1}^{\infty} (-1)^{k-1} \left(O_{kn}^{(1)} - O_{kn-n}^{(1)} \right) = \frac{\pi}{2n} \left(\frac{1}{4}(1-(-1)^n) + \sum_{1 \le 2k-1 < n} \csc \frac{(2k-1)\pi}{2n} \right).$$

Remark 2 Given here formulas (13)–(15) can be generalized for the complex variable $r \in \mathbb{C}$, $\operatorname{Re} r > 1$. To do this we should analyze the performed above discussion starting with formula (2).

1.4 Selected Identities for the Generalized Harmonic Numbers

We have

$$\sum_{k=1}^{n} \frac{H_k^{(a)}}{k^b} = \sum_{k=1}^{n} \frac{\psi_*^{(a-1)}(k+1) - \psi_*^{(a-1)}(1)}{\Gamma(a) k^b} \overset{(11)}{=} \sum_{k=1}^{n} \frac{\psi_*^{(a-1)}(k+1)}{\Gamma(a) k^b} + \zeta(a) H_n^{(b)}$$

for any $a, b > 1$. Hence, if $n \to \infty$, then we get

$$\begin{aligned} \sum_{k=1}^{\infty} \frac{H_k^{(a)}}{k^b} &= \sum_{k=1}^{\infty} \frac{\psi_*^{(a-1)}(k+1)}{\Gamma(a) k^b} + \zeta(a)\zeta(b) \\ &\overset{(10)}{=} \zeta(a)\zeta(b) - \sum_{k=1}^{\infty} \sum_{j=0}^{\infty} \frac{1}{(k+j+1)^a k^b}. \end{aligned} \tag{16}$$

Similarly we can determine the more general sums

$$\begin{aligned} \sum_{k=1}^{n} \frac{H_k^a H_k^b}{k^c} &= \sum_{k=1}^{n} \frac{\left(\psi_*^{(a-1)}(k+1) - \psi_*^{(a-1)}(1) \right) \left(\psi_*^{(b-1)}(k+1) - \psi_*^{(b-1)}(1) \right)}{\Gamma(a)\Gamma(b) k^c} \\ &\overset{(11)}{=} \sum_{k=1}^{n} \frac{\psi_*^{(a-1)}(k+1)\psi_*^{(b-1)}(k+1)}{\Gamma(a)\Gamma(b) k^c} + \sum_{k=1}^{n} \frac{\psi_*^{(a-1)}(k+1)\zeta(a)}{\Gamma(b) k^c} \end{aligned}$$

$$+\sum_{k=1}^{n}\frac{\psi_*^{(b-1)}(k+1)\zeta(b)}{\Gamma(a)k^c}+\zeta(a)\zeta(b)H_n^{(c)}$$

for any $a, b, c > 1$. If $n \to \infty$, then we obtain

$$\begin{aligned}\sum_{k=1}^{\infty}\frac{H_k^a H_k^b}{k^c}&=\sum_{k=1}^{\infty}\frac{\psi_*^{(a-1)}(k+1)\psi_*^{(b-1)}(k+1)}{\Gamma(a)\Gamma(b)k^c}\\&+\sum_{k=1}^{\infty}\frac{\psi_*^{(a-1)}(k+1)\zeta(a)}{\Gamma(b)k^c}+\sum_{k=1}^{\infty}\frac{\psi_*^{(b-1)}(k+1)\zeta(b)}{\Gamma(a)k^c}+\zeta(a)\zeta(b)\zeta(c)\\&\overset{(10)}{=}\zeta(a)\zeta(b)\zeta(c)+\sum_{k=1}^{\infty}\frac{1}{k^c}\cdot\left(\sum_{j=0}^{\infty}\frac{1}{(k+1+j)^a}\cdot\sum_{j=0}^{\infty}\frac{1}{(k+1+j)^b}\right)\\&-\frac{\Gamma(a)\zeta(a)}{\Gamma(b)}\sum_{k=1}^{\infty}\sum_{j=0}^{\infty}\frac{1}{k^c(k+1+j)^a}-\frac{\Gamma(b)\zeta(b)}{\Gamma(a)}\sum_{k=1}^{\infty}\sum_{j=0}^{\infty}\frac{1}{k^c(k+1+j)^b}.\end{aligned}\tag{17}$$

Only when $a, b, c \in \mathbb{N}$, then we can give to the right hand sides of formulas (16), (17) the form using the finite sum, for example (see [4, formula (9)]):

$$\begin{aligned}\sum_{n=1}^{\infty}\frac{H_n}{(n+x)^b}&=\frac{(-1)^b}{(b-1)!}\Bigg[(\psi(x)+\gamma)\psi^{(b-1)}(x)-\frac{1}{2}\psi^{(b)}(x)\\&+\sum_{m=1}^{b-2}\binom{b-2}{m}\psi^{(m)}(x)\psi^{(b-m-1)}(x)\Bigg],\end{aligned}$$

where $b \in \mathbb{N}$, $b \neq 1$, $x \in \mathbb{R}\backslash\{-1, -2, -3, \ldots\}$.

2 Wolstenholme's-Type Relations for the Harmonic Numbers and the Generalized Harmonic Numbers

Definition 3 Let $x, y \in \mathbb{Q}$ and $m \in \mathbb{N}$. The numbers x and y are congruent modulo m if their difference can be expressed as a reduced fraction of the form $\frac{mp}{q}$, where $\gcd(q, m) = \gcd(q, p) = 1$. This definition can be written as follows

$$x \equiv y \pmod m \Leftrightarrow \exists\ p, q \in \mathbb{N}\colon\ \gcd(q, m) = \gcd(q, p) = 1 \text{ and } |x - y| = m\,\frac{p}{q}.$$

We will use also the notation $x \equiv_m y$, which is equivalent to $x \equiv y \pmod m$.

For example, note that $2 \cdot 4 \equiv 1, \quad 3 \cdot 3 \equiv 2, \quad 6 \cdot 6 \equiv 1 \pmod 7$, so we get

$$\frac{1}{2} \equiv 4, \quad \frac{1}{4} \equiv 2, \quad \frac{2}{3} \equiv 3, \quad \frac{1}{6} \equiv 6 \pmod 7.$$

Joseph Wolstenholme in [10] (see also [11, 12]) proved that for $p \in \mathbb{P}$ (where $\mathbb{P}$ denotes the set of all prime numbers), $p \geq 5$, the following congruences hold true

$$H_{p-1} \equiv 0 \pmod{p^2}, \tag{18}$$

$$H_{p-1}^{(2)} \equiv 0 \pmod p. \tag{19}$$

We will apply many times this result in the proofs of congruence relations given in the following subsection.

2.1 Our Results – Congruence Relations for the Harmonic Numbers and the Generalized Harmonic Numbers

The following relations hold true

1. For $p \in \mathbb{P}$, $p \geq 5$, we have $\displaystyle\sum_{k=1}^{p-1} \frac{H_k}{k} \equiv 0 \pmod p$.

Proof Let us note that

$$\sum_{k=1}^{p-1} \left(H_k - \frac{1}{k} \right)^2 - \sum_{k=1}^{p-1} H_k^2 - \sum_{k=1}^{p-1} \frac{1}{k^2} = -2 \sum_{k=1}^{p-1} \frac{H_k}{k},$$

since $H_k - \frac{1}{k} = H_{k-1}$ and $H_{p-1}^{(2)} = \sum\limits_{k=1}^{p-1} \frac{1}{k^2}$. Thus we have

$$\sum_{k=1}^{p-2} H_k^2 - \sum_{k=1}^{p-1} H_k^2 - H_{p-1}^{(2)} = -2 \sum_{k=1}^{p-1} \frac{H_k}{k}.$$

Hence we get

$$H_{p-1}^2 + H_{p-1}^{(2)} = 2 \sum_{k=1}^{p-1} \frac{H_k}{k}.$$

From relations (18) and (19) we conclude the thesis.

2. For $p \in \mathbb{P}$, $p \geq 3$, it holds that $\displaystyle\sum_{k=1}^{p-1} H_k \equiv 1 \pmod p$.

Proof We compute

$$\sum_{k=1}^{p-1} H_k = \sum_{k=1}^{p-1}\sum_{n=1}^{k} \frac{1}{n} = \sum_{n=1}^{p-1}\sum_{k=n}^{p-1} \frac{1}{n} = \sum_{n=1}^{p-1} \frac{p-n}{n} = \sum_{n=1}^{p-1} \left(\frac{p}{n} - 1\right)$$
$$= \left(\sum_{n=1}^{p-1} \frac{p}{n}\right) - (p-1) \equiv_p 1.$$

3. For $p \in \mathbb{P}$, $p \geq 3$, we have $\sum_{k=1}^{p-1} H_k^2 \equiv p-2 \pmod{p}$.

Proof We execute the following transformations

$$\sum_{k=1}^{p-1} H_k^2 = \sum_{k=1}^{p-1}\left(\sum_{n=1}^{k} \frac{1}{n}\right)^2 = \sum_{k=1}^{p-1}\sum_{n=1}^{k} \frac{1}{n^2} + \sum_{k=1}^{p-1} \sum_{1\leq n<m\leq k} \frac{2}{mn}$$
$$= \sum_{n=1}^{p-1}\sum_{k=n}^{p-1} \frac{1}{n^2} + \sum_{k=1}^{p-1}\sum_{n=1}^{k}\sum_{m=n+1}^{k} \frac{2}{mn} = \sum_{n=1}^{p-1} \frac{p-n}{n^2} + \sum_{n=1}^{p-1}\sum_{k=n}^{p-1}\sum_{m=n+1}^{k} \frac{2}{mn}$$
$$\equiv_p \sum_{n=1}^{p-1} \frac{-1}{n} + \sum_{n=1}^{p-1}\sum_{m=n+1}^{p-1} \frac{2(p-m)}{mn} \overset{(18)}{\equiv_p} \sum_{n=1}^{p-1}\sum_{m=n+1}^{p-1} \frac{-2}{n}$$
$$\equiv_p \sum_{n=1}^{p-1} \frac{-2(p-1-n)}{n} \equiv_p \sum_{n=1}^{p-1} \left(\frac{2}{n} + 2\right)$$
$$\equiv_p 2H_{p-1} + 2(p-1) \overset{(18)}{\equiv_p} -2 \equiv_p p-2.$$

Corollary 1 *Let $\{p_n\}_{n\in\mathbb{N}}$ be a sequence of the successive prime numbers and let $S_n \in \{0, 1, \ldots, p_n - 1\}$ be the remainder of dividing the number $\sum_{k=1}^{p_n-1} H_k^2$ by p_n in the sense of Definition 3. Then we have*

$$S_n - S_{n-1} = p_n - p_{n-1}$$

for $n \in \mathbb{N}$, $n \geq 3$.

4. For $p \in \mathbb{P}$, $p \geq 5$ we have $\sum_{k=1}^{p-1} H_k^2 \equiv 2(p-1) \pmod{p^2}$.

Proof Proceeding in the same manner as in the proof of item 3 we obtain

$$\sum_{k=1}^{p-1} H_k^2 = \sum_{n=1}^{p-1} \frac{p-n}{n^2} + \sum_{n=1}^{p-1} \sum_{m=n+1}^{p-1} \frac{2(p-m)}{mn}$$

$$= pH_{p-1}^{(2)} - H_{p-1} + p \sum_{n=1}^{p-1} \sum_{m=n+1}^{p-1} \frac{2}{mn} - \sum_{n=1}^{p-1} \sum_{m=n+1}^{p-1} \frac{2}{n}$$

$$\overset{(18),(19)}{\equiv_{p^2}} 2p \sum_{n=1}^{p-1} \frac{1}{n}(H_{p-1} - H_n) - \sum_{n=1}^{p-1} \frac{2(p-1-n)}{n}$$

$$\equiv_{p^2} 2pH_{p-1}^2 - 2p \sum_{n=1}^{p-1} \frac{H_n}{n} - 2pH_{p-1} + 2H_{p-1} + 2(p-1) \overset{1,(18),(19)}{\equiv_{p^2}} 2(p-1).$$

5. For $p \in \mathbb{P}$, $p \geq 3$, it holds $\sum_{k=1}^{p-1} H_k^3 \equiv \begin{cases} 1 \pmod{p} & \text{for } p \in \{3, 5\}, \\ 6 \pmod{p} & \text{for } p \geq 7. \end{cases}$
   In this case the proof runs analogically like in items 3 and 4 and it is omitted here.
   The following results are just the outcomes of the numerical experiment executed within the range of the initial two hundred prime numbers:
6. For $p \in \mathbb{P}$, $p \geq 7$, it holds $\sum_{k=1}^{p-1} \frac{H_k^2}{k^2} \equiv 0 \pmod{p}$.
7. For $p \in \mathbb{P}$, $p \geq 5$, it holds $\sum_{k=1}^{p-1} \frac{H_k^3}{k} \equiv 0 \pmod{p}$.
8. For $p \in \mathbb{P}$, $p \geq 7$, it holds $\sum_{k=1}^{p-1} \frac{H_k}{k^3} \equiv 0 \pmod{p}$.
9. For $p \in \mathbb{P}$, $p \geq 3$, it holds $\sum_{k=1}^{p-1} \frac{H_k}{k(k+1)} \equiv 0 \pmod{p}$.
10. For $p \in \mathbb{P}$, $p \geq 5$, it holds $\sum_{k=1}^{p-1} \frac{H_k^3}{k(k+1)} \equiv 0 \pmod{p}$.
11. For $p \in \mathbb{P}$, $p \geq 7$, it holds

$$\sum_{k=1}^{p-1} \frac{H_k - H_k^{(2)}}{k^2} \equiv -\sum_{k=1}^{p-1} \frac{H_k^{(2)}}{k} \equiv \sum_{k=1}^{p-2} \frac{H_k}{(k+1)^2} \pmod{p}.$$

At the end let as also present the Maclaurin series expansion of the sum involving the harmonic numbers, in which we are interested in this paper. This expansion reveals the connection between the values of the zeta function for odd positive integers and the harmonic numbers (each coefficient of this expansion possesses this property

which we confirmed numerically for the first twenty coefficients – we present only the first eight coefficients, see also [13]):

$$\sum_{n=1}^{\infty}\frac{H_n}{(n+x)^2}=2\zeta(3)+\sum_{k=1}^{\infty}\sum_{n=1}^{\infty}\frac{(-1)^k(k+1)H_n}{(n+x)^{k+2}}x^k=$$
$$=2\zeta(3)-\frac{\pi^4 x}{36}+\left(-\frac{1}{2}\pi^2\zeta(3)+9\zeta(5)\right)x^2+\left(-\frac{\pi^6}{135}+2\zeta(3)^2\right)x^3+$$
$$+\left(-\frac{1}{18}\pi^4\zeta(3)-\frac{5}{6}\pi^2\zeta(5)+20\zeta(7)\right)x^4+\left(-\frac{\pi^8}{700}+6\zeta(3)\zeta(5)\right)x^5+$$
$$+\left(-\frac{1}{270}\pi^2\left(2\pi^4\zeta(3)+21\pi^2\zeta(5)+315\zeta(7)\right)+35\zeta(9)\right)x^6+$$
$$+\left(-\frac{2\pi^{10}}{8505}+4\zeta(5)^2+8\zeta(3)\zeta(7)\right)x^7+\ldots$$

Let us recall that it remains an open problem whether all the numbers $\zeta(2n-1),\ n\in\mathbb{N}$ are irrational.

Final remark 1 *Some other generalizations of the harmonic numbers are also discussed in literature, for example in papers* [14, 15] *there are defined and investigated the so called Hyperharmonic numbers. Moreover, see the papers:* [16–20].

References

1. Basu, A.: A new method in the study of Euler sums. Ramanujan J. **16**, 7–24 (2008)
2. Borwein, J.M., Bradley, D.M.: Thirty-two Goldbach variations. Int. J. Number Theory **2**, 65–103 (2006)
3. Sofo, A.: Computational Techniques for the Summation of Series. Kluwer Academic/Plenum Publisher, New York (2003)
4. Sofo, A., Cvijovic, D.: Extensions of Euler harmonic sums. Appl. Anal. Discrete Math. **6**, 317–328 (2012)
5. Lagarias, J.C.: An elementary problem equivalent to the Riemann hypothesis. Amer. Math. Monthly **109**(6), 534–543 (2002)
6. Miller K.S., Ross B.: An Introduction to the Fractional Calculus and Fractional Differential Equations. Wiley-Interscience (1993)
7. Rabsztyn, S., Słota, D., Wituła, R.: Gamma and Beta Functions. Silesian University of Technology Press, Gliwice (2012). (in Polish)
8. Wituła, R., Hetmaniok, E., Słota, D.: Generalized Gregory's series. Appl. Math. Comput. **237**, 203–216 (2014)
9. Wituła, R., Gawrońska, N., Słota, D., Zielonka, A.: Some generalizations of Gregory's power series and their applications. J. Appl. Math. Comp. Mech. **12**, 79–91 (2013)
10. Wolstenholme, J.: On certain properties of prime numbers. J. Pure Ap. Mat. **5**, 35–39 (1862)
11. Helou, C., Terjanian, G.: On Wolstenholme's theorem and its converse. J. Number Theory **128**, 475–499 (2008)
12. Wituła, R.: On Some Applications of the Formulas for the Sum of Unimodular Complex Numbers. PK JS Press, Gliwice (2011). (in Polish)

13. Srivastava, H.M.: Certain classes of series associated with the Zeta and relates functions. Appl. Math. Comp. **141**, 13–49 (2003)
14. Dil A., Kurt V.: Polynomials related to harmonic numbers and evaluation of harmonic number series I. arXiv:http://arxiv.org/pdf/0912.1834.pdf
15. Dil, A., Kurt, V.: Polynomials related to harmonic numbers and evaluation of harmonic number series II. Appl. Anal. Discrete Math. **5**, 212–229 (2011)
16. Sofo, A., Srivastava, H.M.: A family of shifted harmonic sums. Ramanujan J. **37**, 89–108 (2015)
17. Sofo, A.: Shifted harmonic sums of order two. Commun. Korean Math. Soc. **29**, 239–255 (2014)
18. Sofo, A.: Summation formula involving harmonic numbers. Anal. Math. **37**, 51–64 (2011)
19. Schmidt, M.D.: Generalized j-factorial functions, polynomials, and applications. J. Integer Seq. **13**(2), 3 (2010)
20. Zheng, D.Y.: Further summation formulae related to generalized harmonic numbers. J. Math. Anal. Appl. **335**, 692–706 (2007)

Cayley–Hamilton Theorem for Fractional Linear Systems

Tadeusz Kaczorek

Abstract The classical Cayley–Hamilton theorem is extended to fractional continuous-time and discrete-time linear systems. It is shown that the Mittag-Leffler functions of the fractional continuous-time linear system and the Φ_i matrices of the fractional discrete-time linear systems satisfy their characteristic equations. The extensions are based on the application of the Lagrange–Sylvester formula of functions of matrices.

Keywords Extension · Cayley–Hamilton theorem · Fractional linear system

1 Introduction

The classical Cayley–Hamilton theorem [1–3] says that every square matrix satisfies its own characteristic equation. The Cayley–Hamilton theorem has been extended to rectangular matrices [4, 5], block matrices [4, 6], pairs of block matrices [6] and standard and singular two-dimensional linear (2-D) systems [7, 8]. The Cayley–Hamilton theorem and its generalizations have been used in control systems, electrical circuits, systems with delays, singular systems, 2-D linear systems, etc. [2, 9–22].

In [23] the Cayley–Hamilton theorem has been extended to n-dimensional (n-D) real polynomial matrices. An extension of the Cayley–Hamilton theorem for continuous-time linear systems with delays has been given in [24].

In this paper the Cayley–Hamilton theorem will be extended to the fractional continuous-time and discrete-time linear systems.

The paper is organized as follows. In Sect. 2 some preliminaries concerning fractional linear systems and the Lagrange–Sylvester formula are recalled. The Cayley–Hamilton theorem for fractional continuous-time linear systems is extended in Sect. 3 and for fractional discrete-time linear systems in Sect. 4. Concluding remarks are given in Sect. 5.

T. Kaczorek (✉)
Faculty of Electrical Engineering, Bialystok University of Technology,
Wiejska 45d, 15-351 Białystok, Poland
e-mail: kaczorek@isep.pw.edu.pl

A. Babiarz et al. (eds.), *Theory and Applications of Non-integer Order Systems*,
Lecture Notes in Electrical Engineering 407, DOI 10.1007/978-3-319-45474-0_5

2 Preliminaries

In this paper the following Caputo definition of the fractional derivative of α order will be used [14]

$$ {}_0D_t^{\alpha} f(t) = \frac{d^{\alpha} f(t)}{dt^{\alpha}} = \frac{1}{\Gamma(1-\alpha)} \int_0^t \frac{\dot{f}(\tau)}{(t-\tau)^{\alpha}} d\tau, \quad 0 < \alpha < 1, \tag{1} $$

where $\dot{f}(\tau) = \frac{df(\tau)}{d\tau}$ and $\Gamma(x) = \int_0^{\infty} t^{x-1} e^{-t} dt$, $Re(x) > 0$ is the Euler gamma function.

Consider the fractional continuous-time linear system

$$ \frac{d^{\alpha} x(t)}{dt^{\alpha}} = Ax(t) + Bu(t), \quad 0 < \alpha < 1, \tag{2} $$

where $x(t) \in \mathbb{R}^n$, $u(t) \in \mathbb{R}^m$ are the state and input vectors and $A \in \mathbb{R}^{n \times n}$, $B \in \mathbb{R}^{n \times m}$.

Theorem 1 ([14]) *The solution to the Eq. (2) has the form*

$$ x(t) = \Phi_0(t) x_0 + \int_0^t \Phi(t-\tau) B u(\tau) d\tau, \quad x(0) = x_0, \tag{3} $$

where

$$ \Phi_0(t) = \sum_{k=0}^{\infty} \frac{A^k t^{k\alpha}}{\Gamma(k\alpha + 1)}, \tag{4} $$

$$ \Phi(t) = \sum_{k=0}^{\infty} \frac{A^k t^{(k+1)\alpha - 1}}{\Gamma[(k+1)\alpha]} \tag{5} $$

are the Mittag-Leffler functions.

Consider the fractional discrete-time linear system

$$ \Delta^{\alpha} x_{i+1} = Ax_i + Bu_i, \quad i \in Z_+ = \{0, 1, \ldots\} \quad 0 < \alpha < 1, \tag{6} $$

where

$$ \Delta^{\alpha} x_i = \sum_{k=0}^{i} (-1)^k \binom{\alpha}{k} x_{i-k}, \quad \binom{\alpha}{k} = \begin{cases} 1 & \text{for} \quad k = 0 \\ \frac{\alpha(\alpha-1)\ldots(\alpha-k+1)}{k!} & \text{for } k = 1, 2, \ldots \end{cases} \tag{7} $$

is the α order difference and $x_i \in \mathbb{R}^n$, $u_i \in \mathbb{R}^m$ are the state and input vectors, $A \in \mathbb{R}^{n\times n}$, $B \in \mathbb{R}^{n\times m}$. Substituting (7) into (6) we obtain

$$x_{i+1} + \sum_{k=1}^{i+1}(-1)^k \binom{\alpha}{k} x_{i-1+k} = Ax_i + Bu_i, \quad i \in Z_+ \tag{8a}$$

and

$$x_{i+1} = A_\alpha x_i + \sum_{k=2}^{i+1}(-1)^{k+1} \binom{\alpha}{k} x_{i-k+1} + Bu_i, \quad i \in Z_+, \tag{8b}$$

where $A_\alpha = A + \alpha I_n$.

Theorem 2 ([14]) *The solution of the Eq. (8) has the form*

$$x_i = \Phi_i x_0 + \sum_{k=0}^{i-1} \Phi_{i-k-1} B u_k, \tag{9}$$

where the matrices Φ_i are determined by the equation

$$\Phi_{i+1} = A_\alpha \Phi_i + \sum_{k=2}^{i+1}(-1)^{k+1} \binom{\alpha}{k} \Phi_{i-k+1}, \quad \Phi_0 = I_n. \tag{10}$$

Consider a matrix $A \in \mathbb{R}^{n\times n}$ with the minimal characteristic polynomial

$$\Psi(\lambda) = (\lambda - \lambda_1)^{m_1}(\lambda - \lambda_2)^{m_2} \ldots (\lambda - \lambda_r)^{m_r}, \tag{11}$$

where $\lambda_1, \lambda_2, \ldots, \lambda_r$ are the eigenvalues of the matrix A and $\sum_{i=1}^r m_i = m \leq n$. It is assumed that the function $f(\lambda)$ is well-defined on the spectrum $\sigma_A = \{\lambda_1, \lambda_2, \ldots, \lambda_r\}$ of the matrix A, i.e.

$$f(\lambda_k), \quad f^{(1)}(\lambda_k) = \frac{df(\lambda)}{d\lambda}|_{\lambda=\lambda_k} \ldots, f^{(m_k-1)}(\lambda_k) = \frac{d^{m_k-1}f(\lambda)}{d\lambda^{m_k-1}}|_{\lambda=\lambda_k}, \tag{12}$$

k $= 1, \ldots, r$, are finite [1, 3].

In this case the matrix $f(A)$ is well-defined and it is given by the Lagrange–Sylvester formula [1, 3]

$$f(A) = \sum_{i=1}^{r} Z_{i1} f(\lambda_i) + Z_{i2} f^{(1)}(\lambda_i) + \cdots + Z_{im_i} f^{(m_i-1)}(\lambda_i), \tag{13}$$

where

$$Z_{ij} = \sum_{k=j-1}^{m_i-1} \frac{\Psi_i(A)(A - \lambda_i I_n)^k}{(k-j+1)!(j-1)!} \frac{d^{k-j+1}}{d\lambda^{k-j+1}} \left[\frac{1}{\Psi_i(\lambda)}\right]_{\lambda=\lambda_i} \tag{14}$$

and

$$\Psi_i(\lambda) = \frac{\Psi(\lambda)}{(\lambda - \lambda_i)^{m_i}}, \quad i = 1, \ldots, r. \tag{15}$$

In particular case where the eigenvalues $\lambda_1, \lambda_2, \ldots, \lambda_n$ of the matrix A are distinct ($\lambda_i \neq \lambda_j, \quad i \neq j$) and

$$\varphi(\lambda) = \Psi(\lambda) = (\lambda - \lambda_1)(\lambda - \lambda_2) \ldots (\lambda - \lambda_n), \tag{16}$$

then the formula (13) has the form

$$f(A) = \sum_{k=1}^{n} Z_k f(\lambda_k), \tag{17}$$

where

$$Z_k = \prod_{\substack{i=1 \\ i \neq k}}^{n} \frac{A - \lambda_i I_n}{\lambda_k - \lambda_i}. \tag{18}$$

It is easy to show [3] that the matrices (18) satisfy the equalities

$$\sum_{k=1}^{n} Z_k = I_n, \tag{19}$$

$$Z_i Z_j = 0 \quad \text{for} \quad i \neq j, \quad i, j = 1, \ldots, n, \tag{20}$$

$$Z_i^k = 0 \quad \text{for} \quad k = 1, 2, \ldots, \quad i = 1, \ldots, n. \tag{21}$$

3 Cayley–Hamilton Theorem for Fractional Continuous-Time linear Systems

Consider a function $f(\lambda)$ well-defined on the spectrum of the matrix $A \in \mathbb{R}^{n \times n}$. The matrix $f(A)$ is given by the formulae (13) and (14).

Theorem 3 *Let*

$$\Psi(\lambda) = \det[I_n \lambda - f(A)] = \lambda^n + a_{n-1}\lambda^{n-1} + \cdots + a_1 \lambda + a_0 \tag{22}$$

be the characteristic polynomial of the matrix $f(A)$. Then the matrix $f(A)$ satisfies its characteristic equation, i.e.

$$[f(A)]^n + a_{n-1}[f(A)]^{n-1} + \cdots + a_1[f(A)] + a_0 I_n = 0. \tag{23}$$

Proof From definition of the inverse matrix we have

$$[I_n\lambda - f(A)]_{ad} = [I_n\lambda - f(A)]^{-1}\det[I_n\lambda - f(A)], \tag{24}$$

where $[I_n\lambda - f(A)]_{ad}$ is the adjoint matrix of $[I_n\lambda - f(A)]$. Note that

$$[I_n\lambda - f(A)]^{-1} = I_n\lambda^{-1} + f(A)\lambda^{-2} + [f(A)]^2\lambda^{-3} + \cdots \tag{25}$$

since

$$[I_n\lambda - f(A)][I_n\lambda - f(A)]^{-1} =$$

$$[I_n\lambda - f(A)]\{I_n\lambda^{-1} + f(A)\lambda^{-2} + [f(A)]^2\lambda^{-3} + \cdots\} = I_n. \tag{26}$$

Substitution of (26) and (22) into (24) yields

$$[I_n\lambda - f(A)]_{ad} =$$

$$\{I_n\lambda^{-1} + f(A)\lambda^{-2} + [f(A)]^2\lambda^{-3} + \cdots\}(\lambda^n + a_{n-1}\lambda^{n-1} + \cdots + a_1\lambda + a_0). \tag{27}$$

The entries of the matrix $[I_n\lambda - f(A)]_{ad}$ are polynomial of λ^k for $k = 0, 1, \ldots, n-1$. Comparison of the coefficients at λ^{-1} of (27) yields (23).

Theorem 4 *Let*

$$\det[I_n\lambda - e^{At}] = \lambda^n + a_{n-1}\lambda^{n-1} + \cdots + a_1\lambda + a_0 \tag{28}$$

be the characteristic polynomial of the matrix e^{At}. Then the matrix e^{At} satisfies its characteristic equation

$$e^{nAt} + a_{n-1}e^{(n-1)At} + \cdots + a_1e^{At} + a_0I_n = 0. \tag{29}$$

Proof The proof follows immediately from Theorem 3 for $f(A) = e^{At}$ and the equality $(e^{At})^k = e^{kAt}$ for $k = 1, 2, \ldots, n$.

Example 1 Using (17) and (18) it is easy to show that for the matrix

$$A = \begin{bmatrix} -2 & -3 \\ 3 & 4 \end{bmatrix} \tag{30}$$

the exponential matrix e^{At} has the form

$$e^{At} = \begin{bmatrix} (1-3t)e^t & -3te^t \\ 3te^t & (1+3t)e^t \end{bmatrix}. \tag{31}$$

The characteristic polynomial of the matrix (31) is

$$\Psi(\lambda)\det[I_2\lambda - e^{At}] = \begin{vmatrix} \lambda - (1-3t)e^t & 3te^t \\ -3te^t & \lambda - (1+3t)e^t \end{vmatrix} = \lambda^2 - 2e^t\lambda + e^{2t}. \quad (32)$$

Taking into account that

$$(e^{At})^2 = e^{2At} = \begin{bmatrix} (1-6t)e^{2t} & 6te^{2t} \\ -6te^{2t} & (1+6t)e^{2t} \end{bmatrix} \quad (33)$$

and using (32) we obtain

$$\begin{aligned} \Psi(e^{At}) = e^{2At} - 2e^t(e^{At}) + e^{2t}I_2 = \begin{bmatrix} (1-6t)e^{2t} & 6te^{2t} \\ -6te^{2t} & (1+6t)e^{2t} \end{bmatrix} \\ -2e^t \begin{bmatrix} (1-3t)e^t & -3te^t \\ 3te^t & (1+3t)e^t \end{bmatrix} + e^{2t}\begin{bmatrix} 1 & 0 \\ 0 & 1 \end{bmatrix} = \begin{bmatrix} 0 & 0 \\ 0 & 0 \end{bmatrix}. \end{aligned} \quad (34)$$

Therefore, the matrix (31) satisfies its characteristic equation.

Theorem 5 *Let*

$$\varphi_0(\lambda) = \det[I_n\lambda - \Phi_0(t)] = \lambda^n + \overline{a}_{n-1}\lambda^{n-1} + \cdots + \overline{a}_1\lambda + \overline{a}_0 = 0 \quad (35)$$

and

$$\varphi(\lambda) = \det[I_n\lambda - \Phi(t)] = \lambda^n + \widehat{a}_{n-1}\lambda^{n-1} + \cdots + \widehat{a}_1\lambda + \widehat{a}_0 = 0 \quad (36)$$

be the characteristic equations of the matrices $\Phi_0(t)$ and $\Phi(t)$ defined by (4) and (5), respectively. Then the matrices $\Phi_0(t)$ and $\Phi(t)$ satisfy their characteristic equations

$$\begin{aligned} \varphi_0[\Phi_0(t)] = \det[I_n\lambda - \Phi_0(t)] \\ = \Phi_0^n(t) + \overline{a}_{n-1}\Phi_0^{n-1}(t) + \cdots + \overline{a}_1\Phi_0(t) + \overline{a}_0 I_n = 0 \end{aligned} \quad (37)$$

and

$$\begin{aligned} \varphi[\Phi(t)] = \det[I_n\lambda - \Phi_0(t)] \\ = \Phi^n(t) + \widehat{a}_{n-1}\Phi^{n-1}(t) + \cdots + \widehat{a}_1\Phi(t) + \widehat{a}_0 I_n = 0. \end{aligned} \quad (38)$$

Proof Using Theorem 3 for $f(A) = \Phi_0(t)$ and $f(A) = \Phi(t)$ we obtain immediately from (22) and (23) the Eqs. (37) and (38), respectively.

Remark 1 If $\alpha = 1$ then $\Phi_0(t) = \Phi(t) = e^{At}$ and

$$\varphi_0[\Phi_0(t)] = \varphi[\Phi(t)] = e^{nAt} + a_{n-1}e^{(n-1)At} + \cdots + a_1e^{At} + a_0I_n = 0, \quad (39)$$

where $a_k = \widehat{a}_k = \overline{a}_k$ for $k = 0, 1, \ldots, n-1$.

Example 2 Consider the fractional system (2) with $0 < \alpha < 1$ and

$$A = \begin{bmatrix} 0 & 1 \\ 0 & 0 \end{bmatrix}. \tag{40}$$

Using (4) and (5) it is easy to show [14] that

$$\Phi_0(t) = \sum_{k=0}^{\infty} \frac{A^k t^{k\alpha}}{\Gamma(k\alpha + 1)} = I_2 + \frac{At^{\alpha}}{\Gamma(\alpha + 1)} = \begin{bmatrix} 1 & at^{\alpha} \\ 0 & 1 \end{bmatrix}, \quad a = \frac{1}{\Gamma(\alpha + 1)} \tag{41}$$

and

$$\begin{gathered} \Phi(t) = \sum_{k=0}^{\infty} \frac{A^k t^{(k+1)\alpha - 1}}{\Gamma[(k+1)\alpha]} = I_2 \frac{t^{\alpha-1}}{\Gamma(\alpha)} + \frac{At^{2\alpha-1}}{\Gamma(2\alpha)} = \begin{bmatrix} a_1 t^{\alpha-1} & a_2 t^{2\alpha-1} \\ 0 & a_1 t^{\alpha-1} \end{bmatrix}, \\ a_1 = \frac{1}{\Gamma(\alpha)}, \quad a_2 = \frac{1}{\Gamma(2\alpha)}. \end{gathered} \tag{42}$$

The characteristic polynomials of the matrices (41) and (42) have the forms

$$\varphi_0(\lambda) = \det[I_2\lambda - \Phi_0(t)] = \begin{vmatrix} \lambda - 1 & -at^{\alpha} \\ 0 & \lambda - 1 \end{vmatrix} = \lambda^2 - 2\lambda + 1 \tag{43}$$

and

$$\varphi(\lambda) = \det[I_2\lambda - \Phi(t)] = \begin{vmatrix} \lambda - at^{\alpha-1} & -a_2 t^{2\alpha-1} \\ 0 & \lambda - a_1 t^{\alpha-1} \end{vmatrix} = \lambda^2 - 2a_1 t^{\alpha-1}\lambda + a_1^2 t^{2(\alpha-1)}. \tag{44}$$

Taking into account that

$$[\Phi_0(t)]^2 = \begin{bmatrix} 1 & at^{\alpha} \\ 0 & 1 \end{bmatrix}^2 = \begin{bmatrix} 1 & 2at^{\alpha} \\ 0 & 1 \end{bmatrix} \tag{45}$$

and using (43) we obtain

$$\begin{gathered} [\Phi_0(t)]^2 - 2\Phi_0(t) + I_2 = \\ \begin{bmatrix} 1 & 2at^{\alpha} \\ 0 & 1 \end{bmatrix} - 2\begin{bmatrix} 1 & at^{\alpha} \\ 0 & 1 \end{bmatrix} + \begin{bmatrix} 1 & 0 \\ 0 & 1 \end{bmatrix} = \begin{bmatrix} 0 & 0 \\ 0 & 0 \end{bmatrix}. \end{gathered} \tag{46}$$

Similarly, taking into account that

$$[\Phi(t)]^2 = \begin{bmatrix} a_1 t^{\alpha-1} & a_2 t^{2\alpha-1} \\ 0 & a_1 t^{\alpha-1} \end{bmatrix} = \begin{bmatrix} a_1^2 t^{2(\alpha-1)} & 2a_1 a_2 t^{3(\alpha-1)} \\ 0 & a_1^2 t^{2(\alpha-1)} \end{bmatrix} \tag{47}$$

and using (44) we obtain

$$[\Phi(t)]^2 - 2a_1 t^{\alpha-1}\Phi(t) + a_1^2 t^{2(\alpha-1)} I_2 = \begin{bmatrix} a_1^2 t^{2(\alpha-1)} & 2a_1 a_2 t^{3(\alpha-1)} \\ 0 & a_1^2 t^{2(\alpha-1)} \end{bmatrix} -$$

$$2a_1 t^{\alpha-1} \begin{bmatrix} a_1 t^{\alpha-1} & a_2 t^{2\alpha-1} \\ 0 & a_1 t^{\alpha-1} \end{bmatrix} + a_1^2 t^{2(\alpha-1)} \begin{bmatrix} 1 & 0 \\ 0 & 1 \end{bmatrix} = \begin{bmatrix} 0 & 0 \\ 0 & 0 \end{bmatrix}. \tag{48}$$

Therefore, the matrices (41) and (42) satisfy their characteristic equations.

4 Cayley–Hamilton Theorem for Discrete-Time Linear Systems

Consider the fractional discrete-time linear system (6) with the matrix Φ_i determined by the Eq. (10) for the given matrix A.

Theorem 6 *Let*

$$\det[I_n\lambda - \Phi_i] = \lambda^n + b_{n-1}\lambda^{n-1} + \cdots + b_1\lambda + b_0 = 0 \tag{49}$$

be the characteristic equation of the matrix Φ_i, $i = 1, 2, \ldots$. Then the matrix Φ_i satisfies its characteristic equation, i.e.

$$\Phi_i^n + b_{n-1}\Phi_i^{n-1} + \cdots + b_1\Phi_i + b_0 I_n = 0. \tag{50}$$

Proof The proof follows immediately from Theorem 3 for $\Psi(\lambda) = \det[I_n\lambda - \Phi_i]$.

Example 3 For

$$A = \begin{bmatrix} 1 & 0 \\ 0 & 0.5 \end{bmatrix} \tag{51}$$

and $\alpha = 0.5$ we have

$$A_\alpha = A + I_n\alpha = \begin{bmatrix} 1.5 & 0 \\ 0 & 1 \end{bmatrix}. \tag{52}$$

Using (52) and (10) we obtain

$$\Phi_1 = A_\alpha \tag{53a}$$

and

$$\Phi_2 = A_\alpha\Phi_1 + \frac{\alpha(1-\alpha)}{2}\Phi_0 = A_\alpha^2 + \frac{\alpha(1-\alpha)}{2} I_2 = \begin{bmatrix} 1.5 & 0 \\ 0 & 1 \end{bmatrix}^2 + 0.125 \begin{bmatrix} 1 & 0 \\ 0 & 1 \end{bmatrix} = \begin{bmatrix} 2.375 & 0 \\ 0 & 1.125 \end{bmatrix}. \tag{53b}$$

The characteristic polynomial of the matrix (53b) has the form

$$\det[I_2\lambda - \Phi_2] = \begin{vmatrix} \lambda - 2.375 & 0 \\ 0 & \lambda - 1.125 \end{vmatrix} = \lambda^2 - 3.5\lambda + 2.6719. \tag{54}$$

Using (54) and (53b) we obtain

$$\Phi_2^2 - 3.5\Phi_2 + 2.6719I_2 = \begin{bmatrix} 2.375 & 0 \\ 0 & 1.125 \end{bmatrix}^2 -$$

$$3.5\begin{bmatrix} 2.375 & 0 \\ 0 & 1.125 \end{bmatrix} + \begin{bmatrix} 2.6719 & 0 \\ 0 & 2.6719 \end{bmatrix} = \begin{bmatrix} 0 & 0 \\ 0 & 0 \end{bmatrix}. \tag{55}$$

Therefore, the matrix (53b) satisfies its characteristic equation.

Consider the fractional discrete-time linear system (6) for $B = 0$.

Theorem 7 *Let*

$$\det\left[\sum_{k=0}^{L+1}(-1)^k\binom{\alpha}{k}I_n z^{-k} - Az^{-1}\right] = a_0 z^{-h} + a_1 z^{1-h} + \cdots + a_{h-1}z^{-1} + a_h \tag{56}$$

be the characteristic polynomial of the system for $i = L$ and $h = (L+1)n$. Then the matrices Φ_i defined by (10) for $i = 0, 1, \cdots, h$ satisfy the equation

$$a_0\Phi_h + a_1\Phi_{h-1} + \cdots + a_{h-1}\Phi_1 + a_h I_n = 0. \tag{57}$$

Proof From definition of inverse matrix we have

$$\begin{aligned} &\left[\sum_{k=0}^{L+1}(-1)^k\binom{\alpha}{k}I_n z^{-k} - Az^{-1}\right]_{ad} \\ &= \left(\sum_{j=0}^{\infty}\Phi_j z^{-j}\right)(a_0\Phi_h + a_1\Phi_{h-1} + \cdots + a_{h-1}\Phi_1 + a_h I_n) \end{aligned} \tag{58}$$

since

$$\left[\sum_{k=0}^{L+1}(-1)^k\binom{\alpha}{k}I_n z^{-k} - Az^{-1}\right]^{-1} = \sum_{j=0}^{\infty}\Phi_j z^{-j}. \tag{59}$$

Note that the degree of the adjoint matrix is less than h. Comparing the coefficients at the power z^{-h} of (58) we obtain (57).

Example 4 Consider the fractional discrete-time linear system with the matrix (51) and $\alpha = 0.5$. Assuming $L = 1$ from (56) and (51) we obtain

$$\left[\sum_{k=0}^{2}(-1)^k\binom{\alpha}{k}I_2z^{-k}-Az^{-1}\right]^{-1}=\det\left[I_2-(I_2\alpha+A)z^{-1}+\frac{\alpha(\alpha-1)}{2}I_2z^{-2}\right]$$

$$=\begin{vmatrix}1-1.5z^{-1}-0.125z^{-2} & 0\\ 0 & 1-z^{-1}-0.125z^{-2}\end{vmatrix}$$

$$=(0.125)^2z^{-4}+0.3125z^{-3}+1.375z^{-2}-2.5z^{-1}+1. \tag{60}$$

Using (52), (53) and (10) for $i=2,3$ we obtain

$$\Phi_3=A_\alpha\Phi_2+\sum_{k=2}^{3}(-1)^{k+1}\binom{\alpha}{k}\Phi_{3-k}=\begin{bmatrix}3.8125 & 0\\ 0 & 1.3125\end{bmatrix}. \tag{61}$$

$$\Phi_4=A_\alpha\Phi_3+\sum_{k=2}^{4}(-1)^{k+1}\binom{\alpha}{k}\Phi_{4-k}=\begin{bmatrix}6.1484 & 0\\ 0 & 1.5547\end{bmatrix}. \tag{62}$$

Taking into account that in this case $h=4$ and

$$a_4=1,\quad a_3=-2.5,\quad a_2=1.25,\quad a_1=0.3125,\quad a_0=0.0156 \tag{63}$$

and using (57) we obtain

$$a_0\Phi_4+a_1\Phi_3+a_2\Phi_2+a_3\Phi_1+a_4I_2=\begin{bmatrix}0 & 0\\ 0 & 0\end{bmatrix}. \tag{64}$$

Therefore, the matrices Φ_i, $i=0,1,\ldots,4$ satisfy the characteristic equation.

5 Concluding Remarks

The classical Cayley–Hamilton theorem has been extended to the fractional continuous-time and discrete-time linear systems. The extension is based on the application of the Lagrange–Sylvester formula of functions of matrices. It has been shown for continuous-time systems that the matrices $\Phi_0(t)$ and $\Phi(t)$ defined by (4) and (5) satisfy also their characteristic equations (35) and (36), respectively (Theorem 4) and for discrete-time systems the matrices Φ_i defined by (10) satisfy their characteristic equation (57) (Theorem 7). The considerations have been illustrated by numerical examples of the fractional linear systems. The considerations can be extended to fractional descriptor linear systems.

Acknowledgments This work was supported by National Science Centre in Poland under work No. 2014/13/B/ST7/03467.

References

1. Gantmacher, F.R.: The Theory of Matrices. Chelsea Pub. Comp, London (1959)
2. Kaczorek, T.: Linear Control Systems, vol. I, II, Research Studies Press (1992/1993)
3. Kaczorek, T.: Vectors and Matrices in Automation and Electrotechnics. WNT, Warsaw (1998). (in Polish)
4. Kaczorek, T.: An existence of the Cayley-Hamilton theorem for non-square block matrices and computation of the left and right inverses of matrices. Bull. Pol. Ac.: Tech. **43**(1), 49–56 (1995)
5. Kaczorek, T.: Generalization of the Cayley–Hamilton theorem for non-square matrices. In: Proceedings International Conference Fundamentals of Electrotechnics and Circuit Theory XVIII-SPETO, pp. 77–83 (1995)
6. Kaczorek, T.: An extension of the Cayley–Hamilton theorem for a standard pair of block matrices. Int. J. Appl. Math. Comput. Sci. **8**(3), 511–516 (1998)
7. Kaczorek, T.: An existence of the Cayley–Hamilton theorem for singular 2D linear systems with non-square matrices. Bull. Pol. Ac.: Tech. **43**(1), 39–48 (1995)
8. Kaczorek, T.: Extensions of Cayley–Hamilton theorem for 2D continuous-discrete linear systems. Int. J. Appl. Math. Comput. Sci. **4**(4), 507–515 (1994)
9. Chang, F.R., Chan, C.M.: The generalized Cayley–Hamilton theorem for standard pencils. Syst. Control Lett. **18**(192), 179–182 (1992)
10. Kaczorek, T.: An extension of the Cayley–Hamilton theorem for nonlinear time-varying systems. Int J. Appl. Math. Comput. Sci. **16**(1), 141–145 (2006)
11. Kaczorek, T.: Generalizations of the Cayley–Hamilton theorem with applications. Arch. Electr. Eng. LV **I**(1), 3–41 (2007)
12. Kaczorek, T.: Positive 2D hybrid linear systems. Bull. Pol. Ac.: Tech. **55**(4), 351–358 (2007)
13. Kaczorek, T.: Positive discrete-time linear Lyapunov systems. J. Autom., Mob. Robot. Intell. Syst. **2**(3), 13–19 (2008)
14. Kaczorek, T.: Selected Problems of Fractional Systems Theory. Springer, Berlin (2012)
15. Kaczorek, T., Przyborowski, P.: Positive continuous-time linear time-varying Lyapunov systems. In: Proceedings of of XVI International Conference on Systems Science, pp. 140–149, 4–6 Sept, Wrocław-Poland (2007)
16. Lancaster, P.: Theory of Matrices. Academic Press, Massachusetts (1969)
17. Lewis, F.L.: Cayley–Hamilton theorem and Fadeev's method for the matrix pencil [sE-A] . In: Proceedings of 22nd IEEE Conference Decision Control, pp. 1282–1288 (1982)
18. Lewis, F.L.: Further remarks on the Cayley–Hamilton theorem and Fadeev's method for the matrix pencil [sE-A]. IEEE Trans. Automat. Control **31**, 869–870 (1986)
19. Mertizios, B.G., Christodoulous, M.A.: On the generalized Cayley–Hamilton theorem. IEEE Trans. Automat. Control **31**, 156–157 (1986)
20. Smart, N.M., Barnett, S.: The algebra of matrices in n-dimensional systems. Math. Control Inform. **6**, 121–133 (1989)
21. Theodoru, N.J.: M-dimensional Cayley–Hamilton theorem. IEEE Trans. Automat. Control **34**(5), 563–565 (1989)
22. Victoria, J.: A block Cayley–Hamilton theorem. Bull. Math. Sco. Sci. Math. Roum **26**(1), 93–97 (1982)
23. Kaczorek, T.: Generalizations of Cayley–Hamilton theorem for n-D polynomial matrices. IEEE Trans. Autom. Contr. **50**(5), 671–674 (2005)
24. Kaczorek, T.: Extension of the Cayley–Hamilton theorem for continuous-time systems with delays. Int. J. Appl. Math. Comput. Sci. **15**(2), 231–234 (2005)

Order Composition Properties for Output-Additive Variable-Order Derivative

Michał Macias

Abstract The paper presents, composition properties of output-additive switching scheme with fractional constant-order differ-integral. It has been shown that composition property is not commutative and depends on the sequence of composition. Considering switching scheme corresponding to particular type of fractional variable-order definition (so-called $\mathcal{E}$-type). Next, the numerical results of composition properties have been shown.

Keywords Fractional calculus · Variable order derivative

1 Introduction

The fractional calculus is a generalization of the traditional differential calculus for a case when integrals and derivatives are not only integer but also fractional order. This generalization can be used to introduce more accurate models or more efficient control algorithms. The approach based on fractional calculus is especially efficient for modeling systems related to diffusion processes. In [1–3], the heat transfer process was successfully modeled with using fractional models based on normal and anomalous diffusion equation. Papers [2, 4, 5] present, also results of very accurate modeling of ultracapacitors, the electrical energy storage elements that base on the Helmholtz effect and diffusion.

When the order is not constant but depends on time, then the various types of fractional variable order derivatives can be distinguished. In literature plenty of such definitions can be encountered, however, authors put only minor emphasis on their interpretations. In [6], nine different variable order derivative definitions are given and in [7, 8], three general types of variable order definitions can be found but without clear interpretation of them. In papers [9–14] the explanation for two main types and two recursive types of derivatives in the form of switching schemes are given. The

M. Macias (✉)
Institute of Control and Industrial Electronics, Warsaw University of Technology,
Koszykowa 75, 00-662 Warsaw, Poland
e-mail: michal.macias@ee.pw.edu.pl

A. Babiarz et al. (eds.), *Theory and Applications of Non-integer Order Systems*,
Lecture Notes in Electrical Engineering 407, DOI 10.1007/978-3-319-45474-0_6

equivalence between particular types of definitions and appropriate switching strategies are proved by authors. Moreover, based on these strategies, analog models of proper types derivatives were build and validated according to their numerical implementations. Another methods for numerical realization of fractional variable order integrators or differentiators can be found in [15, 16]. Paper [17] shows comparison of control system behavior with fractional variable order PID controller designed according to few types of fractional variable order derivatives.

The main contribution of the paper is to prove the composition properties of output-additive switching scheme with fractional constant order differ-integral from both side of switching scheme. Considering switching scheme is equivalent to the $\mathcal{E}$-type fractional variable-order definition.

The rest of the paper is organized as follows: In Sects. 2 and 3 the fractional constant and output-additive fractional variable-order definitions are presented. Section 4 presents the output-additive switching scheme which is equivalent to the $\mathcal{E}$-type fractional variable-order definition. The main contribution of the paper is shown in Sect. 5. At the end, numerical results of order composition properties have been introduced in Sect. 6.

2 Fractional-Order Grunwald–Letnikov Type Derivative

As a base of generalization onto variable-order derivative the following definition is taken into consideration:

Definition 1 Fractional constant order derivative is defined as follows:

$$ {}_0\mathrm{D}_t^{\alpha} f(t) = \lim_{h \to 0} \frac{1}{h^{\alpha}} \sum_{j=0}^{n} (-1)^j \binom{\alpha}{j} f(t - jh), $$

where $n = \lfloor t/h \rfloor$ and h is a step time.

It was shown in [18] that for constant α_1 and α_2 orders the composition property of Grünwald–Letnikov definition holds

$$ {}_0\mathrm{D}_t^{\alpha_1} {}_0\mathrm{D}_t^{\alpha_2} f(t) = {}_0\mathrm{D}_t^{\alpha_2} {}_0\mathrm{D}_t^{\alpha_1} f(t) = {}_0\mathrm{D}_t^{\alpha_1+\alpha_2} f(t). \tag{1} $$

3 The Output-Additive Fractional Variable-Order Derivative

The output-additive fractional variable-order definition (so-called $\mathcal{E}$-type) its switching scheme and analog model has been widely introduces in [9, 19]. More types of fractional variable-order definition can be found in [11, 14, 20].

Definition 2 The $\mathcal{E}$-type fractional variable-order difference is defined as follows:

$$\mathcal{E}\Delta^{\alpha_k} x_k = \frac{x_k}{h^{\alpha_k}} - \sum_{j=1}^{k} (-1)^j \binom{-\alpha_{k-j}}{j} \frac{h^{\alpha_{k-j}}}{h^{\alpha_k}} \mathcal{E}\Delta^{\alpha_{k-j}} x_{k-j}.$$

This type of difference is obtained for all values of previous differences. In continuous-time domain the $\mathcal{E}$-type definition can be as:

Definition 3 The $\mathcal{E}$-type fractional variable-order derivative is defined as follows:

$${}_{\mathcal{E}}^{0}\mathrm{D}_t^{\alpha(t)} f(t) = \lim_{h \to 0} \left(\frac{f(t)}{h^{\alpha(t)}} - \sum_{j=1}^{\frac{t}{h}} (-1)^j \binom{-\alpha(t-jh)}{j} \frac{h^{\alpha(t-jh)}}{h^{\alpha(b)}} {}_{\mathcal{E}}^{0}\mathrm{D}_{t-jh}^{\alpha(t)} f(t) \right)$$

Remark 1 For a fractional constant-order the $\mathcal{E}$-type definition is numerically identical with constant-order fractional derivative given by Definition 1.

4 The Output-Additive Switching Scheme

The output-additive switching scheme equivalent to the $\mathcal{E}$-type fractional variable-order derivative is depicted in Fig. 1. The blocks $\bar{\alpha}_j = \alpha_j - \alpha_{j-1}$, $j = 1, \ldots, k$ represent the constant-order Grünwald–Letnikov derivative of order α_0 and $\bar{\alpha}_j$ for $j = 1, \ldots, k$. In this case we have the following behavior: after switching time the fractional constant-order derivative is added and the end of actual chain.

Based on the output-additive switching scheme the $\mathcal{E}$-type definition can be expressed by

$${}_{t_k}\mathrm{D}_t^{\bar{\alpha}_k} \cdots {}_{t_1}\mathrm{D}_t^{\bar{\alpha}_1} {}_{0}\mathrm{D}_t^{\alpha_0} f(t) = {}_{\mathcal{E}}^{0}\mathrm{D}_t^{\alpha(t)} f(t). \tag{2}$$

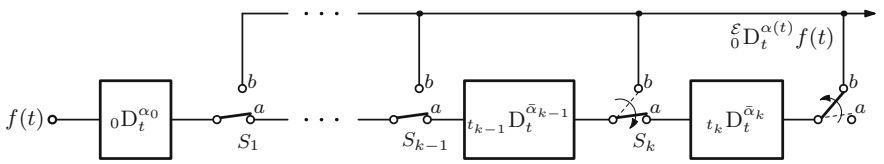

Fig. 1 The output-additive switching scheme corresponding do $\mathcal{E}$-type fractional variable-order derivative, where $\bar{\alpha}_j = \alpha_j - \alpha_{j-1}$, $j = 1, \ldots, k$, (configuration at time $t = t_k$)

5 Orders Composition Properties

For output-additive switching scheme the composition property with constant-order differ-integral holds, but only in one direction, i.e., it is not commutative, and then it depends on the sequence of composition. Two cases of composition orders are depicted in Figs. 2 and 3.

Let consider the switching scheme presented in Fig. 2 with fractional constant-order derivative from the left-hand side. Then, the following theorem can be written:

Theorem 1 *The following composition property holds*

$$ {}_{\mathcal{E}}_{0}\mathrm{D}_{t}^{\alpha(t)}\,{}_{0}\mathrm{D}_{t}^{\beta} f(t) = {}_{\mathcal{E}}_{0}\mathrm{D}_{t}^{\alpha(t)+\beta} f(t), $$

for $\alpha(t) \neq \text{const}$ *and* $\beta \neq 0$.

Proof Directly based on Fig. 2, the following equation can be formulated

$$ {}_{t_k}\mathrm{D}_{t}^{\bar{\alpha}_k} \cdots {}_{t_1}\mathrm{D}_{t}^{\bar{\alpha}_1}\,{}_{0}\mathrm{D}_{t}^{\alpha_0}\,{}_{0}\mathrm{D}_{t}^{\beta} f(t) = {}_{\mathcal{E}}_{0}\mathrm{D}_{t}^{\alpha(t)}\,{}_{0}\mathrm{D}_{t}^{\beta} f(t). \tag{3} $$

Due to the constant-order composition property, (3) can be rewritten to the form

$$ {}_{t_k}\mathrm{D}_{t}^{\bar{\alpha}_k} \cdots {}_{t_1}\mathrm{D}_{t}^{\bar{\alpha}_1}\,{}_{0}\mathrm{D}_{t}^{\alpha_0+\beta} f(t) = {}_{\mathcal{E}}_{0}\mathrm{D}_{t}^{\alpha(t)+\beta} f(t), $$

which ends the proof.

To show that composition property is not commutative it is enough to prove that such property does not holds on time interval for $0 < t \leq t_2$. Then, we can constraint

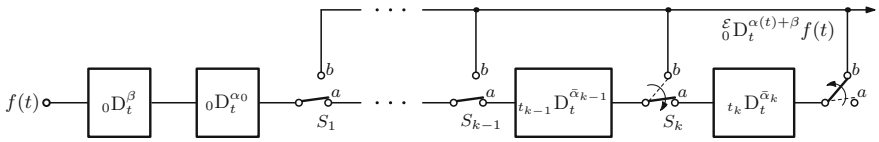

Fig. 2 Composition of output-additive switching scheme with fractional constant-order differ-integral from *left-hand side*, i.e., ${}_{\mathcal{E}}_{0}\mathrm{D}_{t}^{\alpha(t)}\,{}_{0}\mathrm{D}_{t}^{\beta} f(t) = {}_{\mathcal{E}}_{0}\mathrm{D}_{t}^{\alpha(t)+\beta} f(t)$

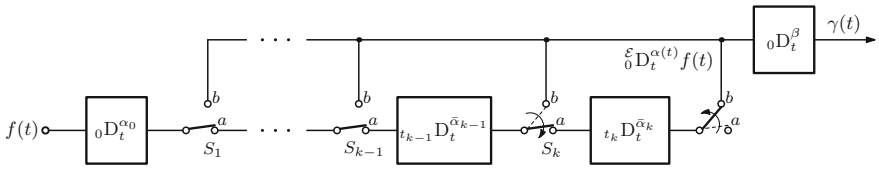

Fig. 3 Composition of output-additive switching scheme with fractional constant-order differ-integral from *right-hand side*, i.e., ${}_{0}\mathrm{D}_{t}^{\beta}\left({}_{\mathcal{E}}_{0}\mathrm{D}_{t}^{\alpha(t)} f(t)\right) = \gamma(t) \neq {}_{\mathcal{E}}_{0}\mathrm{D}_{t}^{\alpha(t)+\beta} f(t)$

the output-additive switching scheme presented in Fig. 3 to time t_2 and formulate a Theorem 2.

Lemma 1 *The fractional constant-order derivative in the Grünwald–Letnikov form given by Definition 1 can be expressed by*

$$\begin{aligned}
{}_0\mathrm{D}_t^{\alpha} f(t) &= \lim_{h\to 0} \frac{1}{h^{\alpha}} \sum_{j=0}^{t} (-1)^j \binom{\alpha}{j} f(t-jh) \\
&= \lim_{h\to 0} \frac{1}{h^{\alpha}} \left(\sum_{j=0}^{\frac{t_1}{h}} (-1)^j \binom{\alpha}{j} f(t-jh) + \sum_{\frac{t_1}{h}+1}^{\frac{t}{h}} (-1)^j \binom{\alpha}{j} f(t-jh) \right) \\
&= \left({}_{t_1}\mathrm{D}_t^{\alpha} + {}_0\mathrm{D}_{t_1-h}^{\alpha} \right) f(t) \implies {}_{t_1}\mathrm{D}_t^{\alpha} f(t) = \left({}_0\mathrm{D}_t^{\alpha} - {}_0\mathrm{D}_{t_1-h}^{\alpha} \right) f(t),
\end{aligned}$$

where h is a step time and $0 < t_1 < t$.

Theorem 2 *The composition of output-additive switching scheme with fractional constant-order differ-integral from right-hand side is expressed by*

$$ {}_0\mathrm{D}_{t_2}^{\beta} {}_{t_1}\mathrm{D}_{t_2}^{\alpha_1} {}_0\mathrm{D}_{t_2}^{\alpha_0} f(t) = \gamma(t) \neq {}_0^{\mathcal{E}}\mathrm{D}_{t_2}^{\alpha(t)+\beta} f(t), \tag{4}$$

for $\alpha(t) \neq \text{const}$ *and* $\beta \neq 0$.

Proof Let us begin with (3), when the composition property holds and time $t = t_2$

$$ {}_{t_1}\mathrm{D}_{t_2}^{\tilde{\alpha}_1} {}_0\mathrm{D}_{t_2}^{\alpha_0} {}_0\mathrm{D}_{t_2}^{\beta} f(t) = {}_0^{\mathcal{E}}\mathrm{D}_{t_2}^{\alpha(t)+\beta} f(t). \tag{5}$$

Applying the commutative property (1) and Lemma 1 to (5), we can extend this equation to the following form

$$\begin{aligned}
\left({}_0\mathrm{D}_{t_2}^{\tilde{\alpha}_1} - {}_0\mathrm{D}_{t_1-h}^{\tilde{\alpha}_1} \right) {}_0\mathrm{D}_{t_2}^{\beta} {}_0\mathrm{D}_{t_2}^{\alpha_0} f(t) &= {}_0\mathrm{D}_{t_2}^{\tilde{\alpha}_1} {}_0\mathrm{D}_{t_2}^{\beta} {}_0\mathrm{D}_{t_2}^{\alpha_0} f(t) - {}_0\mathrm{D}_{t_1-h}^{\tilde{\alpha}_1} {}_0\mathrm{D}_{t_2}^{\beta} {}_0\mathrm{D}_{t_2}^{\alpha_0} f(t) \\
&= {}_0\mathrm{D}_{t_2}^{\beta} \left({}_0\mathrm{D}_{t_1-h}^{\tilde{\alpha}_1} + {}_{t_1}\mathrm{D}_{t_2}^{\tilde{\alpha}_1} \right) {}_0\mathrm{D}_{t_2}^{\alpha_0} f(t) - {}_0\mathrm{D}_{t_1-h}^{\tilde{\alpha}_1} {}_0\mathrm{D}_{t_2}^{\beta} {}_0\mathrm{D}_{t_2}^{\alpha_0} f(t) \\
&= {}_0\mathrm{D}_{t_2}^{\beta} {}_{t_1}\mathrm{D}_{t_2}^{\tilde{\alpha}_1} {}_0\mathrm{D}_{t_2}^{\alpha_0} f(t) + {}_0\mathrm{D}_{t_2}^{\beta} {}_0\mathrm{D}_{t_1-h}^{\tilde{\alpha}_1} {}_0\mathrm{D}_{t_2}^{\alpha_0} f(t) - {}_0\mathrm{D}_{t_1-h}^{\tilde{\alpha}_1} {}_0\mathrm{D}_{t_2}^{\beta} {}_0\mathrm{D}_{t_2}^{\alpha_0} f(t) \\
&= \gamma(t) + {}_0\mathrm{D}_{t_2}^{\beta} {}_0\mathrm{D}_{t_1-h}^{\tilde{\alpha}_1} {}_0\mathrm{D}_{t_2}^{\alpha_0} f(t) - {}_0\mathrm{D}_{t_1-h}^{\tilde{\alpha}_1} {}_0\mathrm{D}_{t_2}^{\beta} {}_0\mathrm{D}_{t_2}^{\alpha_0} f(t) \qquad ,
\end{aligned}$$

comparing above to Theorem 2 ends the proof.

6 Numerical Results of Output-Additive Switching Scheme Composition with Fractional Constant-Order Differ-Integral

This section contains numerical experiment, implemented in Matlab/Simulink environment, with dedicated numerical routines, available under [21]. An numerical example of output-additive switching scheme composition with fractional constant-order differ-integral from left- and right- hand side is depicted in Fig. 4. The simulation parameters take the following values: $f(t)$ is a Heaviside step function, $\beta = -0.4$ and

$$\alpha(t) = \begin{cases} -0.3 & \text{for } t \leq 0.5, \\ -0.8 & \text{for } t > 0.5. \end{cases}$$

Using the parameters from the numerical example the following equation for both cases can be written:

- For a case with fractional constant-order differ-integral from the left-hand side:

$$y(t) = {}_{0}^{\mathcal{E}}\mathrm{D}_{t}^{\alpha(t)-0.4} f(t)$$

- For a case with fractional constant-order differ-integral from the right-hand side:

$$y(t) = {}_{0}\mathrm{D}_{t}^{-0.4}\,{}_{0}^{\mathcal{E}}\mathrm{D}_{t}^{\alpha(t)} f(t)$$

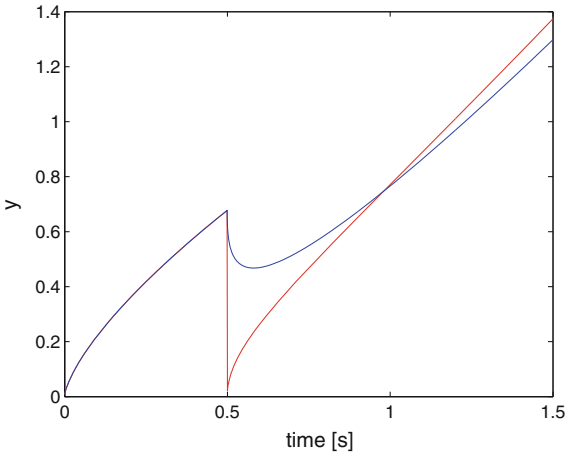

Fig. 4 Composition of output-additive switching scheme with fractional constant-order differ-integral from *left-hand side* ${}_{0}^{\mathcal{E}}\mathrm{D}_{t}^{\alpha(t)+\beta} f(t)$ - *red line*, and *right-hand side* ${}_{0}\mathrm{D}_{t}^{\beta}\left({}_{0}^{\mathcal{E}}\mathrm{D}_{t}^{\alpha(t)} f(t)\right)$ - *blue line*

7 Conclusions

In the paper, the composition properties of output-additive switching scheme with fractional constant-order differ-integral from the left-hand side and right hand side have been proved. It was shown, that for such switching scheme, which is equivalent to the $\mathcal{E}$-type fractional variable-order definition, the composition property holds, but only in one direction, it is not commutative and depends on the sequence of composition. At the end, the composition properties were validated on numerical example.

Acknowledgments This work was supported in part by the Polish National Science Center with the decision number UMO-2014/15/B/ST7/00480, and by the PL - SK cooperation agreement under decision number SK-PL-2015-0038, and by the PL - PT cooperation agreement under decision number 30208/2014.

References

1. Dzielinski, A., Sierociuk, D.: Fractional order model of beam heating process and its experimental verification. In: Baleanu, D., Guvenc, Z.B., Machado, J.A.T. (eds.) New Trends in Nanotechnology and Fractional Calculus Applications, pp. 287–294. Springer, Netherlands (2010)
2. Dzielinski, A., Sierociuk, D., Sarwas, G.: Some applications of fractional order calculus. Bull. Pol. Ac.: Tech. **58**(4), 583–592 (2010)
3. Sierociuk, D., Dzielinski, A., Sarwas, G., Petras, I., Podlubny, I., Skovranek, T.: Modeling heat transfer in heterogeneous media using fractional calculus. In: Proceedings of The Fifth Symposium on Fractional Derivatives and Their Applications (FDTA11) as a part of the Seventh ASME/IEEE International Conference on Mechatronics and Embedded Systems and Applications, pp. 143-147 (2011)
4. Dzielinski, A., Sarwas, G., Sierociuk, D.: Time domain validation of ultracapacitor fractional order model. In: 49th IEEE Conference on Decision and Control (CDC), pp. 3730–3735 (2010)
5. Dzielinski, A., Sierociuk, D.: Ultracapacitor modelling and control using discrete fractional order state-space model. Acta Montan. Slovaca **13**(1), 136–145 (2008)
6. Ramirez, L.E.S., Coimbra, C.F.M.: On the selection and meaning of variable order operators for dynamic modeling. Int. J. Differ. Equ. (2010)
7. Lorenzo, C., Hartley, T.: Variable order and distributed order fractional operators. Nonlinear Dynam. **29**(1–4), 57–98 (2002)
8. Valerio, D., da Costa, J.S.: Variable-order fractional derivatives and their numerical approximations. Signal Process. **91**(3), 470–483 (2011)
9. Macias, M., Sierociuk, D.: An alternative recursive fractional variable-order derivative definition and its analog validation. In: Proceedings of International Conference on Fractional Differentiation and its Applications, pp. 1–6 (2014)
10. Sierociuk, D., Malesza, W., Macias, M.: Equivalent switching strategy and analog validation of the fractional variable order derivative definition. In: Proceedings of European Control Conference, pp. 3464–3469 (2013)
11. Sierociuk, D., Malesza, W., Macias, M.: On a new definition of fractional variable-order derivative. In: Proceedings of the 14th International Carpathian Control Conference (ICCC), pp. 340–345 (2013)
12. Sierociuk, D., Malesza, W., Macias, M.: Derivation, interpretation, and analog modelling of fractional variable order derivative definition. Appl. Math. Model. **39**(13), 3876–3888 (2015)

13. Sierociuk, D., Malesza, W., Macias, M.: Numerical schemes for initialized constant and variable fractional-order derivatives: matrix approach and its analog verification. J. Vib. Control **22**(8), 2032–2044 (2015)
14. Sierociuk, D., Malesza, W., Macias, M.: On the recursive fractional variable-order derivative: equivalent switching strategy, duality, and analog modeling. Circ. Syst. Signal Process. **34**(4), 1077–1113 (2015)
15. Sheng, H., Sun, H., Coopmans, C., Chen, Y., Bohannan, G.W.: Physical experimental study of variable-order fractional integrator and differentiator. In: Proceedings of The 4th IFAC Workshop Fractional Differentiation and its Applications FDA'10 (2010)
16. Tseng, C.C., Lee, S.L.: Design of variable fractional order differentiator using infinite product expansion. In: Proceedings of 20th European Conference on Circuit Theory and Design, pp. 17–20 (2011)
17. Sierociuk, D., Macias, M.: Comparison of variable fractional order PID controller for different types of variable order derivatives. In: 14th International Carpathian Control Conference (ICCC), pp. 334–339 (2013)
18. Podlubny, I.: Fractional Differential Equations. Academic Press, Cambridge (1999)
19. Malesza, W., Macias, M., Sierociuk, D.: Matrix approach and analog modeling for solving fractional variable order differential equations. In: Latawiec, K.J., Lukaniszyn, M., Stanislawski, R. (eds.) Advances in Modelling and Control of Non-integer-Order Systems, Lecture Notes in Electrical Engineering, vol. 320, pp. 71–80. Springer International Publishing (2015)
20. Sierociuk, D., Malesza, W., Macias, M.: Switching scheme, equivalence, and analog validation of the alternative fractional variable-order derivative definition. In: Proceedings of the 52nd IEEE Conference on Decision and Control, pp. 3876-3881 (2013)
21. Sierociuk, D.: Fractional Variable Order Derivative Simulink Toolkit (2012). http://www.mathworks.com/matlabcentral/fileexchange/38801-fractional-variable-order-derivative-simulink-toolkit

Variable-, Fractional-Order Oscillation Element

Dorota Mozyrska and Piotr Ostalczyk

Abstract The dynamic properties of the variable-, fractional-order oscillation element (VFOOE) are investigated in the paper. The equations and the block diagram are derived. Stability and existence conditions of solutions of proposed systems are considered. For the illustration numerical examples are presented.

Keywords Fractional calculus · Discrete linear system · Variable- · Fractional-order backward sum

1 Introduction and Preliminaries

Fractional-order backward differences and sums have become an important mathematical tools in many areas ranged from theoretical to applied sciences [1–3]. Fractional differences provide an excellent instrument for the description of processes of transient behaviours, [4], characterized by a memory of the system states. In the paper we investigate the more general version of fractional difference called the variable-, fractional-order backward difference/sum (VFOBD/S). On the base of defined VFOBS stated for four cases we define the linear time–invariant oscillation element (VFOOE). The oscillation element, among the inertial and integrating ones is one of the most important elements in the analysis and synthesis of dynamical systems, [5]. This can be applied to continuous– and discrete–time systems, linear or nonlinear. We propose the block diagram with two variable fractional-order (VFO) discrete integrators and a negative feedback with a proportional block characterised by a constant coefficients which build the VFOOE.

D. Mozyrska (✉)
Bialystok University of Technology, Wiejska 45A, 15-351 Białystok, Poland
e-mail: d.mozyrska@pb.edu.pl

P. Ostalczyk
Lodz University of Technology, Stefanowskiego 18/22, 90-924 Łódź, Poland
e-mail: piotr.ostalczyk@p.lodz.pl

A. Babiarz et al. (eds.), *Theory and Applications of Non-integer Order Systems*,
Lecture Notes in Electrical Engineering 407, DOI 10.1007/978-3-319-45474-0_7

Definition 1 For $k, l \in \mathbb{N}$ and a given order function $\nu(\cdot)$ we define the coefficient discrete function of two variables by its values $a^{[\nu(l)]}(k)$ by the following

$$a^{[\nu(l)]}(k) = \begin{cases} 1 & \text{for } k = 0 \\ (-1)^k \frac{\nu(l)(\nu(l)-1)\cdots(\nu(l)-k+1)}{k!} & \text{for } k > 0\,. \end{cases} \tag{1}$$

For the case, when $0 < \nu(l) \leq 1$ for $l \in \mathbb{N}$: $a^{[\nu(l)]}(0) = 1$ and $a^{[\nu(l)]}(k) < 0$, for $k > 0$. Consider a discrete–variable bounded real–valued function $f(\cdot)$ defined on a discrete interval $[k_0, k]_{\mathbb{N}} = [k_0, k] \cap \mathbb{N}$. The Grünwald–Letnikov backward–difference (GL–FOBD) is generalized in the next definition to the Grünwald–Letnikov variable-, fractional-order backward difference (GL–VFOBD).

Definition 2 The GL–VFOBD with an order function $\nu(\cdot)$ of a bounded function $f(\cdot)$ is defined as a finite sum

$${}_{k_0}^{GL}\Delta_k^{[\nu(k)]} f(k) = \left[1 \; a^{[\nu(k)]}(1) \; a^{[\nu(k)]}(2) \cdots a^{[\nu(k)]}(k-k_0)\right] \begin{bmatrix} f(k) \\ f(k-1) \\ \vdots \\ f(k_0+1) \\ f(k_0) \end{bmatrix}.$$

Collecting all such equalities in one vector–matrix form we obtain

$${}_{k_0}^{GL}\Delta_k^{[\nu(k)]}\mathbf{f}(k) = {}_{k_0}\mathbf{A}_k^{[\nu(k)]}\mathbf{f}(k)\,, \tag{2}$$

where

$$\mathbf{f}(k) = \begin{bmatrix} f(k) \\ f(k-1) \\ \vdots \\ f(k_0+1) \\ f(k_0) \end{bmatrix}, \quad {}_{k_0}^{GL}\Delta_k^{[\nu(k)]}\mathbf{f}(k) = \begin{bmatrix} {}_{k_0}^{GL}\Delta_k^{[\nu(k)]} f(k) \\ \vdots \\ {}_{k_0}^{GL}\Delta_{k_0+1}^{[\nu(k_0+1)]} f(k_0+1) \\ {}_{k_0}^{GL}\Delta_{k_0}^{[\nu(k_0)]} f(k_0) \end{bmatrix} \tag{3}$$

and

$${}_{k_0}\mathbf{A}_k^{[\nu(k)]} = \begin{bmatrix} 1 & a^{[\nu(k)]}(1) & a^{[\nu(k)]}(2) & \cdots & a^{[\nu(k)]}(k-k_0) & \\ 0 & 1 & a^{[\nu(k-1)]}(1) & \cdots & a^{[\nu(k-1)]}(k-k_0-1) & \\ 0 & 0 & 1 & \cdots & a^{[\nu(k-2)]}(k-k_0-2) & \\ \vdots & \vdots & \vdots & & \vdots & \vdots \\ 0 & 0 & 0 & \cdots & a^{[\nu(k_0+1)]}(1) & \\ 0 & 0 & 0 & \cdots & 1 & \end{bmatrix}. \tag{4}$$

1.1 Variable-, Fractional-Order Linear Integrator

Basing on the definition of the GL–VFOBD we define a variable-, fractional-order linear integrator (VFOI) (acting as a VFO discrete summator). We introduce the following notation

$$ {}_{k_0}\mathbf{B}_k^{(\nu)} = {}_{k_0}\mathbf{A}_k^{[\nu(k)]}, \quad {}_{k_0}\mathbf{B}_k^{(\bar{\nu})} = \left[{}_{k_0}\mathbf{A}_k^{[\nu(k)]} \right]^{-1}. \tag{5} $$

Let now $\xi = (\nu_1, \ldots, \nu_l)$ and $l \in \mathbb{N}_1$. Then we define the following

$$ {}_{k_0}\mathbf{B}_k^{(\xi)} := {}_{k_0}\mathbf{B}_k^{(\nu_1)} \cdot \ldots \cdot {}_{k_0}\mathbf{B}_k^{(\nu_l)}, \tag{6} $$

where it is possible to have some $\nu_i = \bar{\mu}_i$. All order functions are assumed to be positive $\nu_i(k) > 0$. For order functions usually one imposes a condition $0 < \sum_{i=1}^{l} \pm\nu_i(k) \leqslant 1$.

The VFOI is defined by a vector–matrix equation

$$ {}_{k_0}\mathbf{B}_k^{(\xi)}\mathbf{y}(k) = \mathbf{u}(k), \tag{7} $$

where $\mathbf{u}(k)$ and $\mathbf{y}(k)$ are input and output signal vectors, respectively. The order vector ξ is constructed in the same way as presented above. The form used in the oscillation element is given by the vector $\xi = \left[2\nu,\ \bar{\nu}\right]$. The block diagram of the VFOI is presented in Fig. 1.

Proposition 1 *Let the order function $\nu(\cdot)$ be nondecreasing and $\nu(k) \in (0, 1]$. Let ${}_{k_0}\mathbf{B}_k^{(\bar{\nu})} = \left[{}_{k_0}\mathbf{A}_k^{[\nu(k)]} \right]^{-1} = \left(c_{i,j}\right)_{i,j\in\{1,\ldots,k-k_0+1\}}$. Then we have the following properties:*

(a) $c_{i,i} = 1$, *for* $i \in \{1, \ldots, k - k_0 + 1\}$;
(b) $c_{i,i+1} = -a^{[\nu(k-i+1)]}(1) = \nu(k - i + 1)$, *for* $i \in \{1, \ldots, k - k_0\}$;
(c) $c_{i,j} = 0$ *for* $j < i$;
(d) $c_{i,j} \geq 0$ *for all indexes* $i, j \in \{1, \ldots, k - k_0 + 1\}$;
(e) $c_{i,j} = -\sum_{s=1}^{j-i} a^{[\nu(k-i)]}(s)c_{i+s,j}$, *for* $j > i$;
(f) $c_{1,j} = \left[a^{[\nu(k)]}(1) \ldots a^{[\nu(k)]}(k - k_0) \right] {}_{k_0}\mathbf{B}_{k-1}^{(\bar{\nu})}$.

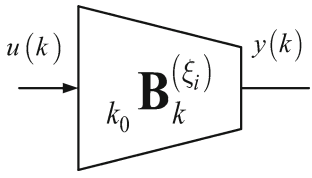

Fig. 1 Block diagram of the VFOI

Proof Points (a)–(d) are obvious. We stay a while with points (e) and (f). For the simplicity we provide the proof with $k_0 = 0$. For points (e) we only need to use the method of backward substitution during solving the problem of inverse matrix as the solution of $k+1$ systems of linear equations. We can state it as follows:

$$ {}_{k_0}\mathbf{A}_k^{[\nu(k)]} \begin{bmatrix} c_{1,j} \\ \vdots \\ c_{k+1,j} \end{bmatrix} = e_j \,, \tag{8} $$

where e_j is column with 1 only in j-th row and we consider systems for $j \in \{1, \ldots, k+1\}$. Then we can formulate the solution of system (8) as it is presented in points (a)–(e).

To prove point (f) we recall the fact that for upper-triangle matrix given in a decomposition of upper-triangle matrices and suitable matrix there is the following formula for the inverse: $\begin{bmatrix} \mathbf{U}_{11} & \mathbf{U}_{12} \\ \mathbf{0} & \mathbf{U}_{22} \end{bmatrix}^{-1} = \begin{bmatrix} \mathbf{U}_{11}^{-1} & -\mathbf{U}_{11}^{-1}\mathbf{U}_{12}\mathbf{U}_{22}^{-1} \\ \mathbf{0} & \mathbf{U}_{22}^{-1} \end{bmatrix}$. Taking $\mathbf{U}_{11} = 1$, $\mathbf{U}_{12} = \left[a^{[\nu(k)]}(1) \ldots a^{[\nu(k)]}(k-k_0) \right]$, $\mathbf{U}_{2,2} = {}_{k_0}\mathbf{A}^{[\nu(k-1)]}$ we receive point (f).

Proposition 2 *Let the order function $\nu(\cdot)$ be nondecreasing and $\nu(k) \in (0, 1]$. Let us consider the following VFOIs:*

$$ {}_{k_0}\mathbf{A}_k^{[\nu(k)]}\mathbf{y}_1(k) = b_0\mathbf{u}(k) \tag{9} $$

$$ {}_{k_0}\mathbf{A}_k^{[0.5\nu(k)]}\,{}_{k_0}\mathbf{A}_k^{[0.5\nu(k)]}\mathbf{y}_2(k) = b_0\mathbf{u}(k) \tag{10} $$

$$ {}_{k_0}\mathbf{A}_k^{[2\nu(k)]}\left[{}_{k_0}\mathbf{A}_k^{[\nu(k)]}\right]^{-1}\mathbf{y}_3(k) = b_0\mathbf{u}(k) \tag{11} $$

$$ {}_{k_0}\mathbf{A}_k^{[2\nu(k)]}\,{}_{k_0}\mathbf{A}_k^{[-\nu(k)]}\mathbf{y}_4(k) = b_0\mathbf{u}(k)\,. \tag{12} $$

Then the unit step responses satisfy inequalities for $k \in \mathbb{N}_0$: $\mathbf{y}_2(k) \geq \mathbf{y}_1(k) \geq \mathbf{y}_4(k) \geq \mathbf{y}_3(k)$ for nondecreasing fractional-order function and $\mathbf{y}_3(k) \geq \mathbf{y}_4(k) \geq \mathbf{y}_1(k) \geq \mathbf{y}_2(k)$ for nonincreasing OFs.

Proof We state here only the proof that for $k \in \mathbb{N}_0$: $\mathbf{y}_2(k) \geq \mathbf{y}_1(k)$ for nondecreasing OF. Let us take for the simplicity $k_0 = 0$. It does not change the generale proof. In the proof let us change notations: $\mathbf{x}(k) := \mathbf{y}_1(k)$ and $\mathbf{y}(k) := \mathbf{y}_2(k)$. Observe that without any assumption we obviously have $x(0) = y(0)$. Nextly, as ${}_0\mathbf{A}_1^{[\nu(1)]} = \left({}_0\mathbf{A}_1^{[0.5\nu(1)]}\right)^2$, then also $x(1) = y(1)$. Let us assume now that for each $l \in \{0, \ldots, k-1\}$: $y(l) \geq x(l)$. Let $R_{\nu(k)} := \left[a^{[\nu(k)]}(1), \ldots, a^{[\nu(k)]}(k)\right]$. Then

$$ {}_0\mathbf{A}_k^{[\nu(k)]} = \begin{bmatrix} 1 & R_{\nu(k)} \\ 0 & \\ \vdots & {}_0\mathbf{A}_{k-1}^{[\nu(k-1)]} \\ 0 & \end{bmatrix}, \quad \left({}_0\mathbf{A}_k^{[0.5\nu(k)]}\right)^2 = \begin{bmatrix} 1 & R_{0.5\nu(k)}\left(I_k + {}_0\mathbf{A}_{k-1}^{[0.5\nu(k-1)]}\right) \\ 0 & \\ \vdots & \left({}_0\mathbf{A}_{k-1}^{[0.5\nu(k-1)]}\right)^2 \\ 0 & \end{bmatrix}. $$

Taking into account Eqs. (9) and (10) we write that

$$x(k) + R_{\nu(k)} \begin{bmatrix} x(k-1) \\ \vdots \\ x(0) \end{bmatrix} = y(k) + R_{0.5\nu(k)} \left(I_k + {}_0\mathbf{A}_{k-1}^{[0.5\nu(k-1)]} \right) \begin{bmatrix} y(k-1) \\ \vdots \\ y(0) \end{bmatrix}.$$

As we assume that $y(l) \geq x(l)$ it follows

$$(x(k) - y(k)) \leq \left(R_{0.5\nu(k)} + R_{0.5\nu(k)0}\mathbf{A}_{k-1}^{[0.5\nu(k-1)]} - R_{\nu(k)} \right) \begin{bmatrix} y(k-1) \\ \vdots \\ y(0) \end{bmatrix}. \quad (13)$$

Let us recall that for constant ν: $R_{0.5\nu(k)} + R_{0.5\nu(k)0}\mathbf{A}_{k-1}^{[0.5\nu(k-1)]} = R_{\nu(k)}$. And for nondecreasing $\nu(\cdot)$ elements of the row $R_{0.5\nu(k)0}\mathbf{A}_{k-1}^{[0.5\nu(k-1)]}$ are less or equal to corresponding elements of $R_{0.5\nu(k)0}\mathbf{A}_{k-1}^{[0.5\nu(k)]}$. Additionally, they are positive as the product of negative values. Hence, $R_{0.5\nu(k)} + R_{0.5\nu(k)0}\mathbf{A}_{k-1}^{[0.5\nu(k-1)]} - R_{\nu(k)} \leq R_{0.5\mu 0}\mathbf{A}_{k-1}^{[0.5\mu]} - R_{\mu} \leq 0$, where $\nu(k) = \mu = const$. What finish the proof that for $k \in \mathbb{N}_0$: $\mathbf{y}_2(k) \geq \mathbf{y}_1(k)$ for for nondecreasing order function.

Example 1 For the following fractional-order functions

$$\nu(k) = \left(1 - e^{-0.1k}\right) \mathbf{1}(k) \text{ and } \nu(k) = 0.25 \left(1 + e^{-0.1k}\right) \mathbf{1}(k) \quad (14)$$

plotted in Figs. 2a and 3a one gets the unit step responses of the VFOIs presented in Figs. 2b and 3b, respectively.

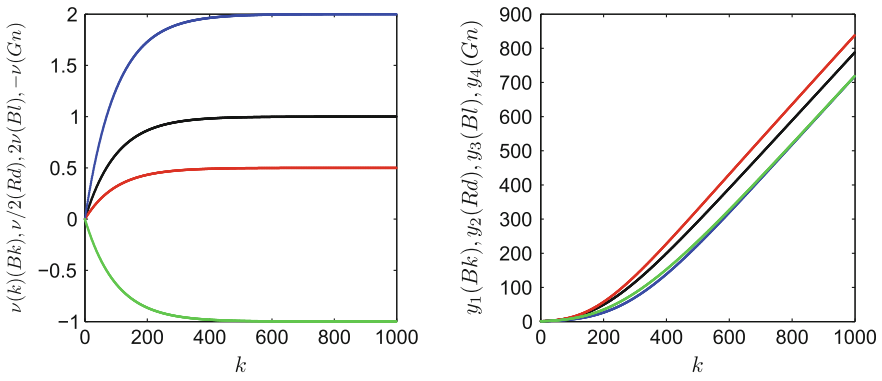

(a) Plot of the fractional–order. (b) VFOIs unit step responses.

Fig. 2 Fractional-order and VFOIs unit step responses for $\nu(k) = \left(1 - e^{-0.01k}\right) \mathbf{1}(k)$

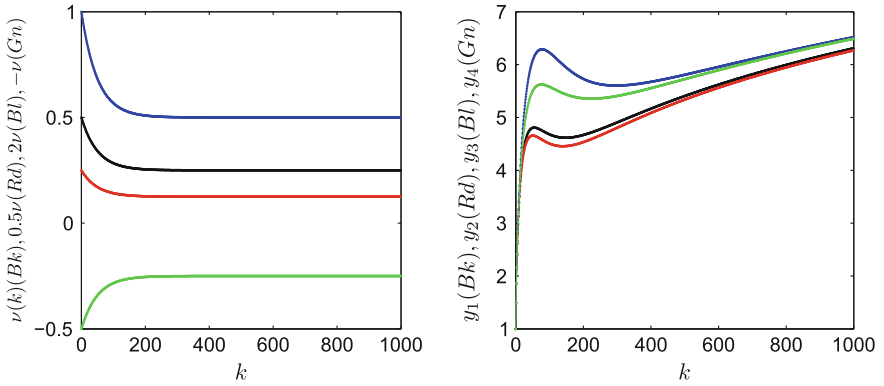

(a) Plot of the fractional–order. (b) VFOIs unit step responses.

Fig. 3 Fractional-order and VFO inertial elements responses for $\nu(k) = 0.25\left(1 + e^{-0.01k}\right)\mathbf{1}(k)$

2 VFO Oscillation Element Description and Response

The block diagram of the VFO oscillation element (VFOOE) is given in Fig. 4. One can see that the VFOIE is created from the VFOI (9)–(12) by adding two negative feedbacks with proportional blocks characterised by constant coefficients a_0 and a_1. Next one adds a proportional block b_0. It is assumed that

$$1 + a_1 + a_0 \neq 0\,. \tag{15}$$

From the block diagram given in Fig. 4 we derive the following equations:

$$\begin{aligned} {}_{k_0}\mathbf{B}_k^{(\xi_2)}\mathbf{x}_2(k) &= \mathbf{x}_1(k)\,,\\ {}_{k_0}\mathbf{B}_k^{(\xi_1)}\mathbf{x}_1(k) &= \mathbf{e}(k)\,,\\ \mathbf{e}(\mathbf{k}) = -a_0\mathbf{x}_2(k) - a_1\mathbf{x}_1(k) &+ b_0\mathbf{u}(k)\,,\\ \mathbf{y}(k) &= \mathbf{x}_2(k)\,. \end{aligned} \tag{16}$$

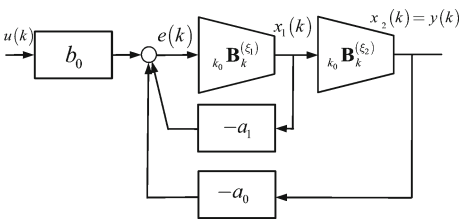

Fig. 4 Block diagram of the VFOOE

Combining the first three equations from (16) we obtain the matrix–vector description of the VFOOE

$$ {}_{k_0}\mathbf{B}_k^{(\xi_1)}\,{}_{k_0}\mathbf{B}_k^{(\xi_2)}\mathbf{y}(k) + a_1\,{}_{k_0}\mathbf{B}_k^{(\xi_2)}\mathbf{y}(k) + a_0\mathbf{y}(k) = b_0\mathbf{u}(k)\,. \tag{17} $$

For ${}_{k_0}\mathbf{B}_k^{(\xi_1)} = {}_{k_0}\mathbf{A}_k^{[2\nu(k)]}\left[{}_{k_0}\mathbf{A}_k^{(\nu(k))}\right]^{-1}$ and ${}_{k_0}\mathbf{B}_k^{(\xi_2)} = {}_{k_0}\mathbf{A}_k^{[\nu(k)]}$ from (17) one obtains

$$ {}_{k_0}\mathbf{A}_k^{[2\nu(k)]}\mathbf{y}(k) + a_1\,{}_{k_0}\mathbf{A}_k^{[\nu(k)]}\mathbf{y}(k) + a_0\mathbf{y}(k) = b_0\mathbf{u}(k)\,. \tag{18} $$

For ${}_{k_0}\mathbf{B}_k^{(\xi_1)} = {}_{k_0}\mathbf{B}_k^{(\xi_2)} = {}_{k_0}\mathbf{A}_k^{[\nu(k)]}$ from (17) we get

$$ {}_{k_0}\mathbf{A}_k^{[\nu(k)]}\,{}_{k_0}\mathbf{A}_k^{[\nu(k)]}\mathbf{y}(k) + a_1\,{}_{k_0}\mathbf{A}_k^{[\nu(k)]}\mathbf{y}(k) + a_0\mathbf{y}(k) = b_0\mathbf{u}(k) \tag{19} $$

and for constant order function $\nu = 1$ one obtains a classical discrete oscillation element. Now we assume zero initial conditions. Simple manipulations on (18) and (19) lead to the solutions of the VFOOE:

$$ \mathbf{y}(k) = b_0\left\{{}_{k_0}\mathbf{A}_k^{[2\nu(k)]} + a_1\,{}_{k_0}\mathbf{A}_k^{[\nu(k)]} + a_0\,{}_{k_0}\mathbf{1}_k\right\}^{-1}\mathbf{u}(k)\,, \tag{20} $$

$$ \mathbf{y}(k) = b_0\left\{{}_{k_0}\mathbf{A}_k^{[\nu(k)]}\,{}_{k_0}\mathbf{A}_k^{[\nu(k)]} + a_1\,{}_{k_0}\mathbf{A}_k^{[\nu(k)]} + a_0\,{}_{k_0}\mathbf{1}_k\right\}^{-1}\mathbf{u}(k)\,, \tag{21} $$

where ${}_{k_0}\mathbf{1}_k$ denotes the identity matrix of degree $k - k_0 + 1$. Note that the inverse matrices exist, when the condition (15) is satisfied. Further analysis is concentrated on the VFOOE form described by (20). Under assumption (15) the VFOOE can be also represented by the variable-, fractional-order difference equation (VFODE)

$$ {}_{k_0}^{GL}\Delta_k^{[2\nu(k)]}y(k) + a_1\,{}_{k_0}^{GL}\Delta_k^{[\nu(k)]}y(k) + a_0 y(k) = b_0 u(k)\,. \tag{22} $$

The coefficients a_1, a_0 in Eq. (22) can be expressed by values w_1, w_2, where $a_1 = -w_1 - w_2$ and $a_0 = w_1 w_2$.

3 VFOOE Stability and Oscillations Criteria

Let us recall the concept of the stability of system (22). System (22) is said to be *asymptotically stable* if $\lim_{k\to\infty} y(k) = 0$.

Let us consider a system described by (22) for constant fractional-order function $\nu(k) = \nu = \text{const}$. Then the stability conditions formulate the following lemma.

Proposition 3 ([3]) *For $a_0, b_0 > 0$ and $a_1 = -w_1 - w_2$, $a_0 = w_1 w_2$ the system is asymptotically stable if and only if roots w_1, w_2 of an algebraic equation $w^2 + a_1 w + a_0 = 0$ are outside the regions given in Fig. 5.*

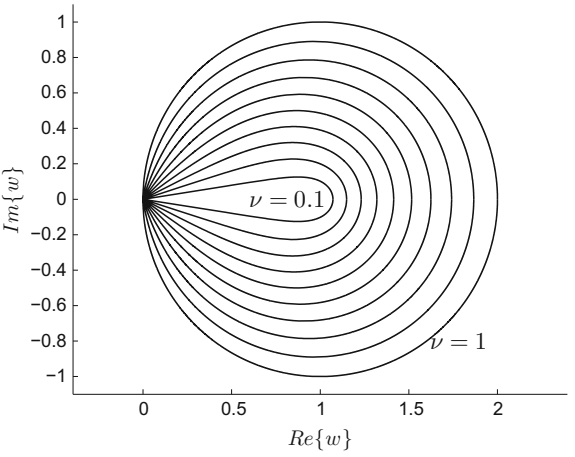

Fig. 5 Stability regions of the fractional-order system

Corollary 1 *If the classical second order–system is stable then the fractional-order system* $(0 < \nu < 1)$ *is also stable.*

For $0 < \nu_{min} \leqslant \nu(k) \leqslant \nu_{max} \leqslant 1$ the system described by Eq. (22) is stable if w_1, w_2 are in the stability region defined by ν_{max}. This is caused by the fact that the stability regions related to every time instant are included in the stability region defined for ν_{max}. Hence, the system is always stable. The system described by Eq. (22) with fractional-order satisfying $\lim\limits_{k\to+\infty} \nu(k) = \nu_{\text{const}} \leqslant 1$ is stable, if the system with constant order ν_{const} is stable. This follows from the fact that transient response tends (with respect to the limit of order function) to the stable solution.

Example 2 Let $\nu(k) = \left[0.8 + 0.2\cos\left(\frac{k}{6}\right)\right]\mathbf{1}(k)$ and $w_1 = -0.1 + j0.1$, $w_2 = -0.1 - j0.1$. In this example $\nu_{max} = 1$ and the roots are inside the stability region defined by ν_{max}. The system is asymptotically stable. The fractional-order, the unit step response and the discrete phase portrait and the classical second order system unit step response are given in Figs. 6a–d, respectively.

The classical second order oscillation element transient properties are characterized by w_1 and w_2. Numerically evaluated area for values w_1 and w_2 for which the unit step response is monotonically increasing is given in Fig. 7. From this figure and the stability regions given in Fig. 5 one concludes the area of w_1 and w_2 for which the unit step response are oscillating.

Proposition 4 *Consider asymptotically stable system described by (22) for* $0 < \nu(k) = \nu_{min} \leqslant 1$. *It is assumed that its unit step response is oscillating. Then the system with* $\nu(k) \geqslant \nu_{min}$ *has also oscillating unit step response.*

Proof Both systems have the same coefficients a_0 and a_1 and equivalently values w_1 and w_2. For $0 < \nu(k) = \nu_{max} \leqslant 1$ values w_1 and w_2 are closer to the stability limits. This intensifies the oscillations.

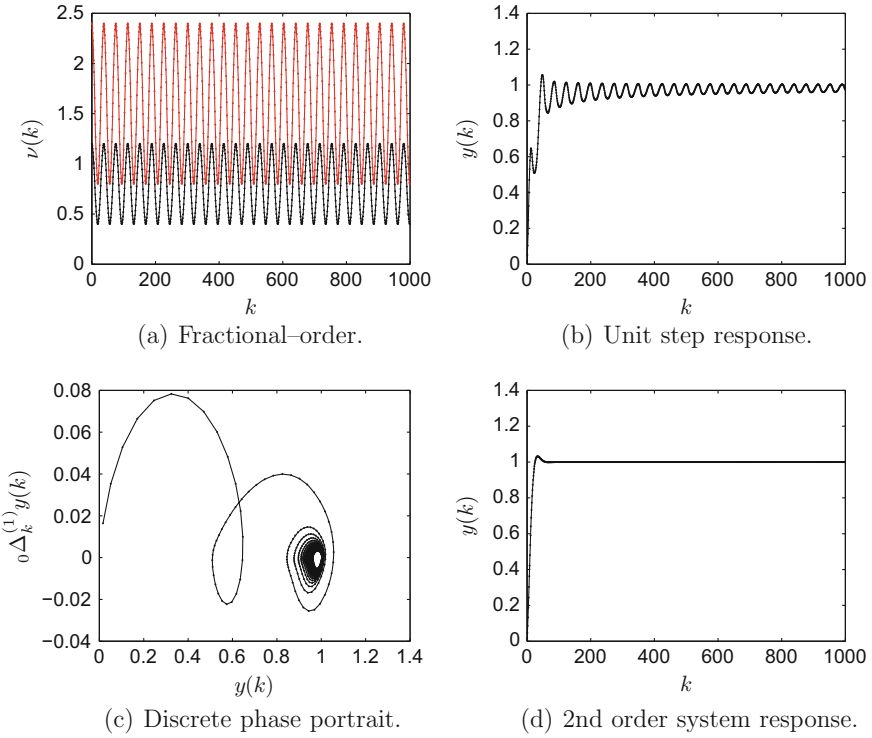

(a) Fractional–order. (b) Unit step response.

(c) Discrete phase portrait. (d) 2nd order system response.

Fig. 6 Fractional-order functions, VFOOE unit step response, related discrete phase portrait and 2nd-order discrete oscillation element response

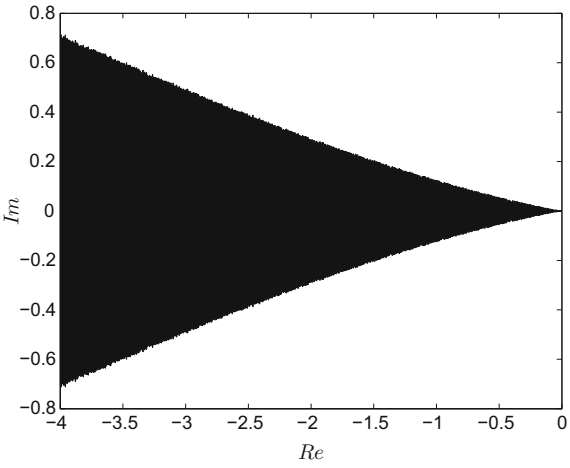

Fig. 7 Monotonic unit step response area for w_1 and w_2

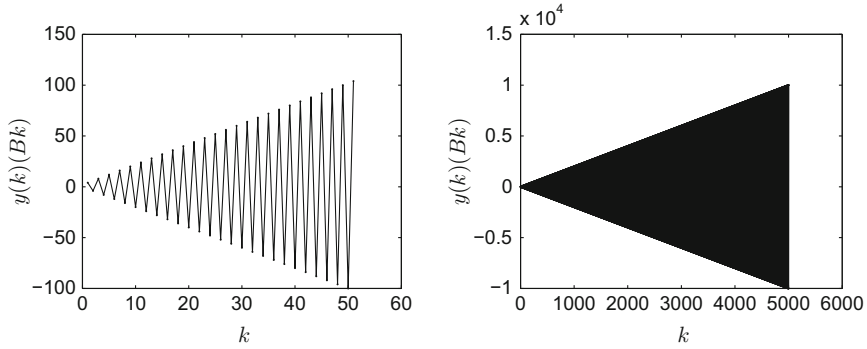

(a) Unit step response of the second-order oscillation element for $k \in \mathcal{T}_1$.

(b) Unit step response of the second-order oscillation element for $k \in \mathcal{T}_2$.

Fig. 8 Unit step response of the second-order oscillation element

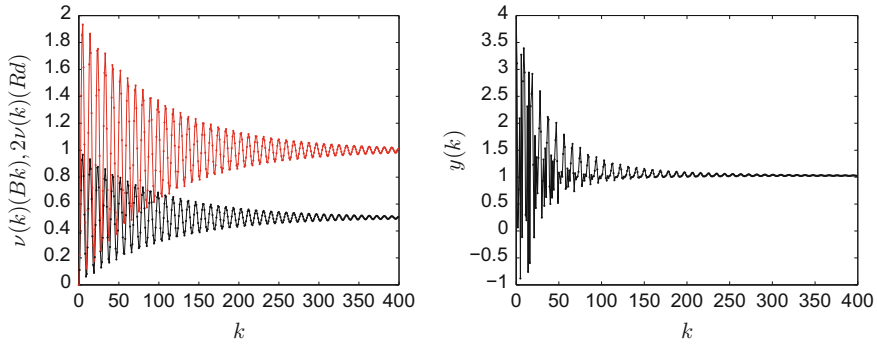

(a) Plot of the fractional–order.

(b) Unit step response.

Fig. 9 Plots of the fractional-order and the unit step response of the VFOOE

Example 3 Consider the second-order discrete oscillation element which is on the stability limit for $a_1 = -4$, $a_0 = 4$. The unit step response simulated for two discrete time ranges $\mathcal{T}_1 = [0, 50]$ and $\mathcal{T}_2 = [0, 500]$ is presented in Fig. 8a, b, respectively. Now one considers fractional-order function $\nu(k) = 0.5 - 0.5\cos(\frac{k}{1.5})e^{-0.01k}$ and the same coefficients. Plots of the fractional-order and the unit step response of the VFOOE are presented in Fig. 9a, b.

4 Final Conclusions

The analysis of the dynamic properties of the VFOOE exhibits almost unlimited possibilities of damped vibration shaping. Such elements can be useful in different kinds of vibrations modelling.

Acknowledgments This research was partially supported by the grant S/WI/1/2016 of the Polish Ministry of Science and Higher Education.

References

1. Agrawal, O., Machado, J.T., Sabatier, J.: Fractional Derivatives and Their Application: Nonlinear Dynamics. Springer, Berlin (2004)
2. Hilfer, R.: Applications of Fractional Calculus in Physics. World Scientific, Singapore (2000)
3. Ostalczyk, P.: Discrete Fractional Calculus. Applications in Control and Image Processing. Series in Computer Vision, vol. 4. World Scientific Publishing, Singapore (2016)
4. Caputo, M., Mainardi, F.: A new dissipation model based on memory mechanism. Pure Appl. Geophys. **91**, 134–147 (1971)
5. Kaczorek, T.: Linear Control Systems: Analysis of Multivariable Systems. Wiley, New York (1992)

Variable-, Fractional-Order Inertial Element

Piotr Ostalczyk and Dorota Mozyrska

Abstract The paper concerns the dynamic properties of the variable-, fractional-order inertial element (VFOIE). The application of a negative feedback to the variable-, fractional-order integrator (VFOI) leads to the VFOIE. The investigations are supported by numerical examples.

Keywords Fractional calculus · Discrete linear systems · Transient characteristics

1 Introduction

In recent decades the application of fractional calculus has attracted interest of researches. In many applications fractional calculus provides a more accurate model of physical systems than ordinary calculus in both cases: continuous-time and discrete-time. Non-integer-order derivatives and differences calculus has become an important tool in many areas of physics, mechanics, chemistry, engineering, finances and image processing [1–4]. Fractional derivatives and differences provide an excellent instrument for the description of memory in various processes [4, 5].

In the paper we investigate elements connected to the more general version of fractional differences admitting variability of the summation order. We work here with variable-, fractional-order inertial elements. The integrator described by the first-order differential equation is the most important element in the analysis and synthesis of dynamic systems [6, 7]. This implies to continuous- and discrete-time systems, linear or nonlinear. We propose inside the creation of variable-, fractional-order inertial elements from variable-, fractional-order integrators by adding a negative feedback with a proportional block characterised by a constant coefficient.

P. Ostalczyk
Lodz University of Technology, Stefanowskiego 18/22, 90-924 Lodz, Poland
e-mail: piotr.ostalczyk@p.lodz.pl

D. Mozyrska (✉)
Bialystok University of Technology, Wiejska 45A, 15-351 Białystok, Poland
e-mail: d.mozyrska@pb.edu.pl

A. Babiarz et al. (eds.), *Theory and Applications of Non-integer Order Systems*,
Lecture Notes in Electrical Engineering 407, DOI 10.1007/978-3-319-45474-0_8

2 Preliminaries

Definition 1 For $k, l \in \mathbb{N}$ and a given order function $\nu(\cdot)$ we define the coefficient discrete function of two variables by its values $a^{[\nu(l)]}(k)$ by the following

$$a^{[\nu(l)]}(k) = \begin{cases} 1 & \text{for } \ k = 0 \\ (-1)^k \frac{\nu(l)(\nu(l)-1)\cdots(\nu(l)-k+1)}{k!} & \text{for } k \in \mathbb{N}_1 \,. \end{cases} \tag{1}$$

For the case when for each $l \in \mathbb{N}$: $0 < \nu(l) \leq 1$ we have that $a^{[-\nu(l)]}(k) > 0$. While $a^{[\nu(l)]}(0) = 1$ and for $k > 0$: $a^{[\nu(l)]}(k) < 0$, for each k, l. Consider a discrete-variable bounded real-valued function $f(\cdot)$ defined on a discrete interval $[k_0, k]_{\mathbb{N}} = [k_0, k] \cap \mathbb{N}$. The Grünwald–Letnikov backward-difference (GL-FOBD) is generalized in the next definition to the Grünwald–Letnikov variable-, fractional-order backward difference (GL-VFOBD).

Definition 2 The GL-VFOBD with an order function $\nu(\cdot)$, with values $\nu(k) \in (0, 1]$ of a bounded function $f(\cdot)$ is defined as a finite sum

$${}_{k_0}^{GL}\Delta_k^{[\nu(k)]} f(k) = \begin{bmatrix} 1 & a^{[\nu(k)]}(1) & a^{[\nu(k)]}(2) & \cdots & a^{[\nu(k)]}(k-k_0) \end{bmatrix} \begin{bmatrix} f(k) \\ f(k-1) \\ \vdots \\ f(k_0+1) \\ f(k_0) \end{bmatrix}.$$

Collecting all such equalities in one vector matrix form we obtain

$${}_{k_0}^{GL}\Delta_k^{[\nu(k)]} \mathbf{f}(k) = {}_{k_0}\mathbf{A}_k^{[\nu(k)]} \mathbf{f}(k) \,, \tag{2}$$

where

$$\mathbf{f}(k) = \begin{bmatrix} f(k) \\ f(k-1) \\ \vdots \\ f(k_0+1) \\ f(k_0) \end{bmatrix}, \quad {}_{k_0}^{GL}\Delta_k^{[\nu(k)]} \mathbf{f}(k) = \begin{bmatrix} {}_{k_0}^{GL}\Delta_k^{[\nu(k)]} f(k) \\ \vdots \\ {}_{k_0}^{GL}\Delta_{k_0+1}^{[\nu(k_0+1)]} f(k_0+1) \\ {}_{k_0}^{GL}\Delta_{k_0}^{[\nu(k_0)]} f(k_0) \end{bmatrix} \tag{3}$$

and

$${}_{k_0}\mathbf{A}_k^{[\nu(k)]} = \begin{bmatrix} 1 & a^{[\nu(k)]}(1) & a^{[\nu(k)]}(2) & \cdots & a^{[\nu(k)]}(k-k_0) & \\ 0 & 1 & a^{[\nu(k-1)]}(1) & \cdots & a^{[\nu(k-1)]}(k-k_0-1) & \\ 0 & 0 & 1 & \cdots & a^{[\nu(k-2)]}(k-k_0-2) & \\ \vdots & \vdots & \vdots & & \vdots & \vdots \\ 0 & 0 & 0 & \cdots & a^{[\nu(k_0+1)]}(1) & \\ 0 & 0 & 0 & \cdots & 1 & \end{bmatrix}. \tag{4}$$

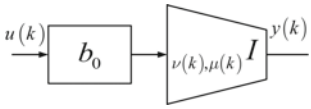

Fig. 1 Block diagram of the VFOI third form

By analogy to formulas (2)–(3) we obtain the vector-matrix description of the VFOBS

$$ {}_{k_0}^{GL}\Delta_k^{[-\mu(k)]}\mathbf{f}(k) = {}_{k_0}\mathbf{A}_k^{[-\mu(k)]}\mathbf{f}(k)\,, \tag{5} $$

where the vector ${}_{k_0}^{GL}\Delta_k^{[-\mu(k)]}\mathbf{f}(k)$ and the matrix ${}_{k_0}\mathbf{A}_k^{[-\mu(k)]}\mathbf{f}(k)$ are defined in a similar way as for the VFOBD.

The matrix (6) defined for $\nu(k), \mu(k) \in (0, 1]$ and $k > 2$ is characterized by following relations: ${}_{k_0}\mathbf{A}_k^{[\nu(k)]}\,{}_{k_0}\mathbf{A}_k^{[-\mu(k)]} \neq {}_{k_0}\mathbf{A}_k^{[-\mu(k)]}\,{}_{k_0}\mathbf{A}_k^{[\nu(k)]}$ and in a special case when $\nu(k) = \mu(k)$ holds: ${}_{k_0}\mathbf{A}_k^{[\nu(k)]}\,{}_{k_0}\mathbf{A}_k^{[-\nu(k)]} \neq {}_{k_0}\mathbf{A}_k^{[-\nu(k)]}\,{}_{k_0}\mathbf{A}_k^{[\nu(k)]} \neq {}_{k_0}\mathbf{1}_k$. However for $\nu(k) = \mu(k) = \text{const}$ all inequalities are replaced by equalities. Basing on the definitions of the VFOD and VFODS we define a variable-, fractional-order linear integrator (VFOI) (acting as a VFO summator). For $0 < \nu(k) + \mu(k) \leqslant 1$ the VFOI is defined by a vector-matrix equation

$$ {}_{k_0}\mathbf{A}_k^{[\nu(k)]}\mathbf{y}(k) = b_0\,{}_{k_0}\mathbf{A}_k^{[-\mu(k)]}\mathbf{u}(k)\,, \tag{6} $$

where b_0 is a constant coefficient. The form described above is called the third form of the VFOI. Its block diagram is presented in Fig. 1.

In formula (6) one can put $\nu(k) = 0$ then one gets a second form of the VFOI. It is denoted in block diagrams as ${}_{\mu(k)}I$ and its written by

$$ \mathbf{y}(k) = b_0\,{}_{k_0}\mathbf{A}_k^{[-\mu(k)]}\mathbf{u}(k)\,. \tag{7} $$

For $\mu(k) = 0$ and $\nu(k) \neq 0$ one obtains the first form of the VFOI which in block diagrams is denoted as ${}_{\nu(k)}I$ and it is written by

$$ {}_{k_0}\mathbf{A}_k^{[\nu(k)]}\mathbf{y}(k) = b_0\mathbf{u}(k)\,. \tag{8} $$

3 VFO Inertial Element

The block diagram of the VFO inertial element (VFOIE) is given in Fig. 2. One can see that the VFOIE is created from the VFOI (6) (where $b_0 = 1$) by adding a negative feedback with a proportional block characterised by a constant coefficient a_0. Next one adds a proportional block b_0. It is assumed that $a_0 \neq -1$.

From block diagram given in Fig. 2 we derive two equations

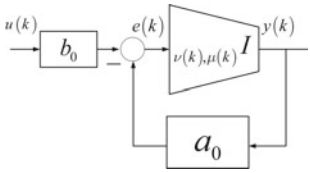

Fig. 2 Block diagram of the VFO inertial element

$$ {}_{k_0}\mathbf{A}_k^{[\nu(k)]}\mathbf{y}(k) = b_{0k_0}\mathbf{A}_k^{[-\mu(k)]}\mathbf{e}(k)\,, \tag{9} $$

$$ \mathbf{e}(k) = b_0\mathbf{u}(k) - a_0\mathbf{y}(k)\,. \tag{10} $$

To simplify a notation we put

$$ {}_{k_0}\mathbf{G}_{o,k}^{[\nu(k),-\mu(k)]} := \left({}_{k_0}\mathbf{A}_k^{[-\mu(k)]}\right)^{-1} {}_{k_0}\mathbf{A}_k^{[\nu(k)]}\,. \tag{11} $$

Combining Eqs. (9) and (10) we obtain the matrix–vector description of the third form of the VFOIE

$$ {}_{k_0}\mathbf{G}_{o,k}^{[\nu(k)]}\mathbf{y}(k) + a_0\mathbf{y}(k) = b_0\mathbf{u}(k)\,. \tag{12} $$

Similar investigations taken into account the first and the second form of the VFOI lead to the vector–matrix description the second

$$ \left[{}_{k_0}\mathbf{A}_k^{[-\mu(k)]}\right]^{-1}\mathbf{y}(k) + a_0\mathbf{y}(k) = b_0\mathbf{u}(k) \tag{13} $$

and the first form of the VFOIE

$$ {}_{k_0}\mathbf{A}_k^{[\nu(k)]}\mathbf{y}(k) + a_0\mathbf{y}(k) = b_0\mathbf{u}(k)\,. \tag{14} $$

Equation (12) can be transformed to an equivalent form

$$ \left[\left({}_{k_0}\mathbf{A}_k^{[-\mu(k)]}\right)^{-1} {}_{k_0}\mathbf{A}_k^{[\nu(k)]} + a_{0k_0}\mathbf{1}_k\right]\mathbf{y}(k) = b_0\mathbf{u}(k) \tag{15} $$

and further

$$ \mathbf{y}(k) = b_0\left[\left({}_{k_0}\mathbf{A}_k^{[-\mu(k)]}\right)^{-1} {}_{k_0}\mathbf{A}_k^{[\nu(k)]} + a_{0k_0}\mathbf{1}_k\right]^{-1}\mathbf{u}(k)\,. \tag{16} $$

Simple matrices manipulations lead to the equivalent form of the VFOIE

$$ \mathbf{y}(k) = b_0\left[{}_{k_0}\mathbf{1}_k + a_0\left({}_{k_0}\mathbf{A}_k^{[-\mu(k)]}\right)^{-1} {}_{k_0}\mathbf{A}_k^{[\nu(k)]}\right]^{-1}\left({}_{k_0}\mathbf{A}_k^{[-\mu(k)]}\right)^{-1} {}_{k_0}\mathbf{A}_k^{[\nu(k)]}\mathbf{u}(k)\,. \tag{17} $$

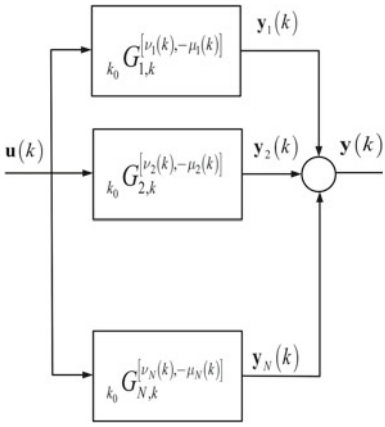

Fig. 3 Parallel connection of the VFOIEs

Introducing a notation one can easily realise a connection to the discrete transfer function description of the closed-loop system

$$\mathbf{y}(k) = b_0 \left[{}_{k_0}\mathbf{1}_k + a_{0k_0} \mathbf{G}_{0,k}^{[\nu(k),-\mu(k)]} \right]^{-1} {}_{k_0}\mathbf{G}_{0,k}^{[\nu(k),-\mu(k)]} \mathbf{u}(k) \,. \tag{18}$$

Denoting

$${}_{k_0}\mathbf{G}_{c,k}^{[\nu(k),-\mu(k)]} := b_0 \left[{}_{k_0}\mathbf{1}_k + a_{0k_0} \mathbf{G}_{0,k}^{[\nu(k),-\mu(k)]} \right]^{-1} {}_{k_0}\mathbf{G}_{0,k}^{[\nu(k),-\mu(k)]} \tag{19}$$

one can establish an input–output relation similar to the discrete transfer function. Figure 3 shows a parallel connection of N VFOIEs.

Each block is described by one of the following equations

$$\mathbf{y}_i(k) = {}_{k_0}\mathbf{G}_{i,k}^{[\nu(k),-\mu(k)]} \mathbf{u}(k), \text{ for } i = 1, 2, \ldots, N \tag{20}$$

and the summator element is given by

$$\mathbf{y}(k) = \sum_{i=1}^{N} \mathbf{y}_i(k) \,. \tag{21}$$

Substitution of (20) into (21) yields

$$\mathbf{y}(k) = \sum_{i=1}^{N} {}_{k_0}\mathbf{G}_{i,k}^{[\nu_i(k),-\mu_i(k)]} \mathbf{u}(k) \,. \tag{22}$$

4 VFOIE Existence Conditions

Similar results as presented in the next Proposition one can find in [8], however for different equation.

Proposition 1 *Let $b_0 > 0$, $u(\cdot)$ be bounded function, and $\nu \in (0, 1]$ be fractional order. The fractional-order discrete linear time-invariant inertial element with constant order ν described by an equation*

$$ {}_0\Delta_k^{[\nu]} y(k) + a_0 y(k) = b_0 u(k) \tag{23} $$

is asymptotically stable if and only if

$$ a_0 \in \mathcal{S}_\nu = (-\infty, -2^\nu) \cup (0, +\infty) \,. \tag{24} $$

Proof Applying to both sides of (23) the one-sided $\mathcal{Z}$-transform, assuming zero initial conditions one gets the discrete transfer function $G_I(z) = \frac{Y(z)}{U(z)} = \frac{b_0}{\left(1-\frac{1}{z}\right)^\nu + a_0}$. The formula for $\mathcal{Z}$-transform of functions $a^{[\nu]}(\cdot)$ comes, for example, from [9]. System is asymptotically stable if and only if every pole lies inside the unit circle, i.e. if modules of solutions of the equation

$$ \left(1 - \frac{1}{z}\right)^\nu + a_0 = 0 \tag{25} $$

are less then 1. Observe that for $a_0 < 0$ we have that $z = \frac{1}{1-(-a_0)^{\frac{1}{\nu}}}$. For $a_0 < 0$ we solve the inequality $|z| < 1$ receiving $a_0 < -2^\nu$. For $a_0 > 0$ Eq. (25) has no roots outside the unite circle. Hence we have got the condition (24).

Corollary 1 *The stability sets (24) satisfy inclusion relations*

$$ \mathcal{S}_1 \subset \mathcal{S}_\nu \subset \mathcal{S}_0 \,. \tag{26} $$

It means that if for some a_0 a classical system is stable then the fractional-order system (with $0 < \nu < 1$) is also stable (assuming the same a_0).

Lemma 1 *Let $b_0 > 0$, $a_0 \neq 0$, $u(\cdot)$ be nondecreasing bounded function, and $\nu(\cdot)$ with values in $(0, 1]$ be fractional nondecreasing order function. Then the solution of equation*

$$ {}_{k_0}\Delta_k^{[\nu(k)]} y(k) + a_0 y(k) = b_0 u(k) \tag{27} $$

is nondecreasing for $y(k_0) \geq 0$.

Proof For the simplicity we take $k_0 = 0$. We use in the proof the following property of coefficients: $-a^{[\nu(k+1)]}(i) \geq -a^{[\nu(k)]}(i) \geq 0$ for nondecreasing order function $\nu(\cdot)$.

Let us assume that for all $s \in \{1, \ldots, k-1\}$ holds $y(s) \geq y(s-1)$. Then we show that also $y(k+1) \geq y(k)$. We have the formulas, for $k \in \mathbb{N}_1$:

$$(1+a_0)y(k+1) = -\sum_{i=1}^{k+1} a^{[\nu(k+1)]}(i)y(k+1-i) + b_0u(k+1)$$

and

$$(1+a_0)y(k) = -\sum_{i=1}^{k} a^{[\nu(k)]}(i)y(k-i) + b_0u(k)\,.$$

Then

$$\begin{aligned}(1+a_0)\left(y(k+1)-y(k)\right) &= -a^{[\nu(k+1)]}(k+1)y(0)\\ &+\sum_{i=1}^{k}\left(-a^{[\nu(k+1)]}(i)y(k+1-i)+a^{[\nu(k)]}(i)y(k-i)\right)\geq 0\,,\end{aligned}$$

as $-a^{[\nu(k+1)]}(k+1)y(0) \geq 0$ and $-a^{[\nu(k+1)]}(i)y(k+1-i) + a^{[\nu(k)]}(i)y(k-i) \geq \left(-a^{[\nu(k+1)]}(i) + a^{[\nu(k)]}(i)\right)y(k-i) \geq 0$. Hence, it means that $y(k+1) \geq y(k)$ and from the mathematical induction principle it holds for all $k \in \mathbb{N}_0$.

Proposition 2 *Let $a_0, b_0 > 0$, $u(\cdot)$ be nondecreasing bounded function, and $\nu(\cdot)$ with values in $(0, 1]$ be fractional nondecreasing order function. The response to the positive input signal $u(k) \geqslant 0$ of the first-order discrete linear inertial element $\overline{y}(k)$ is not less than the response of the VFOIE to the same signal in Eq. (27) i.e. $\overline{y}(k) \geq y(k)$ for $k \in \mathbb{N}$.*

Proof For the simplicity we take $k_0 = 0$. Firstly, let us notice that for fixed $\nu(k) \in (0, 1]$ we have $\forall i \neq 0\ a^{[\nu(k)]}(i) < 0$ and $\sum_{i=0}^{\infty} a^{[\nu(k)]}(i) = 0$. Hence,

$$\sum_{i=0}^{k} a^{[\nu(k)]}(i) = -\sum_{i=k+1}^{\infty} a^{[\nu(k)]}(i) > 0\,.$$

From Lemma 1 we know that sequences $\{y(k)\}_{k\in\mathbb{N}_1}, \{\overline{y}(k)\}_{k\in\mathbb{N}_1}$ are nondecreasing. Then assuming that for all $s \in \{1, \ldots, k-1\}$ holds $\overline{y}(s) \geq y(s)$, we show that also $\overline{y}(k) \geq y(k)$. We have the formulas, for $k \in \mathbb{N}_1$:

$$(1+a_0)y(k) = -\sum_{i=1}^{k} a^{[\nu(k)]}(i)y(k-i) + b_0u(k)\,,\quad (1+a_0)\overline{y}(k) = \overline{y}(k-1) + b_0u(k)\,.$$

Then

$$(1+a_0)\left(\overline{y}(k)-y(k)\right) = \overline{y}(k-1) + \sum_{i=1}^{k} a^{[\nu(k)]}(i)y(k-i)$$

and $y(k-i) \leq y(k-1) < \overline{y}(k-1)$ and $-y(k-i) \geq -\overline{y}(k-1)$. Hence,

$$(1+a_0)\left(\overline{y}(k)-y(k)\right) \geq \overline{y}(k-1) + \sum_{i=1}^{k} a^{[\nu(k)]}(i)\overline{y}(k-1) = \overline{y}(k-1)\sum_{i=0}^{k} a^{[\nu(k)]}(i) \geq 0\,.$$

It means that $\overline{y}(k) \geq y(k)$ and from the mathematical induction principle it holds for all $k \in \mathbb{N}_0$.

Proposition 3 *The VFOIE unit step response of (27) is monotonically increasing for the fractional-order function satisfying a condition* $0 < \nu(k) \leqslant 1$ *and coefficient* $a_0 > 0$.

Proof The monotonic growth is characterized by a permanent positivity of the first-order difference. To prove that the unit step response $h(k)$ of the VFOIE monotonically increases it is sufficient to show that its first-order difference-discrete pulse response $g(k)$ is positive over $(0, +\infty)$. It means that to prove the monotonicity of the unit step response one should prove the positivity of the discrete pulse response. The VFOIE is described by the Eq. (27), which can be transformed to an equivalent form

$$\left[{}_0\mathbf{A}_k^{[\nu(k)]} + a_{00}\mathbf{1}_k\right]\mathbf{g}(k) = b_0\boldsymbol{\delta}(k)\,, \quad \boldsymbol{\delta}(k) = \begin{bmatrix} 0 \\ 0 \\ \vdots \\ 0 \\ \delta(0) \end{bmatrix} = \begin{bmatrix} 0 \\ 0 \\ \vdots \\ 0 \\ 1 \end{bmatrix}. \tag{28}$$

Transcription of Eq. (28) yields

$$\begin{bmatrix} a & a_{k,1} & \cdots & a_{k,k-2} & a_{k,k-1} & a_{k,k} \\ 0 & a & \cdots & a_{k-1,k-3} & a_{k-1,k-2} & a_{k-1,k-1} \\ \vdots & \vdots & & \vdots & \vdots & \cdots \\ 0 & 0 & \cdots & a & a_{2,1} & a_{2,2} \\ 0 & 0 & \cdots & 0 & a & a_{1,1} \\ 0 & 0 & \cdots & 0 & 0 & a \end{bmatrix} \begin{bmatrix} g(k) \\ g(k-1) \\ \vdots \\ g(2) \\ g(1) \\ g(0) \end{bmatrix} = b_0 \begin{bmatrix} 0 \\ 0 \\ \vdots \\ 0 \\ 0 \\ 1 \end{bmatrix}, \tag{29}$$

where $a = 1 + a_0 > 0$ and $a_{i,j} = a^{[\nu(i)]}(j) < 0$ for $i, j = 1, 2, \cdots, k$. The inequalities follow from the asymptotic stability conditions (24) and coefficients (1) properties. Now one calculates $g(0) = \frac{b_0}{a} = \frac{b_0}{1+a_0}$ and assumes that $g(i) > 0$ for $i = 1, 2, \cdots, k-1$. Then from (29) one gets

$$g(k) = -\begin{bmatrix} a_{k,1} & a_{k,2} & \cdots & a_{k,k-1} & a_{k,k} \end{bmatrix} \begin{bmatrix} g(k-1) \\ g(k-2) \\ \vdots \\ g(1) \\ g(0) \end{bmatrix} > 0. \tag{30}$$

The discrete pulse response of the VFOIE is positive. Hence the discrete unit step response is monotonically increasing. This ends the proof.

Corollary 2 *The unit step response of N connected in series and parallel VFOIEs is monotonically increasing.*

5 Numerical Examples

As a support of the analysis, given in previous sections, several numerical examples are given. One considers three variable-, fractional-order inertial elements connected in series. Each element is described by the same Eq. (27). The consecutive outputs are represented by black (Bk), red (Rd) and blue (Bl) plots. In all simulations one assumes $a_0 = 0.005$.

For the fractional-order function

(a)

$$\nu(k) = \left(1 - e^{-0.01k}\right) \mathbf{1}(k) \tag{31}$$

plotted in Fig. 4a one obtains unit step responses presented in Fig. 4b.

(b) For decreasing fractional-order function

$$\nu(k) = \left(1 + 0.52e^{-0.01k}\right) \mathbf{1}(k) \tag{32}$$

plotted in Fig. 5a one obtains unit step responses presented in Fig. 5b.

(c) Finally we analyze the influence of the coefficient a_0 value. In the classical first-order discrete inertial element it is related to so called time constant. For

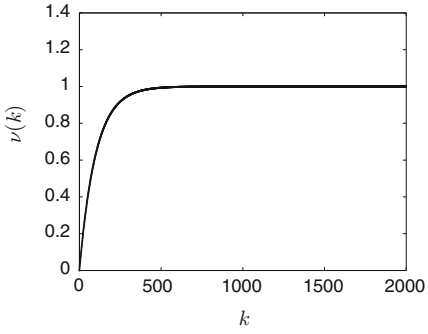

(a) Plot of the fractional–order function.

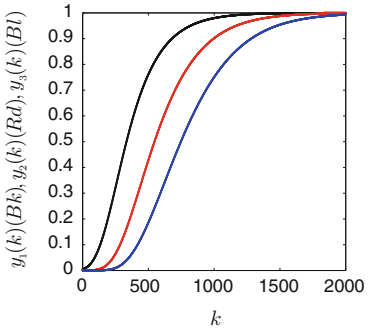

(b) VFO inertial elements responses.

Fig. 4 Fractional-order function and VFO inertial elements responses for $\nu(k) = (1 - e^{-0.01k})\,\mathbf{1}(k)$

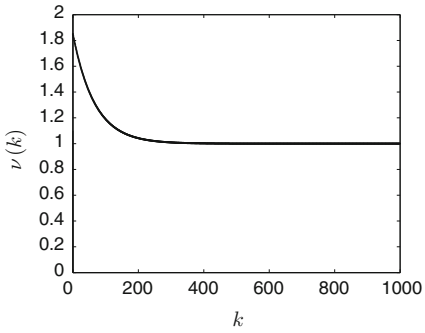

(a) Plot of the fractional–order function.

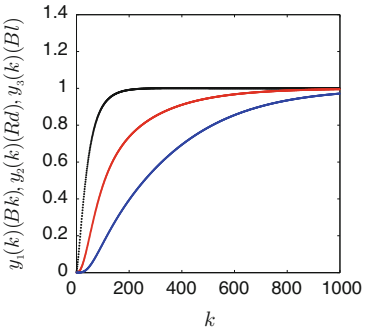

(b) VFOL element unit step response.

Fig. 5 Fractional-order function and VFO inertial elements responses for $\nu(k) = \left(1 + 0.52e^{-0.01k}\right)\mathbf{1}(k)$

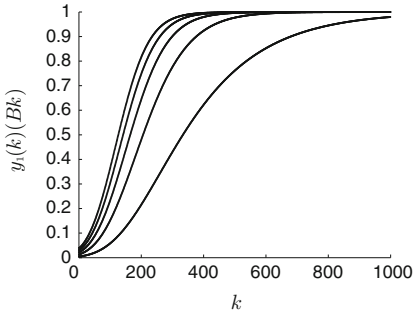

(a) Unit step responses for $a_0 \in \mathcal{A}_1$, $\mathcal{A}_1 = \{0.005, 0.014, 0.023, 0.032, 0.041\}$.

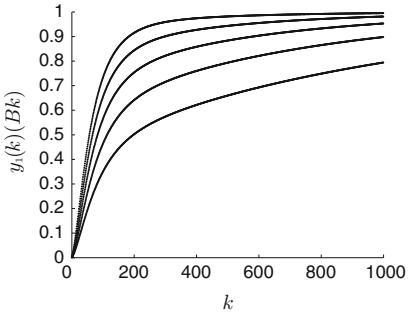

(b) Unit step responses for $a_0 \in \mathcal{A}_2$, $\mathcal{A}_2 = \{0.001, 0.014, 0.018, 0.022, 0.026\}$.

Fig. 6 VFO inertial elements unit step responses of (22) for different a_0 and the same fractional-order functions

two previously considered fractional-order functions we take into account two coefficient a_0 sets: $\mathcal{A}_1$ and $\mathcal{A}_2$ (Fig. 6).

6 Final Conclusions

The paper presents the first basic attempt to the problem of stability of the proposed variable-, fractional-order inertial element (VFOIE) and N-elements parallel connection. We have analyzed the situations accordingly to the corresponding classical difference system.

Acknowledgments This research was partially supported by the grant S/WI/1/2016 of the Polish Ministry of Science and Higher Education.

References

1. Agrawal, O., Machado, J.T., Sabatier, J.: Fractional Derivatives and Their Application: Nonlinear Dynamics. Springer, Berlin (2004)
2. Hilfer, R.: Applications of Fractional Calculus in Physics. World Scientific, Singapore (2000)
3. West, B.J., Grigolini, M.B.P.: Fractional Derivative Simulation Code. Physics of Fractional Operators. Springer, Berlin (2003)
4. Ostalczyk, P.: Discrete Fractional Calculus. Applications in Control and Image Processing. Series in Computer Vision, vol. 4. World Scientific Publishing, Singapore (2016)
5. Caputo, M., Mainardi, F.: A new dissipation model based on memory mechanism. Pure Appl. Geophys. **91**, 134–147 (1971)
6. Kailath, T.: Linear Systems. Prentice-Hall, Inc, Englewood Cliffs (1980)
7. Kaczorek, T.: Linear Control Systems: Analysis of Multivariable Systems. Wiley, New York (1992)
8. Čermák, J., Kisela, T., Nechvatál, L.: Stability and asymptotic properties of a linear fractional difference equation. Adv. Differ. Equ. **1**(122), 1–14 (2012)
9. Mozyrska, D., Wyrwas, M.: Fractional linear equations with discrete operators of positive order. In: Latawiec, K.J., Łukaniszyn, M., Stanisławski, R. (eds.) Advances in the Thoery and Applications of Non-integer Order Systems. Lecture Notes in Electrical Engineering, vol. 320, pp. 47–58. Springer, Berlin (2014)

Remarks on Mittag-Leffler Discrete Function and Putzer Algorithm for Fractional h-Difference Linear Equations

Ewa Pawłuszewicz

Abstract The paper presents some properties of the discrete Mittag-Leffler two parameter function. The extension of the Putzer algorithm onto linear linear fractional order systems is given. This algorithm allows to find the general solution of linear fractional order systems. The problem of approximation of the solutions to fractional linear differential equation with Caputo operator by the solutions to fractional difference equations using the Putzer algorithm is considered.

Keywords Fractional h-difference operators · Discrete Mittag-Leffler function · Fractional linear h-difference equations · Putzer algorithm

1 Introduction

Fractional differential and difference equations describe a lot of phenomena arising in engineering, physics or economics. Mittag-Leffler function naturally occurs as the solution of linear fractional order differential equations. Generally such a solution can be expressed as an infinite series, see [1–3]. So in order to approximate this solution, a truncated form is used, see for example in [3]. In the classical linear differential equation $\dot{x} = Ax$ case the Puzer algorithm can be applied in order to find a general solution, see [4]. This algorithm uses some matrices created based on matrix A, its eigenvalues and a solution of some first order initial value problem, for details see [4, 5]. The algorithm was extended onto linear systems defined on any, even nonhomogeneous, time models, see [6].

E. Pawłuszewicz (✉)
Faculty of Mechanical Engineering, Bialystok University of Technology,
Wiejska 45C, 15-351 Białystok, Poland
e-mail: e.pawluszewicz@pb.edu.pl

A. Babiarz et al. (eds.), *Theory and Applications of Non-integer Order Systems*,
Lecture Notes in Electrical Engineering 407, DOI 10.1007/978-3-319-45474-0_9

Now our goal is to extend Putzer's algorithm onto fractional h-difference linear equations. Since its crucial point concentrates on the discrete Mittag-Leffler function, firstly this function should be studied. Some of its properties were examined in [1]. Now some other properties are discussed.

The paper is organized as follows: in Sect. 2 difference fractional h-operators are introduced. Section 3 presents some properties of discrete Mittag-Leffler function. In Sect. 4 the linear h-difference equation with fractional difference operators is presented. We focus on equations with operators of Caputo-, Riemman–Louville- and Grünwald–Letnikov-type. In [7] it is shown that these operators are related to each other. So, systems with these operators can be studied simultaneously. In Sect. 5 Putzer algorithm for linear fractional order h difference equations is presented. The proof of this algorithm in main part is the same as the proof of Putzer algorithm on time scales, see [6]. In Sect. 6 remarks on Mittag-Leffler continuous function for Caputo operator are presented.

2 Difference Fractional h-Operators

Let α and h be positive real numbers. For $a \in \mathbb{R}$ let $(h\mathbb{N})_a := \{a, a+h, a+2h, \ldots\}$. If $x : (h\mathbb{N})_a \to \mathbb{R}$, then the *forward h-difference operator* is denoted as $(\Delta_h x)(t) := \frac{x(t+h)-x(t)}{h}$, $t = a + kh$, $k \in \mathbb{N}_0$. The *h-difference sum* is defined by

$$\left({}_a\Delta_h^{-1}x\right)(t) := h\sum_{k=0}^{k} x(a+kh)$$
$$\left({}_a\Delta_h^{-1}x\right)(a) := 0$$

for any $t = a + (k+1)h$ and $k \in \mathbb{N}_0$. The *fractional h-sum of order* $\alpha > 0$ for a function $x \in (h\mathbb{N})_a \to \mathbb{R}^p$ is defined as follows

$$\left({}_a\Delta_h^{-\alpha}x\right)(t) := h^\alpha \sum_{k=0}^{n} \binom{n-k+\alpha-1}{n-k} x(a+kh)\,,$$
$$\left({}_a\Delta_h^{0}x\right)(t) := x(t)$$

where $t = a + (\alpha+n)h$ and $n \in \mathbb{N}_0$ and

$$\binom{\alpha}{s} = \begin{cases} 1 & \text{for } s = 0 \\ \frac{\alpha(\alpha-1)\cdots(\alpha-s+1)}{s!} & \text{for } s \in \mathbb{N}. \end{cases}$$

denotes the binomial coefficient.

3 Discrete Mittag-Leffler Function

Let α, β be complex numbers with $\mathrm{Re}\alpha > 0$ and let $\lambda \in \mathbb{R}$. The *discrete Mittag-Leffler two-parameter function* is defined as, see [1, 2]

$$E_{(\alpha,\beta)}(\lambda, n) = \sum_{k=0}^{\infty} \lambda^k (-1)^{n-k} \binom{-k\alpha - \beta}{n-k}. \tag{1}$$

As a special cases of this function one has [1, 2]

$$E_{(\alpha,1)}(\lambda, n) = \sum_{k=0}^{\infty} \lambda^k (-1)^{n-k} \binom{-k\alpha - 1}{n-k}$$

and

$$E_{(\alpha,\alpha)}(\lambda, n) = \sum_{k=0}^{\infty} \lambda^k (-1)^{n-k} \binom{-(k+1)\alpha}{n-k}.$$

Note also that directly from the relation $\binom{-1}{k} = (-1)^k$, $k \in \mathbb{N}_0$, it follows that

$$E_{(0,1)} = \sum_{k=0}^{\infty} \lambda^k (-1)^{n-k} \binom{-1}{n-k} = \sum_{k=0}^{\infty} \lambda^k,$$

i.e. $E_{(0,1)}(\lambda, n)$ is the well known geometrical series.

Proposition 1 *For $\alpha, \beta \in \mathbb{C}$ with $\mathrm{Re}\alpha > 0$ and $\lambda \in \mathbb{R}$, it holds*

$$E_{(\alpha,\beta)}(\lambda, n) = E_{(\alpha,\beta-1)}(\lambda, n) + \sum_{k=0}^{\infty} \lambda^k (-1)^{n-k} \binom{-k\alpha - \beta + 1}{n-k-1}.$$

Proof Since (see for example [8])

$$\binom{-k\alpha - \beta}{n-k} = \binom{-k\alpha - (\beta-1) - 1}{n-k} = \binom{-k\alpha - (\beta-1)}{n-k} + \binom{-k\alpha - (\beta-1)}{n-k-1},$$

then

$$E_{(\alpha,\beta)}(\lambda, n) = E_{(\alpha,\beta-1)}(\lambda, n) + \sum_{k=0}^{\infty} \lambda^k (-1)^{n-k} \binom{-k\alpha - \beta + 1}{n-k-1}$$

Corollary 1 *For $\alpha \in \mathbb{C}$ with $\mathrm{Re}\alpha > 0$ and $\lambda \in \mathbb{R}$, it holds*

$$E_{(1,0)}(\lambda, n) = \frac{\alpha}{\alpha - 1} E_{(1,-1)}(\lambda, n) + n \frac{1-\alpha}{\alpha} \sum_{k=0}^{\infty} \lambda^k (-1)^{n-k} \binom{-k\alpha}{n-k}$$

Proof Since (see for example in [8])

$$\binom{-k\alpha}{n-k} = \binom{-k\alpha-1}{n-k} + \binom{-k\alpha-1}{n-k-1} \quad \text{and} \quad \binom{-k\alpha-1}{n-k-1} = \frac{n-k}{-k\alpha}\binom{-k\alpha}{n-k},$$

then

$$E_{(1,0)}(\lambda, n) = E_{(1,-1)}(\lambda, n) + \sum_{k=0}^{\infty} \lambda^k (-1)^{n-k} \left(\frac{n}{-k\alpha} + \frac{1}{\alpha}\binom{-k\alpha}{n-k} \right).$$

So

$$E_{(1,0)}(\lambda, n) = E_{(1,-1)}(\lambda, n) + \frac{1}{\alpha} E_{(1,0)} - n \sum_{k=0}^{\infty} \frac{1}{k\alpha}\binom{-k\alpha}{n-k}.$$

Proposition 2 *For $-\beta < k\alpha < 1-\beta$ the power series defining Mittag-Leffler function given by (1) is absolutely convergent for any $|\lambda| < 1$.*

Proof In [1] it was shown that for $\alpha \in (0, 1)$ and any $n \in \mathbb{N}$, it holds

$$\left| (-1)^n \binom{-\alpha}{n} \right| \leq 1.$$

Then, for $-\beta < k\alpha < 1-\beta$ one has

$$\begin{aligned} |E_{(\alpha,\beta)}(\lambda, n)| &= \left| \sum_{k=0}^{\infty} \lambda^k (-1)^{n-k} \binom{-k\alpha-\beta}{n-k} \right| \\ &\leq \sum_{k=0}^{\infty} |\lambda^k| \left| (-1)^{n-k} \binom{-k\alpha-\beta}{n-k} \right| \leq \sum_{k=0}^{\infty} |\lambda|^k \end{aligned}$$

Since for $|\lambda| < 1$ series $\sum_{k=0}^{\infty} |\lambda|^k$ converges, hence power series defining Mittag-Leffler function given by (1) is absolutely convergent.

The definition of the discrete Mittag-Leffler two-parameter function can be easily extended to the case when $\lambda \in \mathbb{C}$. In this case Proposition 2 is valid.

4 *h*-Difference Fractional Order Operators

It is known that in literature one can meet several definitions/notations of fractional order differences (see for example [9–12]). Here we focus on Caputo-, Riemman–Louville- and Grünwald–Letnikov-type h-difference operators. h represents a sample step.

Definition 1 ([13]) Let $\alpha \in (0, 1]$ and $a \in \mathbb{R}$. The *Caputo-type fractional h-difference operator* ${}_a^C\Delta_h^\alpha$ of order α for a function $x : (h\mathbb{N})_a \to \mathbb{R}$ is defined by

$$\left({}_a^C\Delta_h^\alpha x\right)(t) = \left({}_a\Delta_h^{-(1-\alpha)}\left(\Delta_h x\right)\right)(t),$$

where $t \in (h\mathbb{N})_{a+(1-\alpha)h}$.

If $\alpha = 1$ then $\left({}_a^C\Delta_h^1 x\right)(t) = \left(\Delta_h x\right)(t)$.

Proposition 3 ([1]) *Let $\alpha \in (0, 1]$ and $\alpha = (\alpha - 1)h$, $h > 0$. The initial value problem*

$$\begin{aligned}\left({}_a^C\Delta_h^\alpha x\right)(t) &= Ax(t + a)\\ x(a) &= x_0 \in \mathbb{R}^p,\end{aligned}$$

where $t \in (h\mathbb{N})_a$ and $x : (h\mathbb{N})_a \to \mathbb{R}^p$, A is $p \times p$ real matrix, has the unique solution:

$$x(t + a) = x(nh + a) = E_{(\alpha,1)}(Ah^\alpha, n)x_0$$

for any $n \in \mathbb{N}_0$.

Definition 2 ([14]) Let $\alpha \in (0, 1]$ and $a \in \mathbb{R}$. The *Riemann–Liouville-type fractional h-difference operator* ${}_a^{RL}\Delta_h^\alpha$ of order α for a function $x : (h\mathbb{N})_a \to \mathbb{R}$ is defined by

$$\left({}_a^{RL}\Delta_h^\alpha x\right)(t) = \left(\Delta_h\left({}_a\Delta_h^{-(1-\alpha)}x\right)\right)(t),$$

where $t \in (h\mathbb{N})_{a+(1-\alpha)h}$.

If $\alpha = 1$ then $\left({}_a^{RL}\Delta_h^1 x\right)(t) = \left(\Delta_h x\right)(t)$. Moreover, for any $t \in (h\mathbb{N})_{a+(1-\alpha)h}$ it holds (see [7]):

$$\left({}_a^C\Delta_h^\alpha x\right)(t) = \left({}_a^{RL}\Delta_h^\alpha x\right)(t) - \frac{x(a)}{h^\alpha}\binom{\frac{t-a}{h}}{-\alpha}. \tag{2}$$

Proposition 4 ([1]) *Let $\alpha \in (0, 1]$ and $\alpha = (\alpha - 1)h$, $h > 0$. The initial value problem*

$$\begin{aligned}\left({}_a^C\Delta_h^\alpha x\right)(t) &= Ax(t + a)\\ x(a) &= x_0,\end{aligned}$$

where $t \in (h\mathbb{N})_a$ and $x : (h\mathbb{N})_a \to \mathbb{R}^p$, A denotes $p \times p$ real matrix, $x_0 \in \mathbb{R}^p$, has the unique solution given as

$$x(t + a) = x(nh + a) = E_{(\alpha,\alpha)}(Ah^\alpha, n)x_0$$

for any $n \in \mathbb{N}_0$.

Definition 3 ([7]) Let $\alpha \in \mathbb{R}$. The *Grünwald–Letnikov-type h-difference operator* ${}_a^{GL}\Delta_h^\alpha$ of order α for a function $x : (h\mathbb{N})_a \to \mathbb{R}$ is defined by

$$\left({}_a^{GL}\Delta_h^\alpha x\right)(t) = \sum_{s=0}^{\frac{t-a}{h}} c_s^{(\alpha)} x(t - sh)$$

where $c_s^{(\alpha)} = (-1)^s \binom{\alpha}{s} \frac{1}{h^\alpha}$.

Let $(\nabla_h x)(t) = \frac{x(t)-x(t-h)}{h}$ denote the h-backward shift operator. If $a = (\alpha - 1)h$, then (see [7]) $\nabla_h \left({}_a\Delta_h^{-(1-\alpha)} x\right)(t) = \left({}_0^{GL}\Delta_h^\alpha y\right)(t)$, where $y(t) := x(t + a)$ for any $t \in (h\mathbb{N})_a$. Moreover,

$$\left({}_0^{GL}\Delta_h^\alpha y\right)(t + h) = \left({}_a^{RL}\Delta_h^\alpha x\right)(t). \tag{3}$$

Additionally if $a = 0$, then (3) and (2) imply that $\left({}_0^{C}\Delta_h^\alpha x\right)(t) = \left({}_0^{RL}\Delta_h^\alpha x\right)(t) = \left({}_0^{GL}\Delta_h^\alpha x\right)(t)$.

Proposition 5 ([1]) *The initial value problem*

$$\begin{aligned} \left({}_0^{GL}\Delta_h^\alpha y\right)(t + h) &= Ay(t) \\ y(0) &= y_0, \end{aligned}$$

where $t \in (h\mathbb{N})_0$, A denotes $p \times p$ real matrix, $y_0 \in \mathbb{R}^p$, has the unique solution given as

$$x(t) = E_{(\alpha,\alpha)}\left(Ah^\alpha, \frac{t}{h}\right) y_0.$$

5 Putzer Algorithm

Since some definitions and facts that we discuss are the same for each type of difference operators, we use the common symbol defined by its values, i.e.

$$\left({}_a\Upsilon^\alpha x\right)(t) = \begin{cases} ({}_a^{C}\Delta_h^\alpha x)(t) \ \text{ or } \ ({}_a^{RL}\Delta_h^\alpha x)(t) & \text{for } a = (\alpha - 1)h; \\ ({}_0^{GL}\Delta_h^\alpha x)(t + h), & \text{for } a = 0. \end{cases}$$

Hence, let us consider the general form of the initial value problem:

$$\begin{aligned} \left({}_a\Upsilon^\alpha x\right)(t) &= Ax(t + a), \\ x(a) &= x_0 \end{aligned}$$

where $x : (h\mathbb{N})_a \to \mathbb{R}^p$. From Propositions 3–5 it follows that for any $t \in (h\mathbb{N})_a$, the solution of the initial value problem

$$\begin{aligned} ({}_a\Upsilon^{\alpha} x)(t) &= \lambda x(t+a), \\ x(a) &= x_0 \end{aligned}$$

with a real scalar λ, has a unique solution

$$x(t+a) = x(nh+a) = E_{(\alpha,\beta)}(\lambda h^{\alpha}, n)x_0,$$

where $\beta = 1$ for the Caputo-type operator, $\beta = \alpha$ for the Riemman–Liouville- and Grünwald–Letnikov-type operators.

Theorem 1 *Let $A \in \mathbb{R}^{p\times p}$ and $t \in (h\mathbb{N})_0$. If $\lambda_1, \ldots, \lambda_n$ are eigenvalues of A, then*

$$E_{(\alpha,\beta)}(Ah^{\alpha}, n) = \sum_{i=0}^{n-1} r_{i+1}(t) P_i, \tag{4}$$

where $\beta = 1$ for the Caputo-type operator, $\beta = \alpha$ for the Riemman–Liouville- and Grünwald–Letnikov-type operators and $r(t) := [r_1(t), \ldots, r_n(t)]^T$ is the solution of the initial value problem

$$\begin{bmatrix} ({}_a\Upsilon^{\alpha} r_1)(t) \\ ({}_a\Upsilon^{\alpha} r_2)(t) \\ ({}_a\Upsilon^{\alpha} r_3)(t) \\ \vdots \\ ({}_a\Upsilon^{\alpha} r_n)(t) \end{bmatrix} = \begin{bmatrix} \lambda_1 & 0 & 0 & \ldots & 0 & 0 \\ 1 & \lambda_2 & 0 & \ldots & 0 & 0 \\ 0 & 1 & \lambda_3 & \ldots & 0 & 0 \\ \vdots & \vdots & \vdots & \ddots & \vdots & \\ 0 & 0 & 0 & \ldots & 1 & \lambda_n \end{bmatrix} \begin{bmatrix} r_1(t+a) \\ r_2(t+a) \\ r_3(t+a) \\ \vdots \\ r_n(t+a) \end{bmatrix}, \tag{5}$$

$$[r_1(a), r_2(a), r_3(a), \ldots, r_n(a)]^T = [1, 0, 0, \ldots, 0]^T$$

and matrices $P_0, P_1, \ldots, P_n$ are recursively defined as

$$\begin{aligned} P_0 &= I \\ P_{k+1} &= (A - \lambda_{k+1} I) P_k, \qquad k = 0, 1, \ldots, n-1. \end{aligned} \tag{6}$$

Proof Let $t \in (h\mathbb{N})_a$. At the beginning note that from Definition 1 one obtains the following

$$\begin{aligned} \left({}_a^C\Delta_h^{\alpha} \sum_{i=0}^{n-1} r_{i+1}\right)(t) &= h^{\alpha} \sum_{k=0}^{n} \binom{n-k+\alpha-1}{n-k} \Delta_h \left(\sum_{i=0}^{n-1} r_{i+1}\right)(kh) \\ &= \sum_{i=0}^{n-1} h^{\alpha} \sum_{k=0}^{n} \binom{n-k+\alpha-1}{n-k} \Delta_h r_{i+1}(kh) \end{aligned}$$

$$= \sum_{i=0}^{n-1} \left({}_a^C\Delta_h^\alpha r_{i+1}\right)(t).$$

Similarly for Riemman–Louiville-type (and Grünwald–Letnikov-type) operator:

$$\begin{aligned}\left({}_a^{RL}\Delta_h^\alpha \sum_{i=0}^{n-1} r_{i+1}\right)(t) &= \left(\Delta_h\left(h^\alpha \sum_{k=0}^{n}\binom{n-k+\alpha-1}{n-k}\sum_{i=0}^{n-1} r_{i+1}\right)\right)(kh+a)\\ &= \sum_{i=0}^{n-1} h^\alpha \sum_{k=0}^{n}\binom{n-k+\alpha-1}{n-k}\left(\Delta_h r_{i+1}\right)(kh+a)\\ &= \sum_{i=0}^{n-1}\left({}_a^{RL}\Delta_h^\alpha r_{i+1}\right)(t).\end{aligned}$$

So, for any $t \in (h\mathbb{N})_a$:

$$\left({}_a\Upsilon^\alpha\left(\sum_{i=0}^{n-1} r_{i+1}\right)\right)(t) = \sum_{i=0}^{n-1}\left({}_a\Upsilon^\alpha r_{i+1}\right)(t). \tag{7}$$

Since the reasoning in the rest of the proof is the same as in the proof of Putzer algorithm on time scales, see [6], we present only the main steps of it.

Let matrices $P_0, P_1, \ldots, P_n$ be defined by (6). From the classical Caley–Hamilton theorem it follows that $P_n = \prod_{i=1}^{n}(A - \lambda_n I) = 0$.

Suppose now that a matrix $X \in \mathbb{R}^{p\times p}$ is defined by the right side of the Eq. (4). We are going to show that this matrix is a solution of the fractional equation $\left({}_a\Upsilon^\alpha X\right)(t) = AX(t+a)$ with the matrix initial condition $X(a) = I$, where I is identity $p \times p$ matrix. Note that $x(a) = P_0 r_1(a) = I$ and (following the reasoning given in [6]) one has

$$\begin{aligned}\left({}_a\Upsilon^\alpha X\right)(t) - AX(t+a) &= \left({}_a\Upsilon^\alpha\left(\sum_{i=0}^{n-1} r_{i+1}P_i\right)\right)(t) - A\sum_{i=0}^{n-1} r_{i+1}(t+a)P_i\\ &= \sum_{i=1}^{n-1} r_i(t+a)P_i + \sum_{i=0}^{n-1}(\lambda_1 I - A)P_i r_{i+1}(t+a)\\ &= \sum_{i=1}^{n-1} r_i(t+a)P_i - \sum_{i=0}^{n-1} P_{i+1}r_{i+1}(t+a) = -r_n(t+a)P_n = 0\end{aligned}$$

Hence, $\left({}_a\Upsilon^\alpha X\right)(t) = AX(t+a)$.

6 Remarks on Mittag-Leffler Continuous Function for Caputo Operator

Recall that the Caputo fractional derivative of the order α, $0 < \alpha \leq 1$, of a real continuous function x is defined as

$$ {}_a^C D^\alpha x(t) = \frac{1}{\Gamma(n-\alpha)} \int_a^1 \frac{x^{(n)}(\tau)}{(t-\tau)^{\alpha+1-n}} d\tau $$

where Γ denotes the gamma function.

Let $\bar{t}_h := a + (1-\alpha)h + nh$ with $n = \left[\frac{t-a}{h}\right] + 1$ and $a = (\alpha - 1)h$, $\alpha \in (0, 1]$. Also let $\overline{x} : (a, T]_{(h\mathbb{N})_a} \to \mathbb{R}^n$.

Proposition 6 ([15]) *The solution of the system*

$$ \left({}_0^C D^\alpha x\right)(t) = f(t, x(t)), x(0) = x_0 . $$

is approximated by the solution of the system

$$ \left({}_a^C \Delta_h^\alpha \overline{x}\right)(t) = f(t, \overline{x}(t)), \overline{x}(a) = x_0 . $$

in values via the limit $\lim_{h\to 0} \overline{x}(t_h) = x(t)$.

Recall that the two parameters continuous Mittang-Leffler function $\mathcal{E}_{(\alpha,\beta)}$ is defined as, see for example [16, 17]

$$ \mathcal{E}_{(\alpha,\beta)}(z) := \sum_{k=0}^{\infty} \frac{z^k}{\Gamma(k\alpha + \beta)}, \quad \alpha, \beta > 0 \tag{8} $$

whenever the series converges.

Corollary 2 ([18]) *Let $\alpha \in (0, 1]$, $h > 0$ and $t \geq a$. If $\bar{t}_h := (1-\alpha)h + nh$, then the continuous Mittang-Leffler function $\mathcal{E}_{(\alpha,\beta)}(At)$ is approximated by the discrete Mittag-Leffler function $E_{(\alpha,\beta)}(A, t_h)$.*

As an immediate consequence of Theorem 1, Corollary 2 and Proposition 6 we obtain the following

Theorem 2 *Let $A \in \mathbb{R}^{p\times p}$ and $t \in (h\mathbb{N})_0$. If $\lambda_1, \ldots, \lambda_n$ are eigenvalues of A then*

$$ \mathcal{E}_{(\alpha,\beta)}(Ah^\alpha, n) = \sum_{i=0}^{n-1} r_{i+1}(t) P_i, \tag{9} $$

where $r(t) := [r_1(t), \ldots, r_n(t)]^T$ *is the solution of the system*

$$\begin{bmatrix} ({}_0D^{\alpha} r_1)(t) \\ ({}_0D^{\alpha} r_2)(t) \\ ({}_0D^{\alpha} r_3)(t) \\ \vdots \\ ({}_0D^{\alpha} r_n)(t) \end{bmatrix} = \begin{bmatrix} \lambda_1 & 0 & 0 & \ldots & 0 & 0 \\ 1 & \lambda_2 & 0 & \ldots & 0 & 0 \\ 0 & 1 & \lambda_3 & \ldots & 0 & 0 \\ \vdots & \vdots & \vdots & \ddots & \vdots & \\ 0 & 0 & 0 & \ldots & 1 & \lambda_n \end{bmatrix} \begin{bmatrix} r_1(t) \\ r_2(t) \\ r_3(t) \\ \vdots \\ r_n(t) \end{bmatrix}, \tag{10}$$

with $t \in (a, T]$ *and initial the initial condition*

$$[r_1(0), r_2(0), r_3(0), \ldots, r_n(0))]^T = [1, 0, 0, \ldots, 0]^T \tag{11}$$

and matrices $P_0, P_1, \ldots, P_n$ *are recursively defined as follows*

$$\begin{aligned} P_0 &= I \\ P_{k+1} &= (A - \lambda_{k+1} I) P_k, \qquad k = 0, 1, \ldots, n-1. \end{aligned} \tag{12}$$

7 Conclusions

The paper studies some properties of the discrete two parameters Mittag-Leffler $E_{(\alpha,\beta)}$ function. In general, this function is a natural extension of the classical exponential function onto the discrete fractional case. Moreover, for $\alpha = 0$ and $\beta = 1$ this function is nothing else but the commonly known geometrical series. Mittag-Leffler function plays a crucial role in the solution of the linear fractional order difference equation. It is shown that it can be determined using the Putzer algorithm.

Acknowledgments The work was supported by Bialystok University of Technology according to the grant no. S/WM/1/2016.

References

1. Mozyrska, D., Wyrwas, M.: The $\mathcal{Z}$-transform method and delta-type fractional difference operators. Discrete Dyn. Natl. Soc. (2015)
2. Mozyrska, D., Pawluszewicz, E.: Local controllability of nonlinear discrete-time fractional order systems. Bull. Pol. Acad.: Tech. **61**(1), 251–256 (2013)
3. Wu, G-Ch., Baleanu, D., Zeng, S.-D., Luo, W.-H.: Mittag-Leffler function for discrete fractional modelling. J. King Saud Univ. Sci. **28**(1), 99–102 (2016)
4. Putzer, E.J.: Avoiding the Jordan canonical form in the discussion of linear systems with constant coefficients. Math. Assoc. Am. **73**(1), 2–7 (1966)
5. Kelley, W.G., Peterson, A.C.: Difference Equations: An Introduction with Applications. Academic Press, New York (2001)
6. Bohner, M., Petersen, A.: Dynamic Equations on Time Scales. Bürkhauser, Boston (2001)

7. Mozyrska, D., Girejko, E., Wyrwas, M.: Comparison of h-difference fractional operators. Advances in the Theory and Applications of Non-integer Order Systems, pp. 191–197. Springer, Berlin (2013)
8. Graham, R.L., Knuth, D.E., Patashnik, O.: Concrete Mathematics: A foundation for Computer Science. Addison-Wesley, Reading (1994)
9. Abdeljawad, T.: On Riemann and Caputo fractional differences. Comput. Math. Appl. **62**(3), 1602–1611 (2011)
10. Atıcı, F.M., Eloe, P.W.: Initial value problems in discrete fractional calculus. Proc. Am. Math. Soc. **137**(3), 981–989 (2009)
11. Kaczorek, T.: Selected Problems of Fractional Systems Theory. Springer, Berlin (2011)
12. Podlubny, I.: Fractional Differential Equations. Mathematics in Sciences and Engineering. Academic Press, New York (1999)
13. Mozyrska D., Girejko E.: Overview of the fractional h-difference operators. In: Advances in Harmonic Analysis and Operator Theory, pp. 253–267. Springer, Berlin (2013)
14. Bastos, N.R.O., Ferreira, R.A.C., Torres, D.F.M.: Necessary optimality conditions for fractional difference problems of the calculus of variations. Discrete Contin. Dyn. Syst. **29**(2), 417–437 (2011)
15. Mozyrska, D., Girejko, E., Wyrwas, M.: Fractional nonlinear systems with sequential operators. Cent. Eur. J. Phys. **11**(10), 1295–1303 (2013)
16. Diethelm, K.: The Analysis of Fractional Differential Equations. Springer, Berlin (2010)
17. Mathai, A.M., Haubold, H.: Special Functions for Applied Scientists. Springer, Berlin (2008)
18. Pawluszewicz, E.: Constrained controllability of fractional h-difference fractional control systems with Caputo type operator. Discrete Dyn. Natl. Soc. (2015)

On the Output-Additive Switching Strategy for a New Variable Type and Order Difference

Dominik Sierociuk, Wiktor Malesza and Michał Macias

Abstract The paper introduces definition of recursive fractional order difference for the case when type of variable order changing is varying in time. The equivalent switching strategies for this definition, which allow to better understand mechanism of type of variable order definition changing, are also given. Numerical results of comparison between given switching schemes and the definition are presented and analyzed.

Keywords Fractional calculus · Variable order derivative

1 Introduction

Fractional calculus is a generalization of traditional differential calculus for the case when order of differentiation and integration is a real or even complex number. The theoretical background for this calculus can be found in [1–5]. One of the most important application areas of fractional calculus is modelling diffusion processes. In [6], results of successful modeling for heat transfer process in solid material were presented. Moreover, in [7] similar results for heat transfer in heterogeneous materials, described by anomalous diffusion using fractional order partial differential equation, were shown. Another example of successful using fractional calculus are ultracapacitors. Modeling of this devices based on anomalous diffusion (fractional order model) was presented in [8, 9]. Despite of modeling, fractional calculus was found interesting also in signal processing [10, 11] and control (e.g. fractional order PID controllers [12]).

D. Sierociuk (✉) · W. Malesza · M. Macias
Institute of Control and Industrial Electronics, Warsaw University of Technology,
Koszykowa 75, 00-662 Warsaw, Poland
e-mail: dsieroci@ee.pw.edu.pl

W. Malesza
e-mail: wmalesza@ee.pw.edu.pl

M. Macias
e-mail: michal.macias@ee.pw.edu.pl

A. Babiarz et al. (eds.), *Theory and Applications of Non-integer Order Systems*,
Lecture Notes in Electrical Engineering 407, DOI 10.1007/978-3-319-45474-0_10

The case when the order is changing in time is more complex to describe than in the constant order case. In [13–17] four different types of variable order derivatives definitions were presented and, what is more important, corresponding with these definitions equivalent switching strategies were introduced and proved. These switching schemes allow to make a clear categorization of definitions, and better understanding their behavior, whose are: input-reductive, input-additive, output-reductive and output-additive. Different type of definition can represent different mechanism of order changing in the real plant or can be used to obtain desired behavior in control algorithm.

We can imagine that in practical application, desired method of order changing can be varying in time, or the system itself changes the switching strategy in time. In order to describe such behavior and processes we will need to define the fractional variable order and variable type difference. Similarly to the variable order case, we can define different manners of type varying. To the best of our knowledge, the pioneer article devoted to the variable type and order differences is [18], where iterative definitions with corresponding input-additive and output-reductive switching schemes were introduced.

In this paper, we will introduce next type of recursive definition of variable order and type difference (other type of recursive definition is presented in [19]). Moreover, we will introduce an equivalent switching strategy that will correspond to this definition. Finally, we will present results of numerical simulations that confirm correctness of obtained theoretical achievements.

The remainder of this paper is structured as follows. In Sect. 2, variable fractional order of constant type difference definitions are recalled. Section 3 presents the main result—definition of recursive fractional variable order and type difference together with corresponding switching strategies. Finally, in Sect. 4, numerical results are presented.

2 Fractional Constant Type Variable Order Differences

The following fractional constant order difference of Grünwald–Letnikov type will be used as a base of generalization onto variable order case

$$\Delta^{\alpha} x_l = \sum_{j=0}^{l} w(j,\alpha) x_{l-j}, \tag{1}$$

where the order $\alpha \in \mathbb{R}$, the values $x_l \in \mathbb{R}$, $l = 0, \ldots, k$, $h > 0$ is a sample time, and

$$w(j,\alpha) = \frac{1}{h^{\alpha}} (-1)^j \binom{\alpha}{j}. \tag{2}$$

For the case of order changing with time (variable order case, with $\alpha_l \in \mathbb{R}$, for $l = 0, \ldots, k$), many different types of differences can be found in literature [20–23]. Among them, we present only four—two iterative and two recursive type definitions. The first one, iterative type, so called $\mathcal{A}$-type difference [21], is the following

$$ {}^{\mathcal{A}}\Delta^{\alpha_l} x_l = \sum_{j=0}^{l} {}^{\mathcal{A}}w(l, j, \alpha_l) x_{l-j}, \tag{3} $$

where

$$ {}^{\mathcal{A}}w(l, j, \alpha_l) = \frac{1}{h^{\alpha_l}} (-1)^j \binom{\alpha_l}{j}. \tag{4} $$

The next iterative type definition, so called $\mathcal{B}$-type difference [24], is the following

$$ {}^{\mathcal{B}}\Delta^{\alpha_l} x_l = \sum_{j=0}^{l} {}^{\mathcal{B}}w(l, j, \alpha_{l-j}) x_{l-j}, \tag{5} $$

where

$$ {}^{\mathcal{B}}w(l, j, \alpha_{l-j}) = \frac{1}{h^{\alpha_{l-j}}} (-1)^j \binom{\alpha_{l-j}}{j}. \tag{6} $$

The recursive type difference definition, so called $\mathcal{D}$-type difference [21], is the following

$$ {}^{\mathcal{D}}\Delta^{\alpha_l} x_l = \frac{x_l}{h^{\alpha_l}} - \sum_{j=1}^{l} {}^{\mathcal{D}}w(l, j, \alpha_l) {}^{\mathcal{D}}\Delta^{\alpha_{l-j}} x_{l-j}, \tag{7} $$

where

$$ {}^{\mathcal{D}}w(l, j, \alpha_l) = (-1)^j \binom{-\alpha_l}{j}. \tag{8} $$

The other type of recursive fractional variable order difference, so called $\mathcal{E}$-type difference [23], is the following

$$ {}^{\mathcal{E}}\Delta^{\alpha_l} x_l = \frac{x_l}{h^{\alpha_l}} - \sum_{j=1}^{l} {}^{\mathcal{E}}w(l, j, \alpha_{l-j}) {}^{\mathcal{E}}\Delta^{\alpha_{l-j}} x_{l-j}, \tag{9} $$

where

$$ {}^{\mathcal{E}}w(l, j, \alpha_{l-j}) = (-1)^j \binom{-\alpha_{l-j}}{j} \frac{h^{\alpha_{l-j}}}{h^{\alpha_l}}. \tag{10} $$

One can see from (9) that for calculation present value of $\mathcal{E}$-type difference all coefficients multiplied by past (early calculated) differences are calculated including the values of past orders.

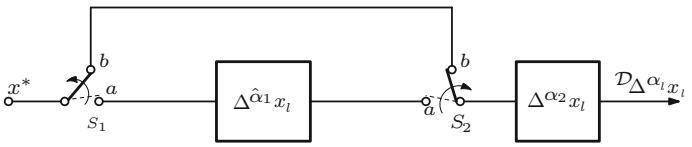

Fig. 1 Simple input-reductive switching scheme of $\mathcal{D}$-type difference (configuration after switching from order α_1 to α_2)

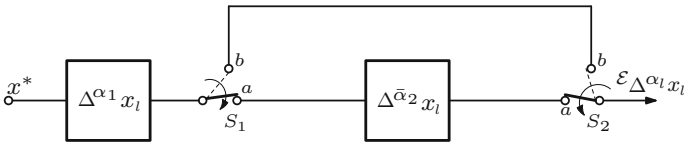

Fig. 2 Simple output-additive switching scheme of $\mathcal{E}$-type difference (configuration after switching from order α_1 to α_2)

2.1 Switching Strategies

In Fig. 1, the simple input-reductive switching scheme equivalent to $\mathcal{D}$-type difference for variable order changing from α_1 to α_2 is presented [21]. The switches S_i, $i = 1, 2$, during the time, take the following positions

$$S_i = \begin{cases} a & \text{for } 0 \le t < T_{\text{sw}}, \\ b & \text{for } t \ge T_{\text{sw}}, \end{cases} \qquad i = 1, 2,$$

where $T_{\text{sw}} = mh$, for some natural number $m \in (0, k)$, and $\hat{\alpha}_1 = \alpha_1 - \alpha_2$.

In Fig. 2, the simple output-additive switching scheme equivalent to $\mathcal{E}$-type difference for variable order changing from α_1 to α_2 is presented [23]. The switches S_i, $i = 1, 2$, during the time, take the following positions

$$S_i = \begin{cases} b & \text{for } 0 \le t < T_{\text{sw}}, \\ a & \text{for } t \ge T_{\text{sw}}, \end{cases} \qquad i = 1, 2,$$

where $T_{\text{sw}} = mh$, for some natural number $m \in (0, k)$, and $\bar{\alpha}_2 = \alpha_2 - \alpha_1$.

3 Fractional Variable Type Differences—Main Result

The $\mathcal{D}$-type and $\mathcal{E}$-type difference definitions differ in the manner of changing in time fractional order. Besides of changing order one can also imagine changing in time the type of difference, that is, for instance,—for some time interval the fractional order can change according to $\mathcal{D}$-type ($\mathcal{E}$-type) difference, and then varied in pursuance

of $\mathcal{E}$-type ($\mathcal{D}$-type) difference. What is crucial in the issue of changing in time type of difference, is (as in the case of changing order) the tactics that can be realized by means of $\mathcal{D}$-type or $\mathcal{E}$-type routines.

3.1 The $\mathfrak{E}$-type Fractional Variable Type and Order Difference

Below, we define variable type difference allowing varying in time a type of changing variable order.

Let $\mathbb{T} = \{\mathcal{D}, \mathcal{E}\}$ be the list of difference definition types symbols, P denotes a sequence of symbols $\mathcal{D}$ and $\mathcal{E}$, and $P_l \in \mathbb{T}$, for $l = 0, \ldots, k$, denote l th element of P.

Definition 1 The $\mathfrak{E}$-type difference of fractional variable type and order is defined as follows

$$^{\mathfrak{E}(P)}\Delta^{\alpha_l} x_l = \frac{x_l}{h^{\alpha_l}} - \sum_{j=1}^{l} {}^{P_{l-j}}w(l, j)\, {}^{\mathfrak{E}(P)}\Delta^{\alpha_{l-j}} x_{l-j}, \tag{11}$$

where

$$^{P_{l-j}}w(l, j) = \begin{cases} {}^{\mathcal{D}}w(l, j, \alpha_l) & \text{for } P_{l-j} = \mathcal{D}, \\ {}^{\mathcal{E}}w(l, j, \alpha_{l-j}) & \text{for } P_{l-j} = \mathcal{E}, \end{cases}$$

according to (8) and (10), respectively.

The definition introduced above is obtained in such a way that all the coefficients multiplied by past (early calculated) differences are calculated for type of changing order that was present for these differences.

3.2 Switching Strategies for Variable Order and Type Differences

In this section, different types of simple switching schemes, that is—switching schemes with only one change of changing order's type, are presented.

In Figs. 3 and 4 are the output-additive switching schemes, where the switches S_i, $i = 1, 2$, during the time, take the following positions

$$S_i = \begin{cases} b & \text{for } 0 \le t < T_{\text{sw}}, \\ a & \text{for } t \ge T_{\text{sw}}, \end{cases} \qquad i = 1, 2,$$

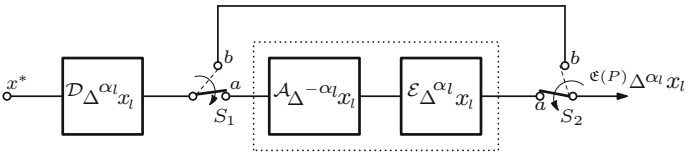

Fig. 3 Simple output-additive switching scheme of $\mathfrak{E}(P)$-type difference, for $P = P^1$ given by (12)

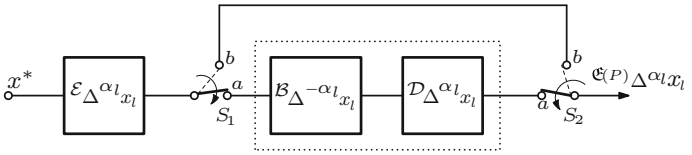

Fig. 4 Simple output-additive switching scheme of $\mathfrak{E}(P)$-type difference, for $P = P^2$ given by (13)

where $T_{\mathrm{sw}} = mh$, for some natural number $m \in (1, k)$. It corresponds, respectively, to the following sequences

$$P_l^1 = \begin{cases} \mathcal{D} & \text{for } l = 0, \ldots, m-1, \\ \mathcal{E} & \text{for } l = m, \ldots, k \end{cases} \tag{12}$$

and

$$P_l^2 = \begin{cases} \mathcal{E} & \text{for } l = 0, \ldots, m-1, \\ \mathcal{D} & \text{for } l = m, \ldots, k. \end{cases} \tag{13}$$

Theorem 1 *The output-additive simple switching schemes presented in Figs. 3 and 4 are equivalent to the $\mathfrak{E}$-type differences for sequences P^1 and P^2 respectively, where the sequences are given by* (12) *and* (13).

Remark 1 The duality property [25] can be applied to obtain the following relation

$$^{\mathcal{A}}\Delta^{\alpha_l\,\mathcal{D}}\Delta^{-\alpha_l}x_l = \sum_{j=0}^{l} {}^{\mathcal{A}}w(l, j, \alpha_l)\,{}^{\mathcal{D}}\Delta^{-\alpha_{l-j}}x_{l-j} = x_l. \tag{14}$$

Proof Let us assume the simple output-reductive switching scheme of $\mathfrak{E}$-type difference, for $P = P^1$ given by (12). For this situation, the variable order and type definition can be rewritten as follows: for $0 \le t < T_{\mathrm{sw}}$ we have

$$^{\mathfrak{E}(P)}\Delta^{\alpha_l}x_l = {}^{\mathcal{D}}\Delta^{\alpha_l}x_l = \frac{x_l}{h^{\alpha_l}} - \sum_{j=1}^{l} {}^{\mathcal{D}}w(l,\, j,\, \alpha_l)\,{}^{\mathcal{D}}\Delta^{\alpha_{l-j}}x_{l-j};$$

for $t \geq T_{\mathrm{sw}}$, where $T_{\mathrm{sw}} = mh$, and $r = l - m + 1$, we have

$$\begin{aligned} ^{\mathfrak{E}(P)}\Delta^{\alpha_l}x_l = \frac{x_l}{h^{\alpha_l}} &- \sum_{j=r}^{l} {}^{\mathcal{D}}w(l,\, j,\, \alpha_l)\,{}^{\mathcal{D}}\Delta^{\alpha_{l-j}}x_{l-j} \\ &- \sum_{j=1}^{r-1} {}^{\mathcal{E}}w(l,\, j,\, \alpha_{l-j})\,{}^{\mathfrak{D}(P)}\Delta^{\alpha_{l-j}}x_{l-j}. \end{aligned} \tag{15}$$

From the switching strategy presented in Fig. 3, and for $0 \leq t < T_{\mathrm{sw}}$, we have:

$$^{\mathfrak{E}(P)}\breve{\Delta}^{\alpha_l}x_l = \frac{x_l}{h^{\alpha_l}} - \sum_{j=1}^{l} {}^{\mathcal{D}}w(l,\, j,\, \alpha_l)\,{}^{\mathfrak{E}(P)}\Delta^{\alpha_{l-j}}x_{l-j} = {}^{\mathcal{D}}\Delta^{\alpha_l}x_l,$$

which is the same as $\mathfrak{E}$-type difference for $0 \leq t < T_{\mathrm{sw}}$.

For $t \geq T_{\mathrm{sw}}$, that is for $l \geq m$, we have

$$^{\mathfrak{E}(P)}\breve{\Delta}^{\alpha_l}x_l = {}_{m}^{\mathcal{E}}\Delta_{l}^{\alpha_l}\,{}_{m}^{\mathcal{A}}\Delta_{l}^{-\alpha_l\,\mathcal{D}}\Delta^{\alpha_l}x_l = \frac{1}{h^{\alpha_l}}\sum_{j=0}^{l-m} {}^{\mathcal{A}}w(l,\, j,\, -\alpha_l)\,{}_{0}^{\mathcal{D}}\Delta_{l}^{-\alpha_{l-j}}x_{l-j} -$$

$$\sum_{j=1}^{l-m} {}^{\mathcal{E}}w(l,\, j,\, \alpha_{l-j})\,{}^{\mathfrak{E}(P)}\breve{\Delta}^{\alpha_{l-j}}x_{l-j} = \frac{1}{h^{\alpha_l}}\sum_{j=0}^{l-m} {}^{\mathcal{A}}w(l,\, j,\, -\alpha_l)\,{}_{0}^{\mathcal{D}}\Delta_{l}^{-\alpha_{l-j}}x_{l-j} +$$

$$\frac{1}{h^{\alpha_l}}\sum_{j=l-m+1}^{l} {}^{\mathcal{A}}w(l,\, j,\, -\alpha_l)\,{}_{0}^{\mathcal{D}}\Delta_{l}^{-\alpha_{l-j}}x_{l-j} -$$

$$\frac{1}{h^{\alpha_l}}\sum_{j=l-m+1}^{l} {}^{\mathcal{A}}w(l,\, j,\, -\alpha_l)\,{}_{0}^{\mathcal{D}}\Delta_{l}^{-\alpha_{l-j}}x_{l-j} -$$

$$\sum_{j=1}^{l-m} {}^{\mathcal{E}}w(l,\, j,\, \alpha_{l-j})\,{}^{\mathfrak{E}(P)}\breve{\Delta}^{\alpha_{l-j}}x_{l-j} = \frac{1}{h^{\alpha_l}}\sum_{j=0}^{l} {}^{\mathcal{A}}w(l,\, j,\, -\alpha_l)\,{}_{0}^{\mathcal{D}}\Delta_{l}^{-\alpha_{l-j}}x_{l-j} -$$

$$\frac{1}{h^{\alpha_l}}\sum_{j=l-m+1}^{l} {}^{\mathcal{A}}w(l,\, j,\, -\alpha_l)\,{}_{0}^{\mathcal{D}}\Delta_{l}^{-\alpha_{l-j}}x_{l-j} - \sum_{j=1}^{l-m} {}^{\mathcal{E}}w(l,\, j,\, \alpha_{l-j})\,{}^{\mathfrak{E}(P)}\breve{\Delta}^{\alpha_{l-j}}x_{l-j} =$$

$$\frac{x_l}{h^{\alpha_l}} - \frac{1}{h^{\alpha_l}} \sum_{j=l-m+1}^{l} {}^{\mathcal{A}}w(l, j-\alpha_l) {}_0^{\mathcal{D}}\Delta_l^{-\alpha_{l-j}} x_{l-j} -$$

$$\sum_{j=1}^{l-m} \mathcal{E}\, w(l, j, \alpha_{l-j})^{\mathfrak{E}(P)} \breve{\Delta}^{\alpha_{l-j}} x_{l-j}.$$

Taking into account that between coefficients of $\mathcal{A}$- and $\mathcal{D}$-type given by (4) and (8) respectively the following holds ${}^{\mathcal{D}}w(l, j, \alpha) = \frac{1}{h^{\alpha_l}} {}^{\mathcal{A}}w(l, j-\alpha_l)$, we obtain

$$\begin{aligned} {}^{\mathfrak{E}(P)}\breve{\Delta}^{\alpha_l} x_l = \frac{x_l}{h^{\alpha_l}} - \sum_{j=1}^{l-m} \mathcal{E}\, w(l, j, \alpha_{l-j})^{\mathfrak{E}(P)} \breve{\Delta}^{\alpha_{l-j}} x_{l-j} \\ - \sum_{j=l-m+1}^{l} {}^{\mathcal{D}}w(l, j, \alpha_l)^{\mathcal{D}} \Delta^{\alpha_{l-j}} x_{l-j}. \end{aligned} \tag{16}$$

By comparison expression (16) from switching strategy with relation (15) from $\mathfrak{E}$-type difference, we obtain ${}^{\mathfrak{E}(P)}\breve{\Delta}^{\alpha_l} x_l = {}^{\mathfrak{E}(P)}\Delta^{\alpha_l} x_l$, which ends the proof.

In the case of equivalence between switching scheme from Fig. 4 and $\mathfrak{E}$-type difference for sequence $P = P^2$ given by (13), the proof is analogous.

4 Numerical Results

Example 1 Let the type of changing the variable order changes at $T_{\mathrm{sw}} = 5\,\mathrm{s}$, the sample time be $h = 0.01\,\mathrm{s}$, the variable order

$$\alpha(t) = \begin{cases} -0.1 & \text{for } 0 \le t < 2, \\ -0.2 & \text{for } 2 \le t < 5, \\ -0.4 & \text{for } 5 \le t < 8, \\ -0.6 & \text{for } 8 \le t < 10, \end{cases}$$

and two sequences P^1 and P^2 given respectively by (12) and (13) for $m = T_{\mathrm{sw}}/h = 500$.

In Fig. 5, the plots of ${}^{\mathfrak{E}(P^1)}\Delta^{\alpha_l} x_l$ and ${}^{\mathfrak{E}(P^2)}\Delta^{\alpha_l} x_l$ compared with corresponding simple switching schemes, realized in Matlab/Simulink [26], are presented.

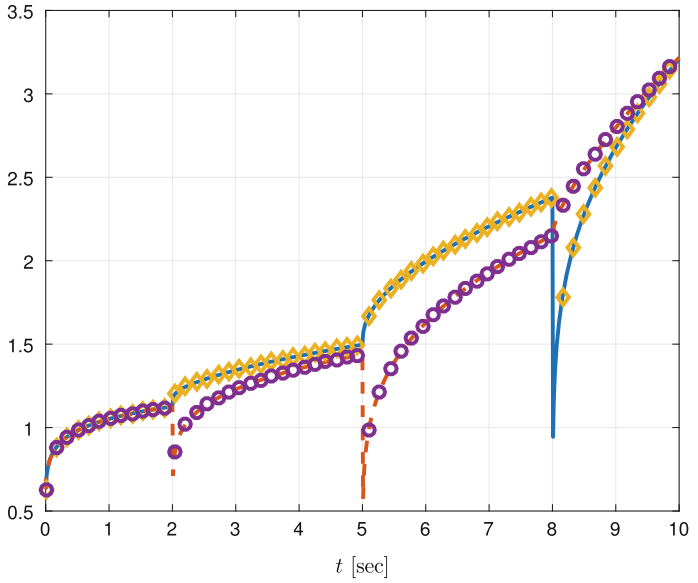

Fig. 5 Plots of ${}^{\mathfrak{E}(P^1)}\Delta^{\alpha_l} x_l$ (*solid line*) and ${}^{\mathfrak{E}(P^2)}\Delta^{\alpha_l} x_l$ (*dashed line*) differences compared with corresponding output-additive switching schemes (*diamonds and circles, respectively*)

5 Conclusion

In the paper, definition of the recursive fractional difference for the case when type of variable order changing is varying in time, has been presented. Definition was introduced together with corresponding equivalent output-additive switching strategies that allow to better understand its dynamical behavior. Proposed definition can be used in control applications, when the type of variable order definition has to be changed in time, and to modelling complex systems, which structure of order changing also depends on time. Finally, numerical results of comparison between definition and corresponding switching schemes were also given.

Acknowledgments This work was supported by the Polish National Science Center with the decision number UMO-2014/15/B/ST7/00480.

References

1. Miller, K., Ross, B.: An Introduction to the Fractional Calculus and Fractional Differential Equations. Wiley, New York (1993)
2. Monje, C.A., Chen, Y., Vinagre, B.M., Xue, D., Feliu, V.: Fractional-Order Systems and Controls. Springer, Berlin (2010)
3. Oldham, K.B., Spanier, J.: The Fractional Calculus. Academic Press, New York (1974)

4. Podlubny, I.: Fractional Differential Equations. Academic Press, San Diego (1999)
5. Samko, S., Kilbas, A., Maritchev, O.: Fractional Integrals and Derivative. Theory and Applications. Gordon & Breach Sci. Publishers, New York (1987)
6. Dzielinski, A., Sierociuk, D.: Fractional order model of beam heating process and its experimental verification. In: Baleanu, D., Guvenc, Z.B., Machado, J.A.T. (eds.) New Trends in Nanotechnology and Fractional Calculus Applications, pp. 287–294. Springer, Netherlands (2010)
7. Sierociuk, D., Dzielinski, A., Sarwas, G., Petras, I., Podlubny, I., Skovranek, T.: Modelling heat transfer in heterogeneous media using fractional calculus. Philos. Trans. Math. Phys. Eng. Sci. **371**(1990), 20120146 (2013)
8. Dzielinski, A., Sarwas, G., Sierociuk, D.: Time domain validation of ultracapacitor fractional order model. In: 49th IEEE Conference on Decision and Control (CDC), pp. 3730–3735 (2010)
9. Dzielinski, A., Sarwas, G., Sierociuk, D.: Comparison and validation of integer and fractional order ultracapacitor models. Adv. Differ. Equ. (2011)
10. Sheng, H., Chen, Y., Qiu, T.: Signal Processing Fractional Processes and Fractional-Order Signal Processing. Springer, London (2012)
11. Sierociuk, D., Macias, M., Malesza, W., Sarwas, G.: Dual estimation of fractional variable order based on the unscented fractional order Kalman filter for direct and networked measurements. Circuit Syst. Signal Process. **35**(6), 2055–2082 (2016)
12. Ostalczyk, P., Rybicki, T.: Variable-fractional-order dead-beat control of an electromagnetic servo. J. Vib. Control **14**(9–10), 1457–1471 (2008)
13. Sierociuk, D., Malesza, W., Macias, M.: Equivalent switching strategy and analog validation of the fractional variable order derivative definition. In: Proceedings of European Control Conference, pp. 3464–3469 (2013)
14. Sierociuk, D., Malesza, W., Macias, M.: On a new definition of fractional variable-order derivative. In: Proceedings of the 14th International Carpathian Control Conference (ICCC), pp. 340–345 (2013)
15. Sierociuk, D., Malesza, W., Macias, M.: Switching scheme, equivalence, and analog validation of the alternative fractional variable-order derivative definition. In: Proceedings of the 52nd IEEE Conference on Decision and Control, pp. 3876-3881 (2013)
16. Sierociuk, D., Macias, M., Malesza, W.: Analog modeling of fractional switched-order derivatives: experimental approach. In: Advances in the Theory and Applications of Non-integer Order Systems, pp. 271–280. Springer International Publishing (2013)
17. Sierociuk, D., Malesza, W., Macias, M.: Derivation, interpretation, and analog modelling of fractional variable order derivative definition. Appl. Math. Model. **39**(13), 3876–3888 (2015)
18. Sierociuk, D., Malesza, W.: On the differences of variable type and variable fractional order. In: Proceedings of European Control Conference. ECC'2016, Aalborg, Denmark (2016, accepted)
19. Malesza, W., Sierociuk, D.: Recursive variable type and order difference, its definition and basic properties. In: 17th International Carpathian Control Conference (ICCC), pp. 473–478 (2016)
20. Lorenzo, C., Hartley, T.: Variable order and distributed order fractional operators. Nonlinear Dyn. **29**(1–4), 57–98 (2002)
21. Sierociuk, D., Malesza, W., Macias, M.: On the recursive fractional variable-order derivative: equivalent switching strategy, duality, and analog modeling. Circuit Syst. Signal Process. **34**(4), 1077–1113 (2015)
22. Valerio, D., da Costa, J.S.: Variable-order fractional derivatives and their numerical approximations. Signal Process. **91**(3), 470–483 (2011)
23. Macias, M., Sierociuk, D.: An alternative recursive fractional variable-order derivative definition and its analog validation. In: Proceedings of International Conference on Fractional Differentiation and its Applications, pp. 1–6 (2014)
24. Malesza, W., Macias, M., Sierociuk, D.: Matrix approach and analog modeling for solving fractional variable order differential equations. In: Latawiec, K.J., Lukaniszyn, M., Stanislawski, R. (eds.) Advances in Modelling and Control of Non-integer-Order Systems. Lecture Notes in Electrical Engineering, vol. 320, pp. 71–80. Springer International Publishing (2015)

25. Sierociuk, D., Twardy, M.: Duality of variable fractional order difference operators and its application to identification. Bull. Pol. Acad.: Tech. **62**(4), 809–815 (2014)
26. Sierociuk, D.: Fractional Variable Order Derivative Simulink Toolkit (2012). http://www.mathworks.com/matlabcentral/fileexchange/38801-fractional-variable-order-derivative-simulink-toolkit

Large Deviations for Stochastic Fractional Differential Equations

Murugan Suvinthra

Abstract In this work, a stochastic fractional differential equation is considered and large deviation principle is established for the corresponding solution distributions. The weak convergence approach, in particular the variational representation for functionals of Brownian motion, is exploited to obtain the large deviation result.

Keywords Large deviation principle · Stochastic fractional differential equations · Weak convergence

1 Introduction

Fractional order models have the tendency to capture non-local relations in space and time, thus forming an improvised model for analyzing complex phenomena. For an introductory study on fractional calculus and fractional derivatives, see the literatures [1, 2]. Inducing randomness into the model helps us to analyze better by taking into consideration the effect of uncertainty, thus leading to stochastic fractional differential equations (refer [3, 4] and references therein). The theory of existence, controllability and stability for fractional differential equations has been studied by many authors (for instance, see [5, 6]). However there seems to be possibly no literature for the study of large deviations for stochastic fractional differential equations.

Large deviations form the study of probabilities of extremely rare events. It is significant to study these rare events because of their heavy impact during their occurrences (one can refer [7–9]). The interlink between the theory of large deviations and stochastic controllability was introduced by Fleming [10]. Following his works, Dupuis and Ellis [11] developed the weak convergence approach to study large deviation principle for random processes. For a detailed description and significance of establishing large deviations using weak convergence approach, one may refer [11, 12]. Using the weak convergence approach, the large deviation principle (LDP)

M. Suvinthra (✉)
Department of Mathematics, Bharathiar University, Coimbatore 641046, India
e-mail: suvinthra@gmail.com

A. Babiarz et al. (eds.), *Theory and Applications of Non-integer Order Systems*,
Lecture Notes in Electrical Engineering 407, DOI 10.1007/978-3-319-45474-0_11

has been established for two-dimensional stochastic Navier–Stokes equations by Sritharan and Sundar [13]; and for stochastic delay differential equations by Mo and Luo [14].

The study of large deviations for stochastic fractional differential equations is a newly emerging area and there seems possibly no previous literature. Introducing non-integer order derivatives in the estimation of rate function using large deviation theory produces relatively good accuracy in the results and can be applied to a variety of problems based on the model chosen. Indeed they can be applied to determine the time of exit of a certain measure from a desired domain, to calculate the entropy in statistical mechanics and also to predict the rate of convergence of a dynamical system to the desired output.

In this paper, we consider the stochastic fractional differential equations with multiplicative type Gaussian noise perturbation and establish the LDP for the solution processes. To deal with this multiplicative noise type, we use the variational representations developed by Budhiraja and Dupuis [15] which require a compactness argument and a weak convergence result. A sequential compactness argument is made by introducing a control term and considering the associated control equation. The weak convergence result is obtained by means of defining measurable maps corresponding to controlled perturbed stochastic differential equations and then studying the convergence of the solution processes.

2 Preliminaries

Consider the nonlinear stochastic fractional differential equation of the form

$$\begin{aligned} {}^{C}D^{\alpha}x(t) &= Ax(t) + f(t, x(t)) + \sigma(t, x(t))\tfrac{\mathrm{d}W(t)}{\mathrm{d}t},\ t \in (0, T], \\ x(0) &= x_0, \end{aligned} \tag{1}$$

where $\frac{1}{2} < \alpha \leq 1, x_0 \in \mathbb{R}^n, A$ is an $n \times n$ matrix and for $J := [0, T], f : J \times \mathbb{R}^n \to \mathbb{R}^n$; $\sigma : J \times \mathbb{R}^n \to \mathbb{R}^{n\times m}$. Also $W(\cdot)$ is an m-dimensional Wiener process.

Assume that the nonlinear drift and diffusion coefficients satisfy Lipschitz condition: For all $x_1, x_2 \in \mathbb{R}^n$ and $t \in J$, there exist constants $L_1, L_2 > 0$ with

$$\|f(t, x_1) - f(t, x_2)\| \leq L_1\|x_1 - x_2\|, \tag{2}$$

$$\|\sigma(t, x_1) - \sigma(t, x_2)\| \leq L_2\|x_1 - x_2\|. \tag{3}$$

The Lipschitz continuity immediately yields the linear growth property and hence, for all $x \in \mathbb{R}^n$, there exists some constant, say $K > 0$ such that

$$\|f(t, x)\|^2 \leq K(1 + \|x\|^2);\ \ \|\sigma(t, x)\|^2 \leq K(1 + \|x\|^2). \tag{4}$$

Let us recall some basic definitions from the fractional calculus. For $\alpha, \beta > 0$, with $n-1 < \alpha < n$, $n-1 < \beta < n$ and $n \in \mathbb{N}$, D is the usual differential operator and suppose $f \in L_1(\mathbb{R}_+), \mathbb{R}_+ = [0, \infty)$. The following definitions and properties are well known (see, for instance, [1, 2]):

(i) Caputo fractional derivative:
The Riemann Liouville fractional integral of a function f is defined by

$$I^{\alpha} f(t) = \frac{1}{\Gamma(\alpha)} \int_0^t (t-s)^{\alpha-1} f(s) \mathrm{d}s,$$

and the Caputo derivative of f is

$${}^{C}D^{\alpha} f = I^{n-\alpha} D^n f = \frac{1}{\Gamma(n-\alpha)} \int_0^t (t-s)^{n-\alpha-1} f^{(n)}(s) \mathrm{d}s,$$

where the function $f(t)$ has absolutely continuous derivatives upto order $n-1$.

(ii) Mittag–Leffler matrix function:

$$E_{\alpha,\beta}(A) = \sum_{k=0}^{\infty} \frac{A^k}{\Gamma(k\alpha + \beta)}.$$

In particular, for $\beta = 1$,

$$E_{\alpha}(A) = \sum_{k=0}^{\infty} \frac{A^k}{\Gamma(k\alpha + 1)}.$$

The solution representation of (1) is given by

$$\begin{aligned} x(t) =& E_{\alpha}(At^{\alpha}) x_0 + \int_0^t (t-s)^{\alpha-1} E_{\alpha,\alpha}(A(t-s)^{\alpha}) f(s, x(s)) \mathrm{d}s \\ &+ \int_0^t (t-s)^{\alpha-1} E_{\alpha,\alpha}(A(t-s)^{\alpha}) \sigma(s, x(s)) \mathrm{d}W(s). \end{aligned} \tag{5}$$

We now present some basic definitions and results from large deviation theory. For this, let $\{\Omega, \mathcal{F}, \mathbf{P}\}$ be a complete filtered probability space equipped with a complete family of right continuous increasing sub σ-algebras $\{\mathcal{F}_t, t \in J\}$ satisfying $\{\mathcal{F}_t \subset \mathcal{F}\}$, and $\{X^{\epsilon}\}$ be a family of random variables defined on this space and taking values in a Polish space E (that is, a complete separable metric space E).

Definition 1 (*Rate Function*) A function $I : E \to [0, \infty]$ is called a rate function if I is lower semicontinuous. A rate function I is called a good rate function if, for each $N < \infty$, the level set $K_N = \{f \in E : I(f) \leq N\}$ is compact in E.

Definition 2 (*Large Deviation Principle*) Let I be a rate function on E. We say the sequence $\{X^\epsilon\}$ satisfies the large deviation principle with rate function I if the following two conditions hold:
(i) *L*arge deviation upper bound. For each closed subset F of E,

$$\limsup_{\epsilon\to 0} \epsilon \log \mathbf{P}(X^\epsilon \in F) \leq -I(F).$$

(ii) *L*arge deviation lower bound. For each open subset G of E,

$$\liminf_{\epsilon\to 0} \epsilon \log \mathbf{P}(X^\epsilon \in G) \geq -I(G).$$

3 Large Deviation Principle

Since X^ϵ is a strong solution to (1) (refer [3]), the Yamada–Watanabe theorem assures that there exists a Borel-measurable function $G^\epsilon : C\big(J;\mathbb{R}^m\big) \to C\big(J;\mathbb{R}^n\big)$ such that $X^\epsilon(\cdot) = G^\epsilon\big(W(\cdot)\big)$ a.s.
Let

$$\mathcal{A} = \left\{ v : v \text{ is } \mathbb{R}^m\text{-valued } \mathcal{F}_t\text{-predictable process and} \int_0^T \|v(s,\omega)\|^2 \mathrm{d}s < \infty \text{ a.s.} \right\},$$

$$S_N = \left\{ v \in L^2\big(0,T;\mathbb{R}^m\big) : \int_0^T |v(s)|^2 \mathrm{d}s \leq N \right\},$$

where $L^2\big(0,T;\mathbb{R}^m\big)$ is the space of all $\mathbb{R}^m$ -valued square integrable functions on J. Then S_N endowed with the weak topology in $L^2\big(0,T;\mathbb{R}^m\big)$ is a compact Polish space. Let us also define

$$\mathcal{A}_N = \{ v \in \mathcal{A} : v(\omega) \in S_N \ \mathbf{P} - a.s \}.$$

We formulate (from Theorem 4.4 in [15]) the following sufficient conditions under which the Laplace principle holds for the family $\{X^\epsilon : \epsilon > 0\}$ (see [14]).
(A) There exists a measurable map $G^0 : C\big(J;\mathbb{R}^m\big) \to C\big(J;\mathbb{R}^n\big)$ such that the following two conditions hold:

(i) Let $\{v^\epsilon : \epsilon > 0\} \subset \mathcal{A}_N$ for some $N < \infty$. If v^ϵ converge to v in distribution as S_N-valued random elements, then

$$G^\epsilon\left(W(\cdot) + \frac{1}{\sqrt{\epsilon}} \int_0^\cdot v^\epsilon(s)\mathrm{d}s\right) \to G^0\left(\int_0^\cdot v(s)\mathrm{d}s\right) \text{ in distribution as } \epsilon \to 0.$$

(ii) For each N$< \infty$, the set $K_N = \left\{ G^0 \left(\int_0^{\cdot} v(s)\mathrm{d}s \right) : v \in S_N \right\}$ is a compact subset of $C\big(J; \mathbb{R}^n\big)$.

Consider the controlled equation associated with (1) with control $v \in S_N$:

$$\begin{aligned} {}^{C}D^{\alpha}x(t) &= Ax(t) + f(t, x(t)) + \sigma(t, x(t))v(t), \\ x(0) &= x_0. \end{aligned} \tag{6}$$

Let x_v denote the solution of the Eq. (6). Now we state the main result in this section, which is a Freidlin–Wentzell type theorem.

Theorem 1 *The family $\{X^{\epsilon}(t)\}$ of (1) satisfies the large deviation principle (equivalently, Laplace principle) in $C\big(J; \mathbb{R}^n\big)$ with good rate function*

$$I(f) := \inf \left\{ \frac{1}{2} \int_0^T \|v(t)\|^2 \mathrm{d}t; x_v = f \right\}, \tag{7}$$

where $v \in L^2\big(0, T; \mathbb{R}^m\big)$; otherwise, $I(f) = \infty$.

In view of Theorem 4.4 in [15], the Proof of Theorem 3.1 is reduced to verifying the two hypotheses in assumption (A). We begin with the following compactness argument.

Lemma 1 (Compactness) *Define $G^0 : C\big(J; \mathbb{R}^m\big) \to C\big(J; \mathbb{R}^n\big)$ by*

$$G^0(g) := \begin{cases} x_v, & \text{if } g = \int_0^{\cdot} v(s)\mathrm{d}s \text{ for some } v \in L^2\big(0, T; \mathbb{R}^m\big), \\ 0\ , & \text{otherwise}. \end{cases}$$

Then, for each $N < \infty$, the set

$$K_N = \left\{ G^0 \left(\int_0^{\cdot} v(s)\mathrm{d}s \right) : v \in S_N \right\}$$

is a compact subset of $C\big(J; \mathbb{R}^n\big)$.

Proof Consider a sequence $\{v_n\} \in S_N$ such that $v_n \to v$ weakly in S_N as $n \to \infty$. Let $x_n(t)$ be the solution of (6) with v replaced by v_n. Define $y_n(t) := x_n(t) - x(t)$. Then

$$\begin{aligned} {}^{C}D^{\alpha}y_n(t) &= Ay_n(t) + f(t, x_n(t)) - f(t, x(t)) + \sigma(t, x_n(t))v_n(t) - \sigma(t, x(t))v(t), \\ y_n(0) &= 0. \end{aligned} \tag{8}$$

The solution representation for the Eq. (8) is given by

$$y_n(t) = \int_0^t (t-s)^{\alpha-1} E_{\alpha,\alpha}(A(t-s)^\alpha)[f(s, x_n(s)) - f(s, x(s))]\mathrm{d}s + \int_0^t (t-s)^{\alpha-1} E_{\alpha,\alpha}(A(t-s)^\alpha)[\sigma(s, x_n(s))v_n(s) - \sigma(s, x(s))v(s)]\mathrm{d}s. \quad (9)$$

Then

$$\begin{aligned}\|y_n(t)\| \leq & M \int_0^t (t-s)^{\alpha-1} \|f(s, x_n(s)) - f(s, x(s))\|\mathrm{d}s \\ & + M \int_0^t (t-s)^{\alpha-1} \|\sigma(s, x_n(s)) - \sigma(s, x(s))\| \|v_n(s)\|\mathrm{d}s \\ & + M \left\| \int_0^t (t-s)^{\alpha-1} \sigma(s, x(s))(v_n(s) - v(s))\mathrm{d}s \right\|. \end{aligned} \quad (10)$$

Using the Lipschitz condition on f and σ given by (2) and (3), we have

$$\begin{aligned}\|y_n(t)\| \leq & ML_1 \int_0^t (t-s)^{\alpha-1} \|y_n(s)\|\mathrm{d}s + ML_2 \int_0^t (t-s)^{\alpha-1} \|y_n(s)\| \|v_n(s)\|\mathrm{d}s \\ & + M \left\| \int_0^t (t-s)^{\alpha-1} \sigma(s, x(s))(v_n(s) - v(s))\mathrm{d}s \right\|. \end{aligned} \quad (11)$$

Applying Gronwall's inequality, we get

$$\begin{aligned}\|y_n(t)\| &\leq M \left\| \int_0^t (t-s)^{\alpha-1} \sigma(s, x(s))(v_n(s) - v(s))\mathrm{d}s \right\| \\ &\quad \times \exp\left(ML_1 \int_0^t (t-s)^{\alpha-1}\mathrm{d}s + ML_2 \int_0^t (t-s)^{\alpha-1} \|v_n(s)\|\mathrm{d}s \right) \\ &\leq M \left\| \int_0^t (t-s)^{\alpha-1} \sigma(s, x(s))(v_n(s) - v(s))\mathrm{d}s \right\| \\ &\quad \times \exp\left(\frac{ML_1 T^\alpha}{\alpha} + \frac{1}{2\alpha - 1} ML_2 T^{2\alpha-1} + MN \right). \end{aligned} \quad (12)$$

Let

$$\zeta^n(t) = \int_0^t (t-s)^{\alpha-1} \sigma(s, x(s))(v_n(s) - v(s))\mathrm{d}s. \quad (13)$$

Observe that $\{\zeta^n(t)\}$ is a family of linear, continuous real-valued functions mapping S_N to $C(J; \mathbb{R}^n)$.

Also notice that the family $\{\zeta^n(t)\}$ is uniformly bounded by C. Hence $\{\zeta^n\}$ is equicontinuous.

Also observe from (13) that as $v_n \to v$ weakly in $L^2\big(0, T; \mathbb{R}^m\big)$, $\zeta^n(t) \to 0$ pointwise for $t \in J$. With these observations, an application of Arzéla-Ascoli theorem immediately implies that $\zeta^n \to 0$ in $C\big(J; \mathbb{R}^n\big)$. Hence

$$\lim_{n\to\infty} \sup_{t\in J} \|\zeta^n(t)\| = 0. \tag{14}$$

Combining this observation with (12) yields the continuity of the map $v \to x_v(t)$. Since the space S_N is compact and since $v \to x_v(t)$ is continuous, the set $K_N = \big\{G^0\big(\int_0^{\cdot} v(s)\mathrm{d}s\big) : v \in S_N\big\}$ for $N < \infty$ is compact.

Lemma 2 (Weak Convergence) *Let $\{v^\epsilon : \epsilon > 0\} \subset \mathcal{A}_N$ for some $N < \infty$. Assume v^ϵ converges to v in distribution as S_N-valued random elements, then*

$$G^\epsilon\left(W(\cdot) + \frac{1}{\sqrt{\epsilon}}\int_0^{\cdot} v^\epsilon(s)\mathrm{d}s\right) \to G^0\left(\int_0^{\cdot} v(s)\mathrm{d}s\right)$$

in distribution as $\epsilon \to 0$.

Proof Consider the nonlinear stochastic fractional differential equation with control $v \in S_N$ of the form

$$\begin{aligned} {}^{C}D^{\alpha}x^\epsilon(t) &= Ax^\epsilon(t) + f(t, x^\epsilon(t)) + \sigma(t, x^\epsilon(t))v^\epsilon(t) + \sqrt{\epsilon}\sigma(t, x^\epsilon(t))\tfrac{\mathrm{d}W(t)}{\mathrm{d}t}, \\ x(0) &= x_0. \end{aligned} \tag{15}$$

The solution representation of (15) is given by

$$\begin{aligned} x^\epsilon(t) = {} & E_\alpha(At^\alpha)x_0 + \int_0^t (t-s)^{\alpha-1}E_{\alpha,\alpha}(A(t-s)^\alpha)f(s, x^\epsilon(s))\mathrm{d}s \\ & + \int_0^t (t-s)^{\alpha-1}E_{\alpha,\alpha}(A(t-s)^\alpha)\sigma(s, x^\epsilon(s))v^\epsilon(s)\mathrm{d}s \\ & + \sqrt{\epsilon}\int_0^t (t-s)^{\alpha-1}E_{\alpha,\alpha}(A(t-s)^\alpha)\sigma(s, x^\epsilon(s))\mathrm{d}W(s). \end{aligned} \tag{16}$$

Take $y^\epsilon(t) = x^\epsilon(t) - x(t)$, where $x(\cdot)$ denotes the solution of the controlled equation (6). Then

$$\begin{aligned} y^\epsilon(t) = {} & \int_0^t (t-s)^{\alpha-1}E_{\alpha,\alpha}(A(t-s)^\alpha)[f(s, x^\epsilon(s)) - f(s, x(s))]\mathrm{d}s \\ & + \int_0^t (t-s)^{\alpha-1}E_{\alpha,\alpha}(A(t-s)^\alpha)[\sigma(s, x^\epsilon(s))v^\epsilon(s) - \sigma(s, x(s))v(s)]\mathrm{d}s \\ & + \sqrt{\epsilon}\int_0^t (t-s)^{\alpha-1}E_{\alpha,\alpha}(A(t-s)^\alpha)\sigma(s, x^\epsilon(s))\mathrm{d}W(s). \end{aligned} \tag{17}$$

Then, using Holder's inequality, the Lipschitz continuity (2) and (3) and further simplifying, we get

$$\begin{aligned}\|y^{\epsilon}(t)\|^2 \leq\, & 4\left\|\int_0^t (t-s)^{\alpha-1}E_{\alpha,\alpha}(A(t-s)^{\alpha})[f(s,x^{\epsilon}(s))-f(s,x(s))]\mathrm{d}s\right\|^2 \\ & + 4\left\|\int_0^t (t-s)^{\alpha-1}E_{\alpha,\alpha}(A(t-s)^{\alpha})[\sigma(s,x^{\epsilon}(s))-\sigma(s,x(s))]v^{\epsilon}(s)\mathrm{d}s\right\|^2 \\ & + 4\left\|\int_0^t (t-s)^{\alpha-1}E_{\alpha,\alpha}(A(t-s)^{\alpha})\sigma(s,x(s))(v^{\epsilon}(s)-v(s))\mathrm{d}s\right\|^2 \\ & + 4\epsilon\left\|\int_0^t (t-s)^{\alpha-1}E_{\alpha,\alpha}(A(t-s)^{\alpha})\sigma(s,x^{\epsilon}(s))\mathrm{d}W(s)\right\|^2 \qquad (18) \\ \leq\, & 4M^2L_1^2\frac{T^{2\alpha-1}}{2\alpha-1}\int_0^t \|y^{\epsilon}(s)\|^2\mathrm{d}s + 4M^2L_2^2\frac{T^{2\alpha-1}}{2\alpha-1}\int_0^t \|y^{\epsilon}(s)\|^2\|v^{\epsilon}(s)\|^2\mathrm{d}s \\ & + 4\left\|\int_0^t (t-s)^{\alpha-1}E_{\alpha,\alpha}(A(t-s)^{\alpha})\sigma(s,x(s))(v^{\epsilon}(s)-v(s))\mathrm{d}s\right\|^2 \\ & + 4\epsilon\left\|\int_0^t (t-s)^{2\alpha-2}E_{\alpha,\alpha}(A(t-s)^{\alpha})\sigma(s,x^{\epsilon}(s))\mathrm{d}W(s)\right\|^2. \qquad (19)\end{aligned}$$

Taking expectation and applying Burkholder–Davis–Gundy inequality for the stochastic integral term, one gets

$$\begin{aligned}\mathrm{e}\|y^{\epsilon}(t)\|^2 \leq\, & 4M^2\frac{T^{2\alpha-1}}{2\alpha-1}\mathrm{e}\int_0^t \|y^{\epsilon}(s)\|^2\left(L_1^2+L_2^2\|v^{\epsilon}(s)\|^2\right)\mathrm{d}s \\ & + 4\left\|\int_0^t (t-s)^{\alpha-1}E_{\alpha,\alpha}(A(t-s)^{\alpha})\sigma(s,x(s))(v^{\epsilon}(s)-v(s))\mathrm{d}s\right\|^2 \\ & + 4\epsilon M^2\frac{T^{2\alpha-1}}{2\alpha-1}\mathrm{e}\int_0^t \|\sigma(s,x^{\epsilon}(s))\|^2\mathrm{d}s. \qquad (20)\end{aligned}$$

Applying Gronwall's inequality and using the linear growth property (4), one gets

$$\begin{aligned}\sup_{t\in J}\mathrm{e}\|y^{\epsilon}(t)\|^2 \leq\, & \left\{4\left\|\int_0^t (t-s)^{\alpha-1}E_{\alpha,\alpha}(A(t-s)^{\alpha})\sigma(s,x(s))(v^{\epsilon}(s)-v(s))\mathrm{d}s\right\|^2\right. \\ & \left. + 8\epsilon M^2K^2\frac{T^{2\alpha-1}}{2\alpha-1}\mathrm{e}\int_0^t (1+\|x^{\epsilon}(s)\|^2)\mathrm{d}s\right\}\exp\left(4M^2\frac{T^{2\alpha-1}}{2\alpha-1}(L_1^2+L_2^2N)\right). \qquad (21)\end{aligned}$$

As before, we define

$$\zeta^{\epsilon}(t) = \int_0^t (t-s)^{\alpha-1}E_{\alpha,\alpha}(A(t-s)^{\alpha})\sigma(s,x(s))(v^{\epsilon}(s)-v(s))\mathrm{d}s.$$

Define

$$f(u) = \int_0^t (t-s)^{\alpha-1} E_{\alpha,\alpha}(A(t-s)^{\alpha})\sigma(s, x(s))u(s)\mathrm{d}s.$$

Due to the linear growth of σ and h, the map $f : S_N \to C\big(J; \mathbb{R}\big)$ is a bounded continuous function. Note that S_N is endowed with the weak topology and v^{ϵ} converge to v in distribution as S_N-valued random elements. Then $\zeta^{\epsilon} \to 0$ in distribution as $\epsilon \to 0$ follows immediately by Theorem A.3.6 in [11].

Using this fact in (21) yields the convergence in distribution of y^{ϵ} to 0 as $\epsilon \to 0$ and the lemma is established.

References

1. Kilbas, A., Srivastava, H.M., Trujillo, J.J.: Theory and Applications of Fractional Differential Equations. Elsevier, New York (2006)
2. Miller, K.S., Ross, B.: An Introduction to the Fractional Calculus and Fractional Differential Equations. Wiley, New York (1993)
3. Mabel Lizzy, R., Balachandran, K., Suvinthra, M.: Controllability of nonlinear stochastic fractional systems. J. Appl. Math. Inform. (under review)
4. Pedjeu, J.C., Ladde, G.S.: Stochastic fractional differential equations: modelling, method and analysis. Chaos Solitons Fract. **45**, 279–293 (2012)
5. Balachandran, K., Kiruthika, S., Trujillo, J.J.: Existence results for fractional impulsive integrodifferential equations in banach spaces. Commun. Nonlinear Sci. Numer. Simul. **16**, 1970–1977 (2011)
6. Kamrani, M.: Numerical solution of stochastic fractional differential equations. Numer. Algorithms **68**, 81–93 (2015)
7. Dembo, A., Zeitouni, O.: Large Deviations Techniques and Applications. Springer, New York (2007)
8. Freidlin, M.I., Wentzell, A.D.: On small random perturbations of dynamical systems. Russ. Math. Surv. **25**, 1–55 (1970)
9. Varadhan, S.R.S.: Asymptotic probabilities and differential equations. Comm. Pure Appl. Math. **19**, 261–286 (1966)
10. Fleming, W.H.: A stochastic control approach to some large deviations problems. In: Dolcetta, C., Fleming, W.H., Zolezzi, T. (eds.) Recent Mathematical Methods in Dynamic Programming, Springer Lecture Notes in Mathematics, vol. 1119, pp. 52–66 (1985)
11. Dupuis, P., Ellis, R.S.: A Weak Convergence Approach to the Theory of Large Deviations. Wiley-Interscience, New York (1997)
12. Boue, M., Dupuis, P.: A variational representation for certain functionals of Brownian motion. Ann. Probab. **26**, 1641–1659 (1998)
13. Sritharan, S.S., Sundar, P.: Large deviations for two dimensional Navier–Stokes equations with multiplicative noise. Stochast. Process. Appl. **116**, 1636–1659 (2006)
14. Mo, C., Luo, J.: Large deviations for stochastic differential delay equations. Nonlinear Anal. **80**, 202–210 (2013)
15. Budhiraja, A., Dupuis, P.: A variational representation for positive functionals of infinite dimensional Brownian motion. Probab. Math. Statist. **20**, 39–61 (2000)

Mean Square Stability of Discrete-Time Fractional Order Systems With Multiplicative Noise

Viorica Mariela Ungureanu and Mădălina Roxana Buneci

Abstract This paper studies stability problems for a class of discrete-time linear fractional systems (LFSs) affected by multiplicative, independent random perturbations. Sufficient conditions for the mean square (MS) stability and mean square asymptotic (MSA) stability properties of the stochastic LFSs are given. A numerical simulation illustrates the effectiveness of the theory.

Keywords Fractional order systems · Discrete-time stochastic systems · Mean square stability · Mean square asymptotic stability

1 Introduction

Fractional calculus (FC) has a long history which goes back to Leibniz who introduced the notion of "$\frac{1}{2}$-order derivative" in a letter to L'Hospital from 1695. Nowadays FC finds important applications in different areas of applied science including electrochemistry, electromagnetism, biophysics, quantum mechanics, radiation physics or control theory (see [1, 2] and the references therein). For example, fractional partial differential equations were used to model the wave propagation in viscoelastic media as well as the dissipation in seismology or in metallurgy [3]. Also, certain adaptive and robust control algorithms (as the one used for the lateral control of autonomous guided vehicle) can be improved by applying various fractional adaptation schemes for the adjustment of the feed-forward gain [4].

In many situations, the real-world phenomena are affected by random factors that exercised a decisive influence in the process evolution. The properties of discrete-time linear systems affected by independent random perturbations and their applications have attracted a lot of interest from the scientific community in the last decades (see

V.M. Ungureanu (✉) · M.R. Buneci
Constantin Brâncuşi University of Târgu-Jiu, Calea Eroilor Nr. 30,
210135 Targu-Jiu, Romania
e-mail: vio@utgjiu.ro

M.R. Buneci
e-mail: ada@utgjiu.ro

A. Babiarz et al. (eds.), *Theory and Applications of Non-integer Order Systems*,
Lecture Notes in Electrical Engineering 407, DOI 10.1007/978-3-319-45474-0_12

for e.g. [5, 6] and the references therein). In this paper we study the asymptotic behavior of the solutions for a class of discrete-time LFSs perturbed by sequences of independent scalars with zero mean and variance $b > 0$. As far as we know this subject seems to be new for linear discrete-time fractional systems (DTFSs) with multiplicative random perturbations. Some recent papers (see for e.g. [7] and the references therein) study various properties of linear stochastic DTFSs only for the case of additive noise.

In the deterministic case, different stability results for linear DTFSs were obtained in [1, 8–11] and the included references. In the stochastic case, we shall prove that similar conditions to those given in the deterministic case (see Criterion 2 from [1], p. 66) are sufficient to ensure the mean square boundedness of the LFSs' solutions (see Proposition 1). Based on Proposition 1, we then derive a mean square stability criterion (see Theorem 1) and sufficient conditions for the MSA stability of the solutions (see Theorem 2). Finally, a numerical simulation is provided to illustrate these results.

2 Notations

As usual, we shall write $\langle ., . \rangle$ for the inner product and $\|.\|$ for norms of elements and operators, unless indicated otherwise. Let $d \in \mathbb{N}^* = \mathbb{N} - \{0\}$ and $L\left(\mathbb{R}^d\right)$ be the real linear space of all linear operators from $\mathbb{R}^d$ to $\mathbb{R}^d$. For any $T \in L\left(\mathbb{R}^d\right)$ we denote by T^* the adjoint operator of T. Through this paper we shall use three norms of an operator $T \in L\left(\mathbb{R}^d\right)$: the operatorial norm $\|T\| = \sup_{x \in \mathbb{R}^d} \frac{\|Tx\|}{\|x\|}$, the nuclear norm $\|T\|_1 = Tr\left[\sqrt{T^*T}\right] < \infty$ and the Hilbert-Schmidt norm $\|T\|_2 = \sqrt{Tr\left[T^*T\right]} < \infty$ [12, 13]. Here Tr [.] is the trace operator. For example, the operator $x \otimes x, x \in \mathbb{R}^d$, defined by $x \otimes x\,(h) = \langle h, x \rangle x$ for all $h \in \mathbb{R}^d$ has the property that $\|x \otimes x\| = \|x \otimes x\|_1 = \|x \otimes x\|_2 = \|x\|^2$.

The convergence of a double sequence $x = \{x_{j,k}\}_{i,j \in \mathbb{N}} \in \mathbb{R}^d$ will be defined in the Pringsheim's sense [14] as it follows: $x = \{x_{j,k}\}_{i,j \in \mathbb{N}} \in \mathbb{R}^d$ is said to *converge* to the limit l if for every $\varepsilon > 0$, there is a positive integer N_ε such that $\left\|x_{j,k} - l\right\| < \varepsilon$ for all $j, k > N_\varepsilon$. If, in addition, the double sequence x is bounded, i.e. $\|x\|_\infty = \sup_{i,j \in \mathbb{N}} \left\|x_{j,k}\right\| < \infty$, then x is said to be *boundedly convergent* to l. A double series $\sum_{i,j=0}^{\infty} x_{j,k}$ is *boundedly convergent*, if its partial sums are boundedly convergent.

Let $(\Omega, \mathcal{F}, P)$ be a probability space. For any integrable random variable ξ on $(\Omega, \mathcal{F}, P)$, we write $E[\xi]$ for its mean (expectation). We will denote by $L^2\left(\Omega, \mathbb{R}^d\right)$, the Hilbert space of all $\mathbb{R}^d$ valued random variables ξ with the property $E\left[\|\xi\|^2\right] < \infty$. For any $\xi \in L^2\left(\Omega, \mathbb{R}^d\right)$, the linear operator $E\,(\xi \otimes \xi)$ defined by $E\,(\xi \otimes \xi)\,(h) = E\,(\langle h, \xi \rangle \xi)\,, h \in H$ has the property that $\|E\,(\xi \otimes \xi)\|_1 = E\,\|\xi\|^2$ and it is called the *correlation operator* of the random variable ξ [4]. If ξ,

$\eta \in L^2(\Omega, \mathbb{R}^p)$, then $E(\xi \otimes \eta)(h) := E(\langle h, \eta \rangle \xi)$, $h \in \mathbb{R}^p$ is a linear operator and $\|E(\xi \otimes \eta)\|_1 \leq E\|\xi\|^2 E\|\eta\|^2$.

3 Discrete-time Fractional Order Systems with Stochastic Perturbations

Let $\mathbb{R}_+^* = \{x \in \mathbb{R}, x > 0\}$ and $\alpha \in \mathbb{R}_+^*$, $\alpha < 2$ be fixed. For all $j \in \mathbb{N}$, let $\binom{\alpha}{j}$ denote the generalized binomial coefficient

$$\binom{\alpha}{j} := \begin{cases} 1, j = 0 \\ \frac{\alpha(\alpha-1)\cdots(\alpha+1-j)}{j!}, j > 0 \end{cases}.$$

In this paper we consider the Grünwald–Letnikov's definition of the fractional-order operators

$$\Delta^{[\alpha]} x_{k+1} = \frac{1}{h^\alpha} \sum_{j=0}^{k+1} (-1)^j \binom{\alpha}{j} x_{k+1-j},$$

where $h \in \mathbb{R}_+^*$ is the sampling period or the time increment.

Let $\{\xi_k\}_{k\in\mathbb{N}}$ be a sequence of real-valued, mutually independent random variables on $(\Omega, \mathcal{F}, P)$ satisfying $E[\xi_k] = 0$ and $E\left[\xi_k^2\right] = b < \infty$ for all $k \in \mathbb{N}$. We consider the discrete-time fractional system

$$\Delta^{[\alpha]} x_{k+1} = \mathbb{A} x_k + \xi_k \mathbb{B} x_k, k \in \mathbb{N} \tag{1}$$

$$x_0 = x \in \mathbb{R}^d, \tag{2}$$

where $\mathbb{A}$, $\mathbb{B}$ are real d-dimensional matrices. Note that in the rest of the paper we do not distinguish between the matrix and the linear operator defined by it.

As in [15], we see that $h^\alpha \Delta^{[\alpha]} x_{k+1} = \sum_{j=0}^{k+1} (-1)^j \binom{\alpha}{j} x_{k+1-j}$. Multiplying (1) by h^α and using the last relation, we get

$$x_{k+1} = (h^\alpha \mathbb{A} + \alpha I_{\mathbb{R}^d}) x_k + \sum_{j=1}^{k} (-1)^j \binom{\alpha}{j+1} x_{k-j} + \xi_k h^\alpha \mathbb{B} x_k.$$

Denoting $A_0 = h^\alpha \mathbb{A} + \alpha I_{\mathbb{R}^d}$, $B = h^\alpha \mathbb{B}$, $c_j := (-1)^j \binom{\alpha}{j+1}$ and $A_j = c_j I_{\mathbb{R}^d}$, system (1) can be equivalently rewritten as

$$x_{k+1} = \sum_{j=0}^{k} A_j x_{k-j} + \xi_k B x_k, \tag{3}$$

$$x_0 = x \in \mathbb{R}^d. \tag{4}$$

Let $\mathcal{F}_n$, $n \in \mathbb{N}^*$ denotes the $\sigma-$ algebra generated by $\{\xi_i, 0 \leq i \leq n-1\}$. Obviously (3)–(4) has a unique solution which belongs to $L^2\left(\Omega, \mathbb{R}^d\right)$. Moreover,

$$x_1 = (A_0 + \xi_0 B)\, x_0, x_2 = (A_0 + \xi_1 B)\, x_1 + A_1 x_0,$$
$$x_3 = (A_0 + \xi_2 B)\, x_2 + A_1 x_1 + A_2 x_0, ..$$

Let us introduce the sequence $G_k, k \in \mathbb{N}$ defined recursively by $G_0 = I_{\mathbb{R}^d}$ and

$$G_{k+1} = (A_0 + \xi_k B)\, G_k + \sum_{j=1}^{k} A_j G_{k-j}, k \geq 1.$$

A simple computation and an induction argument show that $x_k = G_k x_0$ for all $k \in \mathbb{N}$. The operator G_k will be termed *the random solution operator* associated with the fractional system (3). It is not difficult to prove that G_k is $\mathcal{F}_k$-measurable for all $k \in \mathbb{N}^*$ and G_k, ξ_n are independent for $n \geq k$. It follows that x_k is $\mathcal{F}_k$-measurable and ξ_n independent for all $n \geq k > 0$.

Let us introduce the following mean square Lyapunov type stability notions (see for e.g. [16] for deterministic systems).

Definition 1 The null solution of system (3)–(4) is

(a) mean square (MS) stable if for every $\varepsilon > 0$ there is $\delta > 0$ such that if $\|x_0\| \leq \delta$, $x_0 \in \mathbb{R}^d$ then $E\|x_k\|^2 < \varepsilon$ for all $k \in \mathbb{N}$.

(b) mean square asymptotically (MSA) stable if it is stable and there is $\delta_a > 0$ such that $E\|x_k\|^2 \underset{k\to\infty}{\to} 0$ for all $\|x_0\| < \delta_a$.

As usually for linear systems, stability of the null solution $x_k = 0$ is equivalent with stability of any other solution. Then, by a slight abuse of language, we shall use the terms of MS and MSA stability of (3)–(4).

Thus, the aim of this paper is to provide some easy to verify, sufficient conditions for MS and MSA stability of system (3)–(4).

4 Asymptotic Behavior of Solutions

Before giving the main results of this paper we shall establish a useful boundedness property of the solution $x_k, k \in \mathbb{N}$ of (3)–(4). For this we need the following hypothesis.

- (H1) $\|A_0\| + \sum_{j=1}^{n-1} |c_j| + \sqrt{b}\,\|B\| = \gamma < 1$ for all $n \in \mathbb{N}, n \geq 1$.

We recall that $\sum_{j=1}^{\infty} |c_j| = |1-\alpha| < 1$, $\alpha \in (0,2)$ and (H1) is admissible for (3).

Proposition 1 *If (H1) holds, then* $\left\| E\left[x_k \otimes x_p\right]\right\|_1 \leq \|x_0\|^2$ *for all* $k, p \in \mathbb{N}$.

Proof We shall use the induction method. For $k = p = 0$ the statement is obviously true. Assume that $\left\| E\left[x_k \otimes x_p\right]\right\|_1 \leq \|x_0\|^2$ for all $k, p < n$ and let us prove the statement for $k, p < n+1$. Obviously we only have to show the inequalities for $k = n$ or $p = n$. Let $k = p = n$. As mentioned in the above section, ξ_n and x_n are independent random variables for all $n \in \mathbb{N}$. Recalling that $E[\xi_n] = 0$ and $E\left[\xi_n^2\right] = b$ for all $n \in \mathbb{N}$, we have (see [17])

$$E\left[\xi_{n-1}Bx_{n-1} \otimes \xi_{n-1}Bx_{n-1}\right] = E\left[\xi_{n-1}^2\right] E\left[Bx_{n-1} \otimes Bx_{n-1}\right] =$$

$$bBE\left[x_{n-1} \otimes x_{n-1}\right] B^*$$

and $E\left[\xi_{n-1}Bx_{n-1} \otimes A_i x_{n-1-i}\right] = E\left[\xi_{n-1}\right] E\left[Bx_{n-1} \otimes A_i x_{n-1-i}\right] = 0$ for all $i \in \mathbb{N}, i \leq n-1$. Thus

$$E\left[x_n \otimes x_n\right] =$$

$$E\left[\left(\sum_{j=0}^{n-1} A_j x_{n-1-j} + \xi_{n-1}Bx_{n-1}\right) \otimes \left(\sum_{i=0}^{n-1} A_i x_{n-1-i} + \xi_{n-1}Bx_{n-1}\right)\right] =$$

$$E\left[\sum_{j=0}^{n-1}\sum_{i=0}^{n-1} \left(A_j x_{n-1-j}\right) \otimes \left(A_i x_{n-1-i}\right) + bBx_{n-1} \otimes Bx_{n-1}\right]$$

$$= \sum_{j=0}^{n-1}\sum_{i=0}^{n-1} A_j E\left[x_{n-1-j} \otimes x_{n-1-i}\right] A_i^* + bBE\left[x_{n-1} \otimes x_{n-1}\right] B^*.$$

Agreeing that $\sum_{i=r}^{q}$ is 0 if $q < r$, we pass to the norm $\|.\|_1$ and we obtain

$$\|E\left[x_n \otimes x_n\right]\|_1 \leq$$

$$= \sum_{j=0}^{n-1}\sum_{i=0}^{n-1} \left\|A_j E\left[x_{n-1-j} \otimes x_{n-1-i}\right] A_i^*\right\|_1 + b\left\|BE\left[x_{n-1} \otimes x_{n-1}\right] B^*\right\|_1$$

$$= \left\|A_0 E\left[x_{n-1} \otimes x_{n-1}\right] A_0^*\right\|_1 + \sum_{j=1}^{n-1} |c_j| \left\|E\left[x_{n-1-j} \otimes x_{n-1}\right] A_0^*\right\|_1 \tag{5}$$

$$\sum_{i=1}^{n-1} |c_i| \left\|A_0 E\left[x_{n-1} \otimes x_{n-1-i}\right]\right\|_1 + \sum_{j=2}^{n-1}\sum_{i=2}^{n-1} |c_i|\,|c_j| \left\|E\left[x_{n-1-j} \otimes x_{n-1-i}\right]\right\|_1$$

$$+b\left\|BE\left[x_{n-1} \otimes x_{n-1}\right] B^*\right\|_1.$$

We know that $\|AB\|_1 \leq \|A\| \|B\|_1$ for any $A, B \in L\left(\mathbb{R}^d\right)$ [13] and $\left\|A_j\right\| = \left|c_j\right|$, $j \in \mathbb{N}^*$. Thus

$$\begin{aligned}\|E[x_n \otimes x_n]\|_1 \leq \|A_0\|^2 \left\|E\left[x_{n-1} \otimes x_{n-1}\right]\right\|_1 \\ + \sum_{j=1}^{n-1} \left|c_j\right| \|A_0\| \left\|E\left[x_{n-1} \otimes x_{n-1-j}\right]\right\|_1 + \sum_{i=1}^{n-1} |c_i| \|A_0\| \left\|E\left[x_{n-1} \otimes x_{n-1-i}\right]\right\|_1 + \\ \sum_{j=2}^{n-1} \sum_{i=2}^{n-1} |c_i| \left|c_j\right| \left\|E\left[x_{n-1-j} \otimes x_{n-1-i}\right]\right\|_1 + b \|B\|^2 \left\|E\left[x_{n-1} \otimes x_{n-1}\right]\right\|_1 .\end{aligned} \tag{6}$$

From the induction hypothesis, we have

$$\begin{aligned}\|E[x_n \otimes x_n]\|_1 &\leq ((\|A_0\|^2 + 2\sum_{j=1}^{n-1} \left|c_j\right| \|A_0\| + \sum_{j=2}^{n-1} \sum_{i=2}^{n-1} |c_i| \left|c_j\right|) + b \|B\|^2) \|x_0\|^2 \\ &\leq \left(\left(\|A_0\| + \sum_{j=1}^{n-1} \left|c_j\right|\right)^2 + b \|B\|^2\right) \|x_0\|^2 \leq \gamma \|x_0\|^2 \leq \|x_0\|^2\end{aligned}$$

and the conclusion follows. In the case $k = n$ and $p < n$, ξ_{n-1} and x_p are independent and

$$E\left[x_n \otimes x_p\right] = E\left[\left(\sum_{j=0}^{n-1} A_j x_{n-1-j} + \xi_{n-1} B x_{n-1}\right) \otimes x_p\right] = \sum_{j=0}^{n-1} E\left[A_j x_{n-1-j} \otimes x_p\right].$$

Since

$$\left\|E\left[x_n \otimes x_p\right]\right\|_1 \leq \sum_{j=0}^{n-1} \left\|A_j E\left[x_{n-1-j} \otimes x_p\right]\right\|_1 \leq \sum_{j=0}^{n-1} \left\|A_j\right\| \left\|E\left[x_{n-1-j} \otimes x_p\right]\right\|_1 ,$$

we can use again the induction hypothesis to obtain

$$\left\|E\left[x_n \otimes x_p\right]\right\|_1 \leq \left(\|A_0\| + \sum_{j=1}^{n-1} \left|c_j\right|\right) \|x_0\|^2 \leq \gamma \|x_0\|^2 \leq \|x_0\|^2 .$$

Similarly, we can prove that $\left\|E\left[x_p \otimes x_n\right]\right\|_1 \leq \|x_0\|^2$ for all $p < n$. The proof is complete.

The following result is a sufficient criterion for the MS stability of (3)–(4).

Theorem 1 *If (H1) holds, then (3)–(4) is mean square stable.*

Proof Let $\varepsilon > 0$. There is $\delta_\varepsilon = \frac{\varepsilon}{2} > 0$ such that $E\left\|x_p\right\|^2 = \left\|E\left[x_p \otimes x_p\right]\right\|_1 < \varepsilon$ for all $p \in \mathbb{N}$ and $\|x_0\|^2 \leq \frac{\varepsilon}{2}$. The conclusion follows.

Remark 1 (a) From Proposition 1 we get $E\left[\|x(n)\|^2\right] = \|E\left[x_n \otimes x_n\right]\|_1 \leq \|x_0\|^2$ for all $n \in \mathbb{N}$. Consequently, the decreasing, nonnegative sequence defined by $y_n = \sup_{k \geq n} E\left[\|x(k)\|^2\right]$, $n \in \mathbb{N}$ is bounded and has a limit l and $l \leq \|x_0\|^2$ for all fixed $x_0 \in \mathbb{R}^d$.

(b) Using the inequality $\|AB\|_2 \leq \|A\| \|B\|_2$, valid for all $A, B \in L\left(\mathbb{R}^d\right)$ [13], and repeating the arguments from the proof of the inequality (6) with $\|.\|_1$ replaced by $\|.\|_2$, we can establish that

$$\|E\left[x_n \otimes x_n\right]\|_2 \leq \sum_{j=0}^{n-1} \sum_{i=0}^{n-1} B_{i,j} \left\|E\left[x_{n-1-j} \otimes x_{n-1-i}\right]\right\|_2, \tag{7}$$

where $B_{i,j} = \left|c_i c_j\right|$ for $i, j \in \mathbb{N}^*$, $B_{i,0} = B_{0,i} = |c_i| \|A_0\|$, $i \in \mathbb{N}^*$ and $B_{00} = \|A_0\|^2 + b\|B\|^2$.

(c) For all $l, k \in \mathbb{N}$ we have $\|E\left[x_l \otimes x_k\right]\|_2^2 \leq E\left[\|x_l\|^2\right] E\left[\|x_k\|^2\right]$ and

$$\begin{aligned} \sup_{l \geq m, k \geq n} \|E\left[x_l \otimes x_k\right]\|_2^2 &\leq \sup_{l \geq m, k \geq n} E\left[\|x_l\|^2\right] E\left[\|x_k\|^2\right] \\ &= \sup_{l \geq m} E\left[\|x_l\|^2\right] \sup_{k \geq n} E\left[\|x_k\|^2\right] \leq \|x_0\|^4 \end{aligned} \tag{8}$$

Therefore, the double sequence $\sup_{l \geq m, k \geq n} \|E\left[x_l \otimes x_k\right]\|_2^2$, $m, n \in \mathbb{N}$ is bounded and, being decreasing, it is convergent to an $L^2 \in \mathbb{R}$. Passing to the limit as $m, n \to \infty$ in (8), we deduce that $L^2 \leq l^2$ i.e.

$$L = \lim_{i \to \infty, j \to \infty} \sup_{l \geq i, k \geq j} \|E\left[x_l \otimes x_k\right]\|_2 \leq \limsup_{n \to \infty} E\|x_n\|^2 = l. \tag{9}$$

The next result is a version of Mertens Theorem for double sequences (see Theorem 9.17 in [14]).

Lemma 1 *A necessary and sufficient condition that*

$\lim_{n \to \infty, m \to \infty} \sum_{i,j=0}^{n,m} \alpha_{i,j} \Xi_{n-i,m-j} = \sum_{i,j=0}^{\infty} \alpha_{i,j} \lim_{k \to \infty, l \to \infty} \Xi_{k,l}$, for every boundedly convergent sequence $\Xi_{k,l}$ is that $\sum_{i,j=0}^{\infty} \left|\alpha_{i,j}\right| < \infty$.

Indeed, for any boundedly convergent sequence $\Xi_{k,l}$ we can find a double series $\sum_{i,j=0}^{\infty} \beta_{i,j}$ such that $\Xi_{k,l} = \sum_{i,j=0}^{k,l} \beta_{i,j}$ for all $l, k \in \mathbb{N}$. Obviously the series $\sum_{i,j=0}^{\infty} \beta_{i,j}$ is boundedly convergent. A simple computation shows that

$$\sum_{k=0}^{m} \sum_{l=0}^{n} \alpha_{k,l} \Xi_{m-k,n-l}$$

is a partial sum of the Cauchy product double series $\sum_{i,j=0}^{\infty} \alpha_{i,j} * \beta_{i,j}$ and the equivalence of the above lemma with Theorem 9.17 in [14] is evident.

For the next result we need an additional hypothesis

- (H2) $\Gamma := \left(\|A_0\| + \sum_{j=1}^{\infty} |c_j| \right)^2 + b \|B\|^2 < \frac{1}{d}$, where d is the dimension of the state space of (3).

Theorem 2 *Assume that (H1) and (H2). Then (3)–(4) is mean square asymptotically stable.*

Proof Let $B_{i,j}$ be defined as in Remark 1b. An easy computation shows that $\sum_{i,j=0}^{\infty} |B_{i,j}| = \Gamma$. Applying Lemma 1 for $\alpha_{i,j} = B_{i,j}$ and

$$\Xi_{k,l} = \sup_{m \geq l, n \geq k} \|E[x_m \otimes x_n]\|_2$$

and taking into account that $\Xi_{k,l}$ is boundedly convergent, we deduce that

$$\lim_{n,m \to \infty} \sum_{i,j=0}^{n-1,m-1} B_{i,j} \sup_{l \geq n-1-i, k \geq m-1-j} \|E[x_l \otimes x_k]\|_2 =$$
$$\Gamma \lim_{i \to \infty, j \to \infty} \sup_{l \geq i, k \geq j} \|E[x_l \otimes x_k]\|_2 = \Gamma L$$

Hence, for all $\varepsilon_0 > 0$, there is $N_{\varepsilon_0} \in \mathbb{N}$ such that

$$\sum_{i,j=0}^{n-1,m-1} B_{i,j} \sup_{l \geq n-1-i, k \geq m-1-j} \|E[x_l \otimes x_k]\|_2 \leq \Gamma L + \varepsilon_0$$

for all $n, m \geq N_{\varepsilon_0}$. It follows that

$$\sum_{i,j=0}^{n-1} B_{i,j} \sup_{l \geq n-1-i, k \geq n-1-j} \|E[x_l \otimes x_k]\|_2 \leq \Gamma L + \varepsilon_0$$

for all $n \geq N_{\varepsilon_0}$. From (7) we obtain

$$\|E\left[x_n \otimes x_n\right]\|_2 \leq \Gamma L + \varepsilon_0$$

for all $n \geq N_{\varepsilon_0}$. On the other hand $\|E\left[x_n \otimes x_n\right]\|_1 \leq d \|E\left[x_n \otimes x_n\right]\|_2$ and

$$E\left[\|x_n\|^2\right] = \|E\left[x_n \otimes x_n\right]\|_1 \leq d\Gamma L + d\varepsilon_0, n \geq N_{\varepsilon_0}$$

Passing to lim sup as $n \to \infty$, we get

$$\limsup_{n\to\infty} E\left[\|x_n\|^2\right] \leq d\Gamma L + d\varepsilon_0. \tag{10}$$

From Remark 1a we know that

$$L := \lim_{i\to\infty, j\to\infty} \sup_{l\geq i, k\geq j} \|E\left[x_l \otimes x_k\right]\|_2 \leq l := \limsup_{n\to\infty} E\left[\|x_n\|^2\right] \tag{11}$$

and (10) leads to the inequality $l \leq d\Gamma l + d\varepsilon_0$ for all $\varepsilon_0 > 0$. Letting $\varepsilon_0 \to 0$, we obtain $l\,(1 - d\Gamma) \leq 0$ and, by hypothesis (H2), $l = 0$. Therefore $\lim_{n\to\infty} E\,\|x_n\|^2 = 0$ for any $x_0 \in \mathbb{R}^d$. By Theorem 1 we deduce that (3)–(4) is MSA stable with $\delta_a = \infty$.

5 Numerically Simulated Solutions

We shall consider the system (1)–(2) with $d = 1$, $A, B \in \mathbb{R}$ and $\{\xi_k\}_{k\in\mathbb{N}}$ a sequence of real-valued, identically distributed random variables from $L^2(\Omega, \mathbb{R})$. In order to compute its solution $\{x_k\}_{k\in\mathbb{N}}$ we use the below Maple procedure called *DFSsolution*. In this procedure the input parameters are the following: *alpha* is the fractional order of the system, m is the size of the samples drawn from the same distributions as of the stochastic perturbations, $x0$ is a sample of size m of the initial state x_0 given as a vector indexed by $1..m$, A, $B \in \mathbb{R}$ are the coefficients of the above system, $h \in \mathbb{R}_+^*$ is the sampling period or the time increment, n is the maximum k for which we compute a sample from x_k and *distribution* represents the distribution of the stochastic perturbations $\xi_k, k \in \mathbb{N}$. The procedure returns a matrix x having the entries $x\,[i, j] = x_j\,(\omega_i)$, $j = 1..n$, $i = 1..m$ (the column j is a sample from x_j).

```
DFSsolution := proc (alpha, m, x0, A, B, h, n, distribution)
local j, k, i, Xi, S, x, c, A0, B0;
x := array(1 .. m, 0 .. n); c := array(0 .. n);
A0 := h^alpha*A+alpha; B0 := h^alpha*B;
Xi:= Statistics:-RandomVariable(distribution);
S := Statistics:-Sample(Xi, m);
for i to m do x[i,0]:=x0[i]; x[i,1]:=(A0+S[i]*B0)*x0[i] end do;
```

```
c[1]:=-(1/2)*alpha*(alpha-1);
for k to n-1 do
Xi:=Statistics:-RandomVariable(distribution);
S:=Statistics:-Sample(Xi, m);
for i to m do
   x[i,k+1]:=(A0+S[i]*B0)*x[i,k]+sum(c[j]*x[i,k-j],j = 1..k)
end do;
c[k+1]:=-c[k]*(alpha-k-1)/(k+2)
end do;
return x
end proc;
```

Example 1 In (1)–(2) let us consider $h = 1$, $\alpha = \frac{3}{4}$, $A = -\frac{1}{4}$, $B = \frac{1}{16}$, $x_0 \equiv 1$ and let us assume that the distribution of ξ_k is normal $N(0, 1)$ for all k. Then $\|A_0\| = \|h^\alpha A + \alpha\| = \frac{1}{2}$, $\|h^\alpha B\| = \frac{1}{16}$, $b = 1$, and consequently, $\Gamma < \gamma < \frac{1}{2} + \frac{1}{4} + \frac{1}{16} = 0.812 < 1 = min\left(1, \frac{1}{d}\right)$. By Theorem 2, if $\{\xi_k\}_{k\in\mathbb{N}}$ are mutually independent, (1)–(2) is mean square asymptotically stable. If $B = \frac{17}{16}$, then $\gamma = 1.812$ and Theorem 2 does not apply. We use the above Maple procedure to simulate this system. We can represent all samples from $x_0, x_1, \ldots, x_n$ associating a different color to each x_k. The results are presented in Fig. 1.

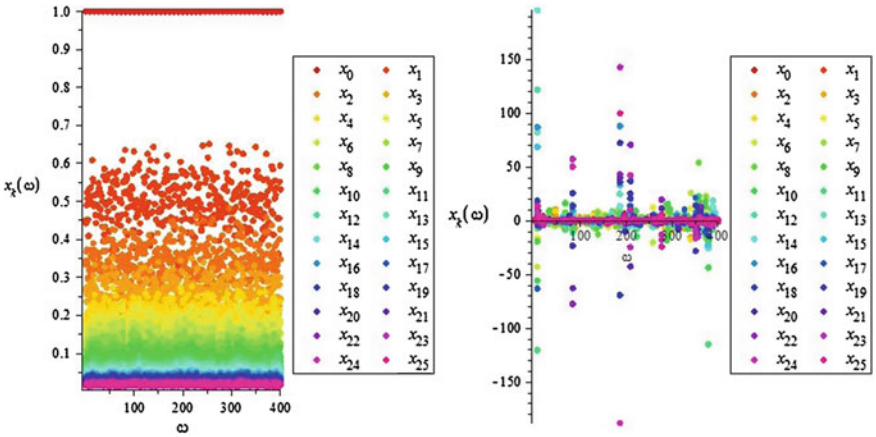

Fig. 1 Samples of size m = 400 from $x_0, x_1 \ldots x_{25}$: *left* $B = \frac{1}{16}$, *right* $B = \frac{17}{16}$

6 Conclusion

This paper studies asymptotic behavior of solutions for linear stochastic DTFSs of the form (3)–(4). Inspired by the deterministic case [1] and using the properties of double series, we derive two simple conditions for the MS and MSA stability. The method could be extended to other type of stochastic systems as nonlinear DTFSs or linear DTFSs with Markovian jumps.

References

1. Monje, C.A., Chen, Y., Vinagre, B.M., Xue, D., Feliu-Batlle, V.: Fractional-Order Systems and Controls: Fundamentals and Applications. Springer, London (2010)
2. Katugampola, U.N.: A new approach to generalized fractional derivatives. Bull. Math. Anal. App. **6**(4), 1–15 (2014)
3. Mainardi, F.: Fractional Calculus and Waves in Linear Viscoelasticity: An Introduction to Mathematical Models. World Scientific, Singapore (2010)
4. Suárez, J.I., Vinagre, B.M., Chen, Y.Q.: A fractional adaptation scheme for lateral control of an AGV. J. Vib. Control. **14**(9–10), 1499–1511 (2008)
5. Dragan, V., Morozan, T., Stoica, A.M.: Mathematical Methods in Robust Control of Discrete-Time Linear Stochastic Systems. Springer, New York (2010)
6. Ungureanu, V.M.: Stability, stabilizability and detectability for Markov jump discrete-time linear systems with multiplicative noise in Hilbert spaces. Optimization **63**(11), 1689–1712 (2014)
7. Sadeghian, H., Salarieh, H., Alasty, A., Meghdari, A.: On the general Kalman filter for discrete time stochastic fractional systems. Mechatronics **23**(7), 764–771 (2013)
8. Buslowicz, M., Ruszewski, A.: Necessary and sufficient conditions for stability of fractional discrete-time linear state-space systems. Bull. Pol. Ac. Tech. **61**(4), 779–786 (2013)
9. Guermah, S., Djennoune, S., Bettayeb, M.: Controllability and observability of linear discrete-time fractional-order systems. Int. J. Appl. Math. Comput. Sci. **18**(2), 213–222 (2008)
10. Guermah, S., Bettayeb, M., Djennoune, S.: Discrete-time Fractional-order Systems: Modeling and Stability Issues. INTECH Open Access Publisher, Croatia (2012)
11. Rivero, M., Rogosin, S.V., Tenreiro Machado, J.A., Trujillo, J.J.: Stability of fractional order systems. Math. Probl. Eng. **2013**, 14 (2013)
12. Kubrusly, C.: The Elements of Operator Theory, 2nd edn. Birkhäuser, Boston (2011)
13. Schaefer, H.H.: Banach Lattices and Positive Operators. Springer, Heidelberg (1974)
14. Mursaleen, M., Mohiuddine, S.A.: Convergence Methods for Double Sequences and Applications. Springer, India (2014)
15. Bandyopadhyay, B., Kamal, S.: Stabilization and Control of Fractional Order Systems: A Sliding Mode Approach. Springer International Publishing, Switzerland (2015)
16. Chen, F., Zhigang, L.: Asymptotic stability results for nonlinear fractional difference equations. J. Appl. Math. **2012**, 1–14 (2012)
17. Ungureanu, V.M.: Representations of mild solutions of time-varying linear stochastic equations and the exponential stability of periodic systems. Electron. J. Qual. Theory Differ. Equ. **4**, 1–22 (2004)

Part II
Modeling and Control

Conformable Fractional Wave-Like Equation on a Radial Symmetric Plate

Derya Avcı, Beyza Billur İskender Eroğlu and Necati Özdemir

Abstract The generalization of physical processes by using local or nonlocal fractional operators has been an attractive research topic over the last decade. Fractionalization of integer order models gives quite reality to mathematical descriptions so that one should obtain the sub/super behaviors of real world problems. In this article, we are motivated to formulate a wave-like equation in terms of the left sequential conformable fractional derivative on a radial plate and also discuss on the differences among the statements of classical, existing fractional and conformable fractional wave equations.

Keywords Sequential conformable fractional derivative · Fractional wave-like equation · Local fractional derivative

1 Introduction

Fractional partial differential equations (FPDEs) have been one of the fascinating topics due to the fact that initial-boundary value problems of FPDEs can give more realistic description to natural phenomenon, such as heat conduction [1], diffusion and wave processes [2–4], optimization and control problems [5–7] and so on. Various types of fractional operators such as Riemann–Liouville, Caputo, Hadamard, Grünwald–Letnikov, Marchaud, Riesz are just a few to name [8–10]. Most of the existing fractional operators are defined via the fractional integrals with singular kernels which is due to their nonlocal structures. This property can be interpreted in two different point of views. Firstly, the nonlocality leads them to give

D. Avcı (✉) · B.B. İskender Eroğlu · N. Özdemir
Department of Mathematics, Faculty of Science and Arts, Balikesir University, Cagis Campus, 10145 Balikesir, Turkey
e-mail: dkaradeniz@balikesir.edu.tr

B.B. İskender Eroğlu
e-mail: biskender@balikesir.edu.tr

N. Özdemir
e-mail: nozdemir@balikesir.edu.tr

A. Babiarz et al. (eds.), *Theory and Applications of Non-integer Order Systems*, Lecture Notes in Electrical Engineering 407, DOI 10.1007/978-3-319-45474-0_13

memory, hereditary effects and future dependence to the real world problems [11–16]. Moreover, sub/super (slow/fast) behaviors of the processes can be investigated by fractional mathematical models. For example, the flow of groundwaters, the flyway of migratory birds, the propagation of sea pollutions are some applications that need to be modelling of sub/super (slow/fast) behaviors. The first point of view emphasizes the advantageous of fractional operators. On the other hand, this property brings the computational difficulties with together. In general, fractional differential equations have been solved by applying numerical methods due to the lack of analytical solutions [17, 18]. This should be considered as a hardness, or i.e. disadvantageous, for nonlocal fractional operators. In addition, most of the nonlocal fractional derivatives don't obey the basic chain, quotient and product rules and also Rolle's and Mean Value Theorems satisfied by integer order derivatives. Over the last decade, new local fractional derivatives have been proposed to overcome these difficulties [19–21]. Khalil et al. [22] came up with a simple and well-behaved definition called as "conformable fractional derivative":

Definition 1 Let $f : [0, \infty) \to \mathbb{R}$ and $t > 0$. Then the conformable derivative of f of order α is defined by,

$$T_\alpha (f)(t) = \lim_{\varepsilon \to 0} \frac{f\left(t + \varepsilon t^{1-\alpha}\right) - f(t)}{\varepsilon}, \tag{1}$$

for $t > 0$, $\alpha \in (0, 1)$. If f is $\alpha-$differentiable in some $(0, a)$, $a > 0$, and $\lim_{t \to 0^+} f^{(\alpha)}(t)$ exists, then define

$$f^{(\alpha)}(0) = \lim_{t \to 0^+} f^{(\alpha)}(t). \tag{2}$$

If the conformable fractional derivative of f of order α exists, then f is said to be $\alpha-$differentiable. Therefore, $T_\alpha (f)(t)$ is sometimes written as $f^{(\alpha)}(t)$ to denote the conformable derivative. $T_\alpha (f)(t)$ satisfies all the basic properties given by the following theorem [22]:

Theorem 1 *Let $\alpha \in (0, 1]$, and f, g be $\alpha - differentiable$ at a point t. Then:*

(1) $T_\alpha (af + bg)(t) = aT_\alpha (f)(t) + bT_\alpha (g)(t)$ *for all* $a, b \in \mathbb{R}$.
(2) $T_\alpha (t^p) = pt^{p-\alpha}$ *for all* $p \in \mathbb{R}$.
(3) $T_\alpha (fg)(t) = fT_\alpha (g) + gT_\alpha (f)$.
(4) $T_\alpha \left(\frac{f}{g}\right)(t) = \frac{gT_\alpha (f) - fT_\alpha (g)}{g^2}$.
(5) $T_\alpha (\lambda) = 0$ *for all constant functions* $f(t) = \lambda$.
(6) If f is differentiable, then $T_\alpha (f)(t) = t^{1-\alpha} \frac{df}{dt}$.

This new definition is very easier to handle and provides some fundamental properties and theorems such as chain rule, integration by parts, Taylor series expansion,

Laplace transform, divergence theorem [23, 24]. However, this fractional derivative has a weakness because all differentiable functions has zero as conformable derivative at the point zero.

In the last few years, there is an increasing interest to new properties and applications of conformable fractional derivative. Abdeljawad [23] improved a remarkable notion "sequential conformable fractional derivative" in the following:

Definition 2 Let $f : [a, \infty) \to \mathbb{R}$ such that $f^{(n)}(t)$ exists and continuous, $0 < \alpha \leq 1$ and $n \in \mathbb{Z}^+$, then the left sequential conformable fractional derivative of order n is defined by

$$^{(n)}T_\alpha^a f(t) = \underbrace{T_\alpha^a T_\alpha^a \dots T_\alpha^a}_{n \text{ times}} f(t). \tag{3}$$

As a special case $n = 2$ and $0 < \alpha \leq \frac{1}{2}$,

$$^{(2)}T_\alpha^a f(t) = T_\alpha^a T_\alpha^a f(t) = \begin{cases} (1-\alpha)(t-a)^{1-2\alpha} f'(t) + (t-a)^{2-2\alpha} f''(t) & t > a \\ 0 & t < a. \end{cases} \tag{4}$$

Note that the second order sequential conformable derivative may not be continuous even f is second continuously differentiable for $\frac{1}{2} < \alpha \leq 1$.

Moreover, the chain rule, integration by parts, Taylor series expansion and Laplace transform for conformable fractional derivative were proposed in [23]. Atangana et al. [24] introduced some useful properties and theorems related to partial and sequential conformable derivatives. Abu Hammad and Khalil [25] introduced different types of heat equation in terms of conformable fractional derivative and proposed Fourier series for conformable fractional derivative (see [26]). By a similar manner, Çenesiz and Kurt researched the solutions of time fractional conformable heat [27] and wave equations [28] in Cartesian coordinates. Kurt et al. [29] also presented the approximate analytical solution of the time conformable Burger's equation. Khalil and Abu–Shaab [30] solved some conformable fractional differential equations by using Fourier series. For more applications on conformable notions we referee to [31–37]. This paper is motivated by the well-description of a conformable fractional wave-like equation on a radial plate. We aim to solve an initial-boundary value problem for a nonhomogeneus wave-like equation in terms of sequential conformable fractional derivative acting on a radial symmetric plate.

2 Statement of the Problem

Let us consider the following conformable fractional wave-like equation

$$\frac{\partial^\alpha}{\partial t^\alpha}\frac{\partial^\alpha}{\partial t^\alpha}u(r,t) = \kappa^2\left(\frac{\partial^2 u}{\partial r^2} + \frac{1}{r}\frac{\partial u}{\partial r}\right) + f(r,t) \tag{5}$$

subjected to the initial and boundary conditions given respectively as

$$u(r,0) = u_0(r), \tag{6}$$

$$\frac{\partial^\alpha}{\partial t^\alpha} u(r,0) = u_1(r), \ 0 < r \le R \tag{7}$$

and

$$u(0,t) = u(R,t) = 0, \ t > 0, \tag{8}$$

where $\frac{\partial^\alpha}{\partial t^\alpha}$ represents the conformable fractional derivative of order $\alpha \left(0 < \alpha \le \frac{1}{2}\right)$, κ is a constant, R is radius of plate and $f(r,t)$ denotes an external force. For simplicity, we assume this function depends only on radius like $f(r)$ in our computations. The solution is found as a linear sum of two separate problem detailed in the following sub sections.

2.1 Homogeneous Conformable Fractional Wave-Like Equation and Non-homogeneous Initial Conditions

Let us consider

$$\frac{\partial^\alpha}{\partial t^\alpha} \frac{\partial^\alpha}{\partial t^\alpha} u(r,t) = \kappa^2 \left(\frac{\partial^2 u}{\partial r^2} + \frac{1}{r} \frac{\partial u}{\partial r} \right) \tag{9}$$

with the initial and boundary conditions

$$u(r,0) = u_0(r), \tag{10}$$

$$\frac{\partial^\alpha}{\partial t^\alpha} u(r,0) = u_1(r), \left(0 < \alpha \le \frac{1}{2}\right), \tag{11}$$

$$u(0,t) = u(R,t) = 0, \ t > 0. \tag{12}$$

We shall assume that the solution is

$$u(r,t) = Q(r) T(t), \tag{13}$$

i.e., u is a product in which the dependence of u on r and t is separated as $Q(r)$ and $T(t)$. By substituting Eq. (13) into Eq. (9), we have the following Bessel ordinary and sequential conformable fractional differential equations

$$\frac{d^2 Q}{dr^2} + \frac{1}{r} \frac{dQ}{dr} + \mu^2 Q = 0, \tag{14}$$

$$\frac{d^{\alpha}}{dt^{\alpha}}\frac{d^{\alpha}}{dt^{\alpha}}T+(\kappa\mu)^{2}T=0. \tag{15}$$

In here, μ^2 is separation constant obtained by solving Eq. (14) as $\mu_i = \frac{\lambda_i}{R}$ in which λ_i denotes the zeros of J_0. The solution of Eq. (14) is well-known zero order Bessel function of first kind

$$Q_i(r) = c_1 J_0(\mu_i r), \tag{16}$$

where c_1 is arbitrary constant which naturally arises in the solution. By using definition of second order sequential conformable fractional derivative in Eqs. (4), (15) can be written as

$$t^{2-2\alpha}T_i''(t)+(1-\alpha)t^{1-2\alpha}T_i'(t)+(\kappa\mu_i)^{2}T_i=0. \tag{17}$$

Making the change of variable $x = \frac{\kappa\mu_i t^{\alpha}}{\alpha}$, Eq. (17) reduces to a differential equation with constant coefficients as follows

$$\frac{d^2T_i}{dx^2}+T_i=0 \tag{18}$$

and so we get

$$T_i(t) = c_2\cos\left(\frac{\kappa\mu_i t^{\alpha}}{\alpha}\right)+c_3\sin\left(\frac{\kappa\mu_i t^{\alpha}}{\alpha}\right), \tag{19}$$

where c_2 and c_3 are arbitrary coefficients. Therefore, the fundamental solution of Problem (9–12) is given by the series

$$u(r,t) = \sum_{i=1}^{\infty}\left[A_i\cos\left(\frac{\kappa\mu_i t^{\alpha}}{\alpha}\right)+B_i\sin\left(\frac{\kappa\mu_i t^{\alpha}}{\alpha}\right)\right]J_0(\mu_i r), \tag{20}$$

where A_i and B_i can be determined by using initial conditions (10) and (11) and also the following orthogonality property of J_0

$$\int_0^R r J_0(\mu_i r)\,J_0(\mu_k r)\,dr = R^2\begin{cases}0, & i\neq k\\ \frac{J_1^2(\lambda_i)}{2}, & i=k\end{cases} \tag{21}$$

where J_1 is first kind Bessel function of order 1. Thus, we have

$$A_i = \frac{2}{R^2J_1^2(\lambda_i)}\int_0^R u_0(r)\,r\,J_0(\mu_i r)\,dr, \tag{22}$$

$$B_i = \frac{2}{R^2\kappa\mu_i J_1^2(\lambda_i)}\int_0^R u_1(r)\,r\,J_0(\mu_i r)\,dr. \tag{23}$$

The critical manner in this work is foundation of B_i. As we noticed that there has been an unawares mistake related to the calculation of B_i because of the description of initial condition given by Eq. (11) in the literature. Heuristically, it seems as if B_i can be calculated by an initial condition $\frac{\partial}{\partial t}u\left(r,0\right)=u_1\left(r\right)$. By checking carefully, first order initial condition only gives the trivial solution for such a problem. However, it is clear that nontrivial solutions of initial-boundary value problems are worth investigating. To find the nontrivial solutions of the present problem, we must choose an initial condition by a conformable fractional derivative of order $0<\alpha\leq\frac{1}{2}$. It should be noted that the choice of initial condition surely depends on the problem statement.

Another remarkable point is that time-fractional wave equations in terms of conventional fractional derivatives as Caputo or RL correspond to classical wave equation for $\alpha=2$. This result changes in the case of conformable fractional differential equations. For instance, the order of sequential conformable fractional derivative as $0<\alpha\leq\frac{1}{2}$ in the present wave formulation. In addition, we see that a damping term arises in reduced Eq. (17) and figures also show this behaviour, clearly. If we take $\alpha=\frac{1}{2}$, then Eq. (17) represents a wave-like equation in classical sense. Note that the choice of α differs from the conventional nonlocal fractional derivatives.

This interesting result for conformable fractional wave-like formulation can not occur in different physical processes. For instance, $\alpha\in(0,1)$ for the conformable fractional heat and Burgers equations and the initial condition is given by $u\left(r,0\right)=u_0\left(r\right)$. Furthermore, these equations reduce to the classical cases for $\alpha=1$. However, we must be careful to define the initial conditions of conformable wave-like equations. It is well known that we need first order initial condition as $u_t\left(r,0\right)=u_1\left(r\right)$ to solve a classical wave equation. Unfortunately, this changes upon the structure of conformable fractional wave equation as seen in this paper.

For the above-mentioned reasons, we must be awake to determine the initial conditions. In this sense, we have tried to give attention to researchers by this article.

As a result, by substituting Eqs. (22) and (23) into Eq. (20) general solution is given as follows

$$u\left(r,t\right)=\sum_{i=1}^{\infty}\frac{2}{R^2J_1^2\left(\lambda_i\right)}\left[\cos\left(\frac{\kappa\mu_it^\alpha}{\alpha}\right)\int_0^R u_0\left(r\right)rJ_0\left(\mu_ir\right)dr\right.$$
$$\left.+\frac{1}{\kappa\mu_i}\sin\left(\frac{\kappa\mu_it^\alpha}{\alpha}\right)\int_0^R u_1\left(r\right)rJ_0\left(\mu_ir\right)dr\right]J_0\left(\mu_ir\right). \tag{24}$$

In the following, we illustrate the behaviors of conformable fractional wave-like equation without an external force under some arbitrary assumptions for problem parameters. Next, we will formulate the 2^{th} part of the problem.

2.2 Non-homogeneous Conformable Fractional Wave-Like Equation and Homogeneous Initial Conditions

In an analogous way, we consider the following problem

$$\frac{\partial^{\alpha}}{\partial t^{\alpha}}\frac{\partial^{\alpha}}{\partial t^{\alpha}}u\left(r,t\right)=\kappa^{2}\left(\frac{\partial^{2}u}{\partial r^{2}}+\frac{1}{r}\frac{\partial u}{\partial r}\right)+f\left(r\right) \tag{25}$$

with the homogeneous initial and boundary conditions

$$u\left(r,0\right)=\frac{\partial^{\alpha}}{\partial t^{\alpha}}u\left(r,0\right)=0,\ 0<r\leq R, \tag{26}$$

$$u\left(0,t\right)=u\left(R,t\right)=0,\ t>0. \tag{27}$$

Similar to Sect. 2.1, $J_0\left(\mu_i r\right)\left(i=1,2,\ldots\right)$ are the basis functions of the 2^{th} part problem and so we aim to find the following solution

$$u\left(r,t\right)=\sum_{i=1}^{\infty}T_i\left(t\right)J_0\left(\mu_i r\right) \tag{28}$$

and also assume that the heat source is represented by the basis functions as follows

$$f\left(r\right)=\sum_{i=1}^{\infty}C_i J_0\left(\mu_i r\right), \tag{29}$$

where

$$C_i=\frac{2}{R^2 J_1^2\left(\lambda_i\right)}\int_0^R f\left(r\right)r J_0\left(\mu_i r\right)dr. \tag{30}$$

A particular assumption for $f\left(r\right)$ is only accepted for simplicity in calculations. We surely obtain the same result for C_i by direct computations without an assumption for $f\left(r\right)$, i.e. $f\left(r\right)$ can be chosen arbitrarily. By substituting Eqs. (28) and (29) into the Eq. (25), the obtained conformable fractional differential equation differs from the Eq. (17) as

$$t^{2-2\alpha}T_i''\left(t\right)+\left(1-\alpha\right)t^{1-2\alpha}T_i'\left(t\right)+\left(\kappa\mu_i\right)^2 T_i=C_i. \tag{31}$$

We then find the solution of Eq. (31)

$$T_i\left(t\right)=k_1\sin\left(\frac{\kappa\mu_i t^{\alpha}}{\alpha}\right)+k_2\cos\left(\frac{\kappa\mu_i t^{\alpha}}{\alpha}\right)+\frac{C_i}{\left(\kappa\mu_i\right)^2}, \tag{32}$$

where k_1 and k_2 can be easily obtained by the homogeneous initial conditions (26). After that we have

$$T_i(t) = \frac{C_i}{(\kappa\mu_i)^2}\left(1 - \cos\left(\frac{\kappa\mu_i t^\alpha}{\alpha}\right)\right). \tag{33}$$

Therefore, the exact solution of 2th case problem is in the following form:

$$u(r,t) = \sum_{i=1}^{\infty} \frac{C_i}{(\kappa\mu_i)^2}\left(1 - \cos\left(\frac{\kappa\mu_i t^\alpha}{\alpha}\right)\right) J_0(\mu_i r). \tag{34}$$

Consequently, we obtain the whole solution of the main problem (5)–(8)

$$\begin{aligned} u(r,t) = \sum_{i=1}^{\infty} \frac{2}{R^2 J_1^2(\lambda_i)} \Bigg[& \cos\left(\frac{\kappa\mu_i t^\alpha}{\alpha}\right) \int_0^R u_0(r)\, r J_0(\mu_i r)\, dr \\ & + \frac{1}{\kappa\mu_i} \sin\left(\frac{\kappa\mu_i t^\alpha}{\alpha}\right) \int_0^R u_1(r)\, r J_0(\mu_i r)\, dr + \frac{1}{(\kappa\mu_i)^2} \\ & \times \left(1 - \cos\left(\frac{\kappa\mu_i t^\alpha}{\alpha}\right)\right) \int_0^R f(r)\, r J_0(\mu_i r)\, dr \Bigg] J_0(\mu_i r). \end{aligned} \tag{35}$$

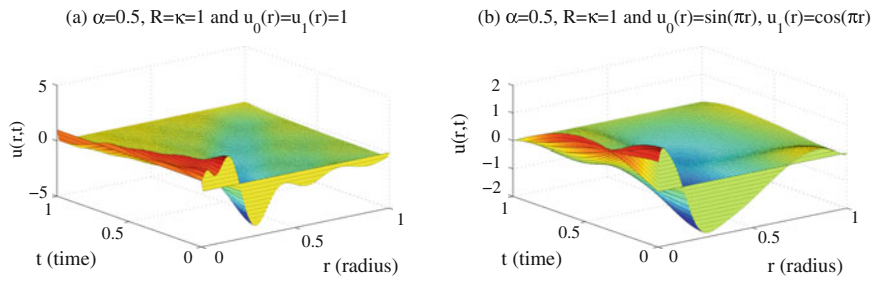

Fig. 1 Behaviours of the wave-like solutions without an external force

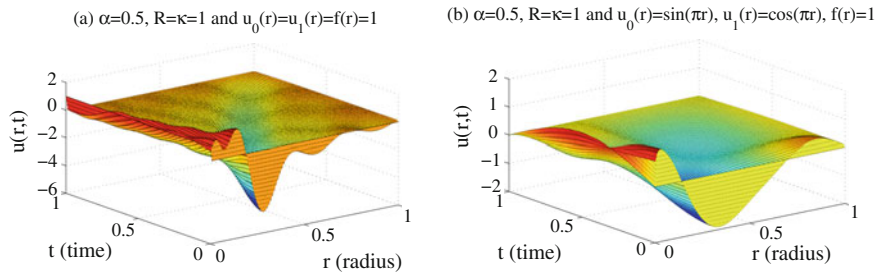

Fig. 2 Behaviours of the wave-like solutions under an external force

We show the numerical results for the solution of conformable fractional wave-like equation are shown in Fig. 1a, b under some assumptions for problem parameters (Fig. 2).

3 Conclusions

In the last decade, local fractional operators have been an increasing interest among the researchers because of their simple and well-behaved definitions. They remove the complexity that naturally arises in the existing fractional operators because of their singular kernels. Conformable fractional derivative is one of these local operators which is based on classical derivative with a fractional parameter. This new derivative quite quickly takes its place in the real world applications defined by partial differential equations. At the beginning, we realized that there is an uncertainty in the description of initial conditions for sequential conformable fractional differential equations. Motivated by this, we aim to give a correct statement for a conformable fractional wave-like equation on a radial symmetric plate. We conclude that we can obtain nontrivial solutions of a sequential conformable fractional wave-like equation if and only if the initial condition is defined in terms of a conformable fractional derivative.

References

1. Povstenko, Y.: Fractional Thermoelasticity. Springer, Switzerland (2015)
2. Povstenko, Y.: Linear Fractional Diffusion-Wave Equation for Scientists and Engineers. Springer, Switzerland (2015)
3. Özdemir, N., Karadeniz, D.: Fractional diffusion-wave problem in cylindrical coordinates. Phys. Lett. A **372**, 5968–5972 (2008)
4. Özdemir, N., Agrawal, O.P., Karadeniz, D., İskender, B.B.: Analysis of an axis-symmetric fractional diffusion-wave problem. J. Phys. A Math. Theor. **42**(35) (2009)
5. Özdemir, N., Karadeniz, D., İskender, B.B.: Fractional optimal control problems of a distributed systems in cylindrical coordinates. Phys. Lett. A **373**, 221–226 (2009)
6. Özdemir, N., İskender, B.B.: Fractional order control of fractional diffusion systems subject to input hysteresis. J. Comput. Nonlinear Dyn. **5**(2), 5 (2010)
7. Evirgen, F., Özdemir, N.: Multistage adomian decomposition method for solving NLP problems over a nonlinear fractional dynamical system. J. Comput. Nonlin. Dyn. **6**(2), 6 (2011)
8. Samko, S.G., Kilbas, A.A., Marichev, O.I.: Fractional Integrals and Derivatives Theory and Applications. Gordon & Breach, Amsterdam (1993)
9. Podlubny, I.: Fractional Differential Equations: An Introduction to Fractional Derivatives, Fractional Differential Equations, to Methods of Their Solution and Some of Their Applications. Academic Press, San Diego (1998)
10. Kilbas, A.A., Srivastava, H.M., Trujillo, J.J.: Theory and Applications of Fractional Differential Equations. Elsevier, Amsterdam (2006)
11. Gorenflo, R.: Fractional calculus: some numerical methods. In: Fractals and Fractional Calculus in Continuum Mechanics, pp. 277–290. Springer, New York (1997)

12. Diethelm, K., Ford, N.J., Freed, A.D., Luchko, Y.: Algorithms for the fractional calculus: a selection of numerical methods. Comput. Methods Appl. Mech. Engrg. **194**, 743–773 (2005)
13. Baleanu, D., Diethelm, K., Scalas, E., Trujillo, J.J.: Fractional Calculus: Models and Numerical Methods. Series on Complexity, Nonlinearity and Chaos, vol. 3. World Scientific Publishing, Singapore (2012)
14. Li, C., Zeng, F.: Numerical Methods for Fractional Calculus. CRC Press, New York (2015)
15. Guo, B., Pu, X., Huang, F.: Fractional Partial Differential Equations and their Numerical Solutions. World Scientific Publishing, Singapore (2015)
16. Atanackovic, T.M., Pipilovic, S., Stankovic, B., Zorica, D.: Fractional Calculus with Applications in Mechanics: Wave Propagation, Impact and Variational Principles. Wiley, London (2014)
17. Hristov, J.: Diffusion models with weakly singular kernels in the fading memories: how the integral-balance method can be applied? Therm. Sci. **19**(3), 947–957 (2015)
18. Hristov, J.: Double integral-balance method to the fractional subdiffusion equation: approximate solutions, optimization problems to be resolved and numerical simulations. J. Vib. Control (2015)
19. Yang, X.J., Baleanu, D., Srivastava, H.M.: Local Fractional Integral Transforms and Their Applications. Elsevier, London (2015)
20. Atangana, A.: Derivative with a New Parameter: Theory, Methods and Applications. Elsevier, London (2015)
21. Katugampola, U.N.: A new fractional derivative with classical properties (2014). arXiv:1410.6535v2
22. Khalil, R., Al Horani, M., Yousef, A., Sababheh, M.: A new definition of fractional derivative. J. Comput. Appl. Math. **264**, 65–70 (2014)
23. Abdeljawad, T.: On conformable fractional calculus. J. Comput. Appl. Math. **279**, 57–66 (2015)
24. Atangana, A., Baleanu, D., Alsaedi, A.: New properties of conformable derivative. Open Math. **13**, 889–898 (2015)
25. Abu Hammad, I., Khalil, R.: Conformable fractional heat differential equation. Int. J Pure Appl. Math. **94**(2), 215–221 (2014)
26. Abu Hammad, I., Khalil, R.: Fractional fourier series with applications. Am. J. Comput. Appl. Math. **4**(6), 187–191 (2014)
27. Çenesiz, Y., Kurt, A.: The solution of time fractional heat equation with new fractional derivative definition. In: 8th International Conference on Applied Mathematics, Simulation, Modelling (ASM 2014), pp. 195–198. WSEAS Press, Florance (2014)
28. Çenesiz, Y., Kurt, A.: The new solution of time fractional wave equation with conformable fractional derivative definition. J. New Theor. **7**, 79–85 (2015)
29. Çenesiz, Y., Kurt, A., Tasbozan, O.: On the solution of burgers equation with the new fractional derivative. Open Phys. **13**(1), 355–360 (2015)
30. Khalil, R., Abu-Shaab, H.: Solution of some conformable fractional differential equations. Int. J. Pure Appl. Math. **103**(4), 667–673 (2015)
31. Zheng, A., Feng, Y., Wang, W.: The Hyers-Ulam stability of the conformable fractional differential equation. Math. Aeterna **5**(3), 485–492 (2015)
32. Neamaty, A., Agheli, B., Darzi, R.: On the determination of the eigenvalues for airy fractional differential equation with turning point. Transylvanian J. Math. Mech. **7**(2), 149–153 (2015)
33. Iyiola, O.S., Ojo, G.O.: On The analytical solution of Fornberg–Whitham equation with the new fractional derivative. Pramana **85**(4), 567–575 (2015)
34. Eslami, M., Rezazadeh, H.: The first integral method for Wu-Zhang system with conformable time-fractional derivative. Calcolo, 1–11 (2015)
35. Benkhettou, N., Hassani, S., Torres, D.F.M.: A conformable fractional calculus on arbitrary time scales. J. King Saud Univ. Sci. **28**(1), 93–98 (2016)
36. Iyiola, O.S., Nwaeza, E.R.: Some new results on the new conformable fractional calculus with application using D'Alambert approach. Progr. Fract. Differ. Appl. **2**(2), 1–7 (2016)
37. Wang, L.-L., Fu, J.-L.: Non-noether symmetries of Hamiltonian systems with conformable fractional derivatives. Chin. Phys. B **25**(1), 7 (2016)

Reconstruction Robin Boundary Condition in the Heat Conduction Inverse Problem of Fractional Order

Rafał Brociek, Damian Słota and Adam Zielonka

Abstract This paper describes a parallel algorithm for reconstruction the boundary condition for the heat conduction equation with derivative of fractional order with respect to the time. The heat transfer coefficient, occurring in the boundary condition of the third kind, was reconstructed. Additional information for the considered inverse problem is given by the temperature measurements at selected points of the domain. The direct problem was solved by using the implicit finite difference method. To minimize functional defining the error of approximate solution parallel Ant Colony Optimization algorithm (ACO) was used. Calculations have been performed in parallel way (multi-threaded). The paper presents examples to illustrate the accuracy and stability of the presented algorithm.

Keywords Inverse problem · Time fractional heat conduction equation · Identification · Heat transfer coefficient

1 Introduction

Artificial intelligence algorithms are widely used in many fields of science [1–4]. Among these algorithms we can distinguish algorithms inspired by behavior of animals in nature, for example Ant Colony Optimization algorithm [5–7], Artificial Bee Colony algorithm [8, 9], firefly algorithm [10]. In many cases, these algorithms are easy to implement and provide better results than conventional methods.

R. Brociek (✉) · D. Słota · A. Zielonka
Institute of Mathematics, Silesian University of Technology, Kaszubska 23,
44-100 Gliwice, Poland
e-mail: rafal.brociek@polsl.pl

D. Słota
e-mail: damian.slota@polsl.pl

A. Zielonka
e-mail: adam.zielonka@polsl.pl

A. Babiarz et al. (eds.), *Theory and Applications of Non-integer Order Systems*,
Lecture Notes in Electrical Engineering 407, DOI 10.1007/978-3-319-45474-0_14

Inverse problems are used in the analysis of various processes, as well as the design of different devices. Solving the inverse problem, we can set boundary conditions or other parameters, so the process described by differential equation, proceeded in a manner specified in advance. In the case of differential equations of integer order, this problem has been described in papers [11–15]. Murio dealt with the inverse problems for the equations with fractional derivatives. The most important of his papers are [16–19]. In these works the mollification method was applied. The heat flux and the temperature on the region boundary are reconstructed in case when the measurements of temperature inside of the domain are known.

In paper [20] the inverse problem of determining the spatial coefficient in source term of the equation and/or the order of Caputo derivative for the time fractional diffusion equation was considered. The authors have shown that for appropriate assumptions, the solution of this problem is unique. Also in the work [21] similar problems are considered. Authors transform the problem into the first kind Volterra integral equation. Then, they used the boundary element method and the generalized Tikhonov regularization to solve this integral equation. Paper [22] describes inverse problem consisting in reconstruction of a spatially varying potential term in the one-dimensional time-fractional diffusion equation. Zheng and Wei in papers [23, 24] describe applications of the Fourier regularization and the convolution method in purpose to reconstruct the value of function and its derivative on the boundary of semi-infinite domain for the time fractional diffusion equation. Similar problem formulated in the bounded domain is considered in paper [25]. For solving this problem the kernel-based meshless method was applied. Xiong et al. [26] discuss the two-dimensional case in the unbounded domain.

In the work [27] authors discussed the problem of determining the thermal conductivity coefficient in the time fractional heat conduction equation. Thermal conductivity coefficient was reconstructed on the grounds of temperature measurements at selected points of the region. The direct problem was solved by applying the finite difference method. To minimize the constructed functional, which expresses the error of approximate solution, the Fibonacci search algorithm was used. Paper [28] describes the reconstruction of the boundary condition for the heat conduction equation of fractional order. To minimize functional defining the error of approximate solution the Nelder-Mead algorithm was used. The paper presents results of computational examples to illustrate the accuracy and stability of the presented algorithm.

In this paper we reconstruct the heat transfer coefficient occurring in the boundary condition for the time fractional heat conduction equation. Fractional derivative with respect to time, occurring in considered equation, has been defined as the Caputo derivative. Additional information for the considered inverse problem was given by the temperature measurements at selected points of the domain. The direct problem was solved by using the implicit finite difference method [29, 30]. To minimize functional defining the error of approximate solution the Ant Colony Optimization algorithm was used [7, 15]. The calculation using this algorithm has been performed in parallel way.

2 Formulation of the Problem

We will consider the following heat conduction equation with a fractional derivative with respect to time

$$c\varrho\frac{\partial^\alpha u(x,t)}{\partial t^\alpha} = \lambda\frac{\partial^2 u(x,t)}{\partial x^2}, \tag{1}$$

defined in domain

$$D = \{(x,t) : x \in [0,L], t \in [0,t^*)\}.$$

In this work, we use the terminology adopted in the case of classical heat conduction equation, despite the change of some units. By c, ϱ, λ we denote the specific heat, the density and thermal conductivity, respectively. The initial condition is posed

$$u(x,0) = f(x), \quad x \in [0,L], \tag{2}$$

as well as the boundary conditions of the second and third kind

$$-\lambda\frac{\partial u}{\partial x}(0,t) = q(t), \quad t \in (0,t^*), \tag{3}$$

$$-\lambda\frac{\partial u}{\partial x}(L,t) = h(t)(u(L,t) - u^\infty), \quad t \in (0,t^*), \tag{4}$$

where h is the heat transfer coefficient and u^∞ is ambient temperature.

As a fractional derivative with respect to time occurring in Eq. (1), we will take the Caputo derivative. For $\alpha \in (0,1)$ the Caputo derivative is defined by the formula

$$\frac{\partial^\alpha u(x,t)}{\partial t^\alpha} = \frac{1}{\Gamma(1-\alpha)}\int_0^t \frac{\partial u(x,s)}{\partial s}(t-s)^{-\alpha}\,ds, \tag{5}$$

where Γ is the Gamma function.

We assume that the function h, describes the heat transfer coefficient, occurs at the boundary condition of the third kind, will depend on two parameters γ_1 and γ_2. Considered inverse problem consists on restore the parameters γ_1, γ_2 (and therefore the boundary condition) on the grounds of known values of the function u in the selected set of points of the domain D. Known values of the function u (input data) in the selected points (x_i, t_j) of the domain D, we denote

$$u(x_i,t_j) = \widehat{U}_{ij}, \quad i = 1,2,\ldots,N_1, \quad j = 1,2,\ldots,N_2, \tag{6}$$

where N_1 is the number of the sensors and N_2 denotes number of measurements at each sensor.

Solving the direct problem for fixed values of h, we obtain a values approximating function u in selected points $(x_i, t_j) \in D$. These values will be denoted by $U_{ij}(h)$.

Using the calculated values of $U_{ij}(h)$ and input data $\widehat{U}_{ij}$, we create functional defining the error of approximate solution

$$J(h) = \sum_{i=1}^{N_1} \sum_{j=1}^{N_2} \left(U_{ij}(h) - \widehat{U}_{ij}\right)^2. \tag{7}$$

After the minimization of the functional (7), we obtain the approximate value of the heat transfer coefficient.

3 Method of Solving

Direct problem, defined by Eqs. (1)–(4), for a fixed value of the heat transfer coefficient was solved using an implicit finite difference method. For this purpose, we built a grid of the form

$$S = \left\{(x_i, t_k),\ x_i = i\,\Delta x,\ t_k = k\,\Delta t, i = 0, 1, \ldots, N,\ k = 0, 1, 2, \ldots, M\right\} \tag{8}$$

with size $N \times M$ and steps $\Delta x = L/N,\ \Delta t = t^*/M$. Fractional derivative (5) was approximated by the formula [29]:

$$D_t^{(\alpha)} u_i^k = \sigma(\alpha, \Delta t) \sum_{j=1}^{k} \omega(\alpha, j) \left(u_i^{k-j+1} - u_i^{k-j}\right), \tag{9}$$

where

$$\sigma(\alpha, \Delta t) = \frac{1}{\Gamma(1-\alpha)\,(1-\alpha)\,(\Delta t)^{\alpha}},$$
$$\omega(\alpha, j) = j^{1-\alpha} - (j-1)^{1-\alpha}.$$

Neumann and Robin boundary condition were approximated in the following way:

$$-\lambda \frac{u_1^k - u_{-1}^k}{2\Delta x} = q_k \implies u_{-1}^k = u_1^k + \frac{2\Delta x q_k}{\lambda}, \tag{10}$$

$$-\lambda \frac{u_{N+1}^k - u_{N-1}^k}{2\Delta x} = h_k(u_N^k - u^{\infty}) \implies u_{N+1}^k = u_{N-1}^k - \frac{2\Delta x h_k}{\lambda}(u_N^k - u^{\infty}). \tag{11}$$

In approximations (10) and (11), we considered additional nodes u_{-1} and u_{N+1}. Next, from (10) and (11), we determine values u_{-1}^k and u_{N+1}^k and use them in discrete form of Eq. (1). Using Eq. (9), an approximation of Neumann and Robin boundary conditions (10), (11) and the difference quotient for the second derivative with respect to the spatial variable, we obtain the following differential equations

$k \geq 1,\ i = 0$:

$$\left(\sigma(\alpha, \Delta t) + \frac{2\,a}{(\Delta x)^2}\right) u_0^k - \frac{2\,a}{(\Delta x)^2}\, u_1^k = \\ = \sigma(\alpha,\, \Delta t)\, u_0^{k-1} - \sigma(\alpha,\, \Delta t) \sum_{j=2}^{k} \omega(\alpha, j) \left(u_0^{k-j+1} - u_0^{k-j}\right) + \frac{2}{c\, \varrho\, \Delta x}\, q_k,$$

$k \geq 1,\ i = 1, 2, \ldots, N-1$:

$$-\frac{a}{(\Delta x)^2}\, u_{i-1}^k + \left(\sigma(\alpha,\, \Delta t) + \frac{2\,a}{(\Delta x)^2}\right) u_i^k - \frac{a}{(\Delta x)^2}\, u_{i+1}^k = \\ = \sigma(\alpha,\, \Delta t)\, u_i^{k-1} - \sigma(\alpha,\, \Delta t) \sum_{j=2}^{k} \omega(\alpha, j) \left(u_i^{k-j+1} - u_i^{k-j}\right),$$

$k \geq 1,\ i = N$:

$$-\frac{2\,a}{(\Delta x)^2}\, u_{N-1}^k + \left(\sigma(\alpha,\, \Delta t) + \frac{2\,a}{(\Delta x)^2} + \frac{2}{c\, \varrho\, \Delta x}\, h_k\right) u_N^k = \\ = \sigma(\alpha,\, \Delta t)\, u_N^{k-1} - \sigma(\alpha,\, \Delta t) \sum_{j=2}^{k} \omega(\alpha, j) \left(u_N^{k-j+1} - u_N^{k-j}\right) + \frac{2}{c\, \varrho\, \Delta x}\, h_k\, u^{\infty},$$

where $u_i^k = u(x_i, t_k)$, $h_k = h(t_k)$ and $a = \frac{\lambda}{c\, \varrho}$ is the thermal diffusivity coefficient.

In order to reconstruct the heat transfer coefficient, we will minimize the functional (7) using the parallel ACO algorithm. It is a heuristic algorithm, so the calculation in each case need to be repeated a certain number of times. To shorten the calculation time, we applied parallel computing. Assume the following symbol

$$F(x) - \text{minimized function}, \quad \mathbf{x} = (x_1, \ldots, x_n) \in D,$$
$$nT - \text{number of threads}, \quad M = nT \cdot p - \text{number of ants in one population},$$
$$I - \text{number of iterations}, \quad \alpha_i - \text{narrowing parameters}$$

Now, we present the steps of the algorithm.

Initialization of the algorithm

(i) Setting parameters of the algorithm, and generate starting population $\mathbf{x}^k = (x_1^k, x_2^k, \ldots, x_n^k)$, where $\mathbf{x}^k \in D$, $k = 1, 2, \ldots, M$.
(ii) Dividing the population on nT groups (groups will be calculated in parallel way) and determining the best solution $\mathbf{x}^{best}$.

The main algorithm

(iii) Random selection of the vector $\mathbf{dx} = (dx_1, dx_2, \ldots, dx_n)$, where $-\alpha_i \leq dx_j \leq \alpha_i$.

(iv) Generate a new population of ants $\mathbf{x}^k = \mathbf{x}^{best} + \mathbf{dx},\ k = 1, 2, \ldots, M$.
(v) Determining the best solution (parallel computing) in the current population. If this solution is better than $\mathbf{x}^{best}$, then we accept this solution as $\mathbf{x}^{best}$.
(vi) Points 3–5 are repeated I^2 times.
(vii) Change the values of narrowing parameters α_i: $\alpha_i = 0.1\alpha_i$.
(viii) Points 3–7 are repeated I times.

4 Numerical Results

Let us consider Eq. (1) with the following data

$$t \in [0, 500],\ x \in [0, 0.2],\ c = 1000,\ \varrho = 2680,$$

$$\lambda = 240,\ q(t) = 0,\ u^{\infty} = 300,\ g(x, t) = 0,\ f(x) = 900,$$

$$h(t) = \gamma_1\ Exp\Big[\frac{t - 45}{455} \ln\Big(\frac{\gamma_2}{\gamma_1}\Big)\Big].$$

The exact values of γ_1, γ_2 are equal to 1400 and 800, respectively.

Solving the direct problem for the exact value of the heat transfer coefficient, we get values of the function in grid points of the region D. Then, from these values, we select only those which correspond to the predetermined grid points (location of the thermocouple).

Selected values of the function will be simulated temperature measurements and will be treated as an exact value (exact input data) and denoted by $\widehat{U}_{ij}$. The grid used to generate these data was of the size 300×5000. We assume one measuring point $x_p = 0.15$ ($N_1 = 1$), the measurements from this point will be read every 0.5, 1, 2 s ($N_2 = 1000, 500, 250$).

In order to investigate the effect of measurement errors on the results of reconstruction and stability of the algorithm, the input data was perturbed by the pseudo-random error of sizes 1 and 2 %. In the process of minimizing functional, the direct problem was solve many times. Used for this purpose grid has size of 100×1000 and a different density than the mesh used to generate the input data.

In order to determine the minimum of the functional (7) ACO algorithm was used. This algorithm is heuristic, therefore required to repeat calculations a certain number of times. In this paper, we assumed that the calculations for each case will be repeated ten times. Algorithm was adapted for parallel computations (calculations on multiple threads), which significantly reduced the computational time. Table 1 presents times of single execution of algorithm depending on different number of threads. The number of ants in each case was 12.

As we can see, use of a larger number of threads significantly reduces the computation time. In case of twelve threads, calculation accelerated nearly 8.6 times than

Table 1 Times of single execution of algorithm depending on different number of threads

Number of threads	Time (s)
1	1826.07
2	914.28
3	610.06
4	477.43
6	348.43
12	211.59

Table 2 Results of calculation in case of measurements every 0.5, 1, 2 s (grid 100×500) in measurement point $x_p = 0.15$ ($\overline{\gamma}_i$ – restored value of γ_i, $\delta_{\overline{\gamma}_i}$ – percentage relative error of γ_i, σ – standard deviation ($i = 1, 2$))

Readings	Noise (%)	$\overline{\gamma}_1$	$\delta_{\overline{\gamma}_1}(\%)$	σ	$\overline{\gamma}_2$	$\delta_{\overline{\gamma}_2}(\%)$	σ
Every 0.5 s	0	1402.58	0.19	0.46	798.94	0.14	0.47
	1	1388.24	0.84	0.46	815.62	1.96	0.52
	2	1371.94	2.01	1.60	813.24	1.66	1.95
Every 1 s	0	1402.22	0.16	0.79	799.35	0.09	0.78
	1	1403.44	0.25	0.76	810.04	1.26	0.76
	2	1382.33	1.27	0.72	817.37	2.18	0.77
Every 2 s	0	1402.17	0.16	0.62	799.26	0.10	0.52
	1	1405.97	0.43	0.75	778.81	2.65	0.64
	2	1398.51	0.11	0.82	797.66	0.30	1.08

in case of calculations without multithreading. Because calculation need to be repeat ten times for each case of input data, benefit from saving time is significant.

Table 2 shows result of determining of γ_1, γ_2 depending on the size of disturbance input data at the measurement point $x_p = 0.15$.

In case of exact input data, the relative errors of the reconstruction of coefficients are minimal and do not exceed 0.2 %. In the case of perturbed input data, relative errors of restoring coefficients γ_i usually are smaller than the input data errors.

One of the main indicators of evaluating the results are errors of reconstruction the temperature in the measurement point $x_p = 0.15$. Table 3 presents errors of the reconstruction the temperature at measurement point in case of measurements every 0.5, 1, 2 s. Based on these results, we can say that the reconstructed temperature at the measurement point is very good. Relative errors of reconstruction the temperature in each case do not exceed 0.05 %.

In Fig. 1 there are shown the relative errors of reconstruction of heat transfer coefficient h for measurements every 0.5, 1, 2 s. In each case under consideration, relative error of reconstruction the heat transfer coefficient is less than 1.5 %.

Table 3 Errors of temperature reconstruction in measurement point $x_p = 0.15$ for measurements every 0.5, 1, 2 s (Δ_{avg} – average absolute error, Δ_{max} – maximum absolute error, δ_{avg} – average relative error, δ_{max} – maximum relative error)

Noise	0 %	1 %	2 %	0 %	1 %	2 %	0 %	1 %	2 %
	0.5 s			1 s			2 s		
Δ_{avg} [K]	0.0093	0.1057	0.2452	0.0084	0.1067	0.1372	0.0081	0.1383	0.0599
Δ_{max} [K]	0.0561	0.2050	0.3696	0.0567	0.2346	0.2283	0.0567	0.4121	0.0780
δ_{avg} [%]	0.0011	0.0121	0.0281	0.0010	0.0123	0.0157	0.0010	0.0160	0.0069
δ_{max} [%]	0.0063	0.0238	0.0423	0.0064	0.0272	0.0260	0.0064	0.0478	0.0091

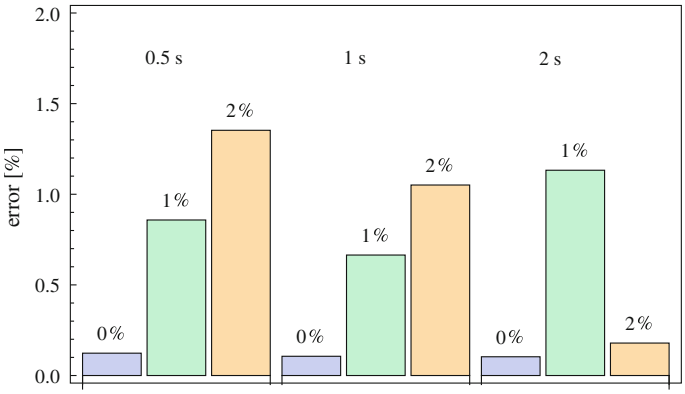

Fig. 1 Relative errors of reconstruction of the heat transfer coefficient for various perturbations of input data and for measurements every 0.5, 1, 2 s

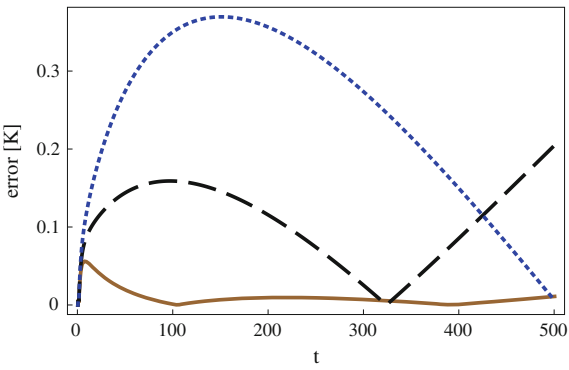

Fig. 2 Distribution of errors of temperature reconstruction in measurement point $x_p = 0.15$ for measurements every 0.5 s and for various perturbations of input data (0 % – *solid line*, 1 % – *dashed line*, 2 % – *dotted line*)

Figure 2 presents the distribution of errors of temperature reconstruction in measurement point $x_p = 0.15$ in case of measurements every 0.5 s.

5 Conclusions

In this paper we considered the inverse problem for the heat conduction equation of fractional order. Heat transfer coefficient, occurring in Robin boundary condition, was reconstructed. Direct problem was solved using the finite difference method, and to minimize the functional, parallel ACO algorithm was used.

Heat transfer coefficient has been reconstructed very well. Errors of this reconstruction in each case are less than 1.5 % and in most cases do not exceed the input data errors. Errors of restore temperature at the measurement point are minimal and do not exceed 0.05 %.

In the paper, parallel ACO algorithm was used, which gives us significant acceleration of computation in compare to the calculation does not use multithreading. Using four threads, algorithm execute nearly 3.8 times faster than calculation does not use multithreading. In case of calculation on 6, 12 threads, time of computation was reduced accordingly 5.2 and 8.6 times.

References

1. Ardakani, M., Khodada, M.: Identification of thermal conductivity and the shape of an inclusion using the boundary elements method and the particle swarm optimization algorithm. Inverse Probl. Sci. Eng. **17**(7), 855–870 (2009)
2. Woźniak, M., Połap, D., Gabryel, M., Nowicki, K., Napoli, C., Tramotana, E.: Can we process 2D images using artificial bee colony? In: Rutkowski, L., Korytkowski, M., Scherer, R., Tadeusiewicz, R., Zadeh, L.A., Zurada, J.M. (eds.) Artificial Intelligent and Soft Computing. Lecture Notes in Computer Science, vol. 9119, pp. 660–671. Springer, Heidelberg (2015)
3. Nowak, A., Woźniak, M., Nowicki, K., Napoli, C.: Can we process 2D images using artificial bee colony? In: Leszek Rutkowski, Marcin Korytkowski, Rafal Scherer, Ryszard Tadeusiewicz, Lotfi A. Zadeh, Jacek M. Zurada (Eds.), Artificial Intelligent and Soft Computing, vol. 9119 of Lecture Notes in Computer Science, pp. 469–480. Springer (2015)
4. Woźniak, M., Połap, D., Napoli, C., Tramotana, E., Damasevicius, R.: Is the colony of ants able to recognize graphic objects? In: Dregvaite, G., Damasevicius, R. (eds.) Information and Software Technologies. Communications in Computer and Information Science, vol. 538, pp. 660–671. Springer, Heidelberg (2015)
5. Toksari, M.D.: Ant colony optimization for finding the global minimum. Appl. Math. Comput. **176**(1), 308–316 (2006)
6. Socha, K., Dorigo, M.: Ant colony optimization in continuous domains. Eur. J. Oper. Res. **185**(3), 1155–1173 (2008)
7. Dorigo, M., Stutzle, T.: Ant Colony Optimization. MIT Press, Cambridge (2004)
8. Karaboga, D., Basturk, B.: On the performance of artificial bee colony (ABC) algorithm. Appl. Soft. Comput. **8**(1), 687–697 (2008)
9. Karaboga, D., Akay, B.: A comparative study of artificial bee colony algorithm. Appl. Math. Comput. **214**(1), 108–132 (2009)
10. Santos, A., Campos Velho, H., Luz, E., Freitas, S., Grell, G., Gan, M.: Firefly optimization to determine the precipitation field on South America. Inverse Probl. Sci. Eng. **21**(3), 451–466 (2013)
11. Hristov, J.: An inverse Stefan problem relevant to boilover: heat balance integral solutions and analysis. Therm. Sci. **11**(2), 141–160 (2007)

12. Grysa, K., Leśniewska, R.: Different finite element approaches for inverse heat conduction problems. Inverse Probl. Sci. Eng. **18**(1), 3–17 (2010)
13. Nowak, I., Smolka, J., Nowak, A.J.: Application of Bezier surfaces to the 3-D inverse geometry problem in continuous casting. Inverse Probl. Sci. Eng. **19**(1), 75–86 (2011)
14. Johansson, B.T., Lesnic, D., Reeve, T.: A meshless regularization method for a two-dimensional two-phase linear inverse Stefan problem. Adv. Appl. Math. Mech. **5**, 825–845 (2013)
15. Hetmaniok, E., Słota, D., Zielonka, A.: Experimental verification of selected artificial intelligence algorithms used for solving the inverse Stefan problem. Numer. Heat Tr. B-Fund. **66**(4), 343–359 (2014)
16. Murio, D.A.: Stable numerical solution of a fractional-diffusion inverse heat conduction problem. Comput. Math. Appl. **53**(10), 1492–1501 (2007)
17. Murio, D.A.: Time fractional IHCP with Caputo fractional derivatives. Comput. Math. Appl. **56**(9), 2371–2381 (2008)
18. Murio, D.A., Mejia, C.E.: Generalized time fractional IHCP with Caputo fractional derivatives. J. Phys. Conf. Ser. **135**, 8 (2008)
19. Murio, D.A.: Stable numerical evaluation of Grünwald–Letnikov fractional derivatives applied to a fractional IHCP. Inverse Probl. Sci. Eng. **17**(2), 229–243 (2009)
20. Miller, L., Yamamoto, M.: Coefficient inverse problem for a fractional diffusion equation. Inverse Probl. **8**(7), 8 (2013)
21. Wei, T., Zhang, Z.Q.: Reconstruction of time-dependent source term in a time-fractional diffusion equation. Eng. Anal. Bound. Elem. **37**(1), 23–31 (2013)
22. Jin, B., Rundell, W.: An inverse problem for a one-dimensional time-fractional diffusion problem. Inverse Probl. **28**(7), 19 (2012)
23. Zheng, G.H., Wei, T.: A new regularization method for the time fractional inverse advection-dispersion problem. SIAM J. Numer. Anal. **49**(5), 1972–1990 (2011)
24. Zheng, G.H., Wei, T.: A new regularization method for solving a time-fractional inverse diffusion problem. J. Math. Anal. Appl. **378**(2), 418–431 (2011)
25. Dou, F.F., Hon, Y.C.: Kernel-based approximation for Cauchy problem of the time-fractional diffusion equation. Eng. Anal. Bound. Elem. **36**(9), 1344–1352 (2012)
26. Xiong, X., Zhoua, Q., Honb, Y.C.: An inverse problem for fractional diffusion equation in 2-dimensional case: stability analysis and regularization. J. Math. Anal. Appl. **393**(1), 185–199 (2012)
27. Brociek, R., Słota, D., Wituła, R.: Reconstruction of the thermal conductivity coefficient in the time fractional diffusion equation. In: Latawiec, K.J., Łukaniszyn, M., Stanisławski, R. (eds.) Advances in Modelling and Control of Non-integer-Order Systems, vol. 320, pp. 239–247. Springer, Heidelberg (2015)
28. Brociek, R., Słota, D.: Reconstruction of the boundary condition for the heat conduction equation of fractional order. Therm. Sci. **19**, 35–42 (2015)
29. Murio, D.A.: Implicit finite difference approximation for time fractional diffusion equations. Comput. Math. Appl. **56**(4), 1138–1145 (2008)
30. Brociek, R.: Implicite finite difference metod for time fractional diffusion equations with mixed boundary conditions. Zesz. Nauk. PŚ. Mat. Stosow. **4**, 73–87 (2014)

Linear and Nonlinear Fractional Voigt Models

Amar Chidouh, Assia Guezane-Lakoud, Rachid Bebbouchi, Amor Bouaricha and Delfim F.M. Torres

Abstract We consider fractional generalizations of the ordinary differential equation that governs the creep phenomenon. Precisely, two Caputo fractional Voigt models are considered: a rheological linear model and a nonlinear one. In the linear case, an explicit Volterra representation of the solution is found, involving the generalized Mittag-Leffler function in the kernel. For the nonlinear fractional Voigt model, an existence result is obtained through a fixed point theorem. A nonlinear example, illustrating the obtained existence result, is given.

Keywords Fractional differential equation · Creep phenomenon · Initial value problem · Mittag-Leffler function · Fixed point theorem

---

This work is part of first author's Ph.D., which is carried out at Houari Boumediene University, Algeria.

A. Chidouh · R. Bebbouchi
Laboratory of Dynamic Systems, Houari Boumediene University, Algiers, Algeria
e-mail: m2ma.chidouh@gmail.com

R. Bebbouchi
e-mail: rbebbouchi@hotmail.com

A. Guezane-Lakoud
Laboratory of Advanced Materials, Badji Mokhtar-Annaba University, Annaba, Algeria
e-mail: a_guezane@yahoo.fr

A. Bouaricha
Laboratory of Industrial Mechanics, Badji Mokhtar-Annaba University, Annaba, Algeria
e-mail: bouarichaa@yahoo.fr

D.F.M. Torres (✉)
Department of Mathematics, Center for Research and Development in Mathematics and Applications (CIDMA), University of Aveiro, 3810-193 Aveiro, Portugal
e-mail: delfim@ua.pt

A. Babiarz et al. (eds.), *Theory and Applications of Non-integer Order Systems*,
Lecture Notes in Electrical Engineering 407, DOI 10.1007/978-3-319-45474-0_15

1 Introduction

To study the behaviour of viscoelastic materials, one often uses rheological models that can be of Voigt or Maxwell type or a combination of these basic models [1]. For example, the classical phenomenon of creep, in its simplest form, is known to be governed by a linear ordinary differential equation of order one, given by the linear Voigt model:

$$\eta \frac{d\epsilon(t)}{dt} + E\epsilon(t) = \sigma(t), \quad \sigma(0) = 0, \tag{1}$$

where η is the viscosity coefficient and E is the modulus of the elasticity. For a given stress history σ, the solution of (1) is given by

$$\epsilon(t) = \frac{1}{\eta} \int_0^t e^{-\frac{t-s}{\tau}} \sigma(s) ds, \quad \tau = \frac{\eta}{E}, \tag{2}$$

where for $t \leq 0$ the material is at rest, without stress and strain. The constant τ is called the retardation time and has an analogous meaning to relaxation: it is an estimation of the time required for the creep process to approach completion. The expression

$$k(t) = \frac{1}{E} \left(1 - \exp\left(-\frac{t}{\tau}\right)\right), \quad t \geq 0, \tag{3}$$

is known as the creep function. In Sect. 2 we generalize (1)–(3).

Fractional calculus has recently become an important tool in the analysis of viscoelastic phenomena, such as stress-strain relationships in polymeric materials: in [2] the connection between the fractional calculus and the theory of Abel's integral equation is shown for materials with memory, while a fractional order Voigt model is proposed in [3] to better simulate the surface wave response of soft tissue-like material phantoms. For an historical survey of the contributions on the applications of fractional calculus in linear viscoelasticty, see [4]. In 1996, Mainardi investigated linear fractional relaxation-oscillation and fractional diffusion-wave phenomena [5]. Several other works in the same direction of research followed: for an introduction to the linear operators of fractional integration and fractional differentiation, accessible to applied scientists, we refer to [6]; for a comprehensive overview of fractional calculus and waves in linear viscoelastic media see [7]; for a book devoted to the description of the properties of the Mittag-Leffler function, its numerous generalizations and their applications in different areas of modern science, we refer to [8]; for a generalization of the partial differential equation of Gaussian diffusion, by using the time-fractional derivative, in both the Riemann–Liouville and Caputo senses, see [9]. Heymans and Podlubny have given a physical interpretation of initial conditions for fractional differential equations with Riemann–Liouville fractional derivatives [10]. Here, motivated by such results, we examine fractional creep equations involving Caputo derivatives of order $\alpha \in (0, 1)$. Caputo derivatives were chosen because they

have a major utility for treating initial-value problems for physical and engineering applications, where initial conditions are usually expressed in terms of integer-order derivatives [11, 12]. Precisely, we begin by considering in Sect. 2 the following extension to (1):

$$\begin{cases} \eta^{\alpha} \left({}^{C}D_{0}^{\alpha} \epsilon \right)(t) + E^{\alpha} \epsilon(t) = \sigma(t), \quad 0 < t \leq 1, \\ \epsilon(0) = 0, \end{cases} \tag{4}$$

where $E, \eta > 0$ and σ is a continuous function defined on $[0, 1]$. While the solution (2) of (1) is described by an exponential function, we show that the solution of (4) is expressed in terms of the Mittag-Leffler function (see Theorem 1), which is a generalization of the exponential function and was introduced by Mittag-Leffler in [13], where he investigated some of their properties. The Mittag-Leffler function $E_{\alpha}(t)$ with $\alpha > 0$ is defined by the series representation

$$E_{\alpha}(t) = \sum_{n=0}^{\infty} \frac{t^n}{\Gamma(\alpha n + 1)}, \quad \alpha > 0, \quad t \in \mathbb{C}, \tag{5}$$

where Γ denotes the Gamma function, valid in the whole complex plane. A straightforward generalization of the Mittag-Leffler function (5), due to Wiman [14] and used here, is obtained by replacing the additive constant 1 in the argument of the Gamma function in (5) by an arbitrary complex parameter β:

$$E_{\alpha,\beta}(t) = \sum_{n=0}^{\infty} \frac{t^n}{\Gamma(\alpha n + \beta)}, \quad \alpha > 0, \quad \beta > 0, \quad t \in \mathbb{C}. \tag{6}$$

Mittag-Leffler functions are considered to be the queen functions of fractional calculus and they play a fundamental role in the solution to (4). Details about the Mittag-Leffler function and their importance when solving fractional differential equations can be found in [15–17] and references therein. Here we transform (4) as a Volterra integral equation to obtain an explicit solution involving the Mittag-Leffler function (see Proof of Theorem 1). Moreover, we give a physical interpretation to the fractional order Voigt model (4) as a creep phenomenon, by finding the corresponding creep function (Theorem 2). Under some assumptions on σ, when it depends on ϵ (nonlinear Voigt model), in Sect. 3 we address the question of existence of positive solutions, which also contributes to the physical interpretation of the model (Theorem 3). Roughly speaking, the existence of nontrivial positive solutions is obtained by means of the Guo–Krasnosel'skii fixed point theorem. We end with an illustrative example and Sect. 4 of conclusions.

2 Solution to the Fractional Rheological Linear Voigt Model

Viscoelastic relations may be expressed in both integral and differential forms. Differential forms are related to rheological models and provide a more direct physical interpretation of the viscoelastic behavior. Integral forms are very general and appropriate for theoretical work. In Sect. 1 we introduced the fractional Voigt model (4) and explained its physical relevance. Here we make use of the corresponding integral representation to obtain an explicit solution to (4).

Theorem 1 (The fractional strain) *Assume that the given stress history σ of the fractional initial value problem (4) is a continuous function on* $[0, 1]$. *Then*

$$\epsilon(t) = \frac{1}{\eta^\alpha} \int_0^t (t-s)^{\alpha-1} E_{\alpha,\alpha} \left(-\left(\frac{t-s}{\tau} \right)^\alpha \right) \sigma(s) ds, \tag{7}$$

$0 \le t \le 1$, *is the fractional strain, that is, is the solution to (4).*

Proof Since σ is a continuous function on $[0, 1]$, then we know from [18, Theorem 3.24] that the fractional initial problem (4) is equivalent to the Volterra integral equation of second kind

$$\epsilon(t) = \frac{1}{\eta^\alpha \Gamma(\alpha)} \int_0^t (t-s)^{\alpha-1} \sigma(s) ds - \frac{1}{\tau^\alpha \Gamma(\alpha)} \int_0^t (t-s)^{\alpha-1} \epsilon(s) ds.$$

To solve this integral equation, we apply the method of successive approximations. Let us consider the sequence defined by the following recurrence relation: $\epsilon_m = \frac{I^\alpha \sigma}{\eta^\alpha} - \frac{I^\alpha \epsilon_{m-1}}{\tau^\alpha}$, where $I^\alpha z(t) = \frac{1}{\Gamma(\alpha)} \int_0^t (t-s)^{\alpha-1} z(s) ds$. Setting $\epsilon_0 = \frac{I^\alpha \sigma}{\eta^\alpha}$, we get $\epsilon_1 = \frac{I^\alpha \sigma}{\eta^\alpha} - \frac{I^{2\alpha} \sigma}{\eta^\alpha \tau^\alpha}$ and $\epsilon_2 = \frac{I^\alpha \sigma}{\eta^\alpha} - \frac{I^{2\alpha} \sigma}{\eta^\alpha \tau^\alpha} + \frac{I^{3\alpha} \sigma}{\eta^\alpha \tau^{2\alpha}}$. Continuing this process, we obtain that

$$\epsilon_m = \frac{1}{\eta^\alpha} \sum_{k=0}^{m} \left(-\frac{1}{\tau^\alpha} \right)^k I^{k\alpha+\alpha} \sigma.$$

Consequently, we have

$$\epsilon_m(t) = \frac{1}{\eta^\alpha} \int_0^t (t-s)^{\alpha-1} \sum_{k=0}^{m} \frac{(t-s)^{k\alpha}}{\Gamma(k\alpha+\alpha)} \left(-\frac{1}{\tau^\alpha} \right)^k \sigma(s) ds.$$

Taking the limit as $m \to \infty$, and by (6), we obtain the explicit solution (7). □

Remark 1 Our fractional problem (4) provides a generalization to the linear Voigt creep model (1). If we take $\alpha = 1$, then Theorem 1 gives the solution (2) to the classical problem (1).

We now generalize the creep function (3) to our fractional Voigt model (4).

Theorem 2 (The fractional creep function) *The creep function associated with the fractional initial value problem (4) is given by*

$$k_\alpha(t) = -\left(\frac{\tau}{\eta}\right)^\alpha \left(E_\alpha\left(-\left(\frac{t}{\tau}\right)^\alpha\right) - 1\right). \tag{8}$$

Proof We find the creep function k_α by using (7), where the latter is defined as

$$\epsilon(t) = \int_0^t k_\alpha(t-s)d\sigma(s), \quad 0 \le t \le 1.$$

Integrating expression (7) by parts, we obtain that

$$\begin{aligned}\epsilon(t) = \frac{1}{\eta^\alpha} t^\alpha E_{\alpha,\alpha+1}\left(-\left(\frac{t}{\tau}\right)^\alpha\right)\sigma(0) \\ + \frac{1}{\eta^\alpha}\int_0^t (t-s)^\alpha E_{\alpha,\alpha+1}\left(-\left(\frac{t-s}{\tau}\right)^\alpha\right)\sigma'(s)ds, \quad 0 \le t \le 1.\end{aligned}$$

The strain is linear in the stress. Therefore, the creep function is given by

$$k_\alpha(t) = \frac{1}{\eta^\alpha} t^\alpha E_{\alpha,\alpha+1}\left(-\left(\frac{t}{\tau}\right)^\alpha\right). \tag{9}$$

Now, by using the definition of Mittag-Leffler function in (9), we obtain that

$$\begin{aligned}k_\alpha(t) &= \frac{1}{\eta^\alpha} t^\alpha \sum_{n=0}^{\infty}(-1)^n \frac{\left(\frac{t}{\tau}\right)^{\alpha n}}{\Gamma(\alpha n + \alpha + 1)} = \left(\frac{\tau}{\eta}\right)^\alpha \sum_{n=0}^{\infty}(-1)^n \frac{\left(\frac{t}{\tau}\right)^{\alpha n+\alpha}}{\Gamma(\alpha n + \alpha + 1)} \\ &= -\left(\frac{\tau}{\eta}\right)^\alpha \sum_{n=1}^{\infty}(-1)^n \frac{\left(\frac{t}{\tau}\right)^{\alpha n}}{\Gamma(\alpha n + 1)} = -\left(\frac{\tau}{\eta}\right)^\alpha \left(E_\alpha\left(-\left(\frac{t}{\tau}\right)^\alpha\right) - 1\right).\end{aligned}$$

The proof is complete. □

Remark 2 If we take $\alpha = 1$, then we obtain from Theorem 2 that

$$k_1(t) = \frac{\tau}{\eta}\left(1 - E_1\left(-\left(\frac{t}{\tau}\right)\right)\right) = \frac{1}{E}\left(1 - \exp\left(-\left(\frac{t}{\tau}\right)\right)\right) = k(t),$$

that is, the creep function (3) is a special case of the $k_\alpha(t)$ given by (8).

Next we generalize (4) to the nonlinear case, where the stress σ depends on the strain ϵ.

3 A Nonlinear Fractional Voigt Model

By applying the method of successive approximations, we have proved in Sect. 2 that the fractional initial value problem (4) has a solution ϵ in $C[0, 1]$ given by (7). Let us now consider (4) as a nonlinear problem, that is, consider a fractional Voigt model described by a differential equation with a nonlinear right-hand side σ depending on ϵ:

$$\begin{cases} \eta^{\alpha} \left({}^{C}D_{0}^{\alpha}\epsilon\right)(t) + E^{\alpha}\epsilon(t) = \sigma(\epsilon(t)), \quad 0 < t \leq 1, \\ \epsilon(0) = 0. \end{cases} \tag{10}$$

We deal with the solvability of the initial value problem (10). Precisely, we are interested in proving the existence of positive solutions, which are the ones that make sense in physics. To establish existence of solutions has been a very active research area in mathematics. This is particularly true with respect to existence of solutions for fractional differential equations [19], which is also explained by the development of other fields of research, such as physics, mechanics and biology [11, 20, 21]. Many methods are used to prove existence of a solution, such as the fixed point technique, for which several theories are available [22–24]. In recent years, there has been many papers investigating the existence of positive solutions: see [25–30] and references therein. In this section, motivated by many papers that discuss the existence of solutions to initial value problems, e.g. [31–33], we focus on the fractional initial value problem (10).

Theorem 3 (Existence of a positive solution to the nonlinear fractional Voigt model (10)) *Assume that $\sigma : \mathbb{R}_+ \to \mathbb{R}_+$ is a continuous, convex and decreasing function. Let $\mathbf{E}_0 := \lim_{\epsilon\to 0} \frac{\sigma(\epsilon)}{\epsilon}$ and $\mathbf{E}_\infty := \lim_{\epsilon\to\infty} \frac{\sigma(\epsilon)}{\epsilon}$. If $\mathbf{E}_0 = \infty$ and $\mathbf{E}_\infty = 0$, then problem (10) has at least one nontrivial positive bounded solution $\epsilon \in X$.*

Our Theorem 3 is proved by the Guo–Krasnosel'skii fixed point theorem [34, 35]. Roughly speaking, our analysis is mainly based on the following result on the monotonicity of the Mittag-Leffler function, which was first proved by Schneider in [36]: the generalized Mittag-Leffler function $E_{\alpha,\beta}(-t)$ with $t \geq 0$ is completely monotonic if and only if $0 < \alpha \leq 1$ and $\beta \geq \alpha$. Thus, if $0 < \alpha \leq 1$ and $\beta \geq \alpha$, then $(-1)^n \frac{d^n}{dt^n} E_{\alpha,\beta}(-t) \geq 0$ for all $n = 0, 1, 2, \ldots$ Note that $\sigma(0) \neq 0$ because our function σ is positive and decreasing and we are interested in a nontrivial solution.

3.1 Auxiliary Results

Let $X = C[0, 1]$ be the Banach space of all continuous real functions defined on $[0, 1]$ with the norm $\|u\| = \sup_{t\in[0,1]} |u(t)|$. Define the operator $T : X \to X$ by

$$T\epsilon(t) = \frac{1}{\eta^\alpha} \int_0^t (t-s)^{\alpha-1} E_{\alpha,\alpha}\left(-\left(\frac{t-s}{\tau}\right)^\alpha\right) \sigma(\epsilon(s))ds, \quad 0 \le t \le 1. \tag{11}$$

Using the Guo–Krasnosel'skii fixed point theorem, we prove existence of nontrivial positive solutions. For that we first present and prove several lemmas. In what follows, K is the cone $K := \{\epsilon \in X : \ \epsilon(t) \ge 0, \ 0 \le t \le 1\}$.

Lemma 1 *The operator $T : K \to K$ is completly continuous.*

Proof Taking into account the monotonicity of the Mittag-Leffler function, we have that the operator $T : K \to K$ is continuous in view of the assumptions of non-negativeness and continuity of σ. Let $B \subset K$ be the bounded set $B := B(0, \eta_0) = \{\epsilon \in K : \|\epsilon\| \le \eta_0, \ \eta_0 > 0\}$, and let $\rho = \max_{0\le t\le 1, 0\le\epsilon\le\eta_0} \sigma(\epsilon(t)) + 1$. Then, for any $\epsilon \in B$, we have

$$\begin{aligned} |T\epsilon(t)| &= \left| \frac{1}{\eta^\alpha} \int_0^t (t-s)^{\alpha-1} E_{\alpha,\alpha}\left(-\left(\frac{t-s}{\tau}\right)^\alpha\right) \sigma(\epsilon(s))ds \right| \\ &\le \frac{1}{\eta^\alpha} \int_0^t (t-s)^{\alpha-1} E_{\alpha,\alpha}\left(-\left(\frac{t-s}{\tau}\right)^\alpha\right) |\sigma(\epsilon(s))| \, ds \\ &\le \frac{\rho}{\eta^\alpha \Gamma(\alpha+1)} t^\alpha \Rightarrow \|T\epsilon\| \le \frac{\rho}{\eta^\alpha \Gamma(\alpha+1)}. \end{aligned}$$

Hence, $T(B)$ is uniformly bounded. Now, we prove that the operator T is equicontinuous for each $\epsilon \in B$, any $\varepsilon > 0$, and $t_1, t_2 \in [0, 1]$ with $t_2 > t_1$. Let $\delta = \left(\frac{\eta^\alpha \Gamma(\alpha+1)\varepsilon}{2\rho}\right)^{\frac{1}{\alpha}}$. Then, for $|t_2 - t_1| < \delta$,

$$\begin{aligned} &|T\epsilon(t_1) - T\epsilon(t_2)| \\ &\quad \le \frac{\rho}{\eta^\alpha \Gamma(\alpha)} \left(\int_0^{t_1} ((t_1-s)^{\alpha-1} - (t_2-s)^{\alpha-1})ds + \int_{t_1}^{t_2} (t_2-s)^{\alpha-1} ds \right) \\ &\quad \le \frac{\rho\left((t_1^\alpha + (t_2 - t_1)^\alpha - t_2^\alpha + (t_2 - t_1)^\alpha\right)}{\eta^\alpha \Gamma(\alpha+1)} \le \frac{2\rho(t_2-t_1)^\alpha}{\eta^\alpha \Gamma(\alpha+1)} = \varepsilon. \end{aligned}$$

Therefore, $T(B)$ is equicontinuous. From the Arzela–Ascoli theorem, it follows that operator T is completely continuous. □

The following results are also used in the proof of our Theorem 3.

Lemma 2 (Jensen's inequality [37]) *Let μ be a positive measure and let Ω be a measurable set with $\mu(\Omega) = 1$. Let I be an interval and suppose that u is a real function in $L^1(\Omega)$ with $u(t) \in I$ for all $t \in \Omega$. If f is convex on I, then*

$$f\left(\int_{\Omega} u(t)d\mu(t)\right) \leq \int_{\Omega} (f \circ u)(t)d\mu(t).$$

Lemma 3 (Guo–Krasnosel'skii's fixed point theorem [34]) *Let X be a Banach space and let $K \subset X$ be a cone. Assume Ω_1 and Ω_2 are bounded open subsets of X with $0 \in \Omega_1 \subset \overline{\Omega}_1 \subset \Omega_2$, and let $T : K \cap (\overline{\Omega}_2 \backslash \Omega_1) \to K$ be a completely continuous operator such that either*

(i) $Tu \leq u$ for any $u \in K \cap \partial\Omega_1$ and $Tu \geq u$ for any $u \in K \cap \partial\Omega_2$, or
(ii) $Tu \geq u$ for any $u \in K \cap \partial\Omega_1$ and $Tu \leq u$ for any $u \in K \cap \partial\Omega_2$.

Then T has a fixed point in $K \cap (\overline{\Omega}_2 \backslash \Omega_1)$.

Since σ is continuous on $\mathbb{R}_+$, we can define the function $\overline{\sigma}(\epsilon) = \max_{0 \leq z \leq \epsilon} \{\sigma(z)\}$. Let $\overline{\mathbf{E}}_0 = \lim_{\epsilon \to 0} \frac{\overline{\sigma}(\epsilon)}{\epsilon}$ and $\overline{\mathbf{E}}_\infty = \lim_{\epsilon \to \infty} \frac{\overline{\sigma}(\epsilon)}{\epsilon}$.

Lemma 4 (See [29]) *Assume σ is continuous. Then $\overline{\mathbf{E}}_0 = \mathbf{E}_0$ and $\overline{\mathbf{E}}_\infty = \mathbf{E}_\infty$.*

We are now in condition to prove Theorem 3.

3.2 *Proof of Theorem 3*

By Lemma 1, we know that the operator (11) is completely continuous. Now, using Lemma 3, we give a proof to our result. Denote $\Omega_{r_i} = \{\epsilon \in X : \|\epsilon\| < r_i\}$. When $\mathbf{E}_0 = \infty$, we can choose $r_1 > 0$ sufficiently small such that $\sigma(\epsilon) \geq \varpi\epsilon$ for $\epsilon \leq r_1$, where ϖ satisfies $\left(\varpi \frac{E_{\alpha,\alpha}(-\frac{1}{\tau^\alpha})}{\eta^\alpha \alpha(\alpha+1)}\right) > 1$. Now let us show that $T\epsilon \leq \epsilon$ for any $\epsilon \in K \cap \partial\Omega_{r_1}$. In fact, if there exists $\epsilon_1 \in \partial\Omega_{r_1}$ such that $T\epsilon_1 \leq \epsilon_1$, the following inequalities hold:

$$\begin{aligned}
\|\epsilon_1\| \geq \|T\epsilon_1\| &\geq \int_0^1 T\epsilon_1(t)dt \\
&\geq \frac{1}{\eta^\alpha} \int_0^1 \int_0^t (t-s)^{\alpha-1} E_{\alpha,\alpha}\left(-\left(\frac{t-s}{\tau}\right)^\alpha\right) \sigma(\epsilon_1(s))dsdt \\
&\geq \frac{1}{\eta^\alpha} E_{\alpha,\alpha}\left(-\frac{1}{\tau^\alpha}\right) \int_0^1 \sigma(\epsilon_1(s)) \left(\int_s^1 (t-s)^{\alpha-1} dt\right) ds \\
&\geq \frac{E_{\alpha,\alpha}\left(-\frac{1}{\tau^\alpha}\right)}{\eta^\alpha \alpha} \int_0^1 (1-s)^\alpha \sigma(\epsilon_1(s))ds \\
&\geq \frac{E_{\alpha,\alpha}\left(-\frac{1}{\tau^\alpha}\right)}{\eta^\alpha \alpha(\alpha+1)} \int_0^1 (\alpha+1)(1-s)^\alpha \sigma(\epsilon_1(s))ds.
\end{aligned}$$

Then, by Lemma 2, we have

$$\begin{aligned}\|\epsilon_1\| &\geq \frac{E_{\alpha,\alpha}(-\frac{1}{\tau^\alpha})}{\eta^\alpha\alpha(\alpha+1)}\sigma\left(\int_0^1(\alpha+1)(1-s)^\alpha\epsilon_1(s)ds\right)\\ &\geq \frac{E_{\alpha,\alpha}(-\frac{1}{\tau^\alpha})}{\eta^\alpha\alpha(\alpha+1)}\sigma\left(\int_0^1(\alpha+1)(1-s)^\alpha r_1 ds\right)\\ &\geq \frac{E_{\alpha,\alpha}(-\frac{1}{\tau^\alpha})}{\eta^\alpha\alpha(\alpha+1)}\sigma\left(r_1\right) \geq \varpi\frac{E_{\alpha,\alpha}(-\frac{1}{\tau^\alpha})}{\eta^\alpha\alpha(\alpha+1)}r_1 > r_1,\end{aligned}$$

which is a contradiction. Since $\mathbf{E}_\infty = 0$, Lemma 4 implies $\overline{\mathbf{E}}_\infty = 0$. Thus, there exists $r_2 \in (r_1, \infty)$ such that $\overline{\sigma}(r_2) < \eta^\alpha\Gamma(\alpha+1)r_2$. Note that $0 < \Gamma(\alpha+1) < 1$ for all $\alpha \in (0, 1)$. We now show that $T\epsilon \geq \epsilon$ for any $\epsilon \in K \cap \partial\Omega_{r_2}$. If there exists $\epsilon_2 \in \partial\Omega_{r_2}$ such that $T\epsilon_2 \geq \epsilon_2$, then

$$\begin{aligned}\|\epsilon_2\| \leq \|T\epsilon_2\| &= \sup_{t\in[0,1]}\frac{1}{\eta^\alpha}\int_0^t(t-s)^{\alpha-1}E_{\alpha,\alpha}\left(-\left(\frac{t-s}{\tau}\right)^\alpha\right)\sigma\left(\epsilon_2(s)\right)ds\\ &\leq \frac{1}{\eta^\alpha\Gamma(\alpha+1)}\max_{0<\epsilon_2<r_2}\sigma(\epsilon_2)\\ &\leq \frac{1}{\eta^\alpha\Gamma(\alpha+1)}\overline{\sigma}(r_2) < r_2,\end{aligned}$$

which is a contradiction. Hence, from the first part of the Lemma 3, T has a fixed point in $K \cap (\overline{\Omega}_{r_2}\backslash\Omega_{r_1})$. Therefore, problem (10) has at least one nontrivial bounded positive solution $\epsilon \in X$.

3.3 An Example

We now take a simple example to illustrate our analysis. Consider problem

$$\begin{cases} {}^C D_0^{\frac{1}{2}}\epsilon(t) + \sqrt{2}\epsilon(t) = \frac{1}{1+\epsilon(t)}, \quad 0 < t \leq 1,\\ \epsilon(0) = 0.\end{cases} \tag{12}$$

As already mentioned, the term $\frac{1}{1+\epsilon(t)}$ is the constitutive equation of the creep. Function $\sigma(\epsilon) = \frac{1}{1+\epsilon} : \mathbb{R}_+ \to \mathbb{R}_+$ is continuous, convex and decreasing with $\sigma(0) \neq 0$. Due to the fact that $\mathbf{E}_0 = \infty$ and $\mathbf{E}_\infty = 0$, it follows from Theorem 3 that (12) has at least one nontrivial bounded positive solution $\epsilon \in C[0, 1]$.

4 Conclusion

In this work we investigated the creep phenomenon described by linear and nonlinear fractional order Voigt models involving the Caputo derivative. We were able to give an integral representation of our initial value problem and to compute the creep function in the linear case. The obtained Volterra integral equation involves the Mittag-Leffler function in the kernel, which is a completely monotonic function in the context of our considerations. This property was the key of our analysis to establish existence of positive solutions.

Acknowledgments This research was finished while Chidouh was visiting University of Aveiro, Portugal. The hospitality of the host institution and the financial support of Houari Boumedienne University, Algeria, are here gratefully acknowledged. Torres was supported by CIDMA and FCT within project UID/MAT/04106/2013. The authors are grateful to two referees for valuable comments and suggestions.

References

1. Marques, S.P.C., Creus, G.J.: Computational Viscoelasticity. Springer Briefs in Applied Sciences and Technology. Springer, Heidelberg (2012)
2. Koeller, R.C.: Applications of fractional calculus to the theory of viscoelasticity. Trans. ASME J. Appl. Mech. **51**(2), 299–307 (1984)
3. Meral, F.C., Royston, T.J., Magin, R.: Fractional calculus in viscoelasticity: an experimental study. Commun. Nonlinear Sci. Numer. Simul. **15**(4), 939–945 (2010)
4. Mainardi, F.: An historical perspective on fractional calculus in linear viscoelasticity. Fract. Calc. Appl. Anal. **15**(4), 712–717 (2012)
5. Mainardi, F.: Fractional relaxation-oscillation and fractional diffusion-wave phenomena. Chaos Solitons Fractals **7**(9), 1461–1477 (1996)
6. Gorenflo, R., Mainardi, F.: Fractional calculus: integral and differential equations of fractional order. In: Fractals and Fractional Calculus in Continuum Mechanics, of CISM Courses and Lectures, vol. 378, pp. 223–276. Springer, Vienna (1997)
7. Mainardi, F.: Fractional Calculus and Waves in Linear Viscoelasticity. Imperial College Press, London (2010)
8. Gorenflo, R., Kilbas, A.A., Mainardi, F., Rogosin, S.V.: Mittag-Leffler Functions, Related Topics and Applications. Springer Monographs in Mathematics. Springer, Heidelberg (2014)
9. Mainardi, F., Mura, A., Pagnini, G., Gorenflo, R.: Time-fractional diffusion of distributed order. J. Vib. Control **14**(9–10), 1267–1290 (2008)
10. Heymans, N., Podlubny, I.: Physical interpretation of initial conditions for fractional differential equations with Riemann–Liouville fractional derivatives. Rheol. Acta **45**(5), 765–771 (2006)
11. Abbas, M.I.: Existence and uniqueness of solution for a boundary value problem of fractional order involving two Caputo's fractional derivatives. Adv. Difference Equ. **2015**(1), 1–19 (2015)
12. Mozyrska, D., Torres, D.F.M.: Minimal modified energy control for fractional linear control systems with the Caputo derivative. Carpathian J. Math. **26**(2), 210–221 (2010)
13. Mittag-Leffler, G.: Sur la représentation analytique d'une branche uniforme d'une fonction monogène. Acta Math. **29**(1), 101–181 (1905)
14. Wiman, A.: Über den Fundamentalsatz in der Teorie der Funktionen $E^a(x)$. Acta Math. **29**(1), 191–201 (1905)
15. Podlubny, I.: Fractional Differential Equations. Mathematics in Science and Engineering, vol. 198. Academic Press, San Diego (1999)

16. Soubhia, A.L., Camargo, R.F., de Oliveira, E.C., Vaz, J.: Theorem for series in three-parameter Mittag-Leffler function. Fract. Calc. Appl. Anal. **13**(1), 9–20 (2010)
17. Yaşar, B.Y.: Generalized Mittag-Leffler function and its properties. New Trends Math. Sci. **3**(1), 12–18 (2015)
18. Kilbas, A.A., Srivastava, H.M., Trujillo, J.J.: Theory and Applications of Fractional Differential Equations. North-Holland Mathematics Studies, vol. 204. Elsevier, Amsterdam (2006)
19. Abbas, S., Benchohra, M.: Advanced Functional Evolution Equations and Inclusions. Developments in Mathematics. Springer, Heidelberg (2015)
20. Jiang, J., Li, C.F., Cao, D., Chen, H.: Existence and uniqueness of solution for fractional differential equation with causal operators in Banach spaces. Mediterr. J. Math. **12**(3), 751–769 (2015)
21. Sidi Ammi, M.R., El Kinani, E.H., Torres, D.F.M.: Existence and uniqueness of solutions to functional integro-differential fractional equations. Electron. J. Differ. Equ. **2012**(103) (2012)
22. Abbas, S., Benchohra, M., N'Guérékata, G.M.: Topics in Fractional Differential Equations. Developments in Mathematics. Springer, New York (2012)
23. Benkhettou, N., Hammoudi, A., Torres, D.F.M.: Existence and uniqueness of solution for a fractional Riemann–Liouville initial value problem on time scales. J. King Saud Univ. Sci. **28**(1), 87–92 (2016)
24. Debbouche, A., Nieto, J.J., Torres, D.F.M.: Optimal solutions to relaxation in multiple control problems of Sobolev type with nonlocal nonlinear fractional differential equations. J. Optim. Theor. Appl., (2016, in press)
25. Chidouh, A., Torres, D.F.M.: A generalized Lyapunov's inequality for a fractional boundary value problem. J. Comput. Appl. Math. (2016, in press)
26. Graef, J.R., Kong, L., Wang, H.: A periodic boundary value problem with vanishing Green's function. Appl. Math. Lett. **21**(2), 176–180 (2008)
27. Li, N., Wang, C.: New existence results of positive solution for a class of nonlinear fractional differential equations. Acta Math. Sci. Ser. B Engl. Ed. **33**(3), 847–854 (2013)
28. Ammi, M.R., Torres, D.F.M.: Existence and uniqueness of a positive solution to generalized nonlocal thermistor problems with fractional-order derivatives. Differ. Equ. Appl. **4**(2), 267–276 (2012)
29. Wang, H.: On the number of positive solutions of nonlinear systems. J. Math. Anal. Appl. **281**(1), 287–306 (2003)
30. Webb, J.R.L.: Boundary value problems with vanishing Green's function. Commun. Appl. Anal. **13**(4), 587–595 (2009)
31. Chidouh, A., Guezane-Lakoud, A., Bebbouchi, R.: Positive solutions for an oscillator fractional initial value problem. J. Appl. Math. Comput. (2016, in press)
32. Chidouh, A., Guezane-Lakoud, A., Bebbouchi, R.: Positive solutions of the fractional relaxation equation using lower and upper solutions. Vietnam J. Math. (2016, in press)
33. Guezane-Lakoud, A.: Initial value problem of fractional order. Cogent Math. **2**(1) (2015)
34. Guo, D.J., Lakshmikantham, V.: Nonlinear Problems in Abstract Cones. Notes and Reports in Mathematics in Science and Engineering, vol. 5. Academic Press, Boston (1988)
35. Sidi Ammi, M.R., Torres, D.F.M.: Existence of positive solutions for non local p-Laplacian thermistor problems on time scales. JIPAM. J. Inequal. Pure Appl. Math. **8**(3) (2007)
36. Schneider, W.R.: Completely monotone generalized Mittag–Leffler functions. Exposition. Math. **14**(1), 3–16 (1996)
37. Rudin, W.: Real and Complex Analysis. McGraw-Hill, New York (1987)

Digital Fractional Integrator

Radosław Cioć

Abstract The paper presents a new approach for determining digital fractional integrator based on the Grünwald–Letnikov differintegrals. The input signal of the integrator includes a sampling time, numerical values and an order of the differintegrals. The present invention pertains generally to the field of integration of digital signals and more particularly to digital signal processing (DSP) and especially to infinite impulse response filters (IIR).

Keywords Grünwald–Letnikov · Differintegrals · DSP · IIR

1 Introduction

A schematic block diagram (Fig. 1) illustrates a prior art implementation of a digital integrator. Mathematical description of the computation performed by digital integrator circuit can be expressed as [1]:

$$y_i = \sum_{i=0}^{n} (x_i + y_{i-1}) \tag{1}$$

Alternatively, (2) is the z-transform of the digital integrator:

$$y(z) = \frac{1}{1 - z^{-1}} x(z) \tag{2}$$

Grünwald–Letnikov differintegral, given by the following (3), is a mathematical definition of the fractional differintegral of functional sequence [2–4]:

R. Cioć (✉)
Faculty of Transport and Electrical Engineering, Kazimierz Pulaski University of Technology and Humanities in Radom, Malczewskiego 29, 26-600 Radom, Poland
e-mail: r.cioc@uthrad.pl
URL: http://www.wtie.pr.radom.pl

A. Babiarz et al. (eds.), *Theory and Applications of Non-integer Order Systems*, Lecture Notes in Electrical Engineering 407, DOI 10.1007/978-3-319-45474-0_16

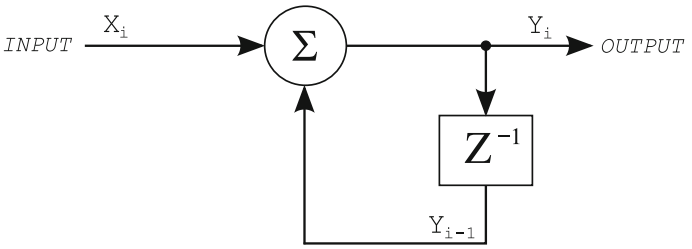

Fig. 1 Implementation of a digital integrator

$$\{f^{(n)}(t)\} = \lim_{dt\to 0} \frac{1}{(dt)^n} \sum_{m=0}^{l} (-1)^m \binom{n}{m} \{f_{l-m}(t_m)\} \equiv {}_{t_l}D^n_{t_0}\{f(t)\}_{0\ldots l} \tag{3}$$

where:
$dt = t_0 - t_1 = t_1 - t_2 = \cdots = t_{l-1} - t_l$;
$m = 0, 1, 2, \ldots, l$;
$l = \lfloor \frac{t_0 - t_l}{dt} \rfloor$ (floor function);
$\{f_{l-m}(t_m)\}$ is the m element of the sequence $\{f(t)\}_{0\ldots l}$;
$l \geq n$;
${}_{t_l}D^n_{t_0}\{f(t)\}_{0\ldots l}$ is Davis notation of the differintegral;
and $f(t)$ can be expressed as a functional sequence:

$$f(t) = \{f(t)\}_{0\ldots l} = \{f_0(t_l), f_1(t_{l-1}) \ldots f_l(t_0)\}. \tag{4}$$

2 Grünwald–Letnikov Integral of Functional Sequence

For $n < 0$, $\binom{n}{m}$ becomes [3, 4]:

$$\binom{-n}{m} = \frac{-n(-n+1)(-n+2)\ldots(-n-m+1)}{m!} = (-1)^m \frac{\Gamma(n+m)}{m!\Gamma(n)} \tag{5}$$

By generalising (3) with the aid of (5) to orders $(-\eta < 0) \in \mathbb{R}$, Grünwald–Letnikov differintegral of a negative order functional sequence is formulated as [2]:

$${}^{l}_{t_l}D^{-\eta}_{t_0}\{f(t)\}_{0\ldots l} = \lim_{dt\to 0} (dt)^{\eta} \sum_{m=0}^{l} \frac{\Gamma(\eta+m)}{m!\Gamma(\eta)} \{f_{l-m}(t_m)\} \tag{6}$$

Symbol l in Davis notation is an additional magnitude which value equals the number of iterations less 1. For the order $\eta = -1$ and $l = 0$ (for a functional sequence of 1 element), (6) becomes:

$$ {}_{(t_l-dt)}^{0}D_{t_l}^{-1}\{f(t)\}_{0\ldots0} = \lim_{dt\to 0} dt\{f_0(t_l)\} \equiv \int\limits_{t_l-dt}^{t_l} \{f(t)\}_{0\ldots0}dt \tag{7} $$

Zero value of the additional magnitude for $\eta < 0$ defines an operation equivalent to integration in the range that equals to the integration step dt. Equation (7) of the order -1 corresponds to quadrature rules for integration of $\{f(t)\}_{0\ldots0}$ and can be represented as a sum total of differintegrals:

$$ \begin{aligned} {}_{t_l}D_{t_0}^{-1}\{f(t)\}_{0\ldots l} &= {}_{t_1}^{0}D_{t_0}^{-1}\{f(t)\}_{l\ldots l} + {}_{t_2}^{0}D_{t_1}^{-1}\{f(t)\}_{(l-1)\ldots(l-1)} + \\ \cdots + {}_{t_l}^{0}D_{(t_l-dt)}^{-1}\{f(t)\}_{0\ldots0} &= \lim_{dt\to 0} dt\{f_l(t_0)\} + \lim_{dt\to 0} dt\{f_{l-1}(t_1)\} + \\ \cdots + \lim_{dt\to 0} dt\{f_0(t_l)\} &= \lim_{dt\to 0} dt \sum_{m=0}^{l}\{f_{l-m}(t_m)\} \equiv \int\limits_{t_l-dt}^{t_0} \{f(t)\}_{0\ldots l}dt \\ &= \int\limits_{t_1}^{t_0}\{f_l(t_0)\}dt + \int\limits_{t_2}^{t_1}\{f_{l-1}(t_1)\}dt + \cdots + \int\limits_{t_l}^{t_l-dt}\{f_0(t_l)\}dt \end{aligned} \tag{8} $$

Following (8) for the orders $(\eta < 0) \in \mathbb{R}$:

$$ \begin{aligned} {}_{t_l}D_{t_0}^{-\eta}\{f(t)\}_{0\ldots l} &= {}_{t_1}^{0}D_{t_0}^{-\eta}\{f(t)\}_{l\ldots l} + {}_{t_2}^{0}D_{t_1}^{-\eta}\{f(t)\}_{(l-1)\ldots(l-1)} + \\ &+ \cdots + {}_{t_l}^{0}D_{(t_l-dt)}^{-\eta}\{f(t)\}_{0\ldots0} = \lim_{dt\to 0}(dt)^{\eta}\{f_l(t_0)\} + \\ &+ \lim_{dt\to 0}(dt)^{\eta}\{f_{l-1}(t_1)\} + \cdots + \lim_{dt\to 0}(dt)^{\eta}\{f_0(t_l)\} \\ &= \lim_{dt\to 0}(dt)^{\eta}\sum_{m=0}^{l}\{f_{l-m}(t_m)\} \equiv \int\limits_{\tau_l-(dt)^{\eta}}^{t_0} \{f(t)\}_{0\ldots l}(dt)^{\eta} \\ &= \int\limits_{\tau_1}^{t_0}\{f_l(t_0)\}(dt)^{\eta} + \int\limits_{\tau_2}^{\tau_1}\{f_{l-1}(t_1)\}(dt)^{\eta} + \\ &+ \cdots + \int\limits_{\tau_l}^{\tau_l-(dt)^{\eta}}\{f_0(t_l)\}(dt)^{\eta}. \end{aligned} \tag{9} $$

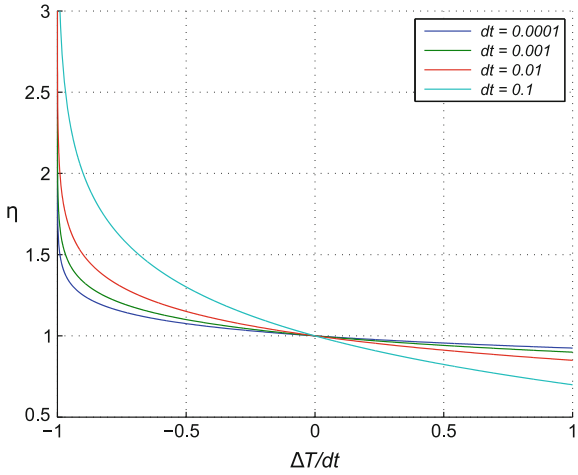

Fig. 2 Dependence of η on $\Delta T/dt$

3 Function $(dt)^{\eta}$

Let ΔT stands for measurement error of dt. ΔT is interpreted as an absolute error and added to dt [2]. Let $(dt)^{\eta}$ stands for variation of dt considering ΔT:

$$(dt)^{\eta} = dt + \Delta T \tag{10}$$

where η is a parameter (as well as the order of Grünwald–Letnikov differintegral) estimating $\{f(t)\}_{0\ldots l}$ at $t_1 + \Delta T$ and derived from (10):

$$\eta = \log_{dt}(dt + \Delta T) \tag{11}$$

Figure 2 shows the dependence of η on the value of ΔT relative to dt.

4 Fractional Integrator

A prior digital integrator (1) hasn't got information about the error of sampling, but if the error is significant in relationship with the sampling time, the result of measuring signal x and the result of signal integration can be twisted (Fig. 3).

Information about value of the error interpreted as function of the order of Grünwald–Letnikov differintegral (10) will precise the final result of integration. The mathematical description for the computation performed by digital fractional integrator circuit can be expressed as [5]:

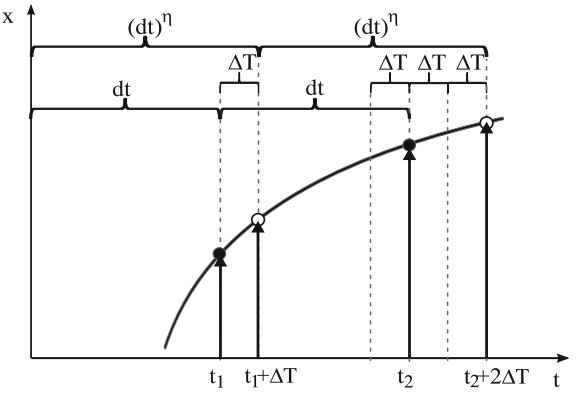

Fig. 3 Digital fractional integrator

$$y_i = h_i \sum_{i=0}^{n} (x_i + y_{i-1}) \tag{12}$$

where the factor h_i is mathematical expression of influence of the sampling time error to the result of integration:

$$h_i = (dt_i)^{\eta_i} - dt_i + 1 \tag{13}$$

For simplifying let dt_i and η_i be constant for each x_i:

$$h_i = h = (dt)^{\eta} - dt + 1 \tag{14}$$

Alternatively the z-transform of the digital fractional integrator is:

$$y(z) = \frac{h(z)}{1 - z^{-1}} x(z) \tag{15}$$

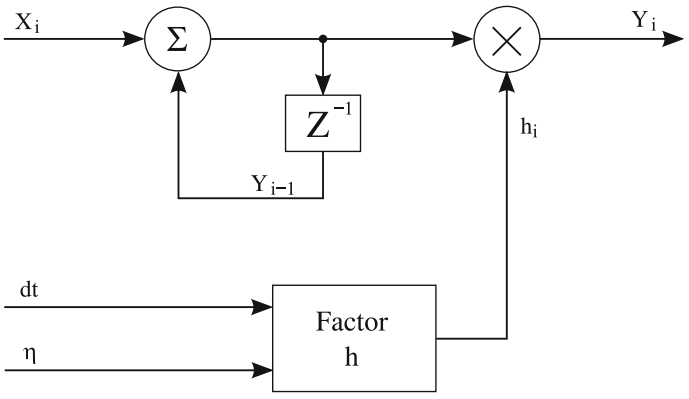

Fig. 4 Digital fractional integrator

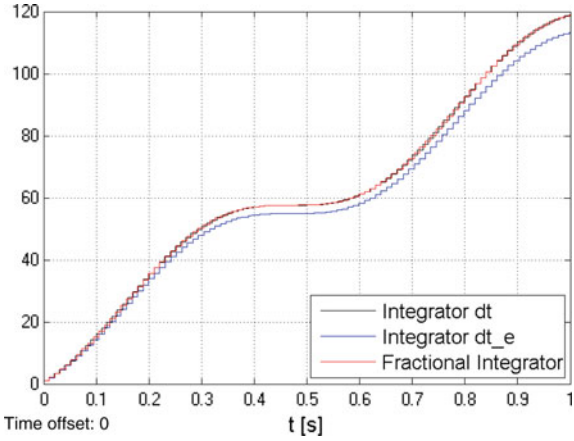

Fig. 5 Digital fractional integrator work: Integrator dt - integration of the input signal for the ideal sampling time dt ($\Delta T = 0$), Integrator dt_e - integration of the input signal for the sampling time dt with the error ($\Delta T/dt = 5\,\%$), Fractional Integrator - integration of the input signal for the sampling time dt with the error by the digital fractional integrator

Figure 4 shows graphical diagram of the digital fractional integrator and Fig. 5 shows effect of its work for sinusoidal input signal, $dt = 0,01$ and $\Delta T/dt = 5\,\%$.

5 Conclusions

Interpretation of the differintegral order as an error of measuring allows to create applications that increase accuracy of measurements. The example of an application is the digital fractional integrator used in the field of digital signal processing (DSP) and especially to Infinite Impulse Response filters (IIR).

References

1. Lyons, R.G.: Understanding Digital Signal Processing. Prentice Hall, Upper Saddle River (2010)
2. Cioć, R.: Physical and geometrical interpretation of Grünwald-Letnikov differintegrals: measurement of path and acceleration. Fract. Calc. Appl. Anal. **19**(1), 161–172 (2016)
3. Das, S.: Functional Fractional Calculus. Springer (2011)
4. Ostalczyk, P.: Zarys Rachunku Różniczkowo-Całkowego Ułamkowych Rzędów. Teoria i Zastosowanie w Praktyce. Wydawnictwo Politechniki Łódzkiej, Łódź (2008)
5. Cioć, R.: Cyfrowy integrator rzeczywistego rzędu pochodno-całki. Zgłoszenie patentowe (Patent Application) P.411354, Urząd Patentowy Rzeczypospolitej Polskiej (2015)

Optimal Control for Discrete Fractional Systems

Andrzej Dzieliński

Abstract In the paper optimal control problem for fractional discrete-time systems with quadratic performance index has been formulated and solved using the dynamic programming approach. New method for numerical computation of optimal control via the solution of dynamic programming problem has been presented. The efficiency of the method has been demonstrated on numerical example and illustrated by graphical representations. Graphs also show the differences between the fractional and integer-order systems theory.

Keywords Discrete-time fractional systems · Optimal control · Dynamic programming

1 Introduction

Optimal control problems aka dynamic optimization problems for integer (not fractional) order systems have been widely considered in literature through recent decades (see e.g. [1, 2]). Mathematical fundamentals of the fractional calculus on the other hand have even more prominent history and can be found e.g. in the monographs [3, 4]. Some optimal control problems for fractional order systems have been investigated e.g. in [5–8]. Fractional Kalman filter and its application have been addressed in [9, 10]. In this paper optimal control problem for fractional discrete-time systems with quadratic performance index will be formulated and solved using dynamic programming approach. A new method for numerical computation of optimal dynamic programming problem will be presented. The efficiency of the method will be demonstrated on numerical example and illustrated by graphs. Graphs also

This work was partially funded with Warsaw University of Technology grant.

A. Dzieliński (✉)
Institute of Control and Industrial Electronics, Warsaw University of Technology,
Kloszykowa 75, 00-662 Warsaw, Poland
e-mail: andrzej.dzielinski@isep.pw.edu.pl
URL: http://www.isep.pw.edu.pl

A. Babiarz et al. (eds.), *Theory and Applications of Non-integer Order Systems*,
Lecture Notes in Electrical Engineering 407, DOI 10.1007/978-3-319-45474-0_17

show the differences between the fractional and classical (standard) systems theory. The paper is organized as follows. In Sect. 2 some preliminaries are recalled and the problem will be formulated. The solutions of the problem are presented in Sect. 3. In Sect. 4 a procedure for computation of the optimal control is proposed and illustrated by numerical example.

Conclusions of the paper are given in Sect. 5.

2 Problem Formulation

The following notation will be used: $\mathbb{R}$ - the set of real numbers, $\mathbb{R}^{n\times n}$ - the set of $n \times n$ real matrices (in particular $\mathbb{R}^n$ is the set of real vectors), I_n - the $n \times n$ identity matrix, $\mathbb{O}$ - the null matrix of appropriate dimensions, W_a^b, V_a^b are $n \times m$ or $n \times n$ matrices and a is the lower right index and b is an upper right index. Power index is not used.

Let us consider a fractional discrete-time system, obtained using Grunwald-Letnikov's (shifted) approximation, described by equations

$$x_{k+1} = \sum_{j=0}^{k} d_j x_{k-j} + Bu_k \,, \qquad k \in \mathbb{Z}_+ \,, \tag{1a}$$

where $x \in \mathbb{R}^n$, $u \in \mathbb{R}^m$ are respectively the state and control vectors, $A \in \mathbb{R}^{n\times n}$, $B \in \mathbb{R}^{n\times m}$ and

$$d_0 = A_\alpha = A + \alpha I_n \,, \qquad 0 < \alpha < 1 \,, \tag{1b}$$

$$d_j = (-1)^j \begin{pmatrix} \alpha \\ j+1 \end{pmatrix} I_n \,, \qquad j = 1, \ldots, k \,. \tag{1c}$$

Further, let us consider a performance index of the form

$$\begin{aligned} J_i(u) &= G(x_N) + \sum_{k=i}^{N-1} F_k(x_k, u_k) \\ &= x_N^T S x_N + \sum_{k=i}^{N-1} \left(x_k^T Q x_k + u_k^T R u_k \right) , \end{aligned} \tag{2}$$

where $R \in \mathbb{R}^{m\times m}$, $Q \in \mathbb{R}^{n\times n}$, $S \in \mathbb{R}^{n\times n}$ and $S \geq 0$, $Q \geq 0$ and $R > 0$.

Optimal trajectory starting at the point x_0 and ending at the point x_k has been divided into N elementary time intervals $[0, N]$. It is desired to find optimal control sequence $u_0, u_1, \ldots, u_{N-1}$, $u \in \mathbb{U}$, $\mathbb{U}$-set of admissible inputs, which minimizes the performance index (2) and satisfies the differential equation (1). The solution of this task by searching for a conditional minimum of the performance index (2) requires

the solution of N equations with N unknown variables of the form

$$\frac{\partial J(u)}{\partial u_k} = 0\,, \quad (k = 0, \ldots, N-1)\,,$$

where $J(u)$ is the performance index (2) with (1) substituted for $k = 1, 2, \ldots, N-1$.

3 Problem Solution

We shall show that the task of determining the $u_0, u_1, \ldots, u_{N-1}$ can be reduced to N tasks of minimizing the functions of one variable.

For $i = N$ the performance index has the form

$$J_N(u) = G(x_N) = x_N^T S x_N\,,$$

which in the general case is a function of final state.

Consider the last N-th section of the optimal trajectory. The corresponding performance index of that section has the form

$$\begin{aligned} J_{N-1}(u) &= J_N(u) + F_{N-1}(x_{N-1}, u_{N-1}) \\ &= x_N^T S x_N + x_{N-1}^T Q x_{N-1} + u_{N-1}^T R u_{N-1}\,, \end{aligned} \tag{3}$$

Denoting $S_{N-1}(\Sigma x_{N-1}) = S_{N-1}(\sum_{j=0}^{N-1} x_{N-1-j})$, as a minimum of the performance index $J_{N-1}(u)$ we can write

$$S_{N-1}(\Sigma x_{N-1}) = \min_{u_{N-1} \in \mathbb{U}} \left\{ J_{N-1}(u) \right\}. \tag{4}$$

Substituting (1) for $k = N-1$ to (4) equation above takes the form

$$\begin{aligned} S_{N-1}(\Sigma x_{N-1}) = \min_{u_{N-1} \in \mathbb{U}} \Big\{ & x_{N-1}^T Q x_{N-1} + u_{N-1}^T R u_{N-1} \\ & + \left(\sum_{j=0}^{N-1} d_j x_{N-1-j} + B u_{N-1} \right)^T S \left(\sum_{j=0}^{N-1} d_j x_{N-1-j} + B u_{N-1} \right) \Big\} \end{aligned} \tag{5}$$

Calculating the first derivative of the Eq. (5) and comparing it to zero we obtain

$$\begin{aligned} 0 = \frac{\partial J_{N-1}(u)}{\partial u_{N-1}} &= \left(R + R^T \right) u_{N-1} \\ &+ B^T \left(S + S^T \right) \left(\sum_{j=0}^{N-1} d_j x_{N-1-j} + B u_{N-1} \right). \end{aligned}$$

We determine u_{N-1} as a function of $x_{N-1}, \ldots, x_0$, i.e.

$$u_{N-1} = \sum_{j=0}^{N-1} W_{N-1}^{1} d_j x_{N-1-j} \,, \tag{6}$$

where

$$W_{N-1}^{1} = -\left[R + R^T + B^T \left(S + S^T\right) B\right]^{-1} B^T \left(S + S^T\right).$$

Substituting (6) to (5) we obtain

$$\begin{aligned} S_{N-1}(\Sigma x_{N-1}) &= x_{N-1}^T Q x_{N-1} \\ &+ \left[\sum_{j=0}^{N-1} V_{N-1}^{R_{01}} d_j x_{N-1-j}\right]^T R \left[\sum_{j=0}^{N-1} V_{N-1}^{R_{01}} d_j x_{N-1-j}\right] \\ &+ \left[\sum_{j=0}^{N-1} V_{N-1}^{S_1} d_j x_{N-1-j}\right]^T S \left[\sum_{j=0}^{N-1} V_{N-1}^{S_1} d_j x_{N-1-j}\right]. \end{aligned} \tag{7}$$

where

$$V_{N-1}^{R_{01}} = W_{N-1}^{1}, \quad V_{N-1}^{S_1} = \left(I_n + B W_{N-1}^{1}\right).$$

Let us consider the N-th and $N-1$-th sections of the optimal trajectory. The corresponding performance index for those sections has the form

$$\begin{aligned} J_{N-2}(u) &= J_{N-1}(u) + F_{N-2}(x_{N-2}, u_{N-2}) \\ &= J_{N-1}(u) + x_{N-2}^T Q x_{N-2} + u_{N-2}^T R u_{N-2} \,. \end{aligned} \tag{8}$$

Denoting $S_{N-2}(\Sigma x_{N-2}) = S_{N-2}(\sum_{j=0}^{N-2} x_{N-2-j})$ as minimum of the performance index $J_{N-2}(u)$ we can write

$$\begin{aligned} S_{N-2}(\Sigma x_{N-2}) &= \min_{\substack{u_{N-1}\in\mathbb{U} \\ u_{N-2}\in\mathbb{U}}} \left\{J_{N-2}(u_{N-2})\right\} \\ &= \min_{u_{N-2}\in\mathbb{U}} \left\{ \min_{u_{N-1}\in\mathbb{U}} J_{N-1}(u_{N-1}) + F_{N-2}(x_{N-2}, u_{N-2})\right\} \\ &= \min_{u_{N-2}\in\mathbb{U}} \left\{S_{N-1}(\Sigma x_{N-1}) + F_{N-2}(x_{N-2}, u_{N-2})\right\}. \end{aligned} \tag{9}$$

Substituting (1) for $k = N-2$ to (9) and calculating the first derivative of the equation and comparing it to zero we obtain

$$0 = \frac{\partial J_{N-2}(u)}{\partial u_{N-2}} = \left(R + R^T\right) u_{N-2} + B^T \left[Q + Q^T\right]$$
$$\left[\sum_{j=0}^{N-2} d_j x_{N-2-j} + B u_{N-2}\right] + \left[V_{N-1}^{R_{01}} d_0 B\right]^T \left[R + R^T\right]$$
$$\left[V_{N-1}^{R_{01}} d_0 \left(\sum_{j=0}^{N-2} d_j x_{N-2-j} + B u_{N-2}\right) + \sum_{j=0}^{N-2} V_{N-1}^{R_{01}} d_{j+1} x_{N-2-j}\right]$$
$$+ \left[V_{N-1}^{S_1} d_0 B\right]^T \left[S + S^T\right] \left[V_{N-1}^{S_1} d_0 \left(\sum_{j=0}^{N-2} d_j x_{N-2-j} + B u_{N-2}\right)\right.$$
$$\left. + \sum_{j=0}^{N-2} V_{N-1}^{S_1} d_{j+1} x_{N-2-j}\right].$$

We determine u_{N-2} as a function of $x_{N-2}, \ldots, x_0$, i.e.

$$u_{N-2} = \sum_{j=0}^{N-2} \left[W_{N-2}^1 d_j + W_{N-2}^2 d_{j+1}\right] x_{N-2-j}\,, \tag{10}$$

Substituting (1) for $k = N-2$ and (10) to (9) we obtain

$$S_{N-2}(\Sigma x_{N-2}) = x_{N-2}^T Q x_{N-2} \tag{11}$$
$$+ \left[\sum_{j=0}^{N-2} \left(V_{N-2}^{Q_{01}} d_j + V_{N-2}^{Q_{02}} d_{j+1}\right) x_{N-2-j}\right]^T \tag{12}$$
$$\times Q \left[\sum_{j=0}^{N-2} \left(V_{N-2}^{Q_{01}} d_j + V_{N-2}^{Q_{02}} d_{j+1}\right) x_{N-2-j}\right] \tag{13}$$
$$+ \left[\sum_{j=0}^{N-2} \left(V_{N-2}^{R_{01}} d_j + V_{N-2}^{R_{02}} d_{j+1}\right) x_{N-2-j}\right]^T \tag{14}$$
$$\times R \left[\sum_{j=0}^{N-2} \left(V_{N-2}^{R_{01}} d_j + V_{N-2}^{R_{02}} d_{j+1}\right) x_{N-2-j}\right] \tag{15}$$
$$+ \left[\sum_{j=0}^{N-2} \left(V_{N-2}^{R_{11}} d_j + V_{N-2}^{R_{12}} d_{j+1}\right) x_{N-2-j}\right]^T \tag{16}$$

$$\times R\left[\sum_{j=0}^{N-2}\left(V_{N-2}^{R_{11}}d_j + V_{N-2}^{R_{12}}d_{j+1}\right)x_{N-2-j}\right] \tag{17}$$

$$+\left[\sum_{j=0}^{N-2}\left(V_{N-2}^{S_1}d_j + V_{N-2}^{S_2}d_{j+1}\right)x_{N-2-j}\right]^T \tag{18}$$

$$\times S\left[\sum_{j=0}^{N-2}\left(V_{N-2}^{S_1}d_j + V_{N-2}^{S_2}d_{j+1}\right)x_{N-2-j}\right], \tag{19}$$

where

$$V_{N-2}^{Q_{01}} = I_n + BW_{N-2}^1\,, \qquad V_{N-2}^{Q_{02}} = BW_{N-2}^2\,,$$
$$V_{N-2}^{R_{01}} = W_{N-2}^1\,, \qquad V_{N-2}^{R_{02}} = W_{N-2}^2\,,$$
$$V_{N-2}^{R_{11}} = V_{N-1}^{R_{01}}d_0V_{N-2}^{Q_{01}}\,, \qquad V_{N-2}^{R_{12}} = V_{N-1}^{R_{01}}d_0V_{N-2}^{Q_{02}} + V_{N-1}^{R_{01}}\,,$$
$$V_{N-2}^{S_1} = V_{N-1}^{S_1}d_0V_{N-2}^{Q_{01}}\,, \qquad V_{N-2}^{S_2} = V_{N-1}^{S_1}d_0V_{N-2}^{Q_{02}} + V_{N-1}^{S_1}\,.$$

In the general case for q last sections of the optimal trajectory the value which minimize performance index (2) with constraints (1) is given by the relation

$$\begin{aligned}
S_{N-q}(\Sigma x_{N-q}) &= x_{N-q}^T Q x_{N-q} \\
&+\sum_{l=0}^{q-2}\left\{\left[\sum_{j=0}^{N-q}\left(\sum_{p=0}^{q-1}V_{N-q}^{Q_{l,p+1}}d_{j+p}\right)x_{N-q-j}\right]^T Q\right. \\
&\left.\times\left[\sum_{j=0}^{N-q}\left(\sum_{p=0}^{q-1}V_{N-q}^{Q_{l,p+1}}d_{j+p}\right)x_{N-q-j}\right]\right\} \\
&+\sum_{r=0}^{q-1}\left\{\left[\sum_{j=0}^{N-q}\left(\sum_{p=0}^{q-1}V_{N-q}^{R_{r,p+1}}d_{j+p}\right)x_{N-q-j}\right]^T R\right. \\
&\left.\times\left[\sum_{j=0}^{N-q}\left(\sum_{p=0}^{q-1}V_{N-q}^{R_{r,p+1}}d_{j+p}\right)x_{N-q-j}\right]\right\} \\
&+\left[\sum_{j=0}^{N-q}\left(\sum_{p=0}^{q-1}V_{N-q}^{S_{p+1}}d_{j+p}\right)x_{N-q-j}\right]^T S \\
&\times\left[\sum_{j=0}^{N-q}\left(\sum_{p=0}^{q-1}V_{N-q}^{S_{p+1}}d_{j+p}\right)x_{N-q-j}\right].
\end{aligned} \tag{20}$$

Control u_{N-q}, which minimizes the performance index $J_{N-q}(u)$, in the general case is given by the relation

$$u_{N-q} = \sum_{j=0}^{N-q} \left(\sum_{p=0}^{q-1} W_{N-q}^{p+1} d_{j+p} \right) x_{N-q-j} \ , \tag{21}$$

4 Procedure and Examples

From the above considerations, following procedure for solving the optimal control problem using the dynamic programming method follows:

Procedure:
Step 1. Knowing the matrices A and B of the system (1) and the coefficient α and the number of elementary sections N of the optimal trajectory, we determine the matrix A_α and coefficients d_j for $j = 0, 1, \ldots, N$.
Step 2. Knowing the matrices R, Q, S of the performance index (2) and the coefficients d_j for $j = 0, 1, \ldots, N$ and using known methods of minimization, we determine the value of the control (6) which minimizes the performance index (3), and its minimum value (7) for $q = 1$. Knowing (7) we determine the value of control (10) which minimizes the performance index (8) and its minimum value (11) for $q = 2$. Continuing the procedure we determine the equations (20) and (21) for $q = 3, 4, \ldots, N$.
Step 3. Using the formula (21) for $q = N$ we determine u_0, the control value in a discrete time $k = 0$ depending on the initial conditions x_0. Using (20) we determine minimum of the performance index $S_0(\Sigma x_0)$. Knowing u_0 and x_0 from the relation (1) for $k = 0$ we determine x_1. Using the formula (21) for $q = N - 1$ we determine u_1 as a function of x_1, x_0. Using (20) we determine the minimum value of the performance index $S_1(\Sigma x_1)$. Knowing u_1 and x_1, x_0 from the relation (1) for $k = 1$ we can find the x_2. Using the formula (21) for $q = N - 2$ we determine u_2 as a function of x_2, x_1, x_0 and using (20) we can determine $S_2(\Sigma x_2)$. Continuing this procedure we can determine the discrete values of control sequence $u_0, u_1, \ldots, u_{N-1} \in \mathbb{U}$, which minimizes the performance index (2) and satisfies the differential equation (1) for given initial conditions x_0 and the subsequent minimum value $S_0(\Sigma x_0), \ldots, S_N(\Sigma x_N)$ of the performance index (2).

Example 1 Consider the fractional discrete-time system (1) with matrices

$$A = \begin{bmatrix} 1 & 2 \\ 3 & 4 \end{bmatrix}, \quad B = \begin{bmatrix} 1 \\ 2 \end{bmatrix}, \quad x_0 = \begin{bmatrix} 0.5 \\ 0.7 \end{bmatrix}, \tag{22}$$

and the performance index (2) with matrices

$$S = \begin{bmatrix} 4 & 1 \\ 1 & 4 \end{bmatrix}, \quad Q = \begin{bmatrix} 3 & 2 \\ 2 & 3 \end{bmatrix}, \quad R = \begin{bmatrix} 1 \end{bmatrix}. \tag{23}$$

Using the above Procedure we obtain.
Step 1. Assuming $\alpha = 0.5$ and $N = 3$, the matrix A_α has the form

$$A_\alpha = A + \alpha I_n = \begin{bmatrix} 1.5 & 2 \\ 3 & 4.5 \end{bmatrix}, \tag{24}$$

and the coefficients d_j for $j = 0, 1, \ldots, N$ are as follows

$$\begin{gathered} d_0 = \begin{bmatrix} 1.5 & 2 \\ 3 & 4.5 \end{bmatrix}, d_1 = \begin{bmatrix} 0.125 & 0 \\ 0 & 0.125 \end{bmatrix}, d_2 = \begin{bmatrix} 0.063 & 0 \\ 0 & 0.063 \end{bmatrix}, \\ d_3 = \begin{bmatrix} 0.039 & 0 \\ 0 & 0.039 \end{bmatrix}. \end{gathered} \tag{25}$$

Step 2. Taking into account the matrices (23) and the coefficients (25) and for $q = 1$ we determine a matrix

$$W_{N-1}^1 = \begin{bmatrix} -0.2400 & -0.3600 \end{bmatrix}, \tag{26}$$

and matrices

$$V_{N-1}^{R_{01}} = \begin{bmatrix} -0.2400 & -0.3600 \end{bmatrix}, \quad V_{N-1}^{S_1} = \begin{bmatrix} 0.7600 & -0.3600 \\ -0.4800 & 0.2800 \end{bmatrix}. \tag{27}$$

for $q = 2$ we determine matrices

$$W_{N-2}^1 = \begin{bmatrix} -0.2677 & -0.3575 \end{bmatrix}, \quad W_{N-2}^2 = \begin{bmatrix} -0.0028 & -0.0474 \end{bmatrix}, \tag{28}$$

and matrices

$$V_{N-2}^{Q_{01}} = \begin{bmatrix} 0.7323 & -0.3575 \\ -0.5353 & 0.2850 \end{bmatrix}, \quad V_{N-2}^{Q_{02}} = \begin{bmatrix} -0.0028 & -0.0474 \\ -0.0055 & -0.0949 \end{bmatrix},$$

$$\begin{aligned} V_{N-2}^{R_{01}} &= \begin{bmatrix} -0.2677 & -0.3575 \end{bmatrix}, \quad V_{N-2}^{R_{02}} = \begin{bmatrix} -0.0028 & -0.0474 \end{bmatrix}, \\ V_{N-2}^{R_{11}} &= \begin{bmatrix} 0.0696 & -0.0836 \end{bmatrix}, \quad V_{N-2}^{R_{12}} = \begin{bmatrix} -0.2244 & -0.0925 \end{bmatrix}, \end{aligned}$$

$$V_{N-2}^{S_1} = \begin{bmatrix} 0.0975 & -0.0499 \\ -0.0727 & 0.0426 \end{bmatrix}, \quad V_{N-2}^{S_2} = \begin{bmatrix} 0.7604 & -0.3534 \\ -0.4820 & 0.2458 \end{bmatrix}. \tag{29}$$

Continuing the procedure for $q = 3$ we obtain

$$\begin{aligned} W_{N-3}^1 &= \begin{bmatrix} -0.2689 & -0.3566 \end{bmatrix}, \quad W_{N-3}^2 = \begin{bmatrix} -0.0187 & -0.0403 \end{bmatrix}, \\ W_{N-3}^3 &= \begin{bmatrix} 0.0019 & -0.0068 \end{bmatrix}, \end{aligned} \tag{30}$$

$$\begin{aligned} V_{N-3}^{Q_{01}} &= \begin{bmatrix} 0.7311 & -0.3569 \\ -0.5378 & 0.2861 \end{bmatrix}, \quad V_{N-3}^{Q_{02}} = \begin{bmatrix} -0.0187 & -0.0403 \\ -0.0373 & -0.0806 \end{bmatrix}, \\ V_{N-3}^{Q_{03}} &= \begin{bmatrix} 0.0019 & -0.0068 \\ 0.0039 & -0.0135 \end{bmatrix}, \quad V_{N-3}^{Q_{11}} = \begin{bmatrix} 0.0994 & -0.0521 \\ -0.0701 & 0.0389 \end{bmatrix}, \\ V_{N-3}^{Q_{12}} &= \begin{bmatrix} 0.7375 & -0.3465 \\ -0.5437 & 0.2668 \end{bmatrix}, \quad V_{N-3}^{Q_{13}} = \begin{bmatrix} -0.0033 & -0.0456 \\ -0.0047 & -0.0979 \end{bmatrix}, \end{aligned}$$

$$\begin{aligned} V_{N-3}^{R_{01}} &= \begin{bmatrix} -0.2689 & -0.3569 \end{bmatrix}, \quad V_{N-3}^{R_{02}} = \begin{bmatrix} -0.0187 & -0.0403 \end{bmatrix}, \\ V_{N-3}^{R_{03}} &= \begin{bmatrix} 0.0019 & -0.0067 \end{bmatrix}, \quad V_{N-3}^{R_{11}} = \begin{bmatrix} 0.0785 & -0.0889 \end{bmatrix}, \\ V_{N-3}^{R_{12}} &= \begin{bmatrix} -0.1599 & -0.1249 \end{bmatrix}, \quad V_{N-3}^{R_{13}} = \begin{bmatrix} -0.0141 & -0.0085 \end{bmatrix}, \\ V_{N-3}^{R_{21}} &= \begin{bmatrix} 0.0062 & -0.0089 \end{bmatrix}, \quad V_{N-3}^{R_{22}} = \begin{bmatrix} 0.0821 & -0.0566 \end{bmatrix}, \\ V_{N-3}^{R_{23}} &= \begin{bmatrix} -0.2257 & -0.0879 \end{bmatrix}, \end{aligned}$$

$$\begin{aligned} V_{N-3}^{S_1} &= \begin{bmatrix} 0.1066 & -0.0538 \\ -0.0718 & 0.0369 \end{bmatrix}, \quad V_{N-3}^{S_2} = \begin{bmatrix} 0.0985 & -0.0477 \\ -0.0748 & 0.0381 \end{bmatrix}, \\ V_{N-3}^{S_3} &= \begin{bmatrix} 0.7603 & -0.3529 \\ -0.4818 & 0.2451 \end{bmatrix}. \end{aligned} \tag{31}$$

Step 3. Using (21) for $q = N = 3$ and (30), (31) we find

$$u_0 = -2.2429. \tag{32}$$

Knowing u_0 and x_0 from (1) for $k = 0$ we determine

$$x_1 = \begin{bmatrix} -0.0929 \\ 0.1642 \end{bmatrix}. \tag{33}$$

Using (20) and (25), (31) we obtain the minimum value of the performance index as

$$J_0(\Sigma x_0) = 8.7699. \tag{34}$$

Continuing this procedure we can determine subsequent discrete values of control as

$$u_1 = -0.2662\,, \quad u_2 = -0.0386. \tag{35}$$

Values of state vector are given as

$$x_2 = \begin{bmatrix} -0.0147 \\ 0.0152 \end{bmatrix}, \quad x_3 = \begin{bmatrix} -0.0106 \\ 0.0114 \end{bmatrix}. \tag{36}$$

Minimum values of the performance index are given as

$$J_1(\Sigma x_1) = 0.1193\,, \quad J_2(\Sigma x_2) = 0.0027, \tag{37}$$

and

$$J_3(u) = G(x_3) = 0.0007. \tag{38}$$

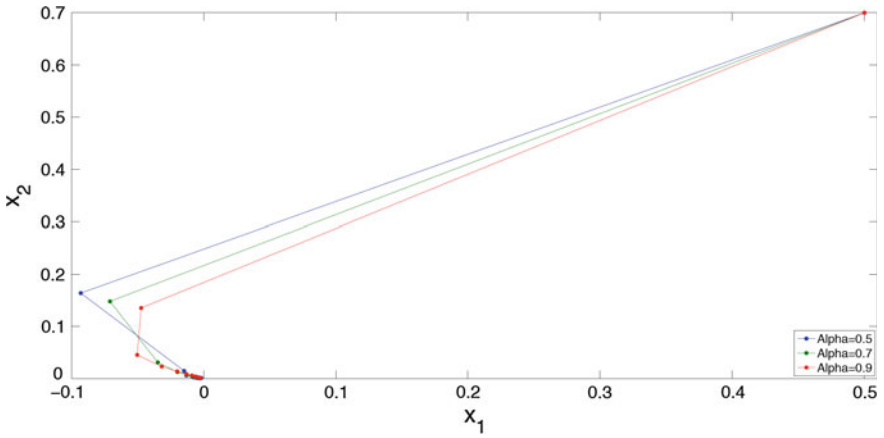

Fig. 1 Optimal trajectories for $\alpha = 0.5, 0.7, 0.9$ and $N = 10$

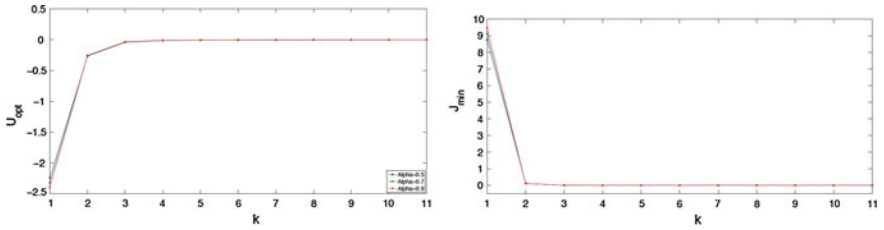

Fig. 2 Optimal control and values of performance index for $\alpha = 0.5, 0.7, 0.9$ and $N = 10$

Figures 1 and 2 illustrate the considerations for the system (1) with matrices (22) and the performance index (2) with matrices (23) for three different values of $\alpha = 0.5, 0.7, 0.9$, and the number of elementary sections of the optimal trajectory $N = 10$.

5 Conclusion

Optimal control problem for fractional discrete-time systems with quadratic performance index has been formulated and solved. A new method based on dynamic programming for numerical computation of optimal control problem has been presented. The efficiency of the method has been demonstrated on numerical example and illustrated by graphs. The differences between the fractional and classical (standard) systems theory have been shown in [11]. A computer algorithm for solving dynamic programming problems with quadratic performance index for fractional discrete-time systems has been tested for different cases of coefficient alpha. The description of a computer algorithm can be found in [12].

References

1. Bellman, R.: Dynamic Programming. Princeton University Press, Princeton (1957)
2. Naidu, D.S.: Optimal Control Systems. Electrical Engineering. CRC Press Inc., Boca Raton (2002)
3. Podlubny, I.: Fractional Differential Equations. An Introduction to Fractional Derivatives, Fractional Differential Equations, Some Methods of Their Solution and Some of Their Applications. Academic Press (1999)
4. Samko, S.G., Kilbas, A.A., Marichev, O.I.: Fractional Integrals and Derivatives: Theory and Applications. Gordon and Breach Science, New York (1993)
5. Agrawal, O.: A general finite element formulation for fractional variational problems. J. Math. Anal. Appl. **337**(1), 1–12 (2008)
6. Frederico, G., Torres, D.: Fractional conservation laws in optimal control theory. Nonlinear Dyn. **53**(3), 215–222 (2008)
7. Jelic, Z., Petrovacki, N.: Optimality conditions and a solution scheme for fractional optimal control problems. Struct. Multidiscip. Optim. **38**(6), 571–581 (2008)
8. Sierociuk, D., Vinagre, B.: Infinite horizon state-feedback LQR controller for fractional problems. In: Proceedings of 49^{th} IEEE Conference on Decision and Control, pp. 6674–6679. Atlanta, USA (2010)
9. Sierociuk, D., Tejado, I., Vinagre, B.: Improved fractional Kalman filter and its application to estimation over lossy networks. Signal Process. **91**(3), 542–552 (2011)
10. Sierociuk, D., Dzielinski, A.: Fractional Kalman filter algorithm for the states, parameters and order of fractional system estimation. International. Int. J. Appl. Math. Comput. Sci. **16**(1), 129–140 (2006)
11. Dzielinski, A., Czyronis, P.: Dynamic programming for discrete-time fractional systems. In: Proceedings of The 19^{th} IFAC World Congress, pp. 2003–2009. Cape Town, South Africa (2014)
12. Dzielinski, A., Czyronis, P.: Computer algorithms for solving optimization problems for discrete-time fractional systems. In: Proceedings of the European Control Conference, pp. 4009–4014. Zurich, Switzerland (2013)

Fractional Order Back Stepping Sliding Mode Control for Blood Glucose Regulation in Type I Diabetes Patients

Hamid Heydarinejad and Hadi Delavari

Abstract In this paper a fractional order backstepping sliding mode controller is proposed for Blood Glucose regulation using Bergman minimal model. A feedback control law is designed based on backstepping algorithm and a fractional order sliding surface is introduced. The backstepping algorithm makes the controller immune to matched and mismatched uncertainties and the fractional order sliding mode control provides robustness. Simulation results show that the proposed fractional order backstepping sliding mode controller are able to reject both matched and mismatched uncertainties and disturbance with a chattering free control law and the simulation results of the proposed controller are compared with the Backstepping sliding mode controller.

Keywords Bergman minimal model · Fractional calculus · Fractional order backstepping sliding mode control · Robust stability · Type I diabetes

1 Introduction

Diabetes mellitus is a metabolic disease characterized by pancreas inability to regulate blood glucose levels within normal range (70–150 mg/dl). Insulin is a hormone generated by specific cells, called beta cells, in the pancreas. Insulin is required to transfer blood glucose into cells, where it is stored and then used for energy. There are two types of diabetes: type I and type II. Type I diabetes or insulin dependent and type II diabetes or non-insulin dependent. In type I diabetes mellitus (T1DM), the immune system attacks and destroys the insulin producing b-cells in the pancreas. Thus, a key issue in diabetes treatment is the delivery of exogenous insulin to obtain glucose levels close to normal. There are two situations depending on glucose

H. Heydarinejad · H. Delavari (✉)
Department of Electrical Engineering,
Hamedan University of Technology, Hamedan 65155, Iran
e-mail: hdelavery@gmail.com

A. Babiarz et al. (eds.), *Theory and Applications of Non-integer Order Systems*,
Lecture Notes in Electrical Engineering 407, DOI 10.1007/978-3-319-45474-0_18

concentration, namely, hyperglycemia and hypoglycemia (Hyperglycemia = Blood glucose concentration >120 (mg/dl)) and Hypoglycemia = Blood glucose concentration <60 (mg/dl)). Chronic elevation of BG level leads to damage of blood vessels (angiopathy), resulting in serious long-term complications, such as blindness, neuropathy, heart disease, and kidney failure.

Continuous glucose monitoring (CGM) systems and insulin pumps technologies have motivated the development of an artificial pancreas system to replace the conventional treatment strategies in T1DM, Therefore, a system that automatically monitors and controls the blood glucose level of a diabetic individual permits the patient to have more participation in the ordinary daily activities with risk reduction of long-term side effects. In recent years, many studies have been made for intelligent control of blood glucose. Among them we focus the 3rd order minimal model of Bergman [1]. From a control viewpoint, the following challenges arise when facing the design of a control algorithm for an artificial pancreas:

- Slow dynamic response to the control action.
- Nonlinear, uncertain and time-varying models.
- Large disturbances (the meals).
- Nonnegative actuation.
- Measurement errors including noise, drift and bias.

Several methods have been previously employed to design the feedback controller for insulin delivery, such as classical methods like PID Switching [2], model predictive control (MPC) [3], Fuzzy logic control [4, 5], Recurrent Neural Net-work [6], High Order Sliding Mode Control [7, 8], Back stepping Sliding Mode Control [9], Optimal control [10], State output Feedback H∞ for Fractional Order Model [11], Hybrid Adaptive PD Controller [12], Reducing Risk of Closed Loop Control of Blood Glucose in Artificial Pancreas using Fractional Calculus [13]. The augmented Bergman minimal model had been used to simulate the 1st type of diabetes. In order to regulate the blood glucose level a fractional order PID controller was employed [14]. The sliding mode control strategy is a systematic approach to retaining asymptotic stability and robust performance in nonlinearities and various uncertainties such as friction, disturbance, and load changing, and it has been attracting considerable interesting. A fractional order Backstepping sliding mode control (FOBSMC) is designed using backstepping sliding mode method and fractional calculus on a fractional order sliding surface based on the Lyapunov's direct stability theorem that guarantees stability and the tracking error to reach the sliding surface in desired time. The main advantages of Backstepping sliding mode controller is robustness against mismatched uncertainties and disturbance [15].

The sensor can measure blood glucose concentration and pass the information to a feedback control system that would calculate the necessary insulin delivery rate using robust fractional order backstepping sliding mode control algorithm, to keep the patient under metabolic control. FOBSMC algorithm, are used to robustly

stabilize the glucose concentration level of a diabetic patient in presence of the parameter variations and meal disturbance. The structure of the proposed FOBSMC is appropriate for making the insulin delivery pumps in closed loop control of diabetes. Therefore, a FOBSMC was designed and tested with them. The designed controller was also applied to Bergman minimal model to check the approach feasibility. Soon after, to reduce the chattering phenomenon, a $tanh$ function is used to replace the discontinuous $signum$ function at the reaching phase in traditional sliding mode control. A computer simulation is performed to manifest the theoretical analysis. The robustness with respect to parameter uncertainties and meal disturbance was tested using Matlab simulation and the simulation results are compared with Backstepping sliding mode control (BSMC). There are some novelty and advantages, which make our proposed method attractive:

- The definition of a new fractional order sliding surface.
- Robustness of the proposed controller against mismatched disturbances and uncertainties.
- Lack of restrictions on the upper limit of disturbances.
- The Blood Glucose concentration (output) and Insulin Injection (control law, Input) are completely stabilized at the basal level (G_b and I_b) in a reasonable time interval.

2 Fractional Calculus

Fractional calculus is an old mathematical topic since the 17th century [16]. The fractional integral-differential operators (fractional calculus) are a generalization of integration and derivation to non-integer order (fractional) operators. There exist many definitions of fractional derivative [17], there are three commonly used definitions for the general fractional differentiation and integration, i.e., the Grünwald–Letnikov (GL), The Riemann–Liouville (RL) and the Caputo [18]. Let us first introduce Caputo definition and results needed here with respect to fractional calculus which will be used later. In spite of intensive researches, the stability of fractional order systems remains an open problem. Stability of fractional order nonlinear dynamic systems are studied in [19, 20].

Definition 1 The fractional integral ${}_0^c D_t^\alpha$ with fractional order $\alpha \in R^+$ of function $x(t)$ is defined as [18]:

$$ {}_0^c D_t^\alpha f(t) = \frac{1}{\Gamma(\alpha)} \int_0^t (t-\tau)^{\alpha-1} x(\tau)\, d\tau. \tag{1} $$

Definition 2 The Caputo derivative of fractional order $\alpha \in R^+$ with function $x(t)$ is defined as [18]:

$$ {}_0^c D_t^{\alpha} x(t) = \frac{1}{\Gamma(m-\alpha)} \int_0^t (t-\tau)^{m-\alpha-1} x^{(m)}(\tau)\, d\tau, \tag{2} $$

$m-1 < \alpha < m \in Z$.

Some of important properties for the Caputo fractional calculus that will use them.

Definition 3 If $x(t) \in C^m[0,1)$ and $m-1 < \alpha < m \in Z^+$, then [21]:

$$ {}_0^c D_t^{\alpha}\ {}_0^c D_t^{-\alpha} x(t) = x(t) \quad \text{for } m = 1, \tag{3} $$

$$ {}_0^c D_t^{-\alpha}\ {}_0^c D_t^{\alpha} x(t) = x(t) - \sum_{k=0}^{m-1} \frac{t^k}{k!} x^{(k)}(0), \tag{4} $$

$$ {}_0^c D_t^{\alpha}\ {}_0^c D_t^{n} x(t) = {}_0^c D_t^{\alpha+n} x(t), \ n \in N, \tag{5} $$

$$ L\left\{ {}_0^c D_t^{\alpha} x(t) \right\} = s^{\alpha} X(s) - \sum_{k=0}^{m-1} s^{\alpha-k-1} x^{(k)}(0), \tag{6} $$

$$ {}_0^c D_t^{\alpha} c = 0, \ \textit{where } c \textit{ is any constant.} \tag{7} $$

Theorem 1 (Fractional-order extension of Lyapunov direct method [19]). *Let $x = 0$ be an equilibrium point for the non-autonomous fractional-order system (8). Assume that there exists a Lyapunov function $V(t, x(t))$ and class-K functions $\gamma_i (i = 1, 2, 3)$ satisfying:*

$$ {}_0^c D_t^{\alpha} x(t) = f(x, t), \tag{8} $$

$$ \gamma_1(\|x\|) \le V_{(x,t)} \le \gamma_2(\|x\|), \tag{9} $$

$$ {}_0^c D_t^{\alpha} V_{(x,t)} \le -\gamma_3(\|x\|), \tag{10} $$

where $a \in (0,1)$. Then the system (8) is asymptotically stable [22].

Using Lemma 1, which allows to find Lyapunov candidate functions for demonstrating the stability of many fractional order systems, using the fractional-order extension of the Lyapunov direct method.

Lemma 1 *Let $x(t) \in R$ be a continuous and derivable function. Then, for any time instant $t \ge t_0$:*

$$ \frac{1}{2}\, {}_0^c D_t^{\alpha} x^2(t) \le x(t)\, {}_0^c D_t^{\alpha} x(t). \tag{11} $$

In proof stability of system with proposed controller, Theorem 1 and Lemma 1 will be used [22].

3 Glucose - Insulin Dynamic

Many models to glucose-insulin process has been presented. Perhaps the most commonly used control relevant model for glucose–insulin dynamics is the minimal model. Bergman's minimal model has been invented in 1980 by Doctor Richard Bergman. The main advantages of the Bergman minimal model are the number of parameters is minimum and it describes the interaction between main components such as insulin and glucose concentrations without getting into biological complexity. Following is the Bergman Minimal Model (BeM) [9, 23, 24]:

$$\begin{aligned}
\dot{B}_1(t) &= -(p_1 + B_2(t))\, B_1(t) + p_1 G_b + D(t), \\
\dot{B}_2(t) &= -p_2 B_2(t) + p_3 (B_3(t) - I_b), \\
\dot{B}_3(t) &= -n (B_3(t) - I_b) + \gamma t\, [B_1(t) - h]^+ + u(t).
\end{aligned} \tag{12}$$

Here $B_1(t)$, $B_2(t)$ and $B_3(t)$ are plasma glucose concentration, the insulin influence on glucose concentration reduction, and insulin concentration in plasma respectively, $u(t) \in R$ is injected insulin rate in (mU/min), G_b is the basal pre-injection level of glucose (mg/dl), I_b is the basal pre-injection level of insulin (μU/ml), p_1 the insulin independent rate constant of glucose uptake in muscles and liver (1/min), p_2 the rate for decrease in tissue glucose uptake ability (1/min), p_3 the insulin-dependent increase in glucose uptake ability in tissue per-unit of insulin concentration above the basal level ((μU/ml)/min). The term $\gamma\, [B_1(t) - h]^+ t$ represents the pancreatic insulin secretion after a meal in take at $t = 0$. As this work is focused on Insulin therapy which is usually administrated to Type I diabetes mellitus patients, γ is assumed to be zero to represent the true dynamic of this disease and p_1 should also be considered zero. The parameter n is the first order decay rate for insulin in blood. This disturbance can be modeled by a decaying exponential function of the following form [9, 25]:

$$D(t) = Ae^{-Bt},\ A, B > 0. \tag{13}$$

We modeled the pump as a first order delay:

$$\dot{u}(t) = \frac{1}{a}(w(t) - u(t)), \tag{14}$$

where $w(t)$ is insulin rate command in pump as input, and a is pump time constant [9]. The fractional oreder Bergman minimal model is used in [11, 26] but the consider the fact that the initialization problem of fractional-order systems remains an open question [11]. One of the advantages of the proposed controller is against other methods of fractional sliding mode, no requirement to calculus of relative degree for Bergman minimal model.

4 Controller Design

4.1 Fractional Order Backstepping Sliding Mode Control

The sliding mode control [27] technique is an effective tool to develop control law insensitive to the matched uncertainties in a system. It is a discontinuous type of control which has found wide applications due to its simplicity and robustness [15, 28]. The aim of developing a sliding mode controller is to achieve robustness against mismatched uncertainty and disturbances. Due to the failure of the sliding mode controller to tackle mismatched uncertainty, the backstepping algorithm is initially used It shows unique advantages in dealing with nonlinear system problems [29]. The fractional order backstepping sliding mode controller to control blood glucose levels in type I diabetes patients in the presence of mismatched uncertainties and disturbances is proposed.

As we mentioned previously, in this paper due to nonlinearities, uncertainties and disturbance of system, we used FOBSMC. Thus, four decouple dynamic models are assumed. The first dynamic part considered as follows:

$$\dot{B}_1(t) = -(p_1 + B_2(t))\, B_1(t) + p_1 G_b + D(t), \tag{15}$$

where $B_2(t)$ is considered as a pseudo control input which should control $B_1(t)$ for tracking desired G_b in presence of $D(t)$ disturbances. Let G_b be a desired constant value of the system output $B_1(t)$, the tracking error of which is defined by:

$$e_1 = B_1(t) - G_d. \tag{16}$$

Thus according to Sliding Mode Control (SMC) theory, the fractional order sliding surface introduced as follows:

$$S_1 = {}_0^c D_t^{-\alpha}\, \dot{e}_1 + \lambda_1 e_1. \tag{17}$$

Taking the time fractional order derivative ${}_0^c D_t^{\alpha}$ of fractional order sliding surface of (17) and using Definition 3, one can obtain:

$${}_0^c D_t^{\alpha} S_1 = \dot{e}_1 + \lambda_1\, {}_0^c D_t^{\alpha} e_1 = 0. \tag{18}$$

With ${}_0^c D_t^{\alpha} S_1 = 0$ and substituting (16) into (18) leads to:

$$\dot{B}_1(t) - \dot{G}_d + \lambda_1\, {}_0^c D_t^{\alpha} e_1 =$$

$$\left(-B_2(t)\, B_1(t) - p_1 B_1(t) + p_1 G_b - \dot{G}_d + \lambda_1\, {}_0^c D_t^{\alpha} e_1\right) = 0. \tag{19}$$

The equivalent pseudo control law based on $B_2(t)$ as follows:

$$B_{2(eq)}(t) = (B_1(t))^{-1}\left(-p_1 B_1(t) + p_1 G_b - \dot{G}_d + \lambda_1 {}_0^c D_t^{\alpha} e_1\right). \tag{20}$$

The next step is to design the reaching mode control scheme, in the proposed method using a switching control law for derives the system trajectories onto the sliding surface ($S(t) = 0$). The reaching law can be chosen as:

$$B_{2(sw)}(t) = (B_1(t))^{-1} k_1 sgn(S_1). \tag{21}$$

Since the reaching law (21) uses the $sign(S)$ function as a hard switcher, the undesirable chattering phenomenon occurs [30]. Hence the $sign(S)$ function, in which S is a fractional order sliding surface, is replaced by the $tanh(S)$ function. So the FOBSMC law can be proposed as:

$$B_{2(sw)}(t) = (B_1(t))^{-1} k_1 tanh(S_1), \tag{22}$$

where k_1 is positive constants and will be determined later. Hence, the overall control law becomes:

$$B_{2(d)}(t) = (B_1(t))^{-1}\left(-p_1 B_1(t) + p_1 G_b - \dot{G}_d + \lambda_1 {}_0^c D_t^{\alpha} e_1 + k_1 tanh(S_1)\right). \tag{23}$$

The desired $B_2(t)$ which is denoted by $B_{2(d)}(t)$. The fractional order term in control signal, i.e. ${}_0^c D_t^{\alpha}$ enhanced the controller robustness. Due to adding the extra degree of freedom, fractional order sliding mode controller can achieve better control performance than integer order sliding mode controller. For the stability analysis of the proposed controller in Theorem 2, we need Lemma 1.

Lemma 2 *The following equality is valid for every positive scalar a and given scalar b [31]:*

$$S(atanh(bS)) = |S(atanh(bS))| = \|S(atanh(bS))\| \geq 0. \tag{24}$$

Theorem 2 ***Stability analysis for the first fractional order sliding surface of proposed controller.***

Consider the Glucose-insulin system with Bergman minimal model (15), first state equation. This system is controlled by the control law $B_{2(d)}(t)$ in (23), then the system trajectories will converge to the sliding surface $S_1(t) = 0$.

Proof Consider a positive definite Lyapunov function candidate in the following form:

$$V_1 = \frac{1}{2} {S_1}^2. \tag{25}$$

To proof stability is done using Theorem 1, Lemmas 1 and 2. Taking the time fractional order derivative ${}_0^cD_t^\alpha$ from both sides of (24), and substitution (14) in it, obtains:

$$ {}_0^cD_t^\alpha V_1 = \frac{1}{2}\,{}_0^cD_t^\alpha {S_1}^2 \le S_1\,{}_0^cD_t^\alpha S_1 = S_1\left(\dot{e}_1 + \lambda_1\,{}_0^cD_t^\alpha e_1\right) = $$

$$ S_1\left(\left(-B_{2(d)}\left(t\right)B_1\left(t\right) - p_1B_1\left(t\right) + p_1G_b\right) - \dot{G}_d + \lambda_1\,{}_0^cD_t^\alpha e_1\right). \tag{26} $$

The substitution pseudo control law (23) into (25), obtains:

$$ S_1\,{}_0^cD_t^\alpha S_1 = S_1\left(\left(-\left(B_1\left(t\right)\right)^{-1}\left(-p_1B_1\left(t\right) + p_1G_b - \dot{G}_d + \lambda_1\,{}_0^cD_t^\alpha e_1 + \right.\right.\right. $$

$$ \left.\left.\left. k_1 tanh(S_1))\,B_1\left(t\right) - p_1B_1\left(t\right) + p_1G_b\right) - \dot{G}_d + \lambda_1\,{}_0^cD_t^\alpha e_1\right). \tag{27} $$

Finally, the simplification (26), obtain:

$$ {}_0^cD_t^\alpha V_1 = \frac{1}{2}\,{}_0^cD_t^\alpha {S_1}^2 \le S_1\,{}_0^cD_t^\alpha S_1 = -k_1 tanh(S_1)\,. \tag{28} $$

According to Lemma 1 it is obvious that the fractional order derivative of Lyapunov function is negative definite [19] and the positive switching gain k_1, guaranties stability of the closed loop system with fractional order sliding mode control [22, 32]. Now the second part of system model is defined as follows:

$$ \dot{B}_2\left(t\right) = -p_2B_2\left(t\right) + p_3\left(B_3\left(t\right) - I_b\right). \tag{29} $$

$B_2\left(t\right)$ is virtual control input for second part of Bergman minimal model, $B_{3(d)}\left(t\right)$ is desired output of the second part control loop of proposed controller, the second error equation introduced as follows:

$$ e_2 = B_2 - B_{2(d)}. \tag{30} $$

The second fractional order sliding surface (31) like the first fractional order sliding surface (17), with the exception that the error dynamic characteristics have changed:

$$ S_2 = {}_0^cD_t^{-\alpha}\dot{e}_2 + \lambda_2 e_2. \tag{31} $$

By using fractional order sliding mode control theory, the desired value of $B_3\left(t\right)$ which consists of equivalent control law and reaching law control, will result as follows:

$$ B_{3(eq)}\left(t\right) = \left(p_3\right)^{-1}\left(p_2B_2\left(t\right) + p_3I_b + \dot{B}_{2(d)} - \lambda_2\,{}_0^cD_t^\alpha e_2\right), \tag{32} $$

$$B_{3(sw)}(t) = -(p_3)^{-1} k_2 tanh(S_2). \tag{33}$$

Theorem 3 ***Stability analysis for the second fractional order sliding surface of proposed controller.***

Consider the second state Eq. (29) of Bergman minimal model (15). This system is controlled by the control law $B_{3(d)}(t)$ in (32) and (33), then the system trajectories will converge to the sliding surface $S_2(t) = 0$.

Proof Consider a positive definite Lyapunov function candidate in the following form [33, 34]:

$$V_2 = V_1 + \frac{1}{2} {S_2}^2. \tag{34}$$

To proof stability is done using Theorem 1, Lemmas 1 and 2. Taking the time fractional order derivative ${}_0^c D_t^\alpha$ from both sides of (34), and substitution (31) in it, obtains:

$${}_0^c D_t^\alpha V_2 = {}_0^c D_t^\alpha V_1 + \frac{1}{2} {}_0^c D_t^\alpha {S_2}^2 \leq S_1 {}_0^c D_t^\alpha S_1 + S_2 {}_0^c D_t^\alpha S_2 =$$

$$-k_1 S_1 tanh(S_1) + S_2 \left(\dot{e}_2 + \lambda_2 {}_0^c D_t^\alpha e_2 \right). \tag{35}$$

The substitution second part of Bergman minimal model (29), error Eq. (30), pseudo control law (32) and (33) into (35), obtains:

$${}_0^c D_t^\alpha V_2 \leq \left(-k_1 tanh(S_1) + S_2 \left(\left(-p_2 B_2(t) + p_3 \left((p_3)^{-1} (p_2 B_2(t) + p_3 I_b + \right. \right. \right. \right.$$

$$\left. \left. \left. \left. \dot{B}_{2d} - \lambda_2 {}_0^c D_t^\alpha e_2 - k_2 tanh(S_2) \right) \right) - p_3 I_b \right) - \dot{B}_{2_d} + \lambda_2 {}_0^c D_t^\alpha e_2 \right) \right). \tag{36}$$

Finally, by simplification of (36), obtains:

$${}_0^c D_t^\alpha V_2 \leq -k_1 S_1 sgn(S_1) - k_2 S_2 sgn(S_2). \tag{37}$$

According to Lemma 1 and Theorem 1, fractional order derivative of Lyapunov function (34) is negative definite and the second part of system is stable [35, 36]. The fractional order sliding surface for state $B_3(t)$ and $u(t)$ is exactly like to state $B_1(t)$ and $B_2(t)$. The process of calculating the control law and stability is in the same case, the sliding variables are defined in:

$$e_3 = B_3(t) - B_{3_d}, e_4 = u(t) - u_d(t), \tag{38}$$

$$S_3 = {}_0^c D_t^{-\alpha} \dot{e}_3 + \lambda_3 e_3, S_4 = {}_0^c D_t^{-\alpha} \dot{e}_4 + \lambda_4 e_4. \tag{39}$$

The $u(t)$ pseudo controller is designed by (39):

$$u_{(d)}(t) = n(B_3(t) - I_b) - \gamma t[B_1(t) - h]^+ + \dot{B}_{3_d} - \lambda_3 {}_0^c D_t^{\alpha} e_3 - k_3 tanh(S_3). \tag{40}$$

Finally, by using sliding mode control theory $w(t)$ is designed as follows:

$$w_d(t) = u(t) + a\dot{u}_d - a\lambda_4 {}_0^c D_t^{\alpha} e_4 - ak_4 tanh(S_4). \tag{41}$$

By applying the proposed controller, by exerting this signal to the system, the system state variables will converge quickly without the normalization of system uncertainties.

Theorem 4 *Consider the fractional order sliding surface (17), (42), using Lyapunov stability theorem in the Theorem 1 and Lemma 1, we guarantee that the fractional order sliding surface (17) is stable and converges to zero.*

$$S_1 = {}_0^c D_t^{-\alpha} \dot{e}_1 + \lambda_1 e_1 = 0. \tag{42}$$

Proof Consider the error fractional order dynamics (43) as follow:

$${}_0^c D_t^q e_1 = -\lambda_1 e_1, 0 < q < 1. \tag{43}$$

Consider a positive definite Lyapunov function candidate for error fractional order dynamics (43) in the following form:

$$V = \frac{1}{2} {e_1}^2. \tag{44}$$

Taking fractional order derivative of both sides of (44) with respect to time, one has:

$${}_0^c D_t^q V = \frac{1}{2} {}_0^c D_t^q {e_1}^2 \leq e_1 {}_0^c D_t^q e_1 = -\lambda_1 {e_1}^2. \tag{45}$$

It implies that the asymptotic stability of the system is guaranteed.

5 Numerical Simulation

In this paper we used nonlinear Bergman minimal model for blood glucose regulation using fractional order backstepping sliding mode control. Fractional calculus is a useful tool to control and to achieve a significant degree of robustness. The control system designed in this paper will be next used as an autonomous blood glucose concentration controller for type I diabetes patients. Consequently, applying fractional order sliding surface to sliding mode control can modify the classical

SMC to more robust controller. In this section we evaluate the proposed design with numerical simulation, and compared them with linear control and the back-stepping sliding mode control method which is introduced on [9]. Simulations were performed using MATLAB software, the specification of Bergman minimal model, FOBSMC parameters is available on Table 1. The simulation results are depicted on Figs. 1, 2, 3, 4, 5, 6, 7 and 8. As it can be seen in Fig. 1 the proposed controller design (FOBSMC) successfully controlled the Blood Glucose concentration and decreased the glucose concentration level from the critical area (hyperglycemia) in initial time and meal disturbance with 80 (mg/dl) amplitude applied at t = 450 min. There is no hypoglycemic undershot, and normoglycemia is achieved in acceptable time. The theoretical analyses and simulations show that the proposed controller achieves set point tracking in the presence of disturbance. The BSMC of the proposed controller (FOBSMC) has better convergence. Both methods have good performance against disturbances applied. This reflects is the robustness of the method against disturbances.

Figure 2 show the insulin infusion (control function) for designed controller and BSMC, it can be seen constrained the nonnegative actuation is regarded, insulin infusion is continues signal and appropriate value. One of the main advantages of the

Table 1 Bergman minimal model parameters value [9] and FOBSMC parameters value

Bergman min. model	$p_1(min^{-1})$	$p_2(min^{-1})$	$p_3(min^{-1})$	$n(min^{-1})$	I_b	G_b	$B_1(0)$	$B_3(0)$
	0	0.0123	8.2×10^{-8}	0.2659	7	70	200	50
FOBSMC	α	a	k_1	k_2	k_3	k_4	λ_1	λ_2
	0.8	2	9×10^{-5}	6.5×10^{-2}	0.03	37	21×10^{-3}	0.85
	λ_3	λ_4	A	B	G_d	$u_{(0)}$	$B_2(0)$	$w_{(0)}$
	2.8×10^{-3}	1	80	−0.5	80	0	0	0

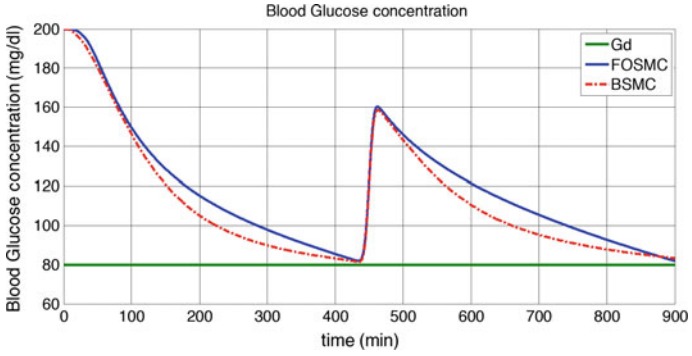

Fig. 1 Patient Blood glucose concentration in FOBSMC and BSMC

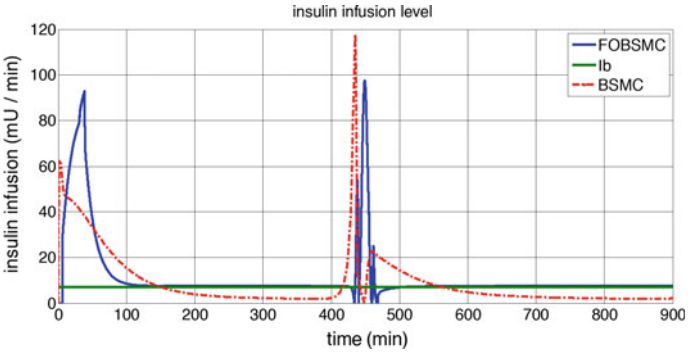

Fig. 2 Control low i.e. Insulin injection with pump in FOBSMC and BSMC

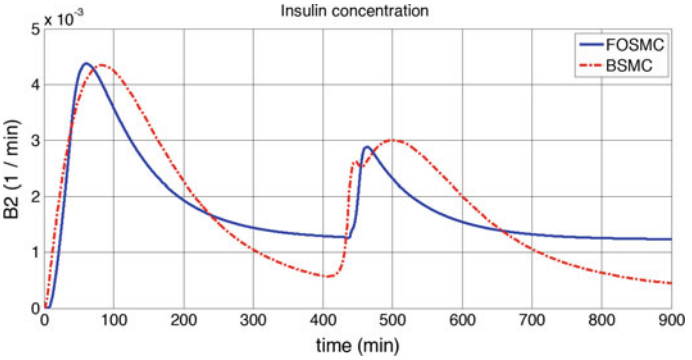

Fig. 3 Patient insulin concentration

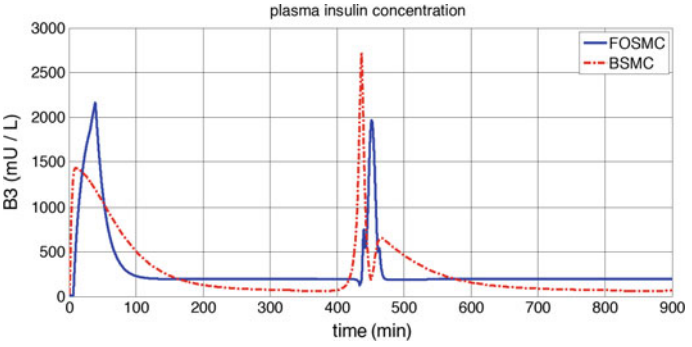

Fig. 4 Plasma insulin concentration

proposed controller, the FOBSMC controller can track the desired value I_b (Insulin basal level). Figure 3 shows the $B_2\,(t)$ state, as it can be seen, the proposed controller Better performance than BSMC controller and closer to real conditions. Figure 4 shows the plasma insulin profile designed controller and BSMC.

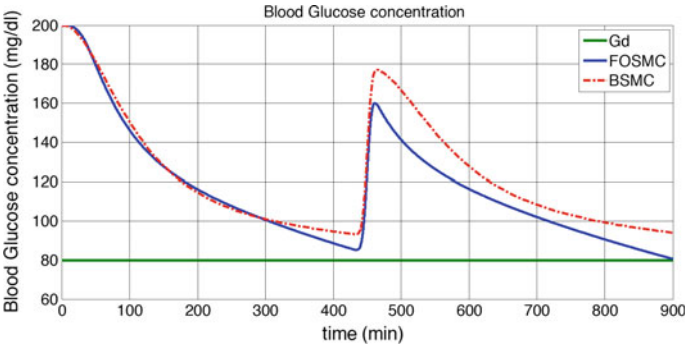

Fig. 5 Patient blood glucose concentration in FOBSMC and BSMC with 30 % Variation in system parameters

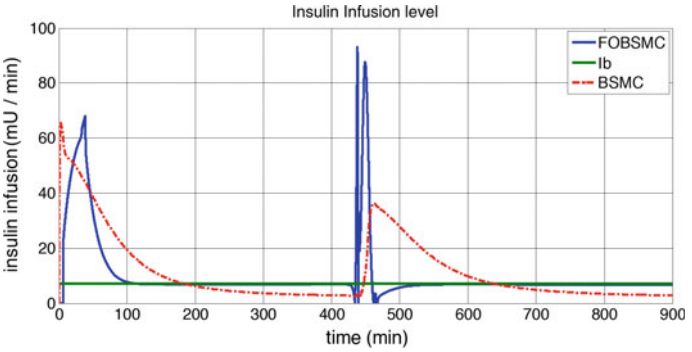

Fig. 6 Insulin injection with pump in FOBSMC and BSMC with 30 % variation in system parameters

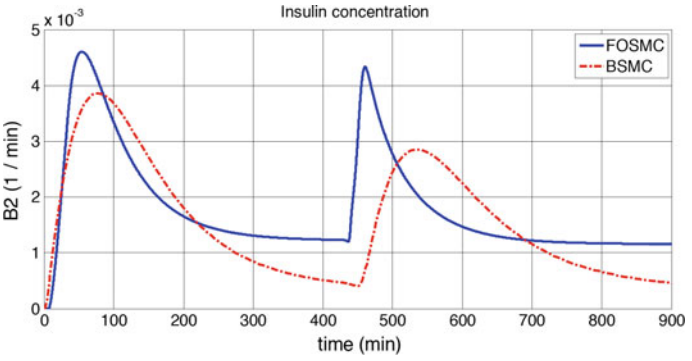

Fig. 7 Patient insulin concentration with 30 % variation in system parameters

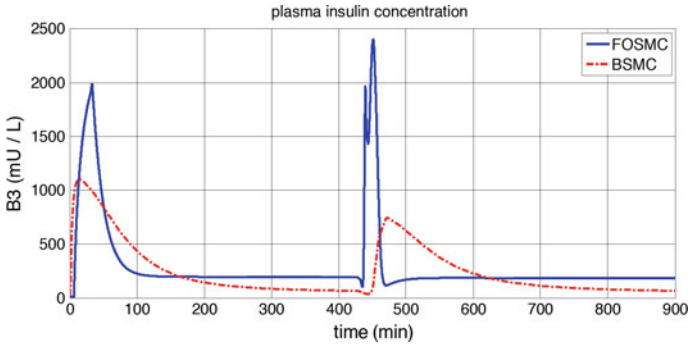

Fig. 8 Plasma insulin concentration with 30 % Variation in system parameters

Table 2 The Controllers performance for Bergman minimal model with 30 % variation in parameters

Controllers	Δ_e
FOBSMC	4157
BSMC	6453

Bergman minimal model parameters in type I diabetics patients due to the physiological condition of the patient will change over time. The Blood glucose controller against parameters uncertainties must also have an appropriate performance and is robust against parametric uncertainties. However, to compare the robust performance of the proposed controller than BSMC controller, meal disturbance of 80 (mg/dl) is applied at t = 450 min, together with 30 % variation in parameters of the system. Responses are shown in Figs. 5, 6, 7 and 8, by combination of the fractional order and Backstepping sliding mode controllers, the performance of the proposed fractional order Backstepping sliding mode controller is much improved with respect to the backstepping sliding mode controller. Simulation results for the proposed controllers are shown in Table 2. It can be seen that the proposed fractional order SMC have the smaller error and more robustness than backstepping sliding mode controllers. The error is defined by:

$$\Delta e = \int |B_1(t) - B_{1vd}(t)|\, dt, \tag{46}$$

where $B_{1vd}(t)$ is $B_1(t)$ after 30 % variation in parameters. Figure 5 the proposed controller design (FOBSMC) successfully controlled the Blood Glucose concentration with 30 % variation in parameters and meal disturbance but BSMC controller with 30 % variation in the parameters, we are seeing an increase tracking error.

6 Conclusion

The diabetes management as one of the challenging control problems in human regulatory systems has been discussed. The treatment of the disease via robust feedback control design using fractional order calculus and sliding mode control has been considered. Stabilization of blood glucose concentration has been dis-cussed in presence of the external disturbances such as food intake and Initial condition critical (Hyperglycemia). From the viewpoint of stability and robust stability analysis and simulation was investigated for the proposed controller. With this aim, a fractional order backstepping sliding mode control design for blood glucose regulation in type I diabetes. The proposed controller design using the four fractional order sliding surfaces for appropriate tracking, robustness against mismatched disturbance and uncertainties. The designed controller is checked and confirmed by computer simulations. According to simulation result the proposed controllers have a good performance in tracking set point in appropriate time, disturbance rejection, non-negative actuator and continuous insulin injected.

References

1. Bergman, R.N., Philips, L.S., Cobelli, C.: Physiologic evaluation of factors controlling glucose tolerance in man. J. Clin. Investig. **68**(6), 1456–1467 (1981)
2. Marchetti, G., Barolo, M., Jovanovic, L., Zisser, H., Seborg, D.E.: An improved PID switching control strategy for type 1 diabetes. IEEE Trans. BioMed. Eng. **55**(3), 857–865 (2008)
3. Parker, R.S., Doyle, F.J., Peppas, N.A.: A model-based algorithm for blood glucose control in type I diabetic patients. IEEE Trans. BioMed. Eng. **46**(2), 148–157 (1999)
4. Wai Ting, C., Quek, C.: A novel blood glucose regulation using TSK-FCMAC: a fuzzy CMAC based on the zero-ordered TSK fuzzy Inference scheme. IEEE Trans. Neural Netw. **20**(5), 856–871 (2009)
5. Grant, P.: A new approach to diabetic control: fuzzy logic and insulin pump technology. Med. Eng. Phys. **29**(7), 824–827 (2007)
6. Allam, F., Nossair, Z., Gomma, H., Ibrahim, I., Abdelsalam, M.: Evaluation of using a recurrent neural network (RNN) and a fuzzy logic controller (FLC) in closed loop system to regulate blood glucose for type-1 diabetic patients. Int. J. Intell. Syst. Appl. **4**(10), 58–71 (2012)
7. Kaveh, P., Shtessel, Y.B.: Blood glucose regulation using higher-order sliding mode control. Int. J. Robust Nonlinear Control **25**(18), 557–569 (2008)
8. Hernandez, A.G.G., Fridman, L., Levant, A., Shtessel, Y.B., Leder, R., Monsalve, C.R., Andrade, S.I.: High-order sliding-mode control for blood glucose: practical relative. Control Eng. Pract. **21**(5), 747–758 (2013)
9. Tadrisi Parsa, N., Vali, A.R., Ghasemi, R.: Back stepping sliding mode control of blood glucose for type I diabetes. Int. J. Med. Health Biomed. Pharm. Eng. **8**(11), 749–753 (2014)
10. Ali, S., Padhi, R.: Optimal blood glucose regulation of diabetic patients using single network adaptive critics. Optim. Control Appl. Methods **32**(2), 196–214 (2009)
11. N'Doye, I., Voos, H., Darouach, M., Schneider, J.G.: Static output feedback H∞ control for a fractional-order glucose-insulin system. Int. J. Control Autom. **13**(4), 798–807 (2015)
12. Leon-Vargasa, F., Garellib, F., De Battistab, H., Vehia, J.: Postprandial blood glucose control using a hybrid adaptive PD controller with insulin-on-board limitation. Biomed. Signal Process. Control **8**(6), 724–732 (2013)

13. Ghorbani, M., Bogdan, P.: Reducing risk of closed loop control of blood glucose in artificial pancreas using fractional calculus. In: 36th Annual International Conference of the Engineering in Medicine and Biology Society, pp. 4839–4842 (2014)
14. Goharimanesh, M., Lashkaripour, A., Abouei Mehrizi, A.: Fractional order PID controller for diabetes patients. J. Comput. Appl. Mech. **46**(1), 69–76 (2015)
15. Adhikary, N., Mahanta, C.: Integral backstepping sliding mode control for underactuated systems: swing-up and stabilization of the cart-pendulum system. ISA Trans. **51**(6), 870–880 (2013)
16. Tenreiro Machado, J., Kiryakova, V., Mainardi, F.: Recent history of fractional calculus. Commun. Nonlinear Sci. Numer. Simulat. **16**(3), 1140–1153 (2011)
17. Monje, C.A., Chen, Y., Vinagre, B.M., Xue, D., Feliu-Batlle, V.: Fractional-Order Systems and Controls. Springer, London (2010)
18. Podlubny, I.: Fractional Differential Equations. Academic Press, San Diego, California (1999)
19. Li, Y., Chen, Y.Q., Podlubny, I.: Stability of fractional-order nonlinear dynamic systems: Lyapunov direct method and generalized Mittag-Leffler stability. Comput. Math. Application. **59**(5), 1810–1821 (2010)
20. Li, Y., Chen, Y.Q., Podlubny, I.: Mittag-Leffler stability of fractional order nonlinear dynamic systems. Automatica **45**(8), 1965–1969 (2009)
21. Li, C., Deng, W.: Remarks on fractional derivatives. Appl. Math. Comput. **187**(2), 777–784 (2007)
22. Aguila-Camacho, N., Duarte-Mermoud, M.A., Gallegos, J.A.: Lyapunov functions for fractional order systems. Commun. Nonlinear Sci. Numer. Simul. **19**(9), 2951–2957 (2014)
23. Palumbo, P., Ditlevsen, S., Bertuzzi, A., De Gaetano, A.: Mathematical modeling of the glucose-insulin system: a review. J. Math. Biosci. **244**(2), 69–81 (2013)
24. Balakrishnan, N.P., Rangaiah, G.P., Samavedham, L.: Review and analysis of blood glucose (BG) models for type 1 diabetic patients. Ind. Eng. Chem. Res. **50**(21), 12041–12066 (2011)
25. Fisher, M.E.: A semi closed-loop algorithm for the control of blood glucose levels in diabetics. IEEE Trans. BioMed. Eng. **38**(1), 57–61 (1991)
26. N'Doye, I., Voos, H., Darouach, M., Schneider, J.G., Knauf, N.: Static output feedback stabilization of nonlinear fractional-order glucose-insulin system. In: IEEE EMBS 19th International Conference on Biomedical Engineering and Sciences, pp. 589–594 (2012)
27. Utkin, V.I.: Sliding Modes in Control and Optimization. Springer, Berlin (1992)
28. Komurcugil, H.: Adaptive terminal sliding-mode control strategy for DC-DC buck converters. ISA Trans. **51**(6), 673–681 (2012)
29. Liang, C., Li, Y.: Attitude analysis and robust adaptive backstepping sliding mode control of spacecrafts orbiting irregular asteroids. Math. Probl. Eng. 15–30 (2014)
30. Delavari, H., Lanusse, P., Sabatier, J.: Fractional order controller design for a flexible manipulator robot. Asian J. Control. **15**(3), 783–795 (2013)
31. Yin, C., Dadras, S., Zhong, S.M., Chen, Y.Q.: Control of a novel class of fractional-order chaotic systems via adaptive sliding mode control approach. Appl. Math. Model. **37**(4), 2469–2483 (2013)
32. Trigeassou, J.C., Maamri, N., Sabatier, J., Oustaloup, A.: A Lyapunov approach to the stability of fractional differential equations. Signal Process. **91**(3), 437–445 (2011)
33. Weia, Y., Chena, Y., Lianga, S., Wanga, Y.: A novel algorithm on adaptive backstepping control of fractional order systems. Neurocomputing **165**, 395–402 (2015)
34. Wang, Z.: Synchronization of an uncertain fractional-order chaotic system via backstepping sliding mode control. Discrete Dyn. Nat. Soc. (2013)
35. Delavari, H.: A novel fractional adaptive active sliding mode controller for synchronization of non-identical chaotic systems with disturbance and uncertainty. Int. J. Dyn. Control. **67**, 2433–2439 (2011)
36. Delavari, H., Ranjbar, A.N., Ghaderi, R., Momani, S.: Fractional order control of a coupled tank. Nonlinear Dyn. **61**(3), 383–397 (2010)

Maximum and Minimum Principles for the Generalized Fractional Diffusion Problem with a Scale Function-Dependent Derivative

Małgorzata Klimek and Kalina Kamińska

Abstract In the paper, we prove the necessary condition for the extremum existence in terms of the generalized function-dependent fractional derivatives. By using these results we extend the maximum and minimum principles, known from the theory of differential equations and from diffusion problems with the Caputo derivative of constant or distributed order. We study the fractional diffusion problem, where time evolution is determined by the scale function-dependent Caputo derivative and show that the maximum or respectively minimum principle is valid, provided the source function is a non-positive or a non-negative one in the domain. As an application, we demonstrate how the sign of the classical solution is controlled by the initial and boundary conditions.

Keywords Maximum principle · Minimum principle · Fractional necessary condition for extremum existence · Generalized diffusion equation · Scale function-dependent fractional derivatives

1 Introduction

The paper is devoted to the discussion of properties of classical solutions to generalized multidimensional time-fractional diffusion problems. We shall derive the corresponding maximum/minimum principles and apply them in control of the sign of the solutions.

M. Klimek (✉)
Institute of Mathematics, Czestochowa University of Technology,
Dabrowskiego 69, 42-201 Czestochowa, Poland
e-mail: mpklimek@o2.pl

K. Kamińska
Faculty of Mechanical Engineering and Computer Science, Czestochowa University of Technology, Dabrowskiego 69, 42-201 Czestochowa, Poland

A. Babiarz et al. (eds.), *Theory and Applications of Non-integer Order Systems*,
Lecture Notes in Electrical Engineering 407, DOI 10.1007/978-3-319-45474-0_19

We consider the time-fractional diffusion problem with the equation including scale function-dependent fractional derivative:

$$ {}^{c}D^{\alpha}_{0+;[z],t}u(x,t) = L(u) + F(x,t) \quad (x,t) \in \Omega_T := G \times (0,T], \tag{1} $$

where operator L looks as follows

$$ L(u) = \sum_{k=1}^{n} \left(p(x) \frac{\partial^2 u}{\partial x_k^2} + \frac{\partial p}{\partial x_k} \frac{\partial u}{\partial x_k} \right) - q(x)u \tag{2} $$

$$ = p(x)\Delta u + (grad(p), grad(u)) - q(x)u, $$

functions $p \in C^1(\bar{G})$, $q \in C(\bar{G})$ fulfill conditions $p(x) > 0$, $q(x) \geq 0$, $\forall x \in \bar{G}$, G is an open and bounded region in R^n, $\bar{G}$ denotes its closure.

Diffusion equation (1) is subjected to the following initial condition

$$ u|_{t=0} = u_0(x), \quad x \in \bar{G} \tag{3} $$

and boundary condition

$$ u|_S = v(x,t), \quad (x,t) \in S \times [0,T], \tag{4} $$

where S is the boundary of region $G \in R^n$.

The diffusion and advection-diffusion including the generalized fractional derivative were introduced in [1, 2]. Their solutions and properties were studied by means of numerical methods [1–3]. Our aim is to derive the analytical results describing the solutions via maximum/minimum principles. These theorems are developed in the classical differential equations theory as well as in the time-fractional diffusion problems [4–7] and are an important tool in proving the uniqueness results and theorems on continuous dependence of solutions on the problem data. We shall obtain analogous maximum/minimum theorems for models with a fractional time-derivative dependent on the scale function.

The paper is organized as follows. Section 2 contains definitions of the classical solution and of the generalized fractional derivative of the Caputo type, its properties and the preliminary results on the existence condition for maximum and minimum. The version, known in calculus for the first-order derivative, is extended to the case of a two function-dependent fractional derivative. The next part, Sect. 3, includes our main results - maximum and minimum principles for the diffusion problem with the generalized Caputo derivative with respect to the time variable and their application in controlling the sign of the classical solution. The brief conclusion section closes the paper.

2 Preliminaries

In this section, we introduce the basic definitions and properties of the generalized fractional derivative and prove the necessary conditions of the extremum existence expressed in terms of this operator.

First, we recall the notion of the classical solution and define the generalized time-fractional derivative appearing in Eq. (1). In the definition of the classical solution, we restrict the source function and the functions determining the initial and boundary conditions to the continuous ones.

Definition 1 Function u, determined in region $\bar{\Omega}_T := \bar{G} \times [0, T]$ will be called a classical solution to problem (1)–(4) with $F \in C(\Omega_T)$, $u_0 \in C(\bar{G})$, $v \in C(S \times [0, T])$ iff

$$u \in CW_T(G) := C(\bar{\Omega}_T) \cap W_t^1((0, T)) \cap C_x^2(G) \tag{5}$$

and u fulfills Eq. (1), initial condition (3) and boundary condition (4). $W_t^1((0, T)) \subset C^1((0, T])$ is a function space such that $f \in W_t^1((0, T)) \Longleftrightarrow f' \in L(0, T)$ i.e. derivatives are determined on $(0, T)$ and absolutely integrable in the Lebesgue sense.

Now, we introduce the scale and weight function-dependent fractional derivative which was defined in [8]. We restrict this brief review to the case of order $\alpha \in (0, 1)$ and the left-sided differential operator of the Caputo type. Let us point out that in fractional calculus analogous derivatives are defined and studied for higher orders, in Caputo and Riemann–Liouville versions and in both cases: as the left- and right-sided operators [8, 9].

Definition 2 Let $\alpha \in (0, 1)$. The generalized (two function-dependent) left derivative of the Caputo type is defined as follows

$${}^{c}D_{0+;[z,w]}^{\alpha} f(t) = I_{0+;[z,w]}^{1-\alpha}(D_{[z,w,L]} f)(t), \tag{6}$$

where $I_{0+;[z,w]}^{1-\alpha}$ denotes the generalized function-dependent integral operator

$$I_{0+;[z,w]}^{1-\alpha} f(t) = \frac{1}{w(t)\Gamma(1-\alpha)} \int_0^t \frac{w(s)z'(s)f(s)}{[z(t) - z(s)]^{\alpha}} ds \tag{7}$$

and the $D_{[z,w,L]}$-operator is given below

$$D_{[z,w,L]} f(t) = \frac{[w(t)f(t)]'}{w(t)z'(t)}, \tag{8}$$

with weight function $w \in C[0, b]$, scale function $z \in C^1[0, b]$ and $w > 0,\ z' > 0$ in interval $[0, b]$.

The above definition extends the notion of the standard Caputo derivative which is recovered in the case:

$$z(t) = t \quad w(t) = 1 \quad t \in [0, b].$$

We refer the reader to the discussion on generalized two-function dependent fractional derivatives (left and right) enclosed in monograph [9] and to further results in [8], where Caputo type derivatives are constructed and studied as well. Let us recall the differentiation formulas for analogs of power functions when $\beta > 0$:

$${}^{c}D^{\alpha}_{0+;[z,w]} \frac{(z(t) - z(0))^{\beta-1}}{w(t)} = \frac{\Gamma(\beta)}{\Gamma(\beta - \alpha)} \frac{(z(t) - z(0))^{\beta-\alpha-1}}{w(t)}. \tag{9}$$

In particular, for $w = 1$ we have the following simpler definition and differentiation formula:

$${}^{c}D^{\alpha}_{0+;[z]} f(t) = I^{1-\alpha}_{0+;[z]} (D_{[z,L]} f)(t), \tag{10}$$

where $I^{1-\alpha}_{0+;[z]}$ denotes the generalized scale function-dependent integral operator

$$I^{1-\alpha}_{0+;[z]} f(t) = \frac{1}{\Gamma(1-\alpha)} \int_0^t \frac{z'(s) f(s)}{[z(t) - z(s)]^{\alpha}} ds \tag{11}$$

and the $D_{[z,L]}$-operator is given below

$$D_{[z,L]} f(t) = \frac{f'(t)}{z'(t)}, \tag{12}$$

with scale function $z \in C^1[0, b]$ and $z' > 0$ in interval $[0, b]$. The differentiation formula (9) is of the form

$${}^{c}D^{\alpha}_{0+;[z]} (z(t) - z(0))^{\beta-1} = \frac{\Gamma(\beta)}{\Gamma(\beta - \alpha)} (z(t) - z(0))^{\beta-\alpha-1}. \tag{13}$$

Now, we shall extend the necessary condition for the maximum existence which was proved in [4–6] in the case of the Caputo derivative and in [7] for the Caputo derivative of distributed order. In the theorem below, we formulate the analogous result for the two-function dependent fractional derivative defined by formula (6). It is a known fact from calculus that if function $f \in W^1_t((0, T)) \cap C[0, T]$ attains a maximum at point $t_0 \in (0, T]$, then $f'(t_0) = 0$. It can be expressed as follows in terms of generalized fractional derivatives.

Theorem 1 *Let function $f \in W^1_t((0, T)) \cap C([0, T])$ attain its maximum on interval $[0, T]$ at point $s = t_0$, $t_0 \in (0, T]$. Then, the generalized two function-dependent Caputo derivative of function f fulfills the following inequality for any order $\alpha \in (0, 1)$*

$${}^{c}D^{\alpha}_{0+;[z,w]} \frac{f}{w}(t_0) \geq 0. \tag{14}$$

Proof We define an auxiliary function:

$$g(s) := \frac{f(t_0) - f(s)}{w(s)} \quad s \in [0, T]. \tag{15}$$

It is easy to check that function g has the following properties:

$$g(s) \geq 0 \quad s \in [0, T] \tag{16}$$

$${}^{c}D^{\alpha}_{0+;[z,w]} g(t) = -{}^{c}D^{\alpha}_{0+;[z,w]} \frac{f}{w}(t) \quad t \in [0, T] \tag{17}$$

$$|g(s)| \leq C_{\epsilon} |z(t_0) - z(s)| \quad s \in [\epsilon, T], \epsilon \in (0, T), \tag{18}$$

which follow from the fact that: $f \in W_t^1((0, t))$, $z \in C^1[0, T]$, $w \in C[0, T]$, $z' > 0$, $w > 0$. Now, we rewrite the derivative and obtain for any $\epsilon \in (0, t_0)$

$${}^{c}D^{\alpha}_{0+;[z,w]} g(t_0) = I^{1-\alpha}_{0+;[z,w]} (D_{[z,w,L]} g)(t_0) \tag{19}$$

$$= \frac{1}{w(t_0)\Gamma(1-\alpha)} \int_0^{t_0} \frac{[w(s)g(s)]'}{[z(t_0) - z(s)]^{\alpha}} ds$$

$$= \frac{1}{w(t_0)\Gamma(1-\alpha)} \int_0^{\epsilon} \frac{[w(s)g(s)]'}{[z(t_0) - z(s)]^{\alpha}} ds + \frac{1}{w(t_0)\Gamma(1-\alpha)} \int_{\epsilon}^{t_0} \frac{[w(s)g(s)]'}{[z(t_0) - z(s)]^{\alpha}} ds$$

$$= I_1 + I_2.$$

Let us note that $f \in W_t^1((0, t))$ yields $wg \in W_t^1((0, t))$, therefore $(wg)' \in L((0, T))$, which means that

$$\forall \delta > 0 \quad \exists \epsilon > 0 \quad |I_1| < \delta. \tag{20}$$

For the I_2 - part we have

$$I_2 = \lim_{s \to t_0} \frac{(z(t_0) - z(s))^{-\alpha} w(s) g(s)}{w(t_0)\Gamma(1-\alpha)} - \frac{(z(t_0) - z(\epsilon))^{-\alpha} w(\epsilon) g(\epsilon)}{w(t_0)\Gamma(1-\alpha)}$$

$$+ \frac{1}{w(t_0)\Gamma(-\alpha)} \int_{\epsilon}^{t_0} \frac{w(s) g(s) z'(s)}{[z(t_0) - z(s)]^{\alpha+1}} ds.$$

The limit in the above equality vanishes:

$$\lim_{s \to t_0} \frac{|(z(t_0) - z(s))^{-\alpha} w(s) g(s)|}{w(t_0)\Gamma(1-\alpha)}$$

$$\leq ||w|| \lim_{s \to t_0} \frac{|(z(t_0) - z(s))^{-\alpha}| \cdot C_{\epsilon} |(z(t_0) - z(s))|}{w(t_0)\Gamma(1-\alpha)} = 0,$$

where we applied property (18) and $||\cdot||$ denotes the supremum norm in the $C[0,T]$-space. From $\Gamma(-\alpha) < 0$ for $\alpha \in (0,1)$ and property (16) we obtain $I_2 \leq 0$ for any $\epsilon \in (0,T)$. Next, from properties (17), (20) we obtain (14). □

The above theorem holds in the case of the scale function-dependent derivative defined by formula (10) when $w = 1$.

Corollary 1 *Let function $f \in W_t^1((0,T)) \cap C([0,T])$ attain its maximum on interval $[0,T]$ at point $s = t_0$, $t_0 \in (0,T]$. Then, the generalized scale function-dependent Caputo derivative of function f fulfills the following inequality for any order $\alpha \in (0,1)$*

$$ {}^cD^{\alpha}_{0+;[z]} f(t_0) \geq 0. \tag{21}$$

The necessary condition for the minimum existence can also be expressed in terms of a two function-dependent derivative.

Theorem 2 *Let function $f \in W_t^1((0,T)) \cap C([0,T])$ attain its minimum on interval $[0,T]$ at point $s = t_0$, $t_0 \in (0,T]$. Then, the generalized two function-dependent Caputo derivative of function f fulfills the following inequality for any order $\alpha \in (0,1)$*

$$ {}^cD^{\alpha}_{0+;[z,w]} \frac{f}{w}(t_0) \leq 0. \tag{22}$$

Proof In the proof, we apply the auxiliary function given in (15). Function g now obeys the inequality:

$$ g(s) \leq 0 \quad s \in [0,T] \tag{23}$$

and it also fulfills (17), (18). Similar to the previous proof, we split the derivative and obtain for any $\epsilon \in (0, t_0)$

$$ {}^cD^{\alpha}_{0+;[z,w]} g(t_0) = \tag{24}$$

$$= \frac{1}{w(t_0)\Gamma(1-\alpha)} \int_0^{\epsilon} \frac{[w(s)g(s)]'}{[z(t_0)-z(s)]^{\alpha}} ds + \frac{1}{w(t_0)\Gamma(1-\alpha)} \int_{\epsilon}^{t_0} \frac{[w(s)g(s)]'}{[z(t_0)-z(s)]^{\alpha}} ds$$

$$= I_1 + I_2.$$

Let us note that again for the first term implication (20) holds. For the I_2 - term we have the equality

$$I_2 = \lim_{s \to t_0} \frac{(z(t_0)-z(s))^{-\alpha} w(s) g(s)}{w(t_0)\Gamma(1-\alpha)} - \frac{(z(t_0)-z(\epsilon))^{-\alpha} w(\epsilon) g(\epsilon)}{w(t_0)\Gamma(1-\alpha)}$$

$$+ \frac{1}{w(t_0)\Gamma(-\alpha)} \int_{\epsilon}^{t_0} \frac{w(s)g(s)z'(s)}{[z(t_0)-z(s)]^{\alpha+1}} ds.$$

The limit in the above equality vanishes as was shown in the previous proof. From $\Gamma(-\alpha) < 0$ for $\alpha \in (0, 1)$ and property (23) we obtain $I_2 \geq 0$ for any $\epsilon \in (0, T)$. Next, from properties (17), (20) we obtain (22). □

From the above necessary condition for the minimum, formulated for the two function-dependent derivative, we obtain the following corollary for the case $w = 1$.

Corollary 2 *Let function* $f \in W_t^1((0, T)) \cap C([0, T])$ *attain its minimum on interval* $[0, T]$ *at point* $s = t_0$, $t_0 \in (0, T]$. *Then, the generalized scale function-dependent Caputo derivative of function* f *fulfills the following inequality for any order* $\alpha \in (0, 1)$

$$ {}^{c}D^{\alpha}_{0+;[z]} f(t_0) \leq 0. \tag{25}$$

3 Main Results

We shall study the generalized fractional diffusion problem with the diffusion equation (1), the initial condition given in (3) and the boundary conditions determined in (4). Our aim is to derive the maximum and minimum principles for the multidimensional case and to apply these results in a preliminary study of the properties of classical solutions to the problem.

First, applying Corollary 1, we prove the theorem which generalizes the classical maximum principle as well as the result proved in [4–6] for fractional diffusion problems. We extend the fractional maximum principle to the case, where in the diffusion equation the Caputo derivative with respect to the time-variable is replaced with the scale function-dependent derivative of the Caputo type given in (10).

Theorem 3 *Let function* $u \in CW_T(G) := C(\bar{\Omega}_T) \cap W_t^1((0, T)) \cap C_x^2(G)$ *be the classical solution of the generalized time-fractional diffusion equation (1) in region* $\Omega_T := G \times (0, T]$, $G \subset R^n$ *and let* $F(x, t) \leq 0, \quad (x, t) \in \Omega_T$. *Then, either solution* u *is non-positive in* $\bar{\Omega}_T$ *or it attains the positive maximum on set* S_G^T *which means*

$$ u(x, t) \leq \max\{0, \max_{(x,t)\in S_G^T} u(x, t)\} \quad (x, t) \in \bar{\Omega}_T, \tag{26}$$

where $S_G^T := (\bar{G} \times \{0\}) \cup (S \times [0, T])$.

Proof Let us assume that thesis (26) is not valid. Then point (x_0, t_0), $x_0 \in G$, $0 \leq t_0 \leq T$ exists such that

$$ u(x_0, t_0) > \max_{(x,t)\in S_G^T} \{0, u(x, t)\} = M > 0. \tag{27}$$

We define number $\epsilon := u(x_0, t_0) - M > 0$ and the following auxiliary function:

$$f(x,t) := u(x,t) + \frac{\epsilon}{2}\frac{z(T)-z(t)}{z(T)} \quad (x,t) \in \bar{\Omega}_T. \tag{28}$$

From this definition and assumptions of the theorem we have:

$$f(x,t) \leq u(x,t) + \frac{\epsilon}{2} \quad (x,t) \in \bar{\Omega}_T$$

$$f(x_0,t_0) \geq u(x_0,t_0) = \epsilon + M \geq \epsilon + u(x,t) \geq \epsilon + f(x,t) - \frac{\epsilon}{2} \quad (x,t) \in S_G^T.$$

From the above inequality we infer that function f cannot attain its maximum on the S_G^T-part of the boundary of region Ω_T. Therefore point $(x_1,t_1) \in \bar{\Omega}_T$ exists such that $x_1 \in G$ and $0 < t_1 \leq T$ and function f attains its maximum at (x_1,t_1). At this point the following inequality is fulfilled

$$f(x_1,t_1) \geq f(x_0,t_0) \geq \epsilon + M > \epsilon.$$

From Corollary 1 and the necessary and sufficient conditions of the existence of the maximum in region Ω_T we obtain the following set of conditions

$${}^cD^{\alpha}_{0+;[z],t} f(x_1,t_1) \geq 0 \quad \alpha \in (0,1)$$

$$grad(f)|_{(x_1,t_1)} = 0 \quad \Delta f|_{(x_1,t_1)} \leq 0$$

and the relations for derivatives

$${}^cD^{\alpha}_{0+;[z],t} u(x,t) = {}^cD^{\alpha}_{0+;[z],t} f(x,t) + \tfrac{\epsilon}{2z(T)} \tfrac{(z(t)-z(0))^{1-\alpha}}{\Gamma(2-\alpha)}, \tag{29}$$

$$grad(f) = grad(u), \qquad \Delta u(x,t) = \Delta f(x,t). \tag{30}$$

Now, we are ready to test the behavior of the generalized diffusion operator at point (x_1,t_1)

$$\left({}^cD^{\alpha}_{0+;[z],t} u(x,t) - L(u)\right)|_{(x_1,t_1)}$$

$$= {}^cD^{\alpha}_{0+;[z],t} f(x_1,t_1) + \frac{\epsilon}{2z(T)} \frac{(z(t_1)-z(0))^{1-\alpha}}{\Gamma(2-\alpha)}$$

$$-p(x_1)\Delta f(x_1,t_1) - \left(grad(p)|_{x_1}, grad(f)|_{(x_1,t_1)}\right)$$

$$+q(x_1)\left(f(x_1,t_1) - \frac{\epsilon}{2}\frac{z(T)-z(t_1)}{z(T)}\right) - F(x_1,t_1)$$

$$\geq \frac{\epsilon}{2z(T)} \frac{(z(t_1)-z(0))^{1-\alpha}}{\Gamma(2-\alpha)} > 0.$$

We note that at point (x_1, t_1) the following inequality holds

$$\left({}^{c}D^{\alpha}_{0+;[z],t}u(x,t) - L(u)\right)|_{(x_1,t_1)} > 0,$$

which means that function u is not a solution to Eq. (1). Therefore the assumption (27) is incorrect and the thesis (26) is valid. □

The above theorem is called the maximum principle. We note that in the case $F(x,t) \geq 0$ an analogous result can be formulated. We prove the minimum principle below. The proof is analogous to the proof of the maximum principle, but we now use the condition from Corollary 2.

Theorem 4 *Let function $u \in CW_T(G) := C(\bar{\Omega}_T) \cap W_t^1((0,T)) \cap C_x^2(G)$ be the classical solution of the generalized time-fractional diffusion equation (1) in the region $\Omega_T := G \times (0,T]$, $G \subset R^n$ and let $F(x,t) \geq 0$, $(x,t) \in \Omega_T$. Then, either solution u is non-negative in $\bar{\Omega}_T$ or it attains the negative minimum on set S_G^T which means*

$$u(x,t) \geq \min\{0, \min_{(x,t)\in S_G^T} u(x,t)\} \quad (x,t) \in \bar{\Omega}_T, \tag{31}$$

where $S_G^T := (\bar{G} \times \{0\}) \cup (S \times [0,T])$.

Proof Let us assume that thesis (31) is not valid. Then point (x_0, t_0), $x_0 \in G$, $0 \leq t_0 \leq T$ exists such that

$$u(x_0,t_0) < \min_{(x,t)\in S_G^T}\{0, u(x,t)\} = M_1 < 0. \tag{32}$$

We define number $\epsilon := u(x_0,t_0) - M_1 < 0$ and the following auxiliary function:

$$f_1(x,t) := u(x,t) + \frac{\epsilon}{2}\frac{z(T) - z(t)}{z(T)} \quad (x,t) \in \bar{\Omega}_T. \tag{33}$$

From this definition and by assumptions we obtain:

$$f_1(x,t) \geq u(x,t) + \frac{\epsilon}{2} \quad (x,t) \in \bar{\Omega}_T$$

$$f_1(x_0,t_0) \leq u(x_0,t_0) = \epsilon + M_1 \leq \epsilon + u(x,t) \leq \epsilon + f_1(x,t) - \frac{\epsilon}{2} \quad (x,t) \in S_G^T.$$

From the above inequality we infer that function f_1 cannot attain its minimum on the S_G^T-part of the boundary of region Ω_T. Therefore point $(x_1, t_1) \in \bar{\Omega}_T$ exists such that $x_1 \in G$ and $0 < t_1 \leq T$ and function f_1 attains its minimum at (x_1, t_1). At this point the following inequality is fulfilled

$$f_1(x_1,t_1) \leq f_1(x_0,t_0) \leq \epsilon + M_1 < \epsilon.$$

From Corollary 2 and the necessary and sufficient conditions of the existence of the minimum in region Ω_T, we obtain the following set of conditions

$$ {}^{c}D^{\alpha}_{0+;[z],t} f_1(x_1, t_1) \leq 0 \quad \alpha \in (0, 1) $$

$$ grad(f_1)|_{(x_1,t_1)} = 0 \quad \Delta f_1|_{(x_1,t_1)} \geq 0 $$

and the relations for derivatives (29), (30), where we have replaced function f by f_1, hold. Now, we analyze the behavior of the generalized diffusion operator at point (x_1, t_1)

$$ \left({}^{c}D^{\alpha}_{0+;[z],t} u(x,t) - L(u)\right)|_{(x_1,t_1)} $$

$$ = {}^{c}D^{\alpha}_{0+;[z],t} f_1(x_1, t_1) + \frac{\epsilon}{2z(T)} \frac{(z(t_1) - z(0))^{1-\alpha}}{\Gamma(2-\alpha)} $$

$$ -p(x_1)\Delta f_1(x_1, t_1) - \left(grad(p)|_{x_1}, grad(f_1)|_{(x_1,t_1)}\right) $$

$$ +q(x_1)\left(f_1(x_1, t_1) - \frac{\epsilon}{2}\frac{z(T) - z(t_1)}{z(T)}\right) - F(x_1, t_1) $$

$$ \leq \frac{\epsilon}{2z(T)} \frac{(z(t_1) - z(0))^{1-\alpha}}{\Gamma(2-\alpha)} < 0. $$

We note that at point (x_1, t_1) the following inequality holds

$$ \left({}^{c}D^{\alpha}_{0+;[z],t} u(x,t) - L(u)\right)|_{(x_1,t_1)} < 0, $$

which means that function u is not a solution to Eq. (1). Therefore the assumption (32) is incorrect and the thesis (31) is valid. □

The derived minimum and maximum principles can be applied in generalized fractional diffusion problems to prove the uniqueness results and properties of classical solutions. One of the applications are the following corollaries on controlling the sign of the classical solution.

Corollary 3 *Let assumptions of Theorem 4 be fulfilled and*

$$ \min_{(x,t)\in S_G^T} u(x, t) \geq 0. $$

Then, the classical solution u is non-negative.

Proof From Theorem 4 we immediately obtain the thesis

$$ u(x, t) \geq \min\{0, \min_{(x,t)\in S_G^T} u(x, t)\} \geq 0 \quad (x, t) \in \bar{\Omega}_T $$

which means that in the case $F(x,t) \geq 0$ we control the value of the classical solution u via the initial and boundary conditions on the S_G^T-part of the boundary. □

Corollary 4 *Let assumptions of Theorem 3 be fulfilled and*

$$\max_{(x,t)\in S_G^T} u(x,t) \leq 0.$$

Then, the classical solution u is non-positive.

4 Conclusion

In the paper, we extended the necessary conditions for the extremum existence to the version expressed in terms of the generalized scale and weight function-dependent fractional derivative. From these conditions, the corollaries follow, where the existence of minimum or maximum at the given point is connected with the corresponding inequality for the left scale and weight function-dependent derivative of the Caputo type.

The obtained necessary conditions were applied in the proof of maximum and minimum principles for time-fractional diffusion problem (1)–(4). These theorems generalize the known classical results as well as the maximum/minimum principle for diffusion problems with a time-fractional Caputo derivative. In the partial differential equations theory, both for the problems of integer and non-integer order, the maximum/minimum principles are applied to prove uniqueness results for classical solutions and to control the sign of the solution. We demonstrated for the generalized diffusion problem of type (1)–(4) that similar results are valid and follow from the maximum/minimum principles. Further applications are still under investigation.

References

1. Xu, Y., He, Zh, Agrawal, O.P.: Numerical and analytical solutions of new generalized fractional diffusion equation. Comput. Math. Appl. **66**(10), 2019–2029 (2013)
2. Xu, Y., Agrawal, O.P.: Numerical solutions and analysis of diffusion for new generalized fractional advection-diffusion equations. Cent. Eur. J. Phys. **11**(10), 1178–1193 (2013)
3. Xu, Y., He, Zh, Xu, Q.: Numerical solutions of fractional advection-diffusion equations with a kind of new generalized fractional derivative. Int. J. Comput. Math. **91**(3), 588–600 (2014)
4. Luchko, Y.: Boundary value problems for the generalized time-fractional diffusion equation of distributed order. Fract. Calc. Appl. Anal. **12**(4), 409–422 (2009)
5. Luchko, Y.: Maximum principle and its application for the time-fractional diffusion equation. Fract. Calc. Appl. Anal. **14**(1), 110–124 (2011)
6. Luchko, Y.: Maximum principle for the generalized time-fractional diffusion equation. J. Math. Anal. Appl. **351**(1), 218–223 (2009)

7. Al-Refai, M., Luchko, Y.: Analysis of fractional diffusion equations of distributed order: maximum principles and their applications. Analysis **36**(2), 123–133 (2015)
8. Agrawal, O.P.: Some generalized fractional calculus operators and their applications in integral equations. Fract. Calc. Appl. Anal. **15**(4), 700–711 (2012)
9. Kilbas, A.A., Srivastawa, H.M., Trujillo, J.J.: Theory and Applications of Fractional Differential Equations. Elsevier, Amsterdam (2006)

On a New Class of Multistage Fractional-Order Phase-Lead Compensators

Guido Maione

Abstract This paper proposes the transfer function forms for implementing a new class of fractional-order phase-lead compensators of analog type. A serial structure of frequency-scaled second-order compensators is defined to reduce the sensitivity to the tolerance of passive components in analog implementations. Compared to conventional multiple realizations, the new structure considerably increases the frequency range in which the phase plot of the compensator shows a flat behavior, and easily locates this range in the desired position. The new compensator gives new chances of flexible and robust control system design.

Keywords Fractional-order lead compensators · Frequency-domain · Multistage compensators · Coefficient sensitivity · Fractional-order control

1 Introduction

After some pioneering results [1, 2], the design and realization approaches of the fractional-order compensators keep on evolving continuously [3]. The fractional integral and derivative actions promise to improve performance, robustness, and flexibility of the phase lead/lag compensators used in industrial loops. However, the implementation of fractional-order compensators requires both the rational realization of irrational transfer functions and new dedicated design solutions. To face the first issue, a popular solution specifies the order and the required precision of the approximating transfer function in a given limited frequency band [1, 4]. A similar approach has been developed by [5]. However, in both methods, the rational transfer functions of order less than six don't lead to satisfactory approximations [6]. There

This work is partly supported by Italian Government funds under the project PON03PE_00067_8 "MEA - Gestione ibrida dell'energia per applicazioni aeronautiche"

G. Maione (✉)
Dipartimento di Ingegneria Elettrica e dell'Informazione, Politecnico di Bari,
Via E. Orabona, 4, 70125 Bari, Italy
e-mail: guido.maione@poliba.it

A. Babiarz et al. (eds.), *Theory and Applications of Non-integer Order Systems*,
Lecture Notes in Electrical Engineering 407, DOI 10.1007/978-3-319-45474-0_20

exist many alternatives, e.g. the truncation of continued fractions expansions [7–10]. Often, however, the zeros and poles of the rational transfer functions become more and more sensitive to the changes of the coefficients of the numerators and of the denominators as the degree of these polynomials increases.

To face the second issue, the design approaches successfully used for integer-order controllers are often adapted to the fractional-order compensators design. Recently, a renewed interest was for fractional-order lead/lag compensators (FLECs/FLACs) [11–13], that are on the background of the CRONE control [1, 14]. The lead/lag compensators are widespread in industry and the prospect of advantages in using FLECs/FLACs is encouraging. Here the focus is on FLECs, because the same pattern provides analogous results for FLACs. A new approach determines the coefficients of the rational transfer function realization of analog FLECs. Then a new class of compensators, consisting of cascaded frequency-scaled sections, is introduced. Two are the main contributions.

Firstly, closed formulas for the coefficients of the rational, N-order, transfer function realization of an analog FLEC are provided. The numerator coefficients are expressed as a linear combination of the numerator coefficients of the transfer function approximating s^{ν}. The denominator coefficients are determined similarly. The formulas, which, in principle, can be applied whatever the approach for approximating s^{ν} will be, are computationally efficient.

A second contribution is underlined. Often the implementation of a FLEC leads to a high-order approximation. However, the higher the order of numerator/denominator polynomials is, the higher the length of their coefficients is and vice-versa. Then the direct realization form shows great sensitivity to the accuracy of the coefficients that change due to the tolerance of passive components whose true values don't match the design. To reduce the undesirable effects, the common practice is to build up a high-order transfer function as a cascade of second-order sections, and a first-order section if necessary.

A new strategy is here proposed. A second-order approximation of the analog FLEC is first determined. Then other second-order sections are designed by frequency-scaling the first one, so that each section dominates on a given frequency interval where it shows a nearly flat phase diagram. The cascade of sections of frequency-scaled second-order approximations of the FLEC generates an analog controller that maintains a flat behavior in a frequency range that is much wider than by conventional series of compensators of the same order.

The paper is organized as follows. Section 2 provides closed formulas for determining the coefficients of the transfer functions realizing the FLECs in the s-domain. Section 3 illustrates the properties of multiple FLECs composed by a cascade of two second-order compensators having Bode plots of the same forms, but appropriately scaled on the frequency axis. Section 4 gives the conclusions.

2 Closed-Form Realization of Fractional-Order Lead Compensators

This section provides closed-form expressions to compute the coefficients of the s-domain transfer function that realizes the FLEC. The closed formulas are useful both to obtain a numerically efficient transfer function realization of the FLECs and to evaluate the sensitivity of the analog implementations to the coefficients variation. So consider the irrational transfer function

$$C_C(s) = \left(\frac{1+\tau s}{1+\Delta\tau s}\right)^{\nu} \tag{1}$$

with $0 < \nu < 1$ and $\tau,\ \Delta \in \mathbb{R}$, that represents a fractional-order lead compensator (FLEC), for $0 < \Delta < 1$, or a fractional-order lag compensator (FLAC), for $\Delta > 1$. Since the (1) is irrational, a rational transfer function approximation must be found. The here proposed realization method is based on a N-order rational transfer function approximation of the basic function x^{ν}, where $x \in \mathbb{C}$:

$$x^{\nu} \approx G(x) = \frac{\beta(x)}{\alpha(x)} = \frac{\sum_{i=0}^{N} b_{N-i}\, x^i}{\sum_{i=0}^{N} a_{N-i}\, x^i}. \tag{2}$$

The coefficients a_{N-i}, b_{N-i} can be obtained by one of the existing methods (see [1, 4, 5, 7, 8] and references therein). The analytical formulas given in [8] (where b_{N-i} and a_{N-i} are respectively denoted by $p_{N,N-i}$ and $q_{N,N-i}$) are

$$b_{N-i} = a_i = (-1)^i \binom{N}{i} (\nu+i+1)_{(N-i)}\, (\nu-N)_{(i)} \tag{3}$$

for $i = 0, \ldots, N$, where $\binom{N}{i}$ is the binomial coefficient, $(\nu+i+1)_{(N-i)} = (\nu+i+1)(\nu+i+2)\cdots(\nu+N)$ and $(\nu-N)_{(i)} = (\nu-N)(\nu-N+1)\cdots(\nu-N+i-1)$, with $(\nu+N+1)_{(0)} = (\nu-N)_{(0)} = 1$. The formulas easily lead to an effective approximation of x^{ν}. Then using the Möbius transformation [15]

$$x = r\,\frac{1+q\,y}{1+p\,y} \tag{4}$$

with $x,\ y \in \mathbb{C}$, to convert transforms (2) in the rational transfer function $G_C(s)$ approximating the FLEC, some preliminary results are shown. Substituting (4) in (2) and reducing it to the same denominator (numerator) give:

$$\left(r\,\frac{1+q\,y}{1+p\,y}\right)^{\nu} \approx G(y) = \frac{Q(y)}{P(y)} = \frac{\sum_{i=0}^{N} b_{N-i}\, r^i\, (1+q\,y)^i\, (1+p\,y)^{N-i}}{\sum_{i=0}^{N} a_{N-i}\, r^i\, (1+q\,y)^i\, (1+p\,y)^{N-i}}. \tag{5}$$

From (5) a closed formula is established for the constants multiplying the powers y^k that appear in the generic terms of both $P(y)$ and $Q(y)$.

Proposition 1 *The $(i+1)$th term of the sum leading to $P(y)$ is a polynomial expressed as sum of $(N+1)$ monomial terms of the form:*

$$a_{N-i}\, L_{ki}\, y^k = a_{N-i}\, r^i \left[\sum_{j=\mu_1}^{\mu_2} \binom{i}{j} \binom{N-i}{k-j} (q)^j\, (p)^{k-j} \right] y^k \tag{6}$$

for $k = 0, 1, \ldots, N$, with $\mu_1 = \max\{0, k+i-N\}$, $\mu_2 = \min\{i, k\}$. Likewise, the sum of monomials terms $b_{N-i}\, L_{ki}\, y^k$ $(k = 0, 1, \ldots, N)$ provides the $(i+1)$th term of the sum defining $Q(y)$.

Proof By the binomial theorem and by the distributive law of the product of sums [16], the generic entry of $P(y)$ can be re-written as:

$$a_{N-i}\, r^i\, (1+q\,y)^i\, (1+p\,y)^{N-i} = a_{N-i}\, r^i \sum_{j=0}^{i} \sum_{m=0}^{N-i} \binom{i}{j} \binom{N-i}{m} (q\,y)^j\, (p\,y)^m, \tag{7}$$

where, for each index i, the second member of (7) represents a polynomial of degree N that adds monomial terms in the form of a constant multiplying y^k. Since the coefficient of y^k adds up in the entries of type (7) for which indices j and m satisfy $j+m=k$, the lower index m in the binomial coefficient in (7) is replaced by $(k-j)$ to underline the role of k explicitly. Thus it holds $a_{N-i}\, r^i\, (1+q\,y)^i\, (1+p\,y)^{N-i} = a_{N-i}\, r^i \sum_{j=0}^{i} \sum_k \binom{i}{j} \binom{N-i}{k-j} (q)^j\, (p)^{k-j}\, y^k$.

Since k does not depend on j, for each m satisfying $0 \le m \le N-i$, there exists one and only one j such that $0 \le k-j \le N-i$, i.e. such that $k+i-N \le j \le k$. These constraints on the index variable j are expected because the bottom index variable of $\binom{N-i}{k-j}$ must be non-negative and not greater than the upper index variable. Since the bottom index of any binomial coefficient must respect this rule, for the indices i and j in $\binom{i}{j}$ it holds $0 \le j \le i$. It follows $j \ge \mu_1 = \max\{0, k+i-N\}$ and $j \le \mu_2 = \min\{i, k\}$, where μ_1 and μ_2 define the start and stop value of the summation (6), respectively.

Finally, (6) holds also true for $Q(y)$ with b_{N-i} replacing a_{N-i}. □

Proposition 2 *The rational approximation of an analog FLEC is given by*

$$\left(\frac{1+\tau\, s}{1+\Delta\, \tau\, s} \right)^{\nu} \approx G_C(s) = \frac{B(s)}{A(s)} = \frac{\sum_{k=0}^{N} B_{N-k}\, s^k}{\sum_{k=0}^{N} A_{N-k}\, s^k}, \tag{8}$$

where

$$A_{N-k} = \sum_{i=0}^{N} a_{N-i}\, L_{ki}^{C},\ B_{N-k} = \sum_{i=0}^{N} b_{N-i}\, L_{ki}^{C},\ L_{ki}^{C} = \tau^{k} \sum_{j=\mu_1}^{\mu_2} \binom{i}{j} \binom{N-i}{k-j} \Delta^{k-j} \tag{9}$$

for $k = 0, 1, \ldots, N$ *and with* $\mu_1 = \max\{0, k+i-N\},\ \mu_2 = \min\{i, k\}$.

Proof Defining $r = 1$, $q = \tau$, $p = \Delta\,\tau$, and $y = s$ and substituting the (4) in $G(y)$ yield:

$$\left(\frac{1+\tau\, s}{1+\Delta\,\tau\, s}\right)^{\nu} \approx \frac{\sum_{i=0}^{N} b_{N-i}\,(1+\tau\, s)^{i}\,(1+\Delta\,\tau\, s)^{N-i}}{\sum_{i=0}^{N} a_{N-i}\,(1+\tau\, s)^{i}\,(1+\Delta\,\tau\, s)^{N-i}}. \tag{10}$$

By Proposition 1 and by the above definitions, the monomial term of degree k of the generic denominator entry in (10) becomes:

$$a_{N-i}\, L_{ki}^{C}\, s^{k} = a_{N-i} \left[\tau^{k} \sum_{j=\mu_1}^{\mu_2} \binom{i}{j} \binom{N-i}{k-j} \Delta^{k-j}\right] s^{k}. \tag{11}$$

Now add the monomial terms involving s^k and belonging to all the entries of the summation in (10) for $i = 0, 1, \ldots, N$. Then, the resulting constant is a linear combination of the $(N+1)$ coefficients a_{N-i} and is named A_{N-k} so that (9) follows. Analogously, the expression of B_{N-k} in (9) follows. Finally, summing the monomials $A_{N-k}\, s^k$ $(B_{N-k}\, s^k)$ for all values of k leads to (8). □

Example 1 This example shows an application of the previously obtained formulas for analog realizations. Let $N = 2$. According to [8], the denominator and numerator coefficients of a second-order approximation of s^{ν} are: $a_0 = (2+\nu)\,(1+\nu)$, $a_1 = 2\,(2+\nu)\,(2-\nu)$, $a_2 = (2-\nu)\,(1-\nu)$, and $b_0 = a_2$, $b_1 = a_1$, $b_2 = a_0$. To obtain A_{N-k} and B_{N-k}, the (9) is used with $L_{00}^{C} = L_{01}^{C} = L_{02}^{C} = 1$, $L_{10}^{C} = 2\,\tau\,\Delta$, $L_{11}^{C} = \tau\,(1+\Delta)$, $L_{12}^{C} = 2\,\tau$ and $L_{20}^{C} = \tau^2\,\Delta^2$, $L_{21}^{C} = \tau^2\,\Delta$, $L_{22}^{C} = \tau^2$. For $\nu = 0.5$, $\tau = 10$ seconds, $\Delta = 0.1$, the following transfer function is obtained:

$$G_C(s) = \frac{153.75\, s^2 + 105\, s + 12}{450.75\, s^2 + 159\, s + 12}$$

which has zeros in $\{-0.5378, -0.1451\}$ and poles in $\{-0.2433, -0.1094\}$.

Remark Closed formulas can also be obtained for a digital realization. The coefficients defining the discrete-time transfer function approximation of a FLEC can be related to A_{N-k} and B_{N-k} in (9). The proof is beyond the scope of this paper and is omitted here for sake of space.

3 Cascade of Frequency-Scaled Compensators

To reduce the undesirable effects due to coefficient variations, high-order transfer functions are often implemented by low-sensitivity structures consisting of a cascade of second-order transfer function sections. Now consider the irrational analog compensator $C_C(s)$. This section introduces a series of frequency-scaled FLECs (FS-FLEC), say $C_C(s\,\omega_s)$, where ω_s is a scale factor. These FLECs are implemented as second-order, frequency-scaled, rational transfer functions, whose coefficients are easily determined by the formulas of Sect. 2. More precisely, each section of the serial structure is realized as an analog second-order transfer function, that is appropriately frequency-scaled with respect to adjacent sections. The series of FS-FLEC realizations not only reduces the errors due to variations in the coefficients of second-order transfer functions, but also exhibits a flat phase plot in a much larger frequency-interval than those guaranteed by the conventional series of multiple identical FLECs (CM-FLEC).

To introduce the new cascade structure, first denote a FLEC as

$$C_{C1}(s) = \left(\frac{1 + \tau s}{1 + \Delta\,\tau s}\right)^{\nu}, \tag{12}$$

where here it is assumed $\Delta < 1$, to fix the ideas and to deal with FLECs only. Then put $s = j\,\omega$. It is well known that the maximum phase-lead ϕ_{m1} of $C_{C1}(s)$ is obtained at the geometric mean of the frequencies $1/\tau$ and $1/(\Delta\,\tau)$ [12, 14]:

$$\omega_{m1} = \frac{1}{\tau\sqrt{\Delta}}. \tag{13}$$

Given ω_{m1}, the maximum magnitude, M_{m1}, and the maximum phase, ϕ_{m1}, of the FLEC can be determined as follows:

$$M_{m1} = |C_{C1}(j\,\omega_{m1})| = (\Delta)^{-0.5\,\nu} \tag{14}$$

$$\phi_{m1} = \nu\left[\tan^{-1}\left(\frac{1}{\sqrt{\Delta}}\right) - \tan^{-1}\left(\sqrt{\Delta}\right)\right] = \nu\,\tan^{-1}\left(\frac{1-\Delta}{2\sqrt{\Delta}}\right) = \nu\,\phi_1. \tag{15}$$

Figure 1 shows the Bode magnitude and phase plots for an analog compensator $C_{C1}(s)$ with $\nu = \{0.3, 0.5, 0.7, 0.9\}$, $\tau = 10\,\text{s}$ and $\Delta = 0.1$ (dashed lines). The plots of a second-order realization $G_{C1}(s)$ of the FLEC are also included (solid lines). As it will be shown below, the accuracy of a second-order $G_{C1}(s)$ is satisfactory in the frequency range of interest for the design purposes of a series of multiple frequency-scaled FLECs. Namely, higher-order, rational transfer function realizations don't significantly improve the approximation of $C_{C1}(s)$ in the frequency range where the phase is nearly flat.

For a given frequency, higher values of ν provide higher phase-leads. However, curves corresponding to lower values of ν exhibit flatter phase plots (see Fig. 1b).

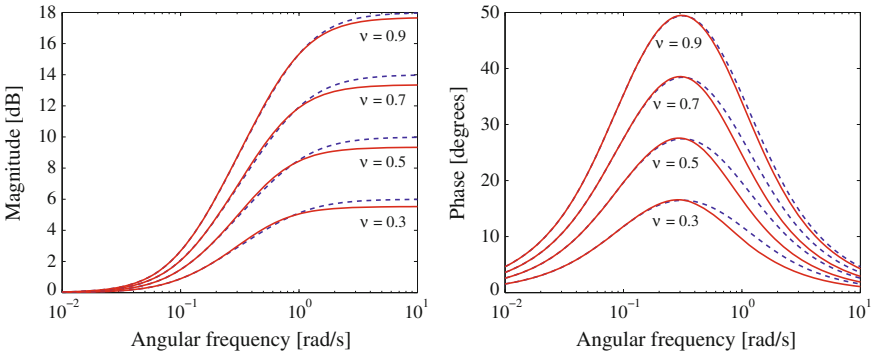

(a) Magnitude plots (b) Phase plots

Fig. 1 Bode plots of the first FLEC compensator in (12) (*dashed lines*) and of its second-order realization given by (8) (*solid lines*)

Now, it is important to recall that the FLECs have an important restriction. Because ϕ_{m1} depends on ν and Δ, the (15) shows that there is a limit in the phase-lead provided by the FLECs. Namely, many authors suggest that the distance between the pole and zero must be such that $\Delta \geq 0.1$ and this value corresponds to $\phi_{m1} \approx \nu\,(54.9)^\circ$. So, if the requested phase-lead is greater than ϕ_{m1}, then a conventional multiple (CM) compensator can be used by arranging a series of two (or more) sections with the same zero-pole pair. Each section of the CM-FLECs has the same phase-lead Bode plots on the same frequency interval, so that the resulting phase plot of the CM-FLECs is the sum of the equal contributions of all the present sections.

Instead, this paper introduces a cascade of two (or more) adjacent FLECs whose Bode plots are equal in form, but properly frequency-scaled. The value of the scale factor for each plot is so chosen that each section dominates on the frequency intervals in which the phase plot is nearly flat. In detail, here $C_{C1}(s)$ has unity scale-factor, while the second FLEC, say $C_{C2}(s)$, is obtained by scaling $C_{C1}(s)$ with the substitution $s \to s\,\omega_s = s\,\Delta$:

$$C_{C2}(s) = \left(\frac{1 + \tau\, s\, \Delta}{1 + \tau\, s\, \Delta^2}\right)^{\nu}. \tag{16}$$

With this value for the scale factor, $C_{C2}(s)$ reaches its maximum phase-lead ϕ_{m2} at the frequency

$$\omega_{m2} = \frac{1}{\tau\, \Delta^{1.5}} = \frac{\omega_{m1}}{\Delta} \tag{17}$$

and the maximum magnitude and phase-lead are

$$M_{m2} = |C_{C2}(j\,\omega_{m2})| = (\Delta)^{-0.5\,\nu} \text{ and } \phi_{m2} = \nu\, \tan^{-1}\left(\frac{1 - \Delta}{2\,\sqrt{\Delta}}\right). \tag{18}$$

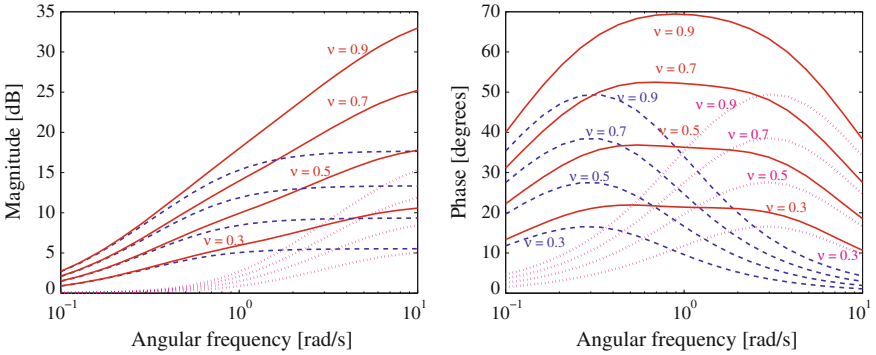

(a) Magnitude plots (b) Phase plots

Fig. 2 Bode plots of the realization of the first compensator in (12) (*dashed lines*), of the second scaled compensator in (16) (*dotted lines*), and of the multiple compensator in (19) (*solid lines*)

Moreover, (18) shows that: $M_{m2} = M_{m1}, \phi_{m2} = \phi_{m1}$. Finally, for a generic frequency $\overline{\omega}$, it can be written $C_{C1}(j\,\overline{\omega}\,\Delta) = C_{C2}(j\,\overline{\omega})$. Figure 2 shows the Bode magnitude and phase plots of the rational transfer function approximation for an analog compensator $C_{C2}(s)$ (see dotted lines in Fig. 2a, b) with the same values of ν, τ, and Δ that are used for $C_{C1}(s)$ in Fig. 1.

With the chosen parameters, the series connection of the two frequency-scaled compensators defines the multiple frequency-scaled FLEC (MFS-FLEC), which has break frequencies in $1/\tau$ and $1/(\tau\,\Delta^2)$. Then it holds:

$$C_{C12}(s) = C_{C1}(s)\,C_{C2}(s\,\Delta) = \left(\frac{1+\tau\,s}{1+\tau\,\Delta^2\,s}\right)^{\nu} \tag{19}$$

and, by (13) and (19), the maximum phase-lead ϕ_{m12} is obtained at the geometric mean of the new break frequencies

$$\omega_{m12} = \frac{1}{\tau\,\Delta} = \frac{\omega_{m1}}{\sqrt{\Delta}} \tag{20}$$

so that the maximum magnitude is

$$M_{m12} = |C_{C12}(j\,\omega_{m12})| = (\Delta)^{-\nu} \tag{21}$$

and the maximum phase-lead is

$$\phi_{m12} = \nu\,\tan^{-1}\left(\frac{1-\Delta^2}{2\,\Delta}\right). \tag{22}$$

As ω_{m12} gives the center of the frequency interval, where the phase diagram is nearly flat, in control system design the value of ω_{m12} is important to locate the MFS-FLEC on the frequency axis.

Analogously, by using the scaled frequency s/Δ, one can obtain the FS-FLEC

$$\tilde{C}_{C2}(s) = \left(\frac{1 + \tau\, s/\Delta}{1 + \tau\, s}\right)^{\nu} \tag{23}$$

with

$$\tilde{\omega}_{m2} = \frac{\sqrt{\Delta}}{\tau} = \omega_{m1}\, \Delta. \tag{24}$$

Hence the transfer function of the MFS-FLEC becomes

$$\tilde{C}_{C12}(s) = C_{C1}(s)\, \tilde{C}_{C2}(s) = \left(\frac{1 + \tau\, s/\Delta}{1 + \tau\, s\, \Delta}\right)^{\nu} \tag{25}$$

and the maximum phase-lead occurs at the angular frequency

$$\tilde{\omega}_{m12} = \frac{1}{\tau} = \omega_{m1}\, \sqrt{\Delta}. \tag{26}$$

Therefore the maximum magnitude is

$$\tilde{M}_{m12} = |\tilde{C}_{C12}(j\, \tilde{\omega}_{m12})| = (\Delta)^{-\nu} = M_{m12} \tag{27}$$

and the maximum phase-lead is

$$\tilde{\phi}_{m12} = \nu\, \tan^{-1}\left(\frac{1 - \Delta^2}{2\, \Delta}\right) = \phi_{m12}. \tag{28}$$

In conclusion, both the sections can be scaled and shifted towards the increasing or decreasing frequencies. Figure 2 shows the Bode plots of the approximations obtained for the FLEC $C_{C1}(s)$, the FS-FLEC $C_{C2}(s)$, and the MFS-FLEC $C_{C12}(s)$, i.e. the Bode plots of $G_{C1}(s)$, $G_{C2}(s)$, and $G_{C12}(s)$, respectively.

Finally, CM-FLECs and MFS-FLECs are compared. Figure 3 shows the Bode diagrams of CM-FLECs, i.e. $C^*_{C12}(j\,\omega) = [C_{C1}(j\,\omega)]^2$, and MFS-FLECs, i.e. $C_{C12}(j\,\omega) = C_{C1}(j\,\omega)\, C_{C2}(j\,\omega)$, for $\nu = \{0.3, 0.5, 0.7, 0.9\}$, $\tau = 10\,\text{s}$, and $\Delta = 0.1$. Compensators $C^*_{C12}(j\,\omega)$ and $C_{C12}(j\,\omega)$ provide the same high-frequency gain, even if the slope of the magnitude plot of $C^*_{C12}(j\,\omega)$ is steeper than that of $C_{C12}(j\,\omega)$. Then, for the magnitude of $C^*_{C12}(j\,\omega)$, the maximum shift upward occurs before the same shift is reached by $C_{C12}(j\,\omega)$. Finally, for a given value of ν, a CM-FLEC provides the maximum phase-lead $\phi^*_{m12} = 2\,\phi_{m1} \approx \nu\,(109.8)^\circ$ that is greater than $\phi_{m12} \approx \nu\,(78.6)^\circ$ given by a MFS-FLEC. However, phase plots of $C_{C12}(j\,\omega)$ are flatter than those of $C^*_{C12}(j\,\omega)$.

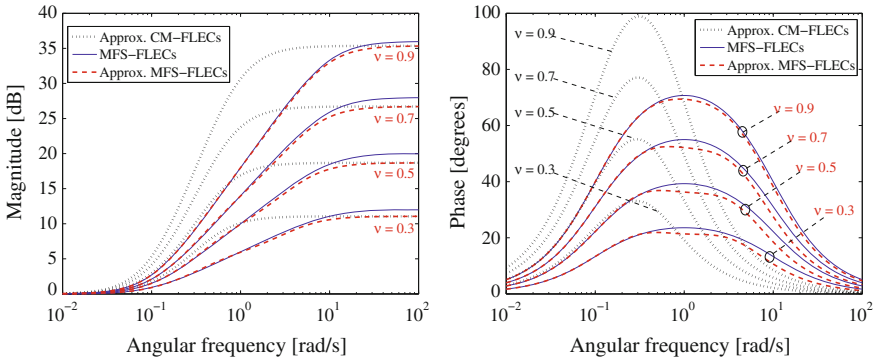

(a) Magnitude plots (b) Phase plots

Fig. 3 Bode plots of approximated CM-FLECs (*dotted lines*), irrational MFS-FLECs (*solid lines*), approximated MFS-FLECs (*dashed lines*)

4 Conclusion

This paper proposes a cascade structure of second-order frequency-scaled sections, which forms the basis of a new implementation approach of fractional-order lead compensators. The resulting transfer functions show flat phase plots in wider frequency ranges than the ones obtained by the high-order direct form transfer functions of FLECs. The width and position of these ranges can be easily adjusted by choosing second-order scaled compensators. Moreover, the cascade form of independent sections limits the negative effects due to coefficient variations. Finally, the closed formulas proven in Sect. 2 make easier the determination of the coefficients of the transfer functions. These results make the proposed structure of fractional compensator very robust and convenient.

A limitation of the proposed approach could be the absence of an explicit integral action in the compensator. In this case, an explicit integrator can be easily added if required. Moreover, if a higher precision in the approximation is desired, then one can increase the order by using more sections (in this paper two sections defined a 4-th order compensator). Nonetheless, practical applications would gain a small benefit. Finally, the proposed compensators are realized by orders higher than those obtained by PID controllers, which however can't yield the same wide frequency range of flat phase, i.e. the same robustness.

Future work will consider digital realization. Namely, not only analogous closed-form expressions can be developed for lag compensators but also for digital compensators. In particular, formulas can be obtained for the coefficients of discrete-time realization of FLECs as linear combination of the coefficients of the analog transfer function approximation. Care will be paid to reduce the typical quantization effects that may lead to poor performance or instability.

References

1. Oustaloup, A.: La commande CRONE. Commande Robuste d'Ordre Non Entiér. Hermés, Paris (1991)
2. Podlubny, I.: Fractional-order systems and $PI^{\lambda}D^{\mu}$-controllers. IEEE Trans. Autom. Control **44**(1), 208–214 (1999)
3. Efe, M.O.: Fractional order systems in industrial automation. A survey. IEEE Trans. Ind. Inf. **7**(4), 582–591 (2011)
4. Oustaloup, A., Levron, F., Nanot, F.M., Mathieu, B.: Frequency band complex noninteger differentiator: characterization and synthesis. IEEE Trans. Circuits Syst. I **47**(1), 25–39 (2000)
5. Charef, A.C., Sun, H.H., Tsao, Y.Y., Onaral, B.: Fractal system as represented by singularity functions. IEEE Trans. Autom. Control **37**(9), 1465–1470 (1992)
6. Cech, M., Schlegel, M.: Optimal continuous approximation of basic fractional elements: theory and applications. In: Proceedings of the 50th IEEE Conference on Decision and Control and European Control Conference (CDC-ECC), Orlando, FL, USA, pp. 7051–7056 (2011)
7. Podlubny, I., Petráš, I., Vinagre, B.M., O'Leary, P., Dorcák, L.: Analogue realizations of fractional-order controllers. Nonlinear Dyn. **29**(1–4), 281–296 (2002)
8. Maione, G.: Continued fractions approximation of the impulse response of fractional order dynamic systems. IET Control Theory Appl. **2**(7), 564–572 (2008)
9. Maione, G.: Conditions for a class of rational approximants of fractional differentiators/integrators to enjoy the interlacing property. In: Bittanti, S., Cenedese, A., Zampieri, S. (eds.) Proceedings of the 18th IFAC World Congress, IFAC Proceedings on line, vol. 18, Part 1, pp. 13984–13989 (2011)
10. Maione, G.: On the Laguerre rational approximation to fractional discrete derivative and integral operators. IEEE Trans. Autom. Control **58**(6), 1579–1585 (2013)
11. Charef, A.C.: Analogue realization of fractional-order integrator, differentiator and fractional $PI^{\lambda}D^{\mu}$ controller. IET Control Theory Appl. **153**(6), 714–720 (2006)
12. Monje, C.A., Calderón, A.J., Vinagre, B.M., Feliu, V.: The fractional order lead compensator. In: The 2nd IEEE International Conference on Computational Cybernetics, Vienna, Austria, pp. 347–352 (2004)
13. Tavazoei, S.M., Tavakoli-Kakhki, M.: Compensation by fractional-order phase-lead/lag compensators. IET Control Theory Appl. **8**(5), 319–329 (2014)
14. Monje, C.A., Chen, Y.Q., Vinagre, B.M., Xue, D., Feliu, V.: Fractional Order Systems and Controls. Fundamentals and Applications. Springer, London (2010)
15. Brown, J.W., Churchill, R.V.: Complex Variables and Application. McGraw-Hill, Int. Ed., Boston (2009)
16. Knuth, D.E.: Fundamental Algorithms. The Art of Computer Programming, vol. 1. Addison-Wesley, Reading (1972)

On the Existence of Optimal Controls for the Fractional Continuous-Time Cucker–Smale Model

Agnieszka B. Malinowska, Tatiana Odzijewicz and Ewa Schmeidel

Abstract In this work the Cucker–Smale fractional optimal control problem is proposed and studied. We show that considered problem has an optimal solution and we derive necessary conditions for this solution.

Keywords Cucker–Smale model · Consensus · Fractional optimal control · Optimal solution · Fractional analysis

Introduction

The collective behavior models describe migration of interacting agents. By following basic local laws they are moving coherently. Such coordinated motion is exhibited by many living beings, e.g., birds, fish, bacteria or insects, and its mathematical modeling is nowadays of strong interest with many authors contributing to the theory (see e.g., [1–7]). One of the simplest and most important models was proposed by Cucker and Smale [3, 8]:

$$\begin{cases} \dot{x}_i(t) = v_i(t) \\ \dot{v}_i(t) = \frac{1}{N} \sum_{j=1}^{N} a(||x_j(t) - x_i(t)||)(v_j(t) - v_i(t)) \quad i = 1, \ldots, N, \end{cases} \tag{1}$$

where $a \in C^1([0; 1))$ is a nonincreasing positive function and $x_i \in \mathbb{R}^d$, $v_i \in \mathbb{R}^d$ are the state and consensus parameters, respectively. The Cucker–Smale model (1) describes

A.B. Malinowska
Faculty of Computer Science, Bialystok University of Technology,
15-351 Bialystok, Poland
e-mail: a.malinowska@pb.edu.pl

T. Odzijewicz (✉)
Department of Mathematics and Mathematical Economics,
Warsaw School of Economics, 02-554 Warsaw, Poland
e-mail: tatiana.odzijewicz@sgh.waw.pl

E. Schmeidel
Faculty of Mathematics and Computer Science, University of Bialystok,
15–245 Bialystok, Poland
e-mail: eschmeidel@math.uwb.edu.pl

A. Babiarz et al. (eds.), *Theory and Applications of Non-integer Order Systems*,
Lecture Notes in Electrical Engineering 407, DOI 10.1007/978-3-319-45474-0_21

the emerging of consensus in a group of N interacting agents described by $2d$ degrees of freedom each, trying to align the consensus parameters v_i with their neighbors. Under certain conditions, Cucker and Smale [3, 8] proved that the system converges to a consensus pattern, characterized by the fact that all the consensus parameters tend, for $t \to \infty$, to the mean consensus parameter $\bar{v} = \frac{1}{n}\sum_{j=1}^{n} v_j(t)$. For the case when a consensus is not achieved it was proposed, in [2], to introduce the external control strategies. The authors considered the optimal control problem of determining a trajectory solution of

$$\begin{cases} \dot{x}_i(t) = v_i(t) \\ \dot{v}_i(t) = \frac{1}{N}\sum_{j=1}^{N} a(||x_j(t) - x_i(t)||)(v_j(t) - v_i(t)) + u_i(t) \quad i = 1, \ldots, N, \end{cases}$$

with the initial condition, and minimizing the cost functional being a combination of a distance from consensus $\bar{v}$ with the $l_1^N - l_2^2$-norm of the control, under the control constraint.

In the above mentioned papers all derivatives are of integer-order. However, it is well known that many phenomena in nature, processes in physics and engineering systems can be modeled more accurately by non-integer-order derivatives [9–13]. This was also observed in the context of consensus of multi-agent systems [14]. Motivated by those papers we propose to study optimal control of the fractional Cucker–Smale model, starting with the simple case of a fractional system of differential equations. Namely, the problem under our consideration is: determine a trajectory solution of

$$\begin{cases} D_{0+}^{\alpha} x_i(t) = v_i(t) \\ D_{0+}^{\alpha} v_i(t) = \frac{1}{N}\sum_{j=1}^{N} (v_j(t) - v_i(t)) + u_i(t) \quad i = 1, \ldots, N, \end{cases} \tag{2}$$

with the initial condition $(I_{0+}^{1-\alpha}[x](0), I_{0+}^{1-\alpha}[v](0)) = (x_0, v_0)$, where D_{0+}^{α}, $I_{0+}^{1-\alpha}$ are the Riemann–Liouville fractional operators, and minimizing the cost functional

$$\int_0^T \left(\sum_{i=1}^{N} \|v_i(t) - \frac{1}{N}\sum_{j=1}^{N} v_j(t)\|_{l_2^d}^2 + \gamma \sum_{i=1}^{N} \|u_i(t)\|_{l_2^d} \right) dt,$$

under the control constraint

$$u(t) \in M := \left\{ u(t) \in (\mathbb{R}^d)^N : \sum_{i=1}^{N} \|u_i(t)\|_{l_2^d} \leq K \right\}, \text{ a.e. on } [0, T],$$

for a given $\gamma, K > 0$. We show that the considered problem has an optimal solution and we derive necessary conditions for this solution.

The paper is organized as follows. In Sect. 1, after a review of basic definitions, we recall theorems on the existence of a solution to the fractional optimal control problem

and a fractional counterpart of Pontryagin's Maximum Principle. Section 2 is devoted to the study of our main problem. We justify the existence of an optimal solution to the Cucker–Smale fractional optimal control problem and derive necessary conditions for this solution. Finally, an illustrative example is given.

1 Preliminaries

In this section we briefly sketch basic definitions and properties from the fractional calculus needed in this paper. Moreover, we recall important theorems regarding the existence of a solution to a fractional optimal control problem and the fractional counterpart of Pontryagin's Maximum Principle. For more information on the fractional calculus and the fractional optimal control we refer the reader to the works [12, 13, 15–19].

1.1 Introduction to Fractional Calculus

Let $\alpha > 0$ and $f \in L^1([a, b]; \mathbb{R}^n)$. We define the left and the right Riemann–Liouville fractional integrals I^{α}_{a+} and I^{α}_{b-} by

$$I^{\alpha}_{a+}[f](t) := \frac{1}{\Gamma(\alpha)} \int_a^t \frac{f(\tau)}{(t-\tau)^{1-\alpha}}\, d\tau,$$

$$I^{\alpha}_{b-}[f](t) := \frac{1}{\Gamma(\alpha)} \int_t^b \frac{f(\tau)}{(\tau-t)^{1-\alpha}}\, d\tau,$$

for almost every $t \in (a, b)$. It is a well known fact that fractional integrals $I^{\alpha}_{a+} : L^p([a, b]; \mathbb{R}^n) \to L^p([a, b]; \mathbb{R}^n)$ and $I^{\alpha}_{b-} : L^p([a, b]; \mathbb{R}^n) \to L^p([a, b]; \mathbb{R}^n)$ are bounded operators for $\alpha > 0$ and $1 \leq p < \infty$, i.e.,

$$\left\| I^{\alpha}_{a+}[f] \right\|_{L^p} \leq K \|f\|_{L^p}, \quad \left\| I^{\alpha}_{b-}[f] \right\|_{L^p} \leq K \|f\|_{L^p},$$

where $K = \frac{(b-a)^{\alpha}}{\Gamma(\alpha+1)}$.

Moreover, let $I^{\alpha}_{a+}(L^p([a, b]; \mathbb{R}^n))$ $\left(I^{\alpha}_{b-}(L^p([a, b]; \mathbb{R}^n))\right)$ denote the set of functions $f : [a, b] \to \mathbb{R}^n$ represented by the left-sided (right-sided) fractional integral of function $g \in L^p([a, b]; \mathbb{R}^n)$. Precisely,

$$I^{\alpha}_{a+}(L^p([a, b]; \mathbb{R}^n)) := \left\{ f : [a, b] \to \mathbb{R}^n : \exists_{g \in L^p([a,b];\mathbb{R}^n)} f = I^{\alpha}_{a+}[g] \right\}$$

and

$$I_{b-}^{\alpha}(L^p([a,b];\mathbb{R}^n)) := \left\{f : [a,b] \to \mathbb{R}^n : \exists_{g \in L^p([a,b];\mathbb{R}^n)} f = I_{b-}^{\alpha}[g]\right\}.$$

Now, let $\alpha \in (0,1)$. The Riemann–Liouville fractional differential operators are given as compositions of classical derivatives and fractional integrals, i.e., the left Riemann–Liouville fractional derivatives D_{a+}^{α} are defined for functions $I_{a+}^{\alpha} f \in AC([a,b];\mathbb{R}^n)$ by

$$D_{a+}^{\alpha}[f](t) := \frac{d}{dt} I_{a+}^{\alpha}[f](t), \quad t \in [a,b] \text{ a.e.}$$

Similarly, the right Riemann–Liouville fractional derivatives D_{b-}^{α} are defined for functions $I_{b-}^{\alpha} f \in AC([a,b];\mathbb{R}^n)$ by

$$D_{b-}^{\alpha}[f](t) := \frac{d}{dt} I_{b-}^{\alpha}[f](t), \quad t \in [a,b] \text{ a.e.}$$

1.2 Fractional Optimal Control Problem

Let us consider the following fractional optimal control problem (FOCP):

$$D_{a+}^{\alpha}[y](t) = g(t, y(t), u(t)), \quad t \in [a,b] \text{ a.e.}, \tag{3}$$

$$I_{a+}^{1-\alpha}[y](a) = y_0, \tag{4}$$

$$u(t) \in M \subset \mathbb{R}^m, \quad t \in [a,b], \tag{5}$$

$$\mathcal{J}(y,u) = \int_a^b f(t, y(t), u(t))\, dt \to \min, \tag{6}$$

where $f : [a,b] \times \mathbb{R}^n \times M \to \mathbb{R}$, $g : [a,b] \times \mathbb{R}^n \times M \to \mathbb{R}^n$ and $\alpha \in (0,1)$. First we recall an existence and uniqueness result to problem (3)–(4).

Theorem 1 (cf. Theorem 8, [16]) *Let $\alpha \in (0,1)$, $1 \leq p < \frac{1}{1-\alpha}$ and $\|\cdot\|$ be the norm in $\mathbb{R}^n$. If*

(i) $t \mapsto g(t,y,u)$ is measurable on $[a,b]$ for all $y \in \mathbb{R}^n$, $u \in M$, $u \mapsto g(t,y,u)$ is continuous on M for $t \in [a,b]$ a.e. and all $y \in \mathbb{R}^n$;

(ii) there exists $L > 0$ such that

$$\|g(t,y_1,u) - g(t,y_2,u)\| \leq L \|y_1 - y_2\|$$

for $t \in [a,b]$ a.e. and all $y_1, y_2 \in \mathbb{R}^n$, $u \in M$;

(ii) there exist $r \in L^p([a,b];\mathbb{R})$ *and* $\gamma \geq 0$ *such that*

$$\|g(t,0,u)\| \leq r(t) + \gamma \|u\|$$

for $t \in [a,b]$ *a.e. and all* $u \in M$,

then problem (3)–(4) has a unique solution $y \in I_{a+}^{\alpha}(L^p) + \left\{ \frac{d}{(t-a)^{1-\alpha}}; d \in \mathbb{R}^n \right\}$ *corresponding to any control* $u \in L^p([a,b];M)$.

For $g(t,y,u) = A(t)y(t) + B(t)u(t)$, where $A : [a,b] \to \mathbb{R}^{n\times m}$, $B : [a,b] \to \mathbb{R}^{n\times m}$ the existence of an optimal solution to problem (3)–(6) is ensured by the following theorem proved in [15].

Theorem 2 (cf. Theorem 19, [15]) *Suppose that* $1 < p < \frac{1}{1-\alpha}$ *and*

(i) M *is convex and compact;*
(ii) $t \mapsto f(t,y,u)$ *is measurable on* $[a,b]$ *for all* $y \in \mathbb{R}^n$ *and* $u \in M$;
(iii) $(y,u) \mapsto f(t,y,u)$ *is continuous on* $\mathbb{R}^n \times M$ *for a.e.* $t \in [a,b]$;
(iv) $u \mapsto f(t,y,u)$ *is convex on* M *for a.e.* $t \in [a,b]$ *and all* $y \in \mathbb{R}^n$;
(v) A, B *are essentially bounded on* $[a,b]$;
(vi) there exists a summable function $\psi_1 : [a,b] \to \mathbb{R}_0^+$ *and a constant* $c_1 \geq 0$ *such that*

$$f(t,y,u) \geq -\psi_1(t) - c_1 \|y\|$$

for a.e. $t \in [a,b]$ *and all* $x \in \mathbb{R}^n$, $u \in M$. *Here,* $\|\cdot\|$ *denotes norm in* $\mathbb{R}^n$.

Then problem (3)–(6) possesses an optimal solution

$$(y_0,u_0) \in \left(I_{a+}^{\alpha}(L^p) + \left\{ \frac{d}{(t-a)^{1-\alpha}}; d \in \mathbb{R}^n \right\} \right) \times \mathcal{U}_M,$$

where

$$\mathcal{U}_M = \left\{ u \in L^1([a,b];\mathbb{R}^m) : u(t) \in M,\ t \in [a,b] \right\}.$$

Theorem 3 (cf. Theorem 9, [16]) *Let* $\alpha \in (0,1)$ *and* $1 \leq p < \frac{1}{1-\alpha}$. *We assume that* M *is compact and*

(i) $g \in C^1$ *with respect to* $y \in \mathbb{R}^n$ *and assumptions (a)–(c) of Theorem 1 are satisfied;*
(ii) $t \mapsto f(t,y,u)$ *is measurable on* $[a,b]$ *for all* $y \in \mathbb{R}^n$, $u \in M$ *and* $u \mapsto f(t,y,u)$ *is continuous on* M *for a.e.* $t \in [a,b]$ *and all* $y \in \mathbb{R}^n$;
(iii) $f \in C^1$ *with respect to* $y \in \mathbb{R}^n$ *and there exist* $\bar{a}_1 \in L^1([a,b],\mathbb{R}_0^+)$, $\bar{a}_2 \in L^{p'}([a,b],\mathbb{R}_0^+)$ $\left(\frac{1}{p} + \frac{1}{p'} = 1\right)$, $\bar{C}_1, \bar{C}_2 \geq 0$ *such that*

$$\|f(t,y,u)\| \leq \bar{a}_1(t) + \bar{C}_1 \|y\|^p , \tag{7}$$

$$\left\| \frac{\partial}{\partial y} f(t,y,u) \right\| \leq \bar{a}_2(t) + \bar{C}_2 \|y\|^{p-1} , \tag{8}$$

for a.e. $t \in [a,b]$ *and all* $y \in \mathbb{R}^n$, $u \in M$;

(iv) $t \mapsto \dfrac{\partial}{\partial y} g(t,y,u)$, $t \mapsto \dfrac{\partial}{\partial y} f(t,y,u)$ *are measurable on* $[a,b]$ *for all* $y \in \mathbb{R}^n$, $u \in M$;

(v) $u \mapsto \dfrac{\partial}{\partial y} g(t,y,u)$, $u \mapsto \dfrac{\partial}{\partial y} f(t,y,u)$ *are continuous on* M *for a.e.* $t \in [a,b]$ *and all* $y \in \mathbb{R}^n$;

(vi) for a.e. $t \in [a,b]$ *and all* $y \in \mathbb{R}^n$ *the set*

$$\tilde{Z} := \left\{ (f(t,y,u), g(t,y,u)) \in \mathbb{R}^{n+1},\ u \in M \right\}$$

is convex.

If the pair

$$(y_*, u_*) \in \left(I^{\alpha}_{a+}(L^p) + \left\{ \frac{d}{(t-a)^{1-\alpha}}; d \in \mathbb{R}^n \right\} \right) \times \mathcal{U}_M$$

is a locally optimal solution to problem (3)–(6)*, then there exists a function* $\lambda \in I^{\alpha}_{b-}(L^{p'})$*, such that*

$$D^{\alpha}_{b-}[\lambda](t) = \frac{\partial}{\partial y} g(t, y_*(t), u_*(t))^T \lambda(t) - \frac{\partial}{\partial y} f(t, y_*(t), u_*(t)) \tag{9}$$

for a.e. $t \in [a,b]$ *and*

$$I^{1-\alpha}_{b-}[\lambda](b) = 0. \tag{10}$$

Moreover,

$$f(t, y_*(t), u_*(t)) - \lambda(t) g(t, y_*(t), u_*(t)) = \min_{u \in M} \{ f(t, y_*(t), u) - \lambda(t) g(t, y_*(t), u) \} \tag{11}$$

for a.e. $t \in [a,b]$.

Remark 1 In [16] the author showed that under certain assumptions FOCP of type (3)–(6) satisfies the Smooth Convex Extremum Principle (SCEP) (see e.g., Theorem 3 of [16]) and as a consequence he obtained the fractional Pontryagin Maximum Principle (see Theorem 9 of [16]). In particular, it is shown that if for a.e. $t \in [a,b]$ and all $y \in \mathbb{R}^n$ the set

$$\tilde{Z} := \left\{ (f(t,y,u), g(t,y,u)) \in \mathbb{R}^{n+1},\ u \in M \right\}$$

is convex, then the convexity assumption in SCEP is satisfied. One can easily check that the convexity of the set $\tilde{Z}$ can be replaced by the condition saying that for any

$u_1, u_2 \in \mathcal{U}_M, y \in \left(I^{\alpha}_{a+}(L^p) + \left\{\frac{d}{(t-a)^{1-\alpha}}; d \in \mathbb{R}^n\right\}\right)$ and $\mu \in [0,1]$ there exists $\tilde{u} \in \mathcal{U}_M$ such that

$$f(t, y, \tilde{u}) \leq \mu f(t, y, u_1) + (1-\mu) f(t, y, u_2), \tag{12}$$

$$g(t, y, \tilde{u}) = \mu g(t, y, u_1) + (1-\mu) g(t, y, u_2). \tag{13}$$

2 Optimal Control Problem of the Fractional Cucker–Smale Model

In this section we shall investigate the Cucker–Smale fractional optimal control problem. Let N denote the number of interacting agents and $(v_i, x_i) \in \mathbb{R}^d \times \mathbb{R}^d$ be understood as the state of each agent (x_i is the main state of an agent and v_i is its consensus parameter). Consequently, for N agents the main state is described by N-uple $x = (x_1, \ldots, x_N)$ and consensus parameter by $v = (v_1, \ldots, v_N)$.

Let $\alpha \in (0,1)$ and $x : [0,T] \longrightarrow (\mathbb{R}^d)^N$, $v : [0,T] \longrightarrow (\mathbb{R}^d)^N$ be measurable. Consider the problem of finding a trajectory solution to the system

$$D^{\alpha}_{0+} \begin{bmatrix} v \\ x \end{bmatrix} (t) = A \begin{bmatrix} v \\ x \end{bmatrix} (t) + Iu(t), \tag{14}$$

describing time evolution of the state (v, x), initialized at

$$I^{1-\alpha}_{0+} \begin{bmatrix} v \\ x \end{bmatrix} (0) = \begin{bmatrix} v_0 \\ x_0 \end{bmatrix} \in (\mathbb{R}^d)^N \times (\mathbb{R}^d)^N. \tag{15}$$

Here $A = \begin{bmatrix} A_N & \mathbf{0}_N \\ \mathbf{I}_N & \mathbf{0}_N \end{bmatrix}$ is the $2dN \times 2dN$ dimensional matrix such that

$$A_N = \begin{bmatrix} (\frac{1}{N}-1)\mathbf{I}_d & \frac{1}{N}\mathbf{I}_d & \ldots & \frac{1}{N}\mathbf{I}_d & \frac{1}{N}\mathbf{I}_d \\ \frac{1}{N}\mathbf{I}_d & (\frac{1}{N}-1)\mathbf{I}_d & \ldots & \frac{1}{N}\mathbf{I}_d & \frac{1}{N}\mathbf{I}_d \\ \vdots & \vdots & \ddots & \vdots & \vdots \\ \frac{1}{N}\mathbf{I}_d & \frac{1}{N}\mathbf{I}_d & \ldots & (\frac{1}{N}-1)\mathbf{I}_d & \frac{1}{N}\mathbf{I}_d \\ \frac{1}{N}\mathbf{I}_d & \frac{1}{N}\mathbf{I}_d & \ldots & \frac{1}{N}\mathbf{I}_d & (\frac{1}{N}-1)\mathbf{I}_d \end{bmatrix}$$

$\mathbf{I}_N$ is the identity $dN \times dN$ matrix, $\mathbf{0}_N$ is the zero $dN \times dN$ matrix, $\mathbf{I}_d$ is the identity $d \times d$ matrix, and $I = \begin{bmatrix} \mathbf{I}_N \\ \mathbf{0}_N \end{bmatrix}$. Note that (14) is system (2) written in matrix notation. A solution to (14) and (15) has to minimize the following cost functional

$$\int_0^T \left(\sum_{i=1}^N \|v_i(t) - \frac{1}{N} \sum_{j=1}^N v_j(t)\|_{l_2^d}^2 + \gamma \sum_{i=1}^N \|u_i(t)\|_{l_2^d} \right) dt, \tag{16}$$

where controls $u = (u_1, \ldots, u_N) : [0, T] \longrightarrow (\mathbb{R}^d)^N$ are integrable functions such that

$$u(t) \in M := \left\{ u(t) \in (\mathbb{R}^d)^N : \sum_{i=1}^N \|u_i(t)\|_{l_2^d} \leq K \right\}, \text{ a.e. on } [0, T], \tag{17}$$

for a given $\gamma, K > 0$. The functional (16) is the combination of the distance from the mean consensus parameter $\bar{v} = \frac{1}{N} \sum_{i=1}^N v_i(t)$ with the $l_1^N - l_2^d$-norm of the control.

2.1 Existence of Solutions to the Cucker–Smale Fractional Optimal Control Problem

We start by showing that an optimal solution to problem (14)–(17) exists.

Theorem 4 *Suppose that* $1 \leq p < \frac{1}{1-\alpha}$. *Then, the Cucker–Smale fractional optimal control problem* (14)–(17) *possesses an optimal solution* (v_*, x_*, u_*) *in the set*

$$\left(I_{0+}^{\alpha} \left(L^p([0, T]; (\mathbb{R}^d)^N \times (\mathbb{R}^d)^N) \right) + \left\{ \frac{c}{t^{1-\alpha}}; c \in (\mathbb{R}^d)^N \times (\mathbb{R}^d)^N \right\} \right) \times \mathcal{U}_M,$$

where

$$\mathcal{U}_M = \left\{ u \in L^1 \left([0, T]; (\mathbb{R}^d)^N \right) : u(t) \in M, \ t \in [0, T] \right\}.$$

Proof The procedure is to apply Theorem 2. First, let us note that the set M given by (17) is compact (as it is closed and bounded) and convex. Now, let us define

$$f(t, v(t), u(t)) := \sum_{i=1}^N \|v_i(t) - \frac{1}{N} \sum_{j=1}^N v_j(t)\|_{l_2^d}^2 + \gamma \sum_{i=1}^N \|u_i(t)\|_{l_2^d}.$$

Clearly, $t \mapsto f(t, v, u)$ is measurable on $[0, T]$ (it is a composition of measurable functions), for all $v \in (\mathbb{R}^d)^N$ and $u \in \mathcal{U}_M$, and $(v, u) \mapsto f(t, v, u)$ is continuous on $(\mathbb{R}^d)^N \times M$ for a.a. $t \in [0, T]$. Moreover, let $u_1, u_2 \in M$ and $\mu \in [0, 1]$, then for a.a. $t \in [0, T]$ and all $v \in (\mathbb{R}^d)^N$ one has

$$
\begin{aligned}
&f(t, v, \mu u_1 + (1-\mu)u_2) \\
&= \sum_{i=1}^{N} \|v_i(t) - \frac{1}{N}\sum_{j=1}^{N} v_j(t)\|_{l_2^d}^2 + \gamma \sum_{i=1}^{N} \|\mu u_{1i}(t) + (1-\mu)u_{2i}(t)\|_{l_2^d} \\
&\leq \sum_{i=1}^{N} \|v_i(t) - \frac{1}{N}\sum_{j=1}^{N} v_j(t)\|_{l_2^d}^2 + \gamma\mu \sum_{i=1}^{N} \|u_{1i}(t)\|_{l_2^d} + \gamma(1-\mu) \sum_{i=1}^{N} \|u_{2i}(t)\|_{l_2^d} \\
&= \mu \left(\sum_{i=1}^{N} \|v_i(t) - \frac{1}{N}\sum_{j=1}^{N} v_j(t)\|_{l_2^d}^2 + \gamma \sum_{i=1}^{N} \|u_{1i}(t)\|_{l_2^d} \right) \\
&+ (1-\mu) \left(\sum_{i=1}^{N} \|v_i(t) - \frac{1}{N}\sum_{j=1}^{N} v_j(t)\|_{l_2^d}^2 + \gamma \sum_{i=1}^{N} \|u_{2i}(t)\|_{l_2^d} \right) \\
&= \mu f(t, v, u_1) + (1-\mu) f(t, v, u_2).
\end{aligned}
$$

Therefore, $u \mapsto f(t, v, u)$ is convex on M for a.a. $t \in [0, T]$ and all $v \in (\mathbb{R}^d)^N$. Clearly, A and I are essentially bounded on $[0, T]$. Finally, observe that

$$
f(t, v, u) = \sum_{i=1}^{N} \|v_i(t) - \frac{1}{N}\sum_{j=1}^{N} v_j(t)\|_{l_2^d}^2 + \gamma \sum_{i=1}^{N} \|u_i(t)\|_{l_2^d} \geq \gamma \sum_{i=1}^{N} \|u_i(t)\|_{l_2^d}.
$$

Hence, by taking $\psi(t) = -\gamma \sum_{i=1}^{N} \|u_i(t)\|_{l_2^d}$ and $c_1 = 0$ we fulfill the last assumption of Theorem 2.

2.2 *Necessary Optimality Conditions for the Fractional Cucker–Smale Optimal Control Problem*

The second step is to state the necessary optimality conditions for an optimal solution to problem (14)–(17).

Theorem 5 *Let* $\alpha \in \left(\frac{1}{2}, 1\right)$. *If*

$$
(v_*, x_*, u_*) \in \left(I_{0+}^{\alpha} \left(L^2([0, T]; (\mathbb{R}^d)^N \times (\mathbb{R}^d)^N) \right) + \left\{ \frac{c}{t^{1-\alpha}}; c \in (\mathbb{R}^d)^N \times (\mathbb{R}^d)^N \right\} \right) \times \mathcal{U}_M
$$

is a locally optimal solution to problem (14)–(17), *then there exists a function* $\lambda \in I_{0+}^{\alpha} \left(L^p([0, T]; (\mathbb{R}^d)^N \times (\mathbb{R}^d)^N) \right)$, *such that*

$$
D_{T-}^{\alpha}[\lambda](t) = A^T \lambda(t) - 2 \left(v_*(t) - \frac{1}{N} \sum_{j=1}^{N} v_{*j}(t) \right)
$$

for a.e. $t \in [0, T]$ *and*

$$I_{T-}^{1-\alpha}[\lambda](T) = 0.$$

Moreover

$$\sum_{i=1}^{N} \|v_{*i}(t) - \frac{1}{N}\sum_{j=1}^{N} v_{*j}(t)\|_{l_2^d}^2 + \gamma \sum_{i=1}^{N} \|u_{*i}(t)\|_{l_2^d} - \lambda(t)\left[A\begin{bmatrix} v_* \\ x_* \end{bmatrix}(t) + Iu_*(t)\right]$$
$$= \min_{u \in M}\left\{\sum_{i=1}^{N} \|v_{*i}(t) - \frac{1}{N}\sum_{j=1}^{N} v_{*j}(t)\|_{l_2^d}^2 + \gamma \sum_{i=1}^{N} \|u_i\|_{l_2^d} - \lambda(t)\left[A\begin{bmatrix} v_* \\ x_* \end{bmatrix}(t) + Iu\right]\right\} \quad (18)$$

for a.e. $t \in [0, T]$.

Proof It is enough to show that the assumptions of Theorem 3 are satisfied. Let

$$g(t, x(t), v(t), u(t)) := A\begin{bmatrix} v \\ x \end{bmatrix}(t) + Iu(t)$$

and the function $f(t, v, u)$ be defined in the same way as in the proof of Theorem 4. Clearly, $(x, v) \mapsto g(t, x, v, u)$ is continuously differentiable and Lipschitz continuous for $t \in [0, T]$ a.e.; all $u \in M$; $t \mapsto g(t, x, v, u)$, $t \mapsto f(t, v, u)$ are measurable on $[0, T]$; functions $u \mapsto g(t, x, v, u)$, $u \mapsto f(t, v, u)$ are continuous on M. Moreover, we have

$$\|g(t, 0, 0, u)\|_{l_1^N - l_2^d} = \|u\|_{l_1^N - l_2^d}.$$

Hence, assumption c of Theorem 1 is satisfied with $r(t) \equiv 0$ and $\gamma = 1$. Observe that function f is continuously differentiable with respect to v and

$$\frac{\partial}{\partial v} f(t, v, u) = 2\left(v - \frac{1}{N}\sum_{j=1}^{N} v_j\right).$$

One has

$$\|f(t, v, u)\|_{l_1^N - l_2^d} = \sum_{i=1}^{N}\left(\|v_i - \tfrac{1}{N}\sum_{j=1}^{N} v_j\|_{l_2^d}^2 + \gamma\|u_i\|_{l_2^d}\right)$$
$$\leq \sum_{i=1}^{N}\left(2\|v_i\|_{l_2^d}^2 + \gamma\|u_i\|_{l_2^d}\right) + 2\|v\|_{l_1^N - l_2^d}^2$$

and

$$\left\| \frac{\partial}{\partial v} f(t, v, u) \right\|_{l_1^N - l_2^d} = 2\|v - \frac{1}{N} \sum_{j=1}^{N} v_j\|_{l_1^N - l_2^d}$$

$$\leq 2 \left(\|v\|_{l_1^N - l_2^d} + \frac{1}{N} \sum_{j=1}^{N} \|v_j\|_{l_2^d} \right) = 2 \left(1 + \frac{1}{N} \right) \|v\|_{l_1^N - l_2^d}.$$

Therefore, choosing $\bar{a}_1(t) = \sum_{i=1}^{N} \|v_i(t)\|_{l_2^d}^2 + \gamma \|u_i(t)\|_{l_2^d}$, $\bar{a}_2(t) \equiv 0$ and $\bar{C}_1 = 2$, $\bar{C}_2 = 2 \left(1 + \frac{1}{N} \right)$ assumption 3 of Theorem 3 is satisfied with $p = 2$. Note that partial derivative of $g(t, x, v, u)$ with respect to (x, v) is equal to A, so it is measurable in t and continuous in u. Moreover, $t \mapsto \frac{\partial}{\partial v} f(t, v, u)$ is measurable on $[0, T]$ for all $v \in (\mathbb{R}^d)^N$, $u \in M$ and $u \mapsto \frac{\partial}{\partial v} f(t, v, u)$ is continuous on M for a.e. $t \in [0, T]$ and all $v \in (\mathbb{R}^d)^N$.

We will finish the proof, showing that conditions (12) and (13) mentioned in Remark 1 are satisfied. Indeed, for every $u_1, u_2 \in \mathcal{U}_M$, $x, v \in I_{0+}^{\alpha} \left(L^2 \left([0, T]; (\mathbb{R}^d)^N \right) \right) + \left\{ \frac{d}{t^{1-\alpha}}; d \in (\mathbb{R}^d)^N \right\}$ and $\mu \in [0, 1]$ one has

$$\mu f(t, v, u_1) + (1 - \mu) f(t, v, u_2) \geq f(t, v, \mu u_1 + (1 - \mu) u_2),$$

$$\mu g(t, x, v, u_1) + (1 - \mu) g(t, x, v, u_2) = g(t, x, v, \mu u_1 + (1 - \mu) u_2)$$

and $\mu u_1 + (1 - \mu) u_2 \in \mathcal{U}_M$, by convexity of M. □

2.3 *Illustrative Example*

Let us consider problem (14)–(17) with $d = 1$ and $N = 3$ (i.e., a model with 3 agents). Then matrix A in system (14) is of the form $A = \begin{bmatrix} A_3 & \mathbf{0}_3 \\ \mathbf{I}_3 & \mathbf{0}_3 \end{bmatrix}$, where

$$A_3 = \begin{bmatrix} -\frac{2}{3} & \frac{1}{3} & \frac{1}{3} \\ \frac{1}{3} & -\frac{2}{3} & \frac{1}{3} \\ \frac{1}{3} & \frac{1}{3} & -\frac{2}{3} \end{bmatrix}.$$

Functional (16) and the set M are given by

$$\int_0^T \left(\sum_{i=1}^3 \left(v_i(t) - \frac{1}{3} \sum_{j=1}^3 v_j(t) \right)^2 + \gamma \sum_{i=1}^3 |u_i(t)| \right) dt, \tag{19}$$

$$M := \left\{ u(t) \in \mathbb{R}^3 : \sum_{i=1}^3 |u_i(t)| \leq K \right\}.$$

By Theorems 4 and 5 we know that the problem possesses an optimal solution (v_*, x_*, u_*) in the set

$$\left(I_{0+}^{\alpha} \left(L^p([0,T]; \mathbb{R}^3 \times \mathbb{R}^3 \right) + \left\{ \frac{c}{t^{1-\alpha}}; c \in \mathbb{R}^3 \times \mathbb{R}^3 \right\} \right) \times \mathcal{U}_M$$

and there exists a function $\lambda \in I_{0+}^{\alpha} \left(L^p([0,T]; \mathbb{R}^3 \times \mathbb{R}^3 \right)$, such that

$$D_{T-}^{\alpha}[\lambda](t) = A^T \lambda(t) - 2 \left(v_*(t) - \frac{1}{3} \sum_{j=1}^3 v_{*j}(t) \right)$$

for a.e. $t \in [0,T]$ and

$$I_{T-}^{1-\alpha}[\lambda](T) = 0.$$

Precisely, the following holds:

$$D_{T-}^{\alpha}[\lambda_1](t) = -\frac{2}{3}\lambda_1(t) + \frac{1}{3}\lambda_2(t) + \frac{1}{3}\lambda_3(t) - 2 \left(v_{1*}(t) - \frac{1}{3} \sum_{j=1}^3 v_{j*}(t) \right), \tag{20}$$

$$D_{T-}^{\alpha}[\lambda_2](t) = \frac{1}{3}\lambda_1(t) - \frac{2}{3}\lambda_2(t) + \frac{1}{3}\lambda_3(t) - 2 \left(v_{2*}(t) - \frac{1}{3} \sum_{j=1}^3 v_{j*}(t) \right), \tag{21}$$

$$D_{T-}^{\alpha}[\lambda_3](t) = \frac{1}{3}\lambda_1(t) + \frac{1}{3}\lambda_2(t) - \frac{2}{3}\lambda_3(t) - 2 \left(v_{3*}(t) - \frac{1}{3} \sum_{j=1}^3 v_{j*}(t) \right) \tag{22}$$

and $I_{T-}^{1-\alpha}[\lambda](T) = 0$. Note that $\lambda_4(t) = \lambda_5(t) = \lambda_6(t) = 0$, for a.e. $t \in [0,T]$, since $D_{T-}^{\alpha}[\lambda_4](t) = 0$, $D_{T-}^{\alpha}[\lambda_5](t) = 0$, $D_{T-}^{\alpha}[\lambda_6](t) = 0$. Clearly, we also have:

$$D_{0+}^{\alpha}[v_{1*}](t) = -\frac{2}{3}v_{1*}(t) + \frac{1}{3}v_{2*}(t) + \frac{1}{3}v_{3*}(t) + u_{1*}(t), \tag{23}$$

$$D^{\alpha}_{0+}[v_{2*}](t) = \frac{1}{3}v_{1*}(t) - \frac{2}{3}v_{2*}(t) + \frac{1}{3}v_{3*}(t) + u_{2*}(t), \tag{24}$$

$$D^{\alpha}_{0+}[v_{3*}](t) = \frac{1}{3}v_{1*}(t) + \frac{1}{3}v_{2*}(t) - \frac{2}{3}v_{3*}(t) + u_{3*}(t), \tag{25}$$

and

$$\begin{aligned} D^{\alpha}_{0+}[x_{1*}](t) &= v_{1*}(t), \\ D^{\alpha}_{0+}[x_{2*}](t) &= v_{2*}(t), \\ D^{\alpha}_{0+}[x_{3*}](t) &= v_{3*}(t). \end{aligned}$$

Let us define the function

$$\begin{aligned} F(v,u,\lambda) := &\sum_{i=1}^{3}\left(v_i - \frac{1}{3}\sum_{i=1}^{3} v_j\right)^2 + \gamma\sum_{i=1}^{3}|u_i| - \lambda_1\left(-\frac{2}{3}v_1 + \frac{1}{3}v_2 + \frac{1}{3}v_3 + u_1\right) \\ &- \lambda_2\left(\frac{1}{3}v_1 - \frac{2}{3}v_2 + \frac{1}{3}v_3 + u_2\right) - \lambda_3\left(\frac{1}{3}v_1 + \frac{1}{3}v_2 - \frac{2}{3}v_3 + u_3\right). \end{aligned}$$

Note that, by Eq. (18), optimal control u_* must be such that

$$F(v_*(t), u_*(t), \lambda(t)) = \min_{u\in M} F(v_*(t), u, \lambda(t)), \text{ for a.e. } t \in [0,T].$$

Variables v do not influence on the point, where the minimum of F is attained, but only on its value. Therefore, every optimal control u_* must be such that

$$Z(u_*(t), \lambda(t)) = \min_{u\in M}\left\{\gamma\sum_{i=1}^{3}|u_i(t)| - \lambda_1(t)u_1(t) - \lambda_2(t)u_2(t) - \lambda_3(t)u_3(t)\right\}$$

for a.e. $t \in [0,T]$, where u_*, λ satisfy Eqs. (20)–(25), and conditions

$$I^{1-\alpha}_{0+}\begin{bmatrix} v \\ x \end{bmatrix}(0) = \begin{bmatrix} v_0 \\ x_0 \end{bmatrix}, \quad I^{1-\alpha}_{T-}[\lambda](T) = 0$$

hold.

Acknowledgments Research supported by the Polish National Science Center grant on the basis of decision DEC-2014/15/B/ST7/05270.

References

1. Aoki, I.: A simulation study on the schooling mechanism in fish. Bull. Jpn. Soc. Sci. Fish **48**(8), 1081–1088 (1982)
2. Caponigro, M., Fornasier, M., Piccoli, B., Trelat, E.: Sparse stabilization and optimal control of the Cucker–Smale model. Math. Control Relat. Fields **3**(4), 447–466 (2013)
3. Cucker, F., Smale, S.: On the mathematics of emergence. Jpn. J. Math. **2**(1), 197–227 (2007)
4. Degond, P., Motsch, S.: Macroscopic limit of self-driven particles with orientation interaction. C.R. Math. Acad. Sci. Paris **345**(10), 555–560 (2007)
5. Milewski, P., Yang, X.: A simple model for biological aggregation with asymmetric sensing. Commun. Math. Sci. **6**(2), 397–416 (2008)
6. Toner, J., Tu, Y.: Flocks, herds, and schools: a quantitative theory of flocking. Phys. Rev. E. **58**(4), 4828–4858 (1998)
7. Vicsek, T., Zafeiris, A.: Collective motion. Phys. Rep. **517**(3–4), 71–140 (2012)
8. Cucker, F., Smale, S.: Emergent behavior in flocks. IEEE Trans. Autom. Control **52**(5), 852–862 (2007)
9. Bagley, R., Calico, R.: Fractional order state equations for the control of viscoelastically damped structures. J. Guid. Control Dyn. **14**(2), 304–311 (1991)
10. Baleanu, D., Tenreiro Machado, J.A., Luo, A.C.J.: Fractional Dynamics and Control. Springer, New York (2012)
11. Domek, S., Dworak, P.: Theoretical Developments and Applications of Non–Integer Order Systems. Lecture Notes in Electrical Engineering, vol. 357. Springer, New York (2015)
12. Kaczorek, T.: Selected Problems of Fractional Systems Theory. Lecture Notes in Control and Information Sciences, vol. 411. Springer, Berlin (2011)
13. Podlubny, I.: Fractional Differential Equations. Mathematics in Science and Engineering, vol. 198. Academic Press, Inc., San Diego (1999)
14. Hongjie, L.: Observer-type consensus protocol for a class of fractional-order uncertain multi-agent systems. Abstr. Appl. Anal. **2012**, 18 p (2012)
15. Kamocki, R.: On the existence of optimal solutions to fractional optimal control problems. Appl. Math. Comput. **35**, 94–104 (2014)
16. Kamocki, R.: Pontryagin maximum principle for fractional ordinary optimal control problems. Math. Methods Appl. Sci. **37**(11), 1668–1686 (2014)
17. Kilbas, A.A., Srivastava, H.M., Trujillo, J.J.: Theory and Applications of Fractional Differential Equations. North-Holland Mathematics Studies, vol. 204. Elsevier Science B.V., Amsterdam (2006)
18. Pooseh, S., Almeida, R., Torres, D.F.M.: Fractional order optimal control problems with free terminal time. J. Ind. Manag. Optim. **10**(2), 363–381 (2014)
19. Samko, S.G., Kilbas, A.A., Marichev, O.I.: Fractional Integrals and Derivatives. Translated from the 1987 Russian Original. Gordon and Breach, Yverdon (1993)

Determining the Time Elapsed Since Sudden Localized Impulse Given to Fractional Advection Diffusion Equation

Marie-Christine Néel

Abstract In some natural media solute transport is ruled by a fractional Advection Diffusion Equation that accounts for fluid and chemicals stored in quiescent zones before being released after random times. An adjoint equation helps us deducing from concentration records where and at what time a solute has been suddenly injected in such media.

Keywords Fractional advection-diffusion equation · Initial Dirac impulse · Data inversion · Adjoint equation

1 Introduction

Fractional equations rule solute spreading in some natural media. An example is the fractional Advection-Diffusion Equation [1, 2] for α in]0, 1[

$$\partial_t u + \Lambda \partial_t^\alpha u = \partial_x \left(-vu + \partial_x Du\right). \tag{1}$$

The Caputo derivative ∂_t^α is usually defined by $\partial_t^\alpha = I_{0,+}^{1-\alpha}\partial_t$ where the fractional Riemann–Liouville integral $I_{0,+}^{1-\alpha}$ satisfies $I_{0,+}^{1-\alpha} f(t) = \frac{1}{\Gamma(1-\alpha)} \int_0^t \frac{f(t')}{(t-t')^\alpha} dt'$ [3]. Having in view initial conditions giving to (1) solutions non-differentiable at $t = 0+$, we use the more general definition [4] $\partial_t^\alpha f(t) = \partial_t I_{0,+}^{1-\alpha} f(t) - \frac{f(0+)t^{-\alpha}}{\Gamma(1-\alpha)}$. It coincides with $I_{0,+}^{1-\alpha}\partial_t f(t)$ when f is differentiable everywhere. For instance, Eq. (1) was found to describe the evolution of a tracer injected at time $t = 0$ in some river flow where its parameters (α, v, D, Λ) could be determined [1]. When fortuitous initially localized contamination invades such medium, finding its origin in time and space conditions remediation and also the assessment of responsibilities: we propose a strategy that finds when and where a solute was injected, assuming local and instantaneous injection.

M.-C. Néel (✉)
University of Avignon, Avignon, France
e-mail: mcneel@avignon.inra.fr

A. Babiarz et al. (eds.), *Theory and Applications of Non-integer Order Systems*,
Lecture Notes in Electrical Engineering 407, DOI 10.1007/978-3-319-45474-0_22

After a brief description of the model, we set the principle of a method that achieves this aim with the help of the numerical solution of an auxiliary equation. We demonstrate the method by applying it on artificial data that mimic a time profile of solute concentration measured at some point. If the data are due to a Dirac impulse $M\delta_{x_0}(x)$ applied at time t_0, we retrieve x_0, t_0 and M. We then justify our approach.

2 The Model and Its Solutions

2.1 Model and Objectives

Equation (1) represents the evolution of the concentration of a solute in a medium where it can be trapped for random times which do not have any finite average. It is equivalent to Fick's law applied to the mobile fraction while u represents the total concentration. We consider it in a one-dimensional finite domain represented by interval $[0, \ell]$, with the boundary conditions

$$(\partial_x Du - vu)(0,t) = 0 \quad , \quad \partial_x u(\ell,t) = 0. \tag{2}$$

We imagine solute concentration recorded at some interior point x_m after a solute amount M has been injected accidentally in the mobile state at some unknown point x_0 at some unknown instant $t_0 > 0$, when the medium was clean: before that instant solute concentration was zero and for $t > t_0$ it is $u(x, t - t_0)$. We want to deduce t_0, x_0 and M from the record.

We ultimately are interested in initial data φ of the form of $M\delta_{x_0}(x)$, δ_b being the Dirac distribution concentrated at point b. Yet, most theoretical materials correspond to initial data $\varphi(x)$ that are at least square integrable functions. Considering such initial data is a necessary step before proceeding to Dirac impulse, of course not included in the domain

$$\mathcal{D}_X(L) = \left\{ f \in H^2(0,\ell) \quad \text{and} \quad D\partial_x f(0,t) - vf(0,t) = \partial_x f(\ell,t) = 0 \right\}$$

of $L \equiv \partial_x^2 D - \partial_x v$ in $X = L^2(0,\ell)$. We note $\langle\cdot\rangle$ the scalar product of X.

The adjoint operator L^* of L in X helps us to describe the solutions of (1) and gives us an auxiliary equation to inspect past history.

2.2 Spectral Properties of L and of Its Adjoint L*

We define the adjoint L^* of L in X by

$$L^* f \equiv \partial_x \left(vf + \partial_x Df \right). \tag{3}$$

Its domain is $\mathcal{D}_X(L^*) = \left\{f \in H^2(0,\ell)/\partial_x f(0,t) = v(f + D\partial_x f)(\ell,t) = 0\right\}$, and it satisfies $\langle Lu \cdot w\rangle = \langle L^* w \cdot u\rangle$ for each (u, w) in $\mathcal{D}_X(L) \times \mathcal{D}_X(L^*)$.

Operators L and L^* are dissipative and invertible. Hence they are closed in X and have compact inverses (by compact inclusion of $H^2(0,\ell)$ in X). Moreover, endowing the set X with the scalar products $\langle u \cdot U\rangle_{\mathcal{H}} \equiv \langle ue^{-x\frac{v}{D}} \cdot U\rangle$ and $\langle u \cdot U\rangle_{\mathcal{H}^*} \equiv \langle ue^{x\frac{v}{D}} \cdot U\rangle$ yields two Hilbert spaces $\mathcal{H}$ and $\mathcal{H}^*$ of norms equivalent to that of X. Operator L (respectively L^*) is self-adjoint in $\mathcal{H}$ (resp. $\mathcal{H}^*$) and has a complete set of eigenfunctions $\{\varphi_i\}$ (resp. $\{\psi_i\}$) associated to eigenvalues $\ldots, -\lambda_{i+1} < -\lambda_i < \cdots < -\lambda_0 < 0$ [5]. We normalize the φ_i with the norm of $\mathcal{H}$ and the ψ_i with that of $\mathcal{H}^*$. Eigenvectors satisfy $\psi_i(x) = e^{-\frac{vx}{D}}\varphi_i(x)$ and

$$\langle \varphi_i \cdot \psi_j\rangle = \langle \varphi_i \cdot \varphi_j\rangle_{\mathcal{H}} = \langle \psi_i \cdot \psi_j\rangle_{\mathcal{H}^*} = \delta_{i,j} \tag{4}$$

for each i and j, $\delta_{i,j}$ being Kronecker index. Thus, each element φ of X expands as $\varphi = \sum\langle \psi_i \cdot \varphi\rangle\varphi_i$ (orthogonal in $\mathcal{H}$) and $\varphi = \sum\langle \varphi_i \cdot \varphi\rangle\psi_i$ (orthogonal in $\mathcal{H}^*$). These expansions give us insight into the solutions of (1) and (2). This due to the asymptotic behavior of the λ_i, equal to the eigenvalues of the Sturm–Liouville operator $\mathcal{L} \equiv -\partial^2_{x^2} + \frac{v^2}{4D^2}$ related to L by $L = -Dm_{-\frac{v}{D}} \circ \mathcal{L} \circ m_{\frac{v}{D}}$, where $m_{\frac{v}{D}}$ represents multiplication by $e^{\frac{-v}{2D}x}$. The eigenvalues satisfy the following property proved in [6].

Property 1: Operators L and L^* of X have complete sets of eigenfunctions φ_i and ψ_i, whose $\mathcal{C}([0,\ell])$ norms are bounded by a quantity $\mathcal{B}$. Eigenvalues satisfy

$$\lambda_i \sim ai^2 \quad \text{when} \quad i \to \infty, \tag{5}$$

a being a positive constant.

These elements help us to describe the solutions of Eq. (1) for $\Lambda \geq 0$.

2.3 Expansion of the Solutions of (1)

Separation of variables based on the φ_i and ψ_i expands each classical [5] solution $u(x,t)$ of (1) and (2) started from initial condition φ in $\mathcal{D}_X(L)$ according to

$$u(x,t) = S(t)\varphi \equiv \sum_{i\geq 0} w_{\lambda_i}(t,\alpha,\Lambda)\langle \varphi \cdot \psi_i\rangle\varphi_i, \tag{6}$$

as in [7] where multi-term fractional equations with different boundary conditions are considered. Yet, the properties of w_λ show that this expansion still describes solutions to (1) and (2) in a mild sense when φ only belongs to X. For convenience we skip the arguments α and Λ of function w_λ.

Function w_λ is equal to $e^{-\lambda t}$ in the conservative case $\Lambda = 0$, and satisfies

$$(\partial_t + \Lambda\partial_t^\alpha + \lambda)w_\lambda(t) = 0. \tag{7}$$

It is linked to the multinomial Mittag-Leffler function $E_{(1-\alpha,1),2}$ [7, 8]

$$w_\lambda(t) = 1 - \lambda t E_{(1-\alpha,1),2}(-\Lambda t^{1-\alpha}, -\lambda t) \tag{8}$$

and has a Laplace transform $\tilde{w}_\lambda$ equal to

$$\tilde{w}_\lambda(s) = \frac{1 + \Lambda s^{\alpha-1}}{s + \Lambda s^\alpha + \lambda}. \tag{9}$$

The latter equality implies

$$w_\lambda(t) = \frac{\lambda}{\pi} \int_0^\infty e^{-rt} \frac{\Lambda r^{\alpha-1} \sin \pi\alpha}{(\lambda - r + \Lambda r^\alpha \cos \pi\alpha)^2 + \Lambda^2 r^{2\alpha} \sin^2 \pi\alpha} dr, \tag{10}$$

where we see a completely monotonous function satisfying $w_\lambda(0+) = 1$ hence $0 \leq w_\lambda(t) \leq 1$ for $t \geq 0$.

For each φ in X with I representing Id or $I_{0,+}^{1-\alpha}$ or integration $I_{0,+}^1$ over $(0, t)$, this implies

$$\sum_{i=0}^{N} I w_{\lambda_i}(t) \langle \varphi \cdot \psi_i \rangle \varphi_i \to I S(t)\varphi \quad \text{when} \quad N \to \infty \tag{11}$$

in $\mathcal{H}$ where the series of (orthogonal) general items $\langle \varphi \cdot \psi_i \rangle \varphi_i$ converges to φ for $t \geq 0$. It also converges in $\mathcal{D}_X(L)$ for $t \geq t^* > 0$ because of the behavior of $\lambda w_\lambda(t)$ at large λ. We find this behavior by splitting the right hand-side of (10) into two integrals $J_{(0,r_\lambda)}$ and $J_{(r_\lambda,+\infty)}$ over $(0, r_\lambda)$ and $(r_\lambda, +\infty)$ separated by $r_\lambda = \text{Min}(\eta\frac{\lambda}{2}, (\frac{\eta\lambda}{2\Lambda|\cos \pi\alpha|})^{\frac{1}{\alpha}})$. We obtain $J_{(r_\lambda,+\infty)} \to 0$ when $\lambda \to +\infty$ and

$$\lambda w_\lambda(t) \to \frac{\Lambda t^{-\alpha}}{\Gamma(1-\alpha)} \quad \text{when} \quad \lambda \to +\infty. \tag{12}$$

Hence $S(t)\varphi$ belongs to $\mathcal{D}_X(L)$ for $t > 0$.

However, $S(t)\varphi$ is not a generalized solution of (1) as defined in [7] when φ is just an element of X. Nevertheless, it is a mild solution, i.e. it solves the time-integrated version [9, 10] of (1)

$$u(x,t) + \Lambda I_{0,+}^{1-\alpha} u(x,t) = \int_0^t Lu(x,t')dt' + \left(1 + \Lambda \frac{t^{1-\alpha}}{\Gamma(2-\alpha)}\right) \varphi(x). \tag{13}$$

Indeed, (7) implies

$$(\text{Id} + \Lambda I_{t_0,+}^{1-\alpha}) w_{\lambda_i}(t) + \lambda_i \int_0^t w_{\lambda_i}(t')dt' = 1 + \Lambda \frac{t^{1-\alpha}}{\Gamma(2-\alpha)},$$

hence $I_1^N + I_2^N = I_3^N$, with $I_1^N = \sum_{i=0}^N (\mathrm{Id} + \Lambda I_{t_0,+}^{1-\alpha}) w_{\lambda_i}(t) b_i$, $b_i = \langle \varphi \cdot \psi_i \rangle \varphi_i$, $I_2^N \int_0^t L \sum_{i=0}^N w_{\lambda_i}(t') b_i dt'$, and $I_3^N = (1 + \Lambda \frac{t^{1-\alpha}}{\Gamma(2-\alpha)}) \sum_{i=0}^N b_i$. When $N \to \infty$, (11) implies that $L \int_0^t \sum_{i=0}^N w_{\lambda_i} b_i dt'$ converges in X. Hence $\int_0^t S(t')\varphi dt'$ belongs to $\mathcal{D}_X(L)$ and $L \int_0^t \sum_{i=0}^N w_{\lambda_i} b_i dt'$ converges to $L \int_0^t \sum_{i=0}^{+\infty} S(t')\varphi dt'$ in X, since L is closed. This proves (13).

The same approach applies to an auxiliary equation.

2.4 Adjoint Equation

For ψ in X, replacing L by its adjoint in (13) yields

$$u^*(x,t) + \Lambda I_{0,+}^{1-\alpha} u^*(x,t) = \int_0^t L^* u^*(x,t')dt' + \left(1 + \Lambda \frac{t^{1-\alpha}}{\Gamma(2-\alpha)}\right) \psi(x), \quad (14)$$

the mild version of the adjoint equation

$$\partial_t u^* + \Lambda I_{0,+}^{1-\alpha} \partial_t u^* = L^* u^*. \quad (15)$$

As in Sect. 2.3, for each ψ in X Property 1 implies that

$$S^*(t)\psi = \sum_{i \geq 0} w_{\lambda_i}(t) \langle \psi \cdot \varphi_i \rangle \psi_i \quad (16)$$

solves (14). Moreover, $S(t)$ and $S^*(t)$ are linear operators (from X to $\mathcal{D}_X(L)$ and $\mathcal{D}_X(L^*)$) adjoint in X since (6) and (16) imply

$$\langle \varphi \cdot S^*(t)\psi \rangle = \langle \psi \cdot S(t)\varphi \rangle \quad (17)$$

for each φ and ψ in X.

Finite difference schemes for spatial derivatives and numerical approximations of Caputo derivatives [11] yield implicit schemes that approximate the solutions of (1) and (15) and return the black/blue lines and symbols of Fig. 1 that illustrate (17) for φ and ψ in X. Moreover, the evolution of $S(t)\varphi$ at point x_m is equivalent to that of $\langle \delta_{x_m} \cdot S(t)\varphi \rangle$, and (17) becomes a tool to investigate φ on the basis of localized records of $S(t)\varphi$ if we replace φ or ψ by Dirac impulses. Section 4 shows that (17) still holds in this case, and Fig. 1 demonstrates this identity at fixed φ when ψ takes the form of $\rho_{x_m,n}(x) \equiv n\rho(n(x - x_m))$, with $\rho(x) = 1$ for $|x| \leq \frac{1}{2}$ and $\rho(x) = 0$ elsewhere. When $n \to \infty$ these ψ approach δ_{x_m}, $\langle \varphi \cdot S^*(t)\psi \rangle$ comes close to $\langle \varphi \cdot S^*(t)\delta_{x_m} \rangle$ and we define $S^*(t)\delta_{x_m}$ by (16) with $\langle \delta_{x_m} \cdot \varphi_i \rangle = \varphi_i(x_m)$. Section 4 proves that $S^*(t)\rho_{x_m,n}$ indeed tends to $S^*(t)\delta_{x_m}$ in X, which moreover satisfies (14) with $\psi = \delta_{x_m}$ in a weak sense.

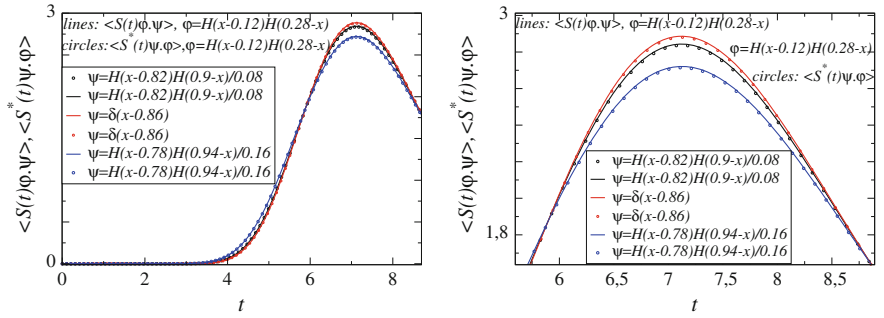

Fig. 1 Numerical illustration of Eq. (17), for fixed initial data φ in $L^2(0, \ell)$, and various examples of ψ function. The latter is either a staircase function, or a Dirac distribution. *Solid lines*/*symbols* represent *right*/*left hand-side* of Eq. (17). Parameters are $D = 0.001$ $v = 0.1$, $\Lambda = 0.1$, and $\alpha = 0.8$

Similar limit yields $S(t)\delta_{x_0}$ and extends (17) to the case when φ and ψ are Dirac measures. In this case (17) gives us insight into the time elapsed since an initial Dirac impulse imposed to (13).

3 Applying (17) to Data Inversion

Indeed, for φ of the form of $\varphi = M\delta_{x_0}$ and applied at instant t_0, later at time $t > t_0$ actual or numerical experiment records $\Phi(t) = M(S(t - t_0)\delta_{x_0})(x_m)$ at point x_m. We do not know x_0, t_0 and M, but equality (17) extended to Dirac measures tells us that $\Phi(t)$ must be equal to $M(S^*(t - t_0)\delta_{x_m})(x_0)$, while we can compute $(S^*(t')\delta_{x_m})(x)$ for each $t' > 0$ and $x \in [0, \ell]$. Comparing Φ with the map of all these $(S^*(t')\delta_{x_m})(x)$ reveals x_0 and t_0 provided we know Λ, α, D and v. We check this on artificial profile Φ computed by numerically solving Eq. (1): we have a series of $\Phi(t^{(i)})$, the $t^{(i)}$ forming a finite increasing sequence of measurement times with $i = 0, \ldots, \mathcal{N}$.

Discretizing Eq. (15) gives us an approximation to $(S^*(t')\delta_{x_m})(x)$ for all $t' > 0$ and x in $[0, \ell]$. Combining Eq. (17) with this discrete field and with profile Φ builds

$$\mathcal{F}(x_0, t_0) \equiv$$
$$\sum_{i\,/\,t^{(i)} \geq t}^{\mathcal{N}} [(S^*(t^{(i+1)} - t_0)\delta_{x_m})(x_0)/\Phi(t^{(i+1)}) - (S^*(t^{(i)} - t_0)\delta_{x_m})(x_0)/\Phi(t^{(i)})]^2.$$

The minimum of $\mathcal{F}(x_0, t_0)$ reveals the best candidate (x_0, t_0) for localization and application time of Dirac impulse at the origin of Φ, since by (17)

$$(S^*(t - t_0)\psi)(x_0)/\Phi(t) \tag{18}$$

must be independent of t.

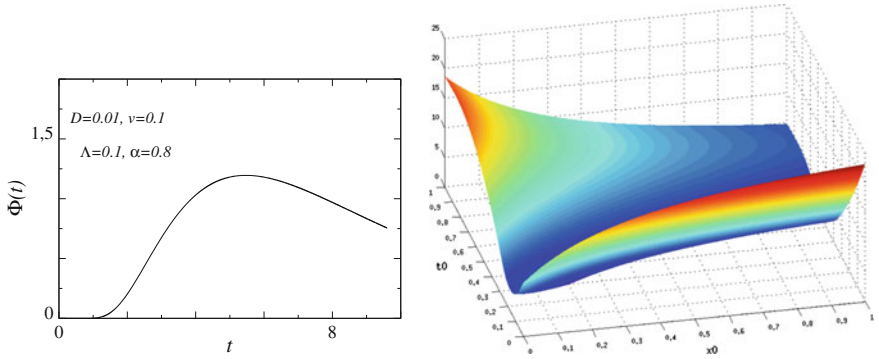

Fig. 2 Profile Φ, and the surface representing function $\mathcal{F}(x_0, t_0)$. Parameters D, v, Λ, α are 0.01, 0.1, 0.1, and 0.8. On the *left* the Φ profile. On the *right* a three-dimensional global view of $\mathcal{F}(x_0, t_0)$. Horizontal/vertical axes represent (x_0, t_0) and $\mathcal{F}$

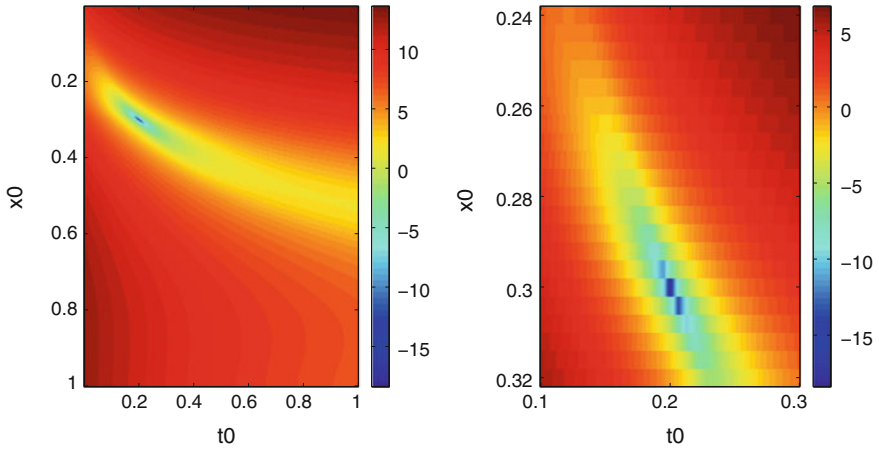

Fig. 3 Logarithmic plot of the levels of the surface representing $\mathcal{F}$ on Fig. 2. The levels of $10.log_{10}(\mathcal{F})$ are reminiscent of the long valley seen on Fig. 2. The *right plot* is a magnification of the *green shape* of *left plot*, and emphasizes the very *thin dark blue pixel* that reveals the true (x_0, t_0)

The minimum of $\mathcal{F}$ is found by just inspecting this function. Figure 2 shows an example of an artificial Φ profile, and a three-dimensional view of the corresponding $\mathcal{F}$ function. We visualize the (x_0, t_0) having the best chance of being injection point and injection time by plotting level contours of $\mathcal{F}$ (in logarithmic form) represented on Fig. 3. The global view (at the left) shows a green zone with a thin blue spot at the minimum of $\mathcal{F}$. Magnifying this zone (on the right) accurately retrieves the actual (x_0, t_0) at the origin of Φ. The value of M immediately follows.

4 The Limit of $S^*(t)\psi$ and $S(t)\varphi$ When φ and ψ are Dirac Measures

This section briefly sets the main steps that give a meaning to $S(t)\delta_{x_0}$ and $S^*(t)\delta_{x_m}$, based on series (6) and (16) and on integral expressions.

4.1 Preliminary: Integral Formulation of $S(t)$

Property 1 For φ and ψ in X,

$$S(t)\varphi = \int_0^\infty g_\alpha(\theta) \sum_{i\geq 0} T(t \cdot h_{\alpha,\Lambda}(t^{\frac{1}{\alpha}-1}\theta))\varphi d\theta, \tag{19}$$

and

$$S^*(t)\psi = \int_0^\infty g_\alpha(\theta) \sum_{i\geq 0} T^*(t \cdot h_{\alpha,\Lambda}(t^{\frac{1}{\alpha}-1}\theta))\psi d\theta, \tag{20}$$

where $T(t)\varphi = \sum_{i=0}^\infty \langle \varphi \cdot \psi_i \rangle e^{-\lambda_i t}\varphi_i$ and $T^*(t)\psi = \sum_{i=0}^\infty \langle \psi \cdot \varphi_i \rangle e^{-\lambda_i t}\psi_i$. Moreover, $h_{\alpha,\Lambda}$ is the function defined in $]0, 1[$ by

$$\theta(\Lambda h_{\alpha,\Lambda}(\theta))^{\frac{1}{\alpha}} + h_{\alpha,\Lambda}(\theta) = 1. \tag{21}$$

Families $T(t)$ and $T^*(t)$ constitute two semi-groups [12] generated by L and L^* in X, equal to $S(t)$ and $S^*(t)$ in the conservative particular case $\Lambda = 0$.

Proof The Laplace transform (9) of $w_\lambda(t)$ writes $\tilde{w}_\lambda(s) = (1 + \Lambda s^{\alpha-1}) \int_0^{+\infty} e^{-(s+\Lambda s^\alpha)\chi - \lambda\chi} d\chi$ where $e^{-(s+\Lambda s^\alpha)\chi}$ is reminiscent of the Laplace transform e^{-s^α} of the probability density function g_α of a positively supported stable probability law of exponent α. It turns out that $e^{-(s+\Lambda s^\alpha)\chi}$ is the Laplace transform of $g_\alpha(\frac{t-\chi}{(\Lambda\chi)^{\frac{1}{\alpha}}})H(t-\chi)\frac{1}{(\Lambda\chi)^{\frac{1}{\alpha}}}$ [1], while $\frac{1}{s+\Lambda s^\alpha+\lambda}$ is that of $\int_0^t e^{-\lambda\chi} g_\alpha(\frac{t-\chi}{(\Lambda\chi)^{\frac{1}{\alpha}}})\frac{1}{(\Lambda\chi)^{\frac{1}{\alpha}}} d\chi$. Also note that $\Lambda s^\alpha e^{-\Lambda\chi s^\alpha} = \frac{-s}{\alpha\chi}\frac{d}{ds}\int_0^{+\infty} e^{-st} g_\alpha(\frac{t}{(\Lambda\chi)^{\frac{1}{\alpha}}})dt$ writes $s\int_0^{+\infty} \frac{t}{\alpha\chi} e^{-st} g_\alpha(\frac{t}{(\Lambda\chi)^{\frac{1}{\alpha}}})\frac{dt}{(\Lambda\chi)^{\frac{1}{\alpha}}}$ because behaviors at infinity allow us exchanging integral and derivative. This implies

$$w_\lambda(t) = \int_0^t \left(1 + \frac{t-\chi}{\alpha\chi}\right) e^{-\lambda\chi} g_\alpha\left(\frac{t-\chi}{(\Lambda\chi)^{\frac{1}{\alpha}}}\right)\frac{d\chi}{(\Lambda\chi)^{\frac{1}{\alpha}}}. \tag{22}$$

Since the derivative of $h_{\alpha,\Lambda}$ satisfies

$$\frac{dh_{\alpha,\Lambda}}{d\theta}(\theta)\left(1 + \frac{1-h_{\alpha,\Lambda}}{\alpha h_{\alpha,\Lambda}(\theta)}\right) = -(\Lambda h_{\alpha,\Lambda}(\theta))^{\frac{1}{\alpha}},$$

setting $\chi = t \cdot h_{\alpha,\Lambda}(t^{\frac{1}{\alpha}-1}\theta')$ in (22) yields

$$w_\lambda(t) = \int_0^\infty g_\alpha(\theta') e^{-\lambda t \cdot h_{\alpha,\Lambda}(t^{\frac{1}{\alpha}-1}\theta')} d\theta'. \tag{23}$$

We finally arrive at (19) by seeing in $\|g_\alpha(\theta')\langle\varphi \cdot \psi_i\rangle\varphi_i\|_{\mathcal{H}}$ the general item of a positive series converging to $g_\alpha(\theta')\|\varphi\|_{\mathcal{H}}$, an integrable function. We similarly obtain (20).

If $T(t)$ and $T^*(t)$ satisfy estimates or preserve positivity, expressions (19) and (20) show that of $S(t)$ and $S^*(t)$ inherit these properties. For instance, computing the resolvent $(\lambda \mathrm{Id} - L)^{-1}$ of L (by Green function) shows that operator $T(t)$ is positivity preserving. Moreover, simple integration (over $(0, \ell)$) of Eq. (1) with $\Lambda = 0$ shows that $T(t)$ satisfies the following property, easily extended to $T^*(t)$.

Property 2 For each non-negative element φ of X, $\|T(t)\varphi\|_{L^1(0,\ell)} \leq \|\varphi\|_{L^1(0,\ell)}$ and $\|T^*(t)\varphi\|_{L^1(0,\ell)} \leq \|\varphi\|_{L^1(0,\ell)}$.

Because g_α is a probability density function, $S(t)$ and $S^*(t)$ are positivity preserving and inherit these estimates.

4.2 The Limit of $S^*(t)\rho_{x_m,n}$ in X Exists

Property 3 For $t > 0$

$$S^*(t)\rho_{x_m,n} \to \sum_{i\geq 0} w_{\lambda_i}(t)\varphi_i(x_m)\psi_i \equiv S^*(t)\delta_{x_m} \tag{24}$$

in $\mathcal{C}([0, \ell])$ (hence in X).

Proof Because of (5) $w_{\lambda_i}(t)(\langle\rho_{x_m,n} \cdot \varphi_i\rangle - \varphi_i(x_m))\psi_i$ has its $\mathcal{C}([0, \ell])$ norm dominated by $2\mathcal{B}^2 w_{\lambda_i}(t)$. Moreover, Property 1 and (12) imply that for each $\varepsilon > 0$ there exists $i_0(\varepsilon, t)$ such that $\sum_{i\geq i_0} w_{\lambda_i}(t) < \frac{\varepsilon}{4\mathcal{B}^2}$. Then, (24) results from the limit $\langle\rho_{x_m,n} \cdot \varphi_i\rangle \to \varphi_i(x_m)$ for each $i < i_0$ when $n \to \infty$.

4.3 The Limit of $S^*(t)\rho_{x_m,n}$ in X Satisfies Eq. (14)

We check that $S^*(t)\delta_{x_m}$ satisfies Eq. (14) in a generalized sense by starting from

$$\begin{aligned} S^*(t)\rho_{x_m,n} + \Lambda I_{0,+}^{1-\alpha} S^*(t)\rho_{x_m,n} - \left(1 + \frac{\Lambda t^{1-\alpha}}{\Gamma(2-\alpha)}\right)\rho_{x_m,n} = \\ L^* \int_0^t S^*(t')\rho_{x_m,n} dt', \end{aligned} \tag{25}$$

where $(1+\frac{\Lambda t^{1-\alpha}}{\Gamma(2-\alpha)})\rho_{x_m,n}$ tends to $(1+\frac{\Lambda t^{1-\alpha}}{\Gamma(2-\alpha)})\delta_{x_m}$ vaguely in the set $\mathcal{M}_b[0,\ell]$ of finite measures on $[0,\ell]$. Moreover, for each $t>0$ the limit $S^*(t)\rho_{x_m,n}\to S^*(t)\delta_{x_m}$ in X holds in $L^1(0,\ell)$. Since $\|S^*(t)\rho_{x_m,n}\|_{L^1(0,\ell)}$ is bounded for $t>0$ by Property 3, dominated convergence implies

$$(I_{0,+}^{1-\alpha}S^*)(t)\rho_{x_m,n}\to(I_{0,+}^{1-\alpha}S^*(t)\delta_{x_m})(t),\quad \int_0^t S^*(t')\rho_{x_m,n}dt'\to\int_0^t S^*(t)\delta_{x_m}(t')dt'$$

in $L^1(0,\ell)$. Hence $L^*\int_0^t S^*(t')\rho_{x_m,n}dt'$ converges vaguely to a finite measure $\mu(t)=((\mathrm{Id}+\Lambda I_{0,+}^{1-\alpha})S(t)^*\delta_{x_m})-(1+\frac{\Lambda t^{1-\alpha}}{\Gamma(2-\alpha)})\delta_{x_m}$, while the limit $\int_0^t S^*(t')\rho_{x_m,n}dt'\to\int_0^t S^*(t)\delta_{x_m}(t')dt'$ in $L^1(0,\ell)$ norm also holds in $\mathcal{M}_b[0,\ell]$. Since L^* is vaguely closed (Prop. 2.7.20 of [13]), the vague limit $\int_0^t S^*(t)\delta_{x_m}(t')dt'$ of $\int_0^t S^*(t')\rho_{x_m,n}dt'$ belongs to the domain of L^* in $\mathcal{M}_b[0,\ell]$ and satisfies $L^*\int_0^t S^*(t)\delta_{x_m}(t')dt'=\mu(t)$.

Hence, for each $t>0$ the strong limit $S^*(t)\delta_{x_m}$ of $S^*(t)\rho_{x_m,n}$ satisfies Eq. (14) in $\mathcal{M}_b[0,\ell]$, with δ_{x_m} instead of ψ. For x_0 in $(0,\ell)$ the strong limit $S(t)\delta_{x_0}$ of $S(t)\rho_{x_0,n}$ similarly solves (13), with $\varphi=\delta_{x_0}$.

4.4 *Equation (17) When ψ and φ are Dirac Measures*

For $t>0$, $S(t)\rho_{x_0,n}\to S(t)\delta_{x_0}$ in $\mathcal{C}[0,\ell]$, and $\rho_{x_m,n}\rightharpoonup\delta_{x_m}$ vaguely in $\mathcal{M}_b[0,\ell]$, the dual of $\mathcal{C}[0,\ell]$. Hence, $\langle\rho_{x_m,n}\cdot S(t)\rho_{x_0,n}\rangle\to\langle\delta_{x_m}\cdot S(t)\delta_{x_0}\rangle$ when $n\to\infty$ by Proposition III.12(iv) of [5]. This proves the following property.

Property 4 For $\psi=\delta_{x_m}$ and $\varphi=\delta_{x_0}$, the strong limits $S^*(t)\delta_{x_m}$ of $S^*(t)\rho_{x_m,n}$ and $S(t)\delta_{x_0}$ of $S(t)\rho_{x_0,n}$ satisfy (14) and (13). Moreover, (17) holds true when φ or ψ or both are Dirac measures.

5 Conclusion

Examining at point x_m the solution of a partial differential equation mimics localized measurement and the x_m value is in fact a duality product involving the fundamental solution of an adjoint equation started from this point. This motivates giving a meaning to such solutions. They are the basis of an inverse method valid for localized initial conditions: it retrieves their track by processing localized observations.

References

1. Schumer, R., Benson, D.A., Meerschaert, M.M., Baeumer, B.: Fractal mobile/immobile solute transport. Water Resour. Res. **39**(10), 1296 (2003)
2. Benson, D.A., Meerschaert, M.M.: A simple and efficient random walk solution of multi-rate mobile/immobile mass transport equations. Adv. Water Resour. **32**(4), 532–539 (2009)
3. Samko, S.G., Kilbas, A.A., Marichev, O.I.: Fractional Integrals and Derivatives: Theory and Applications. Gordon and Breach, New York (1993)
4. Gorenflo, R., Luchko, Y., Yamamoto, M.: Time-fractional diffusion equation in the fractional Sobolev spaces. Fract. Calc. Appl. Anal. **18**(3), 799–820 (2015)
5. Brezis, H.: Analyse Fonctionnelle, théorie et Applications. Masson, Paris (1983)
6. Levitan, B.M., Sargsjan, I.S.: Introduction to Spectral Theory: Selfadjoint Ordinary Differential Operators. Translations of Mathematical Monographs, vol. 39. American Mathematical Society, Providence (1975)
7. Luchko, Y.: Maximum principle for the generalized time-fractional differential diffusion equation. Acta. Math. Vietnam. **24**(2), 141–160 (1999)
8. Luchko, Y., Gorenflo, R.: An operational method for solving fractional differential equations with the Caputo derivatives. J. Math. Anal. Appl. **351**, 218–223 (2009)
9. Arendt, W., Batty, C.J.K., Hieber, M., Neubrander, F.: Vector-Valued Laplace Transforms and Cauchy Problems. Birkhäuser, Basel (2001)
10. Baeumer, B., Meerschaert, M.M.: Stochastic solutions for fractional Cauchy problems. Fract. Calc. Appl. Anal. **4**(4), 481–500 (2001)
11. Diethelm, K., Ford, N.J., Freed, A.D., Luchko, Y.: Algorithms for the fractional calculus: a selection of numerical methods. Comput. Methods Appl. Mech. Eng. **194**(6), 743–773 (2005)
12. Pazy, A.: Semigroups of Linear Operators and Applications to Partial Differential Equations. Applied Mathematical Sciences, vol. 44. Springer, New York (1983)
13. Jacob, N.: Pseudo Differential Operators and Markov Processes. Imperial College Press, London (2001)

Accuracy Analysis for Fractional Order Transfer Function Models with Delay

Krzysztof Oprzędkiewicz and Wojciech Mitkowski

Abstract In the paper a new accuracy estimation method for fractional order transfer functions with delay is presented. Oustaloup's recursive approximation (ORA approximation) and Charef approximation allow us to describe fractional-order systems with the use of integer-order, proper transfer function, a delay is required to be modeled with the use of Pade approximant. Results are by simulations depicted.

Keywords Fractional order transfer function · Oustaloup's recursive approximation · Approximation · Charef approximation · Time-delay systems

1 An Introduction

Fractional order models are able to properly and accurate describe a number of physical phenomena from area of electrotechnics, heat transfer, diffusion etc. Fractional - order approach can be interpreted as generalization of known integer-order models. Fractional order systems has been presented by many Authors [1–5], an example of identification fractional order system can be found in [2, 6] the proposition of generalization the Strejc transfer function model into fractional area was given in [7].

A modeling of fractional-order transfer function in MATLAB/SIMULINK requires us to apply integer order, finite dimensional, proper approximations. An important problem is to assign parameters of approximation and estimating its accuracy. The most known approximants presented by Oustaloup and Charef (see for example [4, 8–11]) base onto frequency approach. This is caused by a fact, that

K. Oprzędkiewicz (✉) · W. Mitkowski
Faculty of Electrotechnics, Automatics, Informatics and Biomedical Engineering, Department of Automatics and Biomedical Engineering, AGH University of Science and Technology, Al. Mickiewicza 30, 30-059 Cracow, Poland
e-mail: kop@agh.edu.pl

W. Mitkowski
e-mail: wojciech.mitkowski@agh.edu.pl

A. Babiarz et al. (eds.), *Theory and Applications of Non-integer Order Systems*, Lecture Notes in Electrical Engineering 407, DOI 10.1007/978-3-319-45474-0_23

for fractional order systems the Bode magnitude plot can be drawn exactly and its parameters can be applied to approximants calculation.

Additionally, for elementary fractional-order elements an analytical form of step and impulse responses can be given (see [8]). These responses can be applied as reference to estimate a correctness of built approximant.

The goal of this paper is to present a new method of accuracy estimation for non integer order transfer function models with delay. The presented method was previously applied to accuracy analysis for Oustaloup's recursive approximation (ORA approximation) and Charef approximation (see [12, 13]). It uses an analytical formula of step response for fractional order system with delay, the Medium Square Error (MSE) cost function and numerical calculations done with the use of MATLAB. The proposed approach does not require the use a step response of modeled plant.

The paper is organized as follows: at the beginning considered transfer functions with delay are presented. Next all the used approximations: ORA, Charef and Pade are remembered. Furthermore numerical calculations done with the use of MATLAB are given and final conclusions are formulated.

2 Considered Non Integer Order Transfer Functions with Delay

Let us consider an elementary fractional - order plant with delay described by the following, non integer order differential equation:

$$y(t) = T_{\alpha_1} {}_0^C D_t^{\alpha_1} u(t-\tau) + u(t-\tau). \tag{1}$$

In (1) $D_t^{\alpha_1}$ denotes an integro - differential operator calculated with the use of Caputo definition (see for example [1, 4]), τ denotes a dead time of plant and T_{α_1} denotes a time constant. If we assume, that all initial conditions are equal zero, then the plant (1) can be described by the following transfer function (2):

$$G_1(s) = \frac{e^{-\tau_1 s}}{T_{\alpha_1} s^{\alpha_1} + 1}. \tag{2}$$

In (2) T_{α_1} and $\tau_1 > 0$ are time constant and dead time respectively, $\alpha_1 \in \mathbf{R}$ is a non integer order of the plant.

The analytical form of the step response $y_{a1}(t)$ for plant described with the use of Eq. (1) and transfer function (2) is a combination of step response of non integer order system without delay (see [8, pp. 8–9]) with step response of pure delay and it can be described as follows:

$$y_{a1}(t) = L^{-1}\left\{\frac{1}{s} G_1(s)\right\} = \left(1(t-\tau_1) - E_{\alpha_1}\left(-\frac{t-\tau_1}{T_{\alpha_1}}\right)\right). \tag{3}$$

In (3) E_α denotes the one parameter Mittag–Leffler function:

$$E_\alpha(x) = \sum_{k=0}^{\infty} \frac{x^k}{\Gamma(k\alpha + 1)} \tag{4}$$

where $\Gamma(\cdot\cdot)$ denotes complete Gamma function described as underneath:

$$\Gamma(\alpha) = \int_0^\infty e^{-x} x^{\alpha-1} dx. \tag{5}$$

The second proposed model with delay has the following form:

$$G_2(s) = \frac{e^{-s\tau_2}}{(T_{\alpha_2} s + 1)^{\alpha_2}}. \tag{6}$$

Parameters of the transfer function (6) are analogical, as transfer function (2): T_{α_2} and $\tau_2 > 0$ denote time constant and dead time respectively, $\alpha_2 \in \mathbf{R}$ is a non integer order of the inertia.

The analytical form of the step response $y_{a2}(t)$ for plant described with the use of (6) follows also directly from step response formula for plant without delay (see [8, p. 9]) and it is expressed as underneath:

$$y_{a2}(t) = L^{-1}\left\{\frac{1}{s} G_2(s)\right\} = \frac{1}{(T_{\alpha_2})^{\alpha_2}} \cdot \frac{\Gamma\left(\alpha_2, \frac{t}{T_{\alpha_2}}\right)}{\Gamma(\alpha_2)}, \tag{7}$$

where $\Gamma(\alpha_2)$ denotes complete Gamma function expressed by (5) and

$$\Gamma\left(\alpha_2, \frac{t}{T_{\alpha_2}}\right)$$

is the incomplete Gamma function:

$$\Gamma\left(\alpha, \frac{t}{T_\alpha}\right) = \int_0^{\frac{t}{T_\alpha}} e^{-x} x^{\alpha-1} dx. \tag{8}$$

Let us assume, that the step responses described by (3) or (7) are accurate responses. This implies, that they can be applied as the reference to estimate an accuracy of approximations.

3 Approximations

3.1 The Oustaloup's Recursive Approximation (ORA Approximation)

The method proposed by Oustaloup (see for example [11]) allows us to approximate an elementary non-integer order transfer function s^α with the use of a finite and integer-order approximation expressed as underneath:

$$s^\alpha \cong G_{ORA}(s) = k_f \prod_{n=1}^{N_{ORA}} \frac{1+\frac{s}{\mu_n}}{1+\frac{s}{\nu_n}} = \frac{L_{ORA}(s)}{D_{ORA}(s)}. \tag{9}$$

In (9) N_{ORA} denotes the order of approximation, μ_n and ν_n denote coefficients calculated as underneath:

$$\begin{gathered} \mu_1 = \omega_l \sqrt{\eta}, \qquad \nu_n = \mu_n \gamma, \qquad n = 1, \ldots, N, \\ \mu_{n+1} = \nu_n \eta, \qquad n = 1, \ldots, N-1 \end{gathered} \tag{10}$$

where:

$$\gamma = \left(\frac{\omega_h}{\omega_l}\right)^{\frac{\alpha}{N}}, \qquad \eta = \left(\frac{\omega_h}{\omega_l}\right)^{\frac{1-\alpha}{N}}. \tag{11}$$

In (11) ω_l and ω_h describe the range of angular frequency, for which parameters are calculated. For convenience during further analysis let us assume, that this frequency range is logarithmically scaled and expressed by the number P:

$$\omega_l = 10^{-P}, \qquad \omega_h = 10^P. \tag{12}$$

A steady–state gain k_f is calculated to assure the convergence the step response of approximation to step response of the real plant in a steady state.

It was proven (see for example [13]) that the frequency range ω_l and ω_h strongly determines the accuracy of ORA approximation.

3.2 The Charef Approximation

The Charef approximation allows us to approximate fractional order transfer function, described by (5) with the use of integer order transfer function $G_{char}(s)$ described as underneath (see [9]):

$$G_{Ch}(s) = \frac{L_{Ch}(s)}{D_{Ch}(s)} = \frac{\prod_{i=0}^{N_{Ch}-1}\left(1+\frac{s}{z_i}\right)}{\prod_{i=0}^{N_{Ch}}\left(1+\frac{s}{p_i}\right)}. \tag{13}$$

In (13) N_{Ch} denotes order of approximation, z_i and p_i denote zeros and poles of approximation. They can be calculated with the use of transfer function (1) pole p_α and fractional order α:

$$\begin{gathered} p_\alpha = \frac{1}{T_\alpha}, \qquad p_0 = p_\alpha \sqrt{b}, \\ p_i = p_0 (ab)^i, \qquad i = 1, \ldots, N, \qquad z_i = a p_0 (ab)^i, \qquad i = 1, \ldots, N-1 \end{gathered} \tag{14}$$

where:

$$a = 10^{\frac{\Delta}{10(1-\alpha)}}, \qquad b = 10^{\frac{\Delta}{10\alpha}}. \tag{15}$$

In (15) Δ denotes a maximal permissible error of approximation, defined as the maximal difference between Bode magnitude plots for model and plant, expressed in [dB].

The order N_{Ch} of Charef approximation can be assigned to minimize the assumed, maximal approximation error Δ (see [9]):

$$N_{Ch} = \left\lceil \frac{\log\left(\frac{\omega_{max}}{p_0}\right)}{\log(ab)} \right\rceil + 1. \tag{16}$$

In (16) ω_{max} denotes the angular frequency, for which the maximal error is achieved. If the value of N_{Ch} with respect to (16) is non-integer, it should be rounded to nearest integer.

3.3 The Pade Approximation

Pade approximation is a classic tool to estimate delay element $e^{-\tau s}$ with the use of rational, integer order transfer function. There are known different versions of this approximant (see for example [14]). The most known is described as underneath:

$$e^{-\tau s} \cong G_p(s) = \frac{2 + \sum_{m=1}^{M} \frac{(-\tau s)^m}{m!}}{2 + \sum_{m=1}^{M} \frac{(\tau s)^m}{m!}} = \frac{L_p(s)}{D_p(s)}, \tag{17}$$

where M denotes the order of Pade approximation.

3.4 The Approximations of the Whole Model

After inserting the both approximants (9) and (17) to the transfer function (2) we obtain:

$$G_{apr1}(s) = \frac{L_p(s)D_{ORA}(s)}{T_\alpha L_{ORA}(s)D_p(s) + D_{ORA}(s)D_p(s)}. \tag{18}$$

The summarized order of approximant transfer function (18) is equal $N_{ORA} + M$. Analogically the approximation of transfer function (5) can be written with the use of (9) and (13):

$$G_{apr2}(s) = \frac{L_p(s)L_{Ch}(s)}{D_p(s)D_{Ch}(s)}. \tag{19}$$

The step response of each approximation (18) or (19) is expressed as underneath:

$$y_{apr_{1,2}}(t) = L^{-1}\left\{\frac{G_{apr_{1,2}}(s)}{s}\right\}. \tag{20}$$

4 Cost Function Describing the Accuracy of Approximations

Let us assume, that the step response $y_a(t)$ described by (3) or (6) is the accurate response. In real situation it is calculated in discrete time moments $k = 1, \ldots, K_s$ and with sample time h. Then $y^+(k) = y(kh)$. Analogically $y^+_{apr}(k)$ is the step response of approximation, described by (20) and calculated along the same, discrete time grid. Consequently the approximation error $e^+(k)$, calculated in discrete time moments $1, \ldots, K_s$ is defined as follows:

$$e^+(k) = y^+_a(k) - y^+_{apr}(k), \qquad k = 1, \ldots, K_s. \tag{21}$$

The accuracy of the approximation can be estimated with the use of typical Medium Square Error (MSE) cost function:

$$MSE = \frac{1}{K_s}\sum_{k=1}^{K_s}\left(e^+(k)\right)^2. \tag{22}$$

The cost function (22) for given plant (described by $\tau_{1,2}$, $T_{\alpha_{1,2}}$ and $\alpha_{1,2}$) is a function of approximation parameters: orders M, N_{Ch}, N_{ORA} and angular frequency range described by P in the case of ORA approximation and maximal error Δ for Charef approximation.

It is known (see [13]) that decreasing P improves the accuracy of ORA approximant for separated element s^{α}, but an influence of this parameter on accuracy of the whole transfer function (2) is not obvious and it should be tested also. The same was checked in the case of Charef approximation (see [12]) and parameter Δ.

Next it can be expected, that increasing both orders N_{Ch}, N_{ORA} and M should increase an approximant quality, described by cost function (22). However, results of previous investigations done by authors point, that too high value of N_{Ch}, or N_{ORA} can cause bad conditioning of a model and consequently, make it useless.

Furthermore – in the considered case an additional problem can appear – for particular values parameters of each applied approximant the cancellation of some poles and roots in approximating transfer function (18) or (19) can appear. This is a separated important problem, close to issue considered in the paper [10]. This will be tried to solve during further investigations.

The fastest method to check proper setting the approximation orders N_{Ch}, or N_{ORA}, M is to calculate the cost function MSE (22) as a function of these orders. Such a setting will be shown in the next section.

5 Examples

As a first example let us consider the optimal order tuning for transfer function in the form (2) with the following values of parameters:

$$G_1(s) = \frac{e^{-22s}}{47s^{1.03} + 1}. \tag{23}$$

The numerical finding of optimal orders M and N can be done with the use of known approach presented for example in [15, p. 572]. It consists in calculating cost function (22) for increasing values of orders M and N_{ORA}. If the significant improvement of cost function during crossing from M to $M + 1$ and analogically between N_{ORA} and $N_{ORA} + 1$ is observed, then estimated orders of model are equal $M + 1$ and $N_{ORA} + 1$ respectively. Optimal orders of model 1 for transfer function (23) obtained with the use of the above approach and cost function (22) are given in Table 1. The comparison of analytical and approximated step response are shown in Fig. 2.

As the second example the model expressed by transfer function (24) was tested. The MSE cost function (22) as a function of both approximation orders is shown in Fig. 3.

Table 1 Optimal orders of approximated model 1

M	N_{ORA}	MSE
4	6	8.0746e-04

Table 2 Optimal orders of approximated model 2

M	N_{Ch}	MSE
6	7	3.0922e-08

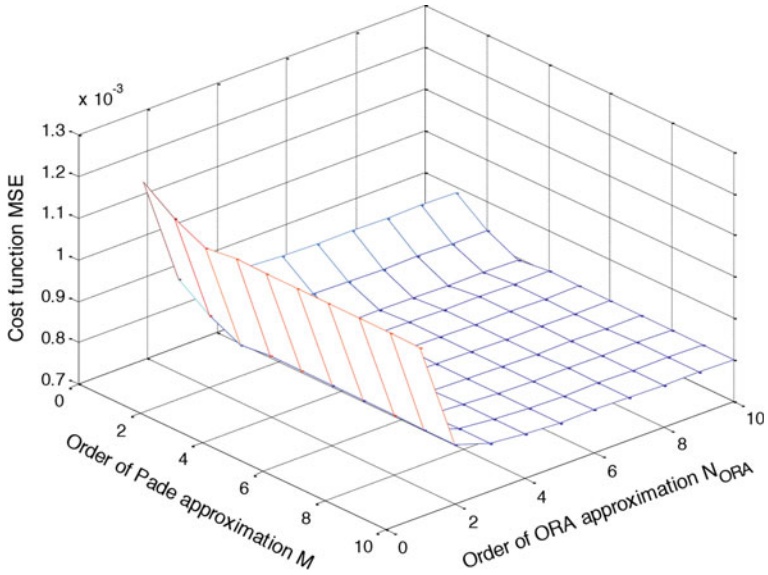

Fig. 1 Cost function (22) as a function of orders: M and N_{ORA} for model 1

$$G_2(s) = \frac{e^{-22s}}{(45s+1)^{0.75}} \tag{24}$$

Optimal orders of model 2 for transfer function (24) obtained with the use of the above approach and cost function (22) are given in Table 2. The comparison of analytical and approximated step response are shown in Fig. 4.

From Tables 1 and 2 and Figs. 1, 2, 3 and 4 it turns out that model 2, described by transfer function (5) and approximated with the use of Charef approximation is much more accurate, than the model 1, described by transfer function (2) and using ORA approximation. Next–the good accuracy of the both tested models is achieved for relatively low orders of all used approximants: Pade, ORA and Charef.

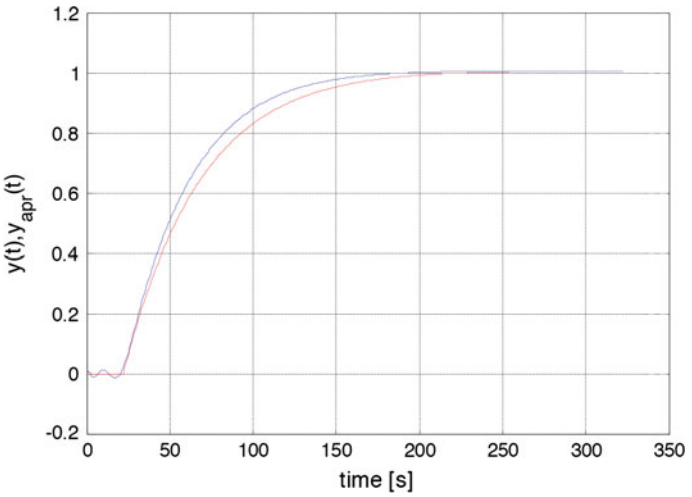

Fig. 2 Analytical (*red*) and approximated (*blue*) step responses for model 1

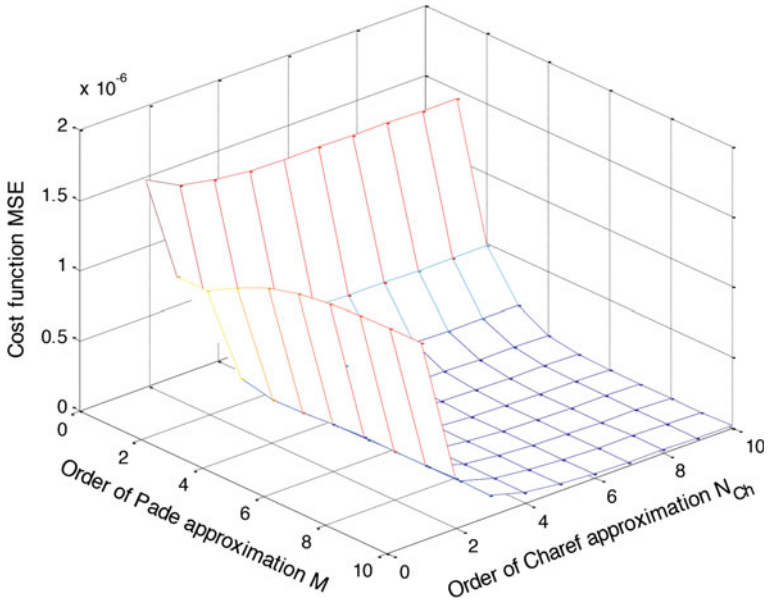

Fig. 3 Cost function (22) as a function of orders: M and N_{Ch} for model 2

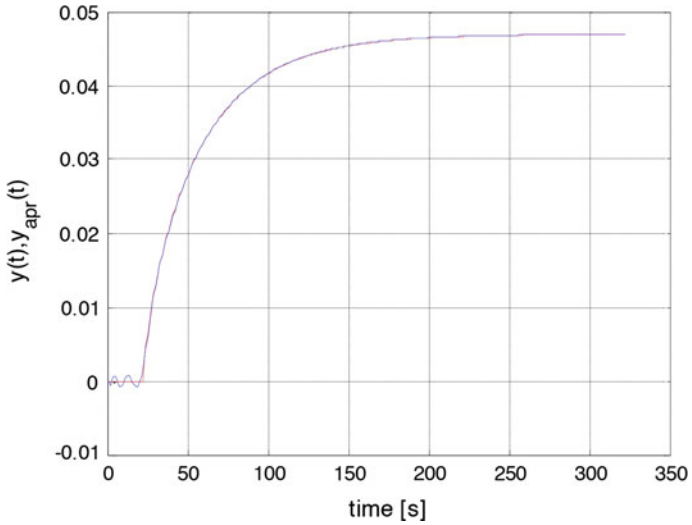

Fig. 4 Analytical (*red*) and approximated (*blue*) step responses for model 2

6 Final Conclusions

The final conclusions for the paper can be formulated as follows:

- The model in the form of non integer order inertial plant with delay (5) is much more accurate in the sense of *MSE* cost function than non integer order model with delay, expressed by transfer function (2).
- The convergence of the both considered models is good, because the good accuracy is achieved for relatively low orders of used approximations.
- Results of tests for the model (2) using ORA approximation point, that the proposed form of non integer order transfer function should be approximated with the use of another methods, which should be proposed. This is going to be the area of further investigations.
- An important issue, which should be considered, is a problem of partial cancellation poles and zeros in transfer functions using both Pade and Charef or ORA approximation. This phenomenon can appear for certain combination of approximation parameters and it will cause the loosing of approximation accuracy. Similar problem during use the Charef approximation was discussed in paper [10]. The analysis of use concatenation of Pade and ORA/Charef approximation should also be presented and it is going to be presented as a sequel of this paper.

Acknowledgments This paper was supported by the AGH (Poland) – project no 11.11.120.817.

References

1. Kaczorek, T.: Selected Problems in Fractional Systems Theory. Springer, New York (2011)
2. Mitkowski, W., Obrączka, A.: Simple identification of fractional differential equation. Solid State Phenom. **180**, 331–338 (2012)
3. Mitkowski, W., Skruch, P.: Fractional-order models of the supercapacitors in the form of RC ladder networks. Bull. Pol. Acad.: Tech. **61**(3), 581–587 (2013)
4. Podlubny, I.: Fractional Differential Equations. Academic Press, San Diego (1999)
5. Vinagre, B.M., Podlubny, I., Hernandez, A., Feliu, V.: Some approximations of fractional order operators used in control theory and applications. Fract. Calc. Appl. Anal. **3**(3), 231–248 (2000)
6. Oprzędkiewicz, K.: A Strejc model-based, semi-fractional (SSF) transfer function model. Automatyka/Automatics; AGH UST **16**(2), 145–154 (2012)
7. Mitkowski, W.: Finite-dimensional approximations of distributed RC networks. Bull. Pol. Acad.: Tech. **62**(2), 263–269 (2014)
8. Caponetto, R., Dongola, G., Fortuna, L., Petras, I.: Fractional Order Systems. Modeling and Control Applications. World Scientific Series on Nonlinear Science, Series A, vol. 72. World Scientific Publishing, Singapore (2010)
9. Charef, A., Sun, H.H., Tsao, Y.Y., Onaral, B.: Fractal system as represented by singularity function. IEEE Trans. Autom. Control **37**(9), 1465–1470 (1992)
10. Oprzędkiewicz, K.: Approximation method for a fractional order transfer function with zero and pole. Arch. Control Sci. **24**(4), 409–425 (2014)
11. Oustaloup, A., Levron, F., Mathieu, B., Nanot, F.M.: Frequency-band complex noninteger differentiator: characterization and synthesis. IEEE Trans. Circuits Syst. I. Fundam. Theory **47**(1), 25–39 (2000)
12. Mitkowski, W., Oprzędkiewicz, K.: An estimation of accuracy of Charef approximation. In: Domek, S., Dworak, P. (eds.) Theoretical Developments and Applications of Non-Integer Order Systems: 7th Conference on Non-Integer Order Calculus and Its Applications. Lecture Notes in Electrical Engineering, vol. 357, pp. 71–80. Springer, New York (2016)
13. Oprzędkiewicz, K., Mitkowski, W., Gawin, E.: An estimation of accuracy of Oustaloup approximation. In: Szewczyk, R., et al. (eds.) Challenges in Automation, Robotics and Measurement Techniques. Advances in Intelligent Systems and Computing, vol. 440, pp. 299–307. Springer, New York (2016)
14. Vajta, M.: Some remarks on Pade-approximations. In: Proceedings of the 3rd TEMPUS-INTCOM Symposium (2000)
15. Isermann, R., Muenchhof, M.: Identification of Dynamic Systems. An Introduction with Applications. Springer, New York (2011)

Accuracy Estimation of Digital Fractional Order PID Controller

Krzysztof Oprzędkiewicz

Abstract In the paper an accuracy estimation method for digital fractional order PID controller is discussed. Integral and derivative parts of a controller are approximated with the use of Power Series Expansion (PSE) and Continuous Fraction Expansion (CFE) methods. These approximations are fundamental tools to modeling fractional-order elements with the use of integer-order, discrete, proper transfer function in the form of FIR or IIR filter. The accuracy of each approximation is a function of its order and other parameters. It can be estimated via comparison of step responses: analytical and approximated in sample moments. The step response expressed by accurate analytical formula can be interpreted as a standard. Approach presented in the paper can be applied during implementation of FO PID at each digital platform (microcontroller, PLC). Results of simulations show, that the CFE approximation allows us to build a FO PID controller so accurate, as constructed with the use of PSE, but much more simple to implementation, because its order is significantly lower.

Keywords Digital fractional order PID controller · PSE approximation · CFE approximation

1 An Introduction

One of main areas of application fractional order calculus in automation is a fractional order PID control (FO PID control). Results presented by many Authors [1–5] show that FO PID controller is able to assure the better control performance than classic integer order PID controller.

An implementation of FO PID controller at each digital platform (PLC, microcontroller) requires us to apply integer order, finite dimensional, discrete approximant.

K. Oprzędkiewicz (✉)
Faculty of Electrotechnics, Automatics, Informatics and Biomedical Engineering,
Deptartment of Automatics and Biomedical Engineering, AGH University
of Science and Technology, Al. Mickiewicza 30, 30-059 Cracow, Poland
e-mail: kop@agh.edu.pl

A. Babiarz et al. (eds.), *Theory and Applications of Non-integer Order Systems*,
Lecture Notes in Electrical Engineering 407, DOI 10.1007/978-3-319-45474-0_24

The most known are: Power Series Expansion (PSE) approximation and Continuous Fraction Expansion (CFE) approximation (see for example [1, 2, 6, 7]). They allow us to estimate a non integer order element with the use of digital filter. The detailed comparison of the both methods was done for example in [2]. In this paper it was marked that the CFE is a more effective method according to the PSE method, but there are some restrictions for the correct choice of the sampling period.

For elementary fractional-order integrator/differentiator an analytical form of step and impulse responses are known (see [1]) These responses can be applied as reference to estimate a correctness and accuracy of tested approximants.

The goal of this paper is to discuss an accuracy estimation of PSE and CFE approximations describing a Fractional Order PID controller (FO PID) with the use of a method proposed by author in papers [8, 9]. The presented approach uses analytical formula of controller's step response, known MSE cost function and numerical calculations done with the use of MATLAB. Proposed method will be also applied to compare of both approximants in the sense of accuracy and numerical complexity.

It is important to notice that the proposed method is dedicated only to optimal tune of approximants, and this problem is independent on optimal tuning FO PID parameters, which should be always dedicated to certain controlled plant.

The paper is organized as follows: at the beginning elementary ideas are remembered. Next the tested PSE and CFE approximations are presented and method of its optimal tuning is proposed. Results are illustrated by simulations done with the use of MATLAB.

2 Preliminaries

A non integer order operator is generally described as underneath (see for example [1]):

$$ {}_aD_t^{\alpha} f(t) = \begin{cases} \frac{d^{\alpha} f(t)}{dt^{\alpha}} & \alpha > 0 \\ 1 & \alpha = 0 \\ \int_a^t f(\tau)(d\tau)^{-\alpha} & \alpha < 0 \end{cases} . \tag{1} $$

In (1) α denotes a non integer order of operation, a, t denote a time interval to calculate operator. The operator (1) can be described by different definitions given by Grünwald and Letnikov (GL definition), Riemann and Liouville (RL definition) and Caputo, but a discretization of the operator (1) can be done most naturally and easily with the use of Grünwald–Letnikov definition, given underneath:

$$ {}_aD_t^{\alpha} f(t) = \lim_{h \to 0} h^{-\alpha} \sum_{j=0}^{\left[\frac{t-a}{h}\right]} (-1)^j \binom{\alpha}{j} f(t - jh). \tag{2} $$

In (2) h is a step of discretization, [..] denotes an integer part, $\binom{\alpha}{j}$ is a generalization of Newton symbol into real numbers:

$$\binom{\alpha}{j} = \begin{cases} 1 & \text{dla } j = 0 \\ \frac{\alpha(\alpha-1)\ldots(\alpha-j+1)}{j!} & \text{dla } j > 0 \end{cases}. \tag{3}$$

For fractional order systems an idea of transfer function can be also given and its form is analogical as for integer order systems.

Let us consider an elementary non-integer order PID controller described by the transfer function (4):

$$G_c(s) = k_p + \frac{k_I}{s^\alpha} + k_D s^\beta. \tag{4}$$

In (4) α, $\beta \in \mathbf{R}$ are fractional-orders of integral and derivative actions, k_P, k_I, k_D are coefficients or proportional, integral and derivative actions of controller. The analytical form of the step response $y_a(t)$ for the above controller can be calculated with the use of [1, p. 5] and it has the following form:

$$y_a(t) = L^{-1}\left\{\frac{1}{s}\left(k_p + \frac{k_I}{s^\alpha} + k_D s^\beta\right)\right\} = k_p + k_I \cdot \frac{t^\alpha}{\Gamma(\alpha+1)} + k_D \cdot \frac{t^{-\beta}}{\Gamma(1-\beta)} \tag{5}$$

where $\Gamma(..)$ denotes complete Gamma function:

$$\Gamma(\alpha) = \int_0^\infty e^{-x} x^{\alpha-1} dx. \tag{6}$$

Let us assume, that the continuous-time step response described by (5) and (6) is the accurate response. It will be applied to accuracy estimation as a standard.

3 The Considered Discrete Approximations

The PSE approximation bases directly onto GL definition given by (2) and it has the following form:

$$\left(k - \frac{L_m}{h}\right)^{D_{kh}^\alpha f(k) \cong h^{-\alpha} \sum_{j=0}^{k} (-1)^j \binom{\alpha}{j} f_{k-j}}. \tag{7}$$

In (7) L_m denotes the "memory length", h is the size of time step, $(-1)^j\binom{\alpha}{j}$ are coefficients calculated as underneath:

$$c_0^{(\alpha)} = 1, \qquad c_j^{(\alpha)} = \left(1 - \frac{1+\alpha}{j}\right) c_{j-1}^{(\alpha)}. \tag{8}$$

It is important to notice that PSE leads to approximation in the form of polynomials, that is, the discretized fractional operator has the form of a FIR filter, which has only zeros. The resulting discrete transfer function, obtained by approximating fractional-order operators, can be expressed in the z-domain as underneath:

$$ {}_0D_{kh}^{\alpha} f(t) \cong h^{-\alpha} PSE \left\{ \left(1 - z^{-1}\right)^{\alpha} \right\}_n = h^{-\alpha} R_n(z^{-1}), \tag{9} $$

where $z = e^{sh}$. Coefficients of the transfer function (9) can be calculated for example with the use of MATLAB function *dfod2* available at [4]. This function will be applied in calculations.

An alternative form of integer order, finite dimensional approximant for non integer order operator can be obtained with the use of Continuous Fraction Expansion (CFE) approximation (see for example [1, p. 14]).

$$ {}_0D_{kh}^{\alpha} f(t) \cong \left(\frac{1+a}{h}\right)^{\pm\alpha} \left(\frac{1-z^{-1}}{1+az^{-1}}\right)^{\pm\alpha} = \left(\frac{1+a}{h}\right)^{\pm\alpha} CFE\{...\}. \tag{10} $$

The CFE transfer function (10) has the form of discrete, n–th order IIR filter containing both poles and zeros. Coefficients of it can be calculated for example with the use of MATLAB function *dfod1* available at [11]. This function will be also applied during numerical optimization of FO PID.

4 Cost Function Describing the Accuracy of Approximations

Denote the step response of considered FO PID calculated in sampling moments by $y^{+}(k)$:

$$ y_a^{+}(k) = y_a(kh), \qquad k = 1, 2, \ldots \tag{11} $$

Let $y_{PSE}^{+}(k)$ or $y_{CFE}^{+}(k)$ denotes the step response of the discrete, approximated controller in k–th time moment. Then the approximation error $e_{PSE,CFE}^{+}(k)$ can be defined as follows:

$$ e_{PSE,CFE}(k) = y_a^{+}(k) - y_{PSE,CFE}^{+}(k). \tag{12} $$

The quality of approximation can be estimated with the use of typical MSE cost function (see for example [12]):

$$ MSE_{PSE,CFE} = \frac{1}{K_s} \sum_{k=1}^{K_s} e_{PSE,CFE}^{+}(k). \tag{13} $$

In (13) K_s denotes a number of all collected samples, $e^{+}_{PSE,CFE}(k)$ is the approximation error of each approximant, described by (12).

To estimate the order of each considered approximant, assuring the reasonable value of cost function (13) can be applied an approach presented in [12, pp. 573, 574].

A criterion to determine an approximation order is the rate of change the cost function (13) as a function of model order. If the increase of order causes firstly big and next small improvement of calculated cost function, then this "threshold" value of order can be interpreted as a its sensible value. This idea will be applied during experiments.

5 Experiments

As an example let us consider an application of both PSE and CFE approximations to model the FO PID controller described by (4). During all experiments the coefficients of controller were constant and equal: $k_p = 1.0$, $k_I = 1.0$ and $k_D = 1.0$, parameters of the approximation for the both parts I and D of controller were the same. All results are collected in the Table 1. Firstly the PSE approximation (9) was tested. Calculations were done for different values of memory length, non integer orders α, β and different values of sample time and with the use of MATLAB function *dfod2* [4]. Results are given in Figs. 1, 2 and 3 and the Table 1.

Next CFE approximation (10) was tested with the use of analogical approach, as above. Calculations were done with the use of MATLAB function *dfod1* [11]. The Euler method (parameter $a = 0$) was applied. Results are shown in Figs. 4, 5 and 6 and Table 1 also.

From Table 1 it can be concluded at once that:

- Shorter sample time assures the better quality of approximation in the sense of MSE cost function, but the convergence of approximation is slower,

Table 1 "Threshold" values of memory length L_m, (PSE) and approximation order (CFE) for different α, β and h in both tested approximations

h [s]	α	β	Threshold value of L_m	MSE_{PSE}	Threshold value of n	MSE_{CFE}
0.1	0.5	0.5	48	$8.3639e-004$	5	$8.6111e-004$
	0.2	0.8	40	$1.0098e-004$	5	$1.1601e-004$
	0.8	0.2	47	0.0039	4	0.0033
0.2	0.5	0.5	25	0.0027	4	0.0027
	0.2	0.8	20	$2.2611e-004$	4	$2.0808e-004$
	0.8	0.2	25	0.0155	2	0.0138

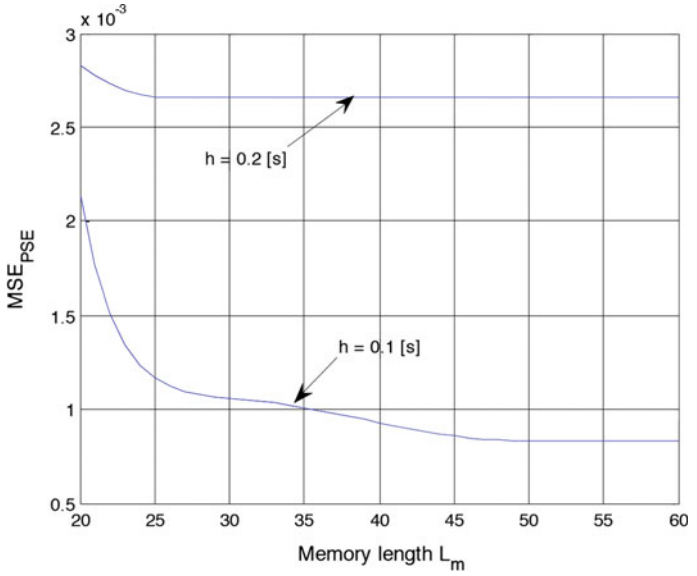

Fig. 1 PSE approximation: MSE cost function for different memory length, different sample time and non integer orders equal: $\alpha = 0.5$, $\beta = 0.5$

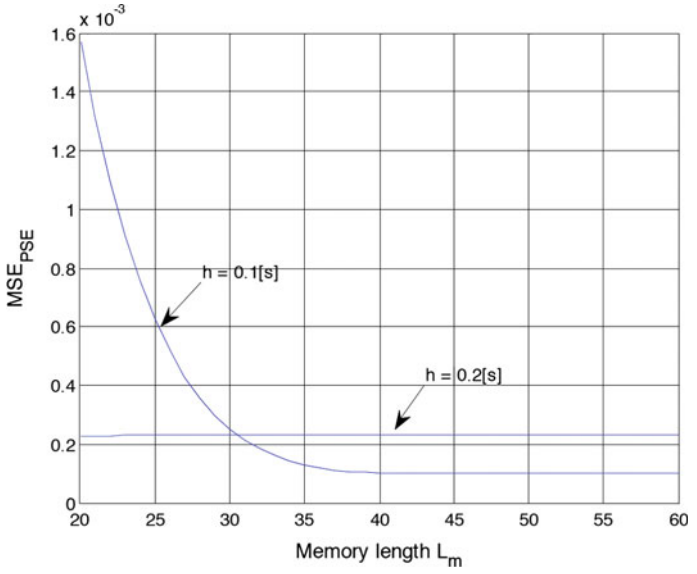

Fig. 2 PSE approximation: MSE cost function for different memory length, different sample time and non integer orders equal: $\alpha = 0.2$, $\beta = 0.8$

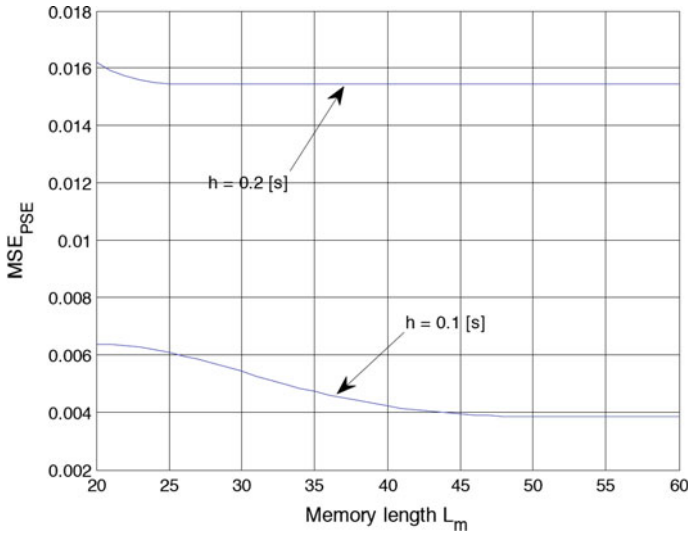

Fig. 3 PSE approximation: MSE cost function for different memory length, different sample time and non integer orders equal: $\alpha = 0.8$, $\beta = 0.2$

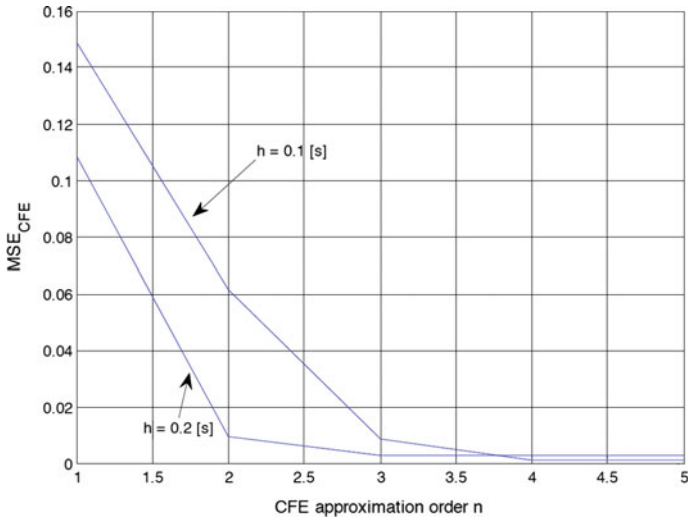

Fig. 4 CFE approximation: MSE cost function for approximation order n, different sample times and non integer orders equal: $\alpha = 0.5$, $\beta = 0.5$

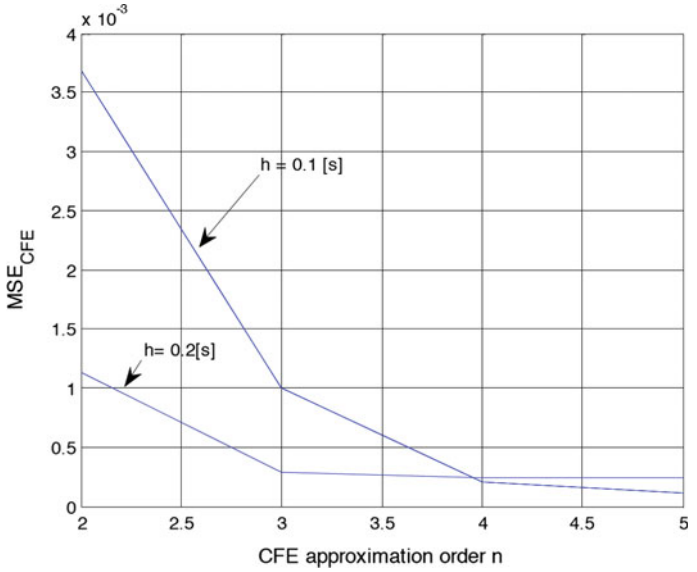

Fig. 5 CFE approximation: MSE cost function for different approximation order n, different sample time and non integer orders equal: $\alpha = 0.2$, $\beta = 0.8$

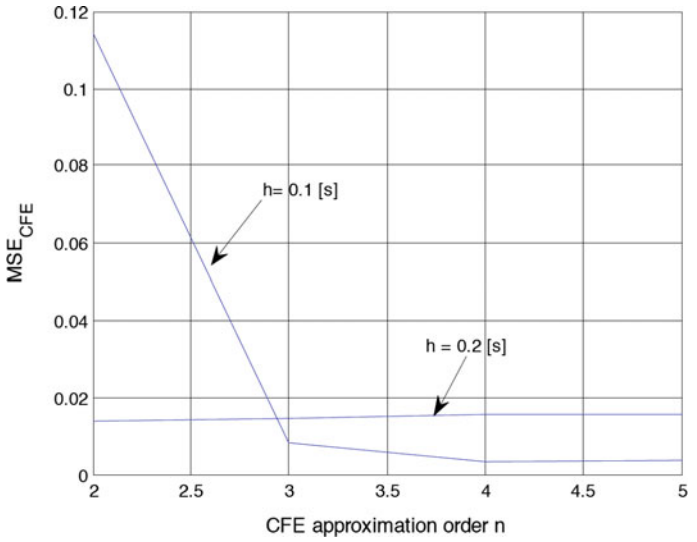

Fig. 6 CFE approximation: MSE cost function for different approximation order n, different sample time and non integer orders equal: $\alpha = 0.8$, $\beta = 0.2$

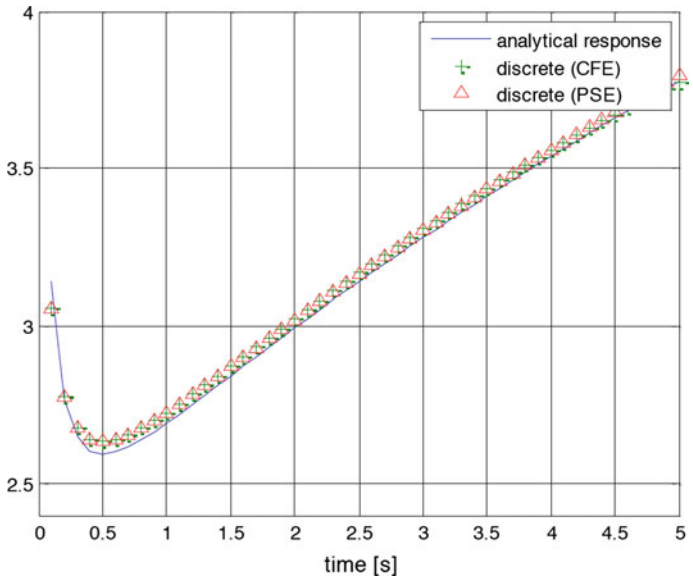

Fig. 7 Step response of FO PID controller and both its approximants, $L_m = 48$, $n = 5$, sample time $h = 0.1[s]$ and non integer orders: $\alpha = 0.5$, $\beta = 0.5$

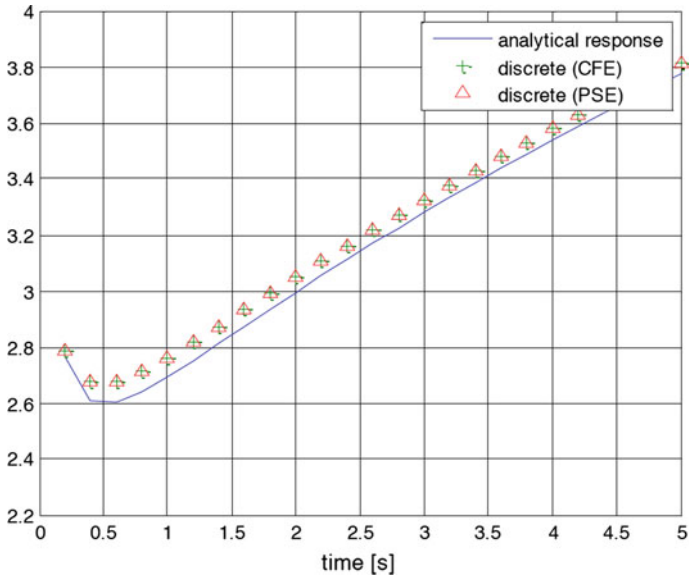

Fig. 8 Step response of FO PID controller and both its approximants, $L_m = 48$, $n = 5$, sample time $h = 0.2[s]$ and non integer orders: $\alpha = 0.5$, $\beta = 0.5$

- The accuracy of the both PSE and CFE methods for the same sample time and non integer orders is very close, but the order of CFE approximation is significantly lower, than PSE approximation.

Examples of step responses of considered FO PID controller for different sample times are given in Figs. 7 and 8.

6 Final Conclusions

The final conclusions from the paper can be formulated as follows: The both tested approximation methods well describe a behavior of a FO PID controller at digital platform.

The order of CFE approximation necessary to obtain the good accuracy is significantly shorter that order of the PSE approximation assuring the close accuracy. This implies that to implementation at digital platform with bounded resources (for example PLC, microcontroller) is recommended the use of CFE.

Results shown in the paper will be applied during implementation FO PID at PLC platform.

Acknowledgments This paper was supported by the AGH (Poland) – project no 11.11.120.815.

References

1. Caponetto, R., Dongola, G., Fortuna, L., Petras, I.: Fractional Order Systems. Modeling and Control Applications. World Scientific Series on Nonlinear Science, Series A, vol. 72. World Scientific Publishing, Singapore (2010)
2. Dorcak, L., Petras, I., Terpak, J., Zbrojovan, M.: Comparison of the methods for discrete approximation of the fractional-order operator. In: Proceedings of the Carpathian Control Conference, pp. 851–856 (2003)
3. Ostalczyk, P.: Discrete Fractional Calculus. Applications in Control and Image Processing Series in Computer Vision, vol. 4. World Scientific Publishing, Singapore (2016)
4. Petras, I.: Realization of fractional order controller based on PLC and its utilization to temperature control. Transfer Inovaci **14**, 34–38 (2009)
5. Vinagre, B.M., Podlubny, I., Hernandez, A., Feliu, V.: Some approximations of fractional order operators used in control theory and applications. Fract. Calc. Appl. Anal. **3**(3), 231–248 (2000)
6. Al Aloui, M.A.: Dicretization methods of fractional parallel PID controllers. In: Proceedings of 6th IEEE International Conference on Electronics, Circuits and Systems, pp. 327–330 (2009)
7. Oustaloup, A., Levron, F., Mathieu, B., Nanot, F.M.: Frequency-band complex noninteger differentiator: characterization and synthesis. IEEE Trans. Circuits Syst. I. Fundam. Theory **47**(1), 25–39 (2000)
8. Mitkowski, W., Oprzędkiewicz, K.: An estimation of accuracy of Charef approximation. In: Domek, S., Dworak, P. (eds.) Theoretical Developments and Applications of Non-integer Order Systems : 7th Conference on Non-integer Order Calculus and Its Applications. Lecture Notes in Electrical Engineering, vol. 357, pp. 71–80. Springer (2016)

9. Oprzędkiewicz, K., Mitkowski, W., Gawin, E.: An estimation of accuracy of Oustaloup approximation. In: Szewczyk, R. et al. (eds.) Challenges in Automation, Robotics and Measurement Techniques. Advances in Intelligent Systems and Computing, vol. 440, pp. 299–307. Springer, Heidelberg (2016)
10. Petras I: http://people.tuke.sk/igor.podlubny/USU/matlab/petras/dfod1.m
11. Petras I: http://people.tuke.sk/igor.podlubny/USU/matlab/petras/dfod2.m
12. Isermann, R., Muenchhof, M.: Identification of Dynamic Systems. An Introduction with Applications. Springer, Heidelberg (2011)

Modeling of Fractional-Order Integrators and Differentiators Using Tustin-Based Approximations and Model Order Reduction Techniques

Marek Rydel, Rafał Stanisławski, Marcin Gałek and Krzysztof J. Latawiec

Abstract This paper presents a set of low-order approximators/dis-cretizers of fractional order derivative and integrator. The approximations are obtained using the Frequency Weighted (FW) reduction method applied to a high order Tustin–Muir based model of fractional-order derivative and integrator. Simulation examples confirm high accuracy of the models both in frequency and time domains. This illustrates the usefulness of the introduced methodology, which can be applied to selection of a set of relatively low order discrete-time approximators of fractional-order derivative and integrator.

Keywords Fractional-order system · Discrete-time systems · Approximation

1 Introduction

Both for integer- and noninteger-order systems there are three main methods for discretization of continuous time systems, providing transformation from the s to z domains. These include (1) the classical transformations based on the rectangular rule, called the Euler method [1], (2) the trapezoidal rule, called the Tustin method [2] and (3) the Al-Alaoui method which combines the above two methods using specific weighting coefficient [3, 4]. The most commonly used method is the rectangular integration rule, which can be simply obtained by the use of the generalized Newton expansion. However, its FIR structure requires a large number of model elements to provide discrete-time 'equivalence' of continuous time system. The trapezoidal integration rule leads to the IIR structured discrete-time model, with relatively low

M. Rydel · R. Stanisławski · M. Gałek · K.J. Latawiec (✉)
Department of Electrical, Control and Computer Engineering,
Opole University of Technology, Opole, Poland
e-mail: k.latawiec@po.opole.pl

M. Rydel
e-mail: m.rydel@po.opole.pl

R. Stanisławski
e-mail: r.stanislawski@po.opole.pl

A. Babiarz et al. (eds.), *Theory and Applications of Non-integer Order Systems*,
Lecture Notes in Electrical Engineering 407, DOI 10.1007/978-3-319-45474-0_25

number of elements. However, it causes the 'wrapping effect' due to its nonlinearity [3, 4]. The Al-Alaoui operator combines the above two methods to minimize the wrapping effect of the Tustin operator. The Al-Alaoui operator is determined by the coefficient $\beta \in [0, 1]$ which weights the shares of of the Euler and Tustin methods in the Al-Alaoui operator. Other approaches behind that research direction are based on the Laguerre functions approach [5, 6] leading to direct discretization of the Grünwald–Letnikov (GL) fractional order derivative. The approach uses the Laguerre filters rather than e.g. FIR ones. It enables to use a low number of elements in the Laguerre-based model and yet to provide a high approximation accuracy [6, 7].

There are two main methods of practical implementation for the Tustin operator i.e. (1) using the continued fraction expansion (CFE) method [8] and (2) using the Muir recursion [7]. The CFE-based Tustin method yields to good approximation accuracy but can cause numerical problems ending up with a low upper limit of implementation length for CFE-Tustin approximator. Accurate approximation in a wide range of frequencies for the fractional-order integrators and differentiators using the recursive Tustin–Muir algorithm requires a very complex model which is not useful from the computational point of view. For this reason, the ability of proper reduction of the model complexity in a given adequacy scope becomes a significant issue. Reduction of a model is not a unique operation and there are several ways to reduce the order of the model [9–11]. Among them, the techniques based on the truncation of balanced realization are given a great interest. The Balanced Truncation Approximation (BTA) method determines the model by eliminating the low-energy and hard-to-reach states in the state space model. The reduction method guarantees that H_∞-norm of difference between full and reduced-order models is upper bounded by twice the sum of the neglected Hankel singular values [11, 12]. However, for the integrator and differentiator the magnitude of frequency response varies significantly with frequency. Therefore, a reduced model obtained by the BTA reduction requires a large number of states to provide an accurate approximation of frequency-domain characteristics in a wide frequency range.

The paper is organized as follows. Having introduced the approximation/discretization problem for fractional-order systems in Sect. 1, the Tustin-based approximations for fractional-order derivative and integrator are recalled in Sect. 2. An application of the SVD-based method in terms of the FW approach to high order Tustin–Muir approximation is presented in Sect. 3. Results and simulation analysis of the introduced methodology is shown in Sect. 4 and conclusions of Sect. 5 complete the paper.

2 Fractional-Order Integrator and Differentiator

One of the most commonly used discretization and practical implementation methods for both 'regular' (integer order) and fractional-order derivatives and integrals is the trapezoidal rule, called the Tustin method. This approach has two advantages (1) the conversion of the left half of the s-plane strictly into the inside of the unit

circle in the textitz-plane (2) warranty that the imaginary axis of the textits-plane is exactly mapped onto the unit circle circumference in the textitz-plane (see e.g. [4]). The disadvantage of the Tustin-based discretization is the occurrence of the wrapping effect in the magnitude characteristic at high frequencies. Discretization of fractional-order derivative and integrator using the Tustin operator is realized as

$$s^{\alpha} \approx \left(\frac{\Delta}{T}\right)^{\alpha} \widehat{=} \left(\frac{2}{T}\right)^{\alpha} \left(\frac{1-z^{-1}}{1+z^{-1}}\right)^{\alpha} \tag{1}$$

where the fractional-order $\alpha \in (0, 1)$ describes fractional-order derivative and $\alpha \in (-1, 0)$ fractional order integrator, T is the sampling period and z is the complex operator. Accurate discretization of fractional-order derivative and integral using the Tustin operator may produce an irrational function leading to infinite lengths of numerator and denominator in Eq. (1). It is well known that the functions in Eq. (1) can be presented in the continued fraction expansion (CFE) form

$$\left(\frac{\Delta}{T}\right)^{\alpha} = \left[a_0(z) + \frac{b_1(z)}{a_1(z) + \frac{b_2(z)}{a_2(z) + \frac{b_3(z)}{a_3(z)+\cdots}}} \right] \tag{2}$$

where the elements $a_i(z)$, $i = 0, 1, \ldots$ and $b_j(z)$, $j = 1, 2, \ldots$ are rational functions in the z domain. By finite implementation length in Eq. (2) we obtain the CFE-based approximation of fractional-order derivative or integrator [13]

$$\left(\frac{\Delta}{T}\right)^{\alpha} \approx w(z) = \left(\frac{2}{T}\right)^{\alpha} CFE_n \left\{ \left(\frac{1-z^{-1}}{1+z^{-1}}\right)^{\alpha} \right\} \tag{3}$$

where T is the sampling period, CFE_n denotes the continued fraction expansion of order n. Of course, the accuracy of the CFE expansion depends on implementation length. Therefore, it is worth emphasizing that due to numerical problems in the Matlab environment an implementation length is bounded and depends on values α.

Another Tustin-based approximation for fractional-order derivative and integrator is based on the Muir recursive scheme. In this case the nominator and denominator of the rational integer-order approximation is calculated in the following way

$$w(z) = \left(\frac{2}{T}\right)^{\alpha} \frac{A_n(z^{-1}, \alpha)}{A_n(z^{-1}, -\alpha)} \tag{4}$$

where $A_n(z^{-1}, \alpha)$ and $A_n(z^{-1}, \alpha)$ are the polynomials of orders n, whose coefficients are calculated in a recursive way

$$A_n(z^{-1}, \alpha) = A_{n-1}(z^{-1}, \alpha) - \gamma_n z^{-n} A_{n-1}(z, \alpha) \tag{5}$$

with

$$\gamma_n = \begin{cases} \frac{\alpha}{n} & \text{n is odd} \\ 0 & \text{n is even} \end{cases}$$

and

$$A_0(z^{-1}, \alpha) = 1$$

The Tustin–Muir approach gives worse performance in comparison to the CFE-Tustin one. However, in contrary to the CFE method the maximum order of implementation length is not limited. Therefore, in order to obtain an accurate approximation of fractional-order derivative in a wide range of frequencies it is necessary to generate very high order approximators.

In the paper we apply model order reduction methods for the Tustin–Muir approximation of the fractional order differentiator and integrator (4). Model order reduction methods require the representation of Eq. (4) in the state space form

$$\begin{aligned} x(t+1) &= Ax(t) + Bu(t) \\ y(t) &= Cx(t) + Du(t) \end{aligned} \tag{6}$$

with the matrices $A \in \Re^{n\times n}$, $B \in \Re^{n\times 1}$, $C \in \Re^{1\times n}$ and $D \in \Re$ given directly from (4).

3 Approximation Procedure

The Frequency Weighted (FW) method is a generalization of the BTA method, which enable to introduce frequency weighting functions [11, 14–18]. Weighting functions are chosen in terms of frequency-domain responses and adequacy scope of the model. A proper selection of weighting functions enables to significantly reduce a relative approximation error for frequency-domain characteristics in a given frequency range [19, 20].

The FW method has been developed for stable models and stable weighting input W_i (state matrices: A_i, B_i, C_i, D_i) and output filters W_o (state matrices: A_o, B_o, C_o, D_o). Introduction of weighting filters modifies the primary model as follows [11, 16]

$$GW_i = \left[\begin{array}{c|c} \hat{A}_i & \hat{B}_i \\ \hline \hat{C}_i & \hat{D}_i \end{array}\right] = \left[\begin{array}{cc|c} A & BC_i & BD_i \\ 0 & A_i & B_i \\ \hline C & DC_i & DD_i \end{array}\right] \tag{7}$$

$$W_oG = \left[\begin{array}{c|c} \hat{A}_o & \hat{B}_o \\ \hline \hat{C}_o & \hat{D}_o \end{array}\right] = \left[\begin{array}{cc|c} A & 0 & B \\ B_oC & A_o & B_oD \\ \hline D_oC & C_o & D_oD \end{array}\right] \tag{8}$$

Controllability and observability gramians of the modified system are computed by taking into account the input and output weights

$$\hat{A}_i \hat{P} \hat{A}_i^T - \hat{P} = -\hat{B}_i \hat{B}_i^T \tag{9}$$

$$\hat{A}_o^T \hat{Q} \hat{A}_o - \hat{Q} = -\hat{C}_o^T \hat{C}_o \tag{10}$$

Introduction of weighed functions changes the order of the model, therefore in the algorithm proposed by Enns [14], as gramians in the reduction algorithm are taken the sub-matrices $\hat{P}_{11}$ and $\hat{Q}_{11}$ of the modified model gramians.

$$P = \hat{P}_{11} \in \mathbb{R}^{n \times n}, \text{ where: } \hat{P} = \begin{bmatrix} \hat{P}_{11} & \hat{P}_{12} \\ \hat{P}_{12}^T & \hat{P}_{22} \end{bmatrix} \tag{11}$$

$$Q = \hat{Q}_{11} \in \mathbb{R}^{n \times n}, \text{ where: } \hat{Q} = \begin{bmatrix} \hat{Q}_{11} & \hat{Q}_{12} \\ \hat{Q}_{12}^T & \hat{Q}_{22} \end{bmatrix} \tag{12}$$

It is worth mentioning that there exist other alternative ways of determination gramians matrices P and Q (see details in Refs. [15–18]).

The Enns algorithm guarantees maintaining of the reduced model stability only for one-side weighing. However, mentioned above modifications provide stability of two-side weighting [15–18].

All the subsequent steps of the reduction algorithms are identical with those for the BTA method and are presented in detail in [21]. As result of the reduction process we obtain an integer-order discrete-time model of order $k \ll n$.

In the paper we use the above presented FW algorithm to model-order reduction of the Tusin-Muir approximation presented in (6). Weighting functions are selected to optimize the approximation performance of the reduced models in the frequency range $\omega \in \frac{1}{T}(10^{-3}, 1)$ [rad/s]. Determination of optimal reduction parameters is a non-convex problem and application of the global optimization algorithms is necessary, so for a solution to this problem we apply the evolutionary algorithm [19].

4 Results and Simulation Analysis

The approximation procedure presented above enables a selection of discrete-time models of fractional-order differentiator and integrator. Tables 1 and 2 present approximators of fractional-order derivative and integration, respectively, for various fractional-orders α and implementation lengths k.

Frequency domain characteristics of the above presented approximators and the actual characteristic of fractional-order derivative are shown in Fig. 1. In order to compare an efficiency of the approximations presented in this paper, the frequency domain characteristics of classical, continued fraction expansion-based (CFE-based)

Table 1 Discrete-time models of fractional-order differentiator

α	k	$w(z)$
0.3	3	$w_3^{0.3}(z) = \left(\frac{2}{T}\right)^{\alpha} \frac{1.231z^3 - 3.127z^2 + 2.578z - 0.6823}{z^3 - 2.023z^2 + 1.112z - 0.08914}$
	5	$w_5^{0.3}(z) = \left(\frac{2}{T}\right)^{\alpha} \frac{1.231z^5 - 4.714z^4 + 6.792z^3 - 4.397z^2 + 1.118z - 0.0304}{z^5 - 3.214z^4 + 3.369z^3 - 0.8003z^2 - 0.6509z + 0.2959}$
0.5	3	$w_3^{0.5}(z) = \frac{2^{\alpha}}{T^{\alpha}} \frac{1.414z^3 - 3.727z^2 + 3.224z - 0.9111}{z^3 - 1.714z^2 + 0.5425z + 0.1718}$
	5	$w_5^{0.5}(z) = \left(\frac{2}{T}\right)^{\alpha} \frac{1.414z^5 - 3.858z^4 + 2.968z^3 + 0.292z^2 - 1.126z + 0.309}{z^5 - 1.719z^4 - 0.1777z^3 + 1.557z^2 - 0.6711z + 0.0111}$
0.7	3	$w_3^{0.7}(z) = \left(\frac{2}{T}\right)^{\alpha} \frac{1.625z^3 - 4.009z^2 + 3.169z - 0.7843}{z^3 - 0.9659z^2 - 0.6408z + 0.6109}$
	5	$w_5^{0.7}(z) = \left(\frac{2}{T}\right)^{\alpha} \frac{1.625z^5 - 4.166z^4 + 2.812z^3 + 0.6622z^2 - 1.21z + 0.2775}{z^5 - 1.161z^4 - 0.8991z^3 + 1.287z^2 - 0.09403z - 0.1317}$

Table 2 Discrete-time models of fractional-order integrator

α	k	$w(z)$
−0.3	3	$w_3^{-0.3}(z) = \left(\frac{2}{T}\right)^{\alpha} \frac{0.8123z^3 - 1.43z^2 + 0.4929z + 0.1248}{z^3 - 2.375z^2 + 1.767z - 0.3926}$
	5	$w_5^{-0.3}(z) = \left(\frac{2}{T}\right)^{\alpha} \frac{0.8123z^5 - 2.523z^4 + 2.435z^3 - 0.2696z^2 - 0.7363z + 0.2812}{z^5 - 3.726z^4 + 5.128z^3 - 3.025z^2 + 0.5685z + 0.05423}$
−0.5	3	$w_3^{-0.5}(z) = \left(\frac{2}{T}\right)^{\alpha} \frac{0.7071z^3 - 0.7562z^2 - 0.4429z + 0.4927}{z^3 - 2.264z^2 + 1.544z - 0.2798}$
	5	$w_5^{-0.5}(z) = \left(\frac{2}{T}\right)^{\alpha} \frac{0.7071z^5 - 1.762z^4 + 0.8233z^3 + 1.093z^2 - 1.143z + 0.2816}{z^5 - 3.534z^4 + 4.428z^3 - 2.074z^2 - 0.001593z + 0.181}$
−0.7	3	$w_3^{-0.7}(z) = \left(\frac{2}{T}\right)^{\alpha} \frac{0.6156z^3 - 0.5102z^2 - 0.582z + 0.478}{z^3 - 2.449z^2 + 1.907z - 0.4583}$
	5	$w_5^{-0.7}(z) = \left(\frac{2}{T}\right)^{\alpha} \frac{0.6156z^5 - 1.368z^4 + 0.3359z^3 + 1.136z^2 - 0.8872z + 0.1669}{z^5 - 3.648z^4 + 4.828z^3 - 2.593z^2 + 0.2921z + 0.1202}$

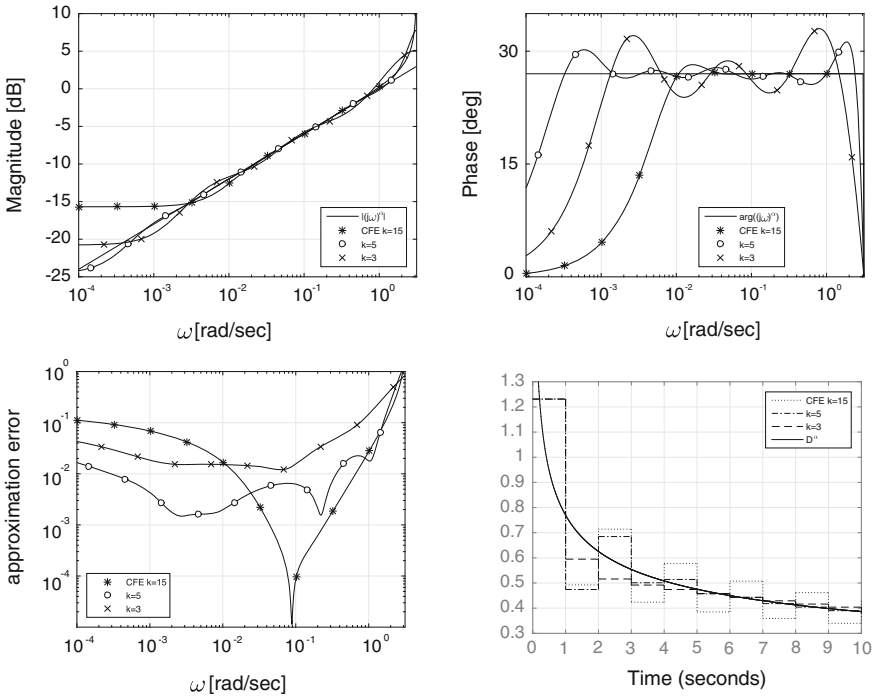

Fig. 1 Frequency responses, approximation errors and step responses for the reduced models of approximation of fractional-order differentiator for $\alpha = 0.3$

Tustin approach [7, 13] of order $k = 15$ are presented in Fig. 1. Moreover, approximation errors related to the actual frequency response of fractional-order derivative as well as the time domain step responses of the approximators are depicted in Fig. 1. Also, characteristics related to approximation of fractional-order integrator are presented in Fig. 2.

The presented results of reduction show that all the obtained reduced models give a very good approximation accuracy both in the frequency domain in the considered range of frequency $\omega \in (10^{-3}, 1)$ [rad/s] and in the time domain. It is worth mentioning that the obtained models give lower approximation errors and better numerical conditioning than the CFE-based Tustin approach. To obtain the equivalent accuracy to the presented in the paper approximators the order of CFE-based Tustin approach would have to be 10 times higher. Moreover, due to the numerical problems it could be infeasible because of the upper limit of order of the CFE-based Tustin approach, e.g. for fractional-order $\alpha = 0.5$ the limit is 41 in the Matlab environment [7]. It can be seen in the magnitude characteristics of Figs. 1 and 2 that properly chosen weighting functions in the FW algorithm enable partial elimination of the wrapping effect affecting the frequency properties of the Tustin approach. Moreover, the reduction process improves time domain properties of modeling due to elimination of some

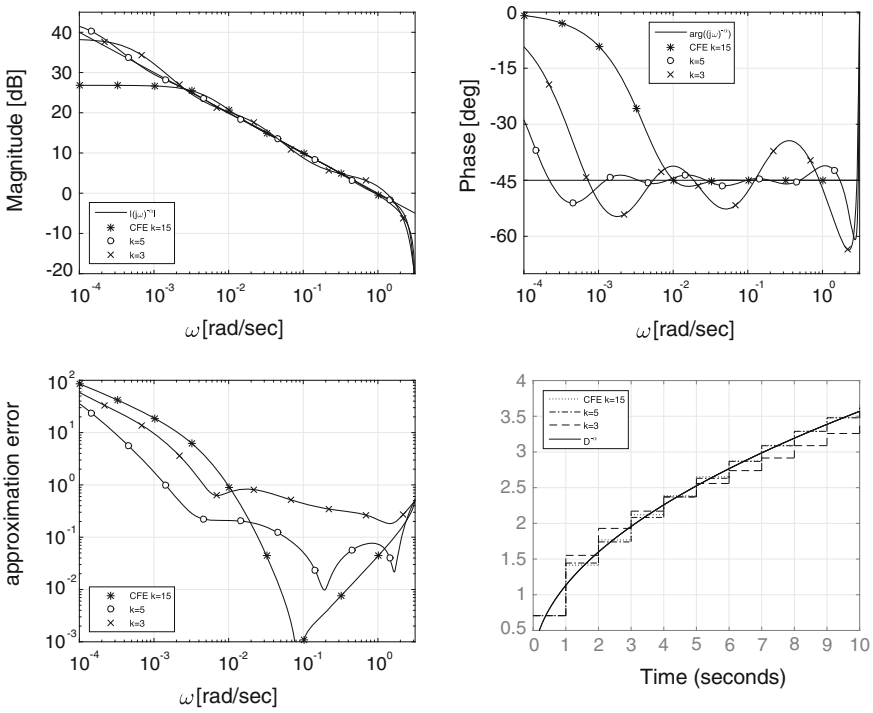

Fig. 2 Frequency responses, approximation errors and step responses for the reduced models of approximation of fractional-order integrator for $\alpha = -0.5$

left half plane poles of the characteristic equation bringing the non-casual properties to the system.

Table 3 shows the approximation errors of the approximators for fractional-order differentiator and integrator for implementation lengths $k = 2$ to $k = 5$. The abbreviations in this table are as follows

- *MSE* - the mean square error of step response,
- *RMSAE* - relative mean square approximation error for the model adequacy range $\omega \in (10^{-3}, 1)$ (rad/s) [22].

The results of Table 3 confirm a very good performance of the proposed approximators both in frequency and time domains.

Table 3 Approximation errors of approximators for fractional-order differentiator and integrator

	$\alpha = 0.3$		$\alpha = 0.5$		$\alpha = 0.7$	
k	*MSE*	*RMSAE*	*MSE*	*RMSAE*	*MSE*	*RMSAE*
2	4.782e−03	0.16912	4.686e−04	0.2331	7.427e−05	0.2200
3	9.262e−04	7.731e−02	1.392e−04	9.792e−02	3.329e−04	0.1011
4	4.493e−04	2.958e−02	3.425e−04	5.961e−02	8.671e−03	9.992e−02
5	3.354e−05	1.424e−02	3.184e−04	5.759e−02	9.864e−03	8.780e−02
	$\alpha = -0.3$		$\alpha = -0.5$		$\alpha = -0.7$	
k	*MSE*	*RMSAE*	*MSE*	*RMSAE*	*MSE*	*RMSAE*
2	49.14	0.1852	266.6	0.3488	1.110e+05	0.3282
3	13.41	8.737e−02	182.5	0.1617	569.3	0.1391
4	1.202	4.130e−02	12.71	6.866e−02	664.1	6.075e−02
5	6.531e−02	1.813e−02	8.896	3.153e−02	226.9	3.076e−02

5 Conclusion

This paper has presented a series of approximators to fractional-order difference and integration for various orders α and implementation lengths k. The proposed models are obtained using the SVD-based reduction method in terms of the Frequency Weighted (FW) approach. However, the procedure to determine the final approximation is time and memory consuming, especially for long implementation lengths of the model used in the reduction process. Nevertheless, high implementation lengths are required in order to obtain an approximation which is adequate in a wide frequency range. Proper selection of weighting functions for the FW method enable to determine a low order model characterized by low approximation errors both in the frequency and time domains. Simulation examples confirm the usefulness of the introduced methodology, which can be applied to selection of a set of relatively low order approximators to fractional-order differentiation and integration.

References

1. Stanisławski, R., Latawiec, K.J.: Normalized finite fractional differences - the computational and accuracy breakthroughs. Int. J. Appl. Math. Comput. Sci. **22**(4), 907–919 (2012)
2. Chen, Y.Q., Vinagre, K.L.: Discretization schemes for fractional-order differentiators and integrators. IEEE Trans. Circuits Syst. I, Fundam. Theory **49**(3), 363–365 (2002)
3. Al-Alaoui, M.A.: Novel digital integrator and differentiator. Electron. Lett. **29**(4), 376–378 (1993)
4. Al-Alaoui, M.A.: Simulation and discretization of fractional-order systems. In: GEM, pp. 249–255 (2009)
5. Stanisławski, R.: New Laguerre filter approximators to the Grünwald–Letnikov fractional difference. Math. Probl. Eng. **2012**, 1–21 (2012)

6. Stanisławski, R., Latawiec, K.J., Łukaniszyn, M.: The steady-state error issue in Laguerre-based modeling of the GL fractional difference. In: Proceedings of the IEEE International Symposium on Industrial Electronics (ISIE), pp. 1–6 (2013)
7. Stanisławski, R., Latawiec, K.J., Łukaniszyn, M.: A comparative analysis of Laguerre-based approximators to the Grünwald–Letnikov fractional-order difference. Math. Probl. Eng. **2015**, 1–10 (2015)
8. Chen, Y.Q., Vinagre, K.L., Podlubny, I.: Continued fraction expansion approaches to discretizing fractional order derivatives - an expository review. Nonlinear Dynam. **38**(1–4), 155–170 (2004)
9. Fortuna, I., Nunnari, G., Gallo, A.: Model Order Reduction Techniques with Applications in Electrical Engineering. Springer, London (1992)
10. Obinata, G., Anderson, B.: Model Reduction for Control System Design. Springer, London (2001)
11. Antoulas, A.: Approximation of Large-Scale Dynamical System. Society for Industrial and Applied Mathematics, Philadelphia (2005)
12. Moore, B.: Principal component analysis in linear systems: controllability, observability and model reduction. IEEE Trans. Automat. Contr. **26**(1), 17–32 (1981)
13. Vinagre, B.M., Chen, Y.Q., Petras, I.: Two direct Tustin discretization methods for fractional-order differentiator/integrator. J. Franklin Inst. **340**(5), 349–362 (2003)
14. Enns, D.: Model reduction with balanced realizations: An error bound and frequency weighted generalization. In: 23rd IEEE Conference on Decision and Control, pp. 127–132 (1984)
15. Lin, C., Chiu, T.: Model reduction via frequency weighted balanced realization. Theory Adv. Technol. **8**(2), 341–451 (1992)
16. Wang, G., Sreeram, V., Liu, W.Q.: A new frequency-weighted balanced truncation method and an error bound. IEEE Trans. Automat. Contr. **44**(9), 1734–1737 (1999)
17. Varga, A., Anderson, B.D.: Accuracy-enhancing methods for balancing-related frequency-weighted model and controller reduction. Automatica **39**(5), 919–927 (2003)
18. Imran, M., Ghafoor, A., Sreeram, V.: A frequency weighted model order reduction technique and error bounds. Automatica **50**(12), 3304–3309 (2014)
19. Rydel, M., Stanisławski, W.: Optimization of reduction parameters of SVD based reduction methods for complex plant mimo lti models. Methods of Applied Computer Science **24**(3), 197–220 (2010) (in Polish)
20. Rydel, M., Stanisławski, W.: Selection of the objective function of reduction parameter optimization algorithm, and its impact on the properties of reduced MIMO models. In: 20th International Conference on Methods and Models in Automation and Robotics, pp. 591–595 (2015)
21. Rydel, M., Stanisławski, R., Bialic, G., Latawiec, K.J.: Modeling of discrete-time fractional-order state space systems using the Balanced Truncation method. Theoretical Developenments and Applications of Non-integer Order Systems. Lecture Notes in Electrical Engineering, vol. 357, pp. 119–127. Springer, Dordrecht (2015)
22. Stanisławski, R., Latawiec, K.J., Łukaniszyn, M., Gałek, M.: Time-domain approximations to the Grünwald–Letnikov difference with application to modeling of fractional-order state space systems. In: 20th International Conference on Methods and Models in Automation and Robotics (MMAR), pp. 579–584 (2015)

Tempered Fractional Model of Transient Current in Organic Semiconductor Layers

Renat Sibatov and Ekaterina Morozova

Abstract This study is devoted to the tempered fractional drift-diffusion of charge carriers in organic semiconductors. The transient current observed in the time-of-flight experiment for the trap-limited transport is related to a solution of the classic Fokker–Planck equation. Using this relationship, we consider photocurrent decay in a multilayered organic samples.

Keywords Tempered fractional equation · Organic semiconductor · Dispersive transport · Time-of-flight

1 Introduction

Study of charge transport and recombination in organic semiconductors is important due to their applications in light-emitting diodes, solar cells and field-effect transistors [1–3]. In recent years, systems based on organic blends (such as P3HT:PCBM) forming bulk heterojunction are actively investigated [1, 4, 5]. Electronic and structural disorder inherent to the systems leads to energy distribution of localized states available for nonequilibrium electrons and holes. The correct interpretation of results of the time-of-flight (ToF) experiments in heterogeneous organic structures is still actual problem [6]. The ToF-method studies a photocurrent response after injection of nonequilibrium carriers by short light pulse. Typically, a strong electric field ($>10^5$ V/cm) close to the dielectric breakdown conditions is applied to a sample in order to avoid space charge effects, bipolar transport of carriers and to reduce contribution of diffusion [6–8]. Among the factors that influence the photocurrent decay

Authors thank the Russian Foundation for Basic Research (project 15-01-99674) and the Ministry of Education and Science of the Russian Federation (state program 2014/296) for financial support. Corresponding author.

R. Sibatov (✉) · E. Morozova
Ulyanovsk State University, Laboratory of Diffusion Processes,
Leo Tolstoy 42, 432017 Ulyanovsk, Russia
e-mail: ren_sib@bk.ru

A. Babiarz et al. (eds.), *Theory and Applications of Non-integer Order Systems*,
Lecture Notes in Electrical Engineering 407, DOI 10.1007/978-3-319-45474-0_26

are density of states (DoS), morphology of percolation area, presence of defective layers, heterogeneity of an electric field, recombination, and others [7–12].

In most cases, classic drift-diffusion equations are not applicable to description of charge carrier kinetics in organic semiconductors. Non-Gaussian (e.g. dispersive) transport regimes are usually observed in these systems [9–11, 13]: the photocurrent decay $I(t)$ essentially differs from the 'normal' step-wise curve corresponding to the Gaussian transport. Universal transient currents (with two power law sections: $I(t) \propto t^{-1+\alpha}$ for $t < t_T$, and $I(t) \propto t^{-1-\alpha}$ for $t > t_T$, α is the dispersion parameter) are typically explained by exponential DoS, but they can also result from percolation of carriers due to structural disorder [11, 14]. For exponential DoS $\rho(\varepsilon) \propto \exp(-\varepsilon/\varepsilon_0)$ with $\varepsilon_0 > kT$, photoinjected carriers never achieve equilibrium distribution on energy, waiting times are characterized by probability density function with power law tail $\psi(t) \propto t^{-\alpha}$, $\alpha = kT/\varepsilon_0 \in (0, 1)$ [9, 15]. The mean localization time diverges in this case.

A universal behavior of the transient photocurrent indicates the self-similarity of charge carrier propagation. The kinetic equation containing derivative of a fractional order α has been derived in [16] from the self-similarity property. The fractional differential model allows to describe normal and dispersive transport within a unified formalism [17]. The fractional differential theory of anomalous charge transport in solids is described in details in recent book [18].

On the other hand, transport of charge carriers in disordered organic media is usually modeled by hopping via localized states with the Gaussian energy distribution [10, 19]. In this case, the equilibrium energy distribution of carriers exists, and it is achieved at times large enough. After equilibration, transport is normal and transient current curves have a plateau. Distributions of sojourn times in some local domains are wide in case $\sigma > kT$, but smoothly truncated [20] and all moments of random waiting times are finite. The Central Limit Theorem is applicable and transport has to be Gaussian at times large enough. To describe results of the ToF-experiment in this case the tempered fractional model was proposed in [20]. The drift-diffusion equation contains tempered fractional derivative, solutions are expressed via tempered fractional stable density. This approach allowed authors to provide probabilistic interpretation of transition from the dispersive regime to the quasi-Gaussian one at decreased voltages.

The approach uses tempered fractional operators [21] and the class of tempered Lévy stable distributions and its inverse [22]. It is originated from the model of truncated Lévy flights [23], a process showing a slow convergence to a Gaussian. The distribution of jump length has a power law behavior up to some large scale, at which it has a cutoff and thus have finite moments of any order. Smoothly (exponentially) truncated Lévy flights, introduced by Koponen [24], provided a convenient analytic representation of results. Authors [25] derived the diffusion equation with the tempered fractional derivative describing the exponentially tempered Lévy flight. In papers [22, 26], the approach based on the tempered fractional calculus [21] was developed to describe crossover from subdiffusive to Gaussian transport. Tempered subdiffusion model assumes exponentially truncated power law distribution of waiting times [20, 27].

Here, using tempered fractional diffusion equation, transport in organic semiconductor layers is described. This consideration is motivated by modification of the ToF-method proposed in [8], which uses an electron beam of high (customizable) energy to generate nonequilibrium charge carriers in a sample. By varying the electron energy, it is possible to change continuously the width of generation region. Authors [13] used this method to analyze surface layers of polymer materials. The experimental results indicated the presence of a defect layer with a higher concentration of localized states. Based on the observed universality of transient current curves, authors believe that the density of localized states (DoS) in a surface layer is described by the same exponential function as in the bulk of the sample, only concentrations of traps are different. We generalize consideration by using tempered Lévy distribution for waiting times.

2 Tempered Fractional Drift-Diffusion Equation

We consider the following drift-diffusion equation [28, 30]:

$$\frac{\partial}{\partial t}\int_0^t p(x,\tau)\,\Phi(t-\tau)d\tau + \frac{\partial}{\partial x}\left\{\mu E(x)p(x,t) - D(x)\frac{\partial}{\partial x}p(x,t)\right\} = G(x)\Phi(t), \tag{1}$$

where $\Phi(t)$ is a kernel of delay caused by the energy distribution of localized states, distribution of random distances between hopping centers, or the presence of dead-ends in a percolation cluster, $E(x)$ is an electric field, μ and D are effective mobility and diffusion coefficient, respectively.

In the Continuous Time Random Walk (CTRW) model [9], the Laplace transform $\tilde{\Phi}(s)$ of kernel is related to transforms of function $P\{\theta > t\} = \Psi(t)$ and pdf $\psi(t)$ of waiting time θ via formula:

$$\tilde{\Phi}(s) = \tilde{\Psi}(s)/\tilde{\psi}(s). \tag{2}$$

In the multiple trapping model, $\Psi_{\mathrm{MT}}(t)$ (see e.g. [11, 14, 15]) can be found as:

$$\Psi_{\mathrm{MT}}(t) = \left\langle \exp\left(-\frac{\omega_\varepsilon t}{\exp(\varepsilon/kT)}\right)\right\rangle_\varepsilon = \int_0^\infty \exp\left\{-\omega_\varepsilon t e^{-\varepsilon/kT}\right\}\rho(\varepsilon)d\varepsilon. \tag{3}$$

Here, $\rho(\varepsilon)$ is DoS, and ω_ε is a trapping rate. For exponential DoS, $\rho(\varepsilon) \propto e^{-\varepsilon/\varepsilon_0}$ and weak dependence of ω_ε on ε ($\omega_\varepsilon \simeq \omega_0$), distribution has the form

$$\Psi_{\mathrm{MT}}(t) = \frac{(c_\alpha t)^{-\alpha}}{\Gamma(1-\alpha)}, \quad c_\alpha = \omega_0\left(\frac{\sin\pi\alpha}{\pi\alpha}\right)^{1/\alpha}, \quad \alpha = \frac{kT}{\varepsilon_0}. \tag{4}$$

Laplace transformation of this kernel is

$$\tilde{\Psi}_{\mathrm{MT}}(s) \sim c_\alpha^{-\alpha} s^{\alpha-1}, \quad \alpha < 0. \tag{5}$$

Using the latter relation, we arrive at the fractional order equation of multiple trapping [18, 28], which contains the Riemann–Liouville derivative

$${}_0\mathsf{D}_t^\alpha p(x,t) + c_\alpha^\alpha \frac{\partial}{\partial x}\left\{\mu E(x) p(x,t) - D(x)\frac{\partial}{\partial x} p(x,t)\right\} = G(x)\delta_\alpha(t), \tag{6}$$

where $\delta_\alpha(t) = t^{-\alpha}/\Gamma(1-\alpha)$.

For Gaussian DoS, after coarse graining procedure [29], waiting time distribution can be approximated by tempered power law within some range of accuracy. If we take pdf $\psi(t)$ in the form of tempered fractional exponent

$$\psi(t) = \nu e^{-\gamma t} t^{\alpha-1} E_{\alpha,\alpha}\left(-(\nu-\gamma^\alpha)t^\alpha\right) \tag{7}$$

having the following Laplace transform

$$\tilde{\psi}(s) = \frac{\nu}{\nu - \gamma^\alpha + (s+\gamma)^\alpha},$$

we obtain tempered fractional equation of dispersive transport

$${}_0\mathsf{D}_t^{\alpha,\gamma} p(x,t) + \nu V \frac{\partial}{\partial x} p(x,t) - \nu C \frac{\partial^2}{\partial x^2} p(x,t) = G(x)\delta_{\alpha,\gamma}(t), \tag{8}$$

where

$${}_0\mathsf{D}_t^{\alpha,\gamma} p(x,t) = e^{-\gamma t}\, {}_0\mathsf{D}_t^\alpha e^{\gamma t} - \gamma^\alpha p(x,t)$$

is the tempered fractional derivative [27]. The Laplace transform of the kernel $\Phi(t)$ in this case has the form

$$\tilde{\Phi}(s) = (\nu s)^{-1}[(s+\gamma)^\alpha - \gamma^\alpha]. \tag{9}$$

3 Transient Current for Tempered Fractional Transport

Laplace transformation of Eq. (1) gives

$$s\tilde{\Phi}(s)\tilde{p}(x,s) - \hat{\mathrm{L}}_{\mathrm{FP}}\tilde{p}(x,s) = G(x)\tilde{\Phi}(s), \tag{10}$$

where we introduced the notation $\hat{\mathrm{L}}_{\mathrm{FP}} = \frac{\partial}{\partial x}\left\{-\mu E(x) + D(x)\frac{\partial}{\partial x}\right\}$. The solution of this Fokker–Planck equation can be written in the form [26, 28]

$$\tilde{p}(x,s) = \int_0^\infty d\tau f(x,\tau)\tilde{q}(\tau,s). \tag{11}$$

Here, $f(x,\tau)$ is a solution to the classic Fokker–Planck equation (i.e. Eq. (1) with the first derivative on operational time τ instead of the integral operator), and $\tilde{q}(\tau,s)$ is the Laplace transform of the probability density function of operational time,

$$\tilde{q}(\tau,s) = \tilde{\Phi}(s)\exp(-\tau s\tilde{\Phi}(s)). \tag{12}$$

Substituting (11) into the Laplace transform of the transient current density [9, 15],

$$I(t) = \frac{1}{L}\int_0^L j(x,t)dx = \frac{e}{L}\frac{d}{dt}\int_0^L (x-L)p(x,t)dx, \tag{13}$$

after integration by parts and inverse Laplace transformation we obtain the following expression

$$I(t) = \int_0^\infty d\tau I_{\mathrm{FP}}(\tau)q(\tau,t), \tag{14}$$

where $I_{\mathrm{FP}}(\tau) = \frac{e}{L}\frac{d}{d\tau}\int_0^L (x-L)f(x,\tau)dx$ is a transient current for normal transport, which can be found by solving classic Fokker–Planck equation. Using the Laplace transform of the latter equation and expression (12), we have

$$\tilde{I}(s) = \tilde{I}_{\mathrm{FP}}(s\tilde{\Phi}(s)).$$

For tempered fractional transport [26]:

$$\tilde{q}(\tau,s) = (\nu s)^{-1}[(s+\gamma)^\alpha - \gamma^\alpha]\exp(-\tau\nu^{-1}[(s+\gamma)^\alpha - \gamma^\alpha]). \tag{15}$$

If E is a homogeneous electric field, $\mu = \mathrm{const}$ and diffusion is absent, transient current of normal drift has the rectangular shape $I_{\mathrm{FP}}(t) = \mu E L^{-1}1_{(0,L/\mu E)}(t)$. Using Laplace transform of this expression, $\tilde{I}_{\mathrm{FP}}(s) = \mu E L^{-1}s^{-1}[1-\exp(-sL/\mu E)]$, we obtain $\tilde{I}(s)$ for tempered fractional drift

$$\tilde{I}(s) = \frac{a\{1-\exp(-[(s+\gamma)^\alpha - \gamma^\alpha]L/a)\}}{L[(s+\gamma)^\alpha - \gamma^\alpha]} = \frac{1}{L}\int_0^L \exp\left(-x\frac{[(s+\gamma)^\alpha - \gamma^\alpha]}{a}\right)dx,$$

where $a = \mu E\nu$. The latter expression can be inverted with the use of the one-sided tempered stable density [21]. Here, we mention only the case $\alpha = 0.5$:

$$I(t) = \frac{ae^{-\gamma t}}{L\sqrt{\pi t}}\left[1-\exp\left(-\frac{L^2}{4a^2 t}+\frac{L\sqrt{\gamma}}{a}\right)\right] + \frac{a\sqrt{\gamma}}{L}\left[\mathrm{erf}(\sqrt{\gamma t}) + \mathrm{erf}\left(\frac{L}{2a\sqrt{t}} - \sqrt{\gamma t}\right)\right]. \tag{16}$$

The corresponding curves are presented in Fig. 1 (left panel).

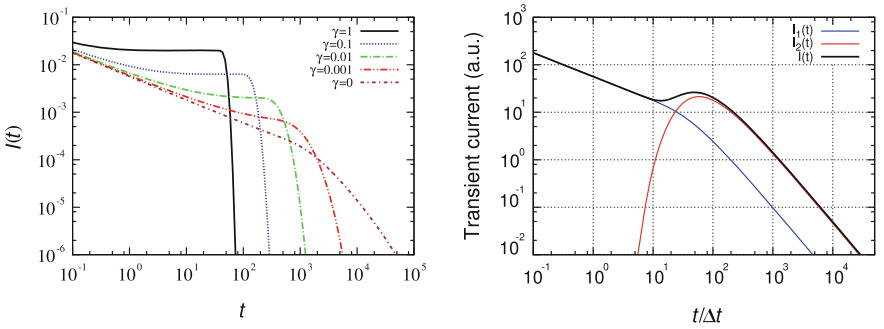

Fig. 1 *Left panel* Transient current (16) for different γ ($L/a = 100$ a.u., $\alpha = 0.5$). *Right panel* Transient current curves (20), $a_1/a_2 = 0.1$, $\alpha = 0.5$, I_i denotes currents in separated layers

4 Transient Current in a Multilayer Sample

Current in a two-layer structure can be found by solving Eq. (1) for each layer with the continuity condition for current density at boundaries. Another way is using modified expression (14) for the non-homogeneous case [30]. Transient current of normal drift in two layers has the form

$$I_{\mathrm{FP}}(t) = \frac{\mu_1 E}{L} 1_{(0,d/\mu_1 E)}(t) + \frac{\mu_2 E}{L} 1_{(d/\mu_1 E, d/\mu_1 E + (L-d)/\mu_2 E)}(t).$$

First and second terms correspond to first and second layers, respectively. So, transient current in case of hereditary drift in two layers has the form:

$$\tilde{I}(s) = \frac{\mu_1 E}{Ls\tilde{\Phi}_1(s)}\left[1 - \exp\left(-\frac{s\tilde{\Phi}_1(s)}{\mu_1 E}d\right)\right] + \\ + \frac{\mu_2 E}{Ls\tilde{\Phi}_2(s)}\left[1 - \exp\left(-\frac{s\tilde{\Phi}_2(s)}{\mu_2 E}(L-d)\right)\right]\exp\left(-\frac{s\tilde{\Phi}_1(s)}{\mu_1 E}d\right). \tag{17}$$

Similarly, in case of distributed generation of charge carriers,

$$\tilde{I}(s) = \frac{\mu_1 E}{Ls\tilde{\Phi}_1(s)}\int_0^d d\xi G(\xi)\left[1 - \exp\left(-\frac{s\tilde{\Phi}_1(s)}{\mu_1 E}(d-\xi)\right)\right] + \\ + \frac{\mu_2 E}{Ls\tilde{\Phi}_2(s)}\int_d^L d\xi G(\xi)\left[1 - \exp\left(-\frac{s\tilde{\Phi}_2(s)}{\mu_2 E}(L-\xi)\right)\right] \\ + \frac{\mu_2 E}{Ls\tilde{\Phi}_2(s)}\left[1 - \exp\left(-\frac{s\tilde{\Phi}_2(s)}{V_2}(L-d)\right)\right]\int_0^d G(\xi)\exp\left(-\frac{s\tilde{\Phi}_1(s)}{\mu_1 E}(d-\xi)\right)d\xi. \tag{18}$$

Here $\tilde{\Phi}_1(s)$, $\tilde{\Phi}_2(s)$ are transforms of memory kernels, $\mu_1 E$, $\mu_2 E$ are advection coefficients in layers 1 and 2, $G(x)$ is a generation function. In case of $d = 0$, we

have the result for homogeneous sample,

$$\tilde{I}(s) = \frac{\mu_2 E}{Ls\tilde{\Phi}(s)} \int_0^L d\xi G(\xi) \left[1 - \exp\left(-\frac{s\tilde{\Phi}(s)}{\mu_2 E}(L-\xi) \right) \right].$$

The analogous expression with μ_1 instead of μ_2 takes place, if $d = L$.

Consider the situation, when both layers are characterized by the same DoS, i.e. $\tilde{\Phi}_1(s) = \tilde{\Phi}_2(s) = \tilde{\Phi}(s)$, but concentrations of localized states are different, and $\mu_1 \neq \mu_2$. Choose the tempered power law for waiting time distribution, $\tilde{\Phi}(s)$ is determined by (9). For the near-surface injection $G(\xi) = N\delta(\xi)$, we have

$$\tilde{I}(s) = \frac{a_1}{L[(s+\gamma)^\alpha - \gamma^\alpha]} \left[1 - \exp\left(-\frac{[(s+\gamma)^\alpha - \gamma^\alpha]}{a_1} d \right) \right]$$
$$+ \frac{a_2 \exp\left(-[(s+\gamma)^\alpha - \gamma^\alpha]d/a_1\right)}{L[(s+\gamma)^\alpha - \gamma^\alpha]} \left[1 - \exp\left(-\frac{[(s+\gamma)^\alpha - \gamma^\alpha]}{a_2}(L-d) \right) \right]. \tag{19}$$

Here, $a_i = \mu_i E \nu$. The inverse Laplace transformation of this function is expressed via the tempered stable density. If $\alpha = 1/2$ and $\gamma = 0$, the current can be presented in terms of elementary functions,

$$I(t) = \frac{a_1}{L\sqrt{\pi t}} \left[1 - \exp\left(-\frac{d^2}{4a_1^2 t} \right) \right]$$
$$+ \frac{a_2}{L\sqrt{\pi t}} \left\{ \exp\left(-\frac{d^2}{4a_1^2 t} \right) - \exp\left[-\frac{1}{4t} \left(\frac{L-d}{a_2} + \frac{d}{a_1} \right)^2 \right] \right\}. \tag{20}$$

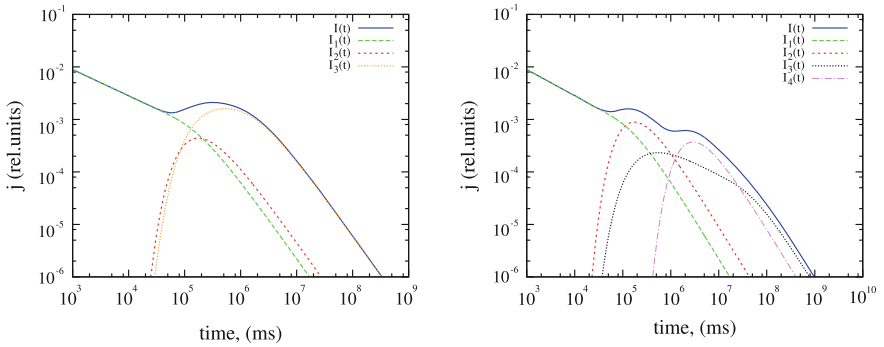

Fig. 2 Transient current curves in 3-layer (*left panel*) and 4-layer (*right panel*) structures with exponentially density of states, $\alpha = kT/\varepsilon_0 = 1/2$ in all layers. I_j are currents in layers. Parameters: 3-layer structure: $d_1 = 10\,\text{nm}, d_2 = 20\,\text{nm}, d_2 = 170\,\text{nm}, L = 200\,\text{nm}, a_1/a_2 = 0.05, a_1/a_3 = 0.5$; 4-layer structure: $d_1 = 10\,\text{nm}, d_2 = 30\,\text{nm}, d_3 = 60\,\text{nm}, d_4 = 120\,\text{nm}, L = 200\,\text{nm}, a_1 = a_3, a_2 = a_4, a_1/a_2 = a_3/a_4 = 0.02$

Graph of this function can have a bump (Fig. 1, right panel). The analogous behavior was observed for the structure with amorphous and crystalline layers in [31].

Similarly, the case of multilayered sample can be considered. Expressions (17), (18) and (20) can be easily generalized for this case. Results of calculations for 3- and 4-layer structures are presented in Fig. 2.

5 Concluding Remarks

Trap-limited transport in organic semiconductors is described by the tempered fractional drift-diffusion equation. Transient current $I(t)$ of the time-of-flight experiment for tempered fractional transport is expressed through a solution of the classic Fokker–Planck equation. Using this relationship, we considered transient current in a multilayered organic samples. For exponential DoS, i.e. when truncation factor is $\gamma = 0$, our calculations agree with the results presented in [13]. For a particular case $\alpha = 1/2$, the solution is expressed via elementary functions. Increased concentration of traps in a surface layer provides the bump on current curves, and it can be explained by shift of the transient current component in the second layer. For $\gamma \neq 0$, current $I(t)$ is expressed through tempered stable densities. Presented results can be useful for analysis of surface defect layers in polymers.

References

1. Yu, G., Gao, J., Hummelen, J.C., Wudl, F., Heeger, A.J.: Polymer photovoltiac cells: Enhanced efficiencies via a network of internal donor-acceptor heterojunctions. Science **270**(5243), 1789 (1995)
2. Klauk, H.: Organic Electronics: Materials, Manufacturing and Applications. Wiley, New York (2006)
3. Günes, S., Neugebauer, H., Sariciftci, N.S.: Conjugated polymer-based organic solar cells. Chem. Rev. **107**(4), 1324–1338 (2007)
4. Dang, M.T., Hirsch, L., Wantz, G.: P3HT:PCBM, best seller in polymer photovoltaic research. Adv. Mater. **23**(31), 3597–3602 (2011)
5. Hwang, I.W., Moses, D., Heeger, A.J.: Photoinduced carrier generation in P3HT/PCBM bulk heterojunction materials. J. Phys. Chem. C. **112**(11), 4350–4354 (2008)
6. Street, R.A., Song, K.W., Northrup, J.E., Cowan, S.: Photoconductivity measurements of the electronic structure of organic solar cells. Phys. Rev. B **83**(16), 165207 (2011)
7. Tiedje, T., Rose, A.: A physical interpretation of dispersive transport in disordered semiconductors. Solid State Commun. **37**(1), 49–52 (1981)
8. Tyutnev, A.P., Saenko, V.S., Pozhidaev, E.D., Kolesnikov, V.A.: Verification of the dispersive charge transport in a hydrazone: polycarbonate molecularly doped polymer. J. Phys. Condens. Matter **21**(11), 115107 (2009)
9. Scher, H., Montroll, E.W.: Anomalous transit-time dispersion in amorphous solids. Phys. Rev. B **12**(6), 2455–2477 (1975)
10. Bässler, H.: Charge transport in disordered organic photoconductors a Monte Carlo simulation study. Phys. Status Solidi (b) **175**(1), 15–56 (1993)

11. Zvyagin, I.P.: Kinetic Phenomena in Disordered Semiconductors. Izd. MGU, Moscow (1984). (in Russian)
12. Arkhipov, V.I., et al.: Nonstationary Injection Currents in Disordered Solids. Shtiintsa, Kishinev (1983)
13. Dunlap, D.H., Schein, L.B., Tyutnev, A., Saenko, V., Pozhidaev, E.D., Parris, P.E., Weiss, D.S.: Two-layer mutiple trapping model for universal current transients in molecularly doped polymers. J. Phys. Chem. C. **114**(19), 9076–9088 (2010)
14. Sibatov, R.T., Morozova, E.V.: Multiple trapping on a comb structure as a model of electron transport in disordered nanostructured semiconductors. J. Exp. Theor. Phys. **120**(5), 860–870 (2015)
15. Tiedje, T. In: The Physics of Hydrogenated Amorphous Silicon, vol. 2 of Electronic and Vibrational Properties. Springer, Berlin (1984)
16. Uchaikin, V.V., Sibatov, R.T.: Fractional differential kinetics of dispersive transport as the consequence of its self-similarity. JETP Lett. **86**(8), 512–516 (2007)
17. Sibatov, R.T., Uchaikin, V.V.: Fractional differential approach to dispersive transport in semiconductors. Physics-Uspekhi **52**(10), 1019–1043 (2009)
18. Uchaikin, V.V., Sibatov, R.T.: Fractional Kinetics in Solids: Anomalous Charge Transport in Semiconductors. Dielectrics and Nanosystems. World Scientific, Singapore (2013)
19. Baranovskii, S.D.: Theoretical description of charge transport in disordered organic semiconductors. Phys. Status Solidi (b) **251**(3), 487–525 (2014)
20. Sibatov, R.T., Uchaikin, V.V.: Truncated Lévy statistics for dispersive transport in disordered semiconductors. Commun. Nonlinear Sci. Numer. Simul. **16**(12), 4564–4572 (2011)
21. Baeumer, B., Meerschaert, M.M.: Tempered stable Lévy motion and transient super-diffusion. J. Comput. Appl. Math. **233**(10), 2438–2448 (2010)
22. Stanislavsky, A., Weron, K., Weron, A.: Diffusion and relaxation controlled by tempered α-stable processes. Phys. Rev. E **78**(5), 051106 (2008)
23. Mantegna, R.N., Stanley, H.E.: Stochastic process with ultraslow convergence to a Gaussian: the truncated Lévy flight. Phys. Rev. Lett. **73**(22), 2946–2949 (1994)
24. Koponen, I.: Analytic approach to the problem of convergence of truncated Lévy flights towards the Gaussian stochastic process. Phys. Rev. E **52**(1), 1197–1199 (1995)
25. Cartea, Á., del-Castillo-Negrete, D.: Fluid limit of the continuous-time random walk with general Lévy jump distribution functions. Phys. Rev. E **76**(4), (2007)
26. Gajda, J., Magdziarz, M.: Fractional Fokker-Planck equation with tempered α-stable waiting times: Langevin picture and computer simulation. Physical Review E **82**(1), (2010)
27. Sabzikar, F., Meerschaert, M.M., Chen, J.: Tempered fractional calculus. J. Comput. Phys. **293**, 14–28 (2015)
28. Sibatov, R.T., Uchaikin, V.V.: Fractional differential kinetics of charge transport in unordered semiconductors. Semiconductors **41**(3), 335–340 (2007)
29. Stodtmann, S.: Stochastic model and intermediate asymptotics for charge transport in organic semiconductors. Ph.D. Thesis (2015)
30. Sibatov, R.T., Uchaikin, V.V.: Dispersive transport of charge carriers in disordered nanostructured materials. J. Comput. Phys. **293**, 409–426 (2015)
31. Kazakova, L.P., Lebedev, E.A.: Transient current in amorphous, porous semiconductor-crystalline semiconductor structures. Semiconductors **32**(2), 169–173 (1998)

Modeling Heat Transfer Process in Grid-Holes Structure Changed in Time Using Fractional Variable Order Calculus

Piotr Sakrajda and Dominik Sierociuk

Abstract The paper presents results of modelling the heat transfer process in specific grid-holes media whose geometry is changed in time. The process will be modeled based on variable fractional order calculus. Responses of variable structure heat transfer system will be obtained from numerical simulation based on finite elements method.

Keywords Heat transfer process · Variable order systems · Modeling

1 Introduction

Modeling of diffusive processes was found as a very promising area of using models based on fractional order calculus. Fractional calculus allows to generalize traditional integer order partial differential equation, which described the diffusion process, onto fractional partial differential equations, who can describe anomalous diffusion processes e.g. sub-diffusion and hyper-diffusion. In [1–3], the heat transfer process was successfully modeled using fractional models based on normal and anomalous diffusion equation. Papers [2, 4, 5] present, also results of models of high accuracy of ultracapacitors, the electrical energy storage elements which base on the Helmholtz effect and diffusion. In [3, 6, 7] anomalous diffusion were used to describe diffusion process in porous, fractal or discontinuous media, e.g. solid bodies consisted of two different materials. The theoretical background for fractional order calculus can be found in [8–10]. The case when the order of the system is varying in time (variable order systems) makes the description much more complicated as for constant order case. In [11–16], four general types of order changing are given. All of these types are corresponded to some particular switching scheme that

P. Sakrajda · D. Sierociuk (✉)
Institute of Control and Industrial Electronics, Warsaw University of Technology,
Koszykowa 75, 00-662 Warsaw, Poland
e-mail: dsieroci@ee.pw.edu.pl

P. Sakrajda
e-mail: sakrajdp@ee.pw.edu.pl

A. Babiarz et al. (eds.), *Theory and Applications of Non-integer Order Systems*,
Lecture Notes in Electrical Engineering 407, DOI 10.1007/978-3-319-45474-0_27

characterize methodology of order changing. Switching schemes present how the chain of constant order differentiators, that represent variable order element, changed its structure in time. Changing of its structure has an effect in changing the order. There are only a few papers presenting experimental results of modelling real plant by variable order model. In [17], experimental studies on an electrochemical example of physical fractional variable-order system are presented. In [18], the variable-order equations were used to describe a history of drug expression. Both papers assume that the order changes very slowly and uses only A-type definition. In [13–16] also analog models of several types of variable order derivatives are presented.

In [19] preliminary results of modeling heat transfer process in variable structure media was presented. Investigated structure of heated media was chosen a plate with central one hole. The best results of modelling were obtained by using D-type variable fractional order derivative.

In this paper, the results of modelling the heat transfer process grid-holes structure of heated medium will be presented. Moreover, the situation when the grid-holes structure is varying (changes dimension of holes) in time will be taken into consideration and modelling results based on fractional variable order calculus will be presented as well. Responses of variable structure heat transfer system will be obtained from numerical simulation based on finite element method.

The paper is organized as follows: Sect. 3 presents a basis of fractional constant and variable order derivative definition. In Sect. 4, short description of modeling heat transfer process based on fractional calculus is recalled and results of approximation the heat transfer process in grid-holes media by anomalous diffusion model. Section 5 contains, the main contribution of the paper—modelling of variable grid-holes structure heat transfer process based on variable fractional order calculus.

2 Problem Statement

Let us investigate the heat transfer process in the medium, which structure is presented in Fig. 1. It is a copper plate with multiple insulator areas λ_i. Moreover, let us assume that the structure of the media is changed in time, what is achieved by changing the size of insulated regions.

The problem, that is investigated in this paper, is modelling the heat transfer process in such defined structure, that is changing in time. Because the modelling of heat transfer process in solid and heterogeneous [3] media was successfully solved based on fractional order calculus, we can expect, that the fractional variable order calculus will be extremely helpful to solve that problem.

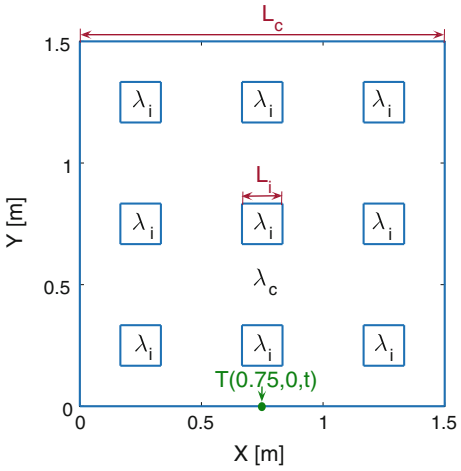

Fig. 1 Scheme of heated plate with measurement point marked

3 The Fractional Constant and Variable Order Derivatives

As an approximations of fractional constant order derivative we will use an iterative definition in Grünwald–Letnikov form.

Definition 1 The iterative fractional order derivative is defined as follows:

$$ {}_0\mathrm{D}_t^{\alpha} f(t) = \lim_{h \to 0} \frac{1}{h^{\alpha}} \sum_{r=0}^{n} (-1)^r \binom{\alpha}{r} f(t - rh), $$

where $h > 0$ is a step time, $\alpha \in \mathbb{R}$, and $n = \lfloor t/h \rfloor$.

There also exists a recursive constant order definition, given as follows:

Definition 2 The recursive fractional order derivative approximation is defined as follows:

$$ {}_0^r\mathrm{D}_t^{\alpha} f(t) = \left(\frac{f(t)}{h^{\alpha}} - \sum_{j=1}^{n} (-1)^j \binom{-\alpha}{j} {}_0^r\mathrm{D}_{t-jh}^{\alpha} f(t - jh) \right). $$

However, for constant order case both definitions are equivalent [16].

The case when the order is changing defining and description is more complicated. We can point out several types of order changing. All of them will be characterized by different mechanism of order changing, and can be intuitive categorized by corresponding switching scheme, as it was presented in [11, 13, 14]. The switching schemes describe how the chain of differentiators is changed during order changes. Because, as it was presented in [19], behavior of $\mathcal{A}$-type, $\mathcal{E}$-type and $\mathcal{B}$-type

definitions is expected to be not suitable in our experiment we will only take into consideration the $\mathcal{D}$-type definition.

The $\mathcal{D}$-type derivative, given by Definition 3, corresponds to the input-reductive switching scheme as it was presented in [16].

Definition 3 ([12]) The $\mathcal{D}$-type of fractional variable order derivative is defined as follows:

$$
\begin{aligned}
&{}_0^{\mathcal{D}}\mathrm{D}_t^{\alpha(t)} f(t) \\
&= \lim_{h\to 0}\left(\frac{f(t)}{h^{\alpha(t)}} - \sum_{r=1}^{n}(-1)^r \binom{-\alpha(t)}{j} {}_0^{\mathcal{D}}\mathrm{D}_{t-rh}^{\alpha(t)} f(t)\right),
\end{aligned}
$$

where $\alpha(t) \in \mathbb{R}$ is an order piecewise constant function.

The input-reductive switching strategy assumes that in differentiators chain for order changing differentiators from the input are reduced. This allows to obtain very intuitive behavior, after switching order output has immediately new order behavior and started from the same point as previous order finished.

4 Fractional Order Approximation of Heat Transfer Process in Grid-Holes Media

The physical process of heat diffusion is described by the heat equation:

$$
\frac{\partial T(x, y, t)}{\partial t} - \lambda \nabla^2 T(x, y, t) = Q(x, y, t), \tag{1}
$$

where $T(x, y, t)$ is temperature at time t and point (x, y), λ is thermal diffusivity of considered material, and $Q(x, y, t)$ is a function describing heat loses.

Because, the analytical description of the heat transfer process in heterogeneous medium can be extremely complicated, let us approximate the heterogeneous medium heat transfer process by homogeneous one and replacing normal heat equation with the fractional order partial differential anomalous diffusion equation:

$$
\frac{\partial^\alpha T(x, y, t)}{\partial t^\alpha} - \lambda_\alpha \nabla^2 T(x, y, t) = Q(x, y, t), \tag{2}
$$

where α is an order of anomalous diffusion, and λ_α is thermal diffusivity for anomalous diffusion model. Coefficient λ_α can differ from λ used in Eq. 1 describing the same problem, but in the classical way. This approximation can be valid only for limited frequency/time range.

In this paper we consider heat transfer in a square-shaped two dimensional structure consisted of two materials: a thermal conductor with very high thermal diffusivity

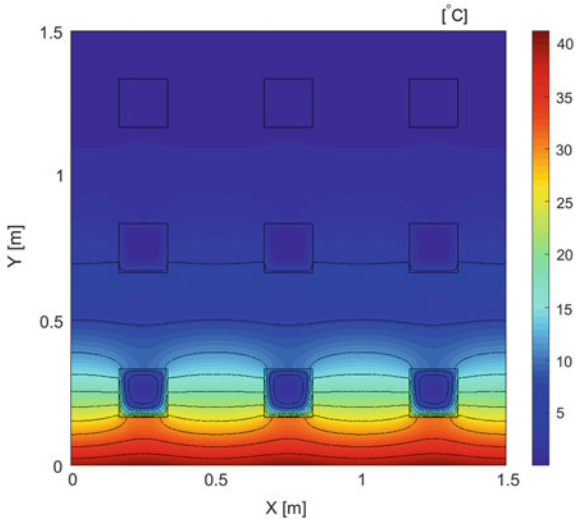

Fig. 2 Heatmap of researched structure after 1000 s of heating. Regions with different heat conduction are clearly visible

λ_c, and thermal insulator with very low thermal diffusivity λ_i. This plate, with the insulator located in multiple areas, is shown in Fig. 2. Such porous-like composition of tested medium results with relatively high anomalous diffusion order α and moderates analytical complexity of the problem, what makes it possible to formulate specific expectations about how this system should react. Also, for the purpose of further description of the system, δ parameter was defined as follows:

$$\delta = \frac{9L_i}{L_c},$$

where L_i and L_c are lengths of the edge of the insulator and conductor region, respectively. In particular $\delta = 3$ and $\delta = 0$ indicate homogeneous plates made of insulator or conductor only, respectively.

Having prepared the medium an input and an output of considered system was defined as follows. The input is a constant heat flux $H(x, 0, t) = H_0 = 0.012 \frac{\mathrm{J}}{\mathrm{s \cdot m^2}}$, that heated the structure at the whole bottom edge of the plate ($y = 0$ in Fig. 1). The output is a temperature $T(0.75, 0, t)$ that is measured at the middle of the heated edge.

Furthermore, it was made an assumption that the structure is perfectly thermally insulated, so the heat losses equals 0.

Having defined all necessary parameters of the researched system, its approximation by one dimensional anomalous diffusion model was made:

$$\frac{\partial^\alpha T(y,t)}{\partial t^\alpha} - \lambda_\alpha \frac{\partial^2 T(y,t)}{\partial y^2} = 0. \tag{3}$$

Knowing that heat flux is given by the equation

$$H(y,t) = -\lambda \frac{\partial T(y,t)}{\partial y}$$

one can solve Eq. 3, eventually deriving relation between temperature and heat flux [3]:

$$T(y,t) = \frac{1}{\sqrt{\lambda_\alpha}} \frac{\partial^{-\alpha/2} H(y,t)}{\partial t^{-\alpha/2}}. \tag{4}$$

The next step was to find values of α and λ_α for various λ_c, λ_i coefficients and geometrical properties of the plate. To achieve it solution of the Eq. 3 was fitted to results of Finite Element Method (FEM) simulation.

Described system was simulated in Matlab environment with Partial Differential Equation toolbox. To provide us with satisfying accuracy the maximum size of edge of finite element was set to 0.01 m. Constant Neumann boundary condition (heat flux heating the plate) was set for bottom ($y = 0$) edge of the plate and the λ_i, λ_c diffusivity coefficients were declared. Results of the FEM simulation are shown in Fig. 2. Temperature for the fitting process was measured at point (0.75, 0).

To fit the mathematical model to the simulation time series Matlab function `fminsearch` was used. As the result the accurate values of order and λ_α coefficient were obtained.

For both cases diffusivity coefficients were chosen as $\lambda_c = 2.3 \times 10^{-4}$ and $\lambda_i = 1.9 \times 10^{-8}$, what corresponds with copper and insulator, respectively. For $\delta = 1$ the following parameters were obtained: $\alpha = 1.09$ and $\lambda_\alpha = 2.96 \times 10^{-4}$, while, for $\delta = 2$, $\alpha = 1.26$ and $\lambda_\alpha = 2.56 \times 10^{-4}$ were obtained. Simulation results and fitted model time series are shown in Fig. 3.

As it can be seen in Fig. 4 approximation of heat in the heterogeneous medium presented in this section gives accurate results.

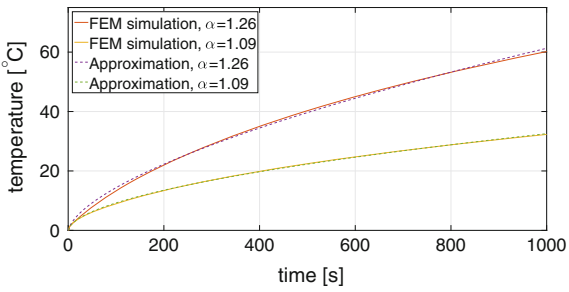

Fig. 3 FEM simulation and fractional approximation results for various α orders

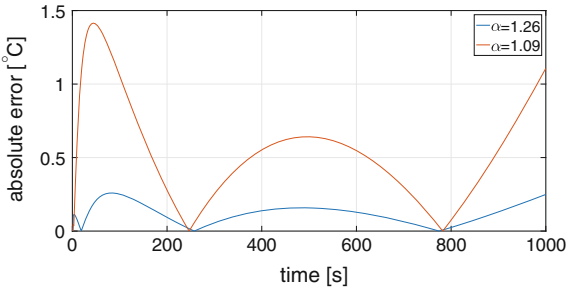

Fig. 4 FEM simulation and fractional approximation absolute error for various α orders

5 Modelling of Heat Transfer Process in Variable Grid-Holes Structure Media

Having fractional order system, that was presented in previous chapter, we created a variable structure system by dynamically changing diffusivity coefficients of heated media. This changing of diffusivity coefficients will have an effect in changing of system order. We can imagine many methods for changing these coefficients, but in this paper the method of changing the part of conductive material into insulator by switching δ coefficient value in time is considered.

5.1 Description of Heat Transfer Process in Variable Structure Media

The simulation methodology, that was used to find coefficients and to validate mathematical model of heat transfer in constant structure media, was applied with modifications to the variable structure problem. By changing δ coefficient the structure shown in Fig. 1 is modified. In our research we switched δ between $\delta_0 = 1$ and $\delta_k = 2$, effectively increasing the cumulative area of insulated regions four times. Values of coefficients λ_c and λ_i were the same as for the constant order problem.

In simulation process, the switching time t_v was set to 1000 s. for the total time of simulation set to 2000 s. For obtaining responses for variable order derivatives, set of dedicated numerical routines [20] implemented in Matlab/Simulink environment was used.

5.2 Results for Modelling Based on $\mathcal{D}$-Type Definition

The model, that was used in identification is given by the following non-stationary fractional variable order differential equation:

$$T(0, 0.75, t) = {}_0^{\mathcal{D}}\mathrm{D}_t^{-\alpha(t)/2} \frac{1}{\sqrt{\lambda_{\alpha(t)}}} H(t),$$

where

$$\lambda_{\alpha(t)} = \begin{cases} \lambda_{1.09} & t < t_v \\ \lambda_{1.26} & t \geqslant t_v \end{cases},$$

and

$$\alpha(t) = \begin{cases} 1.09 & t < t_v \\ 1.26 & t \geqslant t_v \end{cases},$$

Coefficients $\lambda_{1.09}$ and $\lambda_{1.26}$ were obtained during identification of constant structure case.

Results of modelling based on $\mathcal{D}$-type variable order approximations,presented in Fig. 5, confirm that this type of definition is able to describe investigated problem.

Figure 6 shows, that absolute error of this approximation is relatively low. However, the real system reacts more slightly than the variable order differential model. Delay compensation method, researched to solve this problem, was presented in [19].

One can notice, that there are others fractional variable order derivative definitions. However, previous studies on similar problem [19] shows, that $\mathcal{A}$-type, $\mathcal{B}$-type and $\mathcal{E}$-type fail to describe considered process properly.

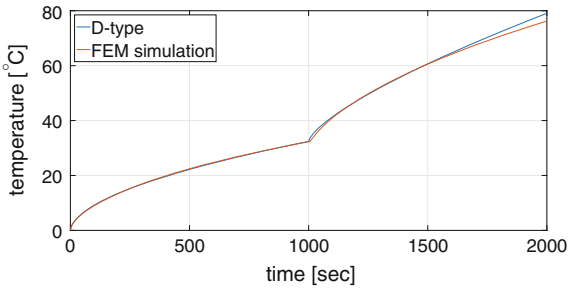

Fig. 5 Comparison of the results of the numerical FEM simulation and $\mathcal{D}$-type variable order model

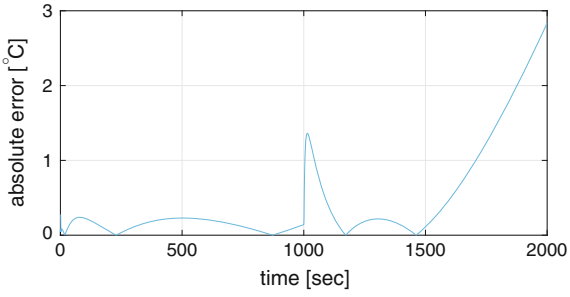

Fig. 6 Absolute error between numerical simulation and $\mathcal{D}$-type variable order model

6 Conclusions

The paper presents a method for modelling the heating process in particular type of variable structure media. The structure of the heated media was changed in time by changing the dimension of holes. In order to obtain responses of variable grid-holes structure heat transfer process Finite Elements Method (FEM) was used. Proposed modelling method based on variable fractional order calculus. Obtained results were compared with proposed variable fractional order model for $\mathcal{D}$-type variable order derivative definition and shows very high accuracy of modelling process.

Acknowledgments This work was partially supported in part by the Polish National Science Center with the decision number UMO-2014/15/B/ST7/00480, and by the PL - SK cooperation agreement under decision number SK-PL-2015-0038.

References

1. Dzielinski, A., Sierociuk, D.: Fractional order model of beam heating process and its experimental verification. In: Baleanu, D., Guvenc, Z.B., Machado, J.A.T. (eds.) New Trends in Nanotechnology and Fractional Calculus Applications, pp. 287–294. Springer, Netherlands (2010)
2. Dzielinski, A., Sierociuk, D., Sarwas, G.: Some applications of fractional order calculus. Bull. Pol. Ac. Tech. **58**(4), 583–592 (2010)
3. Sierociuk, D., Dzielinski, A., Sarwas, G., Petras, I., Podlubny, I., Skovranek, T.: Modelling heat transfer in heterogeneous media using fractional calculus. Phil. Trans. Math. Phys. Eng. Sci. **371** (2013)
4. Dzielinski, A., Sarwas, G., Sierociuk, D.: Time domain validation of ultracapacitor fractional order model. In: 49th IEEE Conference on Decision and Control (CDC), pp. 3730–3735 (2010)
5. Dzielinski, A., Sierociuk, D.: Ultracapacitor modelling and control using discrete fractional order state-space model. Acta Montan. Slovaca **13**(1), 136–145 (2008)
6. Havlin, S., Ben-Avraham, D.: Diffusion in disordered media. Adv. Phys. **36**(6), 695–798 (1987)
7. Koch, D.L., Brady, J.F.: Anomalous diffusion in heterogeneous porous media. Phys. Fluids **31**(5), 965–973 (1988)
8. Monje, C.A., Chen, Y., Vinagre, B.M., Xue, D., Feliu, V.: Fractional-Order Systems and Controls. Springer, Heidelberg (2010)
9. Oldham, K.B., Spanier, J.: The Fractional Calculus. Academic Press, Cambridge (1974)
10. Podlubny, I.: Fractional Differential Equations. Academic Press, Cambridge (1999)
11. Sierociuk, D., Malesza, W., Macias, M.: Equivalent switching strategy and analog validation of the fractional variable order derivative definition. In: Proceedings of European Control Conference, pp. 3464–3469 (2013)
12. Sierociuk, D., Malesza, W., Macias, M.: On a new definition of fractional variable-order derivative. In: Proceedings of the 14th International Carpathian Control Conference (ICCC), pp. 340–345 (2013)
13. Sierociuk, D., Malesza, W., Macias, M.: Switching scheme, equivalence, and analog validation of the alternative fractional variable-order derivative definition. In: Proceedings of the 52nd IEEE Conference on Decision and Control, pp. 3876–3881(2013)
14. Sierociuk, D., Macias, M., Malesza, W.: Analog modeling of fractional switched-order derivatives: Experimental approach. In: Advances in the Theory and Applications of Non-integer Order Systems. pp. 271–280. Springer International Publishing, Heidelberg (2013)

15. Sierociuk, D., Malesza, W., Macias, M.: Derivation, interpretation, and analog modelling of fractional variable order derivative definition. Appl. Math. Model. **39**(13), 3876–3888 (2015)
16. Sierociuk, D., Malesza, W., Macias, M.: On the recursive fractional variable-order derivative: equivalent switching strategy, duality, and analog modeling. Circ. Syst. Signal Pr. **34**(4), 1077–1113 (2015)
17. Sheng, H., Sun, H., Coopmans, C., Chen, Y., Bohannan, G.W.: Physical experimental study of variable-order fractional integrator and differentiator. In: Proceedings of The 4th IFAC Workshop Fractional Differentiation and its Applications FDA'10 (2010)
18. Ramirez, L., Coimbra, C.: On the variable order dynamics of the nonlinear wake caused by a sedimenting particle. Physica D. **240**(13), 1111–1118 (2011)
19. Sierociuk, D., Sakrajda, P.: Modeling of variable structure heat transfer process based on fractional variable order calculus. In: Proceedings of the 55nd IEEE Conference on Decision and Control, Las Vegas, NV, USA (2016). (submitted to)
20. Sierociuk, D.: Fractional Variable Order Derivative Simulink Toolkit (2012). http://www.mathworks.com/matlabcentral/fileexchange/38801-fractional-variable-order-derivative-simulink-toolkit

Analysis of Performance Indicators for Tuning Non-integer Order Controllers

Marta Zagórowska

Abstract Tuning non-integer order controllers using parametric optimization remains a subject of ongoing research. One of the areas of focus concerns analysis of performance indicators ensuring desired behaviour. In this paper we analyze linear, quadratic and quartic performance indicators as tools for finding parameters of PD^{α} and PI^{γ} controllers in RC ladder system of fourth order. Proposed optimization method uses LIRA approximation method and ensures the stability of non-integer closed-loop system.

Keywords Non-integer order controller · Fractional calculus · RC ladder system · Laguerre impulse response approximation

1 Introduction

Tuning controller parameters is one of the most important issues in control theory. Choosing and then calculating the performance indicators for the problem is not obvious and strongly depends on optimized system [1]. The aim of this paper is to show that it is possible to calculate the performance indicators (linear, quadratic and quartic) using an approximation method and use them in optimization method for PD^{α} and PI^{γ} controllers.

Earlier works on parametric optimisation of non-integer order controllers can be found in [2–4] - both in simulational and in experimental setups. An interesting approach to non-integer fractional controllers was investigated in [5], where a concept of robust non-integer controllers is investigated.

Work realised in the scope of project titled "Design and application of non-integer order subsystems in control systems". Project was financed by National Science Centre on the base of decision no. DEC-2013/09/D/ST7/03960.

M. Zagórowska (✉)
AGH University of Science and Technology, Al. Mickiewicza 30,
30-059 Cracow, Poland
e-mail: zagor@agh.edu.pl

A. Babiarz et al. (eds.), *Theory and Applications of Non-integer Order Systems*,
Lecture Notes in Electrical Engineering 407, DOI 10.1007/978-3-319-45474-0_28

The rest of the paper is organised as follows. In the first part of the article, we present a brief description of approximation method for non-integer order systems (LIRA). Then we analyse three performance indicators: integral of impulse response, quadratic performance indicator and integral of fourth order of the impulse response. The paper ends with an example of optimization of PD^{α} and PI^{γ} controllers, followed by conclusion and proposed further works.

2 Optimization Problem

In order to tune the controller, we propose to use parametric optimization methods allowing to minimize chosen performance indicator based e.g. on impulse response of the closed-loop system.

2.1 Laguerre Impulse Approximation Method (LIRA)

Most of previous works focus mainly on quadratic performance indicator. The main purpose of this paper is to provide an extension for other types of performance indices. Contrarily to classical integer order systems, the solution of non-integer order system yields problems either with exact form of the solution or its numerical implementation as it requires the whole "history" beginning with initial conditions (lack of semi-group property). Moreover, even though there are exact solutions presented, e.g., in [6], it is worth notice that they require special functions, i.e. Mittag-Leffler function. Furthermore, taking into account that s^{α} is a multivalued function for complex s and non-integer α, we can notice that direct calculation of integral of impulse response is complicated.

The method used in this paper was first shown in [7]. It uses a set of orthonormal Laguerre functions to approximate a non-integer order system. It concentrates on fitting impulse response of the system in time domain and guarantees, i.a., convergence both in $\mathcal{L}_1$ and $\mathcal{L}_2$ spaces [8].

2.2 Optimization Algorithm

We assume that for given system we have already chosen the structure of $PI^{\mu}D^{\alpha}$ controller (see, e.g. [6]). Let us denote those parameters as $K = [k_i], i = 1, 2, \ldots, n$. For example, fractional $PD^{\alpha} = K_P + K_D s^{\alpha}$ is described with three parameters: $K = \left[k_1, k_2, k_3\right] = \left[K_P, K_D, \alpha\right]$.

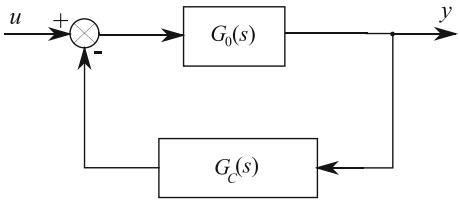

Fig. 1 Impulse response for three integral performance indicators

Before performing optimization method it is necessary to define and/or calculate:

- transfer function $G(s)$ of closed loop system for given system $G_0(s)$ and chosen type of the controller $G_C(s)$.
  For the system depicted in the Fig. 1, we have

$$G(s) = \frac{G_0(s)}{1 + G_0(s)G_C(s)} \tag{1}$$

- optimization method with appropriate parameters, e.g. stop criteria: (see, e.g., [9]):
  - desired accuracy on minimum
  - desired accuracy on function value
  - maximal number of iterations for optimization
- performance indicator that takes into account desired properties

Let us denote the parameters of the controller after j iterations as a vector of n elements $K^j = [k_i^j]$, $i = 1, 2, \ldots, n$. Let us denote the approximation parameters in jth iteration as μ^j, $\mathbf{A}^j$, $\mathbf{B}^j$, $\mathbf{C}^j$.

The algorithm consists of two main steps described below.

(i) Set starting points for controller parameters K^0 in such a way that the system (1) is asymptotically stable.
(ii) Perform the optimization routine calculating the chosen performance indicator. As this step requires more attention, it will be described separately.

The most important part of this method is the algorithm for calculating performance indicator. It consists of three stages. Let us assume that the optimization routine performed j iterations and we have the parameters of the controller from iteration $j - 1$.

(i) For given values of parameters of the controller perform the stability check of the non-integer order system. If the parameters lie outside the asymptotic stability region, set the value of performance indicator to infinity and go to the third step. If the system is asymptotically stable, then go to second step.
(ii) In order to approximate the stable system with LIRA method, find optimal μ^j for K^j. If μ^j is infinite, set the performance indicator to infinity. Otherwise, calculate the value of performance indicator using $\mathbf{A}^j$, $\mathbf{B}^j$, $\mathbf{C}^j$.

(iii) On the basis of value of performance indicator, find K^{j+1} according to chosen optimization routine.

It is important to notice that stability analysis is an essential part of the algorithm. It is worth noticing that although the optimization is performed on approximated system, the stability test is performed for non-integer order one. To verify the stability, we used an original algorithm based on D-partition method for non-integer order systems (see, e.g. [10]).

3 Performance Indicator Analysis

In this section we analysed three performance indicators: linear, quadratic and quartic performance indicators. In this section we present the way for obtaining performance indicators using LIRA approximation.

3.1 Linear Performance Indicator

As a first case we analyse the performance indicator as integral of impulse response.

Theorem 1 *The performance indicator*

$$J = \int_0^\infty y(t)\dot{t} = -\sqrt{\frac{2}{\mu}} \cdot \sum_{i=0}^{n} (-1)^i \beta_i \tag{2}$$

where β_k is given by recurrence formula

$$\beta_k = \frac{\sqrt{2\mu}}{k!} \sum_{j=0}^{k} \begin{bmatrix} k \\ j \end{bmatrix} c_j^k(\mu) \hat{g}^{(k-j)}(\mu) \tag{3}$$

with $c_j^k(\mu) = \frac{k-j+1}{2\mu} c_{j-1}^k$, $c_0^k(\mu) = (2\mu)^k$, $j = 0, 1, 2, \ldots, k$ and μ is a parameter of LIRA method [8]. Here $\hat{g}(\cdot)$ denotes the transfer function of analyzed system.

Proof From [11] we have

$$J = \int_0^\infty y(t)\dot{t} = -\mathbf{C}\mathbf{A}^{-1}\mathbf{B} \tag{4}$$

It can be observed that the product $\mathbf{A}^{-1}\mathbf{B}$ can be computed as a solution of additional system of equations $\mathbf{A}\mathbf{z} = \mathbf{B}$ where z denotes the variable of appropriate dimensions. Matrix $\mathbf{A}$ is a triangular matrix, hence the solution is straightforward.

Using the fact that $\mathbf{A}$ is lower triangular, we have $z_1 = -\sqrt{\frac{2}{\mu}}$ and $z_k = -\sqrt{\frac{2}{\mu}} - 2\sum_{i=1}^{k-1} z_i$ where $k = 1, 2, \ldots, n+1$. Calculating z_k we obtain $z_k = (-1)^k\sqrt{\frac{2}{\mu}}$ where $k = 1, 2, \ldots, n+1$. Thus, from $-\mathbf{C}\mathbf{A}^{-1}\mathbf{B} = -\mathbf{C} \cdot \mathbf{z}$ we have

$$J = -\sum_{i=0}^{n} \beta_i z_i = -\sqrt{\frac{2}{\mu}} \cdot \sum_{i=0}^{n} (-1)^i \beta_i \tag{5}$$

where β_k is given by (3).

3.2 Quadratic Performance Indicators

The optimization consists in minimizing the quadratic performance indicator with respect to the parameters of the controller.

Integral of impulse response It can be observed (for proof see, e.g. [8, 12]) that

$$J = \int_0^\infty y^2(t)dt = ||y||_{\mathcal{L}^2} \approx \sum_{i=1}^{n} \beta_i^2 \tag{6}$$

It is important to notice that during the procedure both types of parameters are optimized - μ and controller parameters.

Integral of impulse response and its derivative In case of quadratic performance indicator, we can take into account more than just impulse response. Here we use also the derivative of impulse response in order to ensure less steep slopes. According to [1], we have:

Theorem 2 *The performance indicator J can be calculated as*

$$J = \int_0^\infty y^2(t) + \dot{y}^2(t)\underline{t} = \int_0^\infty (y(t) + \dot{y}(t))^2 \tag{7}$$

Proof See [1].

The proof from [1] is done for integer order systems. However, it is also valid in our case as we calculate y as impulse response of approximating system. Hence we use this performance indicator for analysis of non-integer order system with approximation.

3.3 Quartic Performance Indicator

The third type of performance measure used in this article is quartic performance indicator.

Theorem 3 *Performance indicator can be calculated as*

$$J = \int_0^\infty y^4(t)\dot{t} = -\mathcal{C}\mathcal{A}^{-1}\mathcal{B} \tag{8}$$

where $\mathcal{A} = \mathbf{A} \otimes I \otimes I \otimes I + I \otimes \mathbf{A} \otimes I \otimes I + I \otimes I \otimes \mathbf{A} \otimes I + I \otimes I \otimes I \otimes \mathbf{A}$, $\mathcal{B} = \mathbf{B} \otimes \mathbf{B} \otimes \mathbf{B} \otimes \mathbf{B}$ *and* $\mathcal{C} = \mathbf{C} \otimes \mathbf{C} \otimes \mathbf{C} \otimes \mathbf{C}$. *The symbol* $\otimes$ *denotes Kronecker product [1].*

Proof For proof see [1].

As previously, it can be observed that the product $\mathcal{A}^{-1}\mathcal{B}$ can be computed as a solution of additional system of equations. Matrix $\mathcal{A}$ is also a triangular matrix, hence the solution is straightforward but tedious. Resulting matrix is sparse triangular matrix of size 625. Let us denote the elements of $\mathbf{A}$ as $a_{k,l}$. To simplify the expression for $\mathcal{A}$ we first need to calculate $\mathcal{A}_2 = \mathbf{A} \otimes I + I \otimes \mathbf{A}$:

$$\mathcal{A}_2(i,j) = \begin{cases} a_{k,l}\ k = i - \lfloor \frac{i}{n} \rfloor \cdot n,\ l = j - \lfloor \frac{i}{n} \rfloor \cdot n \text{ for } 2 \le i \ne mn+1, m \in \mathbb{N}, \\ \qquad \lfloor \frac{i}{n} \rfloor \cdot n + 1 \le j \le i-1; \\ 2a_{kk},\ k = i - \lfloor \frac{i}{n} \rfloor \cdot n,\ \text{for } i = j; \\ a_{k,l}\ k = i + \lfloor \frac{i}{n} \rfloor,\ l = j + \lfloor \frac{j}{n} \rfloor \text{ for } n+1 \le i,\ 1 \le j \le \lfloor \frac{i}{n} \rfloor \cdot n; \\ 0,\ \text{otherwise.} \end{cases} \tag{9}$$

Denoting now elements of $\mathcal{A}_2$ as $\overline{a}_{k,l}$, we can write:

$$\mathcal{A}(i,j) = \begin{cases} 4a_{kk}\ k = i - \lfloor \frac{i}{n^3} \rfloor \cdot n^3, \text{for } i = j; \\ \overline{a}_{k,l},\ k = i - \lfloor \frac{i}{n^2} \rfloor \cdot n^2,\ l = j - \lfloor \frac{i}{n^2} \rfloor \cdot n^2 \text{ for } 2 \le i \ne mn^2+1, m \in \mathbb{N}, \\ \qquad \lfloor \frac{i}{n^2} \rfloor \cdot n^2 + 1 \le j \le i-1; \\ a_{k,l},\ k = i + \lfloor \frac{i}{n^3} \rfloor,\ l = j + \lfloor \frac{j}{n^3} \rfloor \text{ for } n^3+1 \le i, \\ \qquad 1 \le j \le \lfloor \frac{i}{n^3} \rfloor \cdot n^3; \\ 0,\ \text{otherwise.} \end{cases} \tag{10}$$

Calculating $\mathcal{B}$ is straightforward and yields $\mathcal{B} = 4\mu^2 \begin{bmatrix} 1 & 1 & \dots & 1 \end{bmatrix}^\mathsf{T} \in \mathbb{R}_{n^4 \times 1}$.

Matrix $\mathbf{C}$ is a vector of size $n^4 \times 1$ where each element consists of a certain products of β_i^j where the sum of indices j in a single element is four. For now, we have not found explicit analytical formula for $\mathcal{C}$.

4 Optimization of RC Ladder System

In this section we will present the method that uses various performance indicators in order to find optimal values for non-integer *PD* and *PI* controllers. It ends with an example calculated for three integrals - linear, of second power (quadratic) and of fourth power of impulse response.

As optimization method we chose the Nelder–Mead algorithm implemented in Matlab/Simulink software. In this case, the order of the system was fixed and we optimized for controller parameters.

4.1 RC Ladder System

In order to verify the results, we chose an RC ladder system depicted in the Fig. 2 with non-integer order PD controller. This system was widely analysed in literature (see e.g. [13]). Among the others, it is very useful as it allows approximating some distributed systems, e.g., transmission line [14].

We assume that the control acts only on x_4 and we measure the first state, x_1. Therefore, the equations of the system are:

$$\begin{aligned} \dot{\mathbf{x}}(t) &= \mathbf{A}\mathbf{x}(t) + \mathbf{B}u(t) \\ y &= \mathbf{C}\mathbf{x}(t) \end{aligned} \tag{11}$$

where $\mathbf{A} = \begin{bmatrix} -2 & 1 & 0 & 0 \\ 1 & -2 & 1 & 0 \\ 0 & 1 & -2 & 1 \\ 0 & 0 & 1 & -1 \end{bmatrix}$, $\mathbf{B} = \begin{bmatrix} 0 \\ 0 \\ 0 \\ 1 \end{bmatrix}$, $\mathbf{C} = \begin{bmatrix} 1 & 0 & 0 & 0 \end{bmatrix}$. This system is described with transfer function of integer order

$$G_0(s) = \frac{1}{s^4 + 8s^3 + 21s^2 + 20s + 5} \tag{12}$$

Further, we present the analysis of performance indicators for two types of non-integer order controllers: PD^{α} and PI^{γ}.

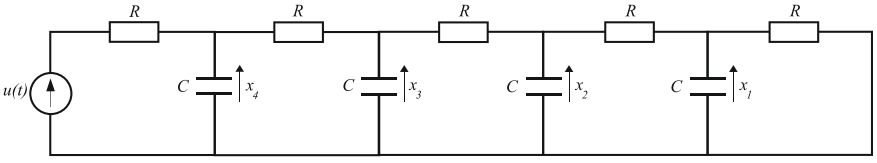

Fig. 2 RC ladder system of fourth order

The above-mentioned optimization routine was analysed for four performance indicators - linear, quadratic and quartic performance indicator. The closed loop system is depicted in the Fig. 1. The approximation order was chosen $n = 4$. Number of iterations was the same for all indicators - 200 and desired accuracy - 10^{-4} both for the value of performance indicator and variables.

PD^{α} controller The transfer function of the controller is $G_R(s) = K_P + K_D s^{\alpha}$ and the transfer function of a closed-loop system is

$$G(s) = \frac{1}{s^4 + 8s^3 + 21s^2 + 20s + K_D s^{\alpha} + 5 + K_P} \tag{13}$$

PI^{γ} controller The transfer function of the controller is $G_C(s) = K_P + K_I s^{-\gamma}$ and the transfer function of a closed-loop system is

$$G(s) = \frac{s^{\gamma}}{s^{4+\gamma} + 8s^{3+\gamma} + 21s^{2+\gamma} + 20s^{1+\gamma} + (5 + K_P)s^{\gamma} + K_I} \tag{14}$$

Results and discussion In both cases, the order of the controller was fixed $\alpha = \gamma = 0.5$. In order to ensure the stability of non-integer order system (13) we choose starting points for parameters of the controllers which guarantee initial stability [15]. The regions of stability for both types of the controller are depicted in the Fig. 3. The results are depicted in the Fig. 4a, b. We show the original impulse response of RC ladder and the impulse response of controlled system tuned according to four types of indicator.

Resulting parameters are gathered in Table 1. Here PI denotes performance indicator value for given parameters.

The performance indicators induced various behaviour depending on type of the controller. Linear performance indicator caused semi-oscillations in the system in

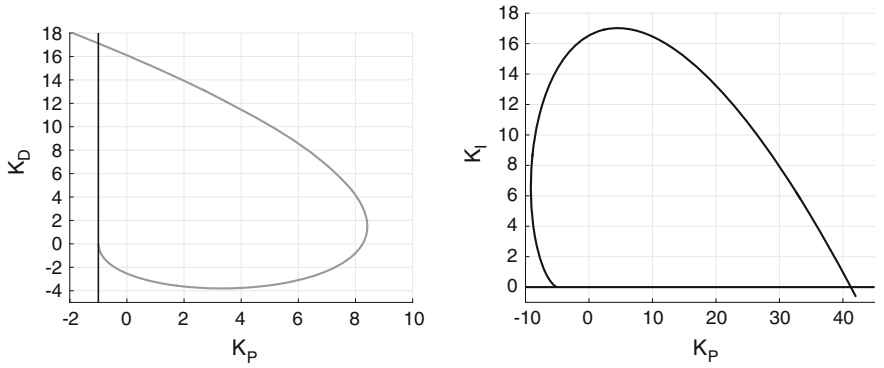

(a) PD^{α} controller (b) PI^{γ} controller

Fig. 3 Stability region obtained with D-partition

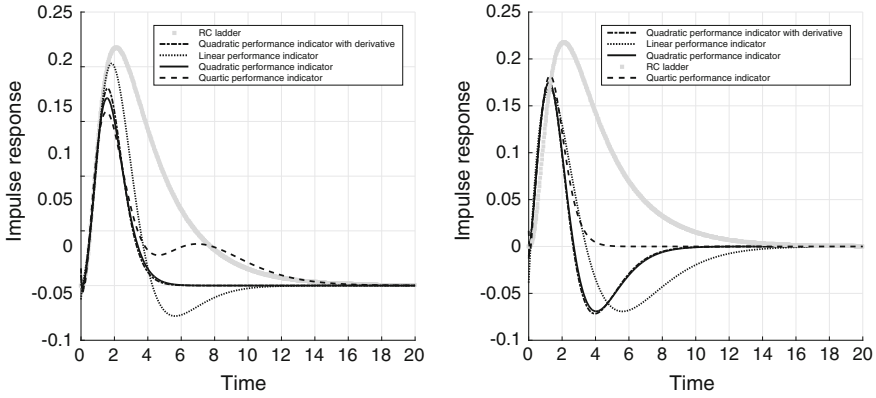

(a) PD^{α} controller (b) PI^{γ} controller

Fig. 4 Impulse response for four integral performance indicators

Table 1 Impulse response for four integral performance indicators

	PD^{α}				PI^{γ}			
	PI	μ	K_P	K_D	PI	μ	K_P	K_I
$\int_0^{\infty} y dt$	0.3606	1.2747	8.1579	–0.8029	–0.0107	0.7825	–0.4742	2.1551
$\int_0^{\infty} y^2 dt$	0.0426	2.5408	3.0970	12.5576	0.0459	1.4627	7.4144	0.000001
$\int_0^{\infty} y^4 dt$	0.0007414	0.8661	–1	17.039	0.0008672	3.1004	1.2782	0.2078
$\int_0^{\infty} \left(y^2 + \dot{y}^2\right) dt$	0.0825	2.7814	5.742	8.9398	0.092	2.9381	7.9787	0.006

both cases. It is consistent with expectations. The indicator given by (2) may be negative. Therefore, in case where there are no additional constraints on the parameters, we can expect that minimum of (2) to be $-\infty$. This result is not desirable as it destabilizes the system. In this system, however, we introduced supplementary information about the parameters as we want to ensure stability of closed-loop system. Hence the optimal impulse response has the form of damped sinusoidal signal.

Quadratic performance indicator is one of the most widely used in control processes. The value of (6) is bounded with 0, therefore, the performance indicator does not require additional constraints. Nevertheless, this indicator behaves differently for PD^{α} and PI^{γ} controller. In the first one, it does not introduce oscillations. The amplitude of the impulse response is smaller and its shape is preserved. For PI^{γ} the indicator introduces oscillations. The amplitude slightly decreases and the convergence to zero is faster for closed-loop system.

Almost the same behaviour comes when we use the performance indicator in form (7). For PD^{α} controller, the amplitude is insignificantly smaller than for classic quadratic performance indicator but the convergence rate stays the same. In the second analysis, for PI^{γ} controller, those two indicators are more similar and yield almost the same response. Therefore, they are not recommended for this problem.

Quartic performance indicator also behaves differently for two kinds of the controllers. For PD controller, it stabilizes the system similarly to open-loop system. Moreover, it minimizes the amplitude. For PI controller, the decrease in amplitude is similar to quadratic performance indicators (slightly bigger). However, it does not introduce oscillations and convergence rate is the fastest. It yields the smallest amplitude of all performance indicators analyzed here as it puts more weight on minimizing large errors. Hence, it may be applicable to a specific class of systems.

5 Conclusion

The aim of this paper was to verify the influence of performance indicators on a method for non-integer order controller tuning. The proposed algorithm is based on parametric optimization and was verified with PD^{α} and PI^{γ} controllers. We used four types of performance indicators to evaluate the quality of the algorithm.

The chosen indicators proved to give valid results for two types of the controller. Their main advantage is that they are based on approximation in form of integer order system.

Nevertheless, there are certain flaws induced by performance indicators. First of all, some of them introduce semi-oscillations. If we want to avoid certain behaviour, it is necessary to introduce additional constraints. Moreover, the use of the quartic performance indicator is limited by numerics. Calculation of Kronecker product increases the dimensions of the problem and requires, i.a., sparse matrices analysis. Hence, it is not directly useful for high approximation orders.

This work is part of wider research concerning on parametric optimization as method for non-integer order controller tuning. Therefore, further works will focus, i.a., on further optimization of linear systems, issues linked with approximation method, stability analysis as one of stop criteria and application in non-linear systems.

References

1. Grabowski, P.: Ćwiczenia Komputerowe z Teorii Sterowania. Wydawnictwa AGH, Kraków (1996)
2. Padula, F., Visioli, A.: Tuning rules for optimal PID and fractional-order PID controllers. J. Process. Contr. **21**(1), 69–81 (2011)
3. Baranowski, J., Zagórowska, M., Bania, P., Bauer, W., Dziwiński, T., Piątek, P.: Impulse response approximation method for bi-fractional filter. In: 19th International Conference on Methods and Models in Automation and Robotics (MMAR), pp. 379–383 (2014)

4. Zagórowska, M., Baranowski, J., Bania, P., Piątek, P., Bauer, W., Dziwiński, T.: Impulse response approximation method for "fractional order lag". In: Latawiec, K.J., Łukaniszyn, M., Stanisławski, R., eds. Advances in Modelling and Control of Noninteger-order Systems - 6th Conference on Non-Integer Orfer Caculus and its Applications, Lecture Notes in Electrical Engineering, vol. 320, pp. 113–122. Springer, Heidelberg (2014)
5. Kesarkar, A.A., Selvaganesan, N.: Novel tuning expressions for fractional order ([pd]ˆbeta and [pi]ˆalpha) controllers using a generalized plant structure. Control Eng. Appl. Inf. **17**(1), 70–80 (2015)
6. Podlubny, I.: Fractional Differential Equations: An Introduction to Fractional Derivatives, Fractional Differential Equations, to Methods of their Solution and Some of their Applications, Mathematics in Science and Engineering. Elsevier Science, Amsterdam (1999)
7. Bania, P., Baranowski, J.: Laguerre polynomial approximation of fractional order linear systems. In: Mitkowski, W., Kacprzyk, J., Baranowski, J. (eds.) Advances in the Theory and Applications of Non-integer Order Systems: 5th Conference on Non-integer Order Calculus and Its Applications, pp. 171–182. Springer, Heidelberg (2013)
8. Baranowski, J., Bauer, W., Zagórowska, M., Piątek, P.: On digital realizations of non-integer order filters. Circuits Syst. Signal Process. **35**(6), 2083–2107 (2016)
9. Nocedal, J., Wright, S.: Numerical Optimization. Springer, Heidelberg (2006)
10. Ruszewski, A.: Stability regions of closed loop system with time delay inertial plant of fractional order and fractional order PI controller. Bull. Pol. Ac. Tech. **56**(4), 329–332 (2008)
11. Grabowski, P.: Control Theory Problem Book (2005). http://www.ia.agh.edu.pl/~pgrab/main.xml
12. Zagórowska, M.: Parametric optimization of non-integer order PD^{μ} controller for delayed system. In: Theoretical Developments and Applications of Non-Integer Order Systems, pp. 259–270. Springer, Heidelberg (2016)
13. Mitkowski, W.: Stabilizacja Systemów Dynamicznych. Wydawnictwa AGH, Kraków (1996)
14. Mitkowski, W.: Remarks about energy transfer in an RC ladder network. Int. J. Appl. Math. Comput. Sci. **13**(2), 193–198 (2003)
15. Zagórowska, M., Baranowski, J., Bania, P., Bauer, W., Dziwiński, T., Piątek, P.: Parametric optimization of pd controller using laguerre approximation. In: 20th International Conference on Methods and Models in Automation and Robotics (MMAR), pp. 104–109 (2015)

Part III
Controllability and Stability

Controllability of Nonlinear Fractional Delay Dynamical Systems with Multiple Delays in Control

Krishnan Balachandran

Abstract This paper describes the controllability of nonlinear fractional delay dynamical systems with multiple delays in control. Necessary and sufficient conditions for the controllability criteria for linear fractional delay system are established. Further sufficient conditions for the controllability of nonlinear fractional delay system are obtained by using fixed point arguments. Examples are provided to illustrate the results.

Keywords Fractional delay differential equation · Laplace transform · Controllability · Mittag-Leffler function · Caputo fractional derivative

1 Introduction

In some real world problems fractional derivative provide an excellent tool for the description of memory and hereditary properties of various materials and processes. The mathematical modeling of systems and processes in the fields of physics, chemistry, aerodynamics, electrodynamics of complex medium, polymer rhenology etc. involves derivative of fractional order.

Controllability is one of the fundamental concept in mathematical control theory, which plays an important role in control systems. The qualitative theory of fractional differential equation has been extensively studied by several authors. An extensive list of these publications can be found. Dauer and Gahl [1] obtained the controllability of nonlinear delay systems. Balachandran and Dauer [2] studied the controllability problems for both linear and nonlinear delay systems. The relative controllability of nonlinear fractional dynamical system with multiple delays and distributive delays in control have been discussed by Balachandran et al. [3, 4]. Klamka [5, 6] established the controllability of both linear and nonlinear system with time variable delay in control. Recently, Mur et al. [7] studied the relative controllability of linear systems

K. Balachandran (✉)
Department of Mathematics, Bharathiar University, Coimbatore, India
e-mail: kb.maths.bu@gmail.com

A. Babiarz et al. (eds.), *Theory and Applications of Non-integer Order Systems*,
Lecture Notes in Electrical Engineering 407, DOI 10.1007/978-3-319-45474-0_29

of fractional order with delay. Babiarz et al. [8] and Klamka et al. [9] gave some results on Schauder's fixed point theorem and Banach fixed point theorem. Detail study on controllability of fractional delay dynamical systems is given in [10].

2 Preliminaries

This section begins with definitions and properties of fractional operator, special functions and its Laplace transformation [11, 12].

(a) The Caputo fractional derivative of order $\alpha > 0, n-1 < \alpha < n$, is defined as

$$^{C}D^{\alpha}f(t) = \frac{1}{\Gamma(n-\alpha)}\int_0^t (t-s)^{n-\alpha-1} f^{(n)}(s)\mathrm{d}s,$$

where the function $f(t)$ has absolutely continuous derivative upto order $n-1$. The Laplace transform of Caputo derivative is in [11].

(b) The Mittag-Leffler functions of various type are defined as

$$E_{\alpha}(z) = E_{\alpha,1}(z) = \sum_{k=o}^{\infty} \frac{z^k}{\Gamma(\alpha k+1)}, z \in \mathbb{C}, Re(\alpha) > 0, \tag{1}$$

$$E_{\alpha,\beta}(z) = \sum_{k=0}^{\infty} \frac{z^k}{\Gamma(\alpha k+\beta)}, z, \beta \in \mathbb{C}, Re(\alpha) > 0, \tag{2}$$

$$E^{\gamma}_{\alpha,\beta}(-\lambda t^{\alpha}) = \sum_{k=0}^{\infty} \frac{(\gamma)_k(-\lambda)^k}{k!\Gamma(\alpha k+\beta)} t^{\alpha k}, \tag{3}$$

where $(\gamma)_n$ is a Pochhamer symbol which is defined as $\gamma(\gamma+1)\cdots(\gamma+n-1)$ and $(\gamma)_n = \dfrac{\Gamma(\gamma+n)}{\Gamma(\gamma)}$. The Laplace transform of Mittag-Leffler functions (1)–(3) are given in [11].

In order to prove our main results we need the following fixed point theorem:

Theorem 1 ([13] Schauder's Fixed Point Theorem) *Let M be a compact, convex set in a Banach space X and $T : M \to M$ be continuous. Then T has a fixed point M.*

3 Linear Delay Systems

Consider the fractional delay dynamical systems with multiple delays in control

$$
\begin{aligned}
{}^{C}D^{\alpha}x(t) &= Ax(t) + Bx(t-h) + \sum_{i=0}^{M} C_i u(\sigma_i(t)), t \in J = [0, T], \\
x(t) &= \phi(t), -h < t \leq 0,
\end{aligned} \tag{4}
$$

where $0 < \alpha < 1, x \in \mathbb{R}^n, u \in \mathbb{R}^m$ A, B are $n \times n$ matrices and C_i are $n \times m$ matrices for $i = 0, 1, 2, \cdots M$. Assume the following conditions
(H1) The functions $\sigma_i : J \to \mathbb{R}, i = 0, 1, 2, \ldots M$ are twice continuously differentiable and strictly increasing in J. Moreover

$$
\sigma_i(t) \leq t, \ i = 0, 1, 2 \ldots M, \ \text{for } t \in J \tag{5}
$$

(H2) Introduce the time lead functions $r_i(t) : [\sigma_i(0), \sigma_i(T)] \to [0, T]$, $i = 0, 1, 2, \ldots M$ such that $r_i(\sigma_i(t)) = t$ for $t \in J$. Further $\sigma_0(t) = t$ and for $t = T$, the following inequality holds

$$
\begin{aligned}
\sigma_M(T) \leq \sigma_{M-1}(T) \leq \cdots \sigma_{m+1}(T) \leq 0 = \sigma_m(T) < \sigma_{m-1}(T) = \cdots \\
= \sigma_1(T) = \sigma_0(T) = T.
\end{aligned} \tag{6}
$$

The following definitions of complete state of the system (4) at time t and relative controllability are assumed.

Definition 1 [14] The set $y(t) = \{x(t), \beta(t, s)\}$, where $\beta(t, s) = u(s)$ for $s \in [\min\ h_i(t), t)$ is said to be the complete state of the system (4) at time t.

Definition 2 System (4) is said to be relatively controllable on $[0, T]$ if for every complete state $y(t)$ and every $x_1 \in \mathbb{R}^n$ there exists a control $u(t)$ defined on $[0, T]$, such that the solution of system (4) satisfies $x(T) = x_1$.

The solution of the system (4) by using Laplace transform is expressed as

$$
\begin{aligned}
x(t) = X_\alpha(t)\phi(0) + B \int_{-h}^{0} (t - s - h)^{\alpha-1} X_{\alpha,\alpha}(t - s - h)\phi(s)\mathrm{d}s \\
+ \int_{0}^{t} (t - s)^{\alpha-1} X_{\alpha,\alpha}(t - s) \sum_{i=0}^{M} C_i u_i(\sigma_i(s))\mathrm{d}s.
\end{aligned} \tag{7}
$$

where

$$
X_\alpha(t) = L^{-1}[s^{\alpha-1}(s^\alpha I - A - Be^{-hs})^{-1}](t),
$$

and

$$X_{\alpha,\alpha}(t) = t^{1-\alpha} \int_0^t \frac{(t-s)^{\alpha-2}}{\Gamma(\alpha-1)} X_\alpha(s)\mathrm{d}s.$$

Using the time lead functions $r_i(t)$, the solution can be written as

$$x(t) = x_L(t;\phi) + \sum_{i=0}^{M} \int_{\sigma_i(0)}^{\sigma_i(t)} (t - r_i(s))^{\alpha-1} X_{\alpha,\alpha}(t - r_i(s)) C_i \dot{r}_i(s) u(s)\mathrm{d}s,$$

where

$$x_L(t;\phi) = X_\alpha(t)\phi(0) + B \int_{-h}^{0} (t - s - h)^{\alpha-1} X_{\alpha,\alpha}(t - s - h)\phi(s)\mathrm{d}s.$$

By using the inequality (6) we get

$$\begin{aligned} x(t) = x_L(t;\phi) &+ \sum_{i=0}^{m} \int_{\sigma_i(0)}^{0} (t - r_i(s))^{\alpha-1} X_{\alpha,\alpha}(t - r_i(s)) C_i \dot{r}_i(s)\beta(s)\mathrm{d}s \\ &+ \sum_{i=0}^{m} \int_{0}^{t} (t - r_i(s))^{\alpha-1} X_{\alpha,\alpha}(t - r_i(s)) C_i \dot{r}_i(s) u(s)\mathrm{d}s \\ &+ \sum_{i=m+1}^{M} \int_{\sigma_i(0)}^{\sigma_i(t)} (t - r_i(s))^{\alpha-1} X_{\alpha,\alpha}(t - r_i(s)) C_i \dot{r}_i(s)\beta(s)\mathrm{d}s. \end{aligned}$$

For simplicity, let us write the solution as

$$x(t) = x_L(t;\phi) + H(t) + \sum_{i=0}^{m} \int_0^t (t - r_i(s)^{\alpha-1} X_{\alpha,\alpha}(t - r_i(s)) C_i \dot{r}_i(s) u(s)\mathrm{d}s, \quad (8)$$

where

$$\begin{aligned} H(t) = &\sum_{i=0}^{m} \int_{\sigma_i(0)}^{0} (t - r_i(s))^{\alpha-1} X_{\alpha,\alpha}(t - r_i(s)) C_i \dot{r}_i(s)\beta(s)\mathrm{d}s \\ &+ \sum_{i=m+1}^{M} \int_{\sigma_i(0)}^{\sigma_i(t)} (t - r_i(s))^{\alpha-1} X_{\alpha,\alpha}(t - r_i(s)) C_i \dot{r}_i(s)\beta(s)\mathrm{d}s. \end{aligned}$$

Now let us define the controllability Grammian matrix

$$W = \sum_{i=0}^{m} \int_0^T (X_{\alpha,\alpha}(T - r_i(s))C_i\dot{r}_i(s))(X_{\alpha,\alpha}(T - r_i(s))C_i\dot{r}_i(s))^* \mathrm{d}s,$$

where the $*$ denotes the matrix transpose.

Theorem 2 *The linear system (4) is relatively controllable on* $[0, T]$ *if and only if the controllability Grammian matrix is positive definite for some* $T > 0$.

Proof Assume W is positive definite. Define the control function by

$$u(t) = (T - r_i(t))^{1-\alpha}(X_{\alpha,\alpha}(T - r_i(t))C_i\dot{r}_i(t))^* W^{-1}\left[x_1 - x_L(T;\phi) - H(T)\right], \tag{9}$$

where the complete state $y(0)$ and the vector $x_1 \in \mathbb{R}^n$ are chosen arbitrary. Taking $t = T$ in (8) and by using (9) we have $X(T) = x_1$.

Thus the control $u(t)$ steers from $x(0)$ to $x(T)$. Hence the system (4) is relatively controllable. On the otherhand if the Grammian matrix is not positive definite, there exists a nonzero vector y such that

$$y^* W y = 0,$$

$$y^* \left[\sum_{i=0}^{m} \int_0^T (X_{\alpha,\alpha}(T - r_i(s))C_i\dot{r}_i(s))(X_{\alpha,\alpha}(T - r_i(s))C_i\dot{r}_i(s))^* \mathrm{d}s \right] y = 0,$$

which implies

$$y^* \sum_{i=0}^{m} (X_{\alpha,\alpha}(T - r_i(s))C_i\dot{r}_i(s)) = 0, \text{ on } [0, T].$$

Consider the zero initial function $\phi = 0$ and $u_0 = 0$ on $[-h, 0]$ and the final point $x_1 = y$. Since the system is controllable there exists a control $u(t)$ on J that steers the response to $x_1 = y$. For $\phi = 0$, $x_L(T;\phi) = 0$, $H(t) = 0$ and on the other hand

$$y = x_L(T) = \sum_{i=0}^{m} \int_0^T (T - r_i(s))^{\alpha-1} X_{\alpha,\alpha}(T - r_i(s))C_i\dot{r}_i(s)u(s)\mathrm{d}s,$$

then

$$y^* y = \sum_{i=0}^{m} \int_0^T y^*(T - r_i(s))^{\alpha-1} X_{\alpha,\alpha}(T - r_i(s))C_i\dot{r}_i(s)u(s)\mathrm{d}s = 0.$$

This contradicts for $y \neq 0$. Hence W is nonsingular.

4 Nonlinear Delay Systems

Consider the nonlinear fractional delay dynamical systems with multiple delays in control of the form

$$
\begin{aligned}
{}^{C}D^{\alpha}x(t) &= Ax(t) + Bx(t-h) + \sum_{i=0}^{M} C_i u(\sigma_i(t)) + f(t, x(t), x(t-h), u(t)), t \in J,\\
x(t) &= \phi(t), -h < t \leq 0.
\end{aligned} \tag{10}
$$

where $0 < \alpha < 1$, $x \in \mathbb{R}^n$, $u \in \mathbb{R}^m$ and A, B are $n \times n$ matrices, C_i for $i = 0, 1, \ldots M$ are $n \times m$ matrices and $f : J \times \mathbb{R}^n \times \mathbb{R}^n \times \mathbb{R}^m \to \mathbb{R}^n$ is a continuous function. Further we impose the following assumption

(H3) The continuous function f satisfies the condition that

$$
||f(t, p)|| \leq \sum_{j=1}^{q} \rho_j(t)\phi_j(p), \tag{11}
$$

where $\phi_j : \mathbb{R}^n \times \mathbb{R}^n \times \mathbb{R}^m \to \mathbb{R}_+$ are measurable functions and $\rho_i : J \to \mathbb{R}_+$ are L_1 functions for $j = 1, 2, \ldots q$.

Denote Q be the Banach space of continuous $\mathbb{R}^n \times \mathbb{R}^m$ valued functions defined on the interval J with the norm

$$
||(x, u)|| = ||x|| + ||u||
$$

where $||x|| = \sup\{x(t) : t \in J\}$ and $||u|| = \sup\{u(t) : t \in J\}$. That is $Q = C_n(J) \times C_m(J)$, where $C_n(J)$ is the Banach space of continuous $\mathbb{R}^n$ valued functions defined on the interval J with the sup norm.

Similar to the linear system, the solution of nonlinear system (10) using time lead function $r_i(t)$ is given as

$$
\begin{aligned}
x(t) = x_L(t; \phi) + H(t) + \sum_{i=0}^{m} \int_0^t (t - r_i(s))^{\alpha-1} X_{\alpha,\alpha}(t - r_i(s)) C_i \dot{r}_i(s) u(s) \mathrm{d}s,\\
+ \int_0^t (t-s)^{\alpha-1} X_{\alpha,\alpha}(t-s) f(s, x(s), x(s-h), u(s)) \mathrm{d}s.
\end{aligned} \tag{12}
$$

Theorem 3 *Assume that the Hypotheses (H1), (H2) and (H3) are satisfied and suppose that*

$$
det W(0, T) > 0. \tag{13}
$$

Then the nonlinear system (10) is relatively controllable on J.

Proof Now, let $\psi_j(r) = \sup\{\phi_j(p); ||p|| \leq r\}$, since (H5) holds, there exists $r_0 > 0$ such that

$$r_0 - \sum_{i=1}^{q} c_j \psi_j(r_0) \geq d,$$

which implies that $\sum_{j=1}^{q} c_j \psi_j(r_0) + d \leq r_0$. Define the operator $\Psi : Q \to Q$ by $\Psi(x, u) = (y, v)$ where y and v are defined as

$$\begin{aligned} v(t) = (T - r_i(t))^{1-\alpha} (X_{\alpha,\alpha}(T - r_i(t)) C_i^* \dot{r}_i(t))^* W^{-1} \Big[& x_1 - x_L(T; \phi) \\ & - \sum_{i=0}^{m} \int_{\sigma_i(0)}^{0} (T - r_i(s))^{\alpha-1} X_{\alpha,\alpha}(T - r_i(s)) C_i \dot{r}_i(s) u_0(s) \mathrm{d}s \\ & - \sum_{i=m+1}^{M} \int_{0}^{T} (T - r_i(s))^{\alpha-1} X_{\alpha,\alpha}(T - r_i(s)) C_i \dot{r}_i(s) u_0(s) \mathrm{d}s \\ & - \int_{0}^{T} (T - s)^{\alpha-1} X_{\alpha,\alpha}(T - s) f(s, x(s), x(s-h), u(s)) \mathrm{d}s \Big], \end{aligned}$$

and

$$\begin{aligned} y(t) = x_L(t; \phi) + & \sum_{i=0}^{m} \int_{\sigma_i(0)}^{0} (t - r_i(s))^{\alpha-1} X_{\alpha,\alpha}(t - r_i(s)) C_i \\ & \times \dot{r}_i(s) u_0(s) \mathrm{d}s + \sum_{i=0}^{m} \int_{0}^{t} (t - r_i(s))^{\alpha-1} X_{\alpha,\alpha}(t - r_i(s)) C_i \dot{r}_i(s) v(s) \mathrm{d}s \\ & + \sum_{i=m+1}^{M} \int_{\alpha_0}^{t} (t - r_i(s))^{\alpha-1} X_{\alpha,\alpha}(t - r_i(s)) C_i \dot{r}_i(s) u_0(s) \mathrm{d}s \\ & + \int_{0}^{t} (t - s)^{\alpha-1} X_{\alpha,\alpha}(t - s) f(s, x(s), x(s-h), v(s)) \mathrm{d}s, \end{aligned}$$

Let

$$\begin{aligned} \lambda &= \sup ||X_{\alpha,\alpha}(T - s)||, \omega = \sup ||x_L(t; \phi)||, \xi_j = 4\lambda\alpha^{-1} T^{\alpha} ||\rho_j|| \\ c_j &= \max\{\xi_j, \delta_{ij}\}, a = \max\{b, 1\}, \delta_{ij} = 4a_i b_i ||C_i^*|| ||W^{-1}|| \lambda\alpha^{-1} T^{\alpha} ||\rho_j|| \\ \nu &= \sup ||u_0(s)||, \mu = \sum_{i=0}^{m} a_i b_i ||C_i^*|| N_i + \sum_{i=m+1}^{M} a_i b_i ||C_i|| M_i, b = \sum_{i=0}^{m} a_i b_i L_i ||C_i|| \\ a_i &= \sup ||X_{\alpha,\alpha}(T - r_i(s))||, b_i = \sup ||\dot{r}_i(s)||, i = 0, 1, \cdots, M. \end{aligned}$$

$$d_i = 4[a_i b_i ||C_i^*|||]||W^{-1}||[|x_1 + \omega + \mu|], i = 0, 1, 2, \ldots m,$$
$$d_2 = 4[\omega + \nu\mu], d = \max\{d_i, d_2\}, i = 0, 1, 2, \ldots m,$$
$$L_i = \int_0^T (T - r_i(s))^{\alpha-1} \mathrm{d}s, i = 0, 1, 2, \ldots m,$$
$$N_i = \int_{\sigma_i(0)}^0 (T - r_i(s))^{\alpha-1} \mathrm{d}s, i = 0, 1, 2 \ldots m,$$
$$M_i = \int_{\sigma_i(0)}^{\sigma_i(T)} (T - r_i(s))^{\alpha-1} \mathrm{d}s, i = m + 1, m + 2, \cdots, M.$$

Then

$$|v(t)| \leq \frac{1}{4a}(d + \sum_{j=1}^{q} c_j \psi_j(r_0)).$$

and

$$|y(t)| \leq \frac{1}{2}(d + \sum_{j=1}^{q} c_j \psi_j(r_0)).$$

Therefore $|v(s)| \leq \frac{r_0}{4a}$ for all $s \in J$ and hence $||v|| \leq \frac{r_0}{4a}$, which gives $||y|| \leq \frac{r_0}{2}$. Thus we have proved that, if $Q(r_0) = \{(x, u) \in Q : ||x|| \leq \frac{r_0}{2}\}$ and $||u|| \leq \frac{r_0}{2}$, then Ψ maps $Q(r_0)$ into itself. Now, let us take $t_1, t_2 \in J$ with $t_1 < t_2$ and for all $(x, u) \in Q(r)$, $r > 0$, we need to show $\Psi(Q(r))$ is equicontinuous.

$$\begin{aligned} ||u(t_1) - u(t_2)|| \leq\ & ||(T - r_i(t_1))^{1-\alpha} C_i^* (X_{\alpha,\alpha}(T - r_i(t_1))\dot{r}_i(t_1))^* \\ & - (T - r_i(t_2))^{1-\alpha} C_i^* (X_{\alpha,\alpha}(T - r_i(t_2))\dot{r}_i(t_2))^*|| \\ & + \times ||W^{-1}|| \Bigg[||x_1|| + ||x_L(T; \phi)|| + \int_0^T (T - s)^{\alpha-1} \\ & \times \sum_{j=1}^{q} ||\rho_i|| ||x_{\alpha,\alpha}(T - s)\psi_j(r)|| \mathrm{d}s \Bigg] \end{aligned} \tag{14}$$

and

$$\begin{aligned} ||x(t_1) - x(t_2)|| \leq\ & ||x_L(t_1; \phi) - x_L(t_2; \phi)|| + \int_{t_1}^{t_2} G(t_2, s) \sum_{j=1}^{p} ||\rho_j|| \psi_j(r) \mathrm{d}s, \\ & + \sum_{i=m+1}^{M} \int_{\sigma_i(0)}^{\sigma_i(t_1)} ||H(t_1, s) - H(t_2, s)|| ||C_i|| ||\dot{r}_i(s)|| ||u_0(s)|| \mathrm{d}s \end{aligned}$$

$$+\sum_{i=0}^{m}\int_{\sigma_i(0)}^{0}||H(t_1,s)-H(t_2,s)||||C_i||||\dot{r}_i(s)||||u_0(s)||\mathrm{d}s$$
$$+\sum_{i=0}^{m}\int_{0}^{t_1}||H(t_1,s)-H(t_2,s)||||C_i||||\dot{r}_i(s)||||u(s)||\mathrm{d}s$$
$$+\int_{0}^{t_1}||G(t_1,s)-G_{t_2,s}||\sum_{j=1}^{q}||\rho_j||\psi_j(r)\mathrm{d}s$$
$$+\sum_{i=0}^{m}\int_{t_1}^{t_2}H(t_2,s)||B_i||||\dot{r}_i(s)||||u(s)||\mathrm{d}s \tag{15}$$

where

$$H(t,s)=(t-r_i(s))^{\alpha-1}X_{\alpha,\alpha}(t-r_i(s)),$$
$$G(t,s)=(t-s)^{\alpha-1}X_{\alpha,\alpha}(t-s).$$

Thus the right hand side of the Eqs. (14) and (15) are independent of $(x,u)\in Q(r)$ and tend to zero as $t_1\to t_2$. Hence $\psi(Q(r))$ is equicontinuous for all $r>0$ and by the regularity assumption of f, the operator is continuous and hence it is completely continuous by the application of Arzela-Ascoli theorem. Since $Q(r_0)$ is closed, bounded and convex, the Schauder fixed point theorem guarantees that Similar to the proof of Theorem 4.1, it can be shown that Ψ has a fixed point $(z,v)\in Q(r)$, such that $\Psi(x,u)=(y,v)=(x,u)$. Hence $x(t)$ is the solution of the system (10) and easy to verify $x(T)=x_1$. Thus the control $u(t)$ steers the system (10) from the initial complete state $y(0)$ to x_1 on J. Hence the system (10) is relatively controllable on J.

5 Examples

In this section, we apply the results obtained in the previous sections to the following fractional dynamical systems with multiple delays in control.

Example 1 Consider the linear fractional delay dynamical system with delay in control of the form

$$^{C}D^{\alpha}x(t)=Ax(t)+Bx(t-1)+C_0u(t)+C_1u(t-1), \tag{16}$$
$$x(t)=\phi(t),$$

where $A=1$, $B=1$, $C_0=1$, $C_1=1$, $h=1$, $\sigma=1$ and $\phi(t)=1$ with the initial point $x(0)=1$ and final point $x(1)=10$. The solution of the Eq. (16) by taking Laplace transform is of the form

$$
\begin{aligned}
x(t) &= \sum_{n=0}^{[t]} (t-n)^{\frac{1}{2}n} E_{\frac{1}{2},\frac{1}{2}n+1}((t-n)^{\frac{1}{2}}), \\
&+ \sum_{n=0}^{[t]} B^{n+1} \int_{-1}^{0} (t-s-n-1)^{\frac{1}{2}n-\frac{1}{2}} E_{\frac{1}{2},\frac{1}{2}(n+1)}((t-s-n-1)^{\frac{1}{2}})\phi(s)\mathrm{d}s, \\
&+ \sum_{n=0}^{[t]} \int_{0}^{t-n} (t-s-n)^{\frac{1}{2}n-\frac{1}{2}} E_{\frac{1}{2},\frac{1}{2}n+\frac{1}{2}}((t-s-n)^{\frac{1}{2}})u(s)\mathrm{d}s \\
&+ \sum_{n=0}^{[t]} \int_{0}^{t-n} (t-s-n)^{\frac{1}{2}n-\frac{1}{2}} E_{\frac{1}{2},\frac{1}{2}n+\frac{1}{2}}((t-s-n)^{\frac{1}{2}})u(s-1)\mathrm{d}s. \qquad (17)
\end{aligned}
$$

Now, consider the controllability on [0, 1], where $[t] = 0$. Then the solution (17), using time lead function the solution can be written as

$$
\begin{aligned}
x(t) &= E_{\frac{1}{2}}(t^{\frac{1}{2}}) + t^{\frac{1}{2}} E_{\frac{1}{2},\frac{3}{2}}(t^{\frac{1}{2}}) \\
&+ \sum_{i=0}^{1} \int_{0}^{t} (t-r_i(s))^{-\frac{1}{2}} E_{\frac{1}{2},\frac{1}{2}}((t-r_i(s))^{\frac{1}{2}})\dot{r}_i(s)u(s)\mathrm{d}s,
\end{aligned}
$$

where $r_0(s) = s$ and $r_1(s) = s - 1$. The controllability Grammian matrix is $W = 86.8522$ is positive definite. Hence by the Theorem 1 the system is controllable on [0, 1].

Figure 1 represent the trajectory of the system without control and Fig. 2 represent the trajectory of the system with control.

Example 2 Consider the nonlinear fractional delay dynamical system represented by the scalar fractional differential equation

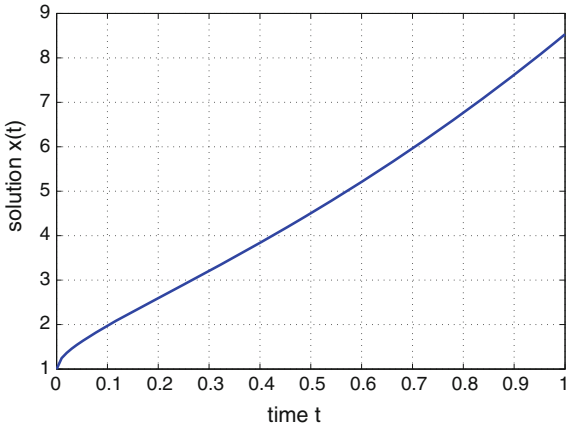

Fig. 1 The trajectory of the system without control

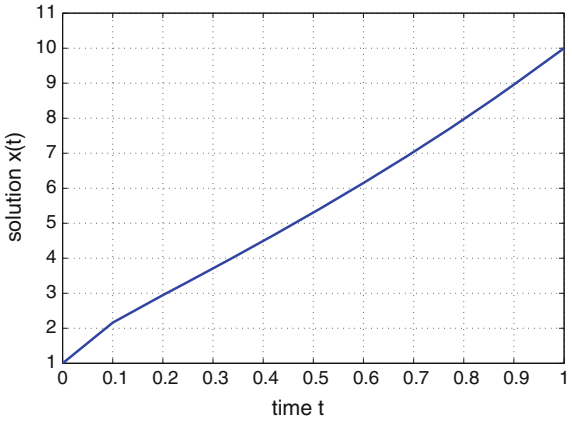

Fig. 2 The trajectory of the system with control

$$
\begin{aligned}
{}^{C}D^{\frac{1}{2}}x(t) &= Ax(t) + Bx(t-1) + C_0u(t) + C_1u(t-1) + f(t, x(t), x(t-1), u(t)),\\
x(t) &= 1
\end{aligned}
\tag{18}
$$

Here, also we consider the controllability on [0, 1] with initial condition $x(0) = x_0$ and final condition $x(1) = x_1$. Take A, B, C_0, C_1 and h as defined in the previous example. Let the nonlinear function

$$
f(t, x(t), x(t-1), u(t)) = \frac{x_1(t)}{x_1(t) + x_2(t)} + \frac{x_2(t)}{1 + x_1(t) + u(t)}. \tag{19}
$$

Since the linear system (16) is controllable on [0, 1] and the nonlinear function (19) satisfies the hypothesis in Theorem 2. Then the nonlinear system (18) is controllable on [0, 1].

6 Conclusion

This paper deals with the controllability of nonlinear fractional delay dynamical systems with multiple delays in control. Grammian matrix is constructed to obtain the controllability results. The control has been designed to steer the system from the initial state to the final state. Further, sufficient conditions are established for the controllability of nonlinear fractional delay dynamical systems.

References

1. Dauer, J.P., Gahl, R.D.: Controllability of nonlinear delay systems. J. Optim. Theory. Appl. **21**(1), 59–68 (1977)
2. Balachandran, K., Dauer, J.P.: Controllability of perturbed nonlinear delay systems. IEEE Trans. Autom. Control **32**, 172–174 (1987)
3. Balachandran, K., Kokila, J., Trujillo, J.J.: Relative controllability of fractional dynamical systems with multiple delays in control. Comput. Math. Appl. **64**(10), 3037–3045 (2012)
4. Balachandran, K., Zhou, Y., Kokila, J.: Relative controllability of fractional dynamical systems with delays in control. Commun. Nonlinear. Sci. Numer. Simul. **17**(9), 3508–3520 (2012)
5. Klamka, J.: Controllability of linear systems with time variable delay in control. Int. J. Control. **24**(6), 869–878 (1976)
6. Klamka, J.: Relative controllability of nonlinear systems with delay in control. Automatica **12**(6), 633–634 (1976)
7. Mur, T., Henriquez, H.R.: Relative controllability of linear systems of fractional order with delay. Math. Control. Relat. F. **5**(4), 845–858 (2015)
8. Babiarz, A., Klamka, J., Niezabitowski, M.: Schauder's fixed point theorem in approximate controllability problems. Int. J. Appl. Math. Comput. Sci. **26**(2), 263–275 (2016)
9. Klamka, J., Babiarz, A, Niezabitowski, M.: Banach fixed point theorem in semilinear controllability problems-a survey. Bull. Pol. Ac. Tech. **64**(1), 21–35 (2016)
10. Nirmala, R.J., Balachandran, K., Germa, L.R., Trujillo, J.J.: Controllability of nonlinear fractional delay dynamical systems. Rep. Math. Phys. **77**(1), 87–104 (2016)
11. Kilbas, A., Srivastava, H.M., Trujillo, J.J.: Theory and Application of Fractional Differential Equations. Elsevier, Amstrdam (2006)
12. Podlubny, I.: Fractional Differential Equations. Academic Press, New York (1999)
13. Granas, A., Dugundji, J.: Fixed Point Theory. Springer, New York (2003)
14. Balachandran, K.: Global relative controllability of non-linear systems with time-varying multiple delays in control. Int. J. Control **46**(1), 193–200 (1987)

New Controllability Criteria for Fractional Systems with Varying Delays

Jerzy Klamka and Beata Sikora

Abstract Finite-dimensional dynamical control systems described by linear fractional-order state equations with multiple delays in control varying in time are presented in the paper. Both the unconstrained and constrained controls are considered. The constraints are put on the control values. The set of admissible control values is assumed to be a convex and compact set containing 0 in its interior and a cone with vertex at zero and a nonempty interior. New necessary and sufficient conditions for unconstrained as well as for constrained relative controllability of fractional-order systems with delayed varying controls are established and proved. A numerical example is presented to illustrate the obtained theoretical results.

Keywords Fractional systems · Linear control systems · Constrained controllability · Varying delays in control · The caputo derivative

1 Introduction

The controllability of dynamical systems is one of the most significant issue in the control theory. The controllability, in short, is a possibility to steer a control system from an initial state into a final state with the aid of admissible controls. Depending on both class of control systems and a set of admissible controls, various controllability definitions have been formulated in subject literature. A review of recently analyzed controllability problems for a broad class of dynamical systems is presented in [1].

J. Klamka
Institute of Automatic Control, Silesian University of Technology,
Akademicka 16, 44-100 Gliwice, Poland
e-mail: jerzy.klamka@polsl.pl

B. Sikora (✉)
Institute of Mathematics, Silesian University of Technology,
Kaszubska 23, 44-100 Gliwice, Poland
e-mail: beata.sikora@polsl.pl

A. Babiarz et al. (eds.), *Theory and Applications of Non-integer Order Systems*,
Lecture Notes in Electrical Engineering 407, DOI 10.1007/978-3-319-45474-0_30

Last decades provide many papers and monographs concerning controllability of dynamical control systems described by fractional-order differential equations. Fractional-order models describe the behavior of many real-life processes more accurately than integer-order ones. Control systems modeled using fractional differential equations occur, among others, in mechanical, biological and chemical problems. Detailed discussions of fractional differential equations and their practical applications can be found, among others, in the monographs: [2–8]. The controllability of discrete-time fractional systems is studied in [9–12], positive fractional discrete-time systems are discussed in [13], positive fractional linear systems, both discrete- and continuous-time, are presented in [14] and [15]. The controllability of continuous-time linear fractional systems is studied, among others, in [16–22].

However, models describing control processes frequently involve delays in state or in control, because very often future states depend on both a present state and on past states of a system. If we have delays in the input function, we deal with control systems with delayed controls. Controllability problems for linear continuous-time fractional systems with delayed control were analyzed in [14, 15, 23–25]. It should be noted, however, that the majority of papers on linear fractional systems controllability address controllability issues for unconstrained controls. The works on controllability of linear fractional systems with bounded inputs are [26] for fractional positive discrete-time linear systems, [27] for fractional positive continuous-time linear systems and [28] for continuous-time linear fractional systems. It should be stressed that, in practice, controls are not completely unconstrained.

The aim of the paper is to give some new criteria for both unconstrained and constrained controllability of continuous-time fractional-order control systems with multiple delays in control varying in time.

The paper is organized as follows. Section 2 recalls some preliminary definitions, formulas and notations. Moreover, it presents the mathematical model of the considered fractional systems and the formula for a solution of the discussed systems. The formula is derived by means of the Laplace transform. Some definitions of relative and constrained relative controllability of the systems are formulated. Constraints are imposed on control values. The main results of the paper, contained in Sect. 3, are the criteria for relative controllability of the fractional system with delayed varying controls and constrained relative controllability when the set of admissible control values U is a convex and compact set containing 0 in its interior and a cone with vertex at zero and nonempty interior. All theorems are proved. The theoretical results are illustrated with a numerical example provided in Sect. 4. Finally, concluding remarks are included in Sect. 5.

2 Preliminaries

Let ${}^{C}D^{\alpha}f(t)$ denote the Caputo fractional derivative of order α ($n<\alpha<n+1$, $n\in\mathbb{N}$) for a function $f:\mathbb{R}^{+}\to\mathbb{R}$.

Definition 1 [3] The Caputo fractional derivative is defined by the formula

$$ {}^{C}D^{\alpha}f(t)=\frac{1}{\Gamma(n-\alpha+1)}\int_{0}^{t}\frac{f^{(n+1)}(\tau)}{(t-\tau)^{\alpha-n}}\,d\tau, $$

where Γ is the gamma function.

In the Caputo approach the initial conditions for fractional differential equations take on the same form as for integer-order differential equations, therefore we use Caputo's fractional derivatives in the paper.

Applying the definition of the Mittag-Leffler function $E_{\alpha,\beta}(z)$ presented, among others, in [3, 14]

$$ E_{\alpha,\beta}(z)=\sum_{k=0}^{\infty}\frac{z^{k}}{\Gamma(\alpha k+\beta)},\ z\in\mathbb{C}, $$

for $\alpha>0$, $\beta>0$ and an arbitrary n-th order square matrix A, we introduce the following notation

$$ \Phi_{0}(t)=E_{\alpha,1}(At^{\alpha})=\sum_{k=0}^{\infty}\frac{A^{k}t^{\alpha k}}{\Gamma(k\alpha+1)}. $$

$\Phi_{0}(t)$ denotes the *pseudo-transition matrix* of the linear fractional system ${}^{C}D^{\alpha}x(t)=Ax(t)$ ([8, 14]). Moreover, let

$$ \Phi(t)=t^{\alpha-1}E_{\alpha,\alpha}(At^{\alpha})=t^{\alpha-1}\sum_{k=0}^{\infty}\frac{A^{k}t^{\alpha k}}{\Gamma((k+1)\alpha)}. $$

The following designation are also used throughout the paper. Let $L^{2}([0,\infty),\mathbb{R}^{m})$ denote the Hilbert spaces of square integrable functions with values in $\mathbb{R}^{m}$ and $L^{2}_{loc}([0,\infty),\mathbb{R}^{m})$ denote the linear space of locally square integrable functions with values in $\mathbb{R}^{m}$.

In the paper we discuss the linear control systems with multiple varying delays in control described by the following fractional differential state equation

$$ {}^{C}D^{\alpha}x(t)=A\,x(t)+\sum_{i=0}^{M}B_{i}(t)\,u(v_{i}(t)) \tag{1} $$

for $t \geq t_0$ and $0 < \alpha < 1$, where

- $x(t) \in \mathbb{R}^n$ is a state vector,
- $u \in L^2_{loc}([t_0, \infty), \mathbb{R}^m)$ is a control,
- A is a $(n \times n)$-matrix with real elements,
- $B_i(t)(i = 0, \ldots, M)$ are $(n \times m)$-matrices with elements $b_{ikj} \in L^2_{loc}([t_0, \infty), \mathbb{R})$, $k = 1, \ldots, M$, $j = 1, \ldots, m$,
- $v_i : [t_0, \infty) \to \mathbb{R}$, $i = 0, 1, \ldots, M$, are absolutely continuous, strictly increasing functions, satisfying the inequalities

$$v_M(t) < v_{M-1} < \cdots < v_k(t) < \cdots < v_1(t) < v_0(t) = t, \ t \in [t_0, \infty),$$

where $v_i(t) = t - h_i(t)$ and $h_i(t) \geq 0$, $i = 0, 1, \ldots, M$, are time-dependent delays in control.

Let be given the initial conditions $z(t_0) = (x(t_0), u_{t_0}) \in \mathbb{R}^M \times L^2([v_M(t_0), t_0], U)$ called the *initial complete state* of the fractional system (1). In the case of dynamical systems with delays, both for integer order and fractional order ones, only a complete state $z(t) = (x(t), u_t(s))$, where $u_t(s) = u(s)$ for $s \in [v_M(t), t)$, fully describes the behavior of the dynamical system at any time t.

Let $U \subset \mathbb{R}^m$ be any non-empty set. The set $L^2([t_0, t_1], U)$ of square integrable functions on $[t_0, t_1]$ with values in U is the *set of admissible controls* for the fractional system (1).

Theorem 1 *For given initial conditions $z(t_0) \in \mathbb{R}^M \times L^2([v_M(t_0), t_0], U)$ and an admissible control $u \in L^2([t_0, t], U)$, for every $t \geq t_0$ there exists a unique, absolutely continuous solution $x(t, z(t_0), u)$ of the differential equation (1) that takes the form*

$$x(t, z(t_0), u) = \Phi_0(t)x(t_0) + \int_{t_0}^{t} \Phi(t - \tau) \sum_{i=0}^{M} B_i(\tau)\, u(v_i(\tau))\, d\tau. \tag{2}$$

Proof In order to prove the theorem we use the method presented in [14] for fractional systems without delays. To simplify the notation, let us denote $x(t, z(t_0), u) = x(t)$. First, we apply the Laplace transform to the fractional equation (1) and we obtain

$$s^{\alpha}\mathcal{L}[x(t)] - s^{\alpha-1}x(t_0) = A\mathcal{L}[x(t)] + \mathcal{L}\Big[\sum_{i=1}^{M} B_i(t)u(v_i(t))\Big],$$

for any fixed $t \geq t_0$. So

$$\mathcal{L}[x(t)] = (s^{\alpha}I - A)^{-1}s^{\alpha-1}x(t_0) + (s^{\alpha}I - A)^{-1}\mathcal{L}\Big[\sum_{i=1}^{M} B_i(t)u(v_i(t))\Big] =$$

$$= \mathcal{L}[\Phi_0(t)x(t_0)] + \mathcal{L}\big[\Phi(t)\big]\mathcal{L}\big[\sum_{i=1}^{M} B_i(t)u(v_i(t))\big],$$

since [8, 14]

$$\mathcal{L}^{-1}[s^{\alpha-1}(s^{\alpha}I - A)^{-1}] = \Phi_0(t)$$

$$\mathcal{L}^{-1}[(s^{\alpha}I - A)^{-1}] = \Phi(t).$$

Next, by the convolution theorem for the Laplace transform, we have

$$\mathcal{L}[x(t)] = \mathcal{L}[\Phi_0(t)x(t_0)] + \mathcal{L}\Big[\int_{t_0}^{t} \Phi(t-\tau)\sum_{i=1}^{M} B_i(\tau)u(v_i(\tau))d\tau\Big].$$

And finally, using the inverse Laplace transform, we have the solution (2). □

As for integer-order dynamical systems, see [29], we can define a set of reachable states called also the attainable set for the fractional system (1).

Definition 2 The attainable set from the initial complete state $z(t_0) = (x(t_0), u_{t_0})$ for the time-delay fractional system (1) is called the set

$$K_U(t) = \{x(t) \in \mathbb{R}^n : x(t) = \Phi_0(t)x(t_0) +$$

$$+ \int_{t_0}^{t} \Phi(t-\tau)\sum_{i=0}^{M} B_i(\tau)\, u(v_i(\tau))\, d\tau : u(t) \in U \text{ for } t \in [t_0, t_1]\Big\}. \tag{3}$$

Analogously to the fractional systems with constant delays in the control (see [28]), we have the definitions of relative controllability and constrained relative controllability of the system (1) on $[t_0, t_1]$.

Definition 3 The fractional system (1) is called relatively controllable on $[t_0, t_1]$ from the initial complete state $z(t_0) = (x(t_0), u_{t_0})$ into $S \subset \mathbb{R}^n$, if for each vector $\widehat{x} \in S$, there exists a control $\widehat{u} \in L^2([t_0, t_1], \mathbb{R}^m)$ such that

$$x(t_1, z(t_0), \widehat{u}) = \widehat{x}.$$

In the paper, constraints put on control values are considered: $u(t) \in U$ for $t \in [t_0, t_1]$. Constraints of this type frequently occur in practical applications concerning problems of optimal control, industrial or biological processes.

Definition 4 The fractional-order system (1) is called relatively U-controllable on $[t_0, t_1]$ from the initial complete state $z(t_0) = (x(t_0), u_{t_0})$ into $S \subset \mathbb{R}^n$, if for each vector $\widetilde{x} \in S$, there exists a control $\widetilde{u} \in L^2([t_0, t_1], U)$ such that

$$x(t_1, z(t_0), \widetilde{u}) = \widetilde{x}.$$

Definition 5 The fractional-order system (1) is called (globally) relatively U-controllable on $[t_0, t_1]$ into $S \subset \mathbb{R}^n$, if it is relatively U-controllable on $[t_0, t_1]$ into the set S for every initial complete state $z(t_0) = (x(t_0), u_{t_0})$.

Remark 1 Definition 2 implies that the system (1) is (globally) relatively U-controllable on $[t_0, t_1]$ if $K_U(t) = \mathbb{R}^n$, see [30].

In case of $S = \mathbb{R}^n$ we say that (1) is relatively or relatively U-controllable on $[t_0, t_1]$ and for $S = \{0\}$, we say that (1) is relatively null controllable or relatively null U-controllability on $[t_0, t_1]$.

3 Main Results

In this main section we discuss relative and constrained relative controllability (relative U-controllability) of the fractional system (1). We establish new criteria of relative controllability of the system with varying delays (1) and relative U-controllability for controls from closed and convex cone with nonempty interior and vertex at zero as well as for controls from a cone with vertex at zero and a nonempty interior.

Before we formulate the first criterion, we transform the formula (2) in the following manner. Let us fix a final time $t_1 > 0$. Using the absolute continuity of v_i and exploiting their inverses $r_i : [v_i(t_0), v_i(t_1)] \to [t_0, t_1]$, $i = 0, 1, 2, \ldots, M$, we can rewrite the solution of (1) in the following form:

$$x(t_1, z(t_0), u) = \Phi_0(t_1)x(t_0) + \sum_{i=0}^{M} \int_{v_i(t_0)}^{v_i(t_1)} \Phi(t_1 - r_i(\tau))B_i(r_i(\tau))\dot{r}_i(\tau)u(\tau)\, d\tau,$$

where $\dot{r}_i$ means the first derivative of r_i.

Without loss of generality, to simplify the notation, we may assume that $t_0 = v_k(t_1)$ for some $k \leq M$. If such a k does not exist, then we introduce an additional delay h_k with control matrix $B_k(t) = 0$. Then the solution (2) of the dynamical system (1) has, at time t_1, the form

$$x(t_1, z(t_0), u) = \Phi_0(t_1)x(t_0) + \sum_{i=0}^{k} \int_{v_i(t_0)}^{t_0} \Phi(t_1 - r_i(\tau))B_i(r_i(\tau))\dot{r}_i(\tau)u_{t_0}(\tau)\, d\tau$$

$$+ \sum_{i=k+1}^{M} \int_{v_i(t_0)}^{v_i(t_1)} \Phi(t_1 - r_i(\tau))B_i(r_i(\tau))\dot{r}_i(\tau)u_{t_0}(\tau)\, d\tau$$

$$+ \sum_{i=0}^{k} \int_{t_0}^{v_i(t_1)} \Phi(t_1 - r_i(\tau))B_i(r_i(\tau))\dot{r}_i(\tau)u(\tau)\, d\tau.$$

The first three terms on the right hand side depend only on $z(t_0) = (x(t_0), u_{t_0})$, We introduce the following denotation

$$q(z(t_0)) = x(t_0)+ \tag{4}$$

$$+\big(\Phi_0(t_1)\big)^{-1}\Bigg[\sum_{i=0}^{k}\int_{v_i(t_0)}^{t_0}\Phi(t_1 - r_i(\tau))B_i(r_i(\tau))\dot{r}_i(\tau)u_{t_0}(\tau)\,d\tau+$$

$$+\sum_{i=k+1}^{M}\int_{v_i(t_0)}^{v_i(t_1)}\Phi(t_1 - r_i(\tau))B_i(r_i(\tau))\dot{r}_i(\tau)u_{t_0}(\tau)\,d\tau\Bigg]$$

and

$$B_{t_1}(t) = \big(\Phi(t_1 - t)\big)^{-1}\sum_{j=0}^{i}\Phi(t_1 - r_i(t))B_i(r_i(t))\dot{r}_i(t), \tag{5}$$

for $t \in [v_{i+1}(t_1), v_i(t_1))$, $i = 0, 1, \ldots, k-1$. $B_{t_1}(t)$ is $(n \times m)$-dimensional matrix defined on $[t_0, t_1]$ (since $t_0 = v_k(t_1)$) with square integrable elements.

As in the case of integer order systems [29, 31], the following lemma holds.

Lemma 1 *Let*

$${}^{C}D^{\alpha}y(t) = Ay(t) + B_{t_1}(t)u(t), \quad t \in [t_0, t_1], \tag{6}$$

be a linear fractional dynamical system without delays in control. Then

$$x(t, z(t_0), u) = y(t, q(z(t_0)), u), \quad t \in [t_0, t_1].$$

Proof The lemma follows immediately from formulas (2), (4) and (5). □

By Lemma 1, the relative controllability on $[t_0, t_1]$ of the fractional system with delays (1) and the controllability on $[t_0, t_1]$ of the fractional system (6) without delays in control are equivalent. It follows that we may apply the method known for fractional-order systems without delays basing on so-called controllability matrix to verify relative controllability of the systems with delays (1).

Let us denote

$$W_k(t_0, t_1) = \int_{t_0}^{t_1}\Phi(t_1 - \tau)B_{t_1}(\tau)B_{t_1}^{T}(\tau)\Phi^{T}(t_1 - \tau)\,d\tau, \tag{7}$$

where $\Phi(t) = t^{\alpha-1}E_{\alpha,\alpha}(At^{\alpha})$, $\Phi^{T}(t) = E_{\alpha,\alpha}(A^{T}t^{\alpha})$ and A^{T} means the transpose of A.

The matrix $W_k(t_0, t_1)$ is called the *relative controllability matrix* of the fractional system (1).

Theorem 2 *The fractional system (1) is relatively controllable on* $[t_0, t_1]$ *if and only if*

$$\operatorname{rank} W_k(t_0, t_1) = n,$$

where $W_k(t_0, t_1)$ *is given by (7).*

Proof Based on Lemma 1, the relative controllability matrix $W_k(t_0, t_1)$ of the system (1) is the controllability matrix of the system without delays (6), simultaneously. We can apply the result for fractional systems without delays presented in [16]. Since $W_k(t_0, t_1)$ is positive definite, it is non-singular, so it is full rank. This completes the proof. □

Now we put constraints on the control values, that is let $u(t) \in U$.

Theorem 3 *Let* $U \subset \mathbb{R}^m$ *be a convex and compact set containing 0 in its interior. If* $\operatorname{rank} W_k(t_0, t_1) = n$ *and the linear fractional dynamical system (1) is asymptotically stable, then the system is relatively null U-controllable on* $[t_0, t_1]$.

Proof Suppose $U \subset \mathbb{R}^m$ be a convex and compact set containing 0 in its interior. Since $\operatorname{rank} W_k(t_0, t_1) = n$, based on Theorem 2, the system (1) is relatively controllable without any constraints on $[t_0, t_1]$. Moreover, owing the asymptotical stability assumption, $x = 0$ is the solution of the system (1) for the admissible control $u(t) = 0$. Using the null control $u(t) = 0$, the solution $x(t, z(t_0), 0)$ of (1) satisfies the conditions

$$\lim_{t \to \infty} x(t, z(t_0), 0) = 0 \quad \textit{and} \quad x(t_1, z(t_0), 0) \in N(0),$$

for some, finite $t_1 \in (t_0, \infty)$, where $N(0)$ is a sufficiently small neighborhood of $0 \in \mathbb{R}^n$. Then, the instantaneous state $x(t_1, z(t_0), 0)$ can be steered to $0 \in \mathbb{R}^n$ in finite time, so the fractional system (1) is relatively null U-controllable. □

Theorem 4 *Let U be a cone with vertex at zero and a nonempty interior in the one-dimensional space* $\mathbb{R}$. *The linear fractional dynamical system (1) is relatively U-controllable on* $[t_0, t_1]$ *if and only if* $\operatorname{rank} W_k(t_0, t_1) = n$ *and the matrix A has only complex eigenvalues.*

Proof The necessary condition follows from the fact that if $\operatorname{rank} W_k(t_0, t_1) < n$ or A has not only complex eigenvalues, no open set about origin can be reached, see [32]. The sufficient condition is satisfied, because if $\operatorname{rank} W_k(t_0, t_1) = n$ (i.e. the fractional system (1) is relatively controllable without any constraints—see Theorem 2) and A has only complex eigenvalues, it is sufficient to reach all states in $\mathbb{R}^n$. In fact, since U is the cone with vertex at the origin and nonempty interior in $\mathbb{R}^n$, for any admissible control u also $ku \in L^2([0, T], U)$ for all $k \geq 0$. The attainable set $K_U(t_1)$ is a convex set containing 0 in its interior (due to the second condition) and it is a cone with vertex at the origin (because it is linear with respect to $u(\cdot)$), hence it has to be a whole space $\mathbb{R}^n$. □

4 Example

In this section we present a numerical example to illustrate the obtained theoretical results.

Example 1 Let be given the following fractional system with the delay in control

$$ {}^{C}D^{\frac{1}{2}}x(t) = Ax(t) + B_0(t)u(t) + B_1(t)u(t-1) + B_2(t)u(-2t), \tag{8} $$

for $t \in [1, 2]$ and $u(t) \in [0, +\infty)$, with initial conditions $z(0) = (0, 0)$, where

$$ A = \begin{bmatrix} 0 & -3 \\ 1 & 0 \end{bmatrix}, \ B_0(t) = \begin{bmatrix} 0 \\ t \end{bmatrix}, \ B_1(t) = \begin{bmatrix} -2t \\ 0 \end{bmatrix}, \ B_2(t) = \begin{bmatrix} t \\ -t \end{bmatrix}. $$

The set of admissible control values $U = [0, +\infty)$ is a cone with vertex at zero and a nonempty interior in the one-dimensional space $\mathbb{R}$. We have $\alpha = \frac{1}{2}$, $n = 2$, $M = 2$. Moreover, $v_0 = t$, $v_1 = t - 1$ and $v_2 = -2t$. As a consequence, $h_0(t) = 0$, $h_1(t) = 1$ and $h_2(t) = 3t$, because $v_i(t) = t - h_i(t)$. We will show, using Theorem 4, that the system (8) is relatively U-controllable on $[1, 2]$.

Since $v_1(2) = 2 - h_1 = 1, k = 1$. Therefore the relative controllability matrix (7) takes the form

$$ W_1(1, 2) = \int_1^2 \Phi(2-\tau)B_{t_1}(\tau)B_{t_1}^T(\tau)\Phi^T(2-\tau)\,d\tau, $$

for $B_{t_1}(t)$ given by formula (5) and $t_1 = 2$, that is

$$ B_{t_1}(t) = \big(\Phi(2-t)\big)^{-1}\Phi(2-t)B_0(t). $$

By the Cayley–Hamilton method we calculate the matrix $E_{\frac{1}{2},\frac{1}{2}}(At^{\frac{1}{2}})$.

$$ E_{\frac{1}{2},\frac{1}{2}}(At^{\frac{1}{2}}) = \sum_{k=0}^{1} \frac{A^k t^{\frac{k}{2}}}{\Gamma(\frac{1}{2}(k+1))} = \begin{bmatrix} 1 & 0 \\ 0 & 1 \end{bmatrix} \frac{t^0}{\sqrt{\pi}} + \begin{bmatrix} 0 & -3 \\ 1 & 0 \end{bmatrix} \frac{t^{\frac{1}{2}}}{1} = \begin{bmatrix} \frac{1}{\sqrt{\pi}} & -3t^{\frac{1}{2}} \\ t^{\frac{1}{2}} & \frac{1}{\sqrt{\pi}} \end{bmatrix} $$

and then

$$ E_{\frac{1}{2},\frac{1}{2}}(A^T t^{\frac{1}{2}}) = \sum_{k=0}^{1} \frac{(A^T)^k t^{\frac{k}{2}}}{\Gamma(\frac{1}{2}(k+1))} = \begin{bmatrix} \frac{1}{\sqrt{\pi}} & t^{\frac{1}{2}} \\ -3t^{\frac{1}{2}} & \frac{1}{\sqrt{\pi}} \end{bmatrix}. $$

As

$$ B_{t_1}(t)B_{t_1}^T(t) = \begin{bmatrix} 0 & 0 \\ 0 & t^2 \end{bmatrix}, $$

we have

$$W_1(1,2) =$$

$$= \int_1^2 (2-\tau)^{-\frac{1}{2}} \begin{bmatrix} \frac{1}{\sqrt{\pi}} & -3(2-\tau)^{\frac{1}{2}} \\ (2-\tau)^{\frac{1}{2}} & \frac{1}{\sqrt{\pi}} \end{bmatrix} \begin{bmatrix} 0 & 0 \\ 0 & \tau^2 \end{bmatrix} \begin{bmatrix} \frac{1}{\sqrt{\pi}} & (2-\tau)^{\frac{1}{2}} \\ -3(2-\tau)^{\frac{1}{2}} & \frac{1}{\sqrt{\pi}} \end{bmatrix} d\tau =$$

$$= \int_1^2 \begin{bmatrix} 9\tau^2(2-\tau)^{\frac{1}{2}} & -\frac{3}{\sqrt{\pi}}\tau^2 \\ -\frac{3}{\sqrt{\pi}}\tau^2 & \frac{1}{\pi}\tau^2(2-\tau)^{-\frac{1}{2}} \end{bmatrix} d\tau = \begin{bmatrix} \frac{426}{35} & -\frac{7}{\sqrt{\pi}} \\ -\frac{7}{\sqrt{\pi}} & \frac{86}{15\pi} \end{bmatrix}.$$

Finally,

$$\operatorname{rank} W_1(1,2) = \operatorname{rank} \begin{bmatrix} \frac{426}{35} & -\frac{7}{\sqrt{\pi}} \\ -\frac{7}{\sqrt{\pi}} & \frac{86}{15\pi} \end{bmatrix} = 2. \tag{9}$$

The matrix A has only complex eigenvalues $\lambda_{1,2} = \pm i\sqrt{3}$. Together with (9), based on Theorem 4, this implies the relative U-controllability of the fractional system (8) on $[1, 2]$ for $U = [0, +\infty)$.

5 Concluding Remarks

The relative and constrained relative controllability of the linear fractional control systems with varying delays in control have been discussed. Constraints imposed on the control values have been considered, i.e. $u(t) \in U$. Definitions of relative controllability the systems in the cases of both unconstrained and constrained control values have been formulated.

New controllability criteria for unconstrained and constrained relative controllability of fractional systems with delays varying in time described by the Eq. (1) have been established and proved. Theorem 2 presents a necessary and sufficient condition for relative controllability of the system (1) without constraints. In Theorem 3, U is assumed to be a convex and compact set containing 0 in its interior. In Theorem 4 the set U is suppose to be a cone with vertex at zero and nonempty interior. The numerical example has been presented to illustrate how to verify the constrained relative controllability of the discussed systems with the use of the established criteria.

Acknowledgments This work was supported by Polish National Science Centre (NCN) research grants according to decisions DEC-2012/07/B/ST7/01404 and DEC-2014/13/B/ ST7/00755, respectively.

References

1. Klamka, J.: Controllability of dynamical systems. A survey. Bull. Pol. Ac.: Tech. **61**(2), 335–342 (2013)
2. Oldham, K.B., Spanier, J.: The Fractional Calculus. Academic Press, Cambridge (1974)
3. Podlubny, I.: Fractional Differential Equations: An Introduction to Fractional Derivatives, Fractional Differential Equations, to Methods of Their Solution and Some of Their Applications. Mathematics in Science and Engineering. Academic Press, Cambridge (1999)
4. Miller, K.S., Ross, B.: An Introduction to the Fractional Calculus and Fractional Differential Calculus. Villey (1993)
5. Samko, S.G., Kilbas, A.A., Marichev, O.I.: Fractional Integrals and Derivatives: Theory and Applications. Gordan and Breach Science Publishers (1993)
6. Kilbas, A.A., Srivastava, H.M., Trujillo, J.J.: Theory and Applications of Fractional Differential Equations. North-Holland Mathematics Studies, vol. 204 (2006)
7. Sabatier, J., Agrawal, O.P., Tenreiro Machado, J.A: Advances in Fractional Calculus. Theoretical Developments and Applications in Physics and Engineering. Springer, Heidelberg (2007)
8. Monje, A., Chen, Y., Viagre, B.M., Xue, D., Feliu, V.: Fractional-order Systems and Controls. Fundamentals and Applications. Springer, Heidelberg (2010)
9. Klamka, J.: Controllability and minimum energy control problem of fractional discrete-time systems. In Baleanu, D., Guvenc, Z., Tenreiro Machado, J.A. (eds.) New Trends Nanotechology and Fractional Calculus Applications, pp. 503–509. Springer, The Netherlands (2010)
10. Klamka, J.: Local controllability of fractional discrete-time semilinear systems. Acta Mech. Autom. **5**, 55–58 (2011)
11. Klamka, J., Czornik, A., Niezabitowski, M., Babiarz, A.: Controllability and minimum energy control of linear fractional discrete-time infinite-dimensional systems. In: Proceedings of the 11th IEEE International Conference on Control and Automation, pp. 1210–1214 (2014)
12. Babiarz, A., Grzejszczak, T., Łęgowski, A., Niezabitowski, M.: Controllability of discrete-time switched fractional order systems. In: Proceedings of the 12th World Congress on Intelligent Control and Automation, pp. 1754–1757 (2016)
13. Trzasko, B.: Reachability and controllability of positive fractional discrete-time systems with delay. J. Autom. Mobile Robot. Intell. Syst. **2**, 43–47 (2008)
14. Kaczorek, T.: Selected Problems of Fractional Systems Theory. Lecture Notes in Control and Information Science, vol. 411 (2011)
15. Kaczorek, T., Rogowski, K.: Fractional Linear Systems and Electrical Circuits. Studies in Systems, Decision and Control, vol. 13 (2015)
16. Balachandran, K., Kokila, J.: On the controllability of fractional dynamical systems. Int. J. Appl. Math. Comput. Sci. **22**(3), 523–531 (2012)
17. Balachandran, K., Park, J.Y., Trujillo, J.J.: Controllability of nonlinear fractional dynamical systems. Nonlinear Anal. Theory Methods Appl. **75**(4), 1919–1926 (2012)
18. Balachandran, K., Kokila, J.: Controllability of fractional dynamical systems with prescribed controls. IET Control Theory A. **7**, 1242–1248 (2013)
19. Chen, Y.Q., Ahn, H.S., Xue, D.: Robust controllability of interval fractional order linear time invariant systems. Signal Process. **86**(10), 2794–2802 (2006)
20. Chikriy, A.A., Matichin, I.I: Presentation of solutions of linear systems with fractional derivatives in the sense of Riemann-Liouville, Caputo and Miller-Ross. J. Autom. Inform. Sci. **40**, 1–11 (2008)
21. Sakthivel, R., Ren, Y., Mahmudov, N.I.: On the approximate controllability of semilinear fractional differential systems. Comput. Math. Appl. **62**(3), 1451–1459 (2011)
22. Wang, J., Zhou, Y.: Complete controllability of fractional evolution systems. Commun. Nonlinear Sci. Numer. Simul. **17**(11), 4346–4355 (2012)
23. Balachandran, K., Zhou, Y., Kokila, J.: Relative controllability of fractional dynamical systems with delays in control. Commun. Nonlinear Sci. Numer. Simul. **17**(9), 3508–3520 (2012)
24. Balachandran, K., Kokila, J., Trujillo, J.J.: Relative controllability of fractional dynamical systems with multiple delays in control. Comput. Math. Appl. **64**(10), 3037–3045 (2012)

25. Wei, J.: The controllability of fractional control systems with control delay. Comput. Math. Appl. **64**(10), 3153–3159 (2012)
26. Kaczorek, T.: An extension of Klamka's method of minimum energy control to fractional positive discrete-time linear systems with bounded inputs. Bull. Pol. Ac. Tech. **62**(2), 227–231 (2014)
27. Kaczorek, T.: Minimum energy control of fractional positive continuous-time linear systems with bounded inputs. Int. J. Appl. Math. Comput. Sci. **24**(2), 335–340 (2014)
28. Sikora, B.: Controllability of time-delay fractional systems with and without constraints. IET Control Theory A. **10**(3), 320–327 (2016)
29. Klamka, J.: Controllability of Dynamical Systems. Kluwer Academic Publishers, Germany (1991)
30. Klamka, J.: Constrained controllability of semilinear systems with delayed controls. Bull. Pol. Ac. Tech. **56**(4), 333–337 (2008)
31. Sikora, B.: On the constrained controllability of dynamical systems with multiple delays in the state. Int. J. Appl. Math. Comput. Sci. **13**(4), 469–479 (2003)
32. Brammer, R.: Controllability in linear autonomous systems with positive controllers. SIAM J. Control **10**(2), 339–353 (1972)

Controllability of Nonlinear Stochastic Fractional Integrodifferential Systems in Hilbert Spaces

Rajendran Mabel Lizzy

Abstract In this paper we obtain the sufficient conditions for the controllability of nonlinear stochastic fractional integrodifferential systems and nonlinear systems with implicit fractional derivative in Hilbert spaces by using the fixed point technique.

Keywords Stochastic fractional differential equation · Controllability · Implicit derivative · Integrodifferential equations

1 Introduction

When it is well-known that the fractional differential equations (FDEs) have attracted considerable interest due to its ability to model complex phenomena by capturing non-local relations in space and time (refer [1]), the fluctuations in nature can be captured only by adding random elements into the differential equations (see for instant [2, 3]). Our motivation for considering FDEs with random elements comes from the fact that many phenomena in science that have been modeled by fractional differential equations have some uncertainty. Therefore for investigating more accurate solutions, we need the solutions of stochastic fractional differential equations (SFDEs) (see [4]).

The concept of controllability of integer-order systems in both finite and infinite dimensional spaces, that is, systems represented by ordinary differential equations and partial differential equations is well established (see [5–8]). The notion of controllability for stochastic differential systems in finite-dimensional spaces was introduced by Kalman in 1960 (see also [9, 10]). Later, it was extended to infinite dimensional spaces and many works appeared on the controllability of both linear and nonlinear stochastic differential systems. We mention a few here [11–13]. Recently, the controllability results for FDEs in finite dimensional spaces for both linear and nonlinear systems are studied by many authors (see for instant [14] and references therein). The controllability of the system,

R.M. Lizzy (✉)
Department of Mathematics, Bharathiar University, Coimbatore 641 046, India
e-mail: kb.maths.bu@gmail.com

A. Babiarz et al. (eds.), *Theory and Applications of Non-integer Order Systems*,
Lecture Notes in Electrical Engineering 407, DOI 10.1007/978-3-319-45474-0_31

$$
\begin{aligned}
{}^{C}D^{\alpha}x(t) &= Ax(t) + Bu(t) + \sigma(t)\frac{\mathrm{d}W(t)}{\mathrm{d}t}, t \in J = [0, T], \\
x(0) &= x_0,
\end{aligned} \tag{1}
$$

where $\frac{1}{2} < \alpha \leq 1$, A and B are bounded linear operators is studied in [15]. Integrodifferential equations and equations with implicit derivative occur naturally while modelling physical and biological phenomenon. The study of controllability of such systems have been of great interest in the recent years, for instant, see [11, 14, 16]. However, no work has been reported on the controllability of nonlinear stochastic fractional integrodifferential systems with implicit derivative in the literature and this work will fill the gap. In this paper we obtain the sufficient conditions for controllability of the nonlinear stochastic fractional integrodifferential system and nonlinear systems with implicit derivative by using the Banach contraction principle. The technique of using fixed point theorems to prove controllability results can be referred in [17].

2 Preliminaries

Let X, U and K be separable Hilbert spaces and for convenience, we will use the same notation $\|\cdot\|$ to represent their norms. $\mathbb{L}(X, U)$ is the space of all bounded linear operators from X to U and $\mathbb{L}(X, X) = \mathbb{L}(X)$.

Let $(\Omega, \mathcal{F}, \mathbf{P}, \{\mathcal{F}_t\}_{t\geq 0})$ be a complete filtered probability space with the probability measure $\mathbf{P}$ on Ω. The filtration $\{\mathcal{F}_t | t \geq 0\}$ is generated by the K-valued Wiener process $(W(t))_{t\geq 0}$ defined on $(\Omega, \mathcal{F}, \mathbf{P}, \{\mathcal{F}_t\}_{t\geq 0})$ with the covariance operator $Q \in \mathbb{L}(K, K)$ such that $\mathrm{Tr}Q < \infty$. Let $\mathbb{L}_2^0 = \mathbb{L}_2(Q^{\frac{1}{2}}K, X)$ be the space of all Hilbert-Schmidt operators with norm denoted by $\|\cdot\|_{\mathbb{L}_2^0}$ (see [2]). Denote,

(i) $Y := \mathbb{L}_2(\Omega, \mathcal{F}_T, X)$, which is the Hilbert space of all $\mathcal{F}_T$-measurable square integrable random variables with values in X.

(ii) $\mathcal{H}_2$ to be the subspace of $C(J, \mathbb{L}_2(\mathcal{F}, X))$ consisting of all $\mathcal{F}_t$-measurable processes with values in X, identifying processes which are $\mathbf{P}_T$ a.s. and endowed with the norm,

$$\|\phi\|^2_{\mathcal{H}_2} = \sup_{t\in J} \mathbf{E}\|\phi\|^2.$$

(iii) $\mathcal{H}_2^{\alpha}$ to be the subspace of $C^{\alpha}(J, \mathbb{L}_2(\mathcal{F}, X)) = \{x \in C(J, \mathbb{L}_2(\mathcal{F}, X)) : {}^{C}D^{\alpha}x \in C(J, \mathbb{L}_2(\mathcal{F}, X))\}$ consisting of all $\mathcal{F}_t$-measurable processes with values in X and endowed with the norm,

$$\|\phi\|^2_{\mathcal{H}_2} = \sup_{t\in J} \mathbf{E}\|\phi\|^2 + \sup_{t\in J} \mathbf{E}\|{}^{C}D^{\alpha}\phi\|^2.$$

(iv) $U_{ad} := \mathbb{L}_2^{\mathcal{F}}(J, U)$, which is a Hilbert space of all square integrable and $\mathcal{F}_t$-measurable processes with values in U.

Let us recall some basic definitions from fractional calculus. Let D denote the usual differential operator and I, the identity operator. Let $\alpha, \beta > 0$, with $n-1 < \alpha < n$, $n-1 < \beta < n$ and $n \in \mathbb{N}$. Suppose $f \in L_1(\mathbb{R}_+)$, $\mathbb{R}_+ = [0, \infty)$. The following definitions and properties are well known (see, for instance, [1]):

(i) Caputo fractional derivative:
The Riemann Liouville fractional integral of a function f is defined as,

$$I^{\alpha} f(t) = \frac{1}{\Gamma(\alpha)} \int_0^t (t-s)^{\alpha-1} f(s) \mathrm{d}s,$$

and the Caputo derivative of f is ${}^{C}D^{\alpha} f = I^{n-\alpha} D^n f$, i.e.

$${}^{C}D^{\alpha} f(t) = \frac{1}{\Gamma(n-\alpha)} \int_0^t (t-s)^{n-\alpha-1} f^{(n)}(s) \mathrm{d}s,$$

where the function $f(t)$ has absolutely continuous derivative up to order $n-1$.

(ii) Mittag-Leffler operator function:
If A is a bounded operator then

$$E_{\alpha,\beta}(A) = \sum_{k=0}^{\infty} \frac{A^k}{\Gamma(k\alpha + \beta)}.$$

In particular, for $\beta = 1$,

$$E_{\alpha,1}(A) = E_{\alpha}(A) = \sum_{k=0}^{\infty} \frac{A^k}{\Gamma(k\alpha + 1)}.$$

(iii) Solution Representation:
Consider the linear stochastic fractional differential equation in the Hilbert space X of the form,

$$\begin{aligned} {}^{C}D^{\alpha} x(t) &= Ax(t) + Bu(t) + f(t) + \sigma(t) \frac{\mathrm{d}W(t)}{\mathrm{d}t}, t \in J, \\ x(0) &= x_0, \end{aligned} \tag{2}$$

where $0 < \alpha \leq 1$, $A : \mathcal{H}_2 \to \mathcal{H}_2$ and $B : U_{ad} \to \mathcal{H}_2$ are bounded linear operators, $\sigma : J \to \mathbb{L}_2^0$ and $W(t)$ is a K-valued Weiner process. In order to find the solution representation we need the following hypothesis and Lemma.

(H1) The operator $A \in \mathbb{L}(\mathcal{H}_2)$ commutes with the fractional integral operator I^{α} on $\mathcal{H}_2$(and$\mathcal{H}_2^{\alpha}$) and $\|A\|^2 \leq \frac{(2\alpha-1)(\Gamma(\alpha))^2}{T^{2\alpha}}$.

Lemma 1 [18] *Suppose that A is a linear bounded operator defined on a Banach space, and assume that $\|A\| < 1$. Then $(I - A)^{-1}$ is linear and bounded. Also*

$$(I - A)^{-1} = \sum_{k=0}^{\infty} A^k.$$

The convergence of the above series is in the operator norm, and $\|(I - A)^{-1}\| \leq (1 - \|A\|)^{-1}$.

We next show that the operator $\|I^{\alpha}A\| \leq 1$ and by the Lemma 1 we obtain $(I - I^{\alpha}A)^{-1}$ is bounded and linear. Let $x(t) \in \mathcal{H}_2$, then by (H1), we have

$$\begin{aligned}\mathbf{E}\|(I^{\alpha}A)x(t)\|_X &\leq \frac{T}{(\Gamma(\alpha))^2} \sup_{t\in J} \int_0^t (t-s)^{2\alpha-2}\mathbf{E}\|Ax(s)\|_X^2 \mathrm{d}s \\ &\leq \frac{T^{2\alpha}}{(2\alpha-1)(\Gamma(\alpha))^2} \sup_{t\in J} \mathbf{E}\|Ax(t)\|_X^2 \leq \|x\|_{\mathcal{H}_2}.\end{aligned}$$

Taking supremum over time on the left hand side of the above inequality we obtain $\|I^{\alpha}A\| \leq 1$. On the other hand, taking I^{α} on both sides of (2), using Lemma 1 and the fact that I^{α} commutes with A, we can get the solution of (2) as in [15],

$$\begin{aligned}x(t) = E_{\alpha}(At^{\alpha})x_0 &+ \int_0^t (t-s)^{\alpha-1}E_{\alpha,\alpha}(A(t-s)^{\alpha})Bu(s)\mathrm{d}s \\ &+ \int_0^t (t-s)^{\alpha-1}E_{\alpha,\alpha}(A(t-s)^{\alpha})f(s)\mathrm{d}s \\ &+ \int_0^t (t-s)^{\alpha-1}E_{\alpha,\alpha}(A(t-s)^{\alpha})\sigma(s)\mathrm{d}W(s). \qquad (3)\end{aligned}$$

Similar to the conventional controllability concept, the controllability of the stochastic fractional dynamical system is defined as follows:
The set of all states attainable from x_0 in time $t > 0$ is given by the set

$$\mathcal{R}_t(x_0) = \{x(t; x_0, u) : u \in U_{ad}\},$$

where $x(t)$ is given in (3).

Definition 1 [12] The stochastic fractional system (2) is said to be completely controllable on the interval J if for every $x_1 \in Y$, there exists a control $u \in U_{ad}$ such that the solution $x(t)$ given in (3) satisfies $x(T) = x_1$.
In other words,

$$\mathcal{R}_T(x_0) = Y.$$

Define the operator $L_T : U_{ad} \to Y$ as (see [12])

$$L_T u = \int_0^T (T-s)^{\alpha-1} E_{\alpha,\alpha}(A(T-s)^{\alpha}) B u(s) \mathrm{d}s.$$

Clearly, the adjoint operator L_T^* of L_T satisfying $L_T^* \in \mathbb{L}(Y, U_{ad})$ is obtained as

$$\left(L_T^* x\right)(t) = (T-t)^{\alpha-1} B^* E_{\alpha,\alpha}(A^*(T-t)^{\alpha}) \mathbf{E}\{x|\mathcal{F}_t\}.$$

Definition 2 The controllability Grammian operator $\mathcal{W}_T : Y \to Y$ is defined as

$$\mathcal{W}_T(x) = \int_0^T (T-s)^{2\alpha-2} E_{\alpha,\alpha}(A(T-s)^{\alpha}) B B^* E_{\alpha,\alpha}(A^*(T-s)^{\alpha}) \mathbf{E}\{x|\mathcal{F}_s\} \mathrm{d}s,$$

where * denotes adjoint operator.

It is clear that the operators are linear bounded for all $\frac{1}{2} < \alpha \leq 1$.

3 Stochastic Fractional Integrodifferential Systems

Consider the nonlinear stochastic fractional integrodifferential system of the form

$$\begin{aligned} {}^{C}D^{\alpha} x(t) &= Ax(t) + Bu(t) + f\left(t, x(t), \int_0^t g(t,s,x(s))\mathrm{d}s\right) \\ &\quad + \sigma\left(t, x(t), \int_0^t h(t,s,x(s))\mathrm{d}s\right) \frac{\mathrm{d}W(t)}{\mathrm{d}t}, \\ x(0) &= x_0, \end{aligned} \tag{4}$$

where $\frac{1}{2} < \alpha \leq 1$ and the nonlinear function $f : J \times \mathcal{H}_2 \times \mathcal{H}_2 \to \mathcal{H}_2$, $\sigma : J \times \mathcal{H}_2 \times \mathcal{H}_2 \to L_3^0$, $g : J \times \mathcal{H}_2 \times \mathcal{H}_2 \to \mathcal{H}_2$ and $h : J \times \mathcal{H}_2 \times \mathcal{H}_2 \to \mathcal{H}_2$ are continuous.

(H2) Assume that there exist constants $N_i > 0$ for $i = 1, \ldots, 4$ such that

$$\begin{aligned} \|f(t, x_1, y_1) - f(t, x_2, y_2)\|^2 &\leq N_1 \left(\|x_1 - x_2\|^2 + \|y_1 - y_2\|^2\right) \\ \|\sigma(t, x_1, y_1) - \sigma(t, x_2, y_2)\|_{\mathbb{L}_2^0}^2 &\leq N_2 \left(\|x_1 - x_2\|^2 + \|y_1 - y_2\|^2\right) \\ \|g(t, s, x_1) - g(t, s, x_2)\|^2 &\leq N_3 \|x_1 - x_2\|^2 \\ \|h(t, s, x_1) - h(t, s, x_2)\|^2 &\leq N_4 \|x_1 - x_2\|^2, \end{aligned}$$

for all $x_1, x_2, y_1, y_2 \in \mathcal{H}_2$.

Let us take, $N_5 = \sup_{t\in J} \|f(t,0,0)\|$, $N_6 = \sup_{t\in J} \|\sigma(t,0,0)\|$, $N_7 = \sup_{t\in J} \| \int_0^t g(t,s,0)\mathrm{d}s\|$ and $N_8 = \sup_{t\in J} \| \int_0^t h(t,s,0)\mathrm{d}s\|$. For each fixed $z \in \mathcal{H}_2$, consider the corresponding linear system of (4) as

$$\begin{aligned} {}^{C}D^{\alpha}x(t) &= Ax(t) + Bu(t) + f\left(t, z(t), \int_0^t g(t,s,z(s))\mathrm{d}s\right) \\ &\quad + \sigma\left(t, z(t), \int_0^t h(t,s,z(s))\mathrm{d}s\right)\frac{\mathrm{d}W(t)}{\mathrm{d}t}, \\ x(0) &= x_0. \end{aligned} \tag{5}$$

The solution of (5) is given by,

$$\begin{aligned} x(t) &= E_{\alpha}(At^{\alpha})x_0 + \int_0^t (t-s)^{\alpha-1}E_{\alpha,\alpha}(A(t-s)^{\alpha})Bu(s)\mathrm{d}s \\ &\quad + \int_0^t (t-s)^{\alpha-1}E_{\alpha,\alpha}(A(T-s)^{\alpha})f\left(s, z(s), \int_0^s g(s,r,z(r))\mathrm{d}r\right)\mathrm{d}s \\ &\quad + \int_0^t (t-s)^{\alpha-1}E_{\alpha,\alpha}(A(T-s)^{\alpha})\sigma\left(s, z(s), \int_0^s h(s,r,z(r))\mathrm{d}r\right)\mathrm{d}W(s). \end{aligned} \tag{6}$$

For convenience let us take $M_1 = \sup_{0\le t\le T} \|E_{\alpha}(At^{\alpha})\|^2$ and $M_2 = \sup_{0\le t\le T} \|E_{\alpha,\alpha}(At^{\alpha})\|^2$. We also assume the following condition,

(H3) Let $\rho_1 = \dfrac{8T^{2\alpha}M_2}{(2\alpha-1)}\left(N_2T^{-1} + N_2N_4 + N_1 + N_1N_3T\right)$ be such that $0 \le \rho_1 < 1$.

Theorem 1 *If the hypothesis* $(H1)$–$(H3)$ *are satisfied and if the linear fractional dynamical system (5) is controllable, then the nonlinear fractional dynamical system (4) is controllable.*

Proof Let x_1 be an arbitrary point in Y. Define the operator Φ on $\mathcal{H}_2$ by

$$\begin{aligned} \Phi x(t) &= E_{\alpha}(At^{\alpha})x_0 + \int_0^t (t-s)^{\alpha-1}E_{\alpha,\alpha}(A(t-s)^{\alpha})Bu(s)\mathrm{d}s \\ &\quad + \int_0^t (t-s)^{\alpha-1}E_{\alpha,\alpha}(A(T-s)^{\alpha})f\left(s, z(s), \int_0^s g(s,r,z(r))\mathrm{d}r\right)\mathrm{d}s \\ &\quad + \int_0^t (t-s)^{\alpha-1}E_{\alpha,\alpha}(A(T-s)^{\alpha})\sigma\left(s, z(s), \int_0^s h(s,r,z(r))\mathrm{d}r\right)\mathrm{d}W(s). \end{aligned}$$

Since the linear system (5) corresponding to the nonlinear system (4) is controllable we have, $\mathcal{W}_T$ is invertible (see [15]) and so we can define the control variable u as

$$u(t) = (T-t)^{\alpha-1}B^*E_{\alpha,\alpha}(A^*(T-t)^\alpha)\mathbf{E}\Bigg\{\mathcal{W}_T^{-1}\Bigg(x_1 - E_\alpha(AT^\alpha)x_0$$
$$-\int_0^T (T-s)^{\alpha-1}E_{\alpha,\alpha}(A(T-s)^\alpha)f\left(s, z(s), \int_0^s g(s,r,z(r))\mathrm{d}r\right)\mathrm{d}s$$
$$-\int_0^T (T-s)^{\alpha-1}E_{\alpha,\alpha}(A(T-s)^\alpha)\sigma\left(s, z(s), \int_0^s h(s,r,z(r))\mathrm{d}r\right)\mathrm{d}W(s)\Bigg)\Bigg|\mathcal{F}_t\Bigg\}.$$

If we obtain a fixed point for Φ, then that fixed point will be a solution of the control problem. Clearly, $\Phi(x(T)) = x_1$, which means that the control u steers the nonlinear system from the initial state x_0 to x_1 in the time T, provided we can obtain a fixed point of the nonlinear operator Φ. First we show that Φ maps $\mathcal{H}_2$ into itself. Estimating $u(t)$ we obtain,

$$\sup_{t\in J}\mathbf{E}\|u(t)\|^2 \le 4\|L_T^*\|^2\|\mathcal{W}_T^{-1}\|^2\Bigg[\mathbf{E}\|x_1\|^2 + M_1\mathbf{E}\|x_0\|^2$$
$$+M_2N\frac{T^{2\alpha}}{2\alpha-1} + M_2N'\frac{T^{2\alpha-1}}{2\alpha-1}\Bigg] = K_1 \ < \infty,$$

where $N = (N_1N_3 + N_1)\sup_{t\in J}\mathbf{E}\|x(t)\|^2 + N_5 + N_1N_7 < \infty$, $N' = (N_2N_4 + N_2)$ $\sup_{t\in J}\mathbf{E}\|x(t)\|^2 + N_2N_8 + N_6 < \infty$. Further from the assumptions we have,

$$\sup_{t\in J}\mathbf{E}\|\Phi x(t)\|^2 \le 4M_1\mathbf{E}\|x_0\|^2 + 4M_2K_1\|B\|^2\frac{T^{2\alpha}}{2\alpha-1}$$
$$+4M_2N\frac{T^{2\alpha}}{2\alpha-1} + 4M_2N'\frac{T^{2\alpha-1}}{2\alpha-1} < \infty.$$

Thus Φ maps $\mathcal{H}_2$ into itself. Now for $x_1, x_2 \in \mathcal{H}_2$, we have

$$\sup_{t\in J}\mathbf{E}\|\Phi x_1(t) - \Phi x_2(t))\|^2$$

$$= \sup_{t\in J}\mathbf{E}\Bigg\|\int_0^t (t-s)^{\alpha-1}E_{\alpha,\alpha}(A(t-s)^\alpha)B\ L_T^*\mathcal{W}_T^{-1}$$
$$\Bigg\{\int_0^T (T-\theta)^{\alpha-1}E_{\alpha,\alpha}(A(T-\theta)^\alpha)$$
$$\Bigg[f\left(\theta, x_1(\theta), \int_0^\theta g(\theta,r,x_1(r))\mathrm{d}r\right) - f\left(\theta, x_2(\theta), \int_0^\theta g(\theta,r,x_2(r))\mathrm{d}r\right)\Bigg]\mathrm{d}\theta$$
$$+\int_0^T (T-\theta)^{\alpha-1}E_{\alpha,\alpha}(A(T-\theta)^\alpha)$$
$$\Bigg[\sigma\left(\theta, x_1(\theta), \int_0^\theta h(\theta,r,x_1(r))\mathrm{d}r\right) - \sigma\left(\theta, x_2(\theta), \int_0^\theta h(\theta,r,x_2(r))\mathrm{d}r\right)\Bigg]\mathrm{d}W(\theta)\Bigg\}\mathrm{d}s$$

$$
\begin{aligned}
&+\int_0^t (t-s)^{\alpha-1} E_{\alpha,\alpha}(A(T-s)^{\alpha}) \\
&\left[f\left(s, x_1(s), \int_0^s g(s,r,x_1(r))\mathrm{d}r\right) - f\left(s, x_2(s), \int_0^s g(s,r,x_2(r))\mathrm{d}r\right)\right]\mathrm{d}s \\
&+\int_0^t (t-s)^{\alpha-1} E_{\alpha,\alpha}(A(T-s)^{\alpha}) \\
&\left[\sigma\left(s, x_1(s), \int_0^s h(s,r,x_1(r))\mathrm{d}r\right) - \sigma\left(s, x_2(s), \int_0^s h(s,r,x_2(r))\mathrm{d}r\right)\right]\mathrm{d}W(s)\Bigg\|^2 \\
&\leq \frac{8T^{2\alpha}M_2}{(2\alpha-1)}\left(N_2T^{-1}+N_2N_4+N_1+N_1N_3T\right)\sup_{t\in J}\mathbf{E}\|x_1(t)-x_2(t)\|^2 \\
&\leq \rho_1\|x_1-x_2\|^2_{\mathcal{H}_2}.
\end{aligned}
$$

Using (H3) we conclude that Φ is a contraction mapping and hence there exists a unique fixed point $x \in \mathcal{H}_2$ for Φ. Any fixed point of Φ satisfies $x(T) = x_1$ for an arbitrary $x_1 \in Y$. Therefore the system (4) is controllable on J.

4 Stochastic Fractional Systems with Implicit Derivative

Consider the nonlinear stochastic fractional differential system with implicit fractional derivative of the form

$$
\begin{aligned}
{}^{C}D^{\alpha}x(t) &= Ax(t) + Bu(t) + f(t, x(t), {}^{C}D^{\alpha}x(t)) + \sigma(t, x(t))\frac{\mathrm{d}W(t)}{\mathrm{d}t}, \\
x(0) &= x_0,
\end{aligned} \tag{7}
$$

where $\frac{1}{2} < \alpha \leq 1$ and the nonlinear functions $f : J \times \mathcal{H}_2^{\alpha} \times \mathcal{H}_2 \to \mathcal{H}_2$, $\sigma : J \times \mathcal{H}_2^{\alpha} \to \mathcal{H}_2$ are continuous.

(H4) Assume that there exist constants $L_1, L_2 > 0$ such that

$$
\begin{aligned}
\|f(t, x_1, {}^{C}D^{\alpha}x_1(t)) - f(t, x_2, {}^{C}D^{\alpha}x_2(t))\|^2 &\leq L_1\left(\|x_1(t)-x_2(t)\|^2\right. \\
&\quad \left.+\|{}^{C}D^{\alpha}x_1(t) - {}^{C}D^{\alpha}x_2(t)\|^2\right) \\
\|\sigma(t, x_1(t)) - \sigma(t, x_2(t))\|^2_{\mathbb{L}_2^0} &\leq L_2\|x_1(t)-x_2(t)\|^2,
\end{aligned}
$$

for all $x_1, x_2 \in \mathcal{H}_2^{\alpha}$.

We denote $L_3 = \sup_{t\in J}\|f(t,0,0)\|$ and $L_4 = \sup_{t\in J}\|\sigma(t,0)\|$. For each fixed $z \in \mathcal{H}_2^{\alpha}$, consider the corresponding linear system of (7):

$$
\begin{aligned}
{}^{C}D^{\alpha}x(t) &= Ax(t) + Bu(t) + f(t, z(t), {}^{C}D^{\alpha}z(t)) + \sigma(t, z(t))\frac{\mathrm{d}W(t)}{\mathrm{d}t}, \\
x(0) &= x_0.
\end{aligned} \tag{8}
$$

The solution of (8) is given by,

$$
\begin{aligned}
x(t) = E_{\alpha}(At^{\alpha})x_0 &+ \int_0^t (t-s)^{\alpha-1}E_{\alpha,\alpha}(A(t-s)^{\alpha})Bu(s)\mathrm{d}s \\
&+ \int_0^t (t-s)^{\alpha-1}E_{\alpha,\alpha}(A(T-s)^{\alpha})f(s, z(s), {}^{C}D^{\alpha}z(s))\mathrm{d}s \\
&+ \int_0^t (t-s)^{\alpha-1}E_{\alpha,\alpha}(A(T-s)^{\alpha})\sigma(s, z(s))\mathrm{d}W(s).
\end{aligned} \tag{9}
$$

We also assume the following condition,

(H5) Let $\rho_2 = \max\left\{\dfrac{8T^{2\alpha}M_2}{(2\alpha-1)}\left(L_1 + L_2T^{-1}\right), \dfrac{8T^{2\alpha}M_2L_1}{(2\alpha-1)}\right\}$ be such that $0 \le \rho_2 < 1$.

Theorem 2 *If the hypothesis* $(H1)$, $(H4)$ *and* $(H5)$ *are satisfied and if the linear fractional dynamical system (8) is controllable, then the nonlinear fractional dynamical system (7) is controllable for* $\frac{1}{2} < \alpha \le 1$.

Proof Let x_1 be an arbitrary point in Y. Define the operator Φ on $\mathcal{H}_2^{\alpha}$ by

$$
\begin{aligned}
\Phi x(t) = E_{\alpha}(At^{\alpha})x_0 &+ \int_0^t (t-s)^{\alpha-1}E_{\alpha,\alpha}(A(t-s)^{\alpha})Bu(s)\mathrm{d}s \\
&+ \int_0^t (t-s)^{\alpha-1}E_{\alpha,\alpha}(A(T-s)^{\alpha})f(s, x(s), {}^{C}D^{\alpha}x(s))\mathrm{d}s \\
&+ \int_0^t (t-s)^{\alpha-1}E_{\alpha,\alpha}(A(T-s)^{\alpha})\sigma(s, x(s))\mathrm{d}W(s).
\end{aligned}
$$

Since the linear system (8) corresponding to the nonlinear system (7) is controllable we have, $\mathcal{W}_T$ is invertible (see [15]) and so we can define the control variable u as

$$
\begin{aligned}
u(t) = (T-t)^{\alpha-1}B^{*}E_{\alpha,\alpha}(A^{*}(T-t)^{\alpha})\mathbf{E}\Big\{\mathcal{W}_T^{-1}\Big(x_1 - E_{\alpha}(AT^{\alpha})x_0 \\
- \int_0^T (T-s)^{\alpha-1}E_{\alpha,\alpha}(A(T-s)^{\alpha})f(s, x(s), {}^{C}D^{\alpha}x(s))\mathrm{d}s \\
- \int_0^T (T-s)^{\alpha-1}E_{\alpha,\alpha}(A(T-s)^{\alpha})\sigma(s, x(s))\mathrm{d}W(s)\Big)\Big|\mathcal{F}_t\Big\}.
\end{aligned}
$$

If we obtain a fixed point for Φ, then that fixed point will be a solution of the control problem. Clearly, $\Phi(x(T)) = x_1$, which means that the control u steers the nonlinear system from the initial state x_0 to x_1 in the time T, provided we can obtain

a fixed point of the nonlinear operator Φ. First we show that Φ maps $\mathcal{H}_2^\alpha$ into itself. Estimating $u(t)$ we obtain,

$$\mathbf{E}\|u(t)\|^2 \leq 4\|L_T^*\|^2\|\mathcal{W}_T^{-1}\|^2\left[\mathbf{E}\|x_1\|^2 + M_1\mathbf{E}\|x_0\|^2 + M_2N\frac{T^{2\alpha}}{2\alpha-1} + M_2N'\frac{T^{2\alpha-1}}{2\alpha-1}\right] = K_2 \ < \infty,$$

where $N = L_1 \sup_{t\in J}\left(\mathbf{E}\|x(t)\|^2 + \mathbf{E}\|{}^C D^\alpha x(t)\|^2\right) + L_3 < \infty$,
$N' = L_2 \sup_{t\in J}\mathbf{E}\|x(t)\|^2 + L_4 < \infty$. Further from the assumptions we have,

$$\sup_{t\in J}\mathbf{E}\|\Phi x(t)\|^2 \leq 4M_1\mathbf{E}\|x_0\|^2 + 4M_2K_2\|B\|^2\frac{T^{2\alpha}}{2\alpha-1} + 4M_2N\frac{T^{2\alpha}}{2\alpha-1} + 4M_2N'\frac{T^{2\alpha-1}}{2\alpha-1} < \infty.$$

Thus Φ maps $\mathcal{H}_2^\alpha$ into itself. Now for $x_1, x_2 \in \mathcal{H}_2^\alpha$, we have

$$\begin{aligned}
&\sup_{t\in J}\mathbf{E}\|\Phi x_1(t) - \Phi x_2(t))\|^2 \\
&= \sup_{t\in J}\mathbf{E}\Bigg\|\int_0^t (t-s)^{\alpha-1}E_{\alpha,\alpha}(A(t-s)^\alpha)B\ L_T^*\mathcal{W}_T^{-1} \\
&\quad\Bigg[\int_0^T (T-\theta)^{\alpha-1}E_{\alpha,\alpha}(A(T-\theta)^\alpha)\,[f(\theta,x_1(\theta)) - f(\theta,x_2(\theta))]\mathrm{d}\theta \\
&\quad + \int_0^T (T-\theta)^{\alpha-1}E_{\alpha,\alpha}(A(T-\theta)^\alpha)[\sigma(\theta,x_1(\theta)) - \sigma(\theta,x_2(\theta))]\mathrm{d}W(\theta)\Bigg]\mathrm{d}s \\
&\quad + \int_0^t (t-s)^{\alpha-1}E_{\alpha,\alpha}(A(T-s)^\alpha)\,[f(s,x_1(s)) - f(s,x_2(s))]\,\mathrm{d}s \\
&\quad + \int_0^t (t-s)^{\alpha-1}E_{\alpha,\alpha}(A(T-s)^\alpha)\,[\sigma(s,x_1(s)) - \sigma(s,x_2(s))]\,\mathrm{d}W(s)\Bigg\|^2 \\
&\leq \frac{8T^{2\alpha}M_2}{(2\alpha-1)}\left(L_1 + L_2T^{-1}\right)\sup_{t\in J}\mathbf{E}\|x_1(t) - x_2(t)\|^2 \\
&\quad + \frac{8T^{2\alpha}M_2L_1}{(2\alpha-1)}\sup_{t\in J}\mathbf{E}\|{}^C D^\alpha x_1(t) - {}^C D^\alpha x_2(t)\|^2 \\
&\leq \rho_2\|x_1 - x_2\|^2_{\mathcal{H}_2^\alpha}.
\end{aligned}$$

Using (H4) we conclude, Φ is a contraction mapping and hence there exists a unique fixed point $x \in \mathcal{H}_2^\alpha$ for Φ. Any fixed point of Φ satisfies $x(T) = x_1$ for any arbitrary $x_1 \in Y$. Therefore the system (7) is controllable on J.

Acknowledgments The work was supported by the [University Grants Commission] under grant [number: MANF-2015-17-TAM-50645] from the government of India.

References

1. Kilbas, A., Srivastava, H.M., Trujillo, J.J.: Theory and Applications of Fractional Differential Equations. Elsevier, New York (2006)
2. Da Prato, G., Zabczyk, J.: Stochastic Equations in Infinite Dimensions. Cambridge University, Press (1992)
3. Oksendal, B.: Stochastic Differential Equations: An Introduction with Applications. Springer, Heidlberg (2000)
4. Kamrani, M.: Numerical solution of stochastic fractional differential equations. Numer. Algorithms **68**(1), 81–93 (2015)
5. Bensoussan, A., Da Prato, G., Delfour, M.C., Mitter, S.K.: Representation and Control of Infinite Dimensional Systems. Birkhäuser, Boston (1993)
6. Curtain, R.F., Zwart, H.: An Introduction to Infinite Dimensional Systems Theory. Springer, New York (1995)
7. Klamka, J.: Constrained controllability of semilinear systems. Nonlinear Anal. **47**, 2939–2949 (2001)
8. Zabczyk, J.: Mathematical Control Theory. Birkhäuser, Boston (1992)
9. Bashirov, A.E., Mahmudov, N.I.: On concepts of controllability for linear deterministic and stochastic system. SIAM J. Control Optim. **37**(6), 1808–1821 (1999)
10. Klamka, J.: Controllability of dynamical systems: a survey. Bull. Pol. Ac. Tech. **61**(2), 221–229 (2013)
11. Balachandran, K., Karthikeyan, S.: Controllability of nonlinear Itô stochastic integrodifferential systems. J. Franklin Inst. **345**(4), 382–391 (2008)
12. Mahmudov, N.I.: Controllability of linear stochastic systems in Hilbert spaces. J. Math. Anal. Appl. **259**(1), 64–82 (2001)
13. Mahmudov, N.I.: Controllability of semilinear stochastic systems in Hilbert spaces. J. Math. Anal. Appl. **288**(1), 197–211 (2003)
14. Balachandran, K., Park, J.Y.: Controllability of fractional integrodifferential systems in Banach spaces. Nonlinear Anal. Hybrid Syst. **3**(4), 363–367 (2009)
15. Mabel Lizzy, R., Balachandran, K., Suvinthra, M.: Controllability of nonlinear stochastic fractional systems. J. Appl. Math. Inf. (under review)
16. Balachandran, K., Divya, S.: Controllability of nonlinear implicit fractional integrodifferential systems. Int. J. Appl. Math. Comput. Sci. **24**(4), 713–722 (2014)
17. Balachandran, K., Dauer, J.P.: Controllability of nonlinear systems in Banach spaces: a survey. J. Optim. Theory Appl. **115**(1), 7–28 (2002)
18. Kreyszig, E.: Introductory Functional Analysis with Applications. Wiley, New York (1978)

Finding a Set of (A, B, C, D) Realisations for Fractional One-Dimensional Systems with Digraph-Based Algorithm

First Approach

Konrad Andrzej Markowski and Krzysztof Hryniów

Abstract This paper presents the first proposition of a method allowing the determination of a set of (**A**, **B**, **C**) realisations of the one-dimensional fractional system from created digraph. The algorithm presented is the extension of previously published algorithm that finds a complete set of all possible realisations, instead of only a few realisations, as was in case of canonical form methods. The advantages of the proposed method are the possibilities of obtaining a set of state matrices directly from digraph form of the system and using fast parallel computing method. The algorithm is presented in pseudo-code and illustrated with example.

Keywords Realisation · Fractional system · Digraphs · Algorithm · One-dimensional system

1 Introduction

One of constant problems in analysis of dynamic systems is the realisation problem. In many research studies, we can find a canonical form of the system, i.e. constant matrix form, which satisfies the system described by the transfer function [1, 2]. With the use of this form we are able to write only one realisation of the system, while there exists a set of solutions.

K. Hryniów—Research has been financed with the funds of the Statutory Research of 2016.

K.A. Markowski (✉) · K. Hryniów
Faculty of Electrical Engineering, Institute of Control and Industrial Electronics, Warsaw University of Technology, Koszykowa 75, 00-662 Warsaw, Poland
e-mail: Konrad.Markowski@ee.pw.edu.pl

K. Hryniów
e-mail: Krzysztof.Hryniow@ee.pw.edu.pl

A. Babiarz et al. (eds.), *Theory and Applications of Non-integer Order Systems*, Lecture Notes in Electrical Engineering 407, DOI 10.1007/978-3-319-45474-0_32

The first definition of the fractional derivative was introduced by Liouville and Riemann at the end of the 19th century [3]. Mathematical fundamentals of fractional calculus are given in [2–8].

In this paper, a new method allowing for determination of a set of minimal realisations of the fractional continuous one-dimensional (1-D) system will be proposed and the procedure for computation of the minimal realisation will be given. The procedure will be illustrated with a numerical example.

This work has been organised as follows: Sect. 2 presents some notations and basic definitions. In Sect. 3 state-of-the-art in the field of determination of realisations is presented. Section 4 presents the main results of the paper – proposition how to find (**A**, **B**, **C**) matrices directly from constructed digraph, pseudo-code of parallel numerical method and illustration of the working of the method with the example. In Sect. 5 concluding remarks and future work is presented.

2 Notation and Definitions

Notion: In this paper the following notion will be used. The matrices will be denoted by the bold font (for example $\mathbf{A}, \mathbf{B}, \ldots$), the sets by the double line (for example $\mathbb{A}, \mathbb{B}, \ldots$), lower/upper indices and polynomial coefficients will be written as a small font (for example $a, b, \ldots$), fractional derivative will be denoted using a mathfrak font $\mathfrak{D}$ and digraph will be denoted using mathcal font $\mathcal{D}$. The set $n \times m$ of real matrices will be denoted by $\mathbb{R}^{n\times m}$ and $\mathbb{R}^n = \mathbb{R}^{n\times 1}$. The $n \times n$ identity matrix will be denoted by $\mathbf{I}_n$. For more information about the matrix theory, an interested reader may be referred to, for instance [9, 10].

Digraph: A directed graph (or just digraph) $\mathcal{D}$ consists of a non-empty finite set $\mathbb{V}(\mathcal{D})$ of elements called vertices and a finite set $\mathbb{A}(\mathcal{D})$ of ordered pairs of distinct vertices called arcs [11]. We call $\mathbb{V}(\mathcal{D})$ the vertex set and $\mathbb{A}(\mathcal{D})$ the arc set of digraph $\mathcal{D}$. We will often write $\mathcal{D} = (\mathbb{V}, \mathbb{A})$ which means that $\mathbb{V}$ and $\mathbb{A}$ are the vertex set and arc set of $\mathcal{D}$, respectively. The order of $\mathcal{D}$ is the number of vertices in $\mathcal{D}$. The size of $\mathcal{D}$ is the number of arcs in $\mathcal{D}$. For an arc (v_1, v_2) the first vertex v_1 is its tail and the second vertex v_2 is its head.

There are two well-known methods of representation of digraph: list and incidence matrix. In this paper we are using incidence matrix to represent all digraphs. Method of constructing digraphs by this method is presented for example in [11]. Adaptation of this well-known method for dynamic systems was first presented in [12].

We present below some basic notions from graph theory which are used in further considerations. A walk in a digraph $\mathcal{D}^{(1)}$ is a finite sequence of arcs in which every two vertices v_i and v_j are adjacent or identical. A walk in which all of the arcs are distinct is called a path. The path that goes through all vertices is called a finite path. If the initial and the terminal vertices of the path are the same, then the path is called a cycle.

Realisation problem: Let us consider the continuous-time fractional linear system described by state-space equations:

$$\begin{aligned} {}_0\mathfrak{D}_t^{\alpha} x(t) &= \mathbf{A}x(t) + \mathbf{B}u(t), \quad 0 < \alpha \leqslant 1, \\ y(t) &= \mathbf{C}x(t) + \mathbf{D}u(t), \end{aligned} \tag{1}$$

where $x(t) \in \mathbb{R}^n$, $u(t) \in \mathbb{R}^m$, $y(t) \in \mathbb{R}^p$ are the state, input and output vectors, respectively and $\mathbf{A} \in \mathbb{R}^{n\times n}$, $\mathbf{B} \in \mathbb{R}^{n\times m}$, $\mathbf{C} \in \mathbb{R}^{p\times n}$ and $\mathbf{D} \in \mathbb{R}^{p\times m}$. The following Caputo definition of the fractional derivative will be used:

$${}_a^C\mathfrak{D}_t^{\alpha} = \frac{d^{\alpha}}{dt^{\alpha}} = \frac{1}{\Gamma(n-\alpha)} \int_a^t \frac{f^{(n)}(\tau)}{(t-\tau)^{\alpha+1-n}} d\tau, \tag{2}$$

where $\alpha \in \mathbb{R}$ is the order of fractional derivative, $f^{(n)}(\tau) = \frac{d^n f(\tau)}{d\tau^n}$ and $\Gamma(x) = \int_0^{\infty} e^{-t} t^{x-1} dt$ is the gamma function. The Laplace transform of the derivative-integral (2) is given in [2].

Transfer matrix of the system (1) has the following form:

$$\mathbf{T}(s) = \mathbf{C}\left[\mathbf{I}_n s^{\alpha} - \mathbf{A}\right]^{-1} \mathbf{B} + \mathbf{D}. \tag{3}$$

Matrices $(\mathbf{A}, \mathbf{B}, \mathbf{C}, \mathbf{D})$ are called realisation of the transfer matrix if they satisfy the equality (3). The realisation is called minimal if the dimension of the state matrix $\mathbf{A}$ is minimal among all possible realisation of $\mathbf{T}(s)$.

3 State–of–the–Art

There are solutions for the problem of determination of entries of the state matrix $\mathbf{A}$ for a given characteristic polynomial. Most of them are based on usage of the canonical forms of the system [13, 14], i.e. constant matrix form, which satisfies the system described by the transfer function. All of the state-of-the-art methods based on canonical forms [15–19] are capable of giving one of possible realisations of the characteristic polynomial. Due to the complexity of the problem there were no classical methods of determination of the whole set of possible realisations for a given characteristic polynomial.

Such solution was proposed for non-fractional 1-D and 2-D systems in [20, 21] and is based on the multi-dimensional $\mathcal{D}^{(n)}$ digraphs theory. In addition to finding all possible solutions for given characteristic polynomial it can also find solutions that are minimal in rank of $\mathbf{A}$ matrix. The parallel algorithm is shown in [22, 23] as superior to methods proposed in [15–19] in both number of obtained realisations and minimality of matrix size.

Algorithm discussed in this paper is an extension of parallel algorithm described in [22–24] that solves the realisation problem for dynamic system and finds not only **A** matrices, but also **B** and **C** matrices from digraph representation of the system.

4 Main Results

4.1 Theory

The essence of the proposed method for determining a minimal realisation for fractional one-dimensional continuous-time system described by the model (1) will be presented in single-input single-output (SISO) systems. The transfer matrix (3) can be considered as a pseudo-rational function of the variable $\lambda = s^{\alpha}$ and for SISO system has the following form:

$$T(\lambda) = \mathbf{C}\left[\mathbf{I}_n\lambda - \mathbf{A}\right]^{-1}\mathbf{B} + \mathbf{D} = \frac{n(\lambda)}{d(\lambda)} = \frac{b_n\lambda^n + b_{n-1}\lambda^{n-1} + \cdots + b_1\lambda + b_0}{\lambda^n + a_{n-1}\lambda^{n-1} + \cdots + a_1\lambda + a_0}. \quad (4)$$

The matrix **D** can be found by the use of the formula:

$$\mathbf{D} = \lim_{\lambda\to\infty} = [b_n]\,. \quad (5)$$

Using (4) and (5) we can determine strictly proper transfer function in the following form:

$$T_{sp}(\lambda) = \frac{\widetilde{b}_{n-1}\lambda^{n-1} + \cdots + \widetilde{b}_1\lambda + \widetilde{b}_0}{\lambda^n + a_{n-1}\lambda^{n-1} + \cdots + a_1\lambda + a_0}, \quad (6)$$

where $\widetilde{b}_{n-i} = b_n \cdot a_{n-i}$ for $i = 1, \ldots, n$.

Creation of digraph structure that allows to determine the **A** matrices was presented in [23, 24]. Digraph structure is build based on the characteristic polynomial of the transfer function. Matrices **B** and **C** can be obtained from digraph by adding two additional types of vertices - input vertex s and output vertex y. Wages of arcs between vertices v_i and s correspond to wages of input matrix **B** and wages of arcs between vertices v_i and y corresponding to wages of output matrix **C**.

Intersection vertices are vertices that belong to the intersection set of all digraph representations of monomials consisting of given characteristic polynomial as presented in [22, 23]. In case where all arcs from input vertex lead to intersection vertices and all arcs to output vertex start in intersection vertices simplified case exists that was earlier discussed in [25, 26]. Otherwise, there is need of tracing all paths on digraph that start in input vertex and end in output vertex, and basing on them solving a set of equations that allow to determine wages in input and output matrices.

To determine **B** and **C** matrices from digraph we create all the possible paths from input vertex to output vertex and multiply all arc wages on the given path to form a monomial form. Then, we add all the created monomials. After that, for each cycle appearing in the digraph, a sub-graph is created by removal of all the vertices belonging to the given cycle. For each of created sub-graphs we determine all the possible paths from input vertex to output vertex, multiply all the arc wages on the given path and then multiply them by (-1) and by the removed cycle to get a monomial form. At the end we add all the monomials obtained from sub-graphs to previously obtained monomials and distribute monomials to form a set of equations from which **B** and **C** matrices can be created.

As can be seen, in simplified case monomials from sub-graphs do not appear, as intersection vertices are removed for every cycle (as they belong to every cycle) and there is no possibility of forming a path starting at input vertex and ending at output vertex in such case.

Details are presented in Sects. 4.2 and 4.3.

4.2 Algorithm

Algorithm presented in [22, 23] starts with creating digraphs for all monomials in the characteristic polynomial, then joins them by the use of disjoint union to create all possible variants of digraphs representing polynomial realisation – which represents the characteristic polynomial given. The algorithm uses growth and prune steps alongside with control sums (hashes) where needed to eliminate redundant solutions before the main computational step. All parts of the algorithm can be paralleled and computed on device's multiple CUDA kernels.

Algorithm 1 presents in pseudo-code basics of the algorithm. Due to lack of space some parts of the algorithm are presented in simplified form and some functions are only mentioned in comment and their working is not presented in detail – interested reader should look into [21] for more precise presentation of the algorithm's code.

Algorithm 1 *DetermineStateMatrices*()

1: Determine number of *cycles* in characteristic polynomial - it is equal to number of monomials;
2: **for** *monomial* $= 1$ **to** *cycles* **do**
3: Determine digraph $\mathcal{D}^{(1)}$ for every monomial;
4: *MonomialRealisation*1*D*(*monomial*);
5: Determine number of variants for each monomial apart from the first and put it into array *variants*(*monomial*);
6: Variants mean different placement positions of the sub-digraph on the final digraph;
7: **end for**
8: Create all possible combinations of variants of all monomials;
9: Remove all redundant variant sets by checking their control sums;
10: [*kernels*, *variant*(*kernel*)] $=$ *VariantsStart*(*cycles*, *variants*)
11: Determine digraph as a combination of the digraph monomial representation and assign each combination to different CUDA kernel;
12: **for** *kernel* $= 1$ **to** *kernels* **do**
13: *PolynomialRealisation*1*D*(*kernel*, *variant*(*kernel*))
14: Check number of cycles in digraph, if differs from *cycles* remove solution as improper;
15: Record as proper realisation of characteristic polynomial – in this moment we have the structure of matrix **A**;
16: **end for**
17: **for all** *realisations* **do**
18: Each realisation gives as a different structure of **A** matrix that can be filled by a set of possible weights;
19: Now the structure of **B** and **C** matrices need to be determined from constructed digraph;
20: [*B*, *C*] = *FullRealisation*1*D*(*realisation*)
21: Determine weights of the arcs in digraph and write state matrices **A**, **B**, **C**;
22: *DetermineWeights*(*realisation*)
23: **end for**

Algorithm is divided into blocks, each realising different part of the operation. Each block is a function and can be switched to another block to deal with different problem efficiently without the need to change whole algorithm and without performing unnecessary operations for simpler problems. Some functions can be run in different order – for example we can determine weights of **A** matrix first and then construct matrices **B** and **C** that match given matrix **A** or we can determine the structure of all three matrices and then at the end fill the weights in all of them.

Algorithm 2 is much simpler from algorithm constructing monomial realisations presented earlier, as in [21] it was proven that for 1D monomials both growth and prune steps can be omitted and only one solution will be created.

Algorithm 2 *MonomialRealisation*1*D*(*monomial*)

1: *size* equals size of the monomial (sum of powers of all the variables);
2: Create digraph $\mathcal{D}^{(n)}$ for given monomial;
3: **for** *node* = 1 **to** *size* **do**
4: **if** *node* == *size* **then**
5: $a_{size,1} = 1$;
6: **else**
7: $a_{size-1,size} = 1$;
8: **end if**
9: **end for**

Algorithm 3 is addition to algorithm presented in [22, 24] and forms next step of the algorithm, allowing for creation of **B** and **C** matrices directly from digraph. In lines (5–12) additional sub-graphs are created from which additional elements are derived. Those elements (line 10) will be with a negative sign as opposed to the elements formed in line 3. All of the created elements in line 14 will be used to create elements from matrices **B** and **C** after assigning wages.

Algorithm 3 *FullRealisation*1*D*(*realisation*)

1: Create all paths from S_b (source) to S_c (sink);
2: **for all** paths **do**
3: Multiply all wages along the path to form monomial;
4: **end for**
5: Create additional paths from sub-graphs;
6: **for all** cycles **do**
7: Remove all nodes belonging to given cycle from digraph creating sub-graph;
8: Create all paths from S_b to S_c through sub-graph;
9: **for all** paths **do**
10: Multiply all wages along the path, then multiply it by -1 and by removed cycle to form monomial;
11: **end for**
12: **end for**
13: Add all monomials created from paths to create a polynomial;
14: Distribute monomials based on b to form a set of equations from which **B** and **C** matrices can be created;

4.3 Example

Let be given the strictly proper transfer function in the form:

$$T_{sp}(s) = \frac{n(s)}{d(s)} = \frac{\widetilde{b}_2 s^{2\cdot\alpha} + \widetilde{b}_1 s^{\alpha} + \widetilde{b}_0}{s^{3\cdot\alpha} - a_2 s^{2\cdot\alpha} - a_1 s^{\alpha} - a_0}, \quad for \;\; 0 < \alpha < 1. \tag{7}$$

Solution: The strictly proper transfer function (7) can be considered as a pseudo-rational strictly proper transfer function $T_{sp}(\lambda)$ of the variable $\lambda = s^{\alpha}$ in the following form:

$$T_{sp}(\lambda) = \frac{n(\lambda)}{d(\lambda)} = \frac{\widetilde{b}_2\lambda^2 + \widetilde{b}_1\lambda + \widetilde{b}_0}{\lambda^3 - a_2\lambda^2 - a_1\lambda - a_0}. \tag{8}$$

Multiplying the denominator of the (8) by λ^{-3} we obtain the characteristic polynomial in the form:

$$d(\lambda) = 1 - a_2\lambda^{-1} - a_1\lambda^{-2} - a_0\lambda^{-3}. \tag{9}$$

In the next step using procedure presented in paper [23] we determine all the possible digraph structures corresponding to the characteristic polynomial (9). From all the potential realisations, we choose the realisation presented in Fig. 1 and we write the state matrix in the form:

$$\mathbf{A} = \begin{bmatrix} w(v_1, v_1) & w(v_2, v_1) & w(v_3, v_1) \\ w(v_1, v_2) & 0 & 0 \\ 0 & w(v_2, v_3) & 0 \end{bmatrix}, \tag{10}$$

where:

$$a_2 = w(v_1, v_1),\ a_1 = w(v_1, v_2) \cdot w(v_2, v_1),\ a_0 = w(v_1, v_2) \cdot w(v_2, v_3) \cdot w(v_3, v_1).$$

In the next step we must determine matrices **B** and **C**. Multiplying nominator of the strictly proper transfer function (8) by λ^{-2} we obtain the following polynomial in the form which is needed to draw the digraph:

$$n(\lambda) = \widetilde{b}_2 + \widetilde{b}_1\lambda^{-1} + \widetilde{b}_0\lambda^{-2}. \tag{11}$$

To the digraph presented in Fig. 1 we add source vertex s and output vertex y and connect them. Assuming that matrix **B** contains one non-zero entry, we obtain the following three cases:

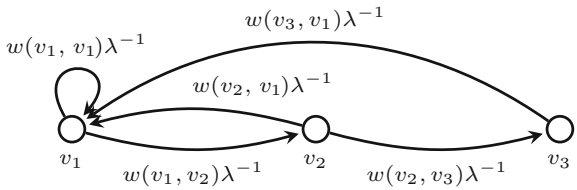

Fig. 1 One of the possible realisation of the characteristic polynomial (9)

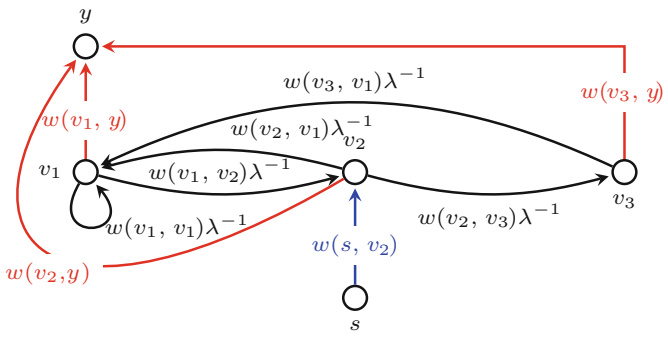

Fig. 2 Realisations of the strictly proper transfer function (7) – Case 2

Case 1: The first case, when source is connected with vertex belonging to intersection set of digraph corresponding monomials (vertex v_1). This case was considered in-detail in papers [25, 26].

Case 2: The second case when source s is connected with vertex v_2 (see Fig. 2). Then, using a created digraph we can write a set of equations in the form:

$$\begin{cases} \lambda^{-1} \left\| \begin{array}{ll} w(s,v_2)w(v_2,y) & = \widetilde{b}_2 \\ w(v_2,v_1)w(s,v_2)w(v_1,y) - w(v_1,v_1)w(s,v_2)w(v_2,y) + & \\ w(v_2,v_1)w(v_2,v_1) & = \widetilde{b}_1 \\ \lambda^{-2} \left\| \begin{array}{ll} w(v_2,v_3)w(v_3,v_1)w(s,v_2)w(v_1,y) - & \\ w(v_1,v_1)w(v_2,v_3)w(s,v_2)w(v_3,y) & = \widetilde{b}_0 \end{array} \right. \end{array} \right. \quad (12)$$

After solving the set of the Eq. (12), we can write the input and output matrices in the following form:

$$\mathbf{B} = \begin{bmatrix} 0 \\ w(s,v_2) \\ 0 \end{bmatrix}, \mathbf{C} = \begin{bmatrix} c_1 & c_2 & c_3 \end{bmatrix}, \quad (13)$$

where:

$$c_1 = \frac{\widetilde{b}_2 w(v_1,v_1)^2 + \widetilde{b}_1 w(v_1,v_1) + \widetilde{b}_0}{w(s,v_2)\left[w(v_1,v_1)w(v_2,v_1) + w(v_2,v_3)w(v_3v_1)\right]}, \quad c_2 = \frac{\widetilde{b}_2}{w(s,v_2)},$$
$$c_3 = \frac{w(v_1,v_1)w(v_2,v_3)w(v_3,v_1)\widetilde{b}_2 + w(v_2,v_3)w(v_3,v_1)\widetilde{b}_1 - w(v_2,v_1)\widetilde{b}_0}{w(v_2,v_3)w(s,v_2)\left[w(v_1,v_1)w(v_2,v_1) + w(v_2v_3)w(v_3,v_1)\right]}.$$

The desired realisation of the (7) is given by (10) and (13).

Case 3: The third case when source s is connected with vertex v_3 (see Fig. 3). Then, using a created digraph we can write a set of equations in the form:

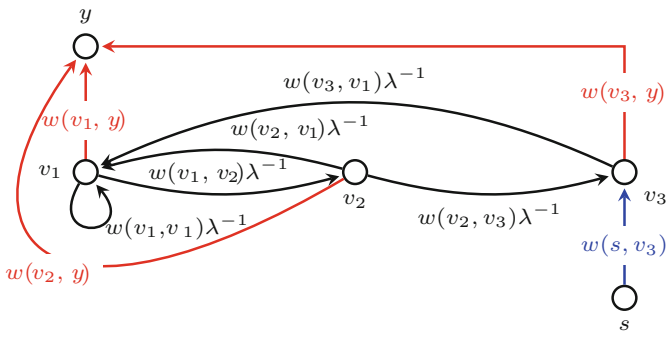

Fig. 3 Realisations of the strictly proper transfer function (7) – Case 3

$$\left\{\begin{array}{l|l|l} & w(s,v_3)w(v_3,y) & = \widetilde{b}_2 \\ \lambda^{-1} & w(v_3,v_1)w(s,v_3)w(v_1,y) - w(v_1,v_1)w(s,v_3)w(v_3,y) & = \widetilde{b}_1 \\ \lambda^{-2} & w(v_1,v_2)w(v_3,v_1)w(s,v_3)w(v_2,y) - & \\ & w(v_1,v_2)w(v_2,v_1)w(s,v_3)w(v_3,y) & = \widetilde{b}_0 \end{array}\right. . \tag{14}$$

After solving the set of the Eq. (14), we can write the input and output matrices in the following form:

$$\mathbf{B} = \begin{bmatrix} 0 \\ 0 \\ w(s,v_3) \end{bmatrix}, \mathbf{C} = \begin{bmatrix} c_1 & c_2 & c_3 \end{bmatrix}, \tag{15}$$

where:

$$c_1 = \frac{\widetilde{b}_1 + w(v_1,v_1)\widetilde{b}_2}{w(v_3,v_1)w(s,v_3)}, \quad c_2 = \frac{\widetilde{b}_0 + w(v_1,v_2)w(v_2,v_1)\widetilde{b}_2}{w(v_1,v_2)w(v_3,v_1)w(s,v_3)}, \quad c_3 = \frac{\widetilde{b}_2}{w(s,v_3)}.$$

The desired realisation of the (7) is given by (10) and (15).

5 Concluding Remarks

In this paper first approach to extending the algorithm presented in [22–24] was presented. Modified method allows for finding (**A**, **B**, **C**) matrices directly from obtained digraph structures of one-dimensional dynamic system. Presented algorithm finds a set of possible realisations instead of just a few, as was in the case of canonical forms approach. Moreover, proposed method is possible to implement numerically in both time and memory efficient way due to it's construction that allows parallelism. Described method was presented along with pseudo-code algorithm and illustrated in the article with numerical example.

Further work includes extension of the algorithm to be able to obtain (**A**, **B**, **C**) matrices of 2-D fractional systems and analysis of reachability of systems, including the experimental evaluation of the reachability index for 2-D systems, which is still an open problem.

References

1. Kaczorek, T.: Selected Problems of Fractional Systems Theory. Springer, Berlin (2011)
2. Kaczorek, T., Sajewski, L.: The Realization Problem for Positive and Fractional Systems. Springer International Publishing, Berlin (2014)
3. Nishimoto, K.: Fractional Calculus. Decartess Press, Koriyama (1984)
4. Miller, K., Ross, B.: An Introduction to the Fractional Calculus and Fractional Differential Equations. Willey, New York (1993)
5. Podlubny, I.: Fractional Differential Equations. Academic, San Diego (1999)
6. Dzieliński, A., Sierociuk, D., Sarwas, G.: Some applications of fractional order calculus. Bull. Pol. Acad. Tech. **58**(4), 583–592 (2010)
7. Das, S.: Functional Fractional Calculus. Springer, Berlin (2011)
8. Ortigueira, M.D.: Fractional Calculus for Scientists and Engineers. Academic, Springer, The Netherlands (2011)
9. Berman, A., Neumann, M., Stern, R.J.: Nonnegative Matrices in Dynamic Systems. Wiley, New York (1989)
10. Horn, R.A., Johnson, C.R.: Topics in Matrix Analysis. Cambridge University Press, Cambridge (1991)
11. Bang-Jensen, J., Gutin, G.: Digraphs: Theory Algorithms and Applications. Springer, London (2009)
12. Fornasini, E., Valcher, M.E.: Directed graphs, 2D state models, and characteristic polynomials of irreducible matrix pairs. Linear Algebra Appl. **263**, 275–310 (1997)
13. Benvenuti, L., Farina, L.: A tutorial on the positive realization problem. IEEE Trans. Autom. Control **49**(5), 651–664 (2004)
14. Kaczorek, T.: Positive 1D and 2D systems. Springer, London (2001)
15. Kaczorek, T.: Realization problem for general model of two-dimensional linear systems. Bull. Pol. Acad. Tech. **35**(11–12), 633–637 (1987)
16. Bisiacco, M., Fornasini, E., Marchesini, G.: Dynamic regulation of 2D systems: a state-space approach. Linear Algebra Appl. **122**, 195–218 (1989)
17. Xu, L., Wu, Q., Lin, Z., Xiao, Y., Anazawa, Y.: Futher results on realisation of 2D filters by Fornasini–Marchesini model. In: 8th International Conference on Control, Automation, Robotics and Vision, pp. 1460–1464 (2004)
18. Xu, L., Wu, L., Wu, Q., Lin, Z., Xiao, Y.: On realization of 2D discrete systems by Fornasini–Marchesini model. Int. J. Control Autom. **4**(3), 631–639 (2005)
19. Kaczorek, T.: Positive realization of 2D general model. Logistyka **3**, 1–13 (2007)
20. Hryniów, K., Markowski, K.A.: Parallel digraphs-building algorithm for polynomial realisations. In: Proceedings of 15th International Carpathian Control Conference (ICCC), pp. 174–179 (2014)
21. Hryniów, K., Markowski, K.A.: Optimisation of digraphs-based realisations for polynomials of one and two variables. In: Szewczyk, R., Zieliński, C., Kaliczyńska, M. (eds.) Progress in Automation, Robotics and Measuring Techniques, Advances in Intelligent Systems and Computing, vol. 350, pp. 73–83. Springer International Publishing, Switzerland (2015)
22. Hryniów, K., Markowski, K.A.: Optimisation of digraphs creation for parallel algorithm for finding a complete set of solutions of characteristic polynomial. In: 20th International Conference on Methods and Models in Automation and Robotics (MMAR), pp. 1139–1144 (2015)

23. Hryniów, K., Markowski, K.A.: Digraphs-building method for finding a set of minimal realisations of positive 2-D dynamic systems. Syst. Control Lett. (2016) (Submitted to)
24. Hryniów, K., Markowski, K.A.: Digraphs minimal positive stable realisations for fractional one-dimensional systems. In: Domek, S., Dworak, P. (eds.) Theoretical Developments and Applications of Non-Integer Order Systems. Lecture Notes in Electrical Engineering, vol. 357, pp. 105–118. Springer International Publishing, Switzerland (2015)
25. Markowski, K.A.: Digraphs structures corresponding to minimal realisation of fractional continuous-time linear systems with all-pole and all-zero transfer function. In: 2016 IEEE International Conference on Automation, Quality and Testing, Robotics (AQTR) (2016)
26. Markowski, K.A.: Two cases of digraph structures corresponding to minimal positive realisation of fractional continuous-time linear systems of commensurate order. J. Appl. Nonlinear Dyn. (2016) (Accepted)

Relative Controllability of Nonlinear Fractional Delay Dynamical Systems with Time Varying Delay in Control

Joice Nirmala Rajagopal

Abstract This paper investigate the relative controllability of nonlinear fractional delay dynamical system with time varying delay in control. The necessary and sufficient conditions for the relative controllability criteria for linear fractional delay system are obtained. The sufficient conditions for the relative controllability of nonlinear fractional delay system are obtained by using Schauder fixed point arguments. Illustrative examples are given to examine the results obtained.

Keywords Controllability · Delay differential equation · Fractional calculus · Laplace transform

1 Introduction

It is evident that many realistic model must include some of the past history of the system. A formulation by a system of ordinary differential equations is not possible to describe physical processes and they can be described by a system of delay differential equations. A related study on analytic solutions of linear delay differential equations has been studied by Bellman and Cooke [1], Smith [2], Halaney [3] Smith and Hale [4]. They have applied the method of steps to find series solution of delay differential equations. Using of Banach and Schauder fixed point theorem we can find in [5, 6].

Fractional differentials and integrals provide more accurate models of systems under consideration. Many authors have demonstrated the dynamics of interfaces between nanoparticles and substrates [7], bioengineering [8], continuum and statistical mechanics [9], filter design, circuit theory and robotics [10]. Differential equations with fractional order have recently proved to be valuable tools to the modeling of many physical phenomena. Moreover, Machoda et al. [11, 12] analysed and designed the fractional order digital control systems and also modeled the fractional dynamics in DNA. Apart from stability, another important qualitative behavior of a dynamical system is controllability. Controllability is used to influence an object behavior so

J.N. Rajagopal (✉)
Department of Mathematics, Bharathiar University, Coimbatore 641046, India
e-mail: joys.maths.bu@gmail.com

A. Babiarz et al. (eds.), *Theory and Applications of Non-integer Order Systems*,
Lecture Notes in Electrical Engineering 407, DOI 10.1007/978-3-319-45474-0_33

as to accomplish a desire goal. Dauer and Gahl [13] obtained the controllability of nonlinear delay systems. Balachandran and Dauer [14] studied the controllability problems for both linear and nonlinear delay systems. The relative controllability of nonlinear fractional dynamical system with multiple delays and distributive delays in control have been discussed by Balachandran et al. [15–17]. Klamka [18, 19] established the controllability of both linear and nonlinear system with time variable delay in control. Manzanilla et al. [20] obtained the controllability of differential equation with delay and advanced arguments. Recently, Mur et al. [21] studied the relative controllability of linear systems of fractional order with delay. Detail study on controllability of fractional delay dynamical systems is given in [22, 23].

2 Preliminaries

This section begins with definitions and properties of fractional operator, special functions and its Laplace transformation. Finally the solution representation of fractional delay differential is given by using Laplace transform [24, 25].

(a) The Caputo fractional derivative of order $\alpha > 0, n-1 < \alpha < n$, is defined as

$$ {}^{C}D^{\alpha} f(t) = \frac{1}{\Gamma(n-\alpha)} \int_0^t (t-s)^{n-\alpha-1} f^{(n)}(s) \mathrm{d}s, $$

where the function $f(t)$ has absolutely continuous derivative upto order $n-1$. The Laplace transform of Caputo derivative is given in [24].

(b) The Mittag-Leffler functions of various type are defined as

$$ E_{\alpha}(z) = E_{\alpha,1}(z) = \sum_{k=o}^{\infty} \frac{z^k}{\Gamma(\alpha k+1)}, z \in \mathbb{C}, Re(\alpha) > 0, \tag{1} $$

$$ E_{\alpha,\beta}(z) = \sum_{k=0}^{\infty} \frac{z^k}{\Gamma(\alpha k+\beta)}, z, \beta \in \mathbb{C}, Re(\alpha) > 0, \tag{2} $$

$$ E^{\gamma}_{\alpha,\beta}(-\lambda t^{\alpha}) = \sum_{k=0}^{\infty} \frac{(\gamma)_k (-\lambda)^k}{k!\Gamma(\alpha k+\beta)} t^{\alpha k}, \tag{3} $$

where $(\gamma)_n$ is a Pochhammer symbol which is defined as $\gamma(\gamma+1)\cdots(\gamma+n-1)$ and $(\gamma)_n = \dfrac{\Gamma(\gamma+n)}{\Gamma(\gamma)}$. The Laplace transform of Mittag-Leffler functions (1), (2) and (3) are given in [24].

In order to prove our main results we need the following fixed point theorem:

Theorem 1 [26] (Schauder's Fixed Point Theorem) *Let M be a compact, convex set in a Banach space X and $T : M \to M$ be continuous. Then T has a fixed point M.*

3 Linear Delay Systems

Consider the fractional delay dynamical systems with multiple delays in control

$$\begin{aligned} {}^{C}D^{\alpha}x(t) &= Ax(t) + Bx(t-h) + \sum_{i=0}^{M} C_i u(\sigma_i(t)), t \in J = [0, T], \\ x(t) &= \phi(t), -h < t \leq 0, \end{aligned} \tag{4}$$

where $0 < \alpha < 1, x \in \mathbb{R}^n, u \in \mathbb{R}^m$ A, B are $n \times n$ matrices and C_i are $n \times m$ matrices for $i = 0, 1, 2, \ldots, M$. Assume the following conditions

(H1) The functions $\sigma_i : J \to \mathbb{R}, i = 0, 1, 2, \ldots, M$ are twice continuously differentiable and strictly increasing in J. Moreover

$$\sigma_i(t) \leq t, \ i = 0, 1, 2 \cdots M, \ \text{for } t \in J \tag{5}$$

(H2) Introduce the time lead functions $r_i(t) : [\sigma_i(0), \sigma_i(T)] \to [0, T]$, $i = 0, 1, 2, \ldots, M$ such that $r_i(\sigma_i(t)) = t$ for $t \in J$. Further $\sigma_0(t) = t$ and for $t = T$, the following inequality holds

$$\begin{aligned} \sigma_M(T) \leq \sigma_{M-1}(T) \leq \cdots \sigma_{m+1}(T) \leq 0 = \sigma_m(T) < \sigma_{m-1}(T) = \cdots = \sigma_1(T) \\ = \sigma_0(T) = T. \end{aligned} \tag{6}$$

The following definitions of complete state of the system (4) at time t and relative controllability are assumed.

Definition 1 [27] The set $y(t) = \{x(t), \beta(t, s)\}$, where $\beta(t, s) = u(s)$ for $s \in [\min h_i(t), t)$ is said to be the complete state of the system (4) at time t.

Definition 2 System (4) is said to be relatively controllable on $[0, T]$ if for every complete state $y(t)$ and every $x_1 \in \mathbb{R}^n$ there exists a control $u(t)$ defined on $[0, T]$, such that the solution of system (4) satisfies $x(T) = x_1$.

The solution of the system (4) by using Laplace transform is expressed as

$$\begin{aligned} x(t) = X_\alpha(t)\phi(0) + B \int_{-h}^{0} (t - s - h)^{\alpha-1} X_{\alpha,\alpha}(t - s - h)\phi(s)\mathrm{d}s \\ + \int_0^t (t - s)^{\alpha-1} X_{\alpha,\alpha}(t - s) \sum_{i=0}^{M} C_i u_i(\sigma_i(s))\mathrm{d}s. \end{aligned} \tag{7}$$

where

$$X_\alpha(t) = L^{-1}[s^{\alpha-1}(s^\alpha I - A - Be^{-hs})^{-1}](t),$$

and

$$X_{\alpha,\alpha}(t) = t^{1-\alpha}\int_0^t \frac{(t-s)^{\alpha-2}}{\Gamma(\alpha-1)} X_\alpha(s)\mathrm{d}s.$$

Using the time lead functions $r_i(t)$, the solution can be written as

$$x(t) = x_L(t;\phi) + \sum_{i=0}^{M}\int_{\sigma_i(0)}^{\sigma_i(t)} (t-r_i(s))^{\alpha-1} X_{\alpha,\alpha}(t-r_i(s))C_i\dot{r}_i(s)u(s)\mathrm{d}s,$$

where

$$x_L(t;\phi) = X_\alpha(t)\phi(0) + B\int_{-h}^{0}(t-s-h)^{\alpha-1}X_{\alpha,\alpha}(t-s-h)\phi(s)\mathrm{d}s.$$

By using the inequality (6) we get

$$\begin{aligned} x(t) = x_L(t;\phi) &+ \sum_{i=0}^{m}\int_{\sigma_i(0)}^{0} (t-r_i(s))^{\alpha-1} X_{\alpha,\alpha}(t-r_i(s))C_i\dot{r}_i(s)\beta(s)\mathrm{d}s \\ &+ \sum_{i=0}^{m}\int_{0}^{t} (t-r_i(s))^{\alpha-1} X_{\alpha,\alpha}(t-r_i(s))C_i\dot{r}_i(s)u(s)\mathrm{d}s \\ &+ \sum_{i=m+1}^{M}\int_{\sigma_i(0)}^{\sigma_i(t)} (t-r_i(s))^{\alpha-1} X_{\alpha,\alpha}(t-r_i(s))C_i\dot{r}_i(s)\beta(s)\mathrm{d}s. \end{aligned}$$

For simplicity, let us write the solution as

$$x(t) = x_L(t;\phi) + H(t) + \sum_{i=0}^{m}\int_0^t (t-r_i(s))^{\alpha-1} X_{\alpha,\alpha}(t-r_i(s))C_i\dot{r}_i(s)u(s)\mathrm{d}s, \quad (8)$$

where

$$\begin{aligned} H(t) = &\sum_{i=0}^{m}\int_{\sigma_i(0)}^{0} (t-r_i(s))^{\alpha-1} X_{\alpha,\alpha}(t-r_i(s))C_i\dot{r}_i(s)\beta(s)\mathrm{d}s \\ &+ \sum_{i=m+1}^{M}\int_{\sigma_i(0)}^{\sigma_i(t)} (t-r_i(s))^{\alpha-1} X_{\alpha,\alpha}(t-r_i(s))C_i\dot{r}_i(s)\beta(s)\mathrm{d}s. \end{aligned}$$

Now let us define the controllability Grammian matrix

$$W = \sum_{i=0}^{m} \int_0^T (X_{\alpha,\alpha}(T - r_i(s))C_i\dot{r}_i(s))(X_{\alpha,\alpha}(T - r_i(s))C_i\dot{r}_i(s))^* \mathrm{d}s,$$

where the $*$ denotes the matrix transpose.

Theorem 2 *The linear system (4) is relatively controllable on* $[0, T]$ *if and only if the controllability Grammian matrix is positive definite for some* $T > 0$.

The proof this statement is similar to proof given by Balachandran et al. [15] by defining the control function as

$$u(t) = (T - r_i(t))^{1-\alpha}(X_{\alpha,\alpha}(T - r_i(t))C_i\dot{r}_i(t))^* W^{-1}\left[x_1 - x_L(T;\phi) - H(T)\right], \tag{9}$$

4 Nonlinear Delay Systems

Consider the nonlinear fractional delay dynamical systems with multiple delays in control of the form

$$\begin{aligned} {}^C D^\alpha x(t) &= Ax(t) + Bx(t-h) + \sum_{i=0}^{M} C_i u(\sigma_i(t)) + f(t, x(t), x(t-h), u(t)), t \in J, \\ x(t) &= \phi(t), -h < t \le 0. \end{aligned} \tag{10}$$

where $0 < \alpha < 1$, $x \in \mathbb{R}^n$, $u \in \mathbb{R}^m$ and A, B are $n \times n$ matrices, C_i for $i = 0, 1, \ldots, M$ are $n \times m$ matrices and $f : J \times \mathbb{R}^n \times \mathbb{R}^n \times \mathbb{R}^m \to \mathbb{R}^n$ is a continuous function. Further we impose the following assumption

(H3) The continuous function f satisfies the condition that

$$\lim_{p \to \infty} \frac{|f(t, p)|}{|p|} = 0, \tag{11}$$

uniformly in $t \in J$, where $p = |x| + |y| + |u|$. Similar to the linear system, the solution of nonlinear system (10) using time lead function $r_i(t)$ is given as

$$\begin{aligned} x(t) = x_L(t;\phi) + H(t) &+ \sum_{i=0}^{m} \int_0^t (t - r_i(s))^{\alpha-1} X_{\alpha,\alpha}(t - r_i(s))C_i\dot{r}_i(s)u(s)\mathrm{d}s \\ &+ \int_0^t (t-s)^{\alpha-1} X_{\alpha,\alpha}(t-s) f(s, x(s), x(s-1), u(s))\mathrm{d}s. \end{aligned} \tag{12}$$

Theorem 3 *Assume that the hypothesis (H1)–(H3) are satisfied and suppose that the linear fractional delay dynamical system (4) is relatively controllable. Then the nonlinear system (10) is relatively controllable on* J.

Proof Define $\Psi : Q \to Q$ by

$$\Psi(x, u) = (y, v)$$

where

$$\begin{aligned} v(t) &= (T - r_i(t))^{1-\alpha}(X_{\alpha,\alpha}(T - r_i(t))C_i^*\dot{r}_i(t))^* \\ &\quad \times W^{-1}\Bigg[x_1 - x_L(T;\phi) - \sum_{i=0}^{m}\int_{\sigma_i(0)}^{0}\Big[(T - r_i(s))^{\alpha-1}X_{\alpha,\alpha}(T - r_i(s)) \\ &\quad \times C_i\dot{r}_i(s)\beta(s)\mathrm{d}s\Bigg] \\ &\quad - \sum_{i=m+1}^{M}\int_0^T (T - r_i(s))^{\alpha-1}X_{\alpha,\alpha}(T - r_i(s))C_i\dot{r}_i(s)\beta(s)\mathrm{d}s \\ &\quad - \int_0^T (T - s)^{\alpha-1}X_{\alpha,\alpha}(T - s)f(s, x(s), x(s-h), u(s))\mathrm{d}s\Bigg], \end{aligned} \tag{13}$$

and

$$\begin{aligned} y(t) &= x_L(t;\phi) + \sum_{i=0}^{m}\int_{\sigma_i(0)}^{0}(t - r_i(s))^{\alpha-1}X_{\alpha,\alpha}(t - r_i(s))C_i\dot{r}_i(s)\beta(s)\mathrm{d}s \\ &\quad + \sum_{i=0}^{m}\int_0^t (t - r_i(s))^{\alpha-1}X_{\alpha,\alpha}(t - r_i(s))C_i\dot{r}_i(s)v(s)\mathrm{d}s \\ &\quad + \sum_{i=m+1}^{M}\int_{\alpha_0}^t (t - r_i(s))^{\alpha-1}X_{\alpha,\alpha}(t - r_i(s))C_i\dot{r}_i(s)\beta(s)\mathrm{d}s \\ &\quad + \int_0^t (t - s)^{\alpha-1}X_{\alpha,\alpha}(t - s)f(s, x(s), x(s-1), v(s))\mathrm{d}s, \end{aligned} \tag{14}$$

Let

$$\begin{aligned} a_i &= \sup||X_{\alpha,\alpha}(T - r_i(s))||, b_i = \sup||\dot{r}_i(s)||, i = 0, 1, 2, \ldots, M, \nu = \sup||\beta(s)|| \\ \vartheta &= \sup||X_{\alpha,\alpha}(T - s)||,\ \mu = \sum_{i=0}^{m} a_i b_i||C_i||N_i + \sum_{i=m+1}^{M} a_i b_i||C_i||M_i, \\ c_i &= 4a_i b_i||C_i^*||||W^{-1}||\nu\alpha^{-1}T^{\alpha}, d_i = 4a_i b_i||C_i^*||||W^{-1}||[|x_1| + \beta + \mu], \\ a &= \max\{b\alpha^{-1}T^{\alpha}||C_i||, 1\}, b = \sum_{i=0}^{m} a_i b_i L_i, c_2 = 4\vartheta\alpha^{-1}T^{\alpha}, d_2 = 4[\beta + \nu\mu], \\ N_i &= \int_{\sigma_i(0)}^{0}(T - r_i(s))^{\alpha-1}\mathrm{d}s, M_i = \int_{\sigma_i(0)}^{\sigma_i(T)}(T - r_i(s))^{\alpha-1}\mathrm{d}s, \end{aligned}$$

$$L_i = \int_0^T (T - r_i(s))^{\alpha-1} \mathrm{d}s, c = \max\{c_i, c_2\}, d = \max\{d_i, d_2\}$$
$$\sup|f| = \{\sup|f(t, x(t), x(t-1), u(t))|, t \in J\}.$$

Then

$$|v(t)| \leq ||C_i^*||a_i b_i||W^{-1}||[||x_1|| + \beta + \mu] + a_i b_i||C_i^*||||W^{-1}||\vartheta\alpha^{-1}T^{\alpha},$$
$$\leq \frac{1}{4a}(d + c\sup|f|)$$

and

$$|y(t)| \leq \beta + \nu\mu + \left(\sum_{i=0}^{m} a_i b_i||C_i||L_i\alpha^{-1}T^{\alpha}\right)v(s) + \vartheta\alpha^{-1}T^{\alpha}\sup|f|,$$
$$\leq \frac{d}{2} + \frac{c}{2}\sup|f|.$$

By Proposition 1 in [28], the function f satisfies the following conditions. For each pair of positive constants c and d, there exists a positive constant r such that for $|p| \leq r$, then

$$c|f(t, p)| + d \leq r \text{ for all } t \in J. \tag{15}$$

Also, for given c and d, if r is a constant such that $r < r_1$ will also satisfy (15). Now take c and d as given above and choose r so that (15) is satisfied. Therefore $||x|| \leq \frac{r}{2}$ and $||u|| \leq \frac{r}{2}$, then $|x(s)| + |y(s)| \leq r$, for all $s \in J$. It follows that $d + c\sup|f| \leq r$. Therefore $|u(s)| \leq \frac{r}{4a}$ for all $s \in J$ and hence $||u|| \leq \frac{r}{4a}$, which gives $||x|| \leq \frac{r}{2}$. Thus,

$$Q(r) = \{(x, u) \in Q : ||x|| \leq \frac{r}{2} \text{ and } ||u|| \leq \frac{r}{2}\},$$

then Ψ maps $Q(r)$ into itself. Our objective is to show that Ψ has a fixed point, since f is continuous, it follows that Ψ is continuous. Let Q_0 be a bounded subset of Q. Consider a sequence $\{(y_j, v_j)\}$ contained in $\Psi(Q_0)$, where we let

$$(y_j, v_j) = \Psi(x_j, u_j),$$

for some $(x_j, u_j) \in Q_0$, for $j = 1, 2, \ldots$. Since f is continuous $|f(s, x_j(s), x_j(s-h), u_j(s))|$ is uniformly bounded for all $s \in J$, and $j = 1, 2, 3, \ldots$. It follows that $\{(y_j, v_j)\}$ is a bounded sequence in Q. Hence $\{v_j(t)\}$ is equicontinuous and a uniformly bounded sequence on $[0, t_1]$. Since $\{y_j(t)\}$ is a uniformly bounded and equicontinuous sequence on $[-h, t_1]$, an application of Ascoli's theorem yield a further subsequence of $\{(y_j, v_j)\}$ which converges in Q to some (y_0, v_0). It follows that $\Psi(Q_0)$ is sequentially compact, hence, the closure is sequentially compact. Thus, Ψ is completely continuous. Since $Q(r)$ is closed, bounded and convex, the

Schauder fixed point theorem implies that Ψ has a fixed point $(x, u) \in Q(r)$, such that $(y, v) = \Psi(x, u) = (x, u)$. It follows that

$$x(t) = x_L(t; \phi) + H(t) + \sum_{i=0}^{m} \int_0^t (t - r_i(s))^{\alpha-1} X_{\alpha,\alpha}(t - r_i(s)) C_i \dot{r}_i(s) u(s) \mathrm{d}s$$
$$+ \int_0^t (t - s)^{\alpha-1} X_{\alpha,\alpha}(t - s) f(s, x(s), x(s - h), u(s)) \mathrm{d}s, \tag{16}$$

for $t \in J$ and $x(t) = \phi(t)$ for $t \in [-h, 0]$

$$X(T) = x_1.$$

Hence the system (10) is relatively controllable on J.

5 Examples

Example 1 Consider the linear fractional delay dynamical systems with delay in control by the fractional differential equation

$${}^{C}D^{\frac{3}{4}} x(t) = \begin{pmatrix} -1 & 0 \\ 0 & -2 \end{pmatrix} x(t) + \begin{pmatrix} 0 & 0 \\ -1 & 0 \end{pmatrix} x(t-1) + \begin{pmatrix} 1 \\ 0 \end{pmatrix} u(t)$$
$$+ \begin{pmatrix} 0 \\ 1 \end{pmatrix} u(t-1), \tag{17}$$

where $\alpha = \frac{3}{4}, h = 1, \sigma = 1, A = \begin{pmatrix} -1 & 0 \\ 0 & -2 \end{pmatrix}, B = \begin{pmatrix} 0 & 0 \\ -1 & 0 \end{pmatrix}, C_0 = \begin{pmatrix} 1 \\ 0 \end{pmatrix}$, and $C_1 = \begin{pmatrix} 0 \\ 1 \end{pmatrix}$ with initial state $x(0) = \begin{pmatrix} 2 \\ 4 \end{pmatrix}$ and final state $x(1) = \begin{pmatrix} 6 \\ 8 \end{pmatrix}$. The solution of the Eq. (17) by using Laplace transform is of the form

$$x(t) = \sum_{n=0}^{[t]} B^n (t - n)^{\frac{3}{4}n} E_{\frac{3}{4}, \frac{3}{4}n+1}(A(t - n)^{\frac{3}{4}})$$
$$+ B \sum_{n=0}^{[t]} B^n \int_{-1}^{0} (t - s - n - 1)^{\frac{3}{4}n + \frac{3}{4} - 1} E_{\frac{3}{4}, \frac{3}{4}(n+1)}(A(t - s - n - 1)^{\frac{3}{4}}) \phi(s) \mathrm{d}s$$
$$+ \sum_{n=0}^{[t]} \sum_{i=0}^{1} B^n C_i \int_0^{t-n} (t - r_i(s) - n)^{\frac{3}{4}n - \frac{1}{4}} (A(t - r_i(s) - n))^{\frac{3}{4}} \dot{r}_i(s) u(s) \mathrm{d}s.$$

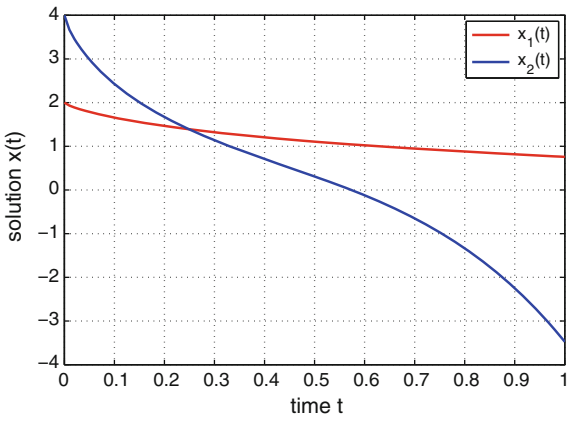

Fig. 1 The trajectory of the dynamical system without control

Now, consider the controllability on [0, 1], where [t] = 0, the solution is of the form

$$x(t) = E_{\frac{3}{4},1}(At^{\frac{3}{4}}) + Bt^{\frac{3}{4}}E_{\frac{3}{4},\frac{3}{4}}(A(t^{\frac{3}{4}})) + \sum_{i=0}^{1} C_i \int_0^t (t - r_i(s))^{-\frac{1}{4}} E_{\frac{3}{4},\frac{3}{4}}(A(t - r_i(s))^{\frac{3}{4}})\dot{r}_i(s)u(s)\mathrm{d}s,$$

The Grammian matrix is defined as

$$W = \sum_{i=0}^{1} \int_0^1 [C_i E_{\frac{3}{4},\frac{3}{4}}(A(1 - r_i(s))^{\frac{3}{4}})\dot{r}_i(s)][C_i E_{\frac{3}{4},\frac{3}{4}}(A(1 - r_i(s))^{\frac{3}{4}})\dot{r}_i(s)]^* \mathrm{d}s,$$

where $r_i(s)$ is a time lead function and it is defined as $r_0(s) = s$ and $r_1(s) = s - 1$. Then the Grammian matrix is

$$W = \begin{pmatrix} 0.1897 & 0 \\ 0 & 86.8973 \end{pmatrix}$$

which is positive definite. Then by the Theorem 1 the system is controllable on [0, 1].

Figure 1 represent the trajectory of the system without control and Fig. 2 represent the trajectory of the system with control.

Example 2 Consider the nonlinear fractional delay dynamical system of the form

$$\begin{aligned} {}^{C}D^{\frac{3}{4}}x(t) &= Ax(t) + Bx(t-1) + C_0u(t) + C_1u(t-1) + f(t, x(t), x(t-1), u(t)), \\ x(t) &= \phi(t) \end{aligned} \tag{18}$$

The matrices A, B, C_0 and C_1 are defined as above and the function f is taken as

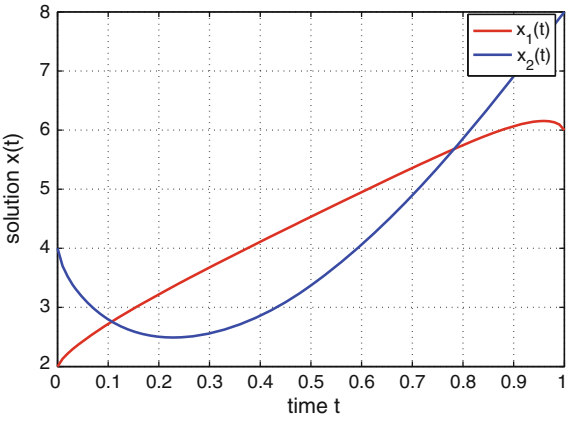

Fig. 2 The trajectory of the dynamical system with control

$$f(t, x(t), x(t-1), u(t)) = \begin{pmatrix} 0 \\ \frac{x_1(t)\sin t}{x_1^2(t)+x_2^2(t)} + \frac{1}{x_1^2(t-1)+u(t)}. \end{pmatrix} \tag{19}$$

Here also we consider the controllability on the [0, 1]. Since the linear system (17) is controllable and the nonlinear function (19) satisfies the hypothesis of the Theorem 2 we say that the nonlinear system (18) is controllable on [0, 1].

6 Conclusion

The relative controllability of nonlinear fractional delay dynamical system with time varying delay in control is discussed. The necessary and sufficient conditions for the relative controllability criteria for linear fractional delay system are obtained by constructing Grammian matrix. The controllability of nonlinear fractional delay dynamical systems is obtained by using the Schauder's fixed point theorem. Examples with numerical simulation is given to examine the results developed.

Acknowledgments The work was supported by the [University Grants Commission] under grant [number: MANF-2013-14-CHR-TAM-25156] from the government of India.

References

1. Bellman, R., Cooke, K.L.: Differential Difference Equations. Academic, New York (1963)
2. Smith, H.: An Introduction to Delay Differential Equations with Application to the Life Sciences. Springer, New York (2011)
3. Halanay, A.: Differential Equations: Stability, Oscillations Time Lags. Academic, New York (1966)

4. Hale, J.: Theory of Functional Differential Equations. Springer, New York (1977)
5. Babiarz, A., Klamka, J., Niezabitowski, M.: Schauder's fixed point theorem in approximate controllability problems. Int. J. Appl. Math. Comput. Sci. **26**(2), 263–275 (2016)
6. Klamka, J., Babiarz, A., Niezabitowski, M.: Banach fixed point theorem in semilinear controllability problems - a survey. Bull. Pol. Ac. Tech. **64**(1), 21–35 (2016)
7. Chow, T.S.: Fractional dynamics of interfaces between soft-nanoparticles and rough substrates. Phys. Lett. A **342**(1), 148–155 (2005)
8. Magin, R.L.: Fractional Calculus in Bioengineering. Begell House, Redding (2006)
9. Mainardi, F.: Fractional calculus: some basic problems in continuum and statistical mechanics. In: Carpinteri, A., Mainardi, F. (eds.) Fractals and Fractional calculus in Continuum Mechanics, vol. 378, pp. 291–348. Springer, New York (1997)
10. Sabatier, J., Agrawal, O.P., Tenreiro-Machado, J.A.: Advances in Fractional Calculus: Theoretical Developments and Applications in Physics and Engineering. Springer, New York (2007)
11. Machado, J.T., Costa, A.C., Quelhas, M.D.: Fractional dynamics in DNA. Commun. Nonlinear. Sci. Numer. Simul. **16**(8), 2963–2969 (2011)
12. Machado, J.T.: Analysis and design of fractional order digital control systems. Syst. Anal. Model. Simul. **27**(2–3), 107–122 (1997)
13. Dauer, J.P., Gahl, R.D.: Controllability of nonlinear delay systems. J. Optim. Theory Appl. **21**(1), 59–68 (1977)
14. Balachandran, K., Dauer, J.P.: Controllability of perturbed nonlinear delay systems. IEEE Trans. Autom. Control **32**, 172–174 (1987)
15. Balachandran, K., Kokila, J., Trujillo, J.J.: Relative controllability of fractional dynamical systems with multiple delays in control. Comput. Math. Appl. **64**(10), 3037–3045 (2012)
16. Balachandran, K., Zhou, Y., Kokila, J.: Relative controllability of fractional dynamical systems with delays in control. Commun. Nonlinear Sci. Numer. Simul. **17**(9), 3508–3520 (2012)
17. Balachandran, K., Zhou, Y., Kokila, J.: Relative controllability of fractional dynamical systems with distributive delays in control. Comput. Math. Appl. **64**(10), 3201–3209 (2012)
18. Klamka, J.: Controllability of linear systems with time variable delay in control. Int. J. Control **24**(6), 869–878 (1976)
19. Klamka, J.: Relative controllability of nonlinear systems with delay in control. Automatica **12**(6), 633–634 (1976)
20. Manzanilla, R., Marmol, L.G., Vanegas, C.J.: On the controllability of differential equation with delayed and advanced arguments. Abstr. Appl. Anal. (2010)
21. Mur, T., Henriquez, H.R.: Relative controllability of linear systems of fractional order with delay. Math. Control Relat. Fields **5**(4), 845–858 (2015)
22. Joice Nirmala, R., Balachandran, K.: Controllability of nonlinear fractional delay integrodifferential systems. J. Appl. Nonlinear Dyn. **5**, 59–73 (2016)
23. Joice Nirmala, R., Balachandran, K., Germa, L.R., Trujillo, J.J.: Controllability of nonlinear fractional delay dynamical systems. Rep. Math. Phys. **77**(1), 87–104 (2016)
24. Kilbas, A., Srivastava, H.M., Trujillo, J.J.: Theory and Application of Fractional Differential Equations. Elsevier, Amstrdam (2006)
25. Podlubny, I.: Fractional Differential Equations. Academic, New York (1999)
26. Granas, A., Dugundji, J.: Fixed Point Theory. Springer, New York (2003)
27. Balachandran, K.: Global relative controllability of non-linear systems with time-varying multiple delays in control. Int. J. Control. **46**(1), 193–200 (1987)
28. Dauer, J.P.: Nonlinear perturbations of quasi-linear control systems. J. Math. Anal. Appl. **54**(3), 717–725 (1976)

Stability Analysis for the New Model of Fractional Discrete-Time Linear State-Space Systems

Andrzej Ruszewski

Abstract In the paper the problem of asymptotic stability of fractional discrete-time linear systems described by the new model are addressed. Necessary and sufficient conditions for asymptotic stability are established. It is shown that location of all eigenvalues of the state matrix in the stability region is necessary and sufficient for asymptotic stability. The parametric description of boundary of this region is given. The considerations are illustrated by numerical examples.

Keywords Linear system · Discrete-time · Fractional-order · Asymptotic stability

1 Introduction

The fractional calculus and its application in many areas in science and engineering have been recently investigated. Fractional differentiation is used in modelling many physical phenomena. A variety of fractional models can be found in various fields (e.g. diffusion, fluid flow, turbulence, viscoelasticity and polymer physics). The state of the art of fractional systems and the application of fractional differentiation has been presented in monographs and papers (see, e.g. [15, 16, 18, 19, 22, 24]).

The fundamental matter in the dynamical systems theory is the stability problem. In the case of linear continuous-time fractional systems this problem has been considered in many publications (see, e.g. [3, 5, 6, 15, 18, 21]). The condition for asymptotic stability and the stability regions in the complex plane of fractional discrete-time systems has been derived in [8, 20, 25]. The conditions for practical stability of fractional discrete-time systems with a given length of practical implementation has been considered in [4, 7, 14, 15] for positive systems and in [4, 11] for non-positive (standard) systems. The robust asymptotic stability of the fractional

A. Ruszewski (✉)
Faculty of Electrical Engineering, Bialystok University of Technology,
Wiejska 45D, 15-351 Białystok, Poland
e-mail: a.ruszewski@pb.edu.pl

A. Babiarz et al. (eds.), *Theory and Applications of Non-integer Order Systems*,
Lecture Notes in Electrical Engineering 407, DOI 10.1007/978-3-319-45474-0_34

continuous-time interval systems has been presented in [1, 10, 17], for the fractional discrete-time interval systems this problem has been analyzed in [2] for positive systems and in [9, 23] for standard systems.

Two fractional order discrete-time state-space models of linear system have been analyzed in the paper [13]. The new model has been introduced and solution of this model has been presented. In this paper the asymptotic stability problem of the new model will be investigated. New necessary and sufficient condition for asymptotic stability will be proposed.

2 Problem Formulation

In the paper [13] was analysed the new model of the of fractional discrete-time linear systems. The state equations of this model has the form

$$\begin{aligned} &\Delta^{\alpha} x(k) = Ax(k) + Bu(k), \quad k = \{0, 1, ...\}, \quad \alpha \in (0,\ 1), \\ &y(k) = Cx(k) + Du(k) \end{aligned} \tag{1}$$

with the initial condition $x(0)$, where $x(k) \in \Re^n$, $u(k) \in \Re^m$, $y(k) \in \Re^p$ are the state, input and output vectors, $A \in \Re^{n \times n}$, $B \in \Re^{n \times m}$, $C \in \Re^{p \times n}$, $D \in \Re^{p \times m}$.

The second model was considered in [13] is better known and more developed. The state equation of this model has the form

$$\Delta^{\alpha} x(k+1) = Ax(k) + Bu(k). \tag{2}$$

The stability conditions of the model (2) was derived in [8, 20, 25].

The following Grünwald-Letnikov fractional difference of $x(k)$ [19] is used

$$\Delta^{\alpha} x(k) = \sum_{l=0}^{k} c_l(\alpha) x(k-l) \tag{3}$$

where $\alpha \in \Re$ is the order of the fractional difference and

$$c_l(\alpha) = \begin{cases} 0 & for\ l < 0 \\ 1 & for\ l = 0 \\ (-1)^l \frac{\alpha(\alpha-1)...(\alpha-l+1)}{l!} & for\ l > 0 \end{cases}$$

The fractional-order discrete transfer functions with zero initial conditions of system (1) has the form [13]

$$G(z) = C[(1 - z^{-1})^{\alpha} I - A]^{-1} B + D. \tag{4}$$

It follows that the characteristic equation of the system (1) has the form

$$w(z) = \det\{(1 - z^{-1})^{\alpha} I - A\}. \tag{5}$$

From the theory of asymptotic stability of discrete-time linear system we have the following definition.

Definition 1 The system (1) is called asymptotically stable if

$$\lim_{k \to \infty} x(k) = 0 \quad \text{for all} \quad x(0) \in \Re^n \quad \text{and} \quad B = 0. \tag{6}$$

The aim of the paper is to give the new necessary and sufficient conditions for asymptotic stability of the fractional system (1). The conditions will be given in terms of eigenvalues of the state matrix A.

3 Solution of the Problem

The characteristic equation $w(z) = 0$ can be written in the form

$$\prod_{i=1}^{n} w_i(z) = 0, \tag{7}$$

where

$$w_i(z) = (1 - z^{-1})^{\alpha} - \lambda_i(A) \tag{8}$$

and $\lambda_i(A)$ denotes i-th eigenvalue of A $(i = 1, 2, \ldots, n)$.

The fractional system (1) is asymptotically stable if and only if all roots of all equations $w_i(z) = 0$ $(i = 1, 2, \ldots, n)$ are stable, i.e. have absolute values less than 1. Therefore, first we consider the problem of stability of roots of the equation

$$(1 - z^{-1})^{\alpha} - \eta = 0 \tag{9}$$

in dependence of $\eta = \lambda_i(A)$.

According to the D-decomposition method [12], the boundary of stability region in the complex η-plane can be determined. Substituting $z = \exp(j\omega)$, $\omega \in [0,\ 2\pi]$ (boundary of the unit circle in the complex z-plane) in Eq. (9) we obtain the parametric description of boundary of stability region in the complex η-plane of the form

$$\eta(\omega) = (1 - e^{-j\omega})^{\alpha}, \quad \omega \in [0,\ 2\pi]. \tag{10}$$

The closed curve (10) divide the complex η-plane into two regions – bounded and unbounded. The boundaries of the stability region for $\alpha = 0.1$, $\alpha = 0.5$ and $\alpha = 0.9$ on the plane of eigenvalues of A are shown in Fig. 1. It is easy to check that (10) for $\alpha = 1$ describes the circle with centre at point (1, 0) and radius 1.

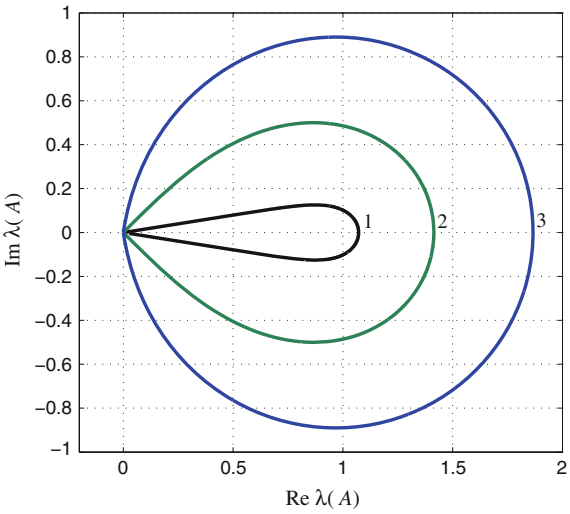

Fig. 1 The boundaries of the stability region of system (1) for $\alpha = 0.1$ (*boundary 1*), $\alpha = 0.5$ (*boundary 2*) and $\alpha = 0.9$ (*boundary 3*)

According to the D-decomposition method for the determination which region is the stability region it is sufficient to show that the system (1) is stable for at least one point in the stability region. The asymptotic stability region is chosen by testing arbitrary points from each region and checking the condition (6).

Let us consider two systems (1) with matrices

$$A = \begin{bmatrix} 1 & -0.24 \\ 1 & 0 \end{bmatrix}, \quad B = \begin{bmatrix} 0 \\ 0 \end{bmatrix} \tag{11}$$

and

$$A = \begin{bmatrix} -1 & -0.24 \\ 1 & 0 \end{bmatrix}, \quad B = \begin{bmatrix} 0 \\ 0 \end{bmatrix}. \tag{12}$$

The matrix A of the system (11) has two eigenvalues $z_1 = 0.4$ and $z_2 = 0.6$ which lie in the bounded region for $\alpha = 0.5$, whereas the system matrix (12) has two eigenvalues $z_1 = -0.4$ and $z_2 = -0.6$ which lie in the unbounded region for all α. The solutions of the system (11) and (12) for initial condition $x(0) = [1 \;\; 0.5]^T$ can be computed [13] and they are shown in Fig. 2a, b, respectively. From Definition 1 and Fig. 2 it follows that the system (1), (11) is not asymptotically stable, while the system (1), (12) is asymptotically stable. Thus, the unbounded region for given α (see Fig. 1) is the stability region of the system (1). This region will be denoted by $S(\alpha)$.

From the above we have the following theorem.

Theorem 1 *The fractional system (1) is asymptotically stable if and only if all eigenvalues* $\lambda_i(A)$ $(i = 1, 2, \ldots, n)$ *are located in the stability region* $S(\alpha)$, *i.e.* $\lambda_i(A) \in S(\alpha)$ *for all* $i = 1, 2, \ldots, n$.

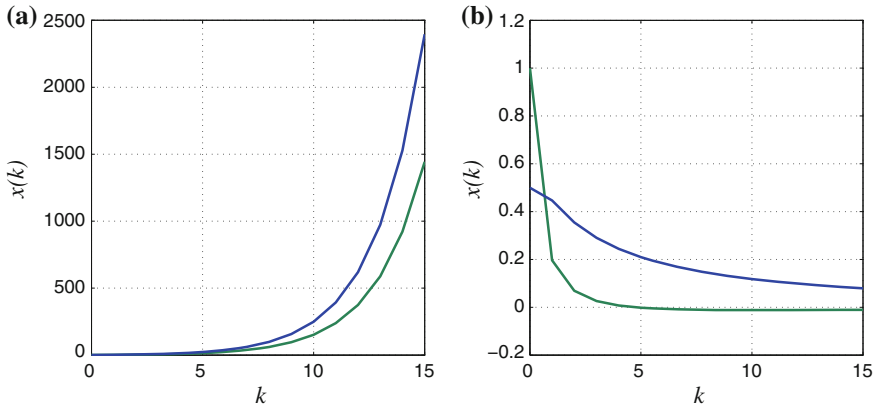

Fig. 2 State vectors for $\alpha = 0.5$; **a** the system (1), (11), **b** the system (1), (12)

From Theorem 1 and Fig. 1 we have the following important remarks.

Remark 1 If the state matrix A has all eigenvalue with negative real part, then the fractional system (1) is asymptotically stable for all $\alpha \in (0,\ 1)$.

Remark 2 If the state matrix A has at least one real eigenvalue $\lambda_i(A) \in (0, 1)$, then the fractional system (1) is not asymptotically stable for all $\alpha \in (0,\ 1)$.

Remark 3 Schur stability of the state matrix A (all eigenvalues have absolute values lees than 1) is neither necessary nor sufficient for asymptotic stability of the fractional system (1).

For $\omega = 0$ and $\omega = \pi$ from (10) we obtain

$$\eta(0) = 0, \tag{13}$$

$$\eta(\pi) = 2^{\alpha}. \tag{14}$$

It is easy to see that $\eta(0) < \eta(\pi)$ and the intervals $(-\infty,\ \eta(0))$ and $(\eta(\pi),\ +\infty)$ of the real axis lies in the stability region $S(\alpha)$ for any fixed $\alpha \in (0,\ 1)$.

Lemma 1 *If all eigenvalues $\lambda_i(A)$ are real, then the fractional system (1) is asymptotically stable if and only if*

$$\lambda_i(A) < 0 \quad or \quad \lambda_i(A) > 2^{\alpha}, \quad i = 1, 2, \ldots, n. \tag{15}$$

From Fig. 1 and Lemma 1 it follows that for any fixed $\alpha \in (0,\ 1)$ there exists a circle $D_1 = D_1(\eta_0, r_1)$ with the centre $\eta_0 = 1$ and radius $r_1 = 1 - 2^{\alpha}$, which entirely lies in the bounded region. If, for example, $\alpha = 0.5$ then $r_1 = 0.4142$. The boundary of the stability region of system (1) with $\alpha = 0.5$ and circle D_1 are shown in Fig. 3.

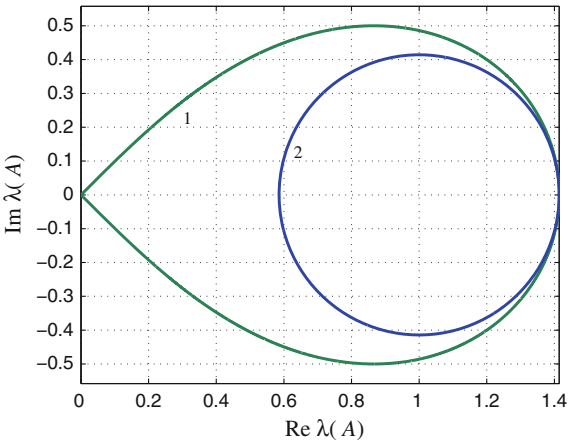

Fig. 3 The boundary of the stability region of system (1) for $\alpha = 0.5$ (*boundary 1*) and circle D_1 (*boundary 2*)

From the above we have the following condition for asymptotic stability, which is easy to apply.

Lemma 2 *The fractional system (1) is not asymptotically stable if all eigenvalues of A are located in circle* $D_1 = D_1(\eta_0, r_1)$, *where* $\eta_0 = 1$ *and* $r_1 = 1 - 2^{\alpha}$.

4 Illustrative Examples

Example 1 Check asymptotic stability of the fractional system (1) with $\alpha = 0.4$ and the state matrix

$$A = \begin{bmatrix} 4 & -6.03 & 4.054 & -1.025 \\ 1 & 0 & 0 & 0 \\ 0 & 1 & 0 & 0 \\ 0 & 0 & 1 & 0 \end{bmatrix}. \tag{16}$$

The matrix A has the following eigenvalues:

$$\lambda_{1,2} = 1.1 \pm j0.2; \quad \lambda_{3,4} = 0.9 \pm j0.1. \tag{17}$$

Circle $D_1 = D_1(1, r_1)$ has radius $r_1 = 1 - 2^{\alpha} = 0.3195$. The boundary of the stability region of system (1) for $\alpha = 0.4$, eigenvalues (17) and circle D_1 are shown in Fig. 4.

From Fig. 4 it follows that eigenvalues (17) lie in the bounded region and circle D_1, therefore the system (1), (16) is not asymptotically stable.

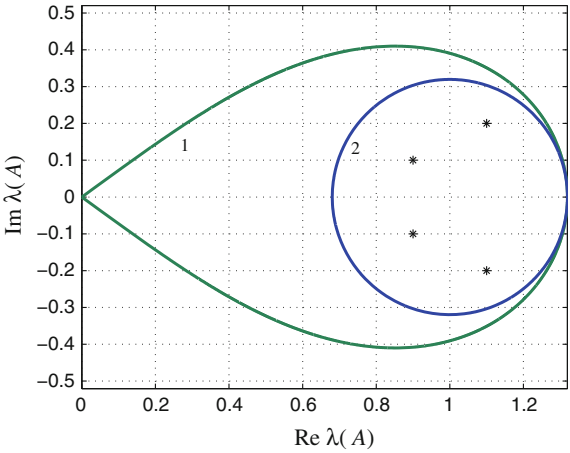

Fig. 4 The boundary of the stability region of system (1) for $\alpha = 0.4$ (*boundary 1*), eigenvalues (17) (*), and circle D_1 (*boundary 2*)

Example 2 Check asymptotic stability of the fractional system (1) with $\alpha = 0.5$ and the state matrix

$$A = \begin{bmatrix} -1.1 & -0.39 & 0.005 & 0.025 \\ 1 & 0 & 0 & 0 \\ 0 & 1 & 0 & 0 \\ 0 & 0 & 1 & 0 \end{bmatrix}. \tag{18}$$

The matrix A has the following eigenvalues:

$$\lambda_1 = -0.5; \quad \lambda_2 = 0.2; \quad \lambda_{3,4} = -0.4 \pm j0.3. \tag{19}$$

From Remark 2 we have that the fractional system (1) with the matrix (18) is not asymptotically stable for any $\alpha \in (0,\ 1)$, because has one real eigenvalue belongs to the interval $(0,\ 1)$. Hence, the system is not asymptotically stable for $\alpha = 0.5$ and for all α.

Note, that the matrix (18) is Schur stable but the system (1), (18) is not asymptotically stable for any $\alpha \in (0,\ 1)$.

5 Concluding Remarks

The asymptotic stability of discrete-time linear system (1) of fractional order $\alpha \in (0,\ 1)$ have been analysed. Necessary and sufficient conditions of asymptotic stability have been established. It is shown that location of all eigenvalues of the state matrix A in the stability region is necessary and sufficient for asymptotic stability. The parametric description of boundary of this region on the plane of eigenvalues of

A has the form (10). Moreover, it has been shown that Schur stability of the state matrix A is neither necessary nor sufficient for asymptotic stability of the fractional system (1).

Acknowledgments This work was supported by the National Science Centre in Poland under the work No. 2014/13/B/ST7/03467.

References

1. Ahn, H.-S., Chen, Y.Q.: Necessary and sufficient stability condition of fractional-order interval linear systems. Automatica **44**(11), 2985–2988 (2008)
2. Busłowicz, M.: Robust stability of positive discrete-time linear systems of fractional order. Bull. Pol. Acad. Tech. **58**(4), 567–572 (2010)
3. Busłowicz, M.: Stability of state-space models of linear continuous-time fractional order systems. Acta Mech. Autom. **5**(2), 15–22 (2011)
4. Busłowicz, M.: Simple analytic conditions for stability of fractional discrete-time linear systems with diagonal state matrix. Bull. Pol. Acad. Tech. **60**(4), 809–814 (2012)
5. Busłowicz, M.: Stability analysis of continuous-time linear systems consisting of n subsystems with different fractional orders. Bull. Pol. Acad. Tech. **60**(2), 279–284 (2012)
6. Busłowicz, M.: Stability conditions for linear continuous-time fractional-order state-delayed systems. Bull. Pol. Acad. Tech. **64**(2), 3–7 (2016)
7. Busłowicz, M., Kaczorek, T.: Simple conditions for practical stability of linear positive fractional discrete-time linear systems. Int. J. Appl. Math. Comput. Sci. **19**(2), 263–269 (2009)
8. Busłowicz, M., Ruszewski, A.: Necessary and sufficient conditions for stability of fractional discrete-time linear state-space systems. Bull. Pol. Acad. Tech. **61**(4), 779–786 (2013)
9. Busłowicz, M., Ruszewski, A.: Robust stability check of fractional discrete-time linear systems with interval uncertainties. In: Latawiec, K.J., et al. (eds.) Advances in Modeling and Control of Non-integer Order Systems. Lecture Notes in Electrical Engineering, vol. 320, pp. 199–208. Springer, Switzerland (2014)
10. Chen, Y.Q., Ahn, H.-S., Podlubny, I.: Robust stability check of fractional order linear time invariant systems with interval uncertainties. Signal Process. **86**(10), 2611–2618 (2006)
11. Dzieliński, A., Sierociuk, D.: Stability of discrete fractional state-space systems. J. Vib. Control **14**(9–10), 1543–1556 (2008)
12. Gryazina, E.N., Polyak, B.T., Tremba, A.A.: D-decomposition technique state-of-the-art. Autom. Remote Control **69**(13), 1991–2026 (2008)
13. Kaczorek, T., Ostalczyk, P.: Responses comparison of the two discrete-time linear fractional state-space models. Int. J. Control (2016, in press)
14. Kaczorek, T.: Practical stability of positive fractional discrete-time systems. Bull. Pol. Acad. Tech. **56**(4), 313–317 (2008)
15. Kaczorek, T.: Selected Problems of Fractional Systems Theory. Springer, Berlin (2011)
16. Kilbas, A.A., Srivastava, H.M., Trujillo, J.J.: Theory and Applications of Fractional Differential Equations. Elsevier, Amsterdam (2006)
17. Liao, Z., Peng, C., Li, W., Wang, Y.: Robust stability analysis for a class of fractional order systems with uncertain parameters. J. Franklin Inst. **348**(6), 1101–1113 (2011)
18. Monje, C., Chen, Y., Vinagre, B., Xue, D., Feliu, V.: Fractional-Order Systems and Controls. Springer, London (2010)
19. Ostalczyk, P.: Epitome of the Fractional Calculus. Publishing Department of Technical University of Łódź, Łódź, Theory and Its Applications in Automatics (2008) (in Polish)
20. Ostalczyk, P.: Equivalent descriptions of a discrete-time fractional-order linear system and its stability domains. Int. J. Appl. Math. Comput. Sci. **22**(3), 533–538 (2012)

21. Petras, I.: Stability of fractional-order systems with rational orders: a survey. Fract. Calc. Appl. Anal. **12**(3), 269–298 (2009)
22. Podlubny, I.: Fractional Differential Equations. Academic, San Diego (1999)
23. Ruszewski, R.: Practical stability and asymptotic stability of interval fractional discrete-time linear state-space system. In: Szewczyk, R., et al. (eds.) Recent Advances in Automation, Robotics and Measuring Techniques. Advances in Intelligent Systems and Computing, vol. 267, pp. 217–227. Springer, Switzerland (2014)
24. Sabatier, J., Agrawal, O.P., Machado, J.A.T. (eds.): Advances in Fractional Calculus: Theoretical Developments and Applications in Physics and Engineering. Springer, London (2007)
25. Stanisławski, R., Latawiec, K.J.: Stability analysis for discrete-time fractional-order LTI state-space systems. Part I: new necessary and sufficient conditions for asymptotic stability. Bull. Pol. Acad. Tech. **61**(2), 353–361 (2013)

Fractional Differential-Algebraic Systems with Delay: Computation of Final Dimension Initial Conditions and Inputs for Given Outputs

Zbigniew Zaczkiewicz

Abstract The paper presents the problems of computation of the initial data of finite dimension and inputs for given outputs of linear stationary fractional differential-algebraic with delay system (FDAD). Necessary and sufficient conditions for existence of solution to the problem are established. Relatively observability of FDAD system is formulated and proved. It is shown that there exist the unique solutions to the problem if FDAD system is relatively observable.

Keywords Fractional differential equations · Differential-algebraic systems · Observability

1 Introduction

Differential equations involving differential operators of fractional (non-integer) order have been proved to be a valuable tool in modeling many phenomena in the fields of physics, chemistry, engineering and others (see, for example, [1–3]). Mathematical aspects of fractional differential equations and methods of their solution were discussed by many authors (see, for example, [4–6] and references cited therein).

Observability for fractional linear system has been proposed in [7–11]. It should be pointed out, that the most observability results are known from theoretical approach. In this paper the problem of computation of initial final conditions and inputs for given outputs of fractional differential-algebraic systems with delay will be formulated and solved. Necessary and sufficient conditions for existence of solutions to the problem will be established. Similar results can be found for fractional continuous [12] and discrete-time [13] systems.

The paper is organized as follows. In Sect. 2 the state equations of FDAD systems and the representation of solutions into series of determining equations solutions are presented. Relative observability and formulation of the problem are introduced in

Z. Zaczkiewicz (✉)
Faculty of Computer Science, Bialystok University of Technology,
15-351 Bialystok, Poland
e-mail: z.zaczkiewicz@pb.edu.pl

A. Babiarz et al. (eds.), *Theory and Applications of Non-integer Order Systems*,
Lecture Notes in Electrical Engineering 407, DOI 10.1007/978-3-319-45474-0_35

Sect. 3. Necessary and sufficient conditions for existence of solutions to the problem are given in Sect. 4. Finally, Sect. 4 contains an example.

2 Preliminaries

Let us introduce the following notation:

${}^{C}D_t^{\alpha}$ is the left-sided Caputo fractional derivatives of order α defined by

$$ {}^{C}D_t^{\alpha} f(t) = \frac{1}{\Gamma(1-\alpha)} \int_0^t \frac{\left(\frac{d}{d\tau} f(\tau)\right)}{(t-\tau)^{\alpha}} d\tau, $$

where $0 < \alpha < 1$, $\alpha \in \mathbb{R}$ and $\Gamma(t) = \int_0^{\infty} e^{-\tau} \tau^{t-1} d\tau$ is the Euler gamma function (see [5] for more details). $T_t = \lim_{\epsilon \to +0} \left[\frac{t-\epsilon}{h}\right]$, where the symbol $[z]$ means entire part of the number z; I_n is the identity n by n matrix.

In this paper, we concentrate on the stationary FDAD system in the form:

$$ \left({}^{C}D_t^{\alpha} x_1\right)(t) = A_{11} x_1(t) + A_{12} x_2(t) + B_1 u(t), \ t > 0, \tag{1a} $$

$$ x_2(t) = A_{21} x_1(t) + A_{22} x_2(t-h) + B_2 u(t), \ t \geq 0, \tag{1b} $$

$$ y(t) = C_1 x_1(t) + C_2 x_2(t) + C_3 u(t), \tag{1c} $$

where $x_1(\cdot) \in \mathbb{R}^{n_1}$, $x_2(\cdot) \in \mathbb{R}^{n_2}$, $u(\cdot) \in \mathbb{R}^{r}$, $y(\cdot) \in \mathbb{R}^{m}$, $A_{11} \in \mathbb{R}^{n_1 \times n_1}$, $A_{12} \in \mathbb{R}^{n_1 \times n_2}$, $A_{21} \in \mathbb{R}^{n_2 \times n_1}$, $A_{22} \in \mathbb{R}^{n_2 \times n_2}$, $B_1 \in \mathbb{R}^{n_1 \times r}$, $B_2 \in \mathbb{R}^{n_1 \times r}$, $C_1 \in \mathbb{R}^{m \times n_1}$, $C_2 \in \mathbb{R}^{m \times n_2}$, $C_3 \in \mathbb{R}^{m \times r}$, are constant (real) matrices, $0 < h$ is a constant delay.

Control and Observation system (1) should be completed with initial conditions:

$$ x_1(+0) = x_0 \in \mathbb{R}^{n_1}, \left[\left({}^{C}D_t^{\alpha-1} x_1\right)(t)\right]_{t=0} = x_0, \ x_2(\tau) = \psi(\tau), \ \tau \in [-h, 0), \tag{2} $$

where $x_0 \in \mathbb{R}^{n_1}$; $\psi \in PC([-h, 0), \mathbb{R}^{n_2})$ and $PC([-h, 0), \mathbb{R}^{n_2})$ denotes the set of piecewise continuous n_2-vector-functions in $[-h, 0]$. Observe that $x_2(t)$ at $t = 0$ is determined from the Eq. (1b).

Definition 1 The solution $x_1(t) = x_1(t; x_0, \psi, u)$, $x_2(t) = x_2(t; x_0, \psi, u)$, to Control and Observation system (1) corresponding to initial condition (2) and an admissible control $u = u(t)$, $t \geq 0$, is a pair of arbitrary vector functions $x_1(t)$ and $x_2(t)$, $t \geq 0$ satisfying the Eq. (1a) for almost all $t > 0$ and (1b) for all $t \geq 0$ under the assumption that $x_1(\cdot)$ is a continuous piecewise-smooth vector function and $x_2(\cdot)$ is piecewise continuous on the interval $[0, +\infty)$. Let $y(t) = y(t; x_0, \psi, u)$ and $\tilde{y}(t) = y(t; \tilde{x}_0, \psi, u)$ denote the outputs corresponding to the solutions $x_1(t) = x_1(t; x_0, \psi, u)$, $x_2(t) = x_2(t; x_0, \psi, u)$ and $\tilde{x}_1(t) = \tilde{x}_1(t; \tilde{x}_0, \psi, u)$, $\tilde{x}_2(t) = \tilde{x}_2(t; \tilde{x}_0, \psi, u)$ respectively.

2.1 Representation of Solutions into Series of Determining Equations Solutions

Let us introduce the determining equations of Control and Observation system (1) (see [14] for more details).

$$\begin{aligned} &X_{1,k}(t) = A_{11}X_{1,k-1}(t) + A_{12}X_{2,k-1}(t) + B_1U_{k-1}(t), \\ &X_{2,k}(t) = A_{21}X_{1,k}(t) + A_{22}X_{2,k}(t-h) + B_2U_k(t),\ k = 0, 1, \ldots; \\ &\text{with initial conditions} \\ &X_{1,k}(t) = 0, X_{2,k}(t) = 0,\ Y_k(t) = 0 \text{ for } t < 0 \text{ or } k \le 0; \\ &U_0(0) = I_{n_1},\ U_k(t) = 0 \text{ for } t^2 + k^2 \neq 0. \end{aligned} \tag{3}$$

Let us introduce the determining equations of homogenous Control and Observation system (1).

$$\begin{aligned} &\widetilde{X}_{1,k}(t) = A_{11}\widetilde{X}_{1,k-1}(t) + A_{12}\widetilde{X}_{2,k-1}(t) + U_{k-1}(t), \\ &\widetilde{X}_{2,k}(t) = A_{21}\widetilde{X}_{1,k}(t) + A_{22}\widetilde{X}_{2,k}(t-h), \\ &Y_k(t) = C_1X_{1,k}(t) + C_2X_{2,k}(t),\ t \ge 0,\ k = 1, 2, \ldots; \end{aligned} \tag{4}$$

with initial conditions

$$\begin{aligned} &\widetilde{X}_{1,k}(t) = 0, \widetilde{X}_{2,k}(t) = 0 \text{ for } t < 0 \text{ or } k \le 0; \\ &U_0(0) = I_{n_1},\ U_k(t) = 0 \text{ for } t^2 + k^2 \neq 0. \end{aligned}$$

Applying the solutions of systems (3), (4) and Laplace transform we can obtain [15]:

Theorem 1 *A solution to Control and Observation system (1) with finite initial conditions (2) for $t \ge 0$ exists, is unique and can be represented in the form of a series in power of solutions to determining systems (3) and (4), in the following form:*

$$\begin{aligned} x_1(t, x_{10}, \psi) = &\sum_{k=0}^{+\infty} \sum_{\substack{i \\ t-ih>0}} X_{1,k+1}(ih) \int_0^{t-ih} \frac{(t-\tau-ih)^{\alpha k}}{\Gamma(\alpha(k+1))} u(\tau)d\tau \\ &+ \sum_{k=0}^{+\infty} \sum_{\substack{j \\ t-jh>0}} \frac{(t-jh)^{\alpha k}}{\Gamma(\alpha k+1)} \widetilde{X}_{1,k+1}(jh)x_{10} \\ &+ \sum_{k=0}^{+\infty} \sum_{\substack{i,j \\ t-(i+j)h>0}} \widetilde{X}_{1,k+1}(ih)A_{12}(A_{22})^{i+1} \int_0^{t-(i+j)h} \frac{(t-\tau-(i+j)h)^{\alpha(k+1)-1}}{\Gamma(\alpha(k+1))} \psi(\tau-h)d\tau, \end{aligned} \tag{5a}$$

$$x_2(t,x_{10},\psi)=\sum_{k=0}^{+\infty}\sum_{\substack{i\\ t-ih>0}}X_{2,k+1}(ih)\int_0^{t-ih}\frac{(t-\tau-ih)^{\alpha k}}{\Gamma(\alpha(k+1))}u(\tau)d\tau+$$

$$+\sum_{\substack{i\\ t-ih>0}}X_{2,0}(ih)u(t-ih) \tag{5b}$$

$$+\sum_{k=0}^{+\infty}\sum_{\substack{j\\ t-jh>0}}\frac{(t-jh)^{\alpha k}}{\Gamma(\alpha k+1)}\widetilde{X}_{2,k+1}(jh)x_{10}+\sum_{i=0}^{+\infty}(A_{22})^{i+1}\psi(t-(i+1)h))$$

$$+\sum_{k=0}^{+\infty}\sum_{\substack{i,j\\ t-(i+j)h>0}}\widetilde{X}_{2,k+1}(ih)A_{12}(A_{22})^{i+1}\int_0^{t-(i+j)h}\frac{(t-\tau-(i+j)h)^{\alpha(k+1)-1}}{\Gamma(\alpha(k+1))}\psi(\tau-h)d\tau,$$

where $\psi(\tau)\equiv 0$ *for* $\tau\notin[-h,0)$.

3 Relative Observability and Problem Formulation

Here, by [16] we establish some algebraic properties of $Y_k(t)$.

Proposition 1 *The solutions* $Y_k(t)$, $t\geq 0$, *of the determining equation (4) satisfy the condition*

$$Y_k(lh)=-\sum_{j=1}^{\Theta_l}r_{0j}Y_k((l-j)h)-\sum_{i=0}^{n_1}\sum_{j=0}^{\Theta_l}r_{ij}Y_{k-i}((l-j)h)$$

for $l=0,1,\ldots$, *where* $\Theta_l=\min\{l,n_1n_2\}$ *and* $k=n_1+1,n_1+2,\ldots$.

Proposition 2 *Solutions* $Y_k(lh)$, $k\geq 1, l\geq 0$, *of determining equation (4) satisfy the following conditions:*

$$Y_k(lh)=-\sum_{j=1}^{\widetilde{\theta}_k}p_{0j}Y_{k-j}(lh)-\sum_{i=1}^{n_2}\sum_{j=0}^{\widetilde{\theta}_k}p_{ij}Y_{k-j}((l..i)h),$$

where $k=1,2,\ldots,l=n_2+1,n_2+2,\ldots$, *and* $\widetilde{\theta}_k=\min\{k-1,n_1(n_2)^2\}$.

Now we introduce two definition that will be applied to the problem of computation of relative initial conditions and inputs for given outputs.

Definition 2 Control and Observation system (1) is said to be $\mathbb{R}^n$-observable with respect to x_1 if for every $x_{10},\tilde{x}_{10}\in\mathbb{R}^{n_1}$, the condition $y(t;x_{10},\psi,u)\equiv\tilde{y}(t;\tilde{x}_{10},\psi,u)$; for every $\psi\in PC([-h;0);\mathbb{R}^{n_2})$, $u\in PC([0;+\infty);\mathbb{R}^r)$ and for $t\geq 0$ implies that $x_{10}=\tilde{x}_{10}$.

Definition 3 Control and Observation system (1) is said to be $\mathbb{R}^n$-observable with respect to x_1 on $[0; T]$ if for every $x_{10}, \tilde{x}_{10} \in \mathbb{R}^{n_1}$, the condition $y(t; x_{10}, \psi, u) \equiv \tilde{y}(t; \tilde{x}_{10}, \psi, u)$; for every $\psi \in PC([-h; 0); \mathbb{R}^{n_2})$, $u \in PC([0; +\infty); \mathbb{R}^r)$ and for $t \in [0; T]$ implies that $x_{10} = \tilde{x}_{10}$.

For the sequel, we need the following result:

Proposition 3 [17] *Functions* $f_{kj}(t) = \frac{(t-jh)^{\alpha k}}{\Gamma(\alpha k+1)}$ *for* $t - jh > 0$ *and* $f_{kj}(t) = 0$ *for* $t - jh \le 0$, *where* $k = 0, 1, \ldots; j = 0, 1, \ldots$, *are linearly independent for* $t > 0$.

Now we may formulate the observability result:

Theorem 2 *Control and Observation system (1) is* $\mathbb{R}^n$*-observable with respect to* x_1 *if and only if*

$$rank \begin{bmatrix} Y_{k+1}(lh), \\ k = 0, 1, \ldots, n_1; \ l = 0, 1, \ldots, n_2 \end{bmatrix} = n_1. \tag{6}$$

Proof By (5) and (1c), $y(t; x_{10}, \psi, u) \equiv \tilde{y}(t; \tilde{x}_{10}, \psi, u)$ is equivalent to the following:

$$\begin{aligned} & C_1 \sum_{k=0}^{+\infty} \sum_{\substack{j \\ t-jh>0}} \frac{(t-jh)^{\alpha(k+1)-1}}{\Gamma(\alpha k+1)} X_{1,k+1}(jh) x_{10} \\ & + C_2 \sum_{k=0}^{+\infty} \sum_{\substack{j \\ t-jh>0}} \frac{(t-jh)^{\alpha(k+1)-1}}{\Gamma(\alpha k+1)} X_{2,k+1}(ih) x_{10} \\ & = C_1 \sum_{k=0}^{+\infty} \sum_{\substack{j \\ t-jh>0}} \frac{(t-jh)^{\alpha(k+1)-1}}{\Gamma(\alpha k+1)} X_{1,k+1}(jh) \tilde{x}_{10} \\ & + C_2 \sum_{k=0}^{+\infty} \sum_{\substack{j \\ t-jh>0}} \frac{(t-jh)^{\alpha(k+1)-1}}{\Gamma(\alpha k+1)} X_{2,k+1}(ih) \tilde{x}_{10}. \end{aligned}$$

It follows from here that

$$\begin{aligned} & \sum_{k=0}^{+\infty} \sum_{\substack{j \\ t-jh>0}} \frac{(t-jh)^{\alpha(k+1)-1}}{\Gamma(\alpha k+1)} [C_1, C_2] \begin{bmatrix} X_{1,k+1}(jh) \\ X_{2,k+1}(jh) \end{bmatrix} (x_{10} - \tilde{x}_{10}) = \\ & \sum_{k=0}^{+\infty} \sum_{\substack{j \\ t-jh>0}} \frac{(t-jh)^{\alpha(k+1)-1}}{\Gamma(\alpha k+1)} Y_{k+1}(jh)(x_{10} - \tilde{x}_{10}) = 0. \end{aligned}$$

By Theorem 2, $\mathbb{R}^n$-observable with respect to x_1 is equivalent to

$$\left[\begin{array}{c} Y_{k+1}(lh), \\ k=0,1,\ldots;\ i=0,1,\ldots \end{array}\right](x_0^* - \tilde{x}_0^*) = 0 \ \Rightarrow\ (x_0^* - \tilde{x}_0^*) = 0.$$

Thus, we have

$$rank\left[\begin{array}{c} Y_{k+1}(lh), \\ k=0,1,\ldots;\ i=0,1,\ldots \end{array}\right] = n_1.$$

Taking into account Propositions 1 and 2, we may claim that the property of $\mathbb{R}^n$-observability with respect to x_1 is saturated and this completes the proof.

Corollary 1 *Control and Observation system (1) is $\mathbb{R}^n$-observable with respect to x_1 on $[0, T_{obs}]$ if and only if*

$$rank\left[\begin{array}{c} Y_{k+1}(lh), \\ k=0,1,\ldots,n_1;\ l=0,1,\ldots,\min\{n_2, T_{obs}\} \end{array}\right] = n_1. \tag{7}$$

The problem of computation of relative initial conditions and inputs for given outputs can be stated as follows:

Given the output vector $y(t) \in \mathbb{R}^m$ for $t \in [0; T_{obs}]$ (T_{obs} is given) of Control and Observation system (1). Compute the initial conditions $x_0 \in \mathbb{R}^{n_1}$, $\psi \equiv 0$ and the input vector

$$u(t) = u_0 + u_1 t^1 + \cdots + u_{n_1-1} t^{n_1-1} \in \mathbb{R}^r,\ t \geq 0 \tag{8}$$

of the system.

In this paper the solvability conditions of the problem will be established for fractional linear differential-algebraic systems with delay.

4 Problem Solution

Applying the solution representation (5) to (1c) we have

$$y(t) = \sum_{k=0}^{+\infty} \sum_{\substack{i,j \\ t-(i+j)h>0}} \left(C_1 \widetilde{X}_{1,k+1}(jh) + C_2 \widetilde{X}_{2,k+1}(jh)\right) A_{12}(A_{22})^{i+1}$$
$$\times \int_0^{t-(i+j)h} \frac{(t-(i+j)h-\tau)^{\alpha(k+1)-1}}{\Gamma(\alpha(k+1))} \psi(\tau - h)d\tau + \sum_{\substack{i=0 \\ t-ih>0}}^{l} C_2 X_{2,0}(ih) u(t-ih)$$

$$+\sum_{k=0}^{+\infty}\sum_{\substack{j\\ t-jh>0}}\frac{(t-jh)^{\alpha k}}{\Gamma(\alpha k+1)}\left(C_1\widetilde{X}_{1,k+1}(jh)+C_2\widetilde{X}_{2,k+1}(jh)\right)x_{10} \tag{9}$$

$$+\sum_{k=0}^{+\infty}\sum_{\substack{i\\ t-ih>0}}\left(C_1X_{1,k+1}(ih)+C_2X_{2,k+1}(ih)\right)\int_0^{t-ih}\frac{(t-ih-\tau)^{\alpha k+}}{\Gamma(\alpha(k+1))}u(\tau)d\tau$$

$$+\sum_{i=0}^{+\infty}C_2(A_{22})^{i+1}\psi(t-(i+1)h)+C_3u(t)$$

Combining (8) and (9) we obtain

$$y(t)=\Omega(t)x_0+F_0(t)u_0+\cdots+F_{n_1-1}(t)u_{n_1-1} \tag{10}$$

where

$$\Omega(t)=\sum_{k=0}^{+\infty}\sum_{\substack{j\\ t-jh>0}}\frac{(t-jh)^{\alpha k}}{\Gamma(\alpha k+1)}Y_{k+1}(jh),$$

$$F_\beta(t)=\sum_{\substack{i=0\\ t-ih>0}}^{l}C_2X_{2,0}(ih)(t-ih)^\beta+C_3t^\beta$$

$$+\sum_{k=0}^{+\infty}\sum_{\substack{i\\ t-ih>0}}\left(C_1X_{1,k+1}(ih)+C_2X_{2,k+1}(ih)\right)\int_0^{t-ih}\frac{(t-ih-\tau)^{\alpha k}}{\Gamma(\alpha(k+1))}\tau^\beta d\tau,$$

$$\alpha=0,\ldots,n_1-1.$$

For the given output vector $y(t)\in\mathbb{R}^m$ for $t\in[0;t_{obs}]$ we choose $t_1,t_2,\ldots,t_{n_1}$ and applying (10) we obtain

$$y=\Upsilon w \tag{11}$$

where

$$\Upsilon=\begin{bmatrix}\Omega(t_1) & F_0(t_1) & \cdots & F_{n_1-1}(t_1)\\ \Omega(t_2) & F_0(t_2) & \cdots & F_{n_1-1}(t_2)\\ \vdots & \vdots & \ddots & \vdots\\ \Omega(t_{n_1}) & F_0(t_{n_1}) & \cdots & F_{n_1-1}(t_{n_1})\end{bmatrix}$$

$$w = \begin{bmatrix} x_0 \\ u_0 \\ \vdots \\ u_{n_1-1} \end{bmatrix} \in \mathbb{R}^{(r+1)n_1}, \; y = \begin{bmatrix} y_1 \\ \vdots \\ y_{n_1} \end{bmatrix}$$

where

$$y_\gamma = y(t_\gamma), \; \Omega(t_\gamma) = \sum_{k=0}^{+\infty} \sum_{\substack{j \\ t_\gamma - jh > 0}} \frac{(t_\gamma - jh)^{\alpha k}}{\Gamma(\alpha k + 1)} Y_{k+1}(jh),$$

$$F_\beta(t_\gamma) = \sum_{\substack{i=0 \\ t_\gamma - ih > 0}}^{l} C_2 X_{2,0}(ih)(t_\gamma - ih)^\beta + C_3 t^\beta$$

$$+ \sum_{k=0}^{+\infty} \sum_{\substack{i \\ t_\gamma - ih > 0}} \left(C_1 X_{1,k+1}(ih) + C_2 X_{2,k+1}(ih) \right) \int_0^{t_\gamma - ih} \frac{(t_\gamma - ih - \tau)^{\alpha k}}{\Gamma(\alpha(k+1))} \tau^\beta d\tau,$$

$$\beta = 0, \ldots, n_1 - 1; \; \gamma = 1, \ldots, n_1.$$

Now we apply the well-knowing Kronecker–Cappelly Theorem [18] the Eq. (11) has a solution w for given Υ and y if and only if

$$\operatorname{rank} \begin{bmatrix} \Upsilon & y \end{bmatrix} = \operatorname{rank} \Upsilon.$$

Theorem 3 *The Eq. (11) for $r + 1 \geq m$ has the solution $w = \begin{bmatrix} x_0^T & u_0^T & \ldots & u_{n_1-1}^T \end{bmatrix}^T$ for any given sequence $y_1, y_2, \ldots, y_{n_1}$ if and only if*

$$rank \Upsilon = m \cdot n_1.$$

Moreover, the solution

$$w = \Upsilon^{-1} y$$

is unique if $r + 1 = m$ and the Eq. (11) has many solutions if $r + 1 > m$.

5 Example

Let us consider the following system:

$$D_t^\alpha x_1(t) = \begin{bmatrix} 0 & 1 \\ 0 & 0 \end{bmatrix} x_1(t) + \begin{bmatrix} 1 & 0 \\ 0 & 0 \end{bmatrix} x_2(t) + \begin{bmatrix} 0 \\ 1 \end{bmatrix} u(t), \; t > 0, \tag{12}$$

$$x_2(t) = \begin{bmatrix} 0 & 0 \\ 1 & 0 \end{bmatrix} x_1(t) + \begin{bmatrix} 0 & 0 \\ 1 & 0 \end{bmatrix} x_2(t-1) + \begin{bmatrix} 1 \\ 0 \end{bmatrix} u(t),\ t \geq 0.$$
$$y(t) = \begin{bmatrix} 1 & 1 \end{bmatrix} x_1(t) + \begin{bmatrix} 1 & 0 \end{bmatrix} x_2(t) + [0]u(t).$$

We put the initial conditions should be completed with final initial conditions:

$$x_0 = \begin{bmatrix} x_{01} \\ x_{02} \end{bmatrix}, \psi(\tau) = \begin{bmatrix} 0 \\ 0 \end{bmatrix},\ \tau \in [-h, 0),$$

and the input in the form (8)

$$u(t) = u_0 + u_1 t,$$

for the given output

$$y(t) = \begin{cases} -16t^2 + 3t,\ t \in [0; 1) \\ -12t,\ t \in [1; 2) \end{cases}$$

First we present the determining equations of System (12):

$$\begin{aligned} X_{1,k}(t) &= [1]X_{1,k-1}(t) + \begin{bmatrix} 0 & -1 \end{bmatrix} X_{2,k-1}(t) + U_{k-1}(t), \\ X_{2,k}(t) &= \begin{bmatrix} 0 \\ 1 \end{bmatrix} X_{1,k}(t) + \begin{bmatrix} 0 & 2 \\ 0 & 0 \end{bmatrix} X_{2,k}(t-1), \\ Y_k(t) &= \begin{bmatrix} 1 & 1 \end{bmatrix} X_{1,k}(t) + \begin{bmatrix} 1 & 0 \end{bmatrix} X_{2,k}(t), \end{aligned} \tag{13}$$

for $k = 0, 1, ...;\ t \geq 0$ with initial conditions

$$X_{1,k}(t) = 0, X_{2,k}(t) = 0,\ Y_k(t) = 0 \text{ for } t < 0 \text{ or } k \leq 0;$$
$$U_0(0) = I_2,\ U_k(t) = 0 \text{ for } t^2 + k^2 \neq 0.$$

Now we compute $Y_k(lh),\ k = 0, 1, 2;\ l = 0, 1, 2$ for the determining system (13) and substituting into (6) we obtain:

$$rank \begin{bmatrix} 1 & 1 \\ 0 & 0 \\ 0 & 0 \\ 0 & 1 \end{bmatrix} = 2.$$

Thus the system (12) is $\mathbb{R}^n$-observable with respect to x_1.

We choose $t_1 = \frac{1}{4},\ t_2 = \frac{5}{4}$ applying to (11) we have:

$$\begin{bmatrix} y_1 \\ y_2 \end{bmatrix} = \begin{bmatrix} \Omega(t_1)\ F_0(t_1)\ F_1(t_1) \\ \Omega(t_2)\ F_0(t_2)\ F_1(t_2) \end{bmatrix} \begin{bmatrix} x_{01} \\ x_{02} \\ u_0 \\ u_1 \end{bmatrix}, \tag{14}$$

$$\text{where } y_1 = -0.25,\ y_2 = -15,\ \Omega(t_1) = \begin{bmatrix} 1 \\ 1.78 \end{bmatrix},\ \Omega(t_2) = \begin{bmatrix} 1 \\ 2.17 \end{bmatrix},$$

$$F_0(t_1) = 1.22,\ F_0(t_2) = 2.29,\ F_1(t_1) = 0.28,\ F_1(t_2) = 2.01.$$

Then the matrix Υ takes the form:

$$\Upsilon = \begin{bmatrix} 1 & 1.78 & 1.22 & 0.28 \\ 1 & 2.17 & 2.29 & 2.01 \end{bmatrix}, \tag{15}$$

The matrix (15) has full row rank and the Eq. (11) has many solutions $x_0,\ u_0,\ u_1$ for any given $y_1,\ y_2$. Applying (15) to (14) we obtain for example

$$\begin{bmatrix} x_{02} \\ u_1 \end{bmatrix} = \begin{bmatrix} 0.68 & -0.09 \\ -0.73 & 0.6 \end{bmatrix} \begin{bmatrix} y_1 \\ y_2 \end{bmatrix} = \begin{bmatrix} 1.18 \\ -8.82 \end{bmatrix}, \text{ for } x_{01} = 0.06 \text{ and } u_0 = 0.05.$$

Theorem 4 *The Eq. (11) has the unique solution only if Control and Observation system (1) is $\mathbb{R}^n$-observable with respect to x_1 on $[0, T_{obs}]$.*

Proof By Theorem 3 the Eq. (11) has the unique solution if only if the matrix Υ has full column rank and this implies that the matrix (7) has full column rank. Thus the Eq. (11) has the unique solution only if Control and Observation system (1) is $\mathbb{R}^n$-observable with respect to x_1 on $[0, T_{obs}]$.

Remark 1 In this paper we presented FDAD systems within Caputo fractional derivatives. The obtained results can be extended to FDAD systems within Riemann–Liouville fractional derivatives (see [19] for the initial conditions problem for the fractional systems).

6 Conclusions

Relative observability with respect to x_1 for Fractional Control and Observation differential-algebraic systems with delay (FDAD) has been presented (Theorem 2). Necessary and sufficient conditions for existence of solution to the problem of computation of the initial data of finite dimension and inputs for given outputs for FDAD systems were established. These considerations will be extended to study the problem on constrained observability problem.

Acknowledgments The present study was supported by a grant S/WI/1/2016 from Bialystok University of Technology and founded from the resources for research by Ministry of Science and Higher Education..

References

1. Baleanu, D., Diethelm, K., Scalas, E., Trujillo, J.J.: Fractional Calculus. Models and Numerical Methods. World Scientific Publishing Co. Pte. Ltd., Singapore (2012)
2. Herrmann, R.: Fractional Calculus. An Introduction for Physicists. World Scientific Publishing Co. Pte. Ltd., Hackensack (2014)
3. Mainardi, F.: Fractional Calculus and Waves in Linear Viscoelasticity. Imperial College Press, London (2010)
4. Diethelm, K.: The Analysis of Fractional Differential Equations. Lecture Notes in Mathematics, vol. 2004. Springer, Berlin (2010)
5. Kilbas, A.A., Srivastava, H.M., Trujillo, J.J.: Theory and Applications of Fractional Differential Equations. North-Holland Mathematics Studies, vol. 204. Elsevier, Amsterdam (2006)
6. Podlubny, I.: Fractional Differential Equations. Academic Press, San Diego (1999)
7. Sajewski, L.: Reachability, observability and minimum energy control of fractional positive continuous-time linear systems with two different fractional orders. Multidimens. Syst. Signal Process. **27**(1), 27–41 (2016)
8. Mozyrska, D., Pawłuszewicz, E., Wyrwas, M.: The h-difference approach to controllability and observability of fractional linear systems with Caputo-type operator. Asian J. Control **17**(4), 1163–1173 (2015)
9. Qun, H., Xianfeng, Z.: Observability of singular fractional linear time-invariant differential systems. Math. Appl. (Wuhan) **27**(3), 581–587 (2014)
10. Tian, G.L.: Controllability and observability of impulsive fractional linear time-invariant system. Comput. Math. Appl. **64**(10), 3171–3182 (2012)
11. Guermah, S., Djennoune, S., Bettayeb, M.: Controllability and observability of linear discrete-time fractional-order systems. Int. J. Appl. Math. Comput. Sci. **18**(2), 213–222 (2008)
12. Kaczorek, T.: Computation of initial conditions and inputs for given outputs of fractional and positive continuous-time linear systems. In: Proceedings of the FSS'11, pp. 119–126 (2011)
13. Kaczorek, T.: Computation of initial conditions and inputs for given outputs of fractional and positive discrete-time linear systems. Arch. Contol Sci. **22**(2), 145–159 (2012)
14. Marchenko, V.M., Poddubnaya, O.N.: Relative controllability of stationary hybrid systems. In: Proceedings of the IEEE Methods and Models in Automation and Robotics (MMAR), pp. 267–272 (2004)
15. Zaczkiewicz, Z.: Representation of solutions for fractional differential-algebraic systems with delays. Bull. Pol. Acad.: Tech. **58**(4), 607–612 (2010)
16. Marchenko, V.M., Poddubnaya, O.N., Zaczkiewicz, Z.: On the observability of linear differential-algebraic systems with delays. IEEE Trans. Autom. Control **51**(8), 1387–1392 (2006)
17. Zaczkiewicz, Z.: Controllability, observability, duality for fractional differential-algebraic systems with delay. JAND **1**, 195–205 (2012)
18. Kaczorek, T.: Vectors and Marices in Autmation and Electrotechnics. WNT Warszawa (1998) (in Polish)
19. Ortigueira, M.D.: Fractional Calculus for Scientists and Engineers. Lecture Notes in Electrical Engineering, vol. 84. Springer, Heidelberg (2011)

Part IV
Applications

Robot Path Control with Al-Alaoui Rule for Fractional Calculus Discretization

Artur Babiarz, Adrian Łęgowski and Michał Niezabitowski

Abstract In this paper an application of the fractional calculus to path control is studied. The integer-order derivative and integral are replaced with the fractional-order ones in order to solve the inverse kinematics problem. As an approximation of the fractional differentiator the Al-Alaoui operator with power series expansion (PSE) is used. The proposed algorithm is a modification of the existing one based on Grünwald–Letnikov formula. In order to maintain the accuracy and to lower the memory requirements a history limit and a combination of fractional- and integer-order derivation are proposed. After reaching assumed accuracy or iteration limit the algorithm switches to integer order derivative and stops after few additional iterations. This approach allows to reduce the positional error and maintain the repeatability of fractional calculus approach. The simulated path in task space have been designed in a way that causes the instability of standard *Closed Loop Pseudoinverse* algorithm. Our study proves that use of fractional calculus may improve the joint paths.

Keywords Fractional calculus · Path planning · Motion planning · Inverse kinematics · Manipulator · Al-Alaoui operator

1 Introduction

A problem of the *inverse kinematics* (IK) is well known and deeply studied. There are many algorithms that find the set of joint values for desired task space coordinates.

Many algorithms have been developed, few of them are presented in [1–5]. New approaches suggest that the topic is still of great importance and that the algorithms

A. Babiarz · A. Łęgowski (✉) · M. Niezabitowski
Institute of Automatic Control, Silesian University of Technology,
16 Akademicka, 44-100 Gliwice, Poland
e-mail: adrian.legowski@polsl.pl

A. Babiarz
e-mail: artur.babiarz@polsl.pl

M. Niezabitowski
e-mail: michal.niezabitowski@polsl.pl

A. Babiarz et al. (eds.), *Theory and Applications of Non-integer Order Systems*,
Lecture Notes in Electrical Engineering 407, DOI 10.1007/978-3-319-45474-0_36

require further improvements. For the problem of uncertainty of joint lengths the efficient method is proposed in [6]. In papers [7, 8] authors prove that for well known structures it is possible to utilize the new neural network based approach. For manipulators with active spherical ball joints the solution is presented in [9]. There are manipulators for which finding the IK solution as closed form formulas may be hard or even impossible and therefore, numerical algorithms for few of them are proposed in [10]. Paper [6] suggests an application of the *Interval Newton* method to solving the IK problem. In order to address the time-efficiency combining the numerical and analytical approach is proposed in paper [11].

The *IK* algorithm should be predictable, repeatable and accurate. The approach presented in this paper allows to meet these requirements with limited memory consumption which is important for implementation in robots' controllers.

Our paper is organized as follows. The second section presents the Grunwald–Letnikov operator with use of the *short memory principle* and Al-Alaoui operator. Third section introduces the standard Jacobian-based inverse kinematics algorithm with integer-order derivative and suggests use of the *Moore–Penrose Pseudoinverse* matrix. The next part proposes replacing integer-order calculus with fractional one and modification of the existing method proposed in [12, 13] by varying the derivative order and modifying the fractional operator. Section five introduces the simulation settings, defines the task and initial conditions. Part six is dedicated to the simulation results and positional accuracy with comparison of two presented methods. The last section summarizes obtained results and underlines the advantages as well as disadvantages of the proposed approach.

2 Fractional Calculus

The idea of non-integer order derivative and integral is nearly as old as well known integer-order calculus. It goes back to the 1695 and Leibniz's letter to L'Hospital [14]. There are many definitions of fractional derivative and integral. The three popular ones are presented in this paper.

The Riemann–Liouville (RL) derivative of non-integer order $0 < \alpha < 1$ is defined as follows [15]:

$$ {}_0D_t^{\alpha} y(t) = \frac{1}{\Gamma(1-\alpha)} \frac{d}{dt} \int_0^t (t-\tau)^{-\alpha} y(\tau) d\tau. \tag{1} $$

The Caputo's definition of derivative has the following form [16]:

$$ {}_0D_t^{\alpha} y(t) = \frac{1}{\Gamma(1-\alpha)} \int_0^t \frac{y'(\tau)}{(t-\tau)^{\alpha}} d\tau. \tag{2} $$

The Grünwald–Letnikov approach is given by the equation [15, 16]:

$$ {}_aD_t^{\alpha} y(t) = \lim_{\Delta t \to 0} \left[\frac{1}{(\Delta t)^{\alpha}} \sum_{k=0}^{\frac{t-a}{\Delta t}} y(t - k\Delta t)\gamma(\alpha, k) \right], \tag{3} $$

$$ \gamma(\alpha, k) = (-1)^k \frac{\Gamma(\alpha + 1)}{\Gamma(k + 1)\Gamma(\alpha - k + 1)}. \tag{4} $$

The function $\Gamma()$ is the Gamma function.

Often, the approximation of expression (3) is implemented with use of the short-memory principle [17] by formula (5):

$$ D^{\alpha} y(t) \approx \frac{1}{(\Delta t)^{\alpha}} \sum_{k=0}^{N} y(t - k\Delta t)\gamma(\alpha, k), \tag{5} $$

where Δt is sampling time and N is the truncation order [12].

The last definition seems to be well suited for software implementation. With use of *lookup table* (*LUT*) there is no need for computing the value of γ in every iteration.

In this paper we compare the operator given by (3) with the Al-Alaoui operator [18] after power series expansion (PSE):

$$ s^{\alpha} \approx \left(\frac{8}{7\Delta t} \frac{1 - z^{-1}}{1 + \frac{z^{-1}}{7}} \right)^{\alpha}. \tag{6} $$

Having the expression (6) we can write that:

$$ D^{\alpha} y(t) \approx \left(\frac{8}{7\Delta t} \right)^{\alpha} \sum_{k=0}^{\infty} \left[\sum_{j}^{k} h(\alpha, j, k) \right] y(t - k\Delta t), \tag{7} $$

where function γ is defined as in (4) and

$$ h(\alpha, j, k) = \left(\frac{1}{7} \right)^{k-j} \gamma(\alpha, j) \frac{\Gamma(-\alpha + 1)}{\Gamma(k - j + 1)\Gamma(-\alpha - k + j + 1)}. \tag{8} $$

This formula is more complicated than Grünwald–Letnikov operator however, with proper implementation and truncation it does not require more time for computation. As earlier, we can use *LUT*.

Currently researchers are looking for new applications of fractional calculus (FC) in various branches of science. Many researchers proved that the FC can be applied in control theory in order to design new type of controllers [19, 20]. In paper [21] fractional continuous models have been studied. Implementation of fractional models requires accurate methods of approximation. Many of them are based on approximating the s^{α} in Laplace domain. They have been studied in [15, 18].

These and many others applications prove the usability of fractional calculus and therefore, need for finding new applications in order to improve solutions for well known problems.

3 Integer-Order Inverse Kinematics

The IK solution can be found in various ways e.g. by finding the analytical formulas [22]. In this paper we focus on differential IK solution. The common approach suggests using the following equation:

$$\frac{dx}{dt} = J(q)\frac{dq}{dt}, \tag{9}$$

where x is the vector of coordinates in task space, q is the vector of coordinates in joint space and $J(q)$ is the Jacobian matrix for given q. For given target manipulator position (X_{ref}) we can rewrite the Eq. (9) as follows:

$$J^{-1}(q_{i-1})\Delta x_i = \Delta q_i, \tag{10}$$

where

$$\begin{aligned} \Delta x_i &= X_{ref} - x_{i-1}, \\ q_i &= \Delta q_i + q_{i-1}, \\ i &= 1, 2, 3, \ldots . \end{aligned}$$

The process of finding solution is iterative and accuracy may be sensitive to number of iterations. Trajectory realization requires computing the IK solution for every given X_{ref}. In every iteration the algorithm takes into account demanded position (X_{ref}) and previous values of task and joint space coordinates. This fact can be written as follows:

$$q_{i-1} + J^{-1}(q_{i-1})(X_{ref}(j\Delta t) - x_{i-1}) = q_i \tag{11}$$

where

$$j = 1, 2, 3, \ldots .$$

It is worth noting that for given $X_{ref}(j\Delta t)$ we use the value of x computed by solving the forward kinematics problem in previous iteration. This is the local nature of integer-order derivative.

Many researchers suggest using *Moore–Penrose pseudoinverse* (*MPp*) of matrix in computations. This approach allows to use the expression (11) for even redundant structures. Considering this we can write:

$$J^{\#}(q_{i-1})\Delta x(i) = \Delta q(i) \tag{12}$$

which can be rewritten as follows:

$$J^{\#}(q_{i-1})(X_{ref} - x_{i-1}) = q_i - q_{i-1}, \tag{13}$$

$$q_{i-1} + J^{\#}(q_{i-1})(X_{ref} - x_{i-1}) = q_i \tag{14}$$

and finally:

$$q_{i-1} + J^{\#}(q_{i-1})(X_{ref}(j\Delta t) - x_{i-1}) = q_i, \tag{15}$$

where $J^{\#}$ is the *MPp* of matrix J. In this paper we assume that q_i represents the $i\text{-}th$ computed value of joints and x_i is the $i\text{-}th$ computed value of task space coordinates. These values are not time-dependent. They hold the computation results.

It has been proven that this simple approach often called *closed loop pseudoinverse* (CLP) leads to an aperiodic joints motion for certain cyclic end-effector trajectories [12]. This problem mostly concerns redundant manipulators and specific trajectories.

4 Inverse Kinematics Based on Fractional Calculus

In paper [12] authors study the application of FC to the CLP method and in paper [23] authors try to have a deep insight into the repeatability problem for the redundant manipulators. The fractional-order derivative is the global operator that has a memory of all past events. This property may force the periodic motion for desired cyclic end-effector trajectories. Considering the approximation of Grünwald–Letnikov derivative, in $j\text{-}th$ time moment, we can rewrite the formula (12) as follows:

$$J^{\#}(q_{i-1})\Delta^{\alpha} x(i) = \Delta^{\alpha} q(i), \tag{16}$$

$$q_i + \sum_{k=1}^{N} \gamma(\alpha, k) q_{i-k} = J^{\#}(q_{i-1}) \left[X_{ref}(j\Delta t) + \sum_{k=1}^{N} \gamma(\alpha, k) x_{i-k} \right], \tag{17}$$

where N is the truncation order and

$$\gamma(\alpha, k) = (-1)^k \frac{\Gamma(\alpha + 1)}{\Gamma(k + 1)\Gamma(\alpha - k + 1)}. \tag{18}$$

Having formula (17) we can compute:

$$q_i = J^{\#}(q_{i-1}) \left[X_{ref}(j\Delta t) + \sum_{k=1}^{N} \gamma(\alpha, k) x_{i-k} \right] - \sum_{k=1}^{N} \gamma(\alpha, k) q_{i-k}. \tag{19}$$

After using Al-Alaoui operator with similar transformations we can rewrite expression (16) as follows:

$$\begin{aligned} q_i =& J^{\#}(q_{i-1}) \left[X_{ref}(j\Delta t) + \sum_{k=1}^{N} \left[\sum_{j}^{k} h(\alpha, j, k) \right] x_{i-k} \right] - \\ & - \sum_{k=1}^{N} \left[\sum_{j}^{k} h(\alpha, j, k) \right] q_{i-k}, \end{aligned} \tag{20}$$

where $h(\alpha, j, k)$ is given by (8).

The Eqs. (19) and (20) allow to design an iterative procedure for finding the solution of IK problem. For given X_{ref} at the time $j\Delta t$ we compute the value of q_i. The only variable that is the function of time is the reference position.

In paper [12] authors suggest that lowering the differential order α lowers the positioning accuracy. We can confirm that for most studied trajectories. To address this issue we propose a variable order α. It has been proven that integer order derivation maintains high positional accuracy. Having that in mind we can write that derivation order is given by the expression (21):

$$\alpha(c) = \begin{cases} 1 & \text{if } c \geq I - d, \\ \alpha_s & \text{if } c < I - d, \end{cases} \tag{21}$$

where α_s is the initial order of derivative, I is the maximal number of iterations, d defines the number of iterations with integer-order derivation and c is the iteration number between $X_{ref}((j-1)\Delta t)$ and $X_{ref}(j\Delta t)$. With that in mind we can rewrite Eq. (19) as follows:

$$q_i = J^{\#}(q_{i-1}) \left[X_{ref}(j\Delta t) + \sum_{k=1}^{N} \gamma(\alpha(c), k) x_{i-k} \right] - \sum_{k=1}^{N} \gamma(\alpha(c), k) q_{i-k} \tag{22}$$

and the Eq. (20) in the following way:

$$\begin{aligned} q_i =& J^{\#}(q_{i-1}) \left[X_{ref}(j\Delta t) + \sum_{k=1}^{N} \left[\sum_{j}^{k} h(\alpha(c), j, k) \right] x_{i-k} \right] - \\ & - \sum_{k=1}^{N} \left[\sum_{j}^{k} h(\alpha(c), j, k) \right] q_{i-k}. \end{aligned} \tag{23}$$

Proposed approach may improve the accuracy. It is worth noting that this method may be more time-efficient since few last iterations consider only previous result.

Table 1 Denavit–Hartenberg (D–H) parameters [24]

i	λ_i (cm)	l_i (cm)	$\alpha_i(^\circ)$	$\theta_i(^\circ)$
1	0	0	0	θ_1
2	λ_2	−3	0	−90
3	0	−3	0	θ_3
4	0	−1	0	θ_4

5 Simulated Path and Settings

In simulation we consider 4 degree of freedom (DOF) manipulator. The task is to follow the given trajectory. The path is generated by periodic functions. It is chosen in a way that allows for periodic motion of joints.

We have omitted the lower and upper bounds for joints in order to ease the task for the algorithm. It is clear that in practical application these constraints have to be included during the path planning. Considering the presented D–H parameters (Table 1) the Jacobian matrix takes the form:

$$J = \begin{bmatrix} -3C_{13} - 3C_1 - C_{134} & 0 & -3C_{13} - C_{134} & -C_{134} \\ -3S_{13} - 3S_1 - S_{134} & 0 & -3S_{13} - S_{134} & -S_{134} \\ 0 & 1 & 0 & 0 \end{bmatrix}, \tag{24}$$

where $C_{lm} = cos(\theta_l + \theta_m)$, $S_{lm} = sin(\theta_l + \theta_m)$, $S_{lmn} = sin(\theta_l + \theta_m + \theta_n)$, $C_{lmn} = cos(\theta_l + \theta_m + \theta_n)$.

The path in task space is given as a location described in Cartesian space:

$$X_{ref}(j\Delta t) = \begin{bmatrix} x_{ref}(j\Delta t) \\ y_{ref}(j\Delta t) \\ z_{ref}(j\Delta t) \end{bmatrix} = \begin{bmatrix} 2.5sin(\omega_1 j\Delta t) + 1 \\ 2.5cos(\omega_2 j\Delta t) + 2.3 \\ 10cos(\omega_3 j\Delta t) \end{bmatrix}, \tag{25}$$

where Δt is the time step, $\omega_1,\ \omega_2,\ \omega_3$ are the angular frequencies and

$$0 \leq j\Delta t \leq 50,$$
$$j = 0, 1, 2, \ldots .$$

The chosen path is designed to cause specific issues. The integer order derivation causes vast growth of joint values. The initial time is $t = 0$. The angular frequencies vary in experiments and therefore, they are specified in every figure or table. We simulate 100 s of robot's motion ($t_{max} = 100\,(\text{s})$). The stop criterion for every given point is defined as a maximal number of iterations $I = 250$. This value has been chosen experimentally.

For every trajectory the initial condition is as follows:

$$q_0 = [6.2024, 10, 5.8199, 3.7168]^T .$$

6 Results

In the first experiment we study the influence of memory length (N) for both fractional operators. Figures 1, 2, 3, 4, 5 and 6 present the trajectories for manipulators' joints. We decided to omit the second joint since its trajectory seems to remain untouched

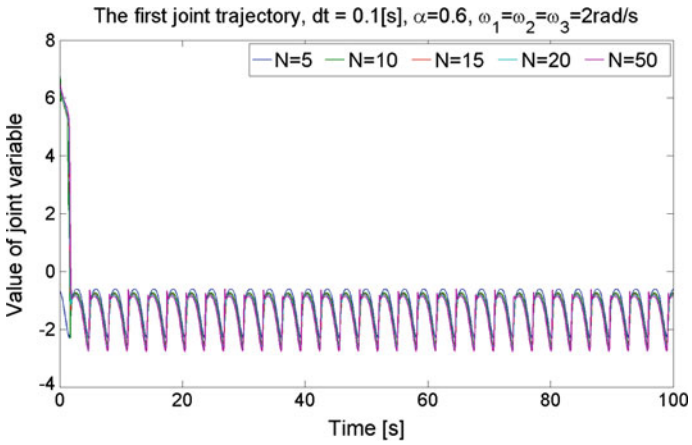

Fig. 1 First joint trajectory with use of Grünwald–Letnikov operator for various N (own source)

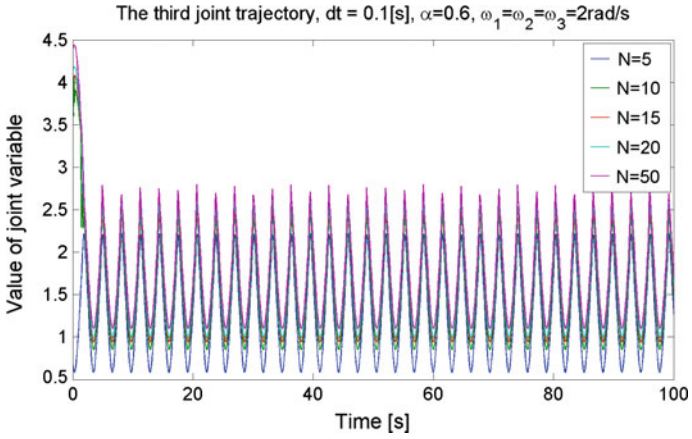

Fig. 2 Third joint trajectory with use of Grünwald–Letnikov operator for various N (own source)

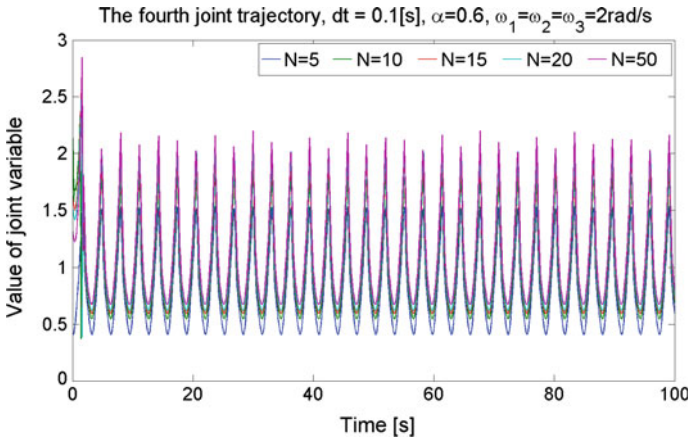

Fig. 3 Fourth joint trajectory with use of Grünwald–Letnikov operator for various N (own source)

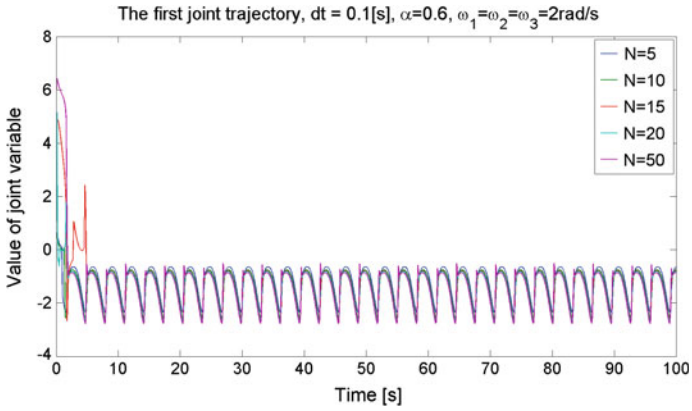

Fig. 4 First joint trajectory with use of Al-Alaoui operator for various N (own source)

by the changes. It is clear that for implementation we would use the smallest N possible.

These Figs. 1, 2, 3, 4, 5 and 6 reveal small differences. For $N = 5$ the algorithm seems to perform sufficiently well. Despite the initial step (i.e. for the first joint from around 6 rad to around -0.5 rad) the trajectory is stable. In this test we require a periodic motion for every joint with extreme values as close to zero as possible. Considering this criterion we conclude that $N = 5$ may be sufficient for our test trajectory. The small number of N meets our other requirement which is small memory consumption. A proper truncation of the sums in (22) and (23) allows for relatively low-cost implementation. With use of the *LUT* there should not be any performance issues during the computation of γ or $h(\alpha, j, k)$.

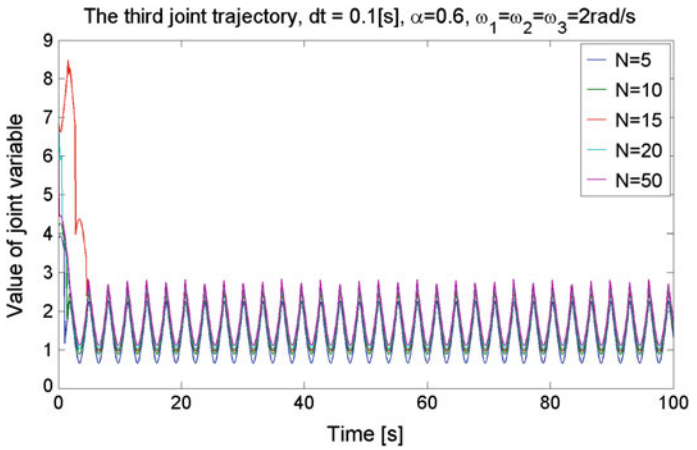

Fig. 5 Third joint trajectory with use of Al-Alaoui operator for various N (own source)

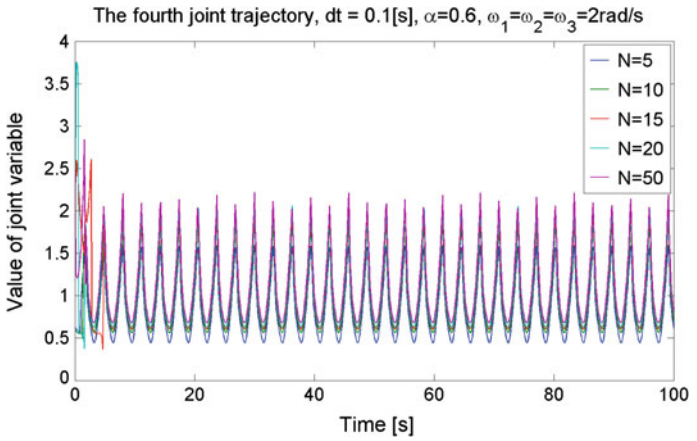

Fig. 6 Fourth joint trajectory with use of Al-Alaoui operator for various N (own source)

Since for $N = 5$ we obtain relatively good results, we decided to use this truncation in other simulations. We conclude that for $\alpha \geq 0.6$ this parameter would have rather poor impact. One must notice that function γ decays slower for lower derivative order (we consider $0 \leq \alpha \leq 1$).

Figures 7, 8 and 9 present the joint trajectories for various order α. In these figures one can observe that integer-order approach causes the multiple rotations for the first joint. We conclude that for specific cases lowering the order may improve the motion performance which can be observed in the Fig. 9 for $\alpha = 0.6$.

Tables 2, 3 and 4 present the accuracy for various alpha with and without integer-order derivation. The accuracy is defined by formula (26).

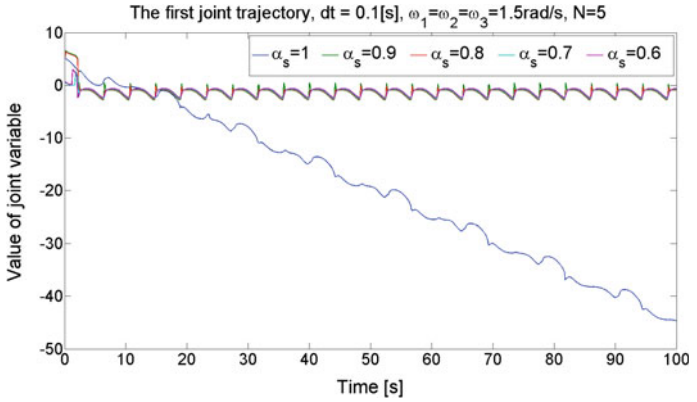

Fig. 7 First joint trajectory with use of Al-Alaoui operator for various α (own source)

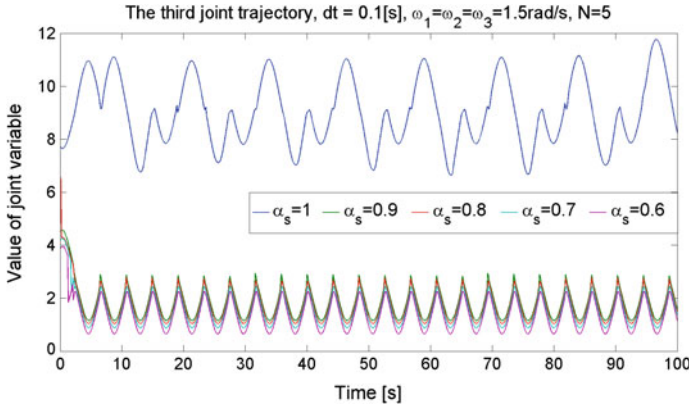

Fig. 8 Third joint trajectory with use of Al-Alaoui operator for various α (own source)

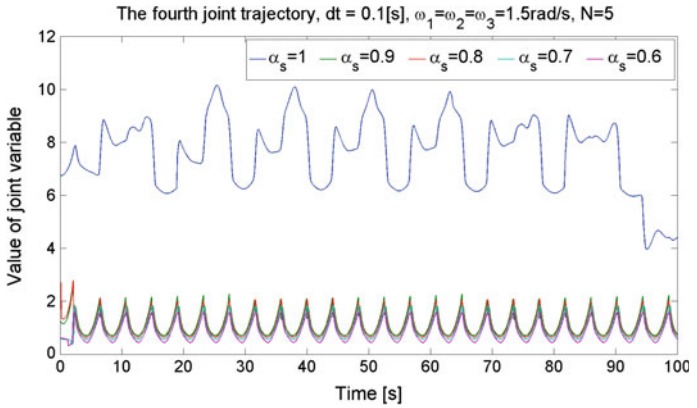

Fig. 9 Fourth joint trajectory with use of Al-Alaoui operator for various α (own source)

Table 2 The positional accuracy for Grünwald–Letnikov approximation, N = 5

ω (rad/s)	$\alpha = 0.99$	$\alpha = 0.9$	$\alpha = 0.8$	$\alpha = 0.7$	$\alpha = 0.6$
2	0.0259	0.2978	0.6908	1.1781	1.7429
4	0.0253	0.2923	0.6809	1.1634	1.7424
5	0.0251	0.2914	0.6784	1.1615	1.7421
6	0.0253	0.2906	0.6772	1.1617	1.7420
8	0.0589	0.2896	0.6760	1.1605	1.7417
9	0.0262	0.2894	0.6757	1.1605	1.7421
10	0.0392	0.2953	0.6744	1.1604	1.7416

Table 3 The positional accuracy for Al-Alaoui operator, N = 5

ω (rad/s)	$\alpha = 0.99$	$\alpha = 0.9$	$\alpha = 0.8$	$\alpha = 0.7$	$\alpha = 0.6$
2	0.0254	0.2595	0.6097	1.0508	1.6103
4	0.0252	0.2545	0.5989	1.0466	1.6078
5	0.0251	0.2536	0.5991	1.0453	1.6041
6	0.0252	0.2529	0.5979	1.0448	1.6055
8	0.0571	0.2520	0.5960	1.0438	1.6038
9	0.0882	0.2518	0.5963	1.0445	1.6038
10	0.0244	0.2902	0.5953	1.0436	1.6040

Table 4 The positional accuracy for Al-Alaoui operator with integer-order derivation in last 10 iterations, N = 5

ω (rad/s)	$\alpha_s = 0.99$	$\alpha_s = 0.9$	$\alpha_s = 0.8$	$\alpha_s = 0.7$	$\alpha_s = 0.6$
2	$4.5754e-16$	$4.9886e-16$	$4.7150e-16$	$4.5578e-16$	$4.4400e-16$
4	$4.5727e-16$	$4.7071e-16$	$4.3854e-16$	$4.4926e-16$	$4.3257e-16$
5	$4.5226e-16$	$4.6581e-16$	$4.4414e-16$	$4.3923e-16$	$4.3683e-16$
6	$4.4739e-16$	$4.6029e-16$	$4.5136e-16$	$4.3621e-16$	$4.1981e-16$
8	$1.5469e-15$	$4.3621e-16$	$4.4384e-16$	$4.3057e-16$	$4.3016e-16$
9	$1.9026e-15$	$4.9731e-16$	$4.5892e-16$	$4.5892e-16$	$4.4340e-16$
10	$4.3797e-16$	$4.8115e-16$	$4.5356e-16$	$4.2807e-16$	$4.3440e-16$

$$
\begin{aligned}
X_d(j) &= X_{ref}(j\Delta t) - X_c(j\Delta t), \\
P_{err} &= \frac{\sum_{j=0}^{J-1} \sqrt{X_d(j)^T X_d(j)}}{J},
\end{aligned}
\tag{26}
$$

where J is the number of points, $X_c(j\Delta t)$ is a direct kinematics result for computed joint variables at j-th point. Results contained in Table 3 reveal that using the Al-Alaoui operator allows to slightly improve the accuracy for most presented simulations. Adding few iterations with integer-order derivation causes further improvements.

7 Conclusions

In this paper we studied the possible application of fractional calculus in solving the inverse kinematics problem and therefore, to manipulator path control. In this paper we presented method based on the existing algorithm. Our experiments confirm that there are benefits of the memory effect. We conclude that lowering the derivation to fractional-order may improve the repeatability of joint trajectories (Figs. 7, 8 and 9) for specified end-effector trajectory but it may increase the positional error. Our modification allows to maintain the accuracy of well known *CLP* algorithm without loosing the cyclic joints motion. The Grünwald–Letnikov and fractional Al-Alaoui operator seem to result in similar trajectories.

The disadvantage of the proposed method is the ignorance of the joint limitations. Properly designed algorithm has to meet these constraints. Moreover, this simple approach does not affect the singular configurations since the Jacobian matrix is computed without any adjustments. This is the reason why presented method may only be the base for more advanced algorithms.

Acknowledgments The work of the second author was supported by Polish Ministry for Science and Higher Education under internal grant for Institute of Automatic Control, Silesian University of Technology, Gliwice, Poland: BKM/506/RAU1/2016 t.1. Moreover, the research was done by the first and the third author as part of the project funded by the National Science Centre in Poland granted according to decisions DEC-2014/13/B/ST7/00755. Finally, the calculations were performed with the use of IT infrastructure of GeCONiI Upper Silesian Centre for Computational Science and Engineering (NCBiR grant no POIG.02.03.01-24-099/13).

References

1. Wang, L.T., Chen, C.: A combined optimization method for solving the inverse kinematics problems of mechanical manipulators. IEEE Trans. Robot. Autom. **7**(4), 489–499 (1991)
2. Manocha, D., Canny, J.F.: Efficient inverse kinematics for general 6R manipulators. IEEE Trans. Robot. Autom. **10**(5), 648–657 (1994)
3. Szkodny, T.: Forward and inverse kinematics of IRb-6 manipulator. Mech. Mach. Theory **30**(7), 1039–1056 (1995)
4. Goldenberg, A.A., Benhabib, B., Fenton, R.G.: A complete generalized solution to the inverse kinematics of robots. IEEE J. Robot. Autom. **1**(1), 14–20 (1985)
5. Szkodny, T.: Basic component of computational intelligence for IRB-1400 robots. In: Proceedings of the first International Conference on Man-Machine Interactions, ICMMI 2009, The Beskids, Poland, September 25–27, pp. 637–646. Springer, Heidelberg (2009)
6. Kumar, V., Sen, S., Shome, S.N., Roy, S.S.: Inverse kinematics of redundant serial manipulators using interval method in handling uncertainties. In: Proceedings of the 2015 Conference on Advances in Robotics, AIR 2015, Goa, India, July 2–4, 2015, pp. 1:1–1:6 (2015)
7. Son, N.N., Anh, H.P.H., Chau, T.D.: Inverse kinematics solution for robot manipulator based on adaptive MIMO neural network model optimized by hybrid differential evolution algorithm. In: 2014 IEEE International Conference on Robotics and Biomimetics, ROBIO 2014, Bali, Indonesia, December 5–10, 2014, pp. 2019–2024 (2014)
8. Köker, R.: A genetic algorithm approach to a neural-network-based inverse kinematics solution of robotic manipulators based on error minimization. Inf. Sci. **222**, 528–543 (2013)

9. Dong, H., Fan, T., Du, Z., Chirikjian, G.S.: Inverse kinematics of active rotation ball joint manipulators using workspaces density functions. In: Advances in Reconfigurable Mechanisms and Robots II, pp. 633–644. Springer International Publishing, Heidelberg (2016)
10. Kucuk, S., Bingul, Z.: Inverse kinematics solutions for industrial robot manipulators with offset wrists. Appl. Math. Model. **38**(78), 1983–1999 (2014)
11. Ananthanarayanan, H., Ordnez, R.: Real-time inverse kinematics of (2n + 1) DOF hyper-redundant manipulator arm via a combined numerical and analytical approach. Mech. Mach. Theory **91**, 209–226 (2015)
12. Duarte, F.B.M., Machado, J.A.T.: Pseudoinverse trajectory control of redundant manipulators: A fractional calculus perspective. In: Proceedings of the 2002 IEEE International Conference on Robotics and Automation, ICRA 2002, May 11-15, 2002, Washington, DC, USA, pp. 2406–2411 (2002)
13. da Graça Marcos, M., Machado, J.T., Azevedo-Perdicoúlis, T.P.: A fractional approach for the motion planning of redundant and hyper-redundant manipulators. Signal Process. **91**(3), 562–570 (2011)
14. Ross, B.: A brief history and exposition of the fundamental theory of fractional calculus. In: Fractional calculus and its applications, pp. 1–36. Springer, Heidelberg (1975)
15. Vinagre, B., Podlubny, I., Hernandez, A., Feliu, V.: Some approximations of fractional order operators used in control theory and applications. Fract. Calc. Appl. Anal. **3**(3), 231–248 (2000)
16. Garrappa, R.: A Grünwald-Letnikov scheme for fractional operators of Havriliak-Negami type. Recent Adv. Appl., Model. Simul. **34**, 70–76 (2014)
17. Podlubny, I.: Fractional Differential Equations: An Introduction to Fractional Derivatives, Fractional Differential Equations, to Methods of Their Solution and Some of Their Applications, vol. 198. Academic Press, San Diego (1998)
18. Barbosa, R.S., Machado, J.A.T.: Implementation of discrete-time fractional-order controllers based on LS approximations. Acta Polytechnica Hungarica **3**(4), 5–22 (2006)
19. Cao, J.Y., Cao, B.G.: Design of fractional order controllers based on particle swarm optimization. In: 2006 1ST IEEE Conference on Industrial Electronics and Applications, pp. 1–6 (2006)
20. Mackowski, M., Grzejszczak, T., Łęgowski, A.: An approach to control of human leg switched dynamics. In: 2015 20th International Conference on Control Systems and Computer Science (CSCS), pp. 133–140 (2015)
21. Aoun, M., Malti, R., Levron, F., Oustaloup, A.: Numerical simulations of fractional systems: an overview of existing methods and improvements. Nonlinear Dyn. **38**(1), 117–131 (2004)
22. Łęgowski, A.: The global inverse kinematics solution in the Adept six 300 manipulator with singularities robustness. In: 2015 20th International Conference on Control Systems and Computer Science, pp. 90–97 (2015)
23. da Graça Marcos, M., Duarte, F.B., Machado, J.T.: Fractional dynamics in the trajectory control of redundant manipulators. Commun. Nonlinear Sci. Numer. Simul. **13**(9), 1836–1844 (2008)
24. Hartenberg, R.S., Denavit, J.: Kinematic Synthesis of Linkages. McGraw-Hill, New York (1964)

Implementation of Bi-fractional Filtering on the Arduino Uno Hardware Platform

Waldemar Bauer and Aleksandra Kawala-Janik

Abstract In this paper application of method based on bi-fractional filtering on the Arduino Uno was proposed. The authors showed that the implementation of a non-integer order filter on a micro-controller hardware platform is possible and gives promising results. Another aspect of potential implementation of such systems involves using biomedical data – in particular EEG signals, which were applied during the research carried out for the purpose of this paper.

Keywords EEG · Bi-fractional filter · Arduino · Time domain Oustaloup

1 Introduction

Nowadays the implementation of non-integer order subsystems on various platform is a broadly researched topic. One of the questions of great importance is to design and develop an algorithm for realisation of non-integer order elements in the discrete implementation (see: [1, 2]).

Only a very few years ago – the technology based on using biomedical data for the purpose of control was very rare and even voice recognition or touch panels were rarely used and nowadays application of brain signals (EEG) as a source data (although very novel) has become in the past two decades very popular due to the growing interest of researchers all over the world [3–5]. This is because (in accordance with multiple studies) not only people, but also animals, are able to communicate with computers using biomedical signals [3]. This particularly important for handicapped users, unable to conduct simple tasks such as using keyboard or mouse [4].

W. Bauer (✉)
Department of Automatics and Biomedical Engineering, AGH University of Science and Technology, Al. Mickiewicza 30, 30-059 Cracow, Poland
e-mail: bauer@agh.edu.pl

A. Kawala-Janik
Faculty of Electrical Engineering, Automatic Control and Informatics, Opole University of Technology, Proszkowska 76/1, 45-758 Opole, Poland
e-mail: kawala84@gmail.com

A. Babiarz et al. (eds.), *Theory and Applications of Non-integer Order Systems*, Lecture Notes in Electrical Engineering 407, DOI 10.1007/978-3-319-45474-0_37

The application of EEG signals is a very difficult task, as it relies on real-time analysis and interpretation a data of (frequently) a very poor quality. Therefore a very important role is to choose appropriate signal processing method (see: [3]), and so the concept of using fractional calculus in technical applications became recently very popular, although regarding it theory was developed already in the 19th century. This is because implementation of such filtering (fractional) allows great flexibility in filter shaping, which is not possible while using traditional filtering methods [6]

The theory of non-integer order systems can be found in e.g.: [7–11] and the Oustaloup method was in more detail described in: [12]. It is important to mention that the Oustaloup approximation can be used in simulations, which were described in: [13–17], in filtering presented in more detail in: [18–20] and with appropriate care in experiments – presented in: [21, 22].

Its sensitivity and stability problems during discretisation were deeply discussed in: [23–25]. Different method of approximation is based on Laguerre functions (see: [1, 26, 27]). The implementation of the algorithm requires the discretisation of the control system designed in a continuous time domain. The earlier results (see: [28]) prove that the transfer function cannot be directly implemented.

The further part of this paper is organised as follows, where the bi-fractional filter is presented in a transmutation and differential equation form. Then the time-domain Oustaloup approximation is shown. The results of experiments are then presented and the main differences between the Matlab-Simulink and the Arduino Uno hardware platform filter realisation are discussed. Finally the conclusions and future works are drawn.

2 Bi-fractional Filter

In this paper the authors focused on the digital realisation of bi-fractional filters. The filter can be given by the following transfer function (see [28]):

$$G(s) = \frac{c}{s^{2\alpha} + 2bs^{\alpha} + c}, \tag{1}$$

where:

- α is base order;
- b is damping coefficient;
- c is free coefficient.

This formula (1) can be represented in the form of a system of differential equation with zero initial conditions:

$$\begin{aligned} {}_0^C\mathrm{D}_t^{\alpha}\mathbf{x}(t) &= \mathbf{A}\mathbf{x}(t) + \mathbf{B}u \\ y(t) &= \mathbf{C}\mathbf{x}(t) \end{aligned} \tag{2}$$

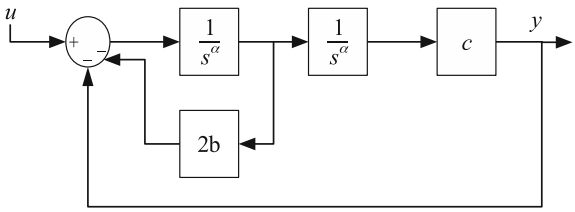

Fig. 1 Block diagram realization of bi-fractional filter in differential equation form

with matrix:

$$\mathbf{A} = \begin{bmatrix} 0 & 1 \\ -c & -2b \end{bmatrix} \quad \mathbf{B} = \begin{bmatrix} 0 \\ 1 \end{bmatrix} \quad \mathbf{C} = \begin{bmatrix} c & 0 \end{bmatrix}$$

Such system can be realized with non-integer order integrators as illustrated with the Fig. 1.

3 The Original Ostaloup Non-integer Time-Domain Approximation

The Oustaloup filter approximation with a fractional-order differentiator $G(s) = s^\alpha$ has a large use of potential, especially in applications [29]. An Oustaloup filter can be designed as [12]:

$$G_f(s) = K \prod_{i=1}^{N} \frac{s + \omega_i'}{s + \omega_i} \tag{3}$$

where:

$$\omega_i' = \omega_b \omega_u^{(2i-1-\alpha)/N} \tag{4}$$

$$\omega_i = \omega_b \omega_u^{(2i-1+\alpha)/N} \tag{5}$$

$$K = \omega_h^\alpha \tag{6}$$

$$\omega_u = \sqrt{\frac{\omega_h}{\omega_b}} \tag{7}$$

Because the poles of this approximation spacing from close to $-\omega_h$ to those very close to $-\omega_b$. This spacing is not-linear and more poles are grouping near $-\omega_b$. This is one of the main reasons of problems in discretisation process.

Time Domain Oustaloup Approximation For zero-initial condition it is possible to describe any part of (3) as follows:

$$\frac{s+\omega_k'}{s+\omega_k} \Longleftrightarrow \begin{cases} \dot{x}_k = A_k x_k + B_k u_k \\ y_k = x_k + u_k \end{cases}$$

where

$$A_k = -\omega_k, \quad B_k = \omega_k' - \omega_k \tag{8}$$

This can be written in vector matrix notation – as below:

$$\begin{aligned} \dot{\mathbf{x}} &= \begin{bmatrix} A_1 & 0 & 0 & \dots & 0 \\ B_2 & A_2 & 0 & \dots & 0 \\ B_3 & B_3 & A_3 & \dots & 0 \\ \vdots & \vdots & \vdots & \ddots & \vdots \\ B_N & B_N & \dots & B_N & A_N \end{bmatrix} \mathbf{x} + \begin{bmatrix} KB_1 \\ KB_2 \\ KB_3 \\ \vdots \\ KB_N \end{bmatrix} u \\ y &= \begin{bmatrix} 1 & 1 & \dots & 1 & 1 \end{bmatrix} \mathbf{x} + Ku \end{aligned} \tag{9}$$

or in brief

$$\begin{aligned} \dot{\mathbf{x}} &= \mathbf{A}\mathbf{x} + \mathbf{B}u \\ y &= \mathbf{C}\mathbf{x} + Du \end{aligned} \tag{10}$$

This approach proved to be more robust to different discretisation schemes (for more details see: [30]). This form will be use in implementation at the Arduino Uno.

4 Digital Realization Bi-fractional Filter at the Arduino Uno

The Arduino Uno is a microcontroller board based on the ATmega328. The Atmega328 has 32 KB of flash memory for storing code (of which 0.5 KB is used for the bootloader). It has also 2 KB of SRAM and 1 KB of EEPROM. The board has 14 digital input/output pins (of which 6 can be used as PWM outputs), 6 analog inputs, a 16 MHz crystal oscillator, a USB connection, a power jack and an ICSP header. It contains everything needed to support the microcontroller and requires simply only USB cable in order to be connected to a computer.

4.1 Algorithm of Calculation Non-integer Integrator

In order to perform the realisation of bi-fractional filtering on the Arduino Uno platform (based on Fig. 1) an algorithm to calculate response of non-integer integrator has to be created. At this stage the time-domain Oustaloup approximation is being used. Because the considered approximation is realised in the time-domain – dif-

ferential scheme can be applied for creating the needed algorithm. The proposed algorithm for the value approximation of response non-integer integrator will have the following form:

Data: N – order of approximation
A, B, C, D – discrete matrix described approximation
xp – integrator state vector
B_u, A_x – local variable
u_t – signal value in time t
x – helper integrator state vector
Result: y_t – non-integer integrator response in time t
$y_t = 0$;
for $i = 0$ *to* $N - 1$ **do**
  $B_u = B[i] * u_t$ $A_x = 0$ **for** $j = 0$ *to* $N - 1$ **do**
    $A_x = A_x + A[i][j] * xp[j]$
  end
  $x[i] = A_x + B_u$ $y_t = y_t + C[i] * x[i]$
end
$xp = x$;
return $y+ = D * u_t$

As it was shown above – the complexity of this algorithm can be clearly seen and it is constant and has a value of $O(n^2)$. One can easily observe the presented algorithm worked only at basic arithmetic operation. For this reasons, it can be easily adapted for any hardware platform e.g.: micro-controllers, PLC, FPGA.

5 Experiments and Results

The tested EEG signal was recorder using inexpensive EEG headset – Emotiv EPOC and was ca. 700 s long. The tests were carried out during imagery left- and right-hand movements [3].

An experiment has been conducted in order to compare the performance of Matlab Simulink and Arduino Uno with the bi-fractional filter implementation for EEG signal. The described time domain Oustaloup approximations has been discretised and implemented on both considered platforms. The scheme of filtering with the use of the Arduino Uno we can seen in Fig. 2.

The bi-fractional filter settings and time-domain Oustaloup approximation parameters are:

- $N = 7$
- $\omega = [10^{-6}, 10^{6}]$
- $\alpha = \{0.1, 0.7\}$
- $b = 1.5$
- $c = 2.24$

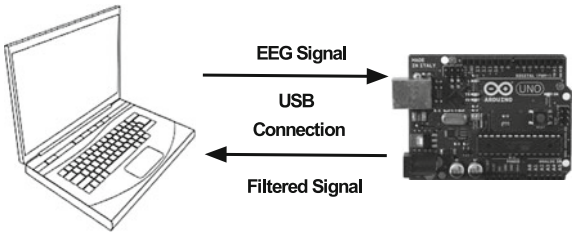

Fig. 2 Arduino Uno/PC connection schema

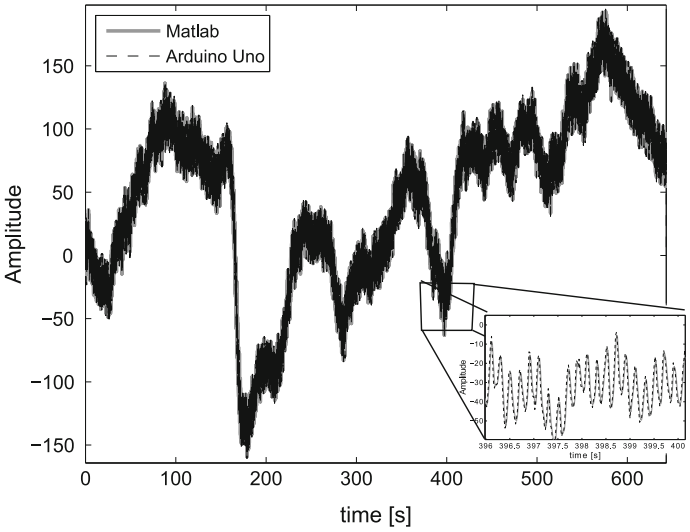

Fig. 3 Comparison filtration result with Oustaloup time domain approximation and Matlab Simulink for $\alpha = 0.1$

Result of the performed filtering for $\alpha = 0.1$ is shown in the Figs. 3, 4 and the results obtained for $\alpha = 0.7$ illustrate the Figs. 5, 6. The average error between Matlab Simulink and Arduino Uno implementation for the filtered signal in time has value of 9.5.

Considering the fact that the Arduino Uno represents the floating-point numbers as float, the presented result is very good. The second case when $\alpha = 0.7$ gives the average error value of 12.48. This shows that such implementation work was correct and was also confirmed with the analysis in the frequency-domain presented in Figs. 4 and 6.

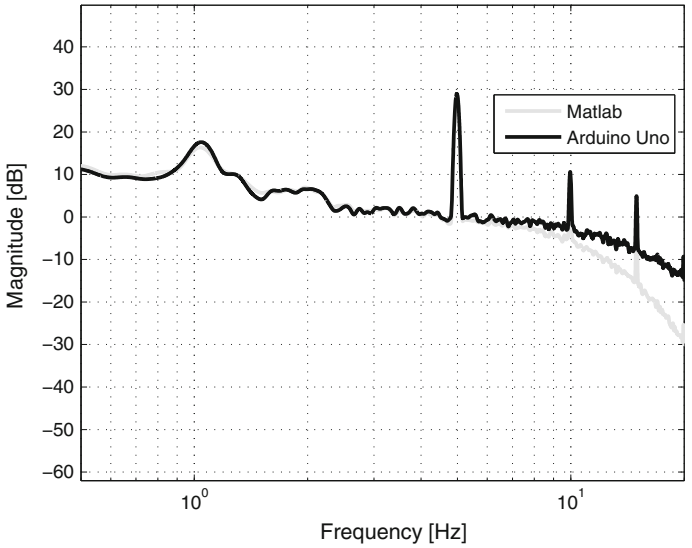

Fig. 4 FFT signal filtered by Oustaloup time domain approximation and Matlab Simulink for $\alpha = 0.1$

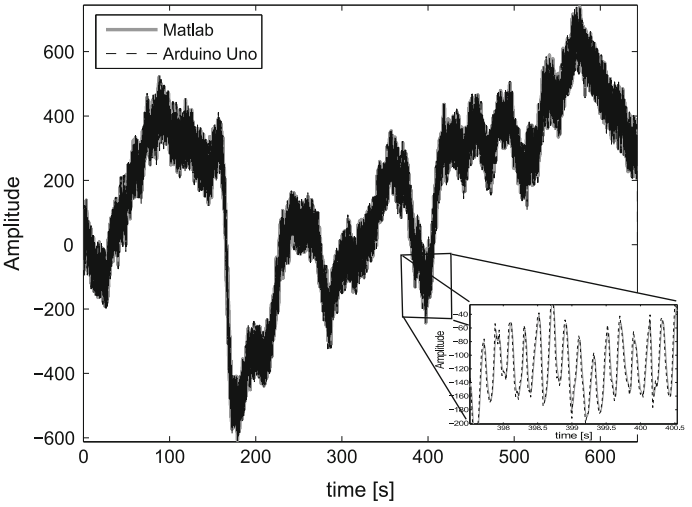

Fig. 5 Comparison filtration result with Oustaloup time domain approximation and Matlab Simulink for $\alpha = 0.7$

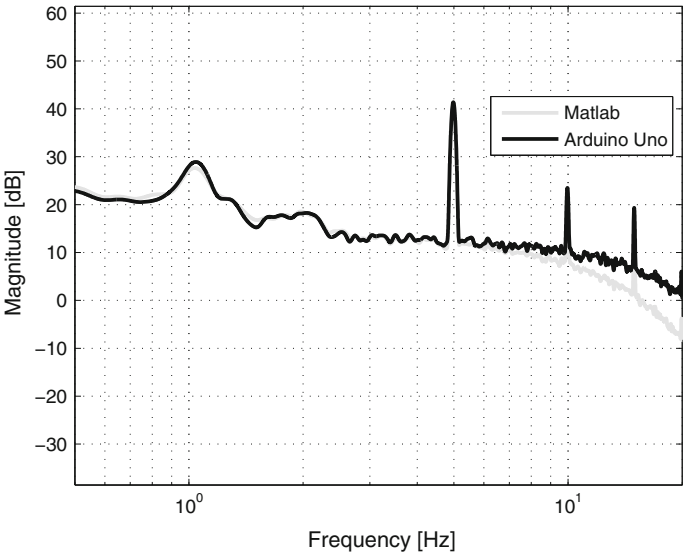

Fig. 6 FFT signal filtered by Oustaloup time domain approximation and Matlab Simulink for $\alpha = 0.7$

6 Conclusions and Further Research

In this paper the implementation method of bi-fractional filter on the Arduino Uno platform was proposed. The authors showed that the implementation of non-integer order filter in micro-controller hardware platform is possible and gives good scientific results.

Further work will include different types of non-integer order filter prototypes, methods of discretisation and implementation on real-time systems hardware platforms.

Acknowledgments Work realised in the scope of project titled "Design and application of non-integer order subsystems in control systems". Project was financed by National Science Centre on the base of decision no. DEC-2013/09/D/ST7/03960.

References

1. Bania, P., Baranowski, J.: Laguerre polynomial approximation of fractional order linear systems. In: Mitkowski, W., Kacprzyk, J., Baranowski, J. (eds.) Advances in the Theory and Applications of Non-integer Order Systems: 5th Conference on Non-integer Order Calculus and Its Applications, Cracow, Poland, pp. 171–182. Springer, Heidelberg (2013)
2. Petráš, I.: Fractional-Order Nonlinear Systems: Modeling, Analysis and Simulation. Nonlinear Physical Science. Springer, Heidelberg (2011)

3. Kawala-Janik, A.: Efficiency evaluation of external environments control using bio-signals. Ph.D. thesis, University of Greenwich (2013)
4. Kawala-Janik, A., Baranowski, J., Podpora, M., Piątek, P., Pelc, M.: Use of a costeffective neuroheadset Emotiv Epoc for pattern recognition purposes. Int. J. Comput. **13**(1), 25–33 (2014)
5. Kawala-Janik, A., Pelc, M., Podpora, M.: Method for EEG signals pattern recognition in embedded systems. Elektronika ir. Elektrotechnika **21**(3), 3–9 (2015)
6. Radwan, A.G., Elwakil, A.S., Soliman, A.M.: On the generalization of second-order filters to the fractional-order domain. J. Circuits, Syst. Comput. **18**(02), 361–386 (2009)
7. Baranowski, J., Zagórowska, M., Bauer, W., Dziwiński, T., Piątek, P.: Applications of direct Lyapunov method in Caputo non-integer order systems. Elektronika ir Elektrotechnika **21**(2), 10–13 (2015)
8. Diethelm, K.: The Analysis of Fractional Differential Equations: An Application- Oriented Exposition Using Differential Operators of Caputo Type. Lecture Notes in Mathematics, vol. 2004. Springer, Heidelberg (2010)
9. Kaczorek, T.: Selected Problems of Fractional Systems Theory. Lecture Notes in Control and Information Sciences. Springer, Heidelberg (2011)
10. Oldham, K., Spanier, J.: The Fractional Calculus. Academic Press, New York (1974)
11. Podlubny, I.: Fractional Differential Equations: An Introduction to Fractional Derivatives, Fractional Differential Equations, to Methods of Their Solution and Some of Their Applications. Mathematics in Science and Engineering. Elsevier Science, Amsterdam (1999)
12. Oustaloup, A., Levron, F., Mathieu, B., Nanot, F.M.: Frequency-band complex noninteger differentiator: characterization and synthesis. IEEE Trans. Circuits Syst. I: Fundam. Theory Appl. **47**(1), 25–39 (2000)
13. Bauer, W., Baranowski, J., Mitkowski, W.: Non-integer order $PI^{\alpha}D^{\mu}$ control ICUMM. In: Mitkowski, W., Kacprzyk, J., Baranowski, J. (eds.) Advances in the Theory and Applications of Non-integer Order Systems: 5th Conference on Non-integer Order Calculus and Its Applications, Cracow, Poland, pp. 171–182. Springer, Heidelberg (2013)
14. Bauer, W., Dziwiński, T., Baranowski, J., Piątek, P., Zagórowska, M.: Comparison of performance indices for tuning of $PI^{\lambda}D^{\mu}$ controller for magnetic levitation system. In: Latawiec, K.J., Łukaniszyn, M., Stanisławski, R. (eds.) Advances in Modelling and Control of Noninteger-order Systems - 6th Conference on Non-Integer Order Caculus and its Applications. Springer, Heidelberg (2014)
15. Dziwiński, T., Bauer, W., Baranowski, J., Piątek, P., Zagórowska, M.: Robust non-integer order controller for air heating process trainer. In: Latawiec, K.J., Łukaniszyn, M., Stanisławski, R. (eds.) Advances in Modelling and Control of Noninteger-order Systems - 6th Conference on Non-Integer Order Caculus and its Applications. Springer, Heidelberg (2014)
16. Mitkowski, W.: Approximation of fractional diffusion-wave equation. Acta Mechanica et Automatica **5**, 65–68 (2011)
17. Zagórowska, M., Baranowski, J., Bania, P., Bauer, W., Dziwiński, T., Piątek, P.: Parametric optimization of PD controller using Laguerre approximation. In: 2015 20th International Conference on Methods and Models in Automation and Robotics (MMAR), pp. 104–109. IEEE, New York (2015)
18. Baranowski, J., Piątek, P., Bauer, W., Dziwiński, T., Zagórowska, M.: Bi-fractional filters, part 2: Right half-plane case. In: 2014 19th International Conference on Methods and Models in Automation and Robotics (MMAR), pp. 369–373. IEEE, New York (2014)
19. Dziwiński, T., Piątek, P., Baranowski, J., Bauer, W., Zagórowska, M.: On the practical implementation of non-integer order filters. In: 2015 20th International Conference on Methods and Models in Automation and Robotics (MMAR), pp. 921–924. IEEE, New York (2015)
20. Kawala-Janik, A., Podpora, M., Baranowski, J., Bauer, W., Pelc, M.: Innovative approach in analysis of EEG and EMG signals - comparision of the two novel methods. In: 2014 19th International Conference on Methods and Models in Automation and Robotics (MMAR), pp. 804–807. IEEE, New York (2014)

21. Dziwiński, T., Bauer, W., Baranowski, J., Piątek, P., Zagórowska, M.: Robust noninteger order controller for air heater. In: 2014 19th International Conference on Methods and Models in Automation and Robotics (MMAR), pp. 434–438. IEEE, New York (2014)
22. Obrączka, A., Mitkowski, W.: The comparison of parameter identification methods for fractional, partial differential equation. Solid State Phenom. **210**, 265–270 (2014)
23. Baranowski, J., Bauer, W., Zagórowska, M., Dziwiński, T., Piątek, P.: Time-domain Oustaloup approximation. In: 2015 20th International Conference on Methods and Models in Automation and Robotics (MMAR), pp. 116–120. IEEE, New York (2015)
24. Bauer, W., Baranowski, J., Dziwiński, T., Piątek, P., Zagórowska, M.: Stabilisation of magnetic levitation with a $PI^{\lambda}D^{\mu}$ controller. In: 2015 20th International Conference on Methods and Models in Automation and Robotics (MMAR), pp. 638–642. IEEE, New York (2015)
25. Piątek, P., Zagórowska, M., Baranowski, J., Bauer, W., Dziwiński, T.: Discretisation of different non-integer order system approximations. In: 2014 19th International Conference on Methods and Models in Automation and Robotics (MMAR), pp. 429–433. IEEE, New York (2014)
26. Baranowski, J., Zagórowska, M., Bania, P., Bauer, W., Dziwiński, T., Piątek, P.: Impulse response approximation method for bi-fractional filter. In: 2014 19th International Conference on Methods and Models in Automation and Robotics (MMAR), pp. 379–383. IEEE, New York (2014)
27. Zagórowska, M., Baranowski, J., Bania, P., Piątek, P., Bauer, W., Dziwiński, T.: Impulse response approximation method for "fractional order lag". In: Latawiec, K.J., Łukaniszyn, M., Stanisławski, R. (eds.) Advances in Modelling and Control of Noninteger-order Systems - 6th Conference on Non-Integer Order Calculus and its Applications. Springer, Heidelberg (2014)
28. Baranowski, J., Bauer, W., Zagórowska, M., Piątek, P.: On digital realizations of non-integer order filters. Circuits Syst. Signal Process (2016)
29. Monje, C.A., Chen, Y., Vinagre, B.M., Xue, D., Feliu, V.: Fractional-Order Systems and Controls. Fundamentals and Applications. Advances in Industrial Control. Springer, London (2010)
30. Baranowski, J., Bauer, W., Zagórowska, M.: Stability properties of discrete time-domain Oustaloup approximation. In: Domek, S., Dworak, P. (eds.) Theoretical Developments and Applications of Non-Integer Order Systems. Lecture Notes in Electrical Engineering, vol. 357, pp. 93–103. Springer International Publishing, Heidelberg (2016)

Fractional Prabhakar Derivative and Applications in Anomalous Dielectrics: A Numerical Approach

Roberto Garrappa and Guido Maione

Abstract Fractional integrals and derivatives based on the Prabhakar function are useful to describe anomalous dielectric properties of materials whose behaviour obeys to the Havriliak–Negami model. In this work some formulas for defining these operators are described and investigated. A numerical method of product-integration type for solving differential equations with the Prabhakar derivative is derived and its convergence properties are studied. Some numerical experiments are presented to validate the theoretical results.

Keywords Havriliak–Negami model · Fractional derivative · Prabhakar function · Numerical method · Product integration

1 Introduction

Complex systems in different areas, such as chemistry, electromagnetism, mechanics, optics and so on, are modelled by means of integral and differential operators of integer or fractional order. Since fractional derivatives and fractional integrals allow to describe anomalous phenomena in a more accurate way, their use for the description of real-life problems is gaining an increasing popularity.

In more recent years, an accurate analysis of experimental data has highlighted the existence of situations in which classical operators of integer or fractional order

Work supported by the Cost Action CA15225.

R. Garrappa (✉)
Dipartimento di Matematica, Università degli Studi di Bari, Via E. Orabona 6, 70125 Bari, Italy
e-mail: roberto.garrappa@uniba.it

G. Maione
Dipartimento di Ingegneria Elettrica e dell'Informazione, Politecnico di Bari, Via E. Orabona 6, 70125 Bari, Italy
e-mail: guido.maione@poliba.it

A. Babiarz et al. (eds.), *Theory and Applications of Non-integer Order Systems*, Lecture Notes in Electrical Engineering 407, DOI 10.1007/978-3-319-45474-0_38

are no more sufficient to fit data in a satisfactory way and more involved operators have been introduced.

This is the case of the dielectric properties of Havriliak–Negami type observed in some polymers [1] whose mathematical description in the time-domain is characterized in terms of the so-called Prabhakar integrals and derivatives [2, 3].

This work reviews the available formulas for defining fractional operators of Prabhakar type involved in the description of Havriliak–Negami models and proposes a numerical method, of product-integration type, for solving the resulting fractional differential equations.

This paper is organized as follows: in Sect. 2 the Prabhakar function is introduced and its main properties are illustrated. Section 3 discusses the applications of the Prabhakar function in modelling some anomalous dielectrics in the Havriliak–Negami model and describes the operators involved in the time-domain representation. Section 4 introduces a product-integration formula for the discretization of these operators and analyses its convergence properties. In Sect. 5 we present some numerical experiments assessing the effectiveness of the proposed approach and validating the theoretical results and we conclude the paper with some concluding remarks in Sect. 6.

2 The Prabhakar Function

The Mittag–Leffler (ML) function is a special function playing a key role in fractional calculus. After the introduction in 1902 of a one parameter version [4], the generalization to two parameters

$$E_{\alpha,\beta}(z) = \sum_{k=0}^{\infty} \frac{z^k}{\Gamma(\alpha k + \beta)}, \quad z \in \mathbb{C}\ , \tag{1}$$

was proposed few years later [5]. In 1971, the Indian mathematician Tialk Raj Prabhakar introduced a three parameter generalization of the ML function [3]

$$E^{\gamma}_{\alpha,\beta}(z) = \frac{1}{\Gamma(\gamma)} \sum_{k=0}^{\infty} \frac{\Gamma(\gamma + k) z^k}{k! \Gamma(\alpha k + \beta)}, \quad z \in \mathbb{C}\ , \tag{2}$$

and studied integral equations of convolution type with $E^{\gamma}_{\alpha,\beta}(z)$ in the kernel.

This function can be defined also for complex parameters α, β and γ under the restriction $\Re\alpha > 0$ and it is an entire function of order $(\Re\alpha)^{-1}$. It is, moreover, a generalization of (1) since $E^{1}_{\alpha,\beta}(z) = E_{\alpha,\beta}(z)$. Nowadays, $E^{\gamma}_{\alpha,\beta}(z)$ is commonly known as the three parameter ML function or Prabhakar function.

The Prabhakar function (2) provides an explicit formulation of the derivatives of the standard ML function (1) since for any $k \in \mathbb{N}$ it is $D^k E_{\alpha,\beta}(z) = k! E^{k+1}_{\alpha,\alpha k+\beta}(z)$ (we refer to the monograph [6] for a comprehensive analysis of the ML functions).

In applications it is usually used a further generalization of (2) given by

$$e^{\gamma}_{\alpha,\beta}(t;\lambda) = t^{\beta-1} E^{\gamma}_{\alpha,\beta}(t^{\alpha}\lambda) \ , \tag{3}$$

where $\lambda \in \mathbb{C}$ is a parameter and $t > 0$ the independent real variable. For the practical computation of $e^{\gamma}_{\alpha,\beta}(t;\lambda)$ formulas (2–3) can be used only for t very close to the origin. An asymptotic expansion holding for large values of t has been derived in [7] for real and negative λ according to

$$e^{\gamma}_{\alpha,\beta}(t;\lambda) = \begin{cases} t^{\beta-\alpha\gamma-1} \displaystyle\sum_{k=0}^{\infty} \binom{-\gamma}{k} \frac{t^{-\alpha k} |\lambda|^{\gamma-k}}{\Gamma(\beta-\alpha k-\alpha\gamma)} & \text{if } \beta \neq \alpha\gamma \\ \displaystyle\sum_{k=1}^{\infty} \binom{-\gamma}{k} \frac{t^{-\alpha k-1} |\lambda|^{\gamma-k}}{\Gamma(-\alpha k)} & \text{if } \beta \neq \alpha\gamma \ . \end{cases}$$

For values of t in a intermediate range both asymptotic expansions (for large and small values) usually fail to provide acceptable results. For this reason a method based on the numerical inversion of the Laplace transform (LT) has been presented in [8]. This method, which allows to compute the Prabhakar function in an accurate way, presents some advantages because the LT of (3) is much more simple than the function itself. One can indeed verify that the following LT pair holds [3, 6]

$$e^{\gamma}_{\alpha,\beta}(t;\lambda) \div \frac{s^{\alpha\gamma-\beta}}{(s^{\alpha}-\lambda)^{\gamma}}, \quad \Re(s) > 0, \quad |\lambda s^{-\alpha}| < 1 \ .$$

By using the LT, it is also simple to verify that the integral of the Prabhakar function is

$$\int_0^t e^{\gamma}_{\alpha,\beta}(u;\lambda)\,\mathrm{d}u = e^{\gamma}_{\alpha,\beta+1}(t;\lambda) \tag{4}$$

and a term by term derivation of the series in (2) allows to compute

$$\frac{\mathrm{d}}{\mathrm{d}t} e^{\gamma}_{\alpha,\beta}(t;\lambda) = e^{\gamma}_{\alpha,\beta-1}(t;\lambda) \ . \tag{5}$$

3 Anomalous Dielectrics and the Prabhakar Derivative

In recent years, applications of the Prabhakar function have been recognized in several fields, ranging from astronomy [9] to physics [10], quantum mechanics [11] and so on. One of the most interesting applications is however related to the description of the relaxation properties of anomalous dielectric materials.

In 1967 a new model of dielectric relaxation, known as Havriliak–Negami (HN), was proposed [1] with the aim of describing in a more realistic way non-typical

behaviours experimentally observed in certain classes of polymers. The complex susceptibility of the HN model (formulated in the frequency domain) is

$$\hat{\chi}(\omega) = \frac{1}{\left(1 + (\mathrm{i}\omega\tau)^{\alpha}\right)^{\gamma}},$$

where τ is the relaxation time and α and γ two real parameters accounting respectively for the asymmetry in the shape of the permittivity spectrum and the broadness of the response. Usually it is assumed $0 < \alpha, \gamma < 1$, although in [7, 12] the extension to $0 < \alpha, \alpha\gamma < 1$ has been also considered.

The HN model generalizes and extends the more familiar Debye and Cole-Cole models for which, however, it is also available a representation in the time-domain by means of differential operators of integer and fractional order. Finding differential operators for the HN model is instead less immediate and the research in this field is still at a very early stage.

From a formal point of view, the relationship in the frequency-domain

$$\hat{y}(\omega) = \hat{\chi}(\omega)\hat{f}(\omega)$$

(in dielectric applications $\hat{y}$ is the polarization and $\hat{f}$ the electric field) is formulated in the time-domain as

$$\left({}_0D_t^{\alpha} + \lambda\right)^{\gamma} y(t) = \frac{1}{\tau^{\alpha\gamma}} f(t)\,,$$

where $\lambda = \tau^{-\alpha}$ and $\left({}_0D_t^{\alpha} + \lambda\right)^{\gamma}$ is just a symbol to denote the fractional pseudo-differential operator resulting from the Fourier inversion of $\left((\mathrm{i}\omega)^{\alpha} + \lambda\right)^{\gamma}$.

Over the years some attempts have been made to provide robust and practical characterizations of $\left({}_0D_t^{\alpha} + \lambda\right)^{\gamma}$. In [13] it was derived

$$\left({}_0D_t^{\alpha} + \lambda\right)^{\gamma} = \exp\left(-\frac{t\lambda}{\alpha}\,{}_0D_t^{1-\alpha}\right) {}_0D_t^{\alpha\gamma} \exp\left(\frac{t\lambda}{\alpha}\,{}_0D_t^{1-\alpha}\right)\,,$$

where the exponential of the Riemann–Liouville (RL) derivative ${}_0D_t^{1-\alpha}$ must be intended in terms of a series representation; the expansion

$$\left({}_0D_t^{\alpha} + \tau^{-\alpha}\right)^{\gamma} = \sum_{k=0}^{\infty} \binom{\gamma}{k} \lambda^k\, {}_0D_t^{\alpha(\gamma-k)};$$

was instead considered in [14, 15] and successively used for numerical simulations in [16]. In both approaches, however, the criteria for truncating the series in order to achieve a given accuracy are not completely clear.

Recently, Garra et al. [2] worked on the integral representation obtained by inversion of the Laplace transform and proposed the following characterization

$$\left({}_0D_t^{\alpha}+\lambda\right)^{\gamma} y(t)=\frac{\mathrm{d}}{\mathrm{d}t}\int_{t_0}^{t} e_{\alpha,1-\alpha\gamma}^{-\gamma}(t-\tau;-\lambda)y(\tau)\,\mathrm{d}\tau\ , \tag{6}$$

where $e_{\alpha,1-\alpha\gamma}^{-\gamma}(t-\tau;-\lambda)$ is the Prabhakar function introduced in the previous section. A regularization in the Caputo sense has also been introduced in [2] according to

$$\left({}_0^{\mathrm{C}}D_t^{\alpha}+\lambda\right)^{\gamma} y(t)=\int_{0}^{t} e_{\alpha,1-\alpha\gamma}^{-\gamma}(t-\tau;-\lambda)y'(\tau)\,\mathrm{d}\tau\ , \tag{7}$$

and it has been shown that (7) is related to (6) by the relationship

$$\left({}_0^{\mathrm{C}}D_t^{\alpha}+\lambda\right)^{\gamma} y(t)=\left({}_0D_t^{\alpha}+\lambda\right)^{\gamma}\left(y(t)-y(0)\right)\ . \tag{8}$$

The derivatives (6) and (7) are clearly generalizations of the classical fractional derivatives of RL and Caputo type. Indeed, since by the Euler's reflection formula $1/\Gamma(-1)=0$, it is immediate to verify that $e_{\alpha,1-\alpha}^{-1}(t;0)=t^{1-\alpha}/\Gamma(1-\alpha)$ and hence when $\gamma=1$ and $\lambda=0$ the derivative (6) coincides with the RL derivative and (7) with the fractional Caputo derivative.

An integral operator $\left({}_0J_t^{\alpha}+\lambda\right)^{\gamma}$ inverting the derivative (6) has been also considered in [2] as

$$\left({}_0J_t^{\alpha}+\lambda\right)^{\gamma} f(t)=\int_{0}^{t} e_{\alpha,\alpha\gamma}^{\gamma}(t-u;-\lambda)f(u)\,\mathrm{d}u\ , \tag{9}$$

thus generalizing the classical RL integral of order α when $\gamma=1$ and $\lambda=0$.

More recently, a further formulation of $\left({}_0D_t^{\alpha}+\lambda\right)^{\gamma}$ has been proposed in terms of fractional differences of Grünwald–Letnikov type [17]

$$\left({}_0D_t^{\alpha}+\lambda\right)^{\gamma} y(t)=\lim_{h\to 0}\frac{(1+h^{\alpha}\lambda)^{\gamma}}{h^{\alpha\gamma}}\sum_{k=0}^{\infty}\Omega_k^{(\alpha,\gamma)}y(t-kh)\ , \tag{10}$$

where

$$\Omega_0^{(\alpha,\gamma)}=1,\quad \Omega_k^{(\alpha,\gamma)}=\frac{1}{1+h^{\alpha}\lambda}\sum_{j=1}^{k}(-1)^j\binom{\alpha}{j}\left(\frac{(1+\gamma)j}{k}-1\right)\Omega_{k-j}^{(\alpha,\gamma)}\ .$$

4 A Product Integration Rule

Let us consider the initial value problem for the pseudo fractional differential equation of Havriliak–Negami type

$$\begin{cases}\left({}_0^{\mathrm{C}}D_t^{\alpha}+\lambda\right)^{\gamma} y(t)=f(t,y(t))\\ y(0)=y_0\end{cases}\ , \tag{11}$$

where $f(t, y)$ is assumed Lipschitz continuous with respect to the second argument. The non-linearity in (11) is motivated by the fact that, in the dielectric applications the right side f is the electric field which, by the Maxwell equations, itself depends on the polarization y. Thanks to (9), the above fractional pseudo-differential equation can be reformulated in the integral form

$$y(t) = y_0 + \left({}_0J_t^{\alpha} + \lambda\right)^{\gamma} f(t, y(t)) \ .$$

In order to numerically approximate the solution of (11) we consider a grid-mesh $t_j = jh$, with a constant step-size $h > 0$. After rewriting, at $t = t_n$, the above integral equation in the piece-wise form

$$y_n = y_0 + \sum_{j=1}^{n} \int_{t_{j-1}}^{t_j} e^{\gamma}_{\alpha,\alpha\gamma}(t_n - u; -\lambda) f(u, y(u)) \, \mathrm{d}u \ ,$$

the vector field $f(u, y(u))$ is approximate, on each interval $[t_{j-1}, t_j]$, by interpolating polynomials and the resulting integrals are evaluated in an exact way. This technique, which is named as product-integration, has been firstly proposed in [18] for the numerical solution of weakly singular Volterra integral equations and hence successfully applied to fractional differential equations [19].

The simplest method of this type is obtained by considering the constant approximation $f(u, y(u)) \equiv f(t_j, y_j)$ on each interval $[t_{j-1}, t_j]$. Since it is

$$\int_{t_{j-1}}^{t_j} e^{\gamma}_{\alpha,\alpha\gamma}(t_n - u; -\lambda) \, \mathrm{d}u = \int_{t_{j-1}}^{t_n} e^{\gamma}_{\alpha,\alpha\gamma}(t_n - u; -\lambda) \, \mathrm{d}u - \int_{t_j}^{t_n} e^{\gamma}_{\alpha,\alpha\gamma}(t_n - u; -\lambda) \, \mathrm{d}u \ ,$$

by applying (4) we obtain

$$\int_{t_{j-1}}^{t_j} e^{\gamma}_{\alpha,\alpha\gamma}(t_n - u; -\lambda) \, \mathrm{d}u = e^{\gamma}_{\alpha,\alpha\gamma+1}(t_n - t_{j-1}; -\lambda) - e^{\gamma}_{\alpha,\alpha\gamma+1}(t_n - t_j; -\lambda)$$

and, since $e^{\gamma}_{\alpha,\alpha\gamma+1}(t_n - t_j; -\lambda) = h^{\alpha\gamma} e^{\gamma}_{\alpha,\alpha\gamma+1}(n - j; -h^{\alpha}\lambda)$, the corresponding numerical scheme, which can be considered as a generalization of the implicit Euler method, reads as

$$y_n = y_0 + h^{\alpha\gamma} \sum_{j=1}^{n} w^{\alpha,\gamma}_{n-j} f(t_j, y_j) \ , \tag{12}$$

where

$$w^{\alpha,\gamma}_n = e^{\gamma}_{\alpha,\alpha\gamma+1}(n + 1; -h^{\alpha}\lambda) - e^{\gamma}_{\alpha,\alpha\gamma+1}(n; -h^{\alpha}\lambda) \ . \tag{13}$$

In the following we will assume that the exact solution of (11) admits an asymptotic expansion in mixed powers of integer order and fractional order, i.e.

$$y(t) = y_0 + \sum_{j=1}^{\infty} c_j t^j + \sum_{j=1}^{\infty} d_j t^{\alpha\gamma j} \tag{14}$$

for some sequences of real coefficients c_j and d_j. To the best of authors' knowledge, there exist no theoretical results on this subject; anyway, the assumption (14) appears reasonable and by no means restrictive since it is congruent with the asymptotic expansion of the solution of simpler weakly singular convolution integral equations (e.g., see [20]).

Theorem 1 *Let $0 < \alpha, \alpha\gamma < 1$, $\lambda > 0$ and assume that the solution $y(t)$ of (11) admits the expansion (14). For any $h > 0$ there exist two positive constants C_1 and C_2 (which do not depend on h) such that*

$$|y(t_n) - y_n| \le C_1 h + C_2 t_n^{\alpha\gamma-1} h^{1+\alpha\gamma} \ .$$

Proof The proof will follow very closely the proof of Theorem 2.1 in [21]. After writing, at $t = t_n$, the exact solution of (11) as

$$y(t_n) = y_0 + h^{\alpha\gamma} \sum_{j=1}^{n} w_{n-j}^{\alpha,\gamma} f(t_j, y(t_j)) + R_n \ , \tag{15}$$

where R_n is the quadrature error

$$R_n = \sum_{j=1}^{n} \int_{t_{j-1}}^{t_j} e_{\alpha,\alpha\gamma}^{\gamma}(t_n - u; -\lambda)\big(f(u, y(u)) - f(t_j, y(t_j))\big)\, \mathrm{d}u \ ,$$

we subtract (12) from (15) and, thanks to the Lipschitzianity of f, for a constant $L > 0$ it is

$$|y(t_n) - y_n| < |R_n| + L \sum_{j=1}^{n} |w_{n-j}^{\alpha,\gamma}| \cdot |y(t_j) - y_j| \ .$$

We put $M_1 = \sup_{0<t<T} E_{\alpha,\alpha\gamma}(-t^\alpha \lambda)$ (the Prabhakar function is indeed bounded [3]) and by using again the Lipschitzianity of f we obtain

$$|R_n| \le M_1 L \sum_{j=1}^{n} \int_{t_{j-1}}^{t_j} \big(t_n - u\big)^{\alpha\gamma-1} \big|y(u) - y(t_j)\big|\, \mathrm{d}u \ ,$$

Note now that $w_1^{\alpha,\gamma} = E_{\alpha,\alpha\gamma}^{\gamma}(-\lambda)$ while for $n > 1$ the Taylor expansion, together with (5), immediately leads to

$$w_n^{\alpha,\gamma} = e_{\alpha,\alpha\gamma}(n + 1 - v; -h^\alpha \lambda), \quad v \in [0, 1]$$

and hence

$$w_n^{\alpha,\gamma} \le M_1 \frac{(n+1-v)^{\alpha\gamma-1}}{\Gamma(\alpha\gamma)} < M_1 \frac{n^{\alpha\gamma-1}}{\Gamma(\alpha\gamma)}$$

from which we infer

$$|y(t_n) - y_n| < |R_n| + M_1 L \sum_{j=1}^{n} (n-j)^{\alpha\gamma} |y(t_j) - y_j| \ .$$

Since $\alpha\gamma < 1$ and the expansion (14), close to the origin it is $|y(u) - y(t_j)| \le M_2 h^{\alpha\gamma}$; away from the origin $y(u)$ is instead smooth and, by the remainder of the polynomial interpolation, it is $|y(u) - y(t_j)| \le M_3 h$. Therefore, given $r \in \mathbb{N}$ such that $y(u)$ can be assumed non smooth for $u \le t_r$ and smooth elsewhere, we have

$$\begin{aligned} |R_n| &\le M_1 L \Big(M_2 h^{\alpha\gamma} \sum_{j=1}^{r-1} \int_{t_{j-1}}^{t_j} \big(t_n - u\big)^{\alpha\gamma-1} \, \mathrm{d}u + M_3 h \sum_{j=r}^{n} \int_{t_{j-1}}^{t_j} \big(t_n - u\big)^{\alpha\gamma-1} \, \mathrm{d}u \Big) \\ &\le M_4 h^{1+\alpha\gamma} t_n^{\alpha\gamma-1} + M_5 h \quad , \end{aligned}$$

and the proof follows in the same way as the proof of Theorem 2.1 in [21]. □

An explicit counterpart of the method (12) can be devised by using in each interval $[t_{j-1}, t_j]$ the approximation $f(u, y(u)) \equiv f(t_{j-1}, y_{j-1})$. The resulting method is

$$y_n = y_0 + h^{\alpha\gamma} \sum_{j=0}^{n-1} w_{n-j-1}^{\alpha,\gamma} f(t_j, y_j) \tag{16}$$

and convergence properties can be proved in a similar way as in Theorem 1.

5 Numerical Experiments

To numerically test the product integration method devised in Sect. 4, we first consider the linear test equation

$$\left({}_0^{\mathrm{C}}D_t^{\alpha} + \lambda\right)^{\gamma} y(t) = -2y(t) + \cos(2\pi t), \quad y(0) = 1 \ . \tag{17}$$

Since the exact solution is not known in an analytical form, for reference we will use the solution obtained by truncating the Grünwald–Letnikov formula (10) with a smaller step-size h. Thanks to the first order convergence of this method [17], it can be considered accurate enough to be used for reference. For some parameters α, γ and λ the solution of this problem is presented in Fig. 1 (all the experiments are made

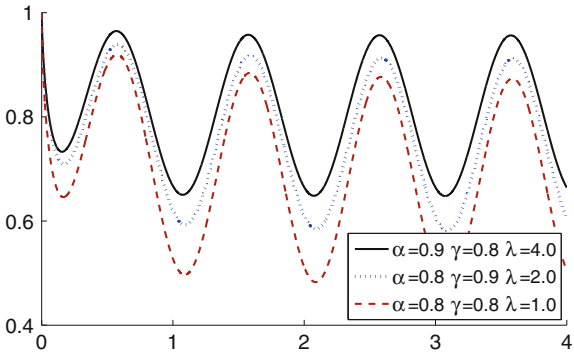

Fig. 1 Solution of the problem (17) for some values of α, γ and λ

by using Matlab and the Prabhakar function for the weights of the rule is evaluated by means of the `ml.m` code devised in [8]).

In Table 1 we report the error $E_h = |y(t_n) - y_n|$ and the estimated order of convergence (EOC) evaluated as $\log_2(E_h/E_{h/2})$ resulting from the application of the product-integration method described in Sect. 4. As we can readily observe, convergence of the first order is clearly achieved, thus confirming the theoretical findings of Theorem 1.

For a second test problem we consider the nonlinear equation

$$\left({}_0^{\mathrm{C}}D_t^{\alpha} + \lambda\right)^{\gamma} y(t) = t^2 - \left(y(t)\right)^2, \quad y(0) = 1 \ , \tag{18}$$

whose solutions are shown in Fig. 2.

Also in this case the theoretical results on the first order convergence are confirmed by the numerical experiments as reported in Table 2, thus validating the effectiveness of the approach proposed in this work.

Table 1 Errors and EOC for problem (17) at $t = 4.0$

h	$\alpha = 0.9 \quad \gamma = 0.8 \quad \lambda = 4.0$		$\alpha = 0.8 \quad \gamma = 0.9 \quad \lambda = 2.0$		$\alpha = 0.8 \quad \gamma = 0.8 \quad \lambda = 1.0$	
	Error	EOC	Error	EOC	Error	EOC
2^{-5}	4.01×10^{-3}		4.08×10^{-3}		3.57×10^{-3}	
2^{-6}	2.02×10^{-3}	0.987	2.04×10^{-3}	0.999	1.73×10^{-3}	1.049
2^{-7}	1.01×10^{-3}	1.000	1.01×10^{-3}	1.008	8.35×10^{-4}	1.047
2^{-8}	5.04×10^{-4}	1.004	5.04×10^{-4}	1.009	4.06×10^{-4}	1.039
2^{-9}	2.51×10^{-4}	1.005	2.51×10^{-4}	1.008	1.99×10^{-4}	1.030
2^{-10}	1.25×10^{-4}	1.004	1.25×10^{-4}	1.006	9.80×10^{-5}	1.022

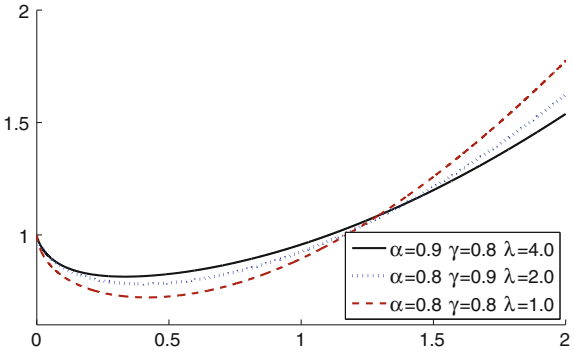

Fig. 2 Solution of the problem (18) for some values of α, γ and λ

Table 2 Errors and EOC for problem (18) at $t = 2.0$

h	$\alpha = 0.9 \quad \gamma = 0.8 \quad \lambda = 4.0$		$\alpha = 0.8 \quad \gamma = 0.9 \quad \lambda = 2.0$		$\alpha = 0.8 \quad \gamma = 0.8 \quad \lambda = 1.0$	
	Error	EOC	Error	EOC	Error	EOC
2^{-5}	6.79×10^{-3}		7.09×10^{-3}		6.62×10^{-3}	
2^{-6}	3.52×10^{-3}	0.947	3.64×10^{-3}	0.961	3.39×10^{-3}	0.965
2^{-7}	1.80×10^{-3}	0.968	1.85×10^{-3}	0.976	1.72×10^{-3}	0.978
2^{-8}	9.12×10^{-4}	0.981	9.34×10^{-4}	0.986	8.70×10^{-4}	0.986
2^{-9}	4.60×10^{-4}	0.989	4.70×10^{-4}	0.992	4.37×10^{-4}	0.991
2^{-10}	2.31×10^{-4}	0.993	2.36×10^{-4}	0.995	2.20×10^{-4}	0.994

6 Concluding Remarks

In this paper we have discussed the problem of numerically solving differential equations with Prabhakar derivatives; problems of this kind arise in the simulation of anomalous relaxation properties in Havriliak–Negami models.

We have devised a product-integration rule with weights expressed in terms of the Prabhakar function and studied the convergence properties. By means of some numerical experiments the effectiveness of the proposed approach has been illustrated. As far as we know, this is one of the very few methods available for solving problems of this kind.

References

1. Havriliak, S., Negami, S.: A complex plane representation of dielectric and mechanical relaxation processes in some polymers. Polymer **8**, 161–210 (1967)
2. Garra, R., Gorenflo, R., Polito, F., Tomovski, Ž.: Hilfer-Prabhakar derivatives and some applications. Appl. Math. Comput. **242**, 576–589 (2014)

3. Prabhakar, T.R.: A singular integral equation with a generalized Mittag-Leffler function in the kernel. Yokohama Math. J. **19**, 7–15 (1971)
4. Mittag-Leffler, M.G.: Sur l'intégrale de Laplace-Abel. C. R. Acad. Sci. Paris (Ser. II) **136**, 937–939 (1902)
5. Wiman, A.: Über den fundamental satz in der teorie der funktionen $E_\alpha(x)$. Acta Math. **29**(1), 191–201 (1905)
6. Gorenflo, R., Kilbas, A.A., Mainardi, F., Rogosin, S.: Mittag-Leffler Functions, Related Topics and Applications. Springer, Berlin (2014)
7. Mainardi, F., Garrappa, R.: On complete monotonicity of the Prabhakar function and non-Debye relaxation in dielectrics. J. Comput. Phys. **293**, 70–80 (2015)
8. Garrappa, R.: Numerical evaluation of two and three parameter Mittag-Leffler functions. SIAM J. Numer. Anal. **53**(3), 1350–1369 (2015)
9. An, J., Van Hese, E., Baes, M.: Phase-space consistency of stellar dynamical models determined by separable augmented densities. Mon. Not. R. Astron. Soc. **422**(1), 652–664 (2012)
10. Saxena, R., Pagnini, G.: Exact solutions of triple-order time-fractional differential equations for anomalous relaxation and diffusion I: the accelerating case. Phys. A: Stat. Mech. Appl. **390**(4), 602–613 (2011)
11. Chaurasia, V., Singh, J.: Application of Sumudu transform in Schrödinger equation occurring in quantum mechanics. Appl. Math. Sci. **4**(57–60), 2843–2850 (2010)
12. Havriliak, S. Jr., Havriliak, S.: Results from an unbiased analysis of nearly 1000 sets of relaxation data. J. Non-Cryst. Solids (PART 1) **172–174**, 297–310 (1994)
13. Nigmatullin, R., Ryabov, Y.: Cole-Davidson dielectric relaxation as a self-similar relaxation process. Phys. Solid State **39**(1), 87–90 (1997)
14. Novikov, V., Wojciechowski, K., Komkova, O., Thiel, T.: Anomalous relaxation in dielectrics. Equations with fractional derivatives. Mater. Sci. Pol. **23**(4), 977–984 (2005)
15. Weron, K., Jurlewicz, A., Magdziarz, M.: Havriliak-Negami response in the framework of the continuous-time random walk. Acta Phys. Pol. B **36**(5), 1855–1868 (2005)
16. Bia, P., Caratelli, D., Mescia, L., Cicchetti, R., Maione, G., Prudenzano, F.: A novel FDTD formulation based on fractional derivatives for dispersive Havriliak-Negami media. Signal Process. **107**, 312–318 (2015)
17. Garrappa, R.: Grünwald-Letnikov operators for fractional relaxation in Havriliak-Negami models. Commun. Nonlinear Sci. Numer. Simul. **38**, 178–191 (2016)
18. Young, A.: Approximate product-integration. Proc. R. Soc. Lond. Ser. A. **224**, 552–561 (1954)
19. Diethelm, K., Ford, N.J., Freed, A.D.: Detailed error analysis for a fractional Adams method. Numer. Algorithms **36**(1), 31–52 (2004)
20. Lubich, C.: Runge-Kutta theory for Volterra and Abel integral equations of the second kind. Math. Comput. **41**(163), 87–102 (1983)
21. Dixon, J.: On the order of the error in discretization methods for weakly singular second kind Volterra integral equations with nonsmooth solutions. BIT **25**(4), 624–634 (1985)

Finite Element Method for Time Fractional Keller–Segel Chemotaxis System

Arumugam Gurusamy

Abstract In this paper, we consider finite element method for time fractional Keller–Segel chemotaxis system. The existence and uniqueness of solutions are proved by using the Schauder's fixed point theorem. The error estimate of the discrete solution is also established.

Keywords Fractional derivative · Existence of solutions · Finite element method · Error estimate

1 Introduction

In recent years, growing attention has been focused on fractional differential equations because they can provide a better approach to describe the complex phenomena in nature, such as viscoelastic materials, anomalous diffusion, signal processing and control theory, etc. Some of the most applications are given in the book of Oldham and Spanier [1], the book of Podlubny [2] and the papers of Bagley and Trovik [3]. Compared to classical integer–order differential equations, the theoretical investigations and establishment of numerical schemes for fractional-order (or fractional for brevity) versions are more complicated due to the special properties of fractional differential operators, such as the non-locality, history dependence, and/or long-range interactions. In general, the fractional partial differential equations (PDEs) can be classified as three categories: time fractional PDEs [4–6], space fractional PDEs [7–9] and space–time fractional PDEs [10]. Chemotaxis is the directed movement of cells as a response to gradients of a chemical signal substance. In 1970 Keller and Segel proposed a mathematical model for the description of such a phenomenon; it takes into account two parabolic differential equations. The main purpose of this paper is to develop a numerical method for a class of time fractional Keller–Segel chemotaxis models.

A. Gurusamy (✉)
DRDO-BU Center for Life Sciences, Bharathiar University Campus,
Coimbatore 641046, India
e-mail: guru.poy@gmail.com

A. Babiarz et al. (eds.), *Theory and Applications of Non-integer Order Systems*,
Lecture Notes in Electrical Engineering 407, DOI 10.1007/978-3-319-45474-0_39

In this paper, we begin with the time fractional Keller–Segel chemotaxis system which can be written in the dimensionless form as:

$$\left.\begin{aligned} \frac{\partial^\alpha u}{\partial t^\alpha} - d_1 \Delta u - \delta \nabla \cdot (\psi(u) \nabla v) = f \quad \text{in } x \in \Omega \times (0, T), \\ \frac{\partial^\alpha v}{\partial t^\alpha} - d_2 \Delta v = \alpha u - \beta v \quad \text{in } x \in \Omega \times (0, T), \end{aligned}\right\} \tag{1}$$

where d_1, d_2, δ, α and β are the positive constants and also we assume that chemotaxis sensitivity function $\psi(u) = \nabla u$. Here, $u(x, t)$ denotes the cell density, $v(x, t)$ stands for a chemoattractant concentration, δ is a chemotactic sensitivity constant and also f is a source term. This system (1) with zero flux boundary conditions and initial conditions

$$\nabla u \cdot \mathbf{n} = \nabla v \cdot \mathbf{n} = 0 \ \text{ on } \partial\Omega, \tag{2}$$

$$u(\cdot, 0) = u_0 \ \text{ and } \ v(\cdot, 0) = v_0 \ \text{ in } \Omega. \tag{3}$$

where $\Omega \subset \mathbb{R}^d$ is a polygonal domain. This system (1) has been discussed theoretically in several papers when $\psi(u) = u$ and $\alpha = 1$. Liu et. al., studied H^1-Galerkin mixed finite element method for time fractional reaction–diffusion equation in [11]. The optimal time convergence order $O(\Delta t^{2-\alpha})$ and the optimal spatial rate of convergence in H^1 and L^2-norms for variable$u$ and its gradient s are derived. The moving finite element methods are studied for a class of time-dependent space fractional differential equations in [12]. As far as our general analysis is concerned, in this investigation we are interested to introduce the gradient of the cell density in the chemotaxis sensitivity function of the original Keller–Segel model. Throughout in this paper $\frac{\partial^\alpha u}{\partial t^\alpha}$ is Caputo fractional-order derivative operator defined by

$$\frac{\partial^\alpha u}{\partial t^\alpha} = \frac{1}{\Gamma(1-\alpha)} \int_0^t \frac{\partial u(x, \tau)}{\partial \tau} \frac{\mathrm{d}\tau}{(t-\tau)^\alpha}, \tag{4}$$

where $0 < \alpha < 1$.

The layout of the paper is as follows. Section 1 is introductory in nature. In Sect. 2, we formulate the weak formulation of the time fractional Keller–Segel chemotaxis system (1). In Sect. 3, we introduce the conforming finite element formulation of the corresponding continuous weak formulation which is derived in the previous section. Finally, in Sect. 4, we derive the existence, uniqueness and error estimate of the discrete solutions of (1).

2 Weak Formulations

In this section, the weak formulation and some auxiliary results are presented.

Let $L^2(\Omega)$, $H_0^1(\Omega)$, denote the usual Sobolev spaces equipped with the norms $\|\cdot\|_{L^2(\Omega)}$, $\|\cdot\|_{H_0^1(\Omega)}$ respectively. Denote $H_0^1(\Omega) := \{v \in H^1(\Omega), v|_{\partial\Omega} = 0\}$.

The weak formulation corresponding to (1) is given by: seek $u, v \in X := H_0^1(\Omega)$ such that

$$a(u, \varphi) + b(u, v, \varphi) = l_1(\varphi) \ \ \forall \varphi \ \in X, \tag{5}$$

$$a(v, \psi) + l_2(u, v, \psi) = 0 \ \ \forall \ \psi \in X, \tag{6}$$

where $\forall \eta, \zeta, \chi \in X$,

$$a(\eta, \zeta) := \int_\Omega {}_0D_t^\alpha \eta \zeta \mathrm{d}x + d_i \int_\Omega \nabla\eta \cdot \nabla\zeta \mathrm{d}x, \ i = 1, 2. \tag{7}$$

$$b(\eta, \zeta, \chi) := \int_\Omega \delta \nabla\eta \nabla\zeta \cdot \nabla\chi \mathrm{d}x, \tag{8}$$

$$l_1(\zeta) := (f, \zeta) \quad l_2(\eta, \zeta, \chi) := \int_\Omega (\eta - \zeta)\chi \mathrm{d}x. \tag{9}$$

In the sequel, let $C_0^\infty(0, T)$ denote the space of all infinitely differentiable functions on $(0, T)$ with compact support in $(0, T]$. Then we introduce the following Sobolev space ${}_0H^\alpha(0, T)$, $0 < \alpha < 1$ which is the closure of ${}_0C^\infty(0, T)$ equipped with the norm $\|\cdot\|_{H^\alpha(0,T)}$, where $\|\cdot\|_{H^\alpha(0,T)}$ denotes the norm in the usual fractional Sobolev space $H^\alpha(0, T)$. Further, define the space with $0 < \alpha < 1$,

$$B^\alpha((0, T) \times \Omega) = {}_0H^\alpha((0, T), L_2(\Omega)) \cap L_2((0, T), H_0^1(\Omega)), \tag{10}$$

where $B^\alpha((0, T) \times \Omega)$ is a Banach space with respect to the norm

$$\|v\|_{B^\alpha((0,T)\times\Omega)} = \left(\|v\|_{H^\alpha((0,T),L^2(\Omega))} + \|v\|_{L^2((0,T),H_0^1(\Omega))}\right)^{1/2}.$$

An equivalent compact vector form corresponding to (5) and (6) is given by: for given $f \in L^2(\Omega)$, seek $\Psi = (u, v) \in \mathcal{K} := X \times X$ such that

$$\mathcal{G}(\Psi, \Phi) := A(\Psi, \Phi) + B(\Psi, \Psi, \Phi) = \mathcal{L}(\Psi, \Psi, \Phi) \ \ \forall \ \Phi \in \mathcal{K}, \tag{11}$$

where $\forall \ \Xi = (\eta_1, \eta_2)$, $\Theta = (\theta_1, \theta_2)$ and $\Phi = (\varphi_1, \varphi_2) \in \mathcal{K}$,

$$A(\Theta, \Phi) := a(\theta_1, \varphi_1) + a(\theta_2, \varphi_2), \tag{12}$$
$$B(\Xi, \Theta, \Phi) := b(\eta_1, \theta_2, \varphi_1), \tag{13}$$
$$\mathcal{L}(\Theta, \Theta, \Phi) := (f, \varphi_1) + (\theta_1 - \theta_2, \varphi_2). \tag{14}$$

The properties of boundedness and coercivity of $A(\cdot, \cdot)$, boundedness of $B(\cdot, \cdot, \cdot)$ and $\mathcal{L}(\cdot, \cdot, \cdot)$ can be easily verified:

$$A(\Theta, \Phi) \leq \|\Theta\|_{H^{\alpha/2}} \|\Phi\|_{H^{\alpha/2}} + \|\Theta\|_{L^2} \|\Phi\|_{L^2}, \tag{15}$$
$$A(\Theta, \Theta) \geq C \|\Theta\|_{H^{\alpha/2}} + \|\Theta\|_{L^2}, \tag{16}$$
$$B(\Xi, \Theta, \Phi) \leq C \|\Xi\|_{L^2} \|\Theta\|_{L^2} \|\Phi\|_{L^2}. \tag{17}$$

A linearization of $\mathcal{G}$ around Ψ in the direction Θ is defined as follows:

$$\mathcal{F}(\Theta, \Phi) := A(\Theta, \Phi) + 2B(\Psi, \Theta, \Phi). \tag{18}$$

3 Conforming Finite Element Methods

Let $\mathcal{T}_h$ be a regular and conforming triangulation of $\overline{\Omega}$ into closed triangles. Let us define the mesh discretization parameter as $h := \max_{T \in \mathcal{T}_h} h_T$. The conforming finite element space is defined as

$$\mathcal{V}_h = \left\{ v \in H^1(\Omega) : v|_T \in \mathcal{T}_h \text{ with } \left.\frac{\partial v}{\partial \nu}\right|_{\partial\Omega} = 0 \right\} \subset H_0^1(\Omega). \tag{19}$$

The conforming finite element formulations corresponding to (6) is defined by: seek $u_h, v_h \in \mathcal{V}_h$ such that

$$a(u_h, \varphi) + b(u_h, v_h, \varphi) = l_1(\varphi) \ \ \forall \varphi \ \in \mathcal{V}_h, \tag{20}$$
$$a(v_h, \psi) + l_2(u_h, v_h, \psi) = 0 \ \ \forall \ \psi \in \mathcal{V}_h, \tag{21}$$

where $a(\cdot, \cdot)$, $b(\cdot, \cdot, \cdot)$, $l_1(\cdot)$ and $l_2(\cdot, \cdot, \cdot)$ are already defined in (7)–(9). An equivalent vector formulation can also be defined as: seek $\Psi_h \in \mathcal{K}_h := \mathcal{V}_h \times \mathcal{V}_h$ such that

$$A(\Psi_h, \Phi) + B(\Psi_h, \Psi_h, \Phi) = \mathcal{L}(\Psi_h, \Psi_h, \Phi) \ \ \forall \ \Phi \in \mathcal{K}_h, \tag{22}$$

where $A(\cdot, \cdot)$, $B(\cdot, \cdot, \cdot)$ and $\mathcal{L}(\cdot, \cdot, \cdot)$ are already defined.

Lemma 1 *Let $\Pi_h : \mathcal{V} \longrightarrow \mathcal{V}$ be the interpolation operator. Then for $\phi \in B^{\alpha/2}((0, T) \times \Omega)$, $0 < \alpha < 1$, it holds:*

$$\|\phi - \Pi_h \phi\|_m \leq C h^{min\{k+1, \alpha/2\} - m} \|\phi\|_{\alpha/2}, for \ \ m = 0, 1, 2. \tag{23}$$

Lemma 2 *If the bilinear form $\mathcal{F}(\cdot,\cdot)$ is nonsingular on $\mathcal{K}\times\mathcal{K}$, then the bilinear form defined by*

$$\mathcal{F}(\Theta,\Phi) := A(\Theta,\Phi) + 2B(\Pi_h\Psi,\Theta,\Phi), \tag{24}$$

is nonsingular on $\mathcal{K}_h\times\mathcal{K}_h$.

4 Existence, Uniqueness and Error Estimate

In this section, we establish that the results concerning the existence, uniqueness and error estimate in $B^{\alpha/2}$ of the discrete solution. For this purpose of the existence of the solution of (22), define the nonlinear map $\Gamma : \mathcal{K}_h \to \mathcal{K}_h$ by

$$\tilde{\mathcal{F}}(\Gamma(\Theta),\Phi) = \mathcal{L}(\Theta,\Theta,\Phi) + 2B(\Pi_h\Psi,\Theta,\Phi) - B(\Theta,\Theta,\Phi). \tag{25}$$

Now we prove contraction result fro the nonlinear map Γ and establish the existence and uniqueness of the solution Ψ_h.

Theorem 1 (Existence and uniqueness) *Let Ψ_h be an isolated solution of (11). Then, for sufficiently small h, the discrete problem (22) possesses a unique solution.*

Proof The proof of this theorem is given in the following 3 steps.

Step 1: (**Mapping of ball to ball**)
Let $\mathbb{B}_R(\Pi_h\Psi) := \{\Phi\in\mathcal{K} : \|\Phi-\Pi_h\Psi\|_{B^{\alpha/2}} \le R\}$. Now we have to show that for sufficiently small mesh parameter h, the map Γ maps the ball $\mathbb{B}_R(\Pi_h\Psi)$ to itself. That is, we show that, for any $\Theta\in\mathcal{K}_h$, there exists a positive constant $R(h)$ such that

$$\|\Theta-\Pi_h\Psi\|_{B^{\alpha/2}} \le R(h) \Rightarrow \|\Gamma(\Theta)-\Pi_h\Psi\|_{B^{\alpha/2}} \le R(h). \tag{26}$$

Since $\tilde{\mathcal{F}}(\cdot,\cdot)$ is nonsingular, there exists $\overline{\Phi}\in\mathcal{K}_h$ with $\|\overline{\Phi}\|_{B^{\alpha/2}} = 1$ such that

$$\beta\|\Gamma(\Theta)-\Pi_h\Psi\|_{B^{\alpha/2}} \le \tilde{\mathcal{F}}(\Gamma(\Theta)-\Pi_h\Psi,\overline{\Phi}), \tag{27}$$

for some positive constant β independent of h. By using the definition of $\tilde{\mathcal{F}}(\cdot,\cdot)$, (11), symmetry of $B(\cdot,\cdot,\cdot)$, we obtain

$$\begin{aligned}\tilde{\mathcal{F}}(\Gamma(\Theta)-\Pi_h\Psi,\overline{\Phi}) &= \mathcal{F}(\Gamma(\Theta)-\Pi_h\Psi,\overline{\Phi})+2B(\Pi_h\Psi,\Gamma(\Theta)-\Pi_h\Psi,\overline{\Phi})\\ &= \mathcal{L}(\Theta,\Theta,\Phi)+2B(\Pi_h\Psi,\Gamma(\Theta)-\Pi_h\Psi,\overline{\Phi})-B(\Theta,\Theta,\overline{\Phi})\\ &\quad -A(\Pi_h\Psi,\overline{\Phi})\\ &= A(\Psi,\overline{\Phi})+B(\Psi,\Psi,\overline{\Phi})+2B(\Pi_h\Psi,\Theta,\overline{\Phi})-A(\Pi_h\Psi,\overline{\Phi})\\ &\quad -B(\Theta,\Theta,\overline{\Phi})-2B(\Pi_h\Psi,\Pi_h\Psi,\overline{\Phi})\\ &= A(\Psi-\Pi_h\Psi,\overline{\Phi})+B(\Psi,\Psi-\Pi_h\Psi,\overline{\Phi})\\ &\quad +B(\Psi-\Pi_h\Psi,\Pi_h\Psi,\overline{\Phi})-B(\Theta-\Pi_h\Psi,\Theta-\Pi_h\Psi,\overline{\Phi}).\end{aligned}$$

Inserting (28) into (27) and simple calculations lead to

$$\beta\|\Gamma(\Theta)-\Pi_h\Psi\|_{B^{\alpha/2}} \le C\ (h+\|\Theta-\Pi_h\Psi\|^2_{B^{\alpha}/2}). \tag{28}$$

This completes the step 1.

Step 2: (**Contraction result**)
For $\Theta_1,\Theta_2\in B_{R(h)}(\Pi_h\Psi)$, the following contraction results holds true: let $\Gamma(\Theta_i)$, $i=1,2$ be the solutions of

$$\tilde{\mathcal{F}}(\Gamma(\Theta_i),\Phi)=\mathcal{L}(\Theta_i,\Theta_i,\Phi)+2B(\Pi_h\Psi,\Theta_i,\Phi)-B(\Theta_i,\Theta_i,\Phi),\ \forall\ \Phi\in\mathcal{K}_h. \tag{29}$$

Using (29), symmetry of $B(\cdot,\cdot,\cdot)$ and boundedness in (17) and the nonsingularity of $\tilde{\mathcal{F}}$, we obtain

$$\begin{aligned}\beta\|\Gamma(\Theta_1)-\Gamma(\Theta_2)\|_{B^{\alpha/2}} &\le \tilde{\mathcal{F}}(\Gamma(\Theta_1)-\Gamma(\Theta_2),\overline{\Phi})\\ &= 2B(\Pi_h\Psi,\Theta_1-\Theta_2,\overline{\Phi})+B(\Theta_2-\Theta_1,\Theta_2-\Theta_1,\overline{\Phi})\\ &= B(\Pi_h\Psi,\Theta_1-\Theta_2,\overline{\Phi})+B(\Pi_h\Psi,\Theta_1-\Theta_2,\overline{\Phi})\\ &\quad +B(\Theta_2,\Theta_1,\overline{\Phi})-B(\Theta_1,\Theta_1,\overline{\Phi})\\ &= B(\Theta_2-\Theta_1,\Theta_1-\Pi_h\Psi,\overline{\Phi})\\ &\quad +B(\Theta_2-\Pi_h\Psi,\Theta_2-\Theta_1,\overline{\Phi})\\ &\le C\|\Theta_2-\Theta_1\|_{B^{\alpha/2}}\big(\|\Theta_1-\Pi_h\Psi\|_{B^{\alpha/2}}\\ &\quad +\|\Theta_2-\Pi_h\Psi\|_{B^{\alpha/2}}\big).\end{aligned} \tag{30}$$

Since $\Theta_1,\Theta_2\in\mathbb{B}_{R(h)}(\Pi_h\Psi)$, we obtain

$$\|\Gamma(\Theta_1)-\Gamma(\Theta_2)\|_{B^{\alpha/2}} \le Ch\|\Theta_2-\Theta_2\|_{B^{\alpha/2}}, \tag{31}$$

for some positive constant C independent of h. This completes the proof of step 2.

Step 3: (**Existence and uniqueness results**)
By using step 1 and an appeal to Schauder fixed point theorem yield that Γ has a fixed point Ψ_h satisfying

$$\|\Psi_h - \Pi_h \Psi\|_{B^{\alpha/2}} \leq R(h). \tag{32}$$

This completes the proof of the existence and uniqueness follows from step 2.

Theorem 2 (Error estimate) *Let Ω be a polygonal domain. Let Ψ be an isolated solution of (11) and Ψ_h be the solution of (22). For sufficiently small h, there hold*

$$\|\Psi - \Psi_h\|_{B^{\alpha/2}} \leq Ch^{\alpha/2}. \tag{33}$$

where C is a positive constant independent of h.

Proof A use of triangle inequality, Lemma 1 and (32) yields the error estimate

$$\begin{aligned} \|\Psi - \Psi_h\|_{B^{\alpha/2}} &= \|\Psi - \Pi_h \Psi + \Pi_h \Psi - \Psi_h\| \\ &\leq \|\Psi - \Pi_h \Psi\|_{B^{\alpha/2}} + \|\Pi_h \Psi - \Psi_h\|_{B^{\alpha/2}} \\ &\leq Ch^{\alpha/2}. \end{aligned} \tag{34}$$

This completes the proof.

5 Conclusion

In this paper, we have used finite element method to discretise the Keller–Segel system (1) and also proved the existence and uniqueness of solutions to the discrete problem (22) by using Schauder fixed point theorem. Finally, we have presented the $B^{\alpha/2}$ norm error estimate to the discrete solutions.

References

1. Oldham, K.B., Spanier, J.: Fractional Calculus: Theory and Application of Differentiation and Integration to Arbitrary Order. Academic Press, London, UK (1974)
2. Podlubny, I.: Fractional Differential Equations. Academic Press, New York (1999)
3. Bagley, R., Torvik, P.: A theoretical basis for the application of fractional calculus to viscoelasticity. J. Rheol. **27**, 201–10 (1983)
4. Jiang, Y.J., Ma, J.T.: Moving finite element methods for time fractional partial differential equations. Sci. China Math. **56**, 1287–1300 (2013)
5. Ford, N.J., Xiao, J.Y., Yan, Y.B.: A finite element method for time fractional partial differential equations. Fract. Calc. Appl. Anal. **14**(3), 454–474 (2011)
6. Zhang, X.D., Huang, P.Z., Feng, X.L., Wei, L.L.: Finite element method for two-dimensional time fractional Tricomi-type equations. Numer. Methods Partial Differ. Equ. **29**, 1081–1096 (2013)
7. Meerschaert, M.M., Tadjeran, C.: Finite difference approximations for two-sided space-fractional partial differential equations. Appl. Numer. Math. **56**(1), 80–90 (2006)
8. Zheng, Y.Y., Li, C.P., Zhao, Z.G.: A note on the finite element method for the space-fractional advection diffusion equation. Comput. Math. Appl. **59**(5), 1718–1726 (2010)

9. Zhang, H., Liu, F., Anh, V.: Galerkin finite element approximation of symmetric space-fractional partial differential equations. Appl. Math. Comput. **217**, 2534–2545 (2010)
10. Zhao, Z.G., Li, C.P.: Fractional difference/finite element approximations for the time-space fractional telegraph equation. Appl. Math. Comput. **219**, 2975–2988 (2012)
11. Liu, Y., Du, Y., Li, H., Wang, J.: An H1-Galerkin mixed finite element method for time fractional reaction-diffusion equation. J. Appl. Math. Comput. **47**, 103–117 (2015)
12. Ma, J., Liu, J., Zhou, Z.: Convergence analysis of moving finite element methods for space fractional differential equations. J. Comp. Appl. Math. **255**, 661–670 (2014)

Adaptive Fractional Order Sliding Mode Controller Design for Blood Glucose Regulation-4-3

Hamid Heydarinejad and Hadi Delavari

Abstract Diabetes is a growing health problem in worldwide. Especially, the patients with Type I diabetes need strict blood glucose level control because the body's production and use of insulin are impaired, causing glucose concentration level to increase in the bloodstream. In this paper, fractional order sliding mode control and adaptive fractional order sliding mode control for robustly stabilize the glucose concentration level of a diabetic patient in presence of the parameter variations and multiple meal disturbance, is proposed. The Bergman minimal model is used to design the proposed controller. The structure of the proposed controllers is appropriate for making the insulin delivery pumps because attenuate the effect of chattering, obtain continuous control law and compliance with constraints insulin pump for subcutaneous injection of insulin. The numerical simulation result shows the advantages proposed controller for example robustness, high accuracy in presence of multiple disturbances with difference value and tracking of a desired glucose concentration in the appropriate time is verified.

Keywords Bergman minimal model · Fractional order sliding mode control · Adaptive control · Robust stability · Type I diabetes mellitus

1 Introduction

Diabetes mellitus is a metabolic disease characterized by pancreas inability to regulate blood glucose levels within normal range (70–150 mg/dl). Insulin is a hormone generated by specific cells, called beta cells, in the pancreas. Insulin is required to transfer blood glucose into cells, where it is stored and then used for energy. There are two types of diabetes: type I and type II. Type I diabetes or insulin dependent and type II diabetes or non-insulin dependent. In type I diabetes mellitus (T1DM), the immune system attacks and destroys the insulin producing b-cells in the pan-

H. Heydarinejad · H. Delavari (✉)
Department of Electrical Engineering, Hamedan University of Technology,
65155 Hamedan, Iran
e-mail: hdelavery@gmail.com

A. Babiarz et al. (eds.), *Theory and Applications of Non-integer Order Systems*,
Lecture Notes in Electrical Engineering 407, DOI 10.1007/978-3-319-45474-0_40

creas. Thus, a key issue in diabetes treatment is the delivery of exogenous insulin to obtain glucose levels close to normal. There are two situations depending on glucose concentration, namely, hyperglycemia and hypoglycemia (Hyperglycemia = Blood glucose concentration $>$ 120 (mg/dl)) and Hypoglycemia = Blood glucose concentration $<$ 60 (mg/dl)). Chronic elevation of BG level leads to damage of blood vessels (angiopathy), resulting in serious long-term complications, such as blindness, neuropathy, heart disease, and kidney failure.

Continuous glucose monitoring (CGM) systems and insulin pumps technologies have motivated the development of an artificial pancreas system to replace the conventional treatment strategies in T1DM, therefore, a system that automatically monitors and controls the blood glucose level of a diabetic individual permits the patient to have more participation in the ordinary daily activities with risk reduction of long-term side effects. The ideal treatment for controlling blood glucose levels in insulin dependent diabetic patients would be the use of an artificial pancreas which would have the following components: (a) a glucose sensor to monitor the blood glucose continuously with sufficient reliability and precision, (b) a computer to calculate the necessary insulin infusion rates by an appropriate feedback algorithm and (c) an insulin infusion pump to supply the required amount of insulin into the blood.

In recent years, many studies have been made for intelligent control of blood glucose. Among them we focus the 3rd order minimal model of Bergman [1]. From a control viewpoint, the following challenges arise when facing the design of a control algorithm for an artificial pancreas:

- Slow dynamic response to the control action.
- Nonlinear, uncertain and time-varying models.
- Large disturbances (the meals).
- Nonnegative actuation.
- Measurement errors including noise, drift and bias.

Several methods have been previously employed to design the feedback controller for insulin delivery, such as classical methods like PID Switching [2], model predictive control (MPC) [3], Fuzzy logic control [4], Recurrent Neural Network [5], High Order Sliding Mode Control [6, 7], Back stepping Sliding Mode Control [8], Optimal control [9], State output Feedback H∞ for Fractional Order Model [10], Hybrid Adaptive PD Controller [11].

The sensor can measure blood glucose concentration and pass the information to a feedback control system that would calculate the necessary insulin delivery rate using robust fractional order sliding mode control (FOSMC) and Adaptive Fractional order Sliding Mode Control (AFOSMC) algorithms, to keep the patient under metabolic control. FOSMC and AFOSMC algorithms, are used to robustly stabilize the glucose concentration level of a diabetic patient in presence of the parameter variations and meal disturbance. The structure of the proposed FOSMC and AFOSMC is appropriate for making the insulin delivery pumps in closed-loop control of diabetes. Therefore, a second order FOSMC was designed and tested with them. The designed controller was also applied to Bergman minimal model to check the approach feasibility. Soon after, to reduce the chattering phenomenon, a $tanh$ function is used to replace the

discontinuous *signum* function at the reaching phase in traditional sliding mode control. A computer simulation is performed to manifest the theoretical analysis. The robustness with respect to parameter uncertainties and meal disturbance was tested using Matlab simulation. There are some novelty and advantages, which make our proposed method attractive:

- The definition of a new fractional sliding surface.
- Robustness of the proposed controller against disturbances.
- Lack of restrictions on the upper limit of disturbances.
- Using fractional order switching control law for achieved states to sliding surface.

2 Fractional Calculus

Fractional calculus is an old mathematical topic since the 17th century [12]. The fractional integral-differential operators (fractional calculus) are a generalization of integration and derivation to non-integer order (fractional) operators. There exist many definitions of fractional derivative [13, 14], there are three commonly used definitions for the general fractional differentiation and integration, i.e., the Grü nwald–Letnikov (GL), The Riemann–Liouville (RL) and the Caputo [15]. Let us first introduce Caputo definition and results needed here with respect to fractional calculus which will be used later.

Definition 1 The fractional integral ${}_0^c D_t^\alpha$ with fractional order $\alpha \in R^+$ of function $x\,(t)$ is defined as [15]:

$$ {}_0^c D_t^\alpha f\,(t) = \frac{1}{\Gamma\,(\alpha)} \int_0^t (t-\tau)^{\alpha-1}\, x\,(\tau)\, d\tau. \tag{1} $$

Definition 2 The Caputo derivative of fractional order $\alpha \in R^+$ with function $x(t)$ is defined as [15, 16]:

$$ {}_0^c D_t^\alpha x\,(t) = \frac{1}{\Gamma\,(m-\alpha)} \int_0^t (t-\tau)^{m-\alpha-1}\, x^{(m)}\,(\tau)\, d\tau, \tag{2} $$

$m-1 < \alpha < m \in Z$.

Here are some of the important properties for the Caputo fractional calculus that will be used.

Definition 3 If $x(t) \in C^m[0, 1)$ and $m-1 < \alpha < m \in Z^+$, then [17]:

$$ {}_0^c D_t^\alpha\ {}_0^c D_t^{-\alpha} x\,(t) = x\,(t)\ \ for\, m = 1, \tag{3} $$

$$ {}_0^c D_t^{-\alpha}\ {}_0^c D_t^{\alpha} x(t) = x(t) - \sum_{k=0}^{m-1} \frac{t^k}{k!} x^{(k)}(0), \tag{4} $$

$$ {}_0^c D_t^{\alpha}\ {}_0^c D_t^{n} x(t) = {}_0^c D_t^{\alpha+n} x(t)\ n \in N, \tag{5} $$

$$ L\left\{ {}_0^c D_t^{\alpha} x(t) \right\} = s^{\alpha} X(s) - \sum_{k=0}^{m-1} s^{\alpha-k-1} x^{(k)}(0). \tag{6} $$

3 Bergman Minimal Model

Many models to glucose-insulin process has been presented, perhaps the most commonly used control relevant model for glucose–insulin dynamics is the minimal model. Bergman's minimal model has been invented in 1980 by Doctor Richard Bergman. The main advantages of the Bergman minimal model are the number of parameters is minimum and it describes the interaction between main components such as insulin and glucose concentrations without getting into biological complexity. The Bergman Minimal Model (BeM) [7, 18, 19] is:

$$ \begin{aligned} \dot{B}_1(t) &= -(p_1 + B_2(t)) B_1(t) + p_1 G_b + D(t), \\ \dot{B}_2(t) &= -p_2 B_2(t) + p_3 (B_3(t) - I_b), \\ \dot{B}_3(t) &= -n (B_3(t) - I_b) + \gamma t [B_1(t) - h]^{+} + u(t). \end{aligned} \tag{7} $$

Here $B_1(t)$, $B_2(t)$ and $B_3(t)$ are plasma glucose concentration, the insulin influence on glucose concentration reduction, and insulin concentration in plasma respectively, $u(t) \in R$ is injected insulin rate in (mU/min), G_b is the basal pre-injection level of glucose (mg/dl), I_b is the basal pre-injection level of insulin (μU/ml), p_1 the insulin independent rate constant of glucose uptake in muscles and liver (1/min), p_2 the rate for decrease in tissue glucose uptake ability (1/min), p_3 the insulin-dependent increase in glucose uptake ability in tissue per-unit of insulin concentration above the basal level ((μU/ml)/min). The term $\gamma [B_1(t) - h]^{+} t$ represents the pancreatic insulin secretion after a meal in take at $t = 0$. As this work is focused on Insulin therapy which is usually administrated to type I diabetes mellitus patients, γ is assumed to be zero to represent the true dynamic of this disease and p_1 should also be considered zero. The parameter n is the first order decay rate for insulin in blood.

First the relative degree of the system must be defined which is required for controller design, Assuming $y = B_1(t)$ the relative degree would be defined with the number of successive differentiation until the control appears in the equation [20, 21]. Relative degree r means that the controller $u(t)$ first appears explicitly in the r-th total derivative of σ. Using (7), the control function appears in the equations after the third differentiation, i.e., [7]:

$$B_1^{(3)}(t) = \varphi_B(B,t) - p_3 B_1(t)\, u(t) \tag{8}$$

$$\begin{aligned}\varphi_{B_{(B,t)}} = {} & B_1\left[-p_1\left({p_1}^2 + 3p_3 I_b\right) - p_3 I_b\,(p_2+n) - p_3\gamma t\,[B_1(t)-h]^+\right] + \\ & B_2\left[-{p_1}^2(1+G_b) + p_1 p_2\,(2G_b-1) + 2D\,(p_1+p_2)\right] + \\ & B_3\left[-2p_3\,(p_1+D)\right] + B_1 B_2\left[-(p_1+p_2)^2 - 3p_3 I_b\right] + \\ & B_1 B_3\left[p_3\,(3p_1+p_2+n)\right] + B_1 {B_2}^2\left[-3\,(p_1+p_2)\right] + \\ & {B_2}^2\,(p_1 G_b + D) + 3p_3 B_1 B_2 B_3 - B_1 {B_2}^3 + \\ & \ddot{D} + (p_1 G_b + D)\left({p_1}^2 + 2p_3 I_b\right).\end{aligned} \tag{9}$$

The relative degree Bergman minimal model is 3 because it is in the third derivative (8) where the input of insulin u first appears. This disturbance can be modeled by a decaying exponential function of the following form [22]:

$$D(t) = Ae^{-Bt}, \quad A, B > 0. \tag{10}$$

We modeled the pump as a first order delay:

$$\dot{u}(t) = \frac{1}{a}\left(w(t) - u(t)\right), \tag{11}$$

where $w(t)$ is insulin rate command in pump input, and a is pump time constant [8].

4 Controller Design

4.1 Fractional Sliding Mode Control

Sliding mode control is a robust nonlinear Lyapunov based control algorithm [23]. In this paper to deal with the disturbances and uncertainties, the FOSMC controller is proposed [24]. Let G_b be a desired constant value of the output of the system $B_1(t)$, the error of which is defined by:

$$e(t) = B_1(t) - G_d. \tag{12}$$

The sliding surface of the proposed FOSMC scheme can be selected as:

$$S(t) = {}_0^c D_t^{\alpha}\,\ddot{e}(t) + \lambda_1 \dot{e} + \lambda_2 e. \tag{13}$$

Taking the time derivative of fractional order sliding surface of (13), one can obtain:

$$\dot{S}(t) = {}_0^c D_t^{\alpha} \dddot{e}(t) + \lambda_1 \ddot{e} + \lambda_2 \dot{e} = 0. \tag{14}$$

With $\dot{S}(t) = 0$ and substituting (12) into (14) leads to:

$${}_0^c D_t^{\alpha} B_1^{(3)}(t) + \lambda_1 \ddot{e} + \lambda_2 \dot{e} = 0. \tag{15}$$

Applying the property (4) of Definition 3 to (15) one can obtain:

$${}_0^c D_t^{-\alpha} {}_0^c D_t^{\alpha} \left(B_1^{(3)}(t) \right) = - {}_0^c D_t^{-\alpha} \left(\lambda_1 \ddot{e} + \lambda_2 \dot{e} \right), \tag{16}$$

$$B_1^{(3)}(t) - \sum_{k=0}^{m-1} \frac{t^k}{k!} \left(B_1^{(3)}(t) \right)^{(k)} (0) = - {}_0^c D_t^{-\alpha} \left(\lambda_1 \ddot{e} + \lambda_2 \dot{e} \right). \tag{17}$$

Substituting (8) into (17) results:

$$\varphi_B(B, t) - p_3 B_1(t) u(t) - w = - {}_0^c D_t^{-\alpha} \left(\lambda_1 \ddot{e} + \lambda_2 \dot{e} \right). \tag{18}$$

By simple manipulation of the above equation one can obtain the following equivalent control law:

$$u_{eq}(t) = (p_3 B_1(t))^{-1} \left(+ \varphi_B(B, t) - w + {}_0^c D_t^{-\alpha} \left(\lambda_1 \ddot{e} + \lambda_2 \dot{e} \right) \right). \tag{19}$$

The next step is to design the reaching mode control scheme, in the proposed method using a new switching control law to derive the system trajectories onto the sliding surface ($S(t) = 0$). The reaching law can be chosen as:

$$u_{sw}(t) = (p_3 B_1(t))^{-1} \; {}_0^c D_t^{-\alpha} \left(k_1 S + k_2 sgn(S) \right). \tag{20}$$

Since the FOSMC law (20) uses the $sign(S)$ function as a hard switcher, the undesirable chattering phenomenon occurs [25]. Hence the $tanh(S)$ function, is replaced by the $sign(S)$ function. So the control law can be proposed as:

$$u_{sw}(t) = (p_3 B_1(t))^{-1} \; {}_0^c D_t^{-\alpha} \left(k_1 S + k_2 tanh(S) \right), \tag{21}$$

where k_1 and k_2 are positive constants and will be determined later. Hence, the overall control law becomes:

$$u(t) = (p_3 B_1(t))^{-1} \left(+ \varphi_B(B, t) - w + {}_0^c D_t^{-\alpha} \left(\lambda_1 \ddot{e} + \lambda_2 \dot{e} \right) + \right.$$

$$\left. {}_0^c D_t^{-\alpha} \left(k_1 S + k_2 tanh(S) \right) \right). \tag{22}$$

The fractional order term in control signal i.e., ${}_0^c D_t^{-\alpha}$ enhanced the controller robustness. Due to adding the extra degree of freedom, fractional order sliding mode controller can achieve better control performance than integer order sliding mode controller.

Consequently, to reduce the chattering effect in the FOSMC, a $tanh\,(S)$ function is proposed in the control signal law, the use of this function causes the creation term tangent hyperbolic at the derivative of Lyapunov function as a result. Using Lemma 1, we guaranties stability glucose insulin system with FOSMC.

Lemma 1 *The following equality is valid for every positive scalar a and given scalar b [26]:*

$$S\,(atanh(bS)) = |S(atanh(bS))| = \|S(atanh(bS))\| \geq 0. \tag{23}$$

Theorem 1 (Stability analysis for the proposed controller) *Consider the Glucose-insulin system with Bergman minimal model (7). This system is controlled by the control law $u(t)$ in (22), then the system trajectories will converge to the sliding surface $S(t) = 0$.*

Proof Consider a positive definite Lyapunov function candidate in the following form:

$$V = \frac{1}{2} S^2\,(t)\,. \tag{24}$$

Taking the time derivative from both sides of (23), and substitution (14) in it, obtains:

$$\dot{V} = S\dot{S} = S\left({}_0^c D_t^{\alpha} \dddot{e}\,(t) + \lambda_1 \ddot{e} + \lambda_2 \dot{e}\right). \tag{25}$$

The substitution (8) and (12) into (24), obtains:

$$\dot{V} = S\left({}_0^c D_t^{\alpha}\left(\varphi_B\,(B,t) - p_3 B_1\,(t)\,u\,(t)\right) + \lambda_1 \ddot{e} + \lambda_2 \dot{e}\right). \tag{26}$$

The substitution (22) into (25), obtains:

$$\dot{V} = S\Big({}_0^c D_t^{\alpha}\Big(\varphi_B(B,t) - p_3 B_1(t)\Big[(p_3 B_1(t))^{-1}(+\varphi_B(B,t) - w +$$

$${}_0^c D_t^{-\alpha}\left(\lambda_1 \ddot{e} + \lambda_2 \dot{e}\right) + {}_0^c D_t^{-\alpha}\left(k_1 S + k_2 tanh\,(S)\right)\Big)\Big]\Big) + \lambda_1 \ddot{e} + \lambda_2 \dot{e}\Big) \tag{27}$$

Finally, by simplification of (26) and using the property (4) of Definition 3, one can obtain:

$$\dot{V} = \left(-k_1 S^2 - k_2 S tanh\,(S)\right) \leq 0. \tag{28}$$

According to Lemma 1 it is obvious that the derivative of Lyapunov function is negative definite [27] and the positive switching gain k_1 and k_2, guaranties stability of the closed loop system with fractional order sliding mode control [28].

In the previous sections, Fractional order sliding mode controller was designed for glucose-insulin system and the system trajectories can be driven onto the predefined sliding surface, but has not provided analysis on the stability of the fractional order sliding surfaces and the error system converge to $S(t) = 0$.

Theorem 2 *Consider the fractional order sliding surface (13) if Laplace transform of the error, $E(s) = L\{e(t)\}$ is bounded, then the state trajectories of the system (13) will converge to zero as $t \to \infty$.*

Proof Let $S(t) = 0$ [24, 29] and using the Laplace transform of the Caputo derivative (the property (4) of Definition 3) for (13), results:

$$E(s) = \frac{\left(s^{q-1}E(0) + s^{q-2}\dot{E}(0) + s^{q-3}\ddot{E}(0) + \lambda_1 E(0)\right)}{(s^q + \lambda_1 s + \lambda_2)}. \tag{29}$$

Using the final-value theorem of the Laplace transformation one can obtain:

$$e(\infty) = \lim_{s\to 0} sE(s) =$$

$$\lim_{s\to 0} s\left[\frac{s^{q-1}E(0) + s^{q-2}\dot{E}(0) + s^{q-3}\ddot{E}(0) + \lambda_1 E(0)}{(s^q + \lambda_1 s + \lambda_2)}\right] = 0 \tag{30}$$

This shows the convergence of the error system trajectories to the fractional sliding surface (13).

Bergman's minimal model parameters are unique to each type I diabetic patients. The result should be the parameters of each patient using clinical data identified, even with accurate identification parameters can change the parameters there during the day but there is no possibility to identify continuous parameters. Using Robust Control Theory and satisfy conditions for the proposed controller, it can be established FOMC is robust controller that the uncertainties parameters and variation parameters.

Theorem 3 *Robust stability analysis for the proposed controller with uncertainty in the Glucose insulin Dynamic with Bergman Minimal Model. In (8) let us assume that Bergman Minimal Model φ_B, p_3 are unknown and we have the estimation of these parameters $\widehat{\varphi}_B$, $\widehat{p}_3$ then we can use these parameters in the controller:*

$$\widetilde{u}(t) = (\widehat{p}_3 B_1)^{-1} \times$$

$$\left(+\widehat{\varphi}_B - w + {}_0^c D_t^{-\alpha}\left(\lambda_1 \ddot{e} + \lambda_2 \dot{e}\right) + {}_0^c D_t^{-\alpha}\left(k_1 S + k_2 tanh(S)\right)\right), \tag{31}$$

where $\widetilde{u}(t)$ is the estimation of control signal. Replacing (8) into (14) and then using (31) instead of $u(t)$ in (8), we have:

$$\dot{S} = \left({}_0^c D_t^{\alpha} \left(\varphi_B - \widehat{p}_3 B_1 \left[(\widehat{p}_3 B_1)^{-1} \left(+\widehat{\varphi}_B - w + \right.\right.\right.\right.$$

$$\left.\left.\left.\left. {}_0^c D_t^{-\alpha} \left(\lambda_1 \ddot{e} + \lambda_2 \dot{e}\right) + {}_0^c D_t^{-\alpha} \left(k_1 S + k_2 sgn\left(S\right)\right)\right)\right]\right) + \lambda_1 \ddot{e} + \lambda_2 \dot{e}\right). \tag{32}$$

The sufficient condition for fractional order sliding surface is:

$$V = \frac{1}{2} S\left(t\right)^2, \qquad \dot{V} = S\left(t\right) \dot{S}\left(t\right) \leq -\eta \left|S_{(t)}\right|. \tag{33}$$

To satisfy (33) the control gain k_2 should satisfy the following condition:

$$k_2 > \max \left| p_3 \widehat{p}_3 \left({}_0^c D_t^{\alpha} \widetilde{P} \widetilde{\varphi}_B + \widetilde{P} \left(\lambda_1 \ddot{e} + \lambda_2 \dot{e}\right) + \right.\right.$$

$$\left.\left. p_3 \widehat{p}_3{}^{-1} k_1 \left({}_0^c D_t^{\alpha} \ddot{e}\left(t\right) + \lambda_1 \dot{e} + \lambda_2 e\right) + \eta\right)\right|, \tag{34}$$

where $\widetilde{\varphi}_B = \varphi_B - \widehat{\varphi}_B$, $\widetilde{P} = 1 - p_3 \widehat{p}_3{}^{-1}$. It means that the proposed controller is stable for unknown glucose - insulin dynamic if k_2 satisfies the (34) condition.

4.2 Adaptive Fractional Sliding Mode Control

In the previous section we have designed a fractional order sliding mode controller for Blood Glucose Regulation with uncertainty and disturbance. The diabetic patient's meal disturbance is unknown value and time varying. In the previous sections, it has been shown knowing the bounds of disturbances is vital to guarantee the system stability and set point tracking [29]. However, in practice it is not simple to determine these bounds precisely. In what follows, we develop an adaptation law to overcome this problem.

Lemma 2 *To tackle the unknown parameters, the following adaptation laws are proposed.*

$$\dot{\widehat{k}}_1 = \gamma_1 S^2, \tag{35}$$

$$\dot{\widehat{k}}_2 = \gamma_2 S tanh\left(S\right), \tag{36}$$

where $\widehat{k}_1, \widehat{k}_2$ are estimations for k_1, k_2 respectively, and γ_1, γ_2 are positive constants.

Proof The chosen a Lyapunov function as follows:

$$V = \frac{1}{2} S^2 + \frac{1}{\gamma_1} \widetilde{k}_1{}^2 + \frac{1}{\gamma_2} \widetilde{k}_2{}^2, \tag{37}$$

where $\widetilde{k}_1 = \widehat{k}_1 - k_1, \widetilde{k}_2 = \widehat{k}_2 - k_2$; taking derivative of both sides of (36) with respect to time yields:

$$\dot{V} = S\dot{S} + \frac{1}{\gamma_1}\widetilde{k}_1\dot{\widehat{k}}_1 + \frac{1}{\gamma_2}\widetilde{k}_2\dot{\widehat{k}}_2. \tag{38}$$

Using fractional order sliding surface (13) and relative degree equation (8):

$$\dot{V} = S\left({}_0^cD_t^{\alpha}\left(\varphi_B(B,t) - p_3B_1(t)u(t)\right) + \lambda_1\ddot{e} + \lambda_2\dot{e}\right) + \frac{1}{\gamma_1}\widetilde{k}_1\dot{\widehat{k}}_1 + \frac{1}{\gamma_2}\widetilde{k}_2\dot{\widehat{k}}_2. \tag{39}$$

The substitution control input (22) into (39):

$$\dot{V} = \Big[S\Big({}_0^cD_t^{\alpha}\Big(\varphi_B(B,t) - p_3B_1(t)\Big[(\widehat{p}_3B_1(t))^{-1}(+\widehat{\varphi}_B(B,t) - w + {}_0^cD_t^{-\alpha}\left(\lambda_1\ddot{e} + \lambda_2\dot{e}\right) + {}_0^cD_t^{-\alpha}\left(\widehat{k}_1S + \widehat{k}_2tanh(S)\right)\Big)\Big]\Big) + \lambda_1\ddot{e} + \lambda_2\dot{e}\Big) + \frac{1}{\gamma_1}\widetilde{k}_1\dot{\widehat{k}}_1 + \frac{1}{\gamma_2}\widetilde{k}_2\dot{\widehat{k}}_2\Big] \tag{40}$$

by simplification of the above equation:

$$\dot{V} = -\widehat{k}_1S^2 - \widehat{k}_2Stanh(S) + \frac{1}{\gamma_1}\widetilde{k}_1\dot{\widehat{k}}_1 + \frac{1}{\gamma_2}\widetilde{k}_2\dot{\widehat{k}}_2 \tag{41}$$

by substitution of the adaptation laws (35), (36) into (41):

$$\dot{V} = -\widehat{k}_1S^2 - \widehat{k}_2Stanh(S) + \widetilde{k}_1S^2 + \widetilde{k}_2Stanh(S) = -k_1S^2 - k_2Stanh(S) \tag{42}$$

This implies that stability of the Bergman minimal model with adaptive fractional order sliding mode control is guaranteed.

5 Numerical Simulation

In this paper we used nonlinear Bergman minimal model for glucose regulation using FOSMC and AFOSMC. Fractional calculus is a useful tool to control and to achieve a significant degree of robustness. The control system designed in this paper will be next used as an autonomous blood glucose controller for type I diabetes patient. Consequently, applying fractional order surface to sliding mode control

Table 1 Bergman minimal model parameters value [6] and FOSMC and AFOSMC parameters value (p_1, p_2, p_3 and n are expressed in (min^{-1}))

Bergman min. model	p_1	p_2	p_3	n	I_b	G_b	$B_1(0)$	$B_3(0)$
	0	0.02	5.3×10^{-7}	0.3	7	70	220	50
FOSMC	α	a	k_1	k_2	λ_1	λ_2	A	G_d
	0.6	2	3.9	5.8	5	9.7	80	80
AFOSMC	α	a	γ_1	γ_2	λ_1	λ_2	B	G_d
	0.6	2	65×10^{-8}	45×10^{-5}	10.85	4.1	−0.5	80

can modify the classical SMC to more robust controller. In this section we evaluate the proposed design with numerical simulation. Simulations were performed using MATLAB software, the specification of Bergman minimal model, FOSMC and AFOSMC parameters is available on Table 1.

The simulation results are depicted on Figs. 1, 2, 3, 4, 5, 6, 7 and 8. As it can be seen in Fig. 1 the proposed controller design (FOSMC) successfully controlled the Blood Glucose and decreased the glucose concentration level from the critical area (hyperglycemia) in initial time and meal disturbance with 80 (mg/dl) amplitude applied at t = 450 min. There is no hypoglycemic undershot, and normoglycemia is achieved in acceptable time. The theoretical analyses and simulations show that the proposed controller achieves set point tracking in the presence of disturbance.

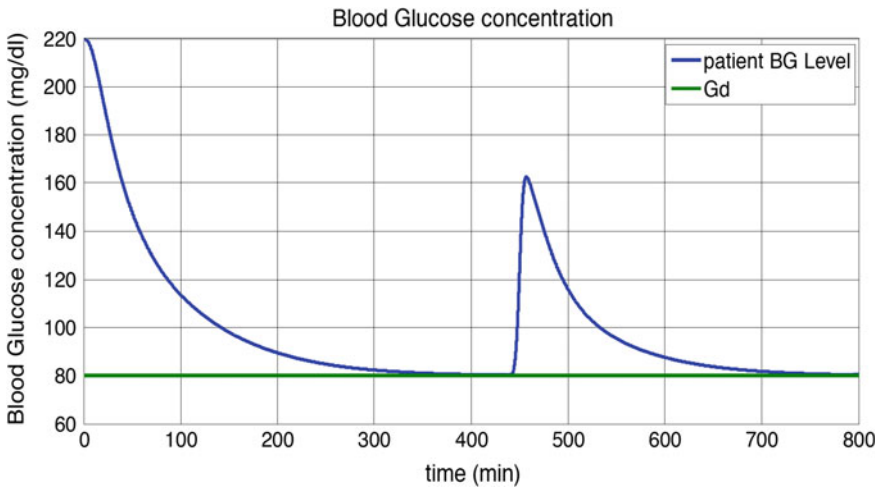

Fig. 1 Patient Blood glucose concentration with FOSMC

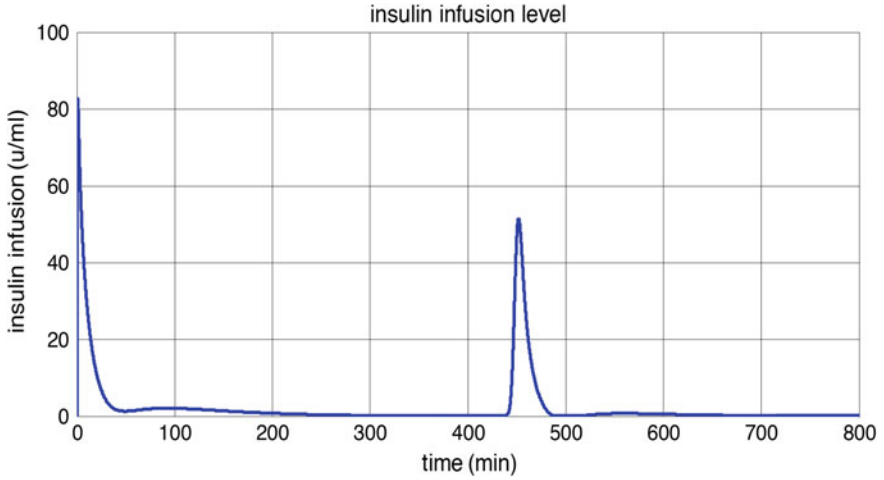

Fig. 2 Control Input (Injected Insulin) with pump in FOSMC

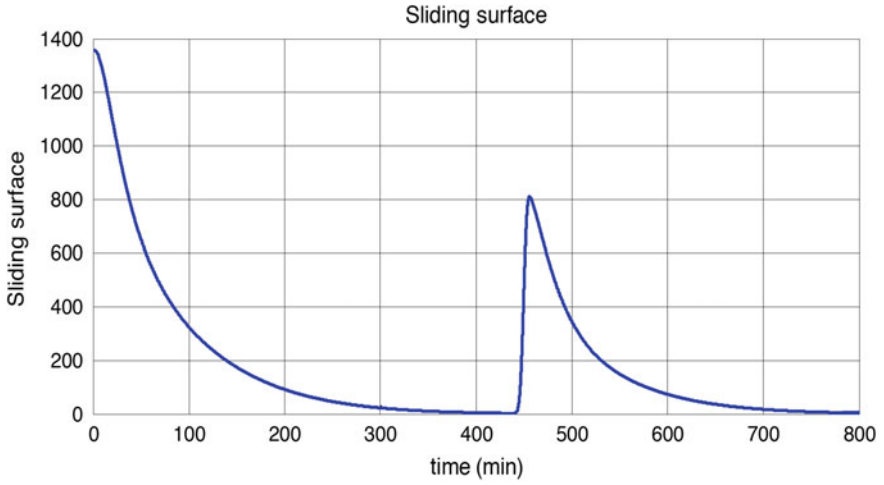

Fig. 3 Sliding surface for FOSMC

Figure 2 shows the insulin infusion (control function) for designed controllers, it can be seen constrained the nonnegative actuation is regarded, insulin infusion is continues signal and appropriate value.

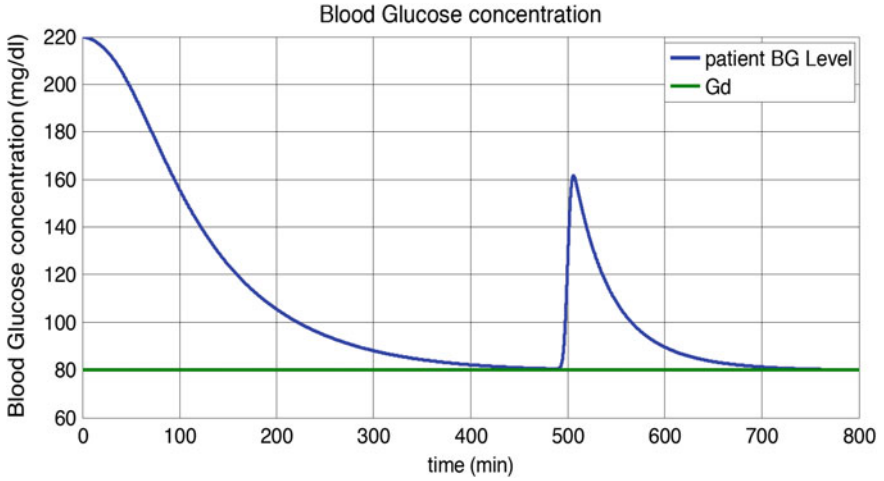

Fig. 4 Patient Blood glucose concentration with AFOSMC

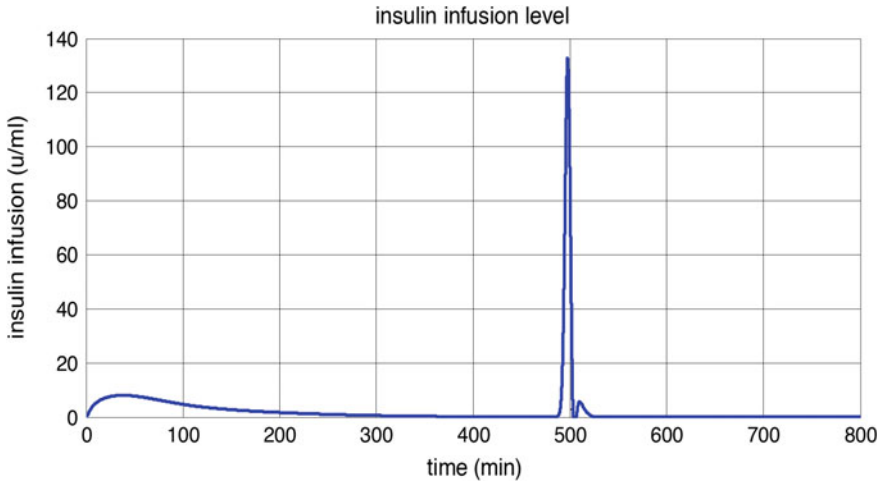

Fig. 5 Control Input (Injected Insulin) with pump in FOSMC

Figure 3 shows the sliding surface $S(t)$, as is obvious sliding surface converges to zero. Figure 4 shown the patient Blood glucose concentration with adaptive fractional order sliding mode control, the patient's blood glucose level could be appropriate tracking under the meal disturbance. There is no hypoglycemic undershot.

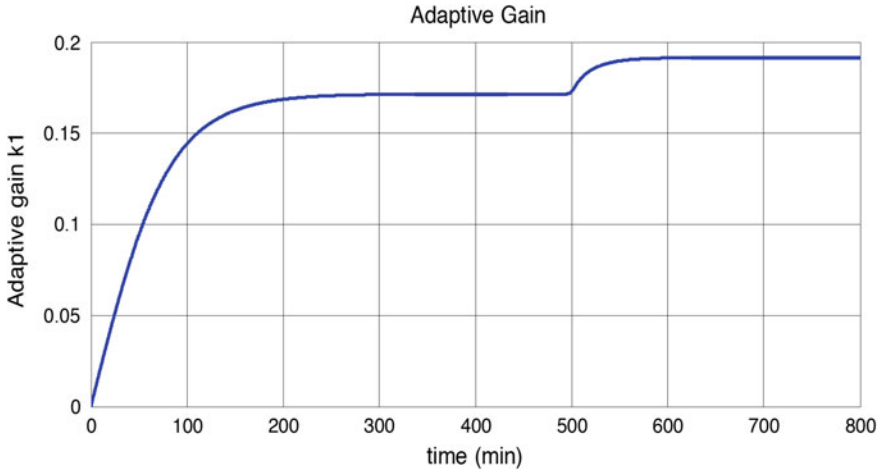

Fig. 6 Adaptive gain K1

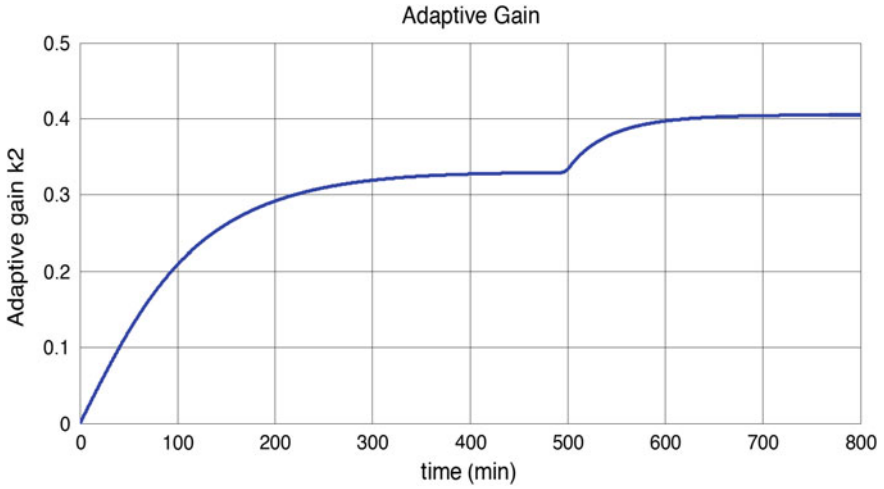

Fig. 7 Adaptive gain K2

Figure 5 shows insulin infusion (control law), the AFOSMC controller has a continuous signal and appropriate insulin injection and patients from an initial state inappropriate (hyperglycemia) eliminate and tracking set point.

Figures 6 and 7 show the adaptation gains k_1 and k_2 of switching control law and their convergence. These coefficients are calculated from Eqs. (34) and (35).

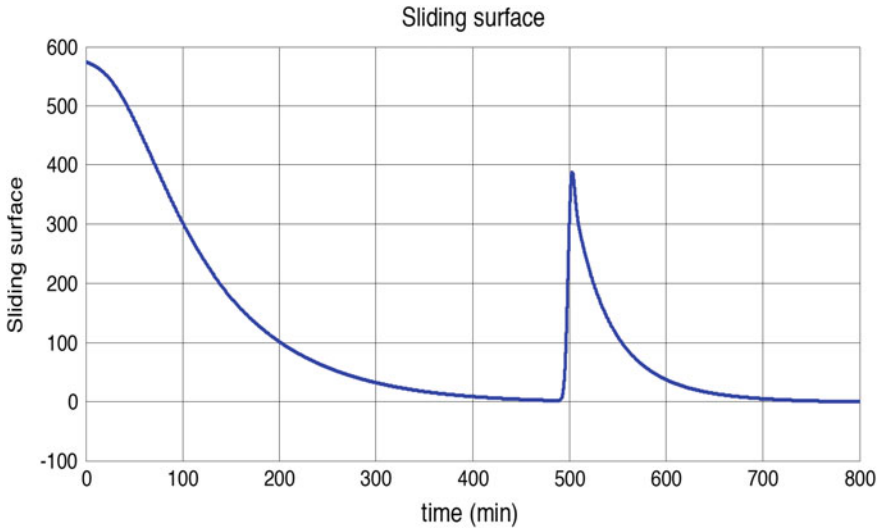

Fig. 8 Sliding surface for AFOSMC

6 Conclusion

The diabetes management as one of the challenging control problems in human regulatory systems has been discussed. The treatment of the disease via robust feedback control design using fractional order calculus and sliding mode control has been considered. Stabilization of blood glucose has been discussed in presence of the external disturbances such as food intake. From the viewpoint of stability and robust stability analysis and simulation was investigated for the proposed controller. With this aim, a fractional sliding mode control and adaptive fractional sliding mode control design for blood glucose regulation in type I diabetes. The proposed controller designed using the new switching control law for reaching states to the fractional order sliding surface. The designed controller is checked and confirmed by computer simulations. According to simulation result the proposed controllers have a good performance in tracking set point in appropriate time, disturbance rejection, non-negative actuator and continuous insulin injected.

References

1. Bergman, R.N., Philips, L.S., Cobelli, C.: Physiologic evaluation of factors controlling glucose tolerance in man. J. Clin. Invest. **68**, 1456–1467 (1981)
2. Marchetti, G., Barolo, M., Jovanovic, L., Zisser, H., Seborg, D.E.: An improved PID switching control strategy for type 1 diabetes. J. IEEE Trans. Biomed. Eng. **55**, 857–865 (2008)

3. Parker, R.S., Doyle, F.J., Peppas, N.A.: A model-based algorithm for blood glucose control in type I diabetic patients. J. IEEE Trans. Biomed. Eng. **46**, 148–157 (1999)
4. Wai, T., Quek, C.: A novel blood glucose regulation using TSK-FCMAC: a fuzzy CMAC based on the zero-ordered TSK fuzzy inference scheme. J. Neural Networks. **20**, 856–871 (2009)
5. Allam, F., Nossair, Z., Gomma, H., Ibrahim, I., Abdelsalam,M.: Evaluation of using a recurrent neural network (RNN) and a fuzzy logic controller (FLC) in closed loop system to regulate blood glucose for type-1 diabetic patients. I.J. Intell. Syst. Appl. **10**, 58–71 (2012)
6. Kaveh, P., Shtessel, Y.B.: Blood glucose regulation using higher-order sliding mode control. Int. J. Robust Nonlinear Control **25**, 557–569 (2008)
7. Hernandez, A.G., Fridman, L., Levant, A., Shtessel, Y.B.: RonLeder: high-order sliding-mode control for blood glucose: practical relative. J. Control Eng. Pract. **21**, 747–758 (2013)
8. Tadrisi Parsa, N., Vali, A.R., Ghasemi, R.: Back stepping sliding mode control of blood glucose for type I diabetes. Int. J. Med. Health Biomed. Pharm. Eng. **8**, 749–753 (2014)
9. Faruque Ali, S.k., Padhi, R.: Optimal blood glucose regulation of diabetic patients using single network adaptive critics. J. Optim. Control Appl. Methods **32**, 196–214 (2009)
10. N'Doye, I., Voos, H., Darouach, M., Schneider, J.G.: Static output feedback H∞ control for a fractional-order glucose-insulin system. Int. J. Control Autom. Syst. **13**, 798–807 (2015)
11. Leon-Vargasa, F., Garellib, F., De Battistab, H., Vehia, J.: Postprandial blood glucose control using a hybrid adaptive PD controller with insulin-on-board limitation. J. Biomed. Signal Process. Control **8**, 724–732 (2013)
12. Tenreiro Machado, J., Kiryakova, V., Mainardi, F.: Recent history of fractional calculus. Commun. Nonlinear Sci. Numer. Simulat. **16**, 1140–1153 (2011)
13. Monje, C.A., Chen, Y., Vinagre, B.M., Xue, D., Feliu-Batlle, V.: Fractional-Order Systems and Controls. Springer, London (2010)
14. Sabatier, J., Agrawal, O.P., Tenreiro Machado, J.: Advances in Fractional Calculus. Springer, Dordrecht (2007)
15. Podlubny, I.: Fractional Differential Equations. Academic Press, San Diego (1999)
16. Faieghi, M.R., Delavari, H., Baleanu, D.: A note on stability of sliding mode dynamics in suppression of fractional-order chaotic systems. J. Comput. Math. Appl. **66**, 832–837 (2013)
17. Li, C., Deng, W.: Remarks on fractional derivatives. J. Appl. Math. Comput. **187**, 777–784 (2007)
18. Palumbo, P., Ditlevsen, S., Bertuzzi, A., De Gaetano, A.: Mathematical modeling of the glucose-insulin system: a review. J. Math. Biosci. **244**, 69–81 (2013)
19. Balakrishnan, N.P., Rangaiah, G.P., Samavedham, L.: Review and analysis of blood glucose (BG) models for type 1 diabetic patients. J. Ind. Eng. Chem. Res. **50**, 12041–12066 (2011)
20. Levant, A.: Higher-order sliding modes, differentiation and output feedback control. Int. J. Control **76**, 924–941 (2003)
21. Shtessel, Y.B., Shkolnikov, I.A., Brown, M.D.J.: An asymptotic second order smooth sliding mode control. Asian J. Control. **5**, 498–504 (2003)
22. Fisher, M.E.: A semi closed-loop algorithm for the control of blood glucose levels in diabetics. IEEE Trans. Biomed. **38**, 57–61 (1991)
23. Faieghi, M.R., Delavari, H., Baleanu, D.: Control of an uncertain fractional-order Liu system via fuzzy fractional-order sliding mode control. J. Vib. Control **18**, 1366–1374 (2011)
24. Delavari, H., Ranjbar, A.N., Ghaderi, R., Momani, S.: Fractional order control of a coupled tank. J. Nonlinear Dyn. **61**, 383–397 (2010)
25. Delavari, H., Lanusse, P., Sabatier, J.: Fractional order controller design for a flexible manipulator robot. Asian J. Control **15**, 783–795 (2013)
26. Yin, C., Dadras, S., Zhong, S.M., Chen, Y.Q.: Control of a novel class of fractional-order chaotic systems via adaptive sliding mode control approach. J. Appl. Math. Model. **37**, 2469–2483 (2013)
27. Li, Y., Chen, Y.Q., Podlubny, I.: Stability of fractional-order nonlinear dynamic systems: Lyapunov direct method and generalized Mittag-Leffler stability. J. Comput. Math. Appl. **59**, 1810–1821 (2010)

28. Trigeassou, J.C., Maamri, N., Sabatier, J., Oustaloup, A.: A Lyapunov approach to the stability of fractional differential equations. J. Signal Process. **91**, 437–445 (2011)
29. Delavari, H.: A novel fractional adaptive active sliding mode controller for synchronization of non-identical chaotic systems with disturbance and uncertainty. J. Nonlinear Dyn. **67**, 2433–2439 (2011)

Expansion of Digraph Size of 1-D Fractional System with Delay

Solutions for Full Characteristic Polynomial

Konrad Andrzej Markowski and Krzysztof Hryniów

Abstract Previous method for determination of state matrices of fractional-order dynamic system by use of digraphs had problems with characteristic polynomials that were of full size (i.e. had all the terms) due to the constraints on matrix size minimality. This article proposes the alternative approach that allows to obtain solutions that can be easily computed even for full polynomials, but creates digraphs (and state matrices) of larger size. Proposed method is illustrated with the symbolic example of full characteristic polynomial showing the difference between the two approaches.

Keywords Fractional system · Delay · Digraphs · Characteristic polynomial · Digraph expansion · One-dimensional system

1 Introduction

One of constant problems in analysis of dynamic systems is the realisation problem. In many research studies, we can find a canonical form of the system, i.e. constant matrix form, which satisfies the system described by the transfer function [1, 2]. With the use of this form we are able to write only one realisation of the system, while there exists a set of solutions. Digraph-based solution allowing for finding a set of possible solutions for fractional systems was presented last year in [3], but as shown later in the article due to different methods of obtaining solutions based on digraph class, as presented in [4], not all solutions can be computed easily. In this paper a method of obtaining a set of solutions belonging to the easiest to compute digraph class by increasing the state matrix size is presented.

Research has been financed with the funds of the Statutory Research of 2016.

K.A. Markowski (✉) · K. Hryniów
Faculty of Electrical Engineering, Institute of Control and Industrial Electronics Koszykowa 75, Warsaw University of Technology, 00-662 Warsaw, Poland
e-mail: Konrad.Markowski@ee.pw.edu.pl

K. Hryniów
e-mail: Krzysztof.Hryniow@ee.pw.edu.pl

A. Babiarz et al. (eds.), *Theory and Applications of Non-integer Order Systems*, Lecture Notes in Electrical Engineering 407, DOI 10.1007/978-3-319-45474-0_41

1.1 Notion

In this paper the following notion will be used. The matrices will be denoted by the bold font (for example $\mathbf{A}, \mathbf{B}, \ldots$), the sets by the double line (for example $\mathbb{A}, \mathbb{B}, \ldots$), lower/upper indices and polynomial coefficients will be written as a small font (for example $a, b, \ldots$), fractional derivative will be denoted using a mathfrak font $\mathcal{D}$ and digraph will be denoted using mathcal font $\mathcal{D}$. The set $n \times m$ of real matrices will be denoted by $\mathbb{R}^{n\times m}$ and $\mathbb{R}^n = \mathbb{R}^{n\times 1}$. The $n \times n$ identity matrix will be denoted by $\mathbf{I}_n$. For more information about the matrix theory, an interested reader may be referred to, for instance: [5, 6].

1.2 One-Dimensional System with Delay

Let us consider a fractional continuous-time linear system with q delays in state vector and input vector described by state-space equations:

$$\begin{aligned} {}_0\mathcal{D}_t^{\alpha} x(t) &= \sum_{k=0}^{q} \mathbf{A}_k x(t-kd) + \sum_{l=0}^{q} \mathbf{B}_l u(t-ld), \\ y(t) &= \mathbf{C}x(t) + \mathbf{D}u(t), \quad 0 < \alpha \leqslant 1, \end{aligned} \tag{1}$$

where $x(t) \in \mathbb{R}^n, u(t) \in \mathbb{R}^m, y(t) \in \mathbb{R}^p$ are the state, input and output vectors respectively and $\mathbf{A}_k \in \mathbb{R}^{n\times n}$, $\mathbf{B}_l \in \mathbb{R}^{n\times m}$, $k, l = 0, 1, \ldots, q$, $\mathbf{C} \in \mathbb{R}^{p\times n}$ and $\mathbf{D} \in \mathbb{R}^{p\times m}$, d is a delay.

Remark 1 In this paper commensurate fractional-order time-delay system is considered.

The following Caputo definition of the fractional derivative will be used:

$${}_a^C\mathcal{D}_t^{\alpha} = \frac{d^{\alpha}}{dt^{\alpha}} = \frac{1}{\Gamma(n-\alpha)} \int_a^t \frac{f^{(n)}(\tau)}{(t-\tau)^{\alpha+1-n}} d\tau, \tag{2}$$

where $\alpha \in \mathbb{R}$ is the order of the fractional derivative, $f^{(n)}(\tau) = \frac{d^n f(\tau)}{d\tau^n}$ and $\Gamma(x) = \int_0^{\infty} e^{-t} t^{x-1} dt$ is the gamma function.

After using the Laplace transform to model (1), Caputo definition (2) and assume zaro initial conditions we can determine the transfer matrix of the considered system in the following form:

$$\mathbf{T}(s) = \mathbf{C}\left[\mathbf{I}_n s^{\alpha} - \sum_{k=0}^{q} \mathbf{A}_k e^{-sdk}\right]^{-1} \sum_{l=0}^{q} \mathbf{B}_l e^{-sdl} + \mathbf{D}. \tag{3}$$

1.3 Digraph

A directed graph (or just digraph) $\mathcal{D}$ consists of a non-empty finite set $\mathbb{V}(\mathcal{D})$ of elements called vertices and a finite set $\mathbb{A}(\mathcal{D})$ of ordered pairs of distinct vertices called arcs [7]. We call $\mathbb{V}(\mathcal{D})$ the vertex set and $\mathbb{A}(\mathcal{D})$ the arc set of digraph $\mathcal{D}$. We will often write $\mathcal{D} = (\mathbb{V}, \mathbb{A})$ which means that $\mathbb{V}$ and $\mathbb{A}$ are the vertex set and arc set of $\mathcal{D}$, respectively. The order of $\mathcal{D}$ is the number of vertices in $\mathcal{D}$. The size of $\mathcal{D}$ is the number of arcs in $\mathcal{D}$. For an arc (v_1, v_2) the first vertex v_1 is its tail and the second vertex v_2 is its head.

There are two well-known methods of representation of digraph: list and incidence matrix. In this paper we are using incidence matrix to represent all digraphs. Method of constructing digraphs by this method is presented for example in [7]. Adaptation of this well-known method for dynamic systems was first presented in [8].

We present below some basic notions from graph theory which are used in further considerations. A walk in a digraph $\mathcal{D}$ is a finite sequence of arcs in which every two vertices v_i and v_j are adjacent or identical. A walk in which all of the arcs are distinct is called a path. The path that goes through all vertices is called a finite path. If the initial and the terminal vertices of the path are the same, then the path is called a cycle.

1.4 Classes of Digraph Structures

Extensive study and experimentation shoved that obtained digraph structures can be grouped into three classes. Some structures are valid for all possible coefficients of characteristic polynomial (given in symbolic form) and have minimal number of arcs needed. Those structures were examined in detail in [4] and [9] and were denoted as class $\mathcal{K}_1$. Some structures give proper solution for given coefficients of characteristic polynomial – their structure can contain some additional arcs and there is need to solve a set of linear equations to get wages of digraph arcs. Those are denoted as class $\mathcal{K}_3$. And there are structures that cannot guarantee proper solution for given characteristic polynomial (or in some specific cases we are unable to determine if the solution is possible) that are denoted as class $\mathcal{K}_2$. More information about digraph structures and how to determine to which class given digraph belongs is presented in [4].

- **Class** $\mathcal{K}_1$: Digraph structures belonging to class $\mathcal{K}_1$ satisfy all characteristic polynomials of given type (with the same number and power of terms) for any $a_{i_1,i_2,\ldots,i_j}! = 0$ wages. Those are digraph structures that are the most thoroughly examined in previous papers and that can be computed quickly using digraph-based GPGPU (General-Purpose Computation on Graphics Processing Units) methods as there is no need of solving a system of polynomial equations. Digraph belongs to class $\mathcal{K}_1$ if the following conditions are satisfied:

(S_{1a}): $\mathbb{V}_1 \cap \mathbb{V}_2 \cap \ldots \cap \mathbb{V}_M \neq \{\emptyset\}$,
(S_{1b}): the number of cycles in digraph $\mathcal{D}^{(n)}$ equals M;

where M is a number of monomials in characteristic polynomial and $\mathbb{V}_k$ is a set of vertices of digraph $\mathcal{D}_k^{(n)}$ of k-th monomial.

- **Class** $\mathcal{K}_2$: Digraph structures belonging to class $\mathcal{K}_2$ cannot satisfy the given characteristic polynomial (or we are unable to determine the solution due to problem with solving a system of under-determined equations) and are considered invalid for given characteristic polynomial.
- **Class** $\mathcal{K}_3$: Digraph structures belonging to class $\mathcal{K}_3$ satisfy given characteristic polynomial with specific $a_{i_1,i_2,\ldots,i_j}$ wages, but unlike class $\mathcal{K}_1$ structures cannot be computed directly using digraph-based method and solving a set of equations is also needed, which significantly slows down the algorithm of finding them.

1.5 Problem Formulation

Although methods presented in [3] allows for obtaining a set of state matrix solutions for given fractional-order dynamic system, some of them are hard to compute and solving a set of equations is needed. In some cases, like in case of system transfer matrix that can be described by full polynomial, there are no solutions belonging to $\mathcal{K}_1$ class and even GPGPU assisted computation cannot obtain numerical solutions quickly. As a solution, expansion of size of the state matrices is proposed, that allows for construction of digraphs that will belong to $\mathcal{K}_1$ class.

2 Solution

Method for determining full characteristic polynomial of the system (1) will be presented for the single-input single-output system (SISO). The transfer matrix (3) can be considered as a function of the operator $\lambda = s^{\alpha}$ and operator $w = e^{sd}$ and for SISO system has the following form:

$$T(\lambda, w) = \mathbf{C}\left[\mathbf{I}_n\lambda - \sum_{k=0}^{q}\mathbf{A}_k w^{-k}\right]^{-1}\sum_{l=0}^{q}\mathbf{B}_l w^{-l} + \mathbf{D} = \frac{n(\lambda, w)}{d(\lambda, w)}, \tag{4}$$

where:

$$
\begin{aligned}
d(\lambda, w) = \lambda^n - a_{n-1}(w)\lambda^{n-1} - a_{n-2}(w)\lambda^{n-2} - \ldots \\
\ldots - a_2(w)\lambda^2 - a_1(w)\lambda - a_0(w) = \\
\lambda^n - \underbrace{\left(1 + w^{-1}\right)}_{a_{n-1}(w)}\lambda^{n-1} - \underbrace{\left(1 + w^{-1} + w^{-2}\right)}_{a_{n-2}(w)}\lambda^{n-2} - \cdots - \\
\ldots - \underbrace{\left(1 + w^{-1} + \cdots + w^{1-n}\right)}_{a_1(w)}\lambda - \underbrace{\left(1 + w^{-1} + \cdots + w^{-n}\right)}_{a_0(w)}
\end{aligned} \tag{5}
$$

is the characteristic polynomial.

By multiplying the nominator and denominator of the strictly transfer function (4) by λ^{-n}, we obtain a characteristic polynomial

$$
d(\lambda, w) = 1 - a_{n-1}(w)\lambda^{-1} - a_{n-2}(w)\lambda^{-2} - \cdots - a_1(w)\lambda^{1-n} - a_0(w)\lambda^{-n} \tag{6}
$$

in the form which is needed to draw the digraph.

During experimentation it appeared that some polynomial solutions cannot be obtained using the minimal possible number of vertices, but were possible to achieve with addition of one or more vertices. Moreover, it is well-known that for full (i.e. with all terms) characteristic polynomial we need the $(2n - 1)$ vertices, where n is the degree of the polynomial, to spin the graph. For such cases previously presented algorithm [3, 10] created digraph structures that belonged only to classes $\mathcal{K}_2$ and $\mathcal{K}_3$, so there was no possibility to obtain easy-to-compute solutions.

A solution to such problems is adding to the previously used method the possibility of spinning the graph on higher number of vertices then the degree of the polynomial n, up to the maximum size of $(2n - 1)$. With such modification it is possible to obtain additional solutions for most characteristic polynomials and to obtain any solutions belonging to $\mathcal{K}_1$ class for full characteristic polynomials. The downside of used method is the enlargement of size of state matrices, as they are directly related to number of vertices in the digraph.

With such approach, when obtaining the state matrix solutions for full characteristic polynomial, we can decide if we want to obtain solutions with minimal size of state matrices equal to n, but that will always belong to $\mathcal{K}_2$ and $\mathcal{K}_3$ classes (Case 1 in the example) or we increase the size of state matrices (and number of vertices in digraph) to $2n - 1$ to achieve some solutions that will belong to $\mathcal{K}_1$ class and can be easily computed (Case 2 in the example).

2.1 Example

For the given characteristic polynomial

$$
d(\lambda, w) = \lambda^2 - \left(a_1 + a_2 w^{-1}\right)\lambda - \left(a_3 + a_4 w^{-1} + a_5 w^{-2}\right), \tag{7}
$$

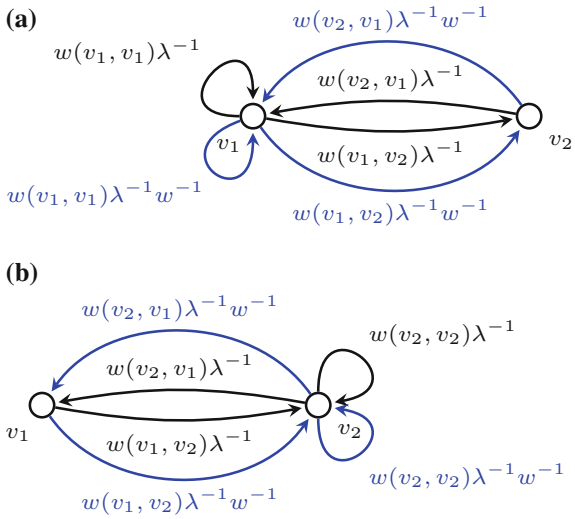

Fig. 1 **a** Possible digraph realisations belonging to class $\mathcal{K}_2$ or $\mathcal{K}_3$: **a** First **b** Second

determine realisation of the fractional continuous-time linear system with one delay $q = 1$ using multi-dimensional digraph theory.

Solution: Multiplying characteristic polynomial (7), by λ^{-2} we obtain:

$$d(\lambda, w) = 1 - \left(a_1 + a_2 w^{-1}\right)\lambda^{-1} - \left(a_3 + a_4 w^{-1} + a_5 w^{-2}\right)\lambda^{-2}. \tag{8}$$

In the first step, we determine possible weights from which we will build digraphs: λ^{-1}–corresponding with matrix $\mathbf{A}_0$ and $\lambda^{-1}w^{-1}$– corresponding with matrix $\mathbf{A}_1$.

Consider the following two cases:

Case 1: Solutions with minimal size of state matrices equal to n, but that will always belong to $\mathcal{K}_2$ and $\mathcal{K}_3$ classes. In the Fig. 1a and Fig. 1b are presented all the possible realisations of the characteristic polynomial (7).

Let us consider the first realisation presented in Fig. 1a. From digraph we can write the following state matrices:

$$\mathbf{A}_0 = \begin{bmatrix} w(v_1, v_1)_{\mathcal{A}_0} & w(v_2, v_1)_{\mathcal{A}_0} \\ w(v_1, v_2)_{\mathcal{A}_0} & 0 \end{bmatrix}, \quad \mathbf{A}_1 = \begin{bmatrix} w(v_1, v_1)_{\mathcal{A}_1} & w(v_2, v_1)_{\mathcal{A}_1} \\ w(v_1, v_2)_{\mathcal{A}_1} & 0 \end{bmatrix}, \tag{9}$$

where:

$$\begin{aligned} a_1 &= w(v_1, v_1)_{\mathcal{A}_0} \neq 0, \\ a_2 &= w(v_1, v_1)_{\mathcal{A}_1} \neq 0, \\ a_3 &= w(v_1, v_2)_{\mathcal{A}_0} \cdot w(v_2, v_1)_{\mathcal{A}_0} \neq 0, \\ a_4 &= w(v_1, v_2)_{\mathcal{A}_0} \cdot w(v_2, v_1)_{\mathcal{A}_1} + w(v_1, v_2)_{\mathcal{A}_1} \cdot w(v_2, v_1)_{\mathcal{A}_0} \neq 0, \\ a_5 &= w(v_1, v_2)_{\mathcal{A}_1} \cdot w(v_2, v_1)_{\mathcal{A}_1} \neq 0. \end{aligned} \tag{10}$$

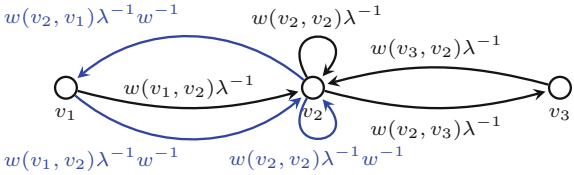

Fig. 2 First of possible digraph realisations belonging to class $\mathcal{K}_1$, spun on 3 vertices

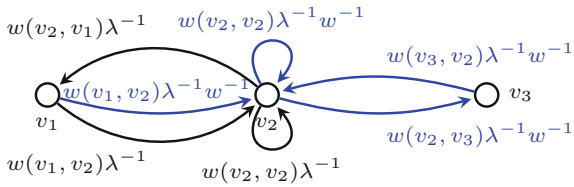

Fig. 3 Second of possible digraph realisations belonging to class $\mathcal{K}_1$, spun on 3 vertices

If the realisation of the characteristic polynomial (7) exist, then the conditions (10) must be satisfied – realisation then belongs to class $\mathcal{K}_3$. Otherwise it belongs to class $\mathcal{K}_2$.

Case 2: Increase the size of state matrices (and number of vertices in digraph) to $2n-1$. In this case we achieve some solutions that will belong to $\mathcal{K}_1$ class and can be easily computed and a solution that belongs to class $\mathcal{K}_2$.

In the Figs. 2 and 3 presented are digraphs which satisfy characteristic polynomial (7) and belong to class $\mathcal{K}_1$. From digraph presented in Fig. 2 we can write the following state matrices:

$$\mathbf{A}_0 = \begin{bmatrix} 0 & 0 & 0 \\ w(v_1, v_2)_{\mathcal{A}_0} & w(v_1, v_2)_{\mathcal{A}_0} & w(v_3, v_2)_{\mathcal{A}_0} \\ 0 & w(v_2, v_3)_{\mathcal{A}_0} & 0 \end{bmatrix}, \tag{11}$$

$$\mathbf{A}_1 = \begin{bmatrix} 0 & w(v_2, v_1)_{\mathcal{A}_1} & 0 \\ w(v_1, v_2)_{\mathcal{A}_1} & w(v_2, v_2)_{\mathcal{A}_1} & 0 \\ 0 & 0 & 0 \end{bmatrix},$$

where:

$$\begin{aligned} a_1 &= w(v_2, v_2)_{\mathcal{A}_0} \neq 0, \\ a_2 &= w(v_2, v_2)_{\mathcal{A}_1} \neq 0, \\ a_3 &= w(v_2, v_3)_{\mathcal{A}_0} \cdot w(v_3, v_2)_{\mathcal{A}_0} \neq 0, \\ a_4 &= w(v_1, v_2)_{\mathcal{A}_0} \cdot w(v_2, v_1)_{\mathcal{A}_1} \neq 0, \\ a_5 &= w(v_1, v_2)_{\mathcal{A}_1} \cdot w(v_2, v_1)_{\mathcal{A}_1} \neq 0. \end{aligned} \tag{12}$$

If the realisation of the characteristic polynomial (7) exist then the conditions (12) must be satisfied – realisation then belongs to class $\mathcal{K}_1$.

For digraph presented on Fig. 3 we have the state matrices in the form:

$$\mathbf{A}_0 = \begin{bmatrix} 0 & w(v_2, v_1)_{\mathcal{A}_0} & 0 \\ w(v_1, v_2)_{\mathcal{A}_0} & w(v_2, v_2)_{\mathcal{A}_0} & 0 \\ 0 & 0 & 0 \end{bmatrix}, \tag{13}$$

$$\mathbf{A}_1 = \begin{bmatrix} 0 & 0 & 0 \\ w(v_1, v_2)_{\mathcal{A}_1} & w(v_2, v_2)_{\mathcal{A}_1} & w(v_3, v_2)_{\mathcal{A}_1} \\ 0 & w(v_2, v_3)_{\mathcal{A}_1} & 0 \end{bmatrix},$$

where:

$$\begin{aligned} a_1 &= w(v_2, v_2)_{\mathcal{A}_0} \neq 0, \\ a_2 &= w(v_2, v_2)_{\mathcal{A}_1} \neq 0, \\ a_3 &= w(v_1, v_2)_{\mathcal{A}_0} \cdot w(v_2, v_1)_{\mathcal{A}_0} \neq 0, \\ a_4 &= w(v_1, v_2)_{\mathcal{A}_1} \cdot w(v_2, v_1)_{\mathcal{A}_0} \neq 0, \\ a_5 &= w(v_2, v_3)_{\mathcal{A}_1} \cdot w(v_3, v_2)_{\mathcal{A}_1} \neq 0. \end{aligned} \tag{14}$$

If the realisation of the characteristic polynomial (7) exist then the conditions (14) must be satisfied – realisation then belongs to class $\mathcal{K}_1$.

As can be seen on Fig. 4, digraph consisting of $2n - 1$ vertices does guarantee that some of the solutions will belong to $\mathcal{K}_1$ class as theory states, but it does not guarantee that all the obtained solutions will belong to that class.

For digraph presented on Fig. 4 we have the state matrices in the form:

$$\mathbf{A}_0 = \begin{bmatrix} w(v_1, v_1)_{\mathcal{A}_0} & w(v_2, v_1)_{\mathcal{A}_0} & 0 \\ w(v_1, v_2)_{\mathcal{A}_0} & 0 & w(v_3, v_2)_{\mathcal{A}_0} \\ 0 & 0 & 0 \end{bmatrix}, \tag{15}$$

$$\mathbf{A}_1 = \begin{bmatrix} w(v_1, v_1)_{\mathcal{A}_1} & 0 & w(v_3, v_1)_{\mathcal{A}_1} \\ 0 & 0 & 0 \\ w(v_1, v_3)_{\mathcal{A}_1} & w(v_2, v_3)_{\mathcal{A}_1} & 0 \end{bmatrix},$$

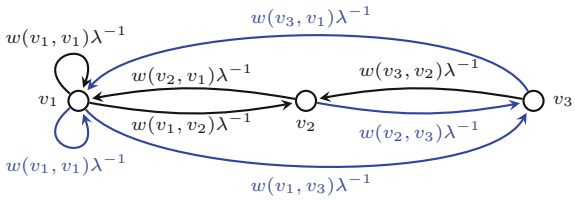

Fig. 4 Possible digraph realisation spun on 3 vertices belonging to class $\mathcal{K}_2$

where:

$$\begin{aligned}
a_1 &= w(v_1, v_1)_{\mathcal{A}_0} \neq 0, \\
a_2 &= w(v_1, v_1)_{\mathcal{A}_1} \neq 0, \\
a_3 &= w(v_1, v_2)_{\mathcal{A}_0} \cdot w(v_2, v_1)_{\mathcal{A}_0} \neq 0, \\
a_4 &= w(v_3, v_2)_{\mathcal{A}_1} \cdot w(v_2, v_3)_{\mathcal{A}_0} \neq 0, \\
a_5 &= w(v_1, v_3)_{\mathcal{A}_1} \cdot w(v_3, v_1)_{\mathcal{A}_1} \neq 0, \\
w(v_1, v_1)_{\mathcal{A}_0} &\cdot w(v_3, v_2)_{\mathcal{A}_0} \cdot w(v_2, v_3)_{\mathcal{A}_1} + \\
-w(v_2, v_1)_{\mathcal{A}_0} &\cdot w(v_3, v_2)_{\mathcal{A}_0} \cdot w(v_1, v_3)_{\mathcal{A}_1} = 0, \\
w(v_3, v_2)_{\mathcal{A}_0} &\cdot w(v_1, v_1)_{\mathcal{A}_1} \cdot w(v_2, v_3)_{\mathcal{A}_1} + \\
-w(v_1, v_2)_{\mathcal{A}_0} &\cdot w(v_2, v_3)_{\mathcal{A}_1} \cdot w(v_3, v_1)_{\mathcal{A}_1} = 0.
\end{aligned} \tag{16}$$

As all of the conditions (16) cannot be satisfied simultaneously, digraph realisation belongs to class $\mathcal{K}_2$ and we cannot obtain a solution.

3 Concluding Remarks

Previous method for determination of state matrices of fractional-order dynamic system using digraph theory presented in [3] allowed for obtaining a set of state matrix solutions, but some of them were hard to compute due to belonging to $\mathcal{K}_3$ class and solving a set of equations was needed. In the paper alternative approach was proposed, that creates both digraph structures and state matrices of larger size ($2n - 1$ instead of n, where n is the degree of the characteristic polynomial), but that creates more solutions and some of them will always belong to easier to compute class $\mathcal{K}_1$. Such approach allows solving one-dimensional fractional-order dynamic systems with delay that are described by characteristic polynomial of full size (i.e. with all the possible terms). Further work includes determination of formal conditions when digraph should be expanded (number of vertices on which it is spun increased in $[n, 2n - 1]$ interval) to generate additional meaningful solutions.

References

1. Kaczorek, T.: Selected Problems of Fractional Systems Theory. Springer, Berlin (2011)
2. Kaczorek, T., Sajewski, L.: The Realization Problem for Positive and Fractional Systems. Springer, Berlin (2014)
3. Hryniów, K., Markowski, K.A.: Digraphs minimal realisations of state matrices for fractional positive systems. In: R. Szewczyk, C. Zieliński, M. Kaliczyńska (eds.) Progress in Automation, Robotics and Measuring Techniques, Advances in Intelligent Systems and Computing, vol. 350, pp. 63–72. Springer International Publishing (2015)

4. Hryniów, K., Markowski, K.A.: Classes of digraph structures corresponding to characteristic polynomials. In: R. Szewczyk, C. Zieliński, M. Kaliczyńska (eds.) Challenges in Automation, Robotics and Measurement Techniques, Advances in Intelligent Systems and Computing, pp. 329–339. Springer International Publishing (2015)
5. Berman, A., Neumann, M., Stern, R.J.: Nonnegative Matrices in Dynamic Systems. Wiley, New York (1989)
6. Horn, R.A., Johnson, C.R.: Topics in Matrix Analysis. Cambridge Univ, Press (1991)
7. Bang-Jensen, J., Gutin, G.: Digraphs: Theory, Algorithms and Applications, 2nd edn. Springer, London (2009)
8. Fornasini, E., Valcher, M.E.: Directed graphs, 2D state models, and characteristic polynomials of irreducible matrix pairs. Linear Algebra and Its Applications **263**, 275–310 (1997)
9. Hryniów, K., Markowski, K.A.: Digraphs-building method for finding a set of minimal realisations of positive 2-D dynamic systems. Systems & Control Letters (Submitted to) (2016)
10. Hryniów, K., Markowski, K.A.: Parallel digraphs-building algorithm for polynomial realisations. In: Proceedings of 2014 15th International Carpathian Control Conference (ICCC), pp. 174–179 (2014)

A Discrete-Time Fractional Order PI Controller for a Three Phase Synchronous Motor Using an Optimal Loop Shaping Approach

Paolo Mercorelli

Abstract The paper presents an implementation of a discrete-time fractional order PI controller based on an optimal loop shape approach. This approach consists of a linearisation of the system using a geometric state feedback and after that a loop shaping problem is formulated in terms of an optimisation problem with constraints. The load sensitivity is minimised with some classical loop shape constraints using a random (genetic) algorithm. The system which is considered is using a synchronous motor with permanent magnets (PMSM). Such kind of motors are commonly used in electric or hybrid road vehicles. For railway vehicles, the PMSM as drive motors have not been widely used yet. The control strategy consists of a combination of a state feedback linearisation together with a PI and a PMW techniques. A fractional PI controller is used to obtain robustness and to guarantee the specification of such kind of strategy. The advantage of using a fractional order PI controller is emphasized using a loop shaping design technique. A feedforward Euler discretisation is used to realise the discrete form of the controller. Simulation analysis is carried out to validate the effectiveness of the proposed application.

Keywords Fractional order PI controller · Electrical motors with permanent magnets · Loop shaping approach · Geometric approach

1 Introduction and Background

The area of fractional calculus (FC) emerged at the same time as the classical differential calculus and it deals with derivatives and integrals to an arbitrary order (real or even complex order) [1–4]. However, its inherent complexity postponed the application of the associated concepts. Nowadays, the FC theory is applied in almost all the areas of science and engineering after recognizing its ability to yield a superior modelling and control in many dynamical systems ([1, 4], and also in [5]). In the

P. Mercorelli (✉)
Institute of Product and Process Innovation, Leuphana University of Lueneburg, Volgershall 1, 21339 Lueneburg, Germany
e-mail: mercorelli@uni.leuphana.de

A. Babiarz et al. (eds.), *Theory and Applications of Non-integer Order Systems*, Lecture Notes in Electrical Engineering 407, DOI 10.1007/978-3-319-45474-0_42

literature we can find several different definitions for the fractional integration and differentiation of arbitrary order ([1], and moreover in [2] and also in [4]). One of the most well-known definitions is given by the Grünwald–Letnikov approach.

The main nomenclature
D^{α} with $\alpha > 0$: partial integration of fractional order α
D^{α} with $\alpha < 0$: partial differentiation of fractional order α
$\mathbf{u}_{in}(t) = [u_a(t), u_b(t), u_0(t)]^T$: three phase input voltage vector
$\mathbf{i}(t) = [i_a(t), i_b(t), i_0(t)]^T$: three phase input current vector
$\mathbf{u}_q(t)$: induced voltage vector
ω_{el}: electrical pulsation
R_s: coil resistance
L_{dq}: dq coil inductance
$\mathbf{A}$: state matrix of the electrical model
$\mathbf{B}$: input matrix of the electrical model
$\mathcal{B} = \mathsf{im}\mathbf{B}$: image of matrix $\mathbf{B}$ (subspace spanned by the columns of matrix $\mathbf{B}$)
$\mathsf{min}\mathcal{I}(\mathbf{A}, \mathcal{B}) = \sum_{i=0}^{n-1} \mathbf{A}^i \mathsf{im}\mathbf{B}$: minimum $\mathbf{A}$-invariant subspace containing $\mathsf{im}(\mathbf{B})$
$\mathbf{F}$: decoupling feedback matrix field
$\mathbf{g}(\omega_{el})$: Park transformation
$\mathbf{T}(\omega_{el})$: decoupling feedforward matrix field

2 PID Controller from the Fractional Derivative and Integral Actions

The mathematical definition of a derivative or integral of fractional order has been the subject of different approaches. One of the most well-known definitions is given by the Grünwald–Letnikov approach. For example, the fractional derivative $\alpha \in \mathbb{R}$ is the following:

$$D^{\alpha} f(t) = \lim_{h \to 0} \left[\frac{1}{h} \sum_{k=0}^{\infty} (-1)^k \binom{\alpha}{k} f(t - hk) \right], \tag{1}$$

where

$$\binom{\alpha}{k} = \frac{\Gamma(\alpha + 1)}{\Gamma(k + 1)\Gamma(\alpha - k + 1)},$$

with $f(t)$ as a function which is indicated, Γ is the Gamma function and h is the time increment. An important property revealed by (1) is that while integer-order operators imply finite series, the fractional order counterparts are defined by infinite series. This means that integer operators are local time operators in opposition with the fractional operators that have, implicitly, a 'memory' of all past events. From a

control and signal processing perspective, the Grünwald–Letnikov approach seems to be the most useful and intuitive, particularly for a discrete-time implementation [4, 6]. Moreover, in the analysis and design of control systems we usually adopt the Laplace transformation ($\mathcal{L}$) method. The definition of the fractional-order operator (1) in the Laplace s-domain, under zero initial conditions, is given by the relation ($\alpha \in \mathbb{R}$):

$$\mathcal{L}\{D^{\alpha} f(t)\} s^{\alpha} F(s), \tag{2}$$

where $F(s) = \mathcal{L}\{F(t)\}$. Note that expression (2) is a direct generalization of the classical integer-order scheme with the multiplication of the signal transform $F(s)$ by the Laplace s-variable raised to a non-integer value α which is more flexible and give the possibility of adjusting more carefully the dynamical properties of a control system. As already referred a fractional derivative and integral can be obtained through the series defined in (1). For a discrete-time algorithm with sampling period T, this formula can be approximated through n-term truncated series, resulting in the following relations in the time and z domains:

$$D^{\alpha} f(t) \approx \frac{1}{T^{\alpha}} \sum_{k=0}^{\infty} (-1)^k \binom{\alpha}{k} f(t - hk),$$

and

$$\mathcal{Z}\{D^{\alpha} f(t)\} \approx \left[\frac{1}{T^{\alpha}} \sum_{k=0}^{\infty} (-1)^k \frac{\Gamma(\alpha + 1)}{k! \Gamma(\alpha - k + 1)} z^{-k} \right] F(z).$$

It is clear that in order to obtain good approximations, a large number of terms should be considered and in the meantime a small sampling time. The simplest approximation which can be done is an interpolation using just the last two samples. In this case just an interpolation of the first order is possible after considering $f(k-1)$ and $f(k)$ in the interval $0 \leq t \leq T$ which results, using a feedforward Euler approximation as follows:

$$f(t) = \big(f(k) - f(k-1)\big) \frac{t}{T} + f(k-1). \tag{3}$$

The integral function of (3), according to the definition of Gamma function, is equal to:

$$\mathcal{I}(f(t)) = \left(\frac{f(k) - f(k-1)}{\Gamma(2+1)} \right) \frac{t+1}{T} + \frac{f(k-1)}{\Gamma(1+1)} t.$$

Considering the α integral function, the following expression is obtained:

$$\mathcal{I}^{\alpha}(f(t)) = \left(\frac{f(k) - f(k-1)}{\Gamma(2+\alpha)} \right) \frac{t^{(1+\alpha)}}{T} + \frac{f(k-1)}{\Gamma(1+\alpha)} t^{\alpha}.$$

Its $\mathcal{Z}$-transformation expression is the following:

$$\mathcal{Z}(\mathcal{I}f(t)) = \frac{\Gamma(\alpha)}{\Gamma(2+\alpha)} z^{-k} F(z).$$

For $\alpha = -1, 0, 1$ these expressions correspond to the differential (D), proportional (P) and integral (I) actions respectively. If at the same time an interval with three elements ($f(k-2)$, $f(k-1)$ and $f(k)$) of the function $f(t)$ is considered, this is equivalent to consider a sampling time which is half of the previous sampling time, an interpolation of the second order is possible as follows:

$$f(t) = \frac{f(k) - 2f(k-1) + f(k-2)}{2} \left(\frac{t}{T}\right)^2 - \big(f(k-1) - 4f(k-1) + 3f(k-2)\big)\frac{t}{T} + f(k-2).$$

In this case it is to consider the interval $2T_s$ even though $T_s = T/2$ and the following two expressions are obtained:

$$\mathcal{I}^{\alpha}(f(t)) = \frac{2^{\alpha}\Gamma(\alpha)}{\Gamma(3+\alpha)} \left((2-\alpha)f(k) + 4\alpha f(k-1) + \alpha^2 f(k-2)\right).$$

Its $\mathcal{Z}$-transformation expression is the following:

$$\mathcal{Z}(\mathcal{I}f(t)) = \frac{2^{\alpha}\Gamma(\alpha)}{\Gamma(3+\alpha)} \left((2-\alpha) + 4\alpha z^{-1} + \alpha^2 z^{-2}\right) F(z). \tag{4}$$

For $\alpha = -1, 0, 1$ these expressions correspond to the differential (D), proportional (P) and integral (I) actions respectively.

3 Model of a Synchronous Motor

Among a variety of models presented in the literature since the introduction of PMSM, the two-axis dq-model, obtained using Park dq-transformation is the most widely used in variable speed PMSM drive control applications as in, for instance, [7]. The Park dq-transformation is a coordinate transformation that converts the three-phase stationary variables into variables in a rotating coordinate system. In dq-transformation, the rotating coordinate is defined relative to a stationary reference angle. The dq-model is considered in this work.

$$\begin{bmatrix} u_d(t) \\ u_q(t) \\ u_0(t) \end{bmatrix} = \begin{bmatrix} \frac{2\sin(\omega_{el}t)}{3} & \frac{2\sin(\omega_{el}-2\pi/3)}{3} & \frac{2\sin(\omega_{el}+2\pi/3)}{3} \\ \frac{2\cos(\omega_{el}t)}{3} & \frac{2\cos(\omega_{el}-2\pi/3)}{3} & \frac{2\cos(\omega_{el}+2\pi/3)}{3} \\ \frac{1}{3} & \frac{1}{3} & \frac{1}{3} \end{bmatrix} \begin{bmatrix} u_a(t) \\ u_b(t) \\ u_c(t) \end{bmatrix},$$

$$\begin{bmatrix} i_d(t) \\ i_q(t) \\ i_0(t) \end{bmatrix} = \begin{bmatrix} \frac{2\cos(\omega_{el}t)}{3} & \frac{2\cos(\omega_{el}-2\pi/3)}{3} & \frac{2\cos(\omega_{el}+2\pi/3)}{3} \\ \frac{-2\sin(\omega_{el}t)}{3} & \frac{-2\sin(\omega_{el}-2\pi/3)}{3} & \frac{-2\sin(\omega_{el}+2\pi/3)}{3} \\ \frac{1}{3} & \frac{1}{3} & \frac{1}{3} \end{bmatrix} \begin{bmatrix} i_a(t) \\ i_b(t) \\ i_c(t) \end{bmatrix}.$$

The dynamic model of the synchronous motor in dq-coordinates can be represented as follows:

$$\begin{bmatrix} \frac{di_d(t)}{dt} \\ \frac{di_q(t)}{dt} \end{bmatrix} = \begin{bmatrix} -\frac{R_s}{L_d} & \frac{L_q}{L_d}\omega_{el}(t) \\ -\frac{R_s}{L_q} & -\frac{L_d}{L_q}\omega_{el}(t) \end{bmatrix} \begin{bmatrix} i_d(t) \\ i_q(t) \end{bmatrix} + \begin{bmatrix} \frac{1}{L_d} & 0 \\ 0 & \frac{1}{L_q} \end{bmatrix} \begin{bmatrix} u_d(t) \\ u_q(t) \end{bmatrix} - \begin{bmatrix} 0 \\ \frac{\Phi\omega_{el}(t)}{L_q} \end{bmatrix} \tag{5}$$

and

$$M_m = \frac{3}{2}p\Big\{\Phi i_q(t) + (L_d - L_q)i_d(t)i_q(t)\Big\}. \tag{6}$$

In (5) and (6), $i_d(t)$, $i_q(t)$, $u_d(t)$ and $u_q(t)$ are the dq-components of the stator currents and voltages in synchronously rotating rotor reference frame, $\omega_{el}(t)$ is the rotor electrical angular speed, the parameters R_s, L_d, L_q, Φ and p are the stator resistance, d-axis and q-axis inductance, the amplitude of the permanent magnet flux linkage, and p the number of couples of permanent magnets, respectively. At the end, M_m indicates the motor torque. Considering an isotropic motor with $L_d \simeq L_q = L_{dq}$, it follows:

$$\begin{bmatrix} \frac{di_d(t)}{dt} \\ \frac{di_q(t)}{dt} \end{bmatrix} = \begin{bmatrix} -\frac{R_s}{L_{dq}} & \omega_{el}(t) \\ -\frac{R_s}{L_{dq}} & \omega_{el}(t) \end{bmatrix} \begin{bmatrix} i_d(t) \\ i_q(t) \end{bmatrix} + \begin{bmatrix} \frac{1}{L_{dq}} & 0 \\ 0 & \frac{1}{L_{dq}} \end{bmatrix} \begin{bmatrix} u_d(t) \\ u_q(t) \end{bmatrix} - \begin{bmatrix} 0 \\ \frac{\Phi\omega_{el}(t)}{L_{dq}} \end{bmatrix} \tag{7}$$

and

$$M_m(t) = \frac{3}{2}p\Phi i_q(t)$$

with the following movement equation

$$M_m(t) - M_w(t) = J\frac{d\omega_{mec}(t)}{dt}$$

where $p\omega_{mech}(t) = \omega_{el}(t)$ and M_w is an unknown mechanical load which consists of a friction part and an external load.

4 Design of the Control Strategy

Figure 1 describes the whole control scheme in which it is possible to see a state feedback linearisation control action in order to obtain the linearisation of the system. The linearisation is obtained using a decoupling control such that a straight-

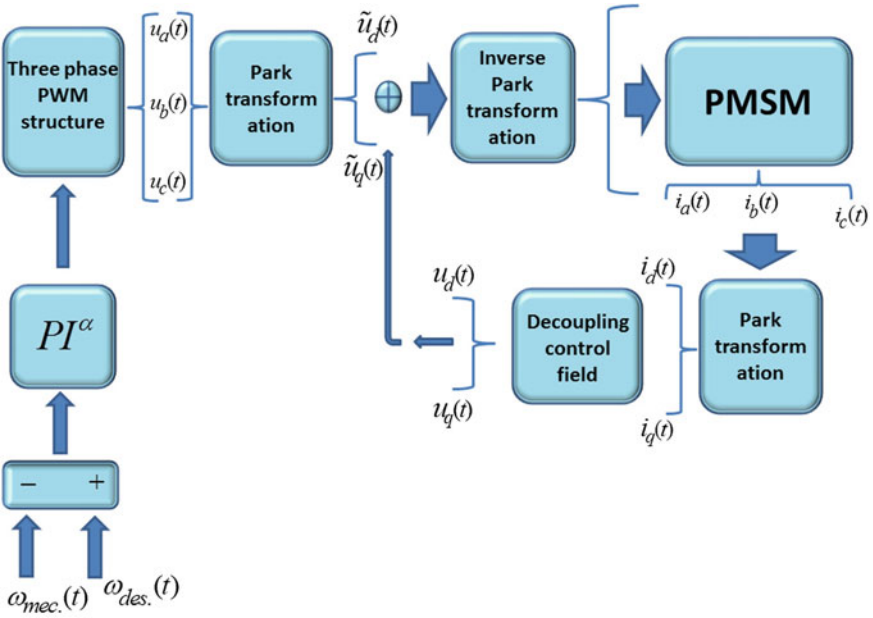

Fig. 1 Control scheme

forward resulting system is obtained. From Fig. 1 also the necessary Park direct and inverse transformations are visible. For achieving a decoupled structure of the system described in (7), a matrix field $\mathbf{F}(\omega_{el})$ is to be calculated such that:

$$\big(\mathbf{A} + \mathbf{BF}(\omega_{el})\big)\mathcal{V} \subseteq \mathcal{V}$$

where $\mathbf{u}(t) = \mathbf{F}(\omega_{el})\mathbf{x}(t)$ is a state feedback with $\mathbf{u}(t) = [u_d(t), u_q(t)]^T$ and $\mathbf{x}(t) = [i_d(t), i_q(t)]^T$,

$$\mathbf{A} = \begin{bmatrix} -\frac{R_s}{L_{dq}} & \omega_{el}(t) \\ -\frac{R_s}{L_{dq}} & \omega_{el}(t) \end{bmatrix} \mathbf{B} = \begin{bmatrix} \frac{1}{L_{dq}} & 0 \\ 0 & \frac{1}{L_{dq}} \end{bmatrix},$$

and $\mathcal{V} = im([0, 1]^T)$ of (4), according to [8], is a controlled invariant subspace. More explicitly it follows:

$$\mathbf{F}(\omega_{el}) = \begin{bmatrix} F_{11} & F_{12} \\ F_{21} & F_{22} \end{bmatrix} \text{and} \begin{bmatrix} u_d(t) \\ u_q(t) \end{bmatrix} = \mathbf{F}(\omega_{el}) \begin{bmatrix} i_d(t) \\ i_q(t) \end{bmatrix},$$

then the decoupling of the dynamics is obtained via the following relationship:

$$\mathrm{im}\left(\begin{bmatrix} -\frac{R_s}{L_{dq}} & \omega_{el}(t) \\ -\frac{R_s}{L_{dq}} & \omega_{el}(t) \end{bmatrix}\right) + \mathrm{im}\left(\begin{bmatrix} \frac{1}{L_{dq}} & 0 \\ 0 & \frac{1}{L_{dq}} \end{bmatrix}\begin{bmatrix} F_{11} & F_{12} \\ F_{21} & F_{22} \end{bmatrix}\begin{bmatrix} 0 \\ 1 \end{bmatrix}\right) \subseteq \mathrm{im}\begin{bmatrix} 0 \\ 1 \end{bmatrix} \quad (8)$$

where parameters F_{11}, F_{12}, F_{21}, and F_{22} are to be calculated in order to guarantee condition (8). Condition (8) is guaranteed if:

$$F_{12} = -\omega_{el}(t)L_{dq},$$

the first relation of (5) becomes as follows:

$$\frac{di_d(t)}{dt} = -\frac{R_s}{L_{dq}}i_d(t) + \frac{u_d(t)}{L_{dq}}.$$

In the same way we can obtain the following condition

$$\mathrm{im}\left(\begin{bmatrix} -\frac{R_s}{L_{dq}} & \omega_{el}(t) \\ -\frac{R_s}{L_{dq}} & \omega_{el}(t) \end{bmatrix}\right) + \mathrm{im}\left(\begin{bmatrix} \frac{1}{L_{dq}} & 0 \\ 0 & \frac{1}{L_{dq}} \end{bmatrix}\begin{bmatrix} F_{11} & F_{12} \\ F_{21} & F_{22} \end{bmatrix}\begin{bmatrix} 1 \\ 0 \end{bmatrix}\right) \subseteq \mathrm{im}\begin{bmatrix} 1 \\ 0 \end{bmatrix}$$

which is guaranteed if

$$F_{11} = R_s.$$

Moreover, considering the following relation

$$F_{21} = -\omega_{el}(t)L_{dq}$$

a feedback linearisation is obtained and the second relation of (5) becomes as follows:

$$\frac{di_q(t)}{dt} = \frac{u_q(t)}{L_{dq}} - \frac{\Phi\omega_{el}(t)}{L_{dq}}. \quad (9)$$

After this decoupling and the geometric feedback linearisation, considering (3), (3) and (9) with a linear friction which depends on the angular velocity of the motor and their Laplace Transformation, then:

$$P(s) = \frac{\Omega_{mec}(s)}{U_q(s)} = \frac{\frac{1}{L_{dq}}}{J\frac{2}{3p\Phi}s^2 + \frac{2}{3p\Phi}s + \frac{\Phi}{L_{dq}}}$$

where $\Omega_{mec.}(s)$ is the Laplace Transformation of variable $\omega_{mec.}(t)$. Moreover, considering the transfer function between torque load and angular velocity, then:

$$S(s) = \frac{\Omega_{mec}(s)}{M_w(s)} = \frac{-\frac{2s}{3p\Phi}}{J\frac{2}{3p\Phi}s^2 + \frac{2}{3p\Phi}s + \frac{\Phi}{L_{dq}}}. \quad (10)$$

5 Design a Fractional PI Controller with a Random Optimisation Algorithm

Considering the following discrete fractional PI$^{\alpha}$ controller in z-domain based on (4):

$$C_d(z) = \frac{U_c(z)}{E(z)} = K_p E(z) + K_i \frac{2^{\alpha}\Gamma(\alpha)}{\Gamma(3+\alpha)}\left((2-\alpha) + 4\alpha z^{-1} + \alpha^2 z^{-2}\right)$$

where $E(z)$ is the error between the desired and measured angular velocity of the motor and $U_c(z)$ is the output of the controller. In this paper the following optimisation problem is considered:

$$\min_{K_p, K_i, \alpha} \left\| \frac{S(s)}{1 + C_d(e^{j\omega_c}) P(j\omega_c)} \right\|_2^2 \quad \text{with} \quad \omega < \omega_c \tag{11}$$

where ω_c is the cross over frequency. Simultaneously the following constraints should be fulfilled. In the literature the transfer function $S(s)$ of (10) is indicated as the load sensitivity function. Three parameters of the controller should be determined such that the following four conditions are satisfied simultaneously:

- The gain crossover frequency of the open-loop system, ω_c, is equal to the desired value, where the equality

  $$|C_d(e^{j\omega_c}) P(j\omega_c)| = 0 \quad \text{dB}$$

  holds for a desired $e^{j\omega_c}$ where $C_d(s)$ and $P(s)$ are the transfer functions of the PI$^{\lambda}$ controller and the motor transfer function respectively.
- The phase margin of the feedback system, ϕ_m, is equal to the desired value

  $$arg\left(C_d(e^{j\omega_c}) P(j\omega_c)\right) > \pi + \phi_m$$

  which holds for the desired ϕ_m.
- The feedback system exhibits a good robustness to variations in the gain of process, which can be achieved by satisfying the following equality

  $$-D < \left(\frac{dC_d(e^{j\omega_c}) P(j\omega_c)}{dw}\right)_{\omega_c} < D$$

  where D is a a positive desired value.
- The feedback system attenuates the high frequency noise, which is achieved by satisfying the inequality:

$$\left| \frac{C_d(e^{j\omega_c})P(j\omega_c)}{1 + C_d(e^{j\omega_c})P(j\omega_c)} \right| < A \quad \text{dB}, \forall \omega > \omega_t$$

where A and ω_t are desired constants.

The cost function in the optimisation problem defined in (11) is of crucial importance because states the insensibility of the controlled system with respect to the disturbances inside the bandwidth of the controlled system. In the presented application a typical case is represented by the change of load to the motor. In the proposed application condition (5) is very important because of the switching functions due to the PMW system which generates high frequency disturbances. The algorithm which is used to find the optimal values of K_p, K_i and α is a random (genetic) one. Basically the random (genetic) algorithm is an evolutionary one, in which starting from a relatively limited number of fathers, in our case 9 fathers (three for each parameter to be optimised), sons are generated to explore the region of optimality. Each father generates three sons which must respect the four conditions mentioned above. After that, the gradients between the sons and the respectively fathers are calculated and the respective two sons with small gradients are not considered for the next generation. The algorithm stops when the gradients reach a minimum predefined threshold.

6 Simulations Results

In this section simulated results are shown. The left part of Fig. 2 represents the loadless case with the obtained velocity tracking in case of a PI^{α} of the first and second order approximation and the right part of Fig. 2 presents the obtained velocity tracking using a PI controller with set up of its parameters using Ziegler-Nichols method. From this figure it is to remark that the second order of approximation of a PI^{α} controller offers the better performance than the first order approximation. On the right part of Fig. 2 the tracking performance of the PI controller set with Ziegler-Nichols is shown. In Fig. 3 the PWM signals related to PI^{α} first order approximation and PI^{α} second order approximation are shown for the loadless case. It is to observe that using the second order PI^{α} the switching time is increasing and that guarantees a finer tracking with respect to the first order approximation of PI^{α}. In Figs. 4 and 5 the load case is shown. In this simulation thanks to the optimal parameter setting due to the minimisation of the sensitivity function, the difference between the performance of the PI^{α} case with respect to the PI parameter set using Ziegler-Nichols method is clearly visible.

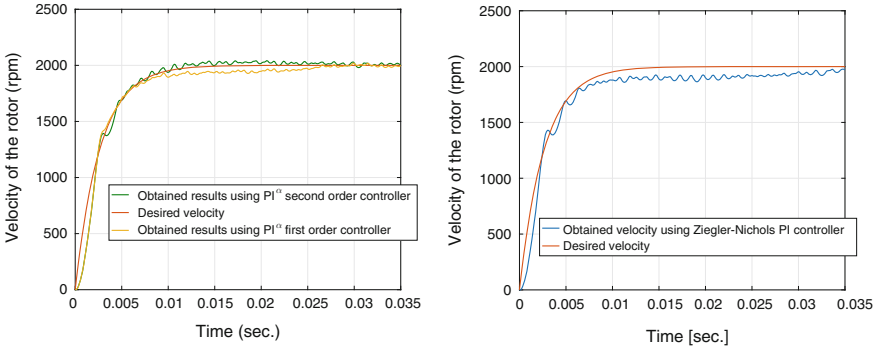

Fig. 2 Loadless case: tracking obtained with PI$^{\alpha}$ first order approximation and PI$^{\alpha}$ second order approximation (*blue*). Tracking obtained using a Ziegler-Nichols PI controller (*right*)

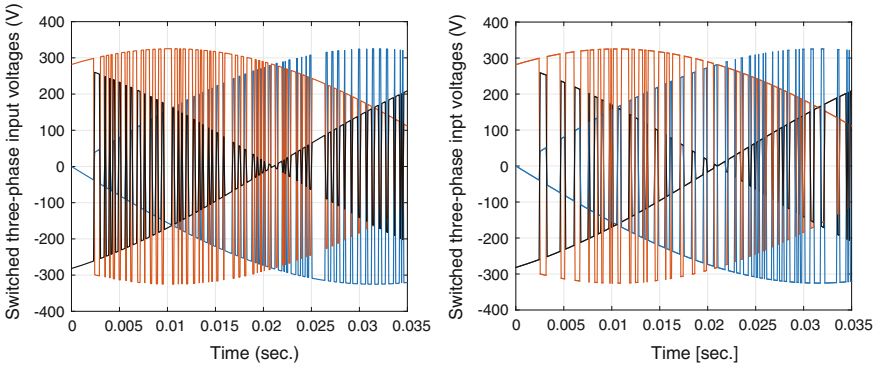

Fig. 3 Loadless case: three phase PWM signal using PI$^{\alpha}$ second order approximation (*left*) and three phase PWM signal using Ziegler-Nichols PI controller (*right*)

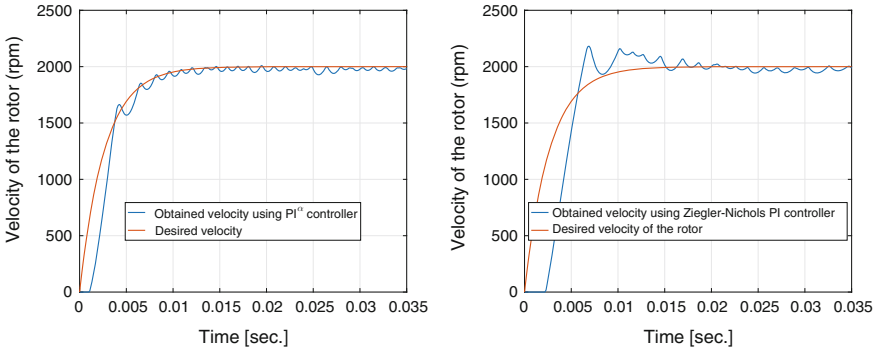

Fig. 4 Load case: tracking obtained with PI$^{\alpha}$ second order approximation (*blue*) (*left*). Tracking obtained using a Ziegler-Nichols PI controller (*right*)

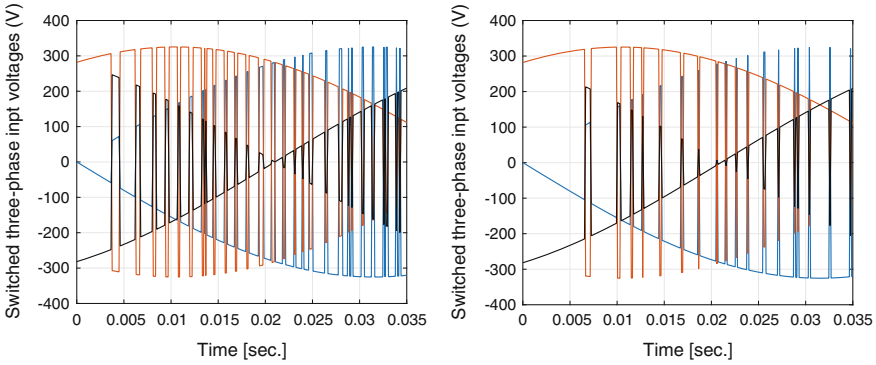

Fig. 5 Load case: three phase PWM signal using PI^{α} second order approximation (*left*) and Three phase PWM signal using Ziegler-Nichols PI controller (*right*)

7 Conclusions

This paper deals with the design of a fractional PI^{α} controller for a three phase synchronous motor using an optimisation problem with loop shaping constraints in which the parameter K_p, K_i and α are calculated using a random (genetic) algorithm implemented in Matlab. The synchronous motor is controlled with a PMW structure and in this context the rejection of high frequency disturbance plays a decisive role for the performance of the controlled system.

References

1. Oldham, K.B., Spanier, J.: The Fractional Calculus. Academic Press, New York (1974)
2. Miller, K.S., Ross, B.: An Introduction to the Fractional Calculus and Fractional Differential Equations. Wiley, New York (1993)
3. Samko, S.G., Kilbas, A.A., Marichev, O.I.: Fractional Integrals and Derivatives: Theory and Applications. Gordon and Breach Science, Amsterdan (1993)
4. Podlubny, I.: Fractional Differential Equations. Academic Press, San Diego (1999)
5. Hilfer, R.: Applications of Fractional Calculus in Physics. World Scientific, Singapore (2000)
6. Barbosa, R.S., Machado, J.A.T.: Implementation of discrete-time fractional order controllers based on LS approximations. Acta Polytechnica Hungarica **3**(4), 5–22 (2006)
7. Khaburi, D.A., Shahnazari, M.: Parameters identification of permanent magnet synchronous machine in vector control. In: Proceedings of the 10th European Conference on Power Electronics and Applications, EPE 2003, Toulouse, France, 2–4 Sept 2003
8. Basile, G., Marro, G.: Controlled and Conditioned Invariants in Linear System Theory. Prentice Hall, New Jersey (1992)

Application of SubIval, a Method for Fractional-Order Derivative Computations in IVPs

Marcin Sowa

Abstract The paper concerns a numerical method for the computations of the fractional derivative in initial value problems. The method bases on a partition of the integrodifferentiation interval into subintervals. It has been referred to previously as the subinterval-based method and is now called SubIval (for simpler reference). The subintervals are modified during a time stepping process – this is determined by an original subinterval dynamics algorithm. The method is mainly built in order to aid in solving problems of circuit theory. Hence, two examples have been introduced to ascertain the method, where both use a fractional order capacitor and a fractional order coil.

Keywords Fractional calculus · Numerical analysis · Circuit analysis · Integrodifferential equations

1 Introduction

The concept of the fractional order derivative is lately becoming more and more popular. In the paper the fractional order derivative of order $\alpha \in (0, 1)$ is considered in Caputo's definition [1]:

$$ {}^{\mathrm{C}}_{t_\mathrm{a}}\mathrm{D}_{t_\mathrm{b}} x(t) = \frac{1}{\Gamma(1-\alpha)} \int_{t_\mathrm{a}}^{t_\mathrm{b}} \frac{x^{(1)}(\tau)}{(t-\tau)^{\alpha}} \mathrm{d}\tau \tag{1} $$

and in the Riemann–Liouville definition [2]:

$$ {}^{\mathrm{RL}}_{t_\mathrm{a}}\mathrm{D}_{t_\mathrm{b}} x(t) = \frac{1}{\Gamma(1-\alpha)} \frac{\mathrm{d}}{\mathrm{d}t} \int_{t_\mathrm{a}}^{t_\mathrm{b}} \frac{x(\tau)}{(t-\tau)^{\alpha}} \mathrm{d}\tau. \tag{2} $$

M. Sowa (✉)
Institute of Electric Engineering and Computer Science,
Silesian University of Technology, Akademicka 10, 44-100 Gliwice, Poland
e-mail: marcin.sowa@polsl.pl

A. Babiarz et al. (eds.), *Theory and Applications of Non-integer Order Systems*,
Lecture Notes in Electrical Engineering 407, DOI 10.1007/978-3-319-45474-0_43

For simplicity the author uses special notations for (1) and (2) when concerning intervals, where for Caputo's definition the fractional derivative is denoted by:

$$ {}^{\mathrm{C}}_{t_\mathrm{a}}\mathrm{D}_{t_\mathrm{b}} = {}^{\mathrm{C}}\mathrm{d}^{\alpha}_{\Xi} x(t), \tag{3} $$

while for the Riemann–Liouville definition:

$$ {}^{\mathrm{RL}}_{t_\mathrm{a}}\mathrm{D}_{t_\mathrm{b}} = {}^{\mathrm{RL}}\mathrm{d}^{\alpha}_{\Xi} x(t), \tag{4} $$

where Ξ denotes the integration interval $[t_\mathrm{a}, t_\mathrm{b}]$. In cases where an equation applies to both definitions – the fractional derivative is simply written as $\mathrm{d}^{\alpha}_{\Xi} x(t)$. In whichever of the thus far proposed definitions ((1), (2) or many others, e.g. given in [3]) the appearance of the fractional derivative greatly increases the problem complexity. The mathematical challenge is not the only reason why fractional calculus has become popular – one can find its usage e.g. in:

- control theory and applications when analyzing fractional order controllers [4, 5],
- circuit theory when modeling lossy coils [6] and supercapacitors [7],
- electromagnetic field analyses where the behavior of some complex materials has been modeled [8],
- temperature field analysis when materials with relevant memory properties are concerned [9],
- in design of various systems using fractional order filters [10].

The context in which the fractional derivative appears is relevant as it can lead to various forms of the Ξ interval – e.g. for initial value problems (IVPs) it is the interval from an initial time instance t_0 to the current time t, while for spatial derivatives the interval can have a different meaning [11]. This (alike the case of either ordinary or partial differential equations) leads to various methods being favorable when solutions are sought. The most commonly considered is the fractional time derivative, in which the author is mostly interested in and which is considered in this paper.

The study presented in this paper concerns a method for the approximation of the fractional time derivative in initial value problems. When it comes to solutions of problems with fractional derivatives – for a limited class of problems (generally linear, with known source time-functions) analytical solutions can be found. For transient problems these base on Mittag-Leffler functions [12], while for AC analyses complex number representations can be used [13]. Analytical solutions can even be found for some more complicated problems e.g. [14]. However, often more demanding problems require them to be treated as an isolated case. For a more general approach (allowing for a wide range of different problems to be solved, including nonlinear problems) numerical methods can be used. Such is also the type of the method proposed in the presented research.

Lead researchers most often mention the following methods for solving fractional differential equations:

- the Adomian decomposition method [15] (which is an analytical technique treating the solution as a series of terms),
- the differential transform method [16] (a numerical method based on Taylor series expansion, constructing the solution as a polynomial),
- the CAS wavelet method [17] (treating the solution in general as a sum of CAS wavelets with unknown coefficients),
- Taylor expansion approach [18] (which bases on Taylor series expansion, leading to a system of equations, where the unknowns are the subsequent derivatives),
- collocation method [19] (where the solution is sought in subintervals, as local polynomials assumed as resulting from interpolations in equidistant nodes),
- methods known as Fractional Linear Multistep Methods (backward difference methods) explained e.g. in general by Lubich [20],
- methods basing on the fractional difference operator [21] (often considered when discussing discrete-time systems [22]).

The method presented in this paper bases on polynomial interpolations (basing on arbitrarily spaced nodes) in designated time subintervals.

2 Basis of the Method

The core of the method relies on the partition of the integrodifferentiation interval $\Xi_{\text{tot}} = [t_{\text{a}}, t_{\text{b}}]$ into $S + 1$ subintervals $\Xi_s = [t_{s,\text{start}}, t_{s,\text{end}}]$, such that $t_{s,\text{start}} = t_{s-1,\text{end}}$. The division yields:

$$\mathrm{d}^{\alpha}_{\Xi_{\text{tot}}} x(t) = \mathrm{d}^{\alpha}_{\Xi_M} x(t) + \sum_{s=1}^{S} \mathrm{d}^{\alpha}_{\Xi_s} x(t). \tag{5}$$

The interval with index $M = S + 1$ is written separately on purpose (it has special properties explained further on). The manner in which the subintervals are categorized and established is explained in Sect. 4. For every subinterval a Lagrange interpolation is performed so that:

$$\mathrm{d}^{\alpha}_{\Xi_{\text{tot}}} x(t) \approx \mathrm{d}^{\alpha}_{\Xi_M} \widetilde{x}_M(t) + \sum_{s=1}^{S} \mathrm{d}^{\alpha}_{\Xi_s} \widetilde{x}_s(t), \tag{6}$$

where $\widetilde{x}_s(t)$ are polynomials defined on subintervals denoted by Θ_s (where $\Xi_s \subseteq \Theta_s$). Assuming that in every subinterval defined on Θ_s there are n_s interpolation nodes, with respect to Lagrange basis polynomials, one can obtain:

$$\widetilde{x}_s(t) = \sum_{i=1}^{n_s} x_{s,i} L_{s,i}(c_s(t - t_{s,1})), \tag{7}$$

where $x_{s,i}$ are values of x at specific time nodes $t_{s,i}$ where the first one is $t_{s,1}$ and the final one is at t_{s,n_s} (if $\Xi_s = \Theta_s$ then $t_{s,1} = t_{s,\text{start}}$ and $t_{s,n_s} = t_{s,\text{end}}$). $L_{s,i}$ is the base Lagrange polynomial taking arguments in [0, 1]. The normalization is made preventively for numerical reasons. c_s is hence the normalization coefficient:

$$c_s = \frac{1}{t_{s,n_s} - t_{s,1}}. \tag{8}$$

The following assumptions are made:

- in the solution process, at each time step, the variable x is computed only for one time instance $t = t_{\text{now}}$,
- only the interpolation resulting in $\widetilde{x}_M$ takes into account the node $t = t_{\text{now}}$.

If all the previous values of x are known then in terms of (6) one can write:

$$\mathrm{d}^{\alpha}_{\Xi_{\text{tot}}} x(t) \approx ax|_{t=t_{\text{now}}} + b, \tag{9}$$

where:

$$a = \mathrm{d}^{\alpha}_{\Xi_M} L_{M,n_M}(c_M(t - t_{M,1})), \tag{10}$$

which is independent on x values, and:

$$b = \mathrm{d}^{\alpha}_{\Xi_M} \sum_{i=1}^{n_M - 1} x_{M,i} L_{M,i}(c_M(t - t_{M,1})) + \sum_{s=1}^{S} \mathrm{d}^{\alpha}_{\Xi_s} \sum_{i=1}^{n_s} x_{s,i} L_{s,i}(c_s(t - t_{s,1})), \tag{11}$$

which (if the mentioned assumptions are true) can be computed at $t = t_{\text{now}}$ since all x values at previous time nodes are known.

3 Analytical Formulae for Integrodifferentiation

If one obtains the Lagrange basis polynomial coefficients alone (or has the polynomials stored in a symbolic form) one can compute a and b from extracted integrodifferentiations of monomials $g\xi^k$ where the local variable $\xi = c_s(t - t_{s,1})$. For an auxiliary variable $\tau_{\text{loc}} = t - t_{s,1}$, for Caputo's definition one obtains:

$${}^{\text{C}}\mathrm{d}^{\alpha}_{\Xi_s}(g\xi_s^k) = \frac{kgc_s^k}{\Gamma(1-\alpha)} \int_0^{\Delta t_{\text{loc},s}} \frac{\tau_{\text{loc}}^{k-1}}{(\Delta T_s - \tau_{\text{loc}})^{\alpha}} \mathrm{d}\tau_{\text{loc}}, \tag{12}$$

where $\Delta t_{\text{loc},s} = t_{s,\text{end}} - t_{s,\text{start}}$ and $\Delta T_s = t - t_{s,\text{start}}$. For an auxiliary variable $\theta = \frac{\tau_{\text{loc}}}{\Delta T_s}$ the above equation takes the form:

$$^{\mathrm{C}}\mathrm{d}^{\alpha}_{\Xi_s}(g\xi_s^k) = \frac{kgc_s^k(\Delta T_s)^{k-\alpha}}{\Gamma(1-\alpha)}\int_0^{\frac{\Delta t_{\mathrm{loc},s}}{\Delta T_s}}\frac{\theta^{k-1}}{(1-\theta)^{\alpha}}\mathrm{d}\theta. \tag{13}$$

The integral represents the incomplete beta function:

$$B_{\frac{\Delta t_{\mathrm{loc},s}}{\Delta T_s}}(k, 1-\alpha) = \int_0^{\frac{\Delta t_{\mathrm{loc},s}}{\Delta T_s}}\frac{\theta^{k-1}}{(1-\theta)^{\alpha}}\mathrm{d}\theta. \tag{14}$$

One can evaluate this by applying the formula [23]:

$$B_{\rho}(k, 1-\alpha) = \frac{\Gamma(k)\Gamma(1-\alpha)}{\Gamma(k+1-\alpha)}(1-(1-\rho)^{1-\alpha}\sum_{j=0}^{k-1}\frac{\rho^j\prod_{i=0}^{j-1}(1-\alpha+i)}{j!}). \tag{15}$$

In conclusion, for already established Θ_s and Ξ_s subintervals, with the help of Lagrange interpolation and the above equation one can compute the a and b coefficients of Eq. (9) leading to a convenient approximation of the fractional derivative in Caputo's definition. For the Riemann–Liouville definition one can do the same and only needs to add the additional term to b according to the relation [24]:

$$^{\mathrm{RL}}\mathrm{d}^{\alpha}_{\Xi_{\mathrm{tot}}}x(t) = ^{\mathrm{C}}\mathrm{d}^{\alpha}_{\Xi_{\mathrm{tot}}}x(t) + \frac{x(t_0)}{\Gamma(1-\alpha)}(t-t_0)^{-\alpha}. \tag{16}$$

4 Subinterval Dynamics

This section explains how the subintervals are established and modified. Θ_s and Ξ_s are combined into subinterval pairs. Four types of subinterval pairs are distinguished:

- the *moving* interval pair: $\Theta_M = \Xi_M$ which is always the rightmost interval on the time axis; its interpolation $\widetilde{x}_M$ is always performed on either the maximum number of nodes (at the beginning of the computations) or an arbitrary number determined by order p (whichever is less); the interpolation is hence made on $[t_{j-p_{\mathrm{mov}}}, t_j]$, with j being the index of the current time step and $p_{\mathrm{mov}} = \min[j, p]$;
- the *built* interval pair: is a state of the S-th interval pair; $t_{s,1}$ is set, while $t_{s,end}$ changes when the interval pair is expanded; while the subinterval pair is built – the number of nodes used for the local interpolation changes;
- the S-th interval pair is *closed* if it can no longer be expanded, Θ_S is not changed; however Ξ_S changes and extends only as far as the beginning of Ξ_M (while it is necessary for Θ subintervals to form a continuous interval and not to overlap, such is not the case for Θ subintervals, where Θ_S will often overlap with Θ_M);
- a subinterval pair is *sealed* if $\Theta_s = \Xi_s$ and changes are no longer made to it.

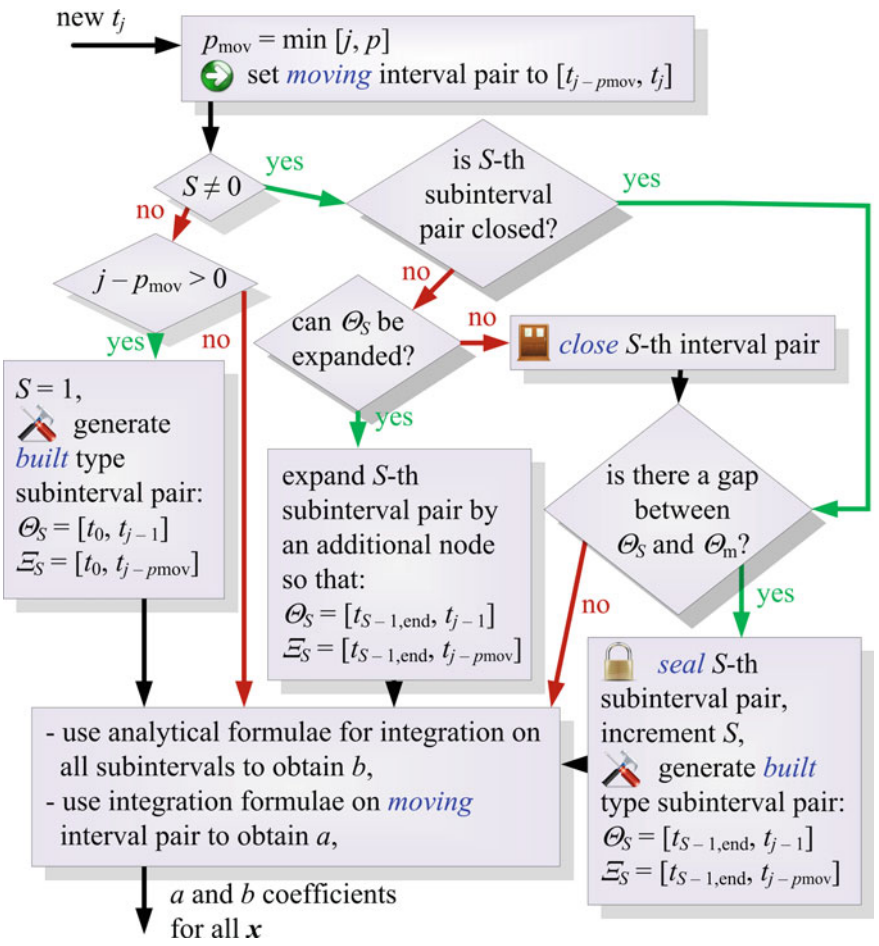

Fig. 1 Algorithm of the subinterval dynamics, which for every new time instance t_j provides a and b coefficients for all the selected variables

The subinterval dynamics algorithm is presented in Fig. 1.

For a new t_j the subintervals are modified and analytical formulae (presented previously in Sect. 3) can be applied to obtain the a and b coefficients of Eq. (9). Because the method fully supports variable time stepping – t_j can be chosen externally according to any algorithm. An example of how the subinterval dynamics work for $p = 3$ is given in Fig. 2.

Fig. 2 Example of subinterval dynamics (maximum order of polynomials $p = 3$)

5 Examples

Two examples are presented in order to verify the method. Both of these have analytical solutions, which will serve as referential ones to be compared with evaluations computed with the application of SubIval. One is a simple transient state problem, which has a well-known and relatively simple analytical solution [25] based on the Mittag-Leffler function. This example is presented in Fig. 3. A comparison of the results (obtained with an application of SubIval with those obtained by computing the analytical solution) is presented in Fig. 4.

When using MATLAB then functions (e.g. [26]) are available for for evaluations of the Mittag-Leffler function.

The second example is more complicated (it is depicted in Fig. 5). Rather than a transient solution the steady state AC solution is compared with the waveforms to which the numerical results tend. The result of this comparison is presented in Fig. 6.

The results presented in Figs. 4 and 6 have been obtained through an adaptive time step technique (as was proposed in [27]), with the core of the computations relying on the implementation of SubIval (taking new t_j values and allowing to obtain a and b coefficients like depicted in Fig. 1). The corrector used a maximum polynomial order of the *moving* subinterval equal to 4, while the predictor's polynomial order was less

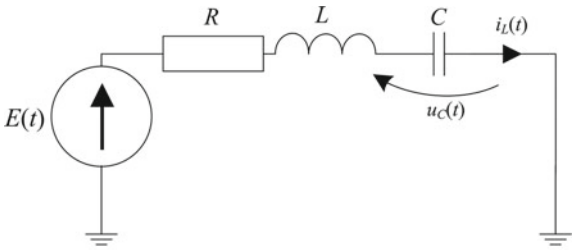

$E(t) = \mathbf{1}(t)$, $R = 2\,\Omega$,
$C = 6.5\,\text{mF}\cdot\text{s}^{\alpha-1}$, $L = 0.6\,\text{H}\cdot\text{s}^{\alpha-1}$, $\alpha = 0.75$

Fig. 3 Exemplary transient problem of an electric circuit supplied by a unit step source

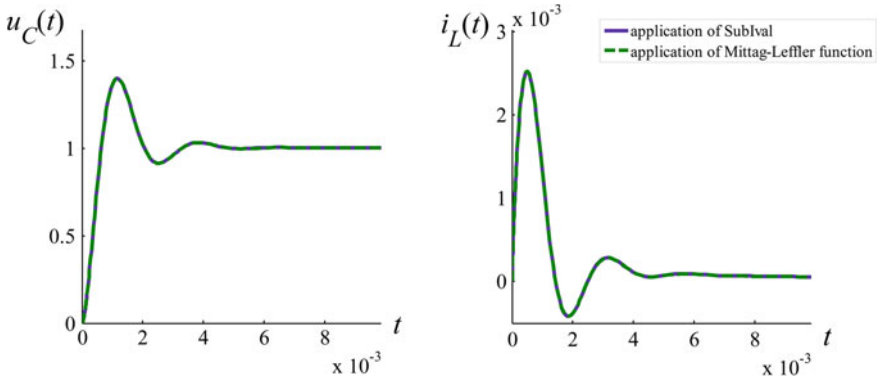

Fig. 4 Comparison of the results for the transient problem

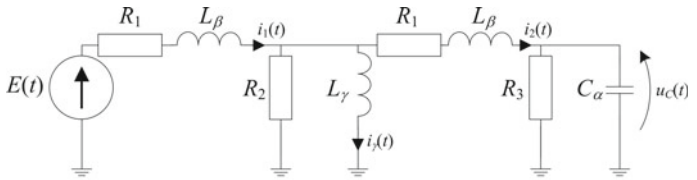

$E(t) = E_{\max}\sin(\omega t)$, $\omega = 2\pi f$, $f = 50$ Hz
$R_1 = 5\,\Omega$, $R_2 = 3\,\text{k}\Omega$, $R_3 = 4\,\Omega$
$L_\beta = 0.05\,\text{H}\cdot\text{s}^{\beta-1}$, $\beta = 0.9$, $L_\gamma = 200\,\text{H}\cdot\text{s}^{\gamma-1}$, $\gamma = 0.4$
$C_\alpha = 0.01\,\text{mF}\cdot\text{s}^{\alpha-1}$, $\alpha = 0.6$

Fig. 5 Exemplary problem with an AC voltage source and fractional order elements

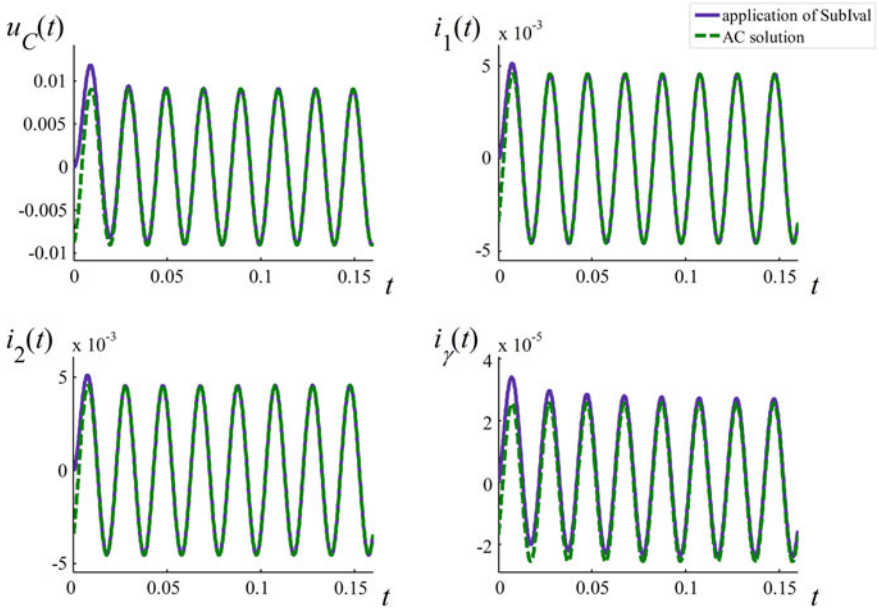

Fig. 6 Comparison of the AC analysis result and the transient numerical solution for 8 periods

by one. The *maximum error* coefficient $e_{\max} = 0.1\,\%$ was used in the computations. $e_{\max}$ determines the maximum allowed difference between the predictor and corrector results. If this value is exceeded then both the predictor and corrector stage must be repeated for a changed, smaller time step Δt. The *control error* $e_{\text{ctrl}} = 0.01\,\%$, which is a coefficient that controls how the time step is modified so that the difference between the predictor and corrector results stays within range of this value. The scheme has been implemented in Matlab, while SubIval computations have been performed through a connection with an ActiveX DLL with its implementation.

The comparison of the obtained results shows a very good resemblance of the entire time function for the transient problem of Fig. 3 and of the steady state for the AC problem of Fig. 5. For all the obtained time functions, when comparing the numerical results with the referential solutions, the maximum errors (relative to their respective maximum absolute values over time) for each time function did not exceed 0.05 %.

6 Conclusions and Remarks

The presented method (SubIval) allows for an approximation of the fractional derivative (in Riemann–Liouville and Caputo definitions) in IVPs. The approximation takes form of a linear dependence (given by (9)) on the variable being computed in

a current time step. This form can be applied in any initial value problem where for a current time step a fractional derivative appears and can be substituted by applying this equation (even in nonlinear problems). SubIval has already been tested for solving systems of fractional differential equations (resulting from circuit analyses) of the form [27]:

$$ {}_0\mathbf{D}_t^{\boldsymbol{\alpha}}\boldsymbol{x}(t) = \boldsymbol{A}\boldsymbol{x}(t) + \boldsymbol{B}\boldsymbol{u}(t) \tag{17} $$

where ${}_0\mathbf{D}_t^{\boldsymbol{\alpha}}\boldsymbol{x}(t)$ is a vector of fractional derivatives ${}_0\mathrm{D}_t^{\alpha_i} x_i(t)$. There, in every time step, the implicit solver leads to a reduction of the problem to a form of a linear system of equations.

When it is possible and when it is desired to have a very accurate result then it is worthwhile to obtain the solution through evaluations of analytical formulae. However, the numerical approach allows to treat various problems in a general manner, where e.g. for the presented problems all could be given in the form of Eq. (17) for numerical computations.

The method fully supports variability of the time step Δt e.g. as it was presented in [27, 28] where the predictor-corrector scheme (applied for the computations whose results are presented in Sect. 5).

In further papers the author plans to present:

- other examples (mainly concerning circuit theory e,g, introducing the fractional derivative to the nonlinear coil model [29]),
- an analysis of the accuracy of the results (ascertained through comparisons with analytical solutions or those obtained by other methods),
- the implementation of improvements like the ones mentioned in [28].

References

1. Caputo, M.: Linear models of dissipation whose Q is almost frequency independent - II. Geophys. J. Int. **13**(5), 529–539 (1967)
2. Munkhammar, J.D.: Riemann-Liouville fractional derivatives and the Taylor-Riemann series. UUDM Proj. Rep. **7**, 1–18 (2004)
3. Katugampola, U.N.: A new approach to generalized fractional derivatives. Bull. Math. Anal. Appl. **6**(4), 1–15 (2014)
4. Spałek, D.: Synchronous generator model with fractional order voltage regulator $\mathrm{PI}^b\mathrm{D}^a$. Acta Energetica **2**(23), 78–84 (2015)
5. Baranowski, J., Bauer, W., Zagórowska, M., Kawala-Janik, A., Dziwiński, T., Piątek, P.: Adaptive non-integer controller for water tank system. Theor. Develop. Appl. Non-Integer Syst. 271–280 (2016)
6. Schäfer, I., Krüger, K.: Modelling of lossy coils using fractional derivatives. Phys. D: Appl. Phys. **41**, 1–8 (2008)
7. Jakubowska, A., Walczak, J.: Analysis of the transient state in a series circuit of the class $\mathrm{RL}_\beta\mathrm{C}_\alpha$. Circuits Syst. Signal Process. **35**, 1831–1853 (2016)
8. Mescia, L., Bia, P., Caratelli, D.: Fractional derivative based FDTD modeling of transient wave propagation in Havriliak–Negami media. IEEE Trans. Microw. Theory Tech. **62**(9), (2014)

9. Brociek, R., Słota, D., Wituła R.: Reconstruction of the thermal conductivity coefficient in the time fractional diffusion equation. In: Advances in Modelling and Control of Non-integer-Order Systems, pp. 239–247 (2015)
10. Kawala-Janik, A., Podpora, M., Gardecki, A., Czuczwara, W., Baranowski, J., Bauer, W.: Game controller based on biomedical signals. In: 2015 20th International Conference on Methods and Models in Automation and Robotics (MMAR), pp. 934–939 (2015)
11. Wang, H., Du, N.: Fast solution methods for space-fractional diffusion equations. J. Comput. Appl. Math. **255**, 376–383 (2014)
12. Kaczorek, T.: Minimum energy control of fractional positive electrical circuits with bounded inputs. Circuits Syst. Signal Process. 1–15 (2015)
13. Zhou, K., Chen, D., Zhang, X., Zhou, R., Iu, H.H.-C.: Fractional-order three-dimensional circuit network. IEEE Trans. Circuits Syst. I Regul. Pap. **62**(10), 2401–2410 (2015)
14. Mitkowski, W., Skruch, P.: Fractional-order models of the supercapacitors in the form of RC ladder networks. Bull. Pol. Acad.: Tech. **61**(3), 580–587 (2013)
15. Momani, S., Noor, M.A.: Numerical methods for fourth order fractional integro-differential equations. Appl. Math. Comput. **182**, 754–760 (2006)
16. Arikoglu, A., Ozkol, I.: Solution of fractional integro-differential equations by using fractional differential transform method. Chaos Solitons Fractals **40**(2), 521–529 (2007)
17. Saeedi, H., Mohseni Moghadam, M.: Numerical solution of nonlinear Volterra integro-differential equations of arbitrary order by CAS wavelets. Commun. Nonlinear Sci. Numer. Simul. **16**, 1216–1226 (2011)
18. Huang, L., Xian-Fang, L., Zhao, Y., Duan, X.-Y.: Approximate solution of fractional integro-differential equations by Taylor expansion method. Comput. Math. Appl. **62**, 1127–1134 (2011)
19. Rawashdeh, E.A.: Numerical solution of fractional integro-differential equations by collocation method. Appl. Math. Comput. **176**, 1–6 (2006)
20. Lubich, C.: Fractional linear multistep methods for Abel-Volterra integral equations of the second kind. Math. Comput. **45**, 463–469 (1985)
21. Cui, M.: Compact finite difference method for the fractional diffusion equation. J. Comput. Phys. **228**, 7792–7804 (2009)
22. Klamka, J., Czornik, A., Niezabitowski, M., Babiarz, A.: Controllability and minimum energy control of linear fractional discrete-time infinite-dimensional systems. In: 11th IEEE International Conference on Control & Automation (ICCA), pp. 1210–1214 (2014)
23. http://functions.wolfram.com/GammaBetaErf/Beta3/03/01/02/0003/
24. Abdeljawad, T.: On Riemann and Caputo fractional differences. Comput. Math. Appl. **62**, 1602–1611 (2011)
25. Włodarczyk, M., Zawadzki, A.: RLC circuits in aspect of positive fractional derivatives. Sci. Works Sil. Univ. Techn.: Electr. Eng. **1**, 75–88 (2011)
26. Podlubny, I., Kacenak, M.: The Matlab mlf code. MATLAB Central File Exchange (2001–2009). File ID 8738 (2001)
27. Sowa, M.: A subinterval-based method for circuits with fractional order elements. Bull. Pol. Acad.: Tech. **62**(3), 449–454 (2014)
28. Sowa, M.: The subinterval-based ("SubIval") method and its potential improvements. In: Proceedings of the 39th Conference on Fundamentals of Electrotechnics and Circuit Theory IC-SPETO (2016)
29. Majka, Ł.: Measurement verification of the nonlinear coil models. In: Proceedings of the 39th Conference on Fundamentals of Electrotechnics and Circuit Theory IC-SPETO (2016)

Application of the Time-Fractional Diffusion Equation to Methyl Alcohol Mass Transfer in Silica

Alexey A. Zhokh, Andrey A. Trypolskyi and Peter E. Strizhak

Abstract Non-usual behavior of methyl alcohol mass transfer in mesoporous silica is experimentally and theoretically investigated. Analysis of the experimental data in terms of the second Fick's law and accounting of various pore geometries demonstrates no correspondence between the experimental data and theoretical solutions. We show that contrary to standard diffusion approach the experimental data are in an excellent coincidence with the solution of the time-fractional diffusion equation, obtained for boundary conditions that correspond to the experimental conditions. Obtained results reveal that methyl alcohol in mesoporous silica may exhibit anomalous features because of geometrical constraints of silica pores.

Keywords Diffusion · Time-fractional diffusion · Anomalous diffusion · Isopropanol · Silica

1 Introduction

Time-fractional diffusion describes mass transfer process with temporal non locality [1], concerning memory effect, which may be determined as a difference between time-scaled intervals of diffusing particle's jump, i.e. if mass transfer process time is depicted on time axis with geometrically equal time intervals, jump's time is shorter or longer than the equal time interval length on time axis [2]. These memory effects govern non-Brownian random walk motion [3]. In this case mean square displacement of particles is nonlinear versus time and the second Fick's law is no more applicable for describing this non-usual diffusion behavior which may occur as faster or slower transport comparably to normal diffusion [1].

Fast and slow non-Fickian transport may be described by the time-fractional diffusion equation with fractional order in range from 1 to 2 and from 0 to 1 respectively [4]. These types of transfer may be present in media with fractal structure

A.A. Zhokh (✉) · A.A. Trypolskyi · P.E. Strizhak
L.V. Pisarzhevsky Institute of Physical Chemistry,
National Academy of Sciences of Ukraine, Prospect Nauki 31, Kiev 03028, Ukraine
e-mail: al.zhokh@gmail.com

A. Babiarz et al. (eds.), *Theory and Applications of Non-integer Order Systems*,
Lecture Notes in Electrical Engineering 407, DOI 10.1007/978-3-319-45474-0_44

[4, 5]. Unlike normal diffusion, governed by the Brownian motion with the variance of probability density function proportional to the first power of time; anomalous transport is characterized by different scaling law [6]. One of the most frequently used statistical models of anomalous diffusion is the continuous time random walk model, corresponding the fractional diffusion equation governed by the Lévy diffusion process [7–9]. The parameters of the fractional integral models may be easily gotten by fitting of the experimental data of mass transfer process. However, like nonlinear equation models, these models are not computationally cheap and are also of a phenomenological description which does not necessarily reflect the physical meaning of the process. Anomalous diffusion through porous media, e.g. silica, is important for chemical engineering, because quantitative study of diffusion gives an opportunity to increase the effectiveness of various industrial processes, sorption and catalysis, only by controlling the regime of mass transport.

Silica is commercially available and extensively used as an effective sorbent because of large surface area, which may be easily controlled during silica synthesis or silica sorbent regeneration. Silica consists of particles typically obtained by sol-gel synthesis with their simultaneous aggregation into clusters [10]. Silica aggregates are well-described by fractal geometry [11]. Silica fractal structure has two different types, mass and surface fractal structures [12]. Fractal silica clusters exhibit self-similar relaxations of density fluctuations, dynamics of which is described by fractal approach [13]. However, the presence of anomalous diffusion in silica fractal structure still is not still fully investigated and a relationship between silica fractal structure and diffusing regime also remains unclear.

The present paper aims to explore the presence of anomalous time-fractional methanol diffusion in mesoporous silica. We show that normal diffusion approach fails describing experimental data. Contrary, we report a good coincidence between experimental results and theoretical analysis developed in the frame of the time-fractional diffusion equation.

2 Preliminaries

2.1 Time-Fractional Diffusion Equation

Time-fractional diffusion kinetics in porous media is described by the time-fractional diffusion equation:

$$\frac{\partial^{\alpha} C}{\partial t^{\alpha}} = K \cdot \frac{\partial^2 C}{\partial x^2}. \tag{1}$$

Here K denotes fractional diffusion coefficient in porous media, $\mathrm{cm}^2/\mathrm{sec}^{\alpha}$, C is the linear concentration of diffusing species, mole/cm; t is time, sec; x is a coordinate, cm; α is an order of the time-fractional derivative ($0 < \alpha < 2$). Time-fractional derivative is used in Caputo sense [14]:

$$\frac{\partial^{\alpha} C\left(x,t\right)}{\partial t^{\alpha}} = \frac{1}{\Gamma\left(m-\alpha\right)} \cdot \int_{0}^{t} \left(t-\tau\right)^{m-\alpha-1} \cdot \frac{\partial^{m} C}{\partial \tau^{m}} d\tau, \tag{2}$$

where $m = 1$ if $0 < \alpha < 1$ and $m = 2$ if $1 < \alpha < 2$, $\Gamma\left(x\right)$ is the Euler gamma function.

Clearly, if $\alpha = 1$ Eq. (1) reduces to standard diffusion equation.

2.2 Green's Function Approach

Applying Fourier-Laplace transforms technique [15–19] to Eq. (1) one may obtain asymptotic Green's functions for short and long times respectively:

$$G^{s}\left(x,t,\epsilon\right) = \frac{\exp\left(-\frac{\left(x-\epsilon\right)^{2}\Gamma\left(m+\alpha\right)}{4\cdot K\cdot t^{\alpha}}\right)}{2\cdot\sqrt{\frac{\pi\cdot K\cdot t^{\alpha}}{\Gamma\left(m+\alpha\right)}}}, \tag{3}$$

$$G^{l}\left(x,t,\epsilon\right) = \frac{x-\epsilon}{2\cdot\Gamma\left(m-\alpha\right)\cdot K\cdot t^{\alpha}}. \tag{4}$$

Here upper index s or l corresponds to short or long time intervals.

For the following initial and boundary conditions:

$$C\left(x,0\right) = C_{0}\left(x\right) = const, \tag{5}$$

$$\left.\frac{\partial C}{\partial x}\right|_{x=0} = 0 \tag{6}$$

the solution of diffusion equation is given in terms of integral formula [20]:

$$C\left(x,t\right) = \int_{0}^{L} \left[G\left(x,t,\epsilon\right) + G\left(x,t,-\epsilon\right)\right] \cdot C_{0}\left(\epsilon\right) d\epsilon. \tag{7}$$

Therefore, substituting Eqs. (3) and (4) into Eq. (7) the solutions of time-fractional diffusion equation at point L are obtained for short and long times respectively:

$$C^{s}\left(L,t\right) = C_{0}\cdot\frac{L}{\sqrt{\frac{\pi\cdot K\cdot t^{\alpha}}{\Gamma\left(m+\alpha\right)}}}, \tag{8}$$

$$C^{l}\left(L,t\right) = C_{0}\frac{L^{2}}{K\cdot t^{\alpha}\cdot\Gamma\left(m-\alpha\right)}. \tag{9}$$

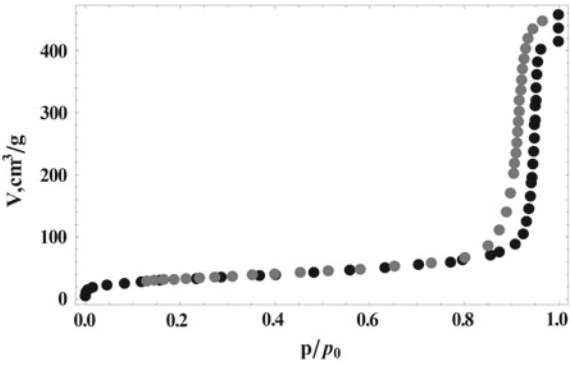

Fig. 1 Sorption isotherm of N_2 on silica surface at 77 K (*black* and *gray circles* correspond to adsorption and desorption data respectively)

3 Materials and Methods

3.1 Porous Silica

Silica sample, used as the porous media for measurement of methanol mass transport in this study, was synthesized by routine sol-gel method [21]. Adsorption–desorption isotherm of silica was obtained using Sorptomatic 1990 instrument. The measurement was made at the boiling point of liquid nitrogen (77 K). Surface area and pore volume were calculated from the isotherm for degassed silica sample.

Silica sample was characterized by adsorption–desorption isotherm of N_2 on silica surface, as shown in Fig. 1. The silica sample has pore volume 0.64 cm^3/g, BET surface area 116 m^2/g, sorption enthalpy 1.16 kJ/mol, mean pore diameter 23.2 nm, maximum pore diameter 23.3 nm, Dubinin and Radushkevich micropore volume 0.0375 cm^3/g, Lippens and de Boer micropore volume 0.0221 cm^3/g, mesopores surface area is 72m^2/g.

3.2 Chromatographic Setup

Gas chromatography is a well-known method for mass transfer processes study [22–24]. Experimental setup is based on gas chromatograph LHM-72, which was rearranged as follows. Chromatograph column was removed from thermostat and diffusion cell was installed. Diffusion cell is a short round steel-made tube, hermetically closed by steel cap from one side, and covered by a steel plate with two inlets from another side. The first inlet is consecutively joined to gas-carrier source and chromatograph evaporator, whereas the second inlet is joined to chromatograph flame-ionization detector. Schematically, the experimental setup is shown in Fig. 2. Silica grain 0.45 cm in diameter was placed inside the diffusion cell. Inert nonporous sodium silicate was used to fix the grain inside the cell and to cover half surface

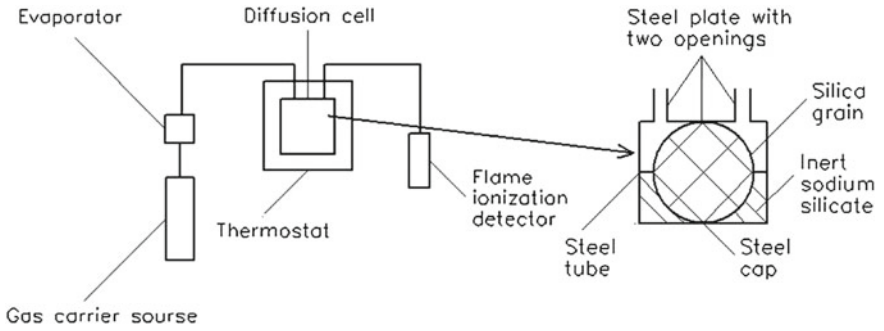

Fig. 2 Experimental setup, based on upgraded LHM-72 chromatograph

of the grain in order to block it from one side and to prevent diffusing species from penetration through both ends. This configuration corresponds to reflecting boundary condition.

Methanol mass transfer was studied at 373 K, 0.5 cm^3/s gas-carrier (argon) flow. The study was performed for two different methanol concentrations that correspond to the methanol injection into the diffusion cell as 0.3 and 0.5 μl.

4 Results and Discussion

An intensity of a chromatograph detector signal versus time is obtained for amount of methanol injected. After injection almost all methanol amount is absorbed by silica during very short time. All phenomena governed by methanol adsorption, methanol pulse flow through the grain, convection in gas phase, and other possible fast mass transfer phenomena, except diffusion, occur on the time scale of few seconds which is mainly defined by the methanol pulse flow through the grain. This time interval is order of linear grain size divided by linear gas flow velocity.

An attempt to fit the experimental results by normal diffusion approach is illustrated in Fig. 3. The data are presented as time dependence of normalized methanol concentration, $Cb(t)/C_0$, where C_0 corresponds to methanol at $t = 0$. Noisy solid line in Fig. 3 represents the experimental kinetics, solid line gives the best fit for the Cartesian coordinates, dashed line presents the simulations results in spherical coordinates, and semidashed line gives the simulations results in cylindrical coordinates. The presented results show that there is a slight almost insignificant difference in simulations performed in various coordinates.

It is evident from the data presented in Fig. 3 that normal diffusion approach, accounted by the second Fick's law, fails to describe mass transfer kinetics of methanol in silica. Also accounting for any geometry of pores does not lead to better fit of the experimental data.

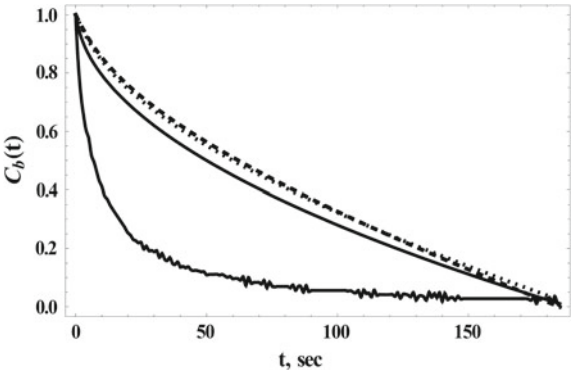

Fig. 3 Experimental data (*solid noisy line*), fitted by the solution of diffusion equation in Cartesian coordinates (*solid line*), spherical coordinates (*dashed line*), and cylindrical coordinates (*semidashed line*) for 0.5μl methanol injected. Values of diffusion coefficient: $1.7 \cdot 10^{-4}$ cm^2/s for Cartesian coordinates, $7.5 \cdot 10^{-6}$ cm^2/s for spherical coordinates, $8.5 \cdot 10^{-6}$ cm^2/s for cylindrical coordinates

The data presented in Fig. 3 demonstrate that methanol concentration time decay much faster comparing to theoretical models described by normal diffusion. Therefore, methanol diffusion in silica may be characterized as anomalous fast diffusion. This conclusion is approved by the following asymptotic analysis of the experimental results.

According to Eqs. (8) and (9) the relevant solutions for short and long times are linearized in logarithmic coordinates, $Ln(C/C_0) - Ln(t)$. The corresponding equations are given by:

$$\ln\left[\frac{C\,(L,t)}{C_0}\right] = \ln\left[\frac{L}{\sqrt{\frac{\pi \cdot K}{\Gamma(m+\alpha)}}}\right] - \frac{\alpha}{2} \cdot \ln t, \tag{10}$$

$$\ln\left[\frac{C\,(L,t)}{C_0}\right] = \ln\left[\frac{L^2}{K \cdot \Gamma\,(m-\alpha)}\right] - \alpha \cdot \ln t. \tag{11}$$

According to Eq. (10) the short time solution has a slope $\alpha/2$ in $Ln(C/C_0) - Ln(t)$ coordinates and intercept corresponds to the diffusion coefficient. Long time asymptotic solution is characterized by the slope α also in $Ln(C/C_0) - Ln(t)$ coordinates.

Figures 4 and 5 demonstrate the fitting of the experimental data by Eqs. (10) and (11) for short and long times. A correspondence between experimental data and fittings by these time-fractional is very high.

Values of fractional order α, calculated from linear equations, are 1.3 and 1.2 for short and long times respectively. Fractional diffusion constant values, obtained in the same manner, are 1.9 and 1.3 for short and long times respectively. A fairly good correspondence for the values of the fractional diffusion constant and fractional order,

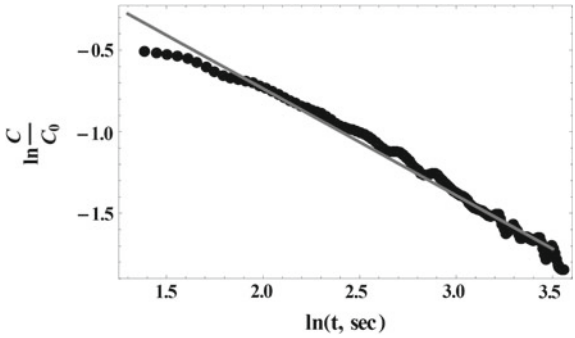

Fig. 4 Normalized methanol concentration time dependencies of experimental data (*points*) and fitted model according to Eq. (10) (*line*) in $Ln(C/C_0) - Ln(t)$ coordinates for short time. Linear equation $y = 0.641 - 0.676 \cdot x$, correlation coefficient $R^2 = 98.8\,\%$

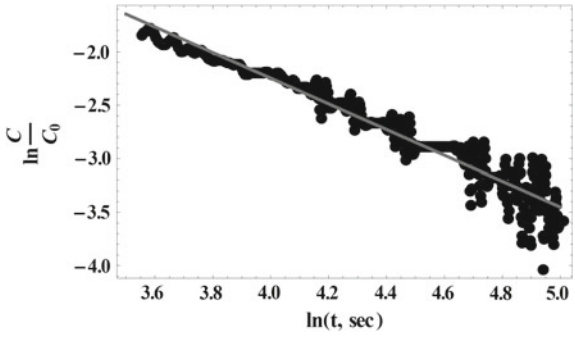

Fig. 5 Normalized methanol concentration time dependencies of experimental data (*points*) and fitted model according to Eq. (10) (*line*) in $Ln(C/C_0) - Ln(t)$ coordinates for short time. Linear equation $y = 2.564 - 1.2 \cdot x$, correlation coefficient $R^2 = 98.9\,\%$

measured for different times, may be concluded. Obtained fractional order values α are typical for anomalous fast diffusive regime [25].

Finally, analytical solution of the time-fractional diffusion equation was obtained by the Laplace transform method in analogously to method proposed by Crank [26] for normal diffusion on a semi-infinite media:

$$C(x,t) = C_0 \cdot \mathrm{erf}\left[\frac{x}{2 \cdot \sqrt{\frac{K \cdot t^{\alpha}}{\Gamma(m+\alpha)}}}\right]. \tag{12}$$

The solution of the time-fractional diffusion equation, plotted under Eq. (12), together with the experimental data is presented in Fig. 6. The coincidence between experimental data and time-fractional diffusion approach is also evident, as it is shown in Fig. 6 where dashed line corresponds to the analytical solution of time-fractional diffusion problem described by Eq. (1) with initial and boundary conditions (5) and (6).

Asymptotic analysis of experimental results for short and long times together with the fitting of the experimental data by the analytical solution clearly demonstrate that normal diffusion approach fails to describe the experimental results. It worse noting that, contrary to normal diffusion approach, there is a good agreement between the

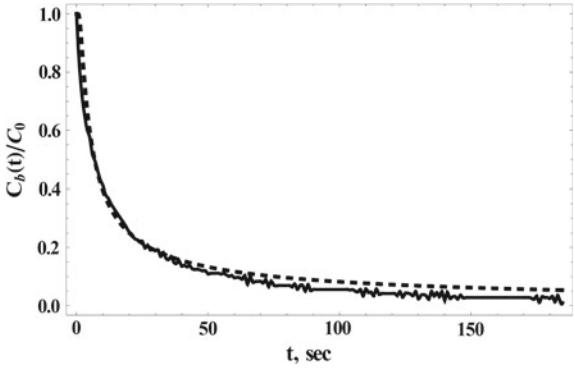

Fig. 6 Experimental data (*solid noisy line*) fitted by analytical solution of the time-fractional diffusion equation in Cartesian coordinates (*dashed line*). Values of fractional diffusion coefficient and fractional order are $4.5 \cdot 10^{-2}$ cm^2/s$^\alpha$ and 1.4

values of fractional diffusion coefficients and fractional order α obtained from short and long time analysis of experimental data as well as from the data presented in Fig. 6. Evidently, methanol diffusion in silica for conditions reported in this paper is characterized as anomalous fast diffusion, or super-diffusion [27]. It is characterized by fractional order value in the range of 1.2–1.3 as it follows from the short and long concentration time scaling, which is in a good agreement with the value 1.4 obtained by fitting the whole curve presented in Fig. 6. Anomalous transport strongly connected with continuous time random walk model, which describes random particle displacement and takes into account the jump time and the waiting time of a particle, before it makes the next movement [28]. This random process does not correspond to normal Gaussian probability distribution, typical for Fickian transport. In this case each jump time is independent of previous jumps [29]. That results to non-integer order of power law kernel for waiting time probability distribution [29]. Therefore, normal differential time operator is replaced by time-fractional integral and we arrive to time-fractional diffusion equation.

The measured values of fractional order α for the methanol super-diffusion in silica, obtained in terms of Caputo fractional derivative, underline the value of distribution exponent of random time intervals for which molecules stay at one particular site on the surface of porous media. As demonstrated by Hilfer [30] mass-conservation law in terms of fractional diffusion holds only for Caputo fractional integral, because not all continuous time random walks with power-law kernels are equal to time-fractional diffusion equation [31]. Distribution exponent of random time intervals for which methanol molecules stay at one particular site on the surface of porous media may concern alcohol adsorption on silica, which is associated with energetic disorder of corresponding adsorption sites [32].

5 Conclusion

Analysis of the experimental data for the methanol transport in silica demonstrates that standard diffusion approach based on the second Fick's law fails to describe experimental data whereas approach based on the time-fractional diffusion equation fits experimental data very well. We have shown that methanol mass transfer in silica is described by the time-fractional diffusion equation. We have shown that applying various types of analysis leads to self-consistent results. The present study reveals that methyl alcohol transport in silica is characterized as superdiffusion, which is significantly faster comparing to standard Fickian diffusion. Experimental evidence for the anomalous diffusion of methanol in silica presented in our study is important for fundamental understanding of the basis of mass transport phenomena in porous media and mass transfer modeling in porous media in the frame fractional calculus, which might be important for chemical engineering applications.

References

1. Metzler, R., Klafter, J.: Boundary value problems for fractional differential equations. Phys. A **278**, 107–125 (2000)
2. Podlubny, I.: Geometric and physical interpretation of fractional integration and fractional differentiation. Frac. Calc. Appl. Anal. **5**(4), 367–386 (2002)
3. Vlahos, L., Isliker, H., Kominis, Y., Hizanidis, K.: Normal and anomalous diffusion: a tutorial. Order Chaos **10**, 1–40 (2008)
4. Ciesielski, M., Leszczynski, J.: Numerical simulations of anomalous diffusion. Comput. Methods Mech. (3–6), pp. 1–5 (2003)
5. O'Shaughnessy, B., Procaccia, I.: Diffusion on fractals. Phys. Rev. A **32**(5), 3073–3083 (1985)
6. Płociniczak, ŁÂĄ: Analytical studies of a time-fractional porous medium equation. Derivation, approximation and applications. Commun. Nonlinear Sci. Numer. Simul. **24**(1–3), 169–183 (2015)
7. Chen, W., Sun, H., Zhang, X., Korosak, D.: Anomalous diffusion modeling by fractal and fractional derivatives. Comput. Math. Appl. **59**(5), 1754–1758 (2010)
8. Paradisi, P., Cesari, R., Mainardi, F., Tampieri, F.: The fractional Fick's law for non-local transport processes. Phys. A **293**, 130–142 (2001)
9. Zhang, H., Liu, F., Anh, V.: Numerical approximation of Levy-Feller diffusion equation and its probability interpretation. J. Comput. Appl. Math. **206**, 1098–1115 (2007)
10. Rodriguez, R., Rojas, G., Estevez, M., Vargas, S.: Fractal characterization of silica sol prepared by the sol-gel method: From the sol formation to the flocculation process. J. Sol-Gel Sci. Technol. **23**, 99–105 (2002)
11. Hinic, I.: Behavior of fractal structure characteristics for neutral silica aero-gels during the sintering process. Phys. State Solid **144**, 59–63 (1994)
12. Sintes, T., Toral, R., Chakrabarti, A.: Fractal structure of silica colloids re-visited. J. Phys. A: Math. Gen. **29**(3), 533–540 (1996)
13. Martin J.E., Wilcoxon, J.: Fractal structure and fractal time in silica sol-gels, In: MRS Proceedings, vol. 180 (1990)
14. Li, C., Qian, D., Chen, Y., On Riemann-Liouville and Caputo derivatives, Discrete Dyn. Nat. Soc. **15** (2011)
15. Han, B.: The time-space fractional diffusion equation with an absorption term. In: 2012 24th Chinese Control and Decision Conference, vol. 2, no. 3, pp. 1054–1056 (2012)

16. Huang, F., Liu, F.: The space-time fractional diffusion equation with Caputo derivatives. J. Appl. Math. Comput. **19**(1), 179–190 (2005)
17. Pagnini, G.: Short note on the emergence of fractional kinetics. Phys. A **409**, 29–34 (2014)
18. Metzler, R., Klafter, J.: The restaurant at the end of the random walk: recent developments in the description of anomalous transport by fractional dynamics. J. Phys. A: Math. Gen. **37**, 161–208 (2004)
19. Atkinson, C., Osseiran, A.: Rational solutions for the time-fractional diffusion equation. SIAM J. Appl. Math. **71**(1), 92–106 (2011)
20. Mainardi, F., Pagnini, G.: The Wright functions as solutions of the time-fractional diffusion equation. Appl. Math. Comput. **141**, 51–62 (2003)
21. Trewyn, B.G., Slowing, I.I., Giri, S., Chen, H., Lin, V.S.: Synthesis and functionalization of a mesoporous silica nanoparticle based on the sol-gel process and applications in controlled release. Acc. Chem. Res. **40**, 846–853 (2007)
22. Marrero, T.R., Mason, E.A.: Gaseous diffusion coefficients. J. Phys. Chem. Ref. Data **1**(1), 117 (1972)
23. Katsanos, N.A.: Studies of diffusion and other rate processes by gas chromatography. Pure Appl. Chem. **65**(10), 2245–2252 (1993)
24. Khalid, K., Khan, R.A., Zain, S.M.: Analysis of diffusion coefficient using reversed-flow gas chromatography-a review. Am. J. Appl. Sci. **8**(5), 428–435 (2011)
25. Tadjeran, C., Meerschaert, M.M.: A second-order accurate numerical method for the two-dimensional fractional diffusion equation. J. Comput. Phys. **220**, 813–823 (2007)
26. Crank, J.: The Mathematics of Diffusion, 2nd edn. Clarendon Press, Oxford (1975)
27. Metzler, R., Klafter, J.: The random walk's guide to anomalous diffusion: a fractional dynamics approach. Phys. Rep. **339**, 77 (2000)
28. Su, N.: Mass-time and space-time fractional partial differential equations of water movement in soils: Theoretical framework and application to infiltration. J. Hydrol. **519**, 1792–1803 (2014)
29. Hapca, S., Crawford, J.W., Macmillan, K., Wilson, M.J., Young, I.M.: Modeling nematode movement using time-fractional dynamics. J. Theor. Biol. **248**, 212–224 (2007)
30. Hilfer, R.: Fractional diffusion based on Riemann-Liouville fractional derivatives. J. Phys. Chem. B **104**(16), 3914–3917 (2000)
31. Scalas, E., Gorenflo, R., Mainardi, F.: Uncoupled continuous-time random walks: Solution and limiting behavior of the master equation. Phys. Rev. E **69**, 011107 (2004)
32. Cruz, M.I., Stone, W.E.E., Fripiat, J.J.: The methanol-silica gel system. II. The molecular diffusion and proton exchange from pulse proton magnetic resonance data. J. Phys. Chem. **76**(21), 3078–3088 (1972)

Author Index

A. Babiarz et al. (eds.), *Theory and Applications of Non-integer Order Systems*,
Lecture Notes in Electrical Engineering 407, DOI 10.1007/978-3-319-45474-0